マイクロフィルム用資料

ISSN 0386-5878
Technical Memorandum
of PWRI No.3906

UJNR

TSUKUBA 2003

PROCEEDINGS OF THE 35TH JOINT MEETING OF U.S. - JAPAN PANEL ON WIND AND SEISMIC EFFECTS UJNR

May 12 - 14, 2003

Tsukuba, Japan

Public Works Research Institute

Copyright © (2003) by P.W.R.I.
All rights reserved. No part of this book may be reproduced by any means, nor transmitted, nor translated into a machine language without the written permission of the Chief Executive of P.W.R.I.

この報告書は、土木研究所理事長の承認を得て刊行したものである。したがって、本報告書の全部又は一部の転載、複製は、土木研究所理事長の文書による承認を得ずしてこれを行ってはならない。

Technical Memorandum
of PWRI No. 3906

PROCEEDINGS OF THE 35TH JOINT MEETING OF U.S.-JAPAN PANEL ON WIND AND SEISMIC EFFECTS UJNR

Edited by

Michio Okahara, Secretary-General
Japan-side Panel on Wind and Seismic Effects

Synopsis

This publication contains the proceedings of the 35th Joint Meeting of the U.S.-Japan Panel on Wind and Seismic Effects, UJNR. The meeting was held at the National Institute for Land and Infrastructure Management, Tsukuba, Japan during May 12-14, 2003. Thirty-one technical papers were authored for the meeting, which were organized into seven themes; Geotechnical Engineering and Ground Motion, Next-Generation Building and Infrastructure Systems, Dams, Wind Engineering, Advanced Information and Communication Technology for Disaster Prevention and Public Health Evaluation, Transportation Systems and Progressive Collapse of Buildings.

Keywords: *Wind engineering, earthquake engineering, information technology, progressive collapse, UJNR*

PREFACE

This publication contains the proceedings of the 35th Joint Meeting of the U.S.-Japan Panel on Wind and Seismic Effects, UJNR. The meeting was held at the National Institute for Land and Infrastructure Management, Tsukuba, Japan during May 12-14, 2003. The proceedings include the program, list of members, task committee reports, and technical papers submitted to the Joint Panel Meeting, and a summary of the technical site visits.

BACKGROUND

Responding to the need for improving engineering and scientific practices through exchange of technical data and information, research personnel and research equipments, the United States and Japan created the U.S.-Japan Cooperative Science Program in 1961. The U.S.-Japan Cooperative Program in Natural Resources (UJNR) was created in January 1964. The objective of UJNR is to exchange information on research results and scientists and engineers in natural resources for benefit of both countries. UJNR is of 18 Panels each responsible for specific technical subjects.

The Panel on Wind and Seismic Effects was established in 1969. Seventeen U.S. and eight Japanese agencies currently participate to develop and exchange technologies aimed at reducing damage from high winds, earthquakes, storm surge, and tsunamis. This work is produced through collaboration between U.S. and Japanese member researchers working in five Task Committees. Each Task Committee focuses on specific technical issues, e.g., geotechnical engineering and ground motion. The Panel provides the vehicle to exchange technical date and information on design and construction of civil engineering infrastructures, buildings, and to exchange high wind and seismic measurement records. Annual Joint Panel Meetings alternate in the U.S. and Japan. These one-week technical meetings including technical site visits provide the forum to discuss on-going research and research results.

The National Institute of Standards and Technology (NIST) provides the U.S.-side chairman and secretary-general. The Public Works Research Institute (PWRI) provides the Japan-side chairman and secretary-general.

Annual Joint Panel Meetings provide the mechanism for interaction between U.S. and Japanese researchers in wind and earthquake engineering which provides opportunities to gain valuable information and to engage in cooperative research. Through these opportunities the Panel member organizations have realized important advances in building and structure technology. The Panel's activities have resulted in improved building and structure codes and standards in both countries.

The Panel's efforts are exemplary of effective joint research and of technology delivery between researchers in the U.S. and Japan. Since its creation, about 2000 papers were presented in 34 Joint Panel

Meetings and Task Committee Workshops and over 250 guest researchers were exchanged. The Panel provides important information about the U.S. and Japan's civil engineering thrusts which influence both countries' research and provide the basis for improvements in building and structure codes and standards.

HIGHLIGHTS OF THE 35TH JOINT PANEL MEETING

- Thirty technical papers were presented orally, 15 by each side. The papers were organized into seven Technical Sessions; Geotechnical Engineering and Ground Motion, Next-Generation Building and Infrastructure Systems, Dams, Wind Engineering, Advanced Information and Communication Technology for Disaster Prevention and Public Health Evaluation, Transportation Systems and Progressive Collapse of Buildings.

- Panel Task Committees (T/C) activities grow in strength and are working well under current structure. They are an effective vehicle to exchange in-depth advanced seismic and wind technologies being used by both countries. They increasingly seek partnering activities with other Panel T/Cs and other UJNR Panels. A new T/C was created on Advanced Information and Communication Technology for Disaster prevention and public Health Evaluation. Four T/C workshops are planned for the coming year.

- The Panel has successfully implemented the recommendations of the Strategic Plan, which was approved at its Thirty-third Joint Panel Meeting.

- The Panel's web site will be expanded with Panel and T/C achievements through regular focused broadcast of its contributions targeted to its member organizations and other customers on its activities and results.

TABLE OF CONTENTS

PREFACE i

AGENDA OF JOINT MEETING AND TECHNICAL SITE VISITS 1

LIST OF PANEL MEMBERS 11

RESOLUTIONS 31

PAPERS 37

THEME 1. Geotechnical Engineering and Ground Motion 39

Status Report on Strong Motion Recording for Buildings in Japan
Izuru Okawa*, Toshihide Kashima, Kuniaki Yamagishi and Morimasa Watakabe 41

Real-Time Seismic Monitoring Needs of a Building Owner and the Solution
Mehmet Çelebi*, Ahmet Sanli, Mark Sinclair, Sharon Gallant and Dan Radulescu 45

Study of Full-Scale / Big-Scale Experiment (Report of US-Japan Symposium on the Seismic Performance of Urban, Reclaimed and Port Areas - Full-Scale Experiment at Tokachi Port -)
Takahiro Sugano* and Eiji Kohama 58

Seismic Response of Earth Dams on Liquefiable Foundation and Compaction Remediation
Michael Sharp* and Korhan Adalier 61

THEME 2. Dams 71

Current U.S. Army Corps of Engineers' Policy and Guidance for Seismic Design of Dams
Anjana Chudgar* and Enrique E. Matheu 73

Advanced Research Activities on Dynamic Analysis for Concrete Dams in Japan and A Study on Seismic Performance of Concrete Gravity Dams by Smeared Crack Model
Ken-ichi Kanenawa*, Takashi Sasaki and Yoshikazu Yamaguchi 82

The Value Added of Field Testing on Concrete Dams
Ziyad H. Duron*, Enrique E. Matheu and Robert L. Hall 94

Characteristics of Seismic Vibrations on Rock Foundation of Dam Sites and Attenuation Relationships of Acceleration Response Spectra at Dam Foundations in Japan
Hideaki Kawasaki, Kenji Inagaki*, Yoshikazu Yamaguchi and Takashi Sasaki 108

THEME 3. Next-Generation Building and Infrastructure Systems 119

Construction, Operation and Application of the George E. Brown, Jr. Network for Earthquake Engineering Simulation
Steven McCabe* and Joy Pauschke 121

Project on 3-D Full-Scale Earthquake Testing Facility (Third Report)
Keiichi Ohtani*, Nobuyuki Ogawa, Tsuneo Katayama and Heki Shibata 133

MCEER Advanced Technology Research for Next Generation Seismic Resilient Buildings

Gary Dargush* and George C. Lee 140
Research and Development in the US-Japan Cooperative Structural Testing Research Program on Smart Structural Systems
Shunsuke Otani, Akira Wada, Yoshikazu Kitagawa, Takafumi Fujita, Mitsumasa Midorikawa*, Masaomi Teshigawara and Masanori Iiba 155
Potential of Satellite and Aerial Remote Sensing Technologies for Earthquake Disaster Management
K. Thirumalai* 185
THEME 4. Transportation Systems 191
Seismic Performance of RC Bridge Columns Subjected to Bilateral Excitation
Kazuhiko Kawashima*, Gakuho Watanabe and Ryoji Hayakawa 193
Multi Hazard Dynamic Testing for Bridge Piers
Phillip Yen* and Kornel Kerenyi 208
Site-Specific Design Earthquake Ground Motion and Seismic Design Technology in Next Generation
Shigeki Unjoh*, Takaaki Kusakabe, Shoichi Nakatani, Takeshi Ohshita, Yasuhiko Wakizaka, Keiichi Tamura and Jiro Fukui 213
Seismic Analysis and Design of Flared Bridge Columns
Hisham Nada, David Sanders* and M. Saiid Saiidi 224
THEME 5. Advanced Information and Communication Technology for Disaster prevention and public Health Evaluation 239
General Overviews and Future Perspectives of Disaster Information Systems in Japan
Hiroaki Miyatake* and Akihiko Nunomura 241
Mortality during Landslides, Chuuk, Federated States of Micronesia, 2002
Carlos Sanchez, Stacy Young, Nachsa Siren, Tzesan Lee, Dahna Batts-Osborne and Josephine Malilay* 254
Application of Remote Sensing and Information & Communication Technologies for Disaster Response
Takaaki Kusakabe and Akihiro Sanada* 261
Spatial Data Fusion for Infrastructure Condition Assessment
William Roper* 270
Geomorphologic Survey for Hazard Mapping and Real-Time GIS, Aided with LiDAR Technology
Sotoshi Nakata, Seiji Ichikawa, Koji Sango, Masaharu Tsuzawa*, Jun-ichi Kisanuki and Soichiro Sato 289
THEME 6. Wind Engineering 297
Wind-Induced Vibration of Stay Cables: Summary of FHWA Study
Nicholas Jones* 299
Utilization of Digital Surface Model in Urban Area for Wind Engineering
Yasuo Okuda*, Hisashi Okada, Kikitsu Hitomitsu, Tetsuro Tamura, Masamiki Ohashi,

Takahisa Kobayashi, Osamu Suzuki, Hiroshi Yamauchi and Naoki Shirai 312
A Model to Predict Hurricanes Induced Losses for Residential Struc*tures*
Jean-Paul Pinelli, Chelakaran Subramanian, Liang Zhang, Kurtis Gurley, Anne Cope, Emil Simiu, Sofia Diniz and Shahid Hamid 322
Calculation of Unsteady Aerodynamic Forces by CFD and Their Comparison with Measured Values
Hiroshi Sato, Jun Murakoshi, Koichiro Fumoto* and Masao Miyazaki 336
THEME 7. Progressive Collapse of Buildings 345
Fire Resistance of Stell Frames
Yosifumi Sakumoto*, Taro Nishigaki and Ken-ichi Ikeda 347
Best Practices Guidelines for Mitigation of Building Progressive Collapse
H. S. Lew* 358
Study on High-Rise Steel Building Structure that Excels in Redundancy
Akira Wada, Ken-ichi Ohi, Hiroyuki Suzuki, Isao Nishiyama, Takashi Hasegawa, Yoshifumi Sakumoto, Mitsuo Fusimi and Hisaya Kamura* 366
Applicability of Seismic Design in Mitigating Progressive Collapse
W. Gene Corley 380
Plastic Deformation Capacity of Welded Beam-End Limited by Brittle Fracture
Takahiro Szuki, Takumi Ishii, Yoshifumi Sakumoto and Akiyoshi Mukai 391
APPENDIX 401
TASK COMMITTEE REPORTS 403
TECHNICAL SITE VISITS 419
STRATEGIC PLAN 431

AGENDA OF JOINT MEETING AND TECHNICAL SITE VISITS

JOINT MEETING

May 11 (Sunday)

Arrival of U.S.-side Delegation
Hotel: Hotel Grand Shinonome
TEL/FAX: +81-29-856-2211/+81-29-856-2679

May 12 (Monday)

10:00 **Opening Ceremonies** [8F Conference Room]

Call to order by Michio Okahara, Secretary-General, Japan-side Panel

Opening remarks by Hisakazu Ohishi, Vice-Minister for Engineering Affairs, Ministry of Land, Infrastructure and Transport

Remarks by Kevin Maher, Minister-Counselor for Environment, Science and Technology Affairs, Embassy of the United States of America

Remarks by Tadahiko Sakamoto, Chairman, Japan-side Panel on Wind and Seismic Effects, Chief Executive, Public Works Research Institute

Remarks by H. S. Lew, Acting Chairman, U.S.-side Panel on Wind and Seismic Effects, Materials and Construction Research Division, National Institute of Standards and Technology, Department of Commerce

Introduction of Japan-side Members by Japan-side Panel Chairman

Introduction of U.S.-side Members by U.S.-side Panel Chairman

Elect Joint Panel Meeting Chairman

Adopt Agenda

Adjourn

11:10 Group Photograph

11:30 **Technical Session 1 - Geotechnical Engineering and Ground Motion**
Chairman - H. S. Lew

11:30 *Status Report on Strong Motion Recording for Buildings in Japan*, Izuru Okawa*, Toshihide Kashima, BRI; Kuniaki Yamagishi, Mitsui Corporation; and Morimasa Watakabe, Toda Corporation

11:45 *Real-Time Seismic Monitoring Needs of a Building Owner and the Solution*, Mehmet Çelebi*, Ahmet Sanli, Mark Sinclair, Sharon Gallant and Dan Radulescu, USGS

12:00 *Study of Full-Scale / Big-Scale Experiment (Report of US-Japan Symposium on the Seismic Performance of Urban, Reclaimed and Port Areas - Full-Scale Experiment at Tokachi Port -)*, Takahiro Sugano* and Eiji Kohama, PARI

12:15 *Seismic Response of Earth Dams on Liquefiable Foundation and Compaction Remediation*, Michael Sharp*, ERDC; and Korhan Adalier, Rensselaer Polytechnic Institute

12:30 Discussion

12:50 Lunch [1F Conference Room]

13:50 **Technical Session 2 - Dams**

Chairman - H. S. Lew

13:50 *Current U.S. Army Corps of Engineers' Policy and Guidance for Seismic Design of Dams*, Anjana Chudgar*, CORPS; and Enrique E. Matheu, Louisiana State University

14:05 *Advanced Research Activities on Dynamic Analysis for Concrete Dams in Japan and A Study on Seismic Performance of Concrete Gravity Dams by Smeared Crack Model*, Ken-ichi Kanenawa*, Takashi Sasaki and Yoshikazu Yamaguchi, PWRI

14:20 *The Value Added of Field Testing on Concrete Dams*, Ziyad H. Duron*, Harvey Mudd College; Enrique E. Matheu, Louisiana State University; and Robert L. Hall, ERDC

14:35 *Characteristics of Seismic Vibrations on Rock Foundation of Dam Sites and Attenuation Relationships of Acceleration Response Spectra at Dam Foundations in Japan*, Hideaki Kawasaki, Kenji Inagaki*, NILIM; Yoshikazu Yamaguchi and Takashi Sasaki, PWRI

14:50 Discussion

15:10 Break

15:20 **Task Committee Meetings**

A: Geotechnical Engineering and Ground Motion [Room #725]

B: Next-Generation Building and Infrastructure Systems [Room #610]

C: Dams [Room #617]

D: Wind Engineering [Room #727]

F: Advanced Information and Communication Technology for Disaster Prevention and Public Health Evaluation [Room #730]

G: Transportation Systems [8F Conference Room]

17:00 Conclusion of Day 1

18:30 Japan-side Panel Hosted Reception
(Okura Frontier Hotel Tsukuba, Phone: 029-852-1112)

May 13 (Tuesday)

9:00 **Technical Session 3 - Next-Generation Building and Infrastructure Systems**
Chairman - Tadahiko Sakamoto

9:00 *Construction, Operation and Application of the George E. Brown, Jr. Network for Earthquake Engineering Simulation*, Steven McCabe* and Joy Pauschke, NSF

9:15 *Project on 3-D Full-Scale Earthquake Testing Facility (Third Report)*, Keiichi Ohtani*, Nobuyuki Ogawa, Tsuneo Katayama and Heki Shibata, NIED

9:30 *MCEER Advanced Technology Research for Next Generation Seismic Resilient Buildings*, Gary Dargush* and George C. Lee, MCEER, SUNY at Buffalo

9:45 *Research and Development in the US-Japan Cooperative Structural Testing Research Program on Smart Structural Systems*, Shunsuke Otani, University of Tokyo; Akira Wada, Tokyo Institute of Technology; Yoshikazu Kitagawa, Keio University; Takafumi Fujita, University of Tokyo; Mitsumasa Midorikawa*, Masaomi Teshigawara and Masanori Iiba, BRI

10:00 *Potential of Satellite and Aerial Remote Sensing Technologies for Earthquake Disaster Management*, K. Thirumalai*, DOT

10:15 Discussion

10:40 Break

11:00 **Technical Session 4 - Transportation Systems**
Chairman - Tadahiko Sakamoto

11:00 *Seismic Performance of RC Bridge Columns Subjected to Bilateral Excitation*, Kazuhiko Kawashima*, Gakuho Watanabe and Ryoji Hayakawa, Tokyo Institute of Technology

11:15 *Multi Hazard Dynamic Testing for Bridge Piers*, Phillip Yen*, FHWA; and Kornel Kerenyi, GKY and Associates, Inc.

11:30 *Site-Specific Design Earthquake Ground Motion and Seismic Design Technology in Next Generation*, Shigeki Unjoh*, PWRI; Takaaki Kusakabe, Shoichi Nakatani, NILIM; Takeshi Ohshita, Yasuhiko Wakizaka, Keiichi Tamura and Jiro Fukui, PWRI

11:45 *Seismic Analysis and Design of Flared Bridge Columns*, Hisham Nada, Alrabiah-Cowi Consulting Engineers; David Sanders* and M. Saiid Saiidi, University of Nevada at Reno

12:00 Discussion

12:20 Lunch [1F Conference Room]

13:20 **Technical Session 5 - Advanced Information and Communication Technology for Disaster Prevention and Public Health Evaluation**
Chairman - Tadahiko Sakamoto

13:20 *General Overviews and Future Perspectives of Disaster Information Systems in Japan*, Hiroaki Miyatake* and Akihiko Nunomura, Cabinet Office

13:35 *Mortality during Landslides, Chuuk, Federated States of Micronesia, 2002*, Carlos Sanchez, Stacy Young, CDC; Nachsa Siren, Department of Health, Chuuk State; Tzesan Lee, Dahna Batts-Osborne and Josephine Malilay*, CDC

13:50 *Application of Remote Sensing and Information & Communication Technologies for Disaster Response*, Takaaki Kusakabe and Akihiro Sanada*, NILIM

14:05 *Spatial Data Fusion for Infrastructure Condition Assessment*, William Roper*, George Washington University

14:20 *Geomorphologic Survey for Hazard Mapping and Real-Time GIS, Aided with LiDAR Technology*, Sotoshi Nakata, Seiji Ichikawa, Koji Sango, Masaharu Tsuzawa*, Jun-ichi Kisanuki and Soichiro Sato, GSI

14:35 Discussion

15:00 Break

15:20 **Strategic Planning Session**

16:40 Conclusion of Day 2

18:30 Individual Japan-side Members Hosted Dinners

May 14 (Wednesday)

9:00 **Technical Session 6 - Wind Engineering**
Chairman - H. S. Lew

9:00 *Wind-Induced Vibration of Stay Cables: Summary of FHWA Study*, Nicholas Jones*, University of Illinois

9:15 *Utilization of Digital Surface Model in Urban Area for Wind Engineering*, Yasuo Okuda*, Hisashi Okada, Kikitsu Hitomitsu, BRI; Tetsuro Tamura, Shuyang Cao, Tokyo Institute of Technology; Masamiki Ohashi, NILIM; Takahisa Kobayashi, Osamu Suzuki, Hiroshi Yamauchi, MRI; and Naoki Shirai, Kokusai Kogyo Co.

9:30 *A Model to Predict Hurricanes Induced Losses for Residential Structures*, Jean-Paul

Pinelli, Chelakaran Subramanian, Liang Zhang, Florida Institute of Technology; Kurtis Gurley, Anne Cope, University of Florida; Emil Simiu, Sofia Diniz, NIST; and Shahid Hamid, Florida International University (Presented by Nicholas Jones)

9:45 *Calculation of Unsteady Aerodynamic Forces by CFD and Their Comparison with Measured Values*, Hiroshi Sato, Jun Murakoshi, Koichiro Fumoto*, PWRI; and Masao Miyazaki, Sumitomo Heavy Industries Ltd.

10:00 Discussion

10:20 Break

10:40 **Technical Session 7 - Progressive Collapse of Buildings**
Chairman - H. S. Lew

10:40 *Fire Resistance of Stell Frames*, Yosifumi Sakumoto*, Nippon Steel Corporation; Taro Nishigaki, Taisei Corporation; Ken-ichi Ikeda, Shimizu Corporation; and Mamoru Kohno, BRI

10:55 *Best Practices Guidelines for Mitigation of Building Progressive Collapse*, H. S. Lew*, NIST

11:10 *Study on High-Rise Steel Building Structure that Excels in Redundancy*, Akira Wada, Tokyo Institute of Technology; Ken-ichi Ohi, University of Tokyo; Hiroyuki Suzuki, Tsukuba University; Isao Nishiyama, BRI; Takashi Hasegawa, NILIM; Yoshifumi Sakumoto, Mitsuo Fusimi, Nippon Steel Corporation; and Hisaya Kamura*, JFE R&D Corporation

11:25 *Applicability of Seismic Design in Mitigating Progressive Collapse*, W. Gene Corley, CTL Engineering (Presented by H. S. Lew)

11:40 Discussion

12:00 Lunch [1F Conference Room]

13:00 **Workshop and Task Committee Reports**
Chairman - Tadahiko Sakamoto

14:10 **Adoption of Final Resolutions**
Chairman - Tadahiko Sakamoto

15:30 Break

15:50 **Closing Ceremonies**
Call to order by Michio Okahara, Secretary-General, Japan-side Panel

Remarks by H. S. Lew, Acting Chairman, U.S.-side Panel on Wind and Seismic Effects

Remarks by Tadahiko Sakamoto, Chairman, Japan-side Panel on Wind and Seismic Effects

16:20 Conclusion of 35th Joint Panel Technical Sessions

18:30 U.S.-side Panel Hosted Reception
(Hotel Grand Shinonome, Phone: 029-856-2211)

TECHNICAL SITE VISITS

May 15 (Thursday)

9:20	Lv. Hotel by NILIM and BRI Buses
9:30-11:15	Visit to Tsukuba Express Train Construction Project
11:15-12:30	Move to Ariake and Kawasaki City by NILIM and BRI Buses
12:30-13:30	Lunch at Ariake Washington Hotel, Tokyo Bay Area
13:30-14:00	Move to Site at Kashimada Station (JR Nanbu-line)
14:00-15:30	Visit to Seismic Isolation High-rise Buildings, Kawasaki City
15:30-16:30	Move to Tokyo/Haneda Airport by NILIM and BRI Buses
17:30	Lv. Tokyo for Hokkaido by Airplane (ANA75)
19:00	Ar. Chitose Airport
19:00-20:30	Move to Muroran City by HCERI Bus
	Hotel: Muroran Prince Hotel
	TEL/FAX: +81-143-22-5555/+81-143-22-5560

May 16 (Friday)

8:00	Lv. Hotel by HCERI Bus
8:30-10:00	Visit to Muroran Institute of Technology
10:00-11:30	Visit to Muroran Highway Construction Office, Traffic Control System for Hakucho Bridge
11:30-12:30	Visit to Muroran-Highway (Weather Resistance Steel Structures)
12:30-13:30	Lunch hosted by Hokkaido Development Bureau
13:30-14:00	Introduction of Dam Project in Hokkaido Area
14:00-15:30	Visit to Japan Steel Works Co., Muroran Plant
16:00-17:00	Visit to Hakucho Suspension Bridge
17:00-18:00	Move to Abuta Town by HCRI Bus
18:00	Ar. Hotel
	Hotel: Toya Lake-side Hotel
	TEL/FAX: +81-142-75-2211/+81-142-75-2753

May 17 (Saturday)

8:30	Lv. Hotel by HCERI Bus
9:00-9:40	Explanation of Usu Volcano and Tunnel Works
9:40-10:10	Visit to Mitoyo Tunnel
10:20-11:45	Visit to the summit of Mt. Usu and the foot of Mt. Showa
11:50-12:05	Visit to Sankei Hospital
12:10-13:10	Lunch
13:20-13:50	Visit to Onsen-cho (Mud flooded area)

13:55-15:00	Visit to the trail on the west foot of Usu Volcano
15:00-16:30	Move to Chitose Airport
(In case of rain)	
13:20-14:00	Visit to Usu Volcanic Museum
14:05-14:25	Visit to Onsen-cho (Mud flooded area)
14:30-14:50	Visit to Kako-numa on the west foot of Usu Volcano
14:50-16:30	Move to Chitose Airport

17:30	Lv. Hokkaido for Tokyo by Airplane (ANA72)
19:00	Ar. Tokyo/Haneda Airport
20:00	Ar. Hotel
	Hotel: Yaesu Fujiya Hotel
	TEL/FAX: +81-3-3273-2111/+81-3-3273-2180

May 18 (Sunday)

Departure of U.S.-side Delegation

LIST OF PANEL MEMBERS

U.S.-SIDE DELEGATION

Dr. H. S. Lew
Acting Chairman, U.S.-side Panel
Senior Research Structural Engineer
Materials and Construction Research Division
Building and Fire Research Laboratory
National Institute of Standards and Technology
100 Bureau Drive Stop 8611
Gaithersburg, MD 20899-861
301-975-6060 (F) 301-869-6275
hai.lew@nist.gov

Mr. Stephen A. Cauffman
Secretary-General, U.S.-side Panel
Research Engineer
Materials and Construction Research Division
Building and Fire Research Laboratory
National Institute of Standards and Technology
100 Bureau Drive, Stop 8611
Gaithersburg, MD 20899-8611
301-975-6051 (F) 301-869-6275
stephen.cauffman@nist.gov

Dr. Jon P. Ake
Geophysicist
Seismotectonics and Geophysics Section
Code D-8330
P.O. Box 25007
Bureau of Reclamation
U.S. Department of the Interior
Denver, CO 80225
303-445-3169 (F) 303-236-9127
jake@do.usbr.gov

Dr. Mehmet K. Celebi
Research Civil Engineer
Earthquake Hazards Team
U.S. Geological Survey
U.S. Department of the Interior
345 Middlefield Road, MS 977
Menlo Park, CA 94025
650-329-5623 (F) 650-329-5163
celebi@usgs.gov

Dr. Anjana Chudgar
U.S. Army Corps of Engineers
Headquarters, 441 G Street NW
ATTN: CECW-EWS
Washington, DC 20314
202-761-0250 (F) 202-761-0633
anjana.k.chudgar@hq02.usace.army.mil

Dr. Gary Dargush
Department of Civil, Structural, and Environmental Engineering
State University of New York at Buffalo
135 Ketter Hall, Buffalo, NY 14260
716-645-2114 ext.2405 (F) 716-645-3733
gdargush@eng.buffalo.edu

Dr. Nicholas P. Jones
Professor and Head
Department of Civil and Environmental Engineering
University of Illinois
205 N. Mathews Avenue
Urbana, IL 61801
217-333-9896 (F) 217-265-0318
217-714-0227
npjones@uiuc.edu

Dr. Josephine N. Malilay
Epidemiologist, Environmental Hazards Epidemiology Section
National Center for Environmental Health
Centers for Disease Control and Prevention
1600 Clifton Rd. NE (Mail stop E-23)
Atlanta, GA 30333
404-498-1359 (F) 404-498-1355
JMalilay@cdc.gov

Dr. Enrique E. Matheu
Research Assistant Professor
Department of Civil and Environmental Engineering
Louisiana State University
Office address:
U.S. Army Engineer Research and Development Center
3909 Halls Ferry Road, ATTN: CEERD-GS-E
Vicksburg, MS 39180
601-634-3235 (F) 601-634-4656
Enrique.E.Matheu@erdc.usace.army.mil

Dr. Steven McCabe
Program Director
Structural Systems and Hazard Mitigation of Structures Program (ENG/CMS)
Room 545 S
National Science Foundation
4201 Wilson Boulevard
Arlington, VA 22230
703-292-7003 (F) 703-292-9053
smccabe@nsf.gov

Mr. Noel J. Raufaste
Guest Researcher
Building and Fire Research Laboratory
National Institute of Standards and Technology
100 Bureau Drive, Stop 8611
Gaithersburg, MD 20899-8611
301-975-6062
noel.raufaste@nist.gov

Dr. William E. Roper
Professor and Chairman
Department of Civil and Environmental Engineering
George Washington University
Phillips Hall, Room 643
The Academic Center
801 22nd St., N.W.
Washington, DC 20052
202-994- 4901 (F) 202-994-0127
wroper@gwu.edu

Dr. David H. Sanders

Associate Professor
Department of Civil Engineering
Mail Stop 258
University of Nevada
Reno, NV 89557
775-784-4288 (F) 775-784-1390
sanders@unr.edu

Dr. K. Thirumalai
Chief Engineer, U.S. DOT/RSPA
U.S. Department of Transportation
400 Seventh Street SW, Suite 7110
Washington DC 20590-0001
202-366-0375
K.Thirumalai@rspa.dot.gov

Dr. W. Phillip Yen
Research Structural Engineer
Structures Division
Turner-FairBank Highway Research Center
Federal Highway Administration
6300 Georgetown Pike
McLean, VA 22101
202-493-3056 (F) 202-493-3442
Wen-huei.Yen@fhwa.dot.gov

Dr. Donald E. Yule
U.S. Army Corps of Engineers
U.S. Army Engineer Research and Development Center
3909 Halls Ferry Road
ATTN: CEERD-GS-E
Vicksburg, MS 39180
601-634-2964 (F) 601-634-4656
don.e.yule@erdc.usace.army.mil

U.S.-SIDE PANEL ON WIND AND SEISMIC EFFECTS
MEMBERSHIP LIST

Dr. S. Shyam Sunder
Chairman, U.S.-side Panel
Chief, Materials and Construction Research Division
Building and Fire Research Laboratory
National Institute of Standards and Technology
100 Bureau Drive, Stop 8611
Gaithersburg, MD 20899-8611
301-975-6061 (F) 301-869-6275
sunder@nist.gov

Mr. Stephen A. Cauffman
Secretary-General, U.S.-side Panel
Research Engineer
Materials and Construction Research Division
Building and Fire Research Laboratory
National Institute of Standards and Technology
100 Bureau Drive, Stop 8611
Gaithersburg, MD 20899-8611
301-975-6051 (F) 301-869-6275
stephen.cauffman@nist.gov

Dr. Daniel P. Abrams
Director, Mid-America Earthquake Center
Hanson Engineers Professor of Civil Engineering
University of Illinois
1241 Newmark Laboratory
205 North Mathews Avenue
Urbana, IL 61801
(F) 217-333-3821
d-abrams@uiuc.edu

Dr. Kharaiti L. Abrol
Principal Structural Engineering Consultant
Room 475
Department of Veterans Affairs
810 Vermont Avenue, NW
Washington, DC 20420
202-565-5579 (F) 202-565-5478
abrkha@hq.med.va.gov

Dr. Jon P. Ake
Geophysicist
Seismotectonics and Geophysics Section
Code D-8330
P.O. Box 25007
Bureau of Reclamation
U.S. Department of the Interior
Denver, CO 80225
303-445-3169 (F) 303-236-9127
jake@do.usbr.gov

Dr. Clifford J. Astill
Program Director
Division of Civil and Mechanical Systems
National Science Foundation
4201 Wilson Boulevard - Room 545
Arlington, VA 22230
703-306-1361 (F) 703-306-0291
castill@nsf.gov

Mr. John R. Baals
Seismic Safety Coordinator
P.O. Box 25007 (D-8110)
Bureau of Reclamation
U.S. Department of the Interior
Denver, CO 80225
303-236-3999 x534 (F) 303-236-9099
jbaals@do.usbr.gov

Dr. Celso S. Barrientos
Physical Scientist
National Environmental Satellite, Data, and
Information Service - Code E/RA28
National Oceanic and Atmospheric Administration
U.S. Department of Commerce
5200 Auth Road
Camp Springs, MD 20746
301-713-9384 x109 (F) 301-713-4598
Celso.S.Barrientos@noaa.gov

Dr. Eddie N. Bernard
Director, Pacific Marine Environmental Laboratory
National Oceanic and Atmospheric Administration
U.S. Department of Commerce
7600 Sand Point Way, NE
BIN C15700/Building 3
Seattle, WA 98115-0070
206-526-6800 (F) 206-526-4576
Eddie.N.Bernard@noaa.gov

Dr. David M. Boore
Geophysicist
U.S. Geological Survey
345 Middlefield Road MS 977
Menlo Park, CA 94025
650-329-5616 (F) 650-329-5163
boore@usgs.gov

Dr. Roger D. Borcherdt
Senior Researcher
Engineering Seismology Geophysics
U.S. Geological Survey
U.S. Department of the Interior
345 Middlefield Road, MS 977
Menlo Park, CA 94025
650-329-5619 (F) 650-329-5163
borcherdt@usgs.gov

Dr. Mehmet K. Celebi
Research Civil Engineer
Earthquake Hazards Team
U.S. Geological Survey
U.S. Department of the Interior
345 Middlefield Road, MS 977
Menlo Park, CA 94025
650-329-5623 (F) 650-329-5163
celebi@usgs.gov

Mr. Harish Chander
Civil/Structural Engineer
Office of Nuclear Safety Policy and Standards
U.S. Department of Energy (EH-53),
Room 3097
270 Corporate Center
20300 Century Boulevard
19901 Germantown Road
Germantown, MD 20874
301-903-6681 (F) 301-903-6172
harish.chander@hq.doe.gov

Dr. C. Y. Chen
Senior Civil/Geotechnical Engineer
Office of Foreign Buildings
Department of State
Code SA-6, Rm. 347
Washington, DC 20520
703-875-6207 (F) 703-875-6204
chency@state.gov

Dr. Ken P. Chong
Director of Mechanics and Materials Program
Engineering Directorate
National Science Foundation
4201 Wilson Boulevard - Room 545
Arlington, VA 22230
703-292-7008 (F) 703-292-9053
kchong@nsf.gov

Dr. James F. Costello
Senior Structural Engineer
Division of Engineering Technology
Office of Nuclear Regulatory Research
U.S. Nuclear Regulatory Commission
Mail Stop T10-L1
Washington, DC 20555
301-415-6009
jfc@nrc.gov

Mr. William E. Freeborne
Mechanical Engineer, Policy Development and Research
Department of Housing and Urban Development
Room 8132
451 Seventh Street, SW
Washington, DC 20410
202-708-4370 x5725 (F) 202-708-5873
william_e._freeborne@hud.gov

Dr. Hamid Ghasemi
Research Structural Engineer
Bridge Safety, Reliability and Security Team
Turner-FairBank Highway Research Center
Federal Highway Administration
6300 Georgetown Pike
McLean VA 22101
202-493-3042 (F) 202-493-3443
hamid.ghasemi@fhwa.dot.gov

Dr. Joseph H. Golden
Director, National Oceanic and Atmospheric
Administration
Rm. DSRC-2B133
325 Broadway Street, Boulder, CO 80302
303-497-6098
jgolden@fsl.noaa.gov

Dr. John L. Gross
Leader
Materials and Construction Research Division
Structures Group
Building and Fire Research Laboratory
National Institute of Standards and Technology
100 Bureau Drive, Stop 8611
Gaithersburg, MD 20899-8611
301-975-6068 (F) 301-869-6275
john.gross@nist.gov

Dr. Robert L. Hall
Chief, Geosciences and Structures Division
Geotechnical and Structures Laboratory
U.S. Army Engineer Research and Development Center
CEERD-GS
3909 Halls Ferry Road
Vicksburg, MS 39180-6199
601-634-2567 (F) 601-634-3412
Robert.L.Hall@erdc.usace.army.mil

Dr. John R. Hays
Seismic and Structural Engineering Group
U.S. Army Engineer Research and Development Center
CEERD-CF-M
Construction Engineering Research Laboratory
2902 Newmark Drive
Champaign, IL 61822-1076
217-373-7248
john.r.hays@erdc.usace.army.mil

Dr. Allen M. Hittelman
Chief, Solid Earth Geophysics Division
E/GC1, National Geophysical Data Center
NOAA, NESDIS
325 Broadway
Boulder, CO 80303-3328
303-497-6591 (F) 303-497-6513
allen.m.hittelman@noaa.gov

Dr. Mary E. Hynes
Chief, Earthquake Engineering and Geophysics Branch
Geotechnical Laboratory
CEERD-GS-R
U.S. Army Engineer Research and Development Center
3909 Halls Ferry Road
Vicksburg, MS 39180
601-634-2280 (F) 601-634-3453
mary.e.hynes@erdc.usace.army.mil

Dr. Nicholas P. Jones
Professor and Head
Department of Civil and Environmental Engineering
University of Illinois
205 N. Mathews Avenue
Urbana, IL 61801
217-333-9896 (F) 217-265-0318
217-714-0227
npjones@uiuc.edu

Mr. Michael Keever
Supervisory Bridge Design Engineer
Office of Earthquake Engineering
California Department of Transportation Division of
Engineering Services, MS9-2/7J

P.O. Box 168041
Sacramento, CA 95816
916-227-8806 (F) 916-227-8242
mike_keever@dot.ca.gov

Mr. Roger M. Kenneally
Senior Structural Engineer
Structural and Geological Engineering Branch
Mail Stop T10-L1
U.S. Nuclear Regulatory Commission
Washington, DC 20555
301-415-6303
rmk@nrc.gov

Dr. George C. Lee
Director, Multidisciplinary Center for Earthquake Engineering Research (MCEER)
State University of New York at Buffalo
Red Jacket Quadrangle
Buffalo, NY 14261
716-645-3391 x111 (F) 716-645-3399
gclee@mceermail.buffalo.edu

Dr. H. S. Lew
Senior Research Structural Engineer
Materials and Construction Research Division
Building and Fire Research Laboratory
National Institute of Standards and Technology
100 Bureau Drive Stop 8611
Gaithersburg, MD 20899-861
301-975-6060 (F) 301-869-6275
hai.lew@nist.gov

Mr. Michael G. Mahoney
Physical Scientist
Mitigation Directorate
Federal Emergency Management Agency
500 C Street, SW
Washington, DC 20472
202-646-2794 (F) 202-646-4387
mike.mahoney@fema.gov

Dr. Josephine N. Malilay
Epidemiologist, Environmental Hazards Epidemiology Section
National Center for Environmental Health
Centers for Disease Control and Prevention
1600 Clifton Rd. NE (Mail stop E-23)
Atlanta, GA 30333
404-498-1359 (F) 404-498-1355
JMalilay@cdc.gov

Dr. Enrique E. Matheu
Research Assistant Professor
Department of Civil and Environmental Engineering
Louisiana State University
Office address:
U.S. Army Engineer Research and Development Center
3909 Halls Ferry Road, ATTN: CEERD-GS-E
Vicksburg, MS 39180
601-634-3235 (F) 601-634-4656
Enrique.E.Matheu@erdc.usace.army.mil

Dr. Steven McCabe
Program Director
Structural Systems and Hazard Mitigation of Structures Program (ENG/CMS)
Room 545 S
National Science Foundation
4201 Wilson Boulevard
Arlington, VA 22230
703-292-7003 (F) 703-292-9053
smccabe@nsf.gov

Dr. Francis G. McLean
Reclamation Value Engineering Program Manager
Code D-8170
P.O. Box 25007
Bureau of Reclamation
Department of the Interior
Denver, CO 80225-5007
303-445-3091 (F) 303-6475
FMCLEAN@do.usbr.gov

Dr. Raymond E. Meyer
Senior Program Manager for Famine Mitigation and Natural Resources Assessment
Department of State
SA14/Room 1705
USAID/Washington, DC 20523-1443
202-712-1078 (F) 202-216-3707
Rmeyer@usaid.gov

Dr. Jack P. Moehle
Director and Principal Investigator, Pacific Earthquake Engineering Research Center (PEER)
1301 South 46th Street
Richmond, CA 94804-4698
510-231-9554 (F) 510-231-9471
moehle@eerc.berkeley.edu

Mr. Noel J. Raufaste
Guest Researcher
Building and Fire Research Laboratory
National Institute of Standards and Technology
100 Bureau Drive, Stop 8611
Gaithersburg, MD 20899-8611
301-975-6062
noel.raufaste@nist.gov

Dr. William E. Roper
Professor and Chairman
Department of Civil and Environmental Engineering
George Washington University
Phillips Hall, Room 643
The Academic Center
801 22nd St., N.W.
Washington, DC 20052
202-994- 4901 (F) 202-994-0127
wroper@gwu.edu

Dr. Erdal Safak
Research Structural Engineer
U.S. Geological Survey
Box 25046, MS 966
Denver Federal Center
Denver, CO 80225
303-273-8593 (F) 303-273-8600
safak@usgs.gov

Dr. Michael K. Sharp
Director, Centrifuge Research Center

Geotechnical and Structures Laboratory
U.S. Army Engineer Research and Development Center
3909 Halls Ferry Road
Vicksburg, MS 39180-6199
601-634-4127 (F) 601-634-4894
michael.k.sharp@erdc.usace.army.mil

Dr. Charles E. Smith
Research Program Manager
Engineering and Research Branch
Minerals Management Service
U.S. Department of the Interior
381 Elden Street, MS 4021
Herndon, VA 20170-4817
703-787-1561 (F) 703-787-1549
smithc@mms.gov or Charles.E.Smith@mms.gov

Dr. W. Phillip Yen
Research Structural Engineer
Structures Division
Turner-FairBank Highway Research Center
Federal Highway Administration
6300 Georgetown Pike
McLean, VA 22101
202-493-3056 (F) 202-493-3442
Wen-huei.Yen@fhwa.dot.gov

JAPAN-SIDE PANEL ON WIND AND SEISMIC EFFECTS MEMBERSHIP LIST

STEERING COMMITTEE MEMBERS

Dr. Tadahiko Sakamoto
Chairman, Japan-side Panel on Wind and Seismic Effects
Chief Executive, Public Works Research Institute
1-6 Minamihara, Tsukuba-shi, Ibaraki-ken 305-8516
Tel: 029-879-6700
Fax: 029-879-6741
E-mail: sakamoto@pwri.go.jp

Dr. Michio Okahara
Secretary-General, Japan-side Panel on Wind and Seismic Effects
Deputy Chief Executive, Public Works Research Institute
1-6 Minamihara, Tsukuba-shi, Ibaraki-ken 305-8516
Tel: 029-879-6700
Fax: 029-879-6702
E-mail: okahara@pwri.go.jp

Mr. Hideaki Akitsune
Director, Planning and Research Administration Department
National Institute for Land and Infrastructure Management
Ministry of Land, Infrastructure and Transport
1 Asahi, Tsukuba-shi, Ibaraki-ken 305-0804 Japan
Tel: 029-864-2826
Fax: 029-864-1527
E-mail: akitsune-h92bn@nilim.go.jp

Mr. Ippei Eguchi
Senior Assistant for Disaster Prevention, Planning Division
Administration Department
Japan Meteorological Agency
1-3-4 Ohte-machi, Chiyoda-ku, Tokyo 100-8918
Tel: 03-3212-8341
Fax: 03-3211-2032
E-mail: ippei.eguchi-a@met.kishou.go.jp

Mr. Yoshihiro Fujimori
Director, International Division for Infrastructure
Policy Bureau
Ministry of Land, Infrastructure and Transport
2-1-3 Kasumigaseki, Chiyoda-ku, Tokyo 100-8918
Tel: 03-5253-8315
Fax: 03-5253-1562
E-mail: fujimori-y2jp@mlit.go.jp

Mr. Takayuki Goto
Director, Building Disaster Prevention Office
Housing Bureau
Ministry of Land, Infrastructure and Transport
2-1-3 Kasumigaseki, Chiyoda-ku, Tokyo 100-8918
Tel: 03-5253-8514
Fax: 03-5253-1630
E-mail: gotou-t2gr@mlit.go.jp

Dr. Nobuo Hamada
Director, Seismological and Volcanological Research Department
Meteorological Research Institute
Japan Meteorological Agency
1 Nagamine, Tsukuba-shi, Ibaraki-ken 305-0052
Tel: 029-853-8675
Fax: 029-853-3730
E-mail: nhamada@mri-jma.go.jp

Prof. Masaya Hirosawa
Professor, Department of Architecture
Kogakuin University
1-24-2 Nishi-Shinjuku, Shinjuku-ku, Tokyo 160-0023
Tel: 03-3342-1211
Fax: 03-3340-0149
E-mail: dt10760@ccs.kogakuin.ac.jp

Dr. Koji Ichii
Senior Researcher, Structural Dynamics Division
Geotechnical and Structural Engineering Department
Port and Airport Research Institute
3-1-1 Nagase, Yokosuka-shi, Kanagawa-ken 239-0826
Tel: 0468-44-5058
Fax: 0468-44-0839
E-mail: ichii@pari.go.jp

Dr. Masanori Iiba
Research Coordinator for Advanced Building Technology
Building Department
National Institute for Land and Infrastructure Management
Ministry of Land, Infrastructure and Transport
1 Tachihara, Tsukuba-shi, Ibaraki-ken 305-8020
Tel: 029-864-4387
Fax: 029-864-6774
E-mail: iiba-m92hx@nilim.go.jp

Dr. Toshio Iwasaki
President, Civil Engineering Research Laboratory
1-18 Kanda Suda-cho Chiyoda-ku, Tokyo 101-0041
Tel: 03-3254-9481
Fax: 03-3254-9448
E-mail: iwasaki@crl.or.jp

Mr. Takashi Kaminosono
Research Coordinator for Disaster Mitigation of Buildings
Research Center for Disaster Risk Management
National Institute for Land and Infrastructure Management
Ministry of Land, Infrastructure and Transport
1 Asahi, Tsukuba-shi, Ibaraki-ken 305-0804
Tel: 029-864-4963
Fax: 029-864-0598
E-mail: kaminosono-t92rx@nilim.go.jp

Prof. Kazuhiko Kawashima
Professor, Department of Civil Engineering
Tokyo Institute of Technology
2-12-1 O-okayama, Meguro-ku, Tokyo 152-0033

Tel: 03-5734-2922
Fax: 03-3729-0728
E-mail: kawasima@cv.titech.ac.jp

Mr. Takaaki Kusakabe
Head, Earthquake Disaster Prevention Division
Research Center for Disaster Risk Management
National Institute for Land and Infrastructure Management
Ministry of Land, Infrastructure and Transport
1 Asahi, Tsukuba-shi, Ibaraki-ken 305-0804
Tel: 029-864-2211
Fax: 029-864-0598
E-mail: ksakabe-t88d8@nilim.go.jp

Mr. Hiromichi Maruyama
Director, Geographic Department
Geographical Survey Institute
Ministry of Land, Infrastructure and Transport
1 Kitasato, Tsukuba-shi, Ibaraki-ken 305-0811
Tel: 029-864-1111
Fax: 029-864-1804
E-mail: maruyama@gsi.go.jp

Mr. Osamu Matsuo
Research Coordinator for Earthquake Disaster Prevention
Research Center for Disaster Risk Management
National Institute for Land and Infrastructure Management
Ministry of Land, Infrastructure and Transport
1 Asahi, Tsukuba-shi, Ibaraki-ken 305-0804
Tel: 029-864-2926
Fax: 029-864-0598
E-mail: matsuo-o92rm@nilim.go.jp

Mr. Chikahiro Minowa
Scientific Research Advisor
National Research Institute for Earth Science and Disaster Prevention
3-1 Tennodai, Tsukuba-shi, Ibaraki-ken 305-0006
Tel: 029-851-1611
Fax: 029-851-1674
E-mail: minowa@bosai.go.jp

Mr. Kenji Morita
Director, Office for Disaster Reduction Research
Research and Development Bureau
Ministry of Education, Culture, Sports, Science and Technology
1-3-2 Kasumigaseki, Chiyoda-ku, Tokyo 100-8966
Tel: 03-5253-4111
Fax: 03-5253-4139
E-mail: kmorita@mext.go.jp

Mr. Akiyoshi Mukai
Chief Research Engineer, Department of Structural Engineering
Building Research Institute
1 Tachihara, Tsukuba-shi, Ibaraki-ken 305-0802
Tel: 029-864-6662
Fax: 029-864-6773
E-mail: mukai@kenken.go.jp

Mr. Jun Murakoshi
Team Leader, Bridge Structure Research Team
Structures Research Group
Public Works Research Institute
1-6 Minamihara, Tsukuba-shi, Ibaraki-ken 305-8516
Tel: 029-879-6792
Fax: 029-879-6739
E-mail: murakosi@pwri.go.jp

Mr. Isao Nagayama
Director, Hydraulic Engineering Research Group
Public Works Research Institute
1-6 Minamihara, Tsukuba-shi, Ibaraki-ken 305-0804
Tel: 029-879-6723
Fax: 029-879-6737
E-mail: nagayama@pwri.go.jp

Mr. Takashi Nanba
Director, Disaster Prevention Office
Coast Administration and Disaster Prevention Division
Ports and Harbors Bureau
Ministry of Land, Infrastructure and Transport
2-1-3 Kasumigaseki, Chiyoda-ku, Tokyo 100-8918
Tel: 03-5253-8689
Fax: 03-5253-1654
E-mail: nanba-t24x@mlit.go.jp

Dr. Junichi Nishikawa
Director, Structure Department
Civil Engineering Research Institute of Hokkaido
1-3 Hiragishi, Toyohira-ku, Sapporo-shi Hokkaido 062-8601
Tel: 011-841-5175
Fax: 011-820-2714
E-mail: nishikaw@ceri.go.jp

Dr. Isao Nishiyama
Chief Research Engineer, Department of Production Engineering
Building Research Institute
1 Tachihara, Tsukuba-shi, Ibaraki-ken 305-0802
Tel: 029-864-6681
Fax: 029-864-6772
E-mail: isao@kenken.go.jp

Dr. Setsuo Noda
Advisor, Mitsubishi Heavy Industries, Ltd.
2-5-1 Marunouchi, Chiyoda-ku, Tokyo 102-0092
Tel: 03-3212-9378
Fax: 03-3212-9833
E-mail: setsuo_noda@mhi.co.jp

Mr. Akihiko Nunomura
Director, Volcanic and Earthquake Disaster Management
Disaster Prevention Bureau
Cabinet Office
1-2-2 Kasumigaseki, Chiyoda-ku, Tokyo 100-8918
Tel: 03-3501-5693
Fax: 03-3501-5199
E-mail: anunomu@op.cao.go.jp

Mr. Keiichi Ohtani
Project-Director, Project of 3-D Full-Scale Earthquake Testing Facility
National Research Institute for Earth Science and Disaster Prevention
3-1 Tennodai, Tsukuba-shi, Ibaraki-ken 305-0006
Tel: 029-856-6234
Fax: 029-852-8512
E-mail: ohtani@bosai.go.jp

Dr. Takaaki Ohyama
Senior Researcher, Infectious Disease Surveillance Center
National Institute of Infectious Diseases
Ministry of Health, Labor and Welfare
1-23-1 Toyama, Shinjuku-ku, Tokyo 162-8640
Tel: 03-5285-1268
Fax: 03-5285-1129
E-mail: Ohyamat@nih.go.jp

Dr. Hisashi Okada
Director, Department of Structural Engineering
Building Research Institute
1 Tachihara, Tsukuba-shi, Ibaraki-ken 305-0802
Tel: 029-864-6633
Fax: 029-864-6773
E-mail: okada@kenken.go.jp

Dr. Shin Okamoto
Director General
Central Research Institute for Construction Technology
Japan Association of Representative General Contractors
1-6-35 Shinsuna, Kouto-ku, Tokyo 136-0075
Tel: 03-5634-8681
Fax: 03-5634-8682
E-mail: shin-okamoto@chugiken.or.jp

Dr. Izuru Okawa
Senior Research Fellow
Department of Structural Engineering
Building Research Institute
1 Tachihara, Tsukuba-shi, Ibaraki-ken 305-0802
Tel: 029-864-6627
Fax: 029-864-6773
E-mail: okawa@kenken.go.jp

Mr. Haruhiko Okuno
Director-General, National Institute for Land and Infrastructure Management
Ministry of Land, Infrastructure and Transport
1 Asahi, Tsukuba-shi, Ibaraki-ken 305-0804
Tel: 029-864-2211
Fax: 029-864-2148
E-mail: okuno-h8310@nilim.go.jp

Ms. Akiko Saito
International Cooperation Coordinator
International Science and Technology Affairs Division
Science and Technology Policy Bureau
Ministry of Education, Culture, Sports, Science and Technology
1-3-2 Kasumigaseki, Chiyoda-ku, Tokyo 100-8918
Tel: 03-5253-4055
Fax: 03-3581-5909
E-mail: saitoaki@mext.go.jp

Mr. Toshio Sakai
Director, Road Emergency Management Office
Road Bureau
Ministry of Land, Infrastructure and Transport
2-1-3 Kasumigaseki, Chiyoda-ku, Tokyo 100-8918
Tel: 03-5253-8111
Fax: 03-5253-1618
E-mail: sakai-t2bp@mlit.go.jp

Dr. Hiroshi Sato
Director, Structures Research Group
Public Works Research Institute
1-6 Minamihara, Tsukuba-shi, Ibaraki-ken 305-8516
Tel: 029-879-6726
Fax: 029-879-6739
E-mail: hsato@pwri.go.jp

Mr. Masahiro Takano
Director, Disaster Risk Management Division
River Bureau
Ministry of Land, Infrastructure and Transport
2-1-3 Kasumigaseki, Chiyoda-ku, Tokyo 100-8918
Tel: 03-3580-8111
Fax: 03-5253-1608
E-mail: takano-m8310@mlit.go.jp

Mr. Yukio Takemura
Director, Typhoon Research Division
Meteorological Research Institute
Japan Meteorological Agency
1 Nagamine, Tsukuba-shi, Ibaraki-ken 305-0052
Tel: 0298-53-8663
Fax: 0298-53-8735
E-mail: ytakemur@mri-jma.go.jp

Dr. Keiichi Tamura
Team Leader, Ground Vibration Research Team
Earthquake Disaster Prevention Research Group
Public Works Research Institute
1-6 Minamihara, Tsukuba-shi, Ibaraki-ken 305-8516
Tel: 029-879-6770
Fax: 029-879-6735
E-mail: tamura@pwri.go.jp

Dr. Masaomi Teshigawara
Chief Research Engineer, Department of Structural Engineering
Building Research Institute
1 Tachihara, Tsukuba-shi, Ibaraki-ken 305-0802
Tel: 029-864-6753
Fax: 029-864-6773
E-mail: teshi@kenken.go.jp

Mr. Ken-ichi Tokida
Director, Earthquake Disaster Prevention Research Group
Public Works Research Institute
1-6 Minamihara, Tsukuba-shi, Ibaraki-ken 305-8516
Tel: 029-879-6700
Fax: 029-879-6736
E-mail: tokida@pwri.go.jp

Dr. Takashi Tomita
Head, Storm Surge and Tsunami Division
Marine Environment Engineering Department
Port and Airport Research Institute
3-1-1 Nagase, Yokosuka-shi, Kanagawa-ken 239-0826
Tel: 0468-44-5052
Fax: 0468-44-1274
E-mail: tomita@pari.go.jp

Dr. Shigeki Unjoh
Team Leader, Earthquake Engineering Research Team
Earthquake Disaster Prevention Research Group
Public Works Research Institute
1-6 Minamihara, Tsukuba-shi, Ibaraki-ken 305-8516
Tel: 029-879-6773
Fax: 029-879-6736

E-mail: unjoh@pwri.go.jp

Dr. Yoshikazu Yamaguchi
Team Leader, Dam Structure Research Team
Hydraulic Engineering Research Group
Public Works Research Institute
1-6 Minamihara, Tsukuba-shi, Ibaraki-ken 305-8516
Tel: 029-879-6780
Fax: 029-879-6737
E-mail: yamaguti@pwri.go.jp

Dr. Hiroyuki Yamanouchi
Chief Executive, Building Research Institute
1 Tachihara, Tsukuba-shi, Ibaraki-ken 305-0802
Tel: 029-864-2151
Fax: 029-864-2989
E-mail: yamanoch@kenken.go.jp

Prof. Koichi Yokoyama
Professor, Department of Urban and Civil Engineering
Ibaraki University
4-12-1 Nakanarusawa, Hitachi-shi, Ibaraki-ken 316-0033
Tel: 0294-38-5161
Fax: 0294-38-5268
E-mail: yokoyama@mx.ibaraki.ac.jp

SECRETARIES COMMITTEE MEMBERS

Dr. Michio Okahara
Secretary-General, Japan-side Panel on Wind and Seismic Effects
Deputy Chief Executive, Public Works Research Institute
1-6 Minamihara, Tsukuba-shi, Ibaraki-ken 305-8516
Tel: 029-879-6700
Fax: 029-879-6702
E-mail: okahara@pwri.go.jp

Mr. Jiro Fukui
Team Leader, Foundation Engineering Team
Structures Research Group
Public Works Research Institute
1-6 Minamihara, Tsukuba-shi, Ibaraki-ken 305-8516
Tel: 029-879-6794
Fax: 029-879-6739
E-mail: fukui@pwri.go.jp

Mr. Kenji Ikeda
Director, Structures Division
Structures Department
Civil Engineering Research Institute of Hokkaido
1-3 Hiragishi, Toyohira-ku, Sapporo-shi Hokkaido 062-8602
Tel: 011-841-1115
Fax: 011-820-2714
E-mail: ikedak@ceri.go.jp

Dr. Naohito Kawai
Head, Structural Standard Division
Building Department
National Institute for Land and Infrastructure Management
Ministry of Land, Infrastructure and Transport
1 Tachihara, Tsukuba-shi, Ibaraki-ken 305-0802
Tel: 029-864-4299
Fax: 029-864-6774
E-mail:kawai-n92hp@nilim.go.jp

Mr. Takaaki Kusakabe
Head, Earthquake Disaster Prevention Division
Research Center for Disaster Risk Management
National Institute for Land and Infrastructure Management
Ministry of Land, Infrastructure and Transport
1 Asahi, Tsukuba-shi, Ibaraki-ken 305-0804
Tel: 029-864-2211
Fax: 029-864-0598
E-mail: ksakabe-t88d8@nilim.go.jp

Mr. Osamu Matsuo
Research Coordinator for Earthquake Disaster Prevention
Research Center for Disaster Risk Management
National Institute for Land and Infrastructure Management
Ministry of Land, Infrastructure and Transport
1 Asahi, Tsukuba-shi, Ibaraki-ken 305-0804
Tel: 029-864-2926
Fax: 029-864-0598
E-mail: matsuo-o92rm@nilim.go.jp

Mr. Chikahiro Minowa
Scientific Research Advisor
National Research Institute for Earth Science and Disaster Prevention
3-1 Tennodai, Tsukuba-shi, Ibaraki-ken 305-0006
Tel: 029-851-1611
Fax: 029-851-1674
E-mail: minowa@bosai.go.jp

Mr. Jun Murakoshi
Team Leader, Bridge Structure Research Team
Structures Research Group
Public Works Research Institute
1-6 Minamihara, Tsukuba-shi, Ibaraki-ken 305-8516
Tel: 029-879-6792
Fax: 029-879-6739
E-mail: murakosi@pwri.go.jp

Mr. Katsuto Nakagawa
Head, Planning Division, Geographic Department
Geographical Survey Institute
Ministry of Land, Infrastructure and Transport
1 Kitasato, Tsukuba-shi, Ibaraki-ken 305-0811
Tel: 029-864-5917
Fax: 029-864-1804
E-mail: k-nakagawa@gsi.go.jp

Dr. Tetsuo Nakazawa
Head, The Second Research Laboratory
Typhoon Research Department
Meteorological Research Institute
Japan Meteorological Agency
Ministry of Land, Infrastructure and Transport
1-1 Nagamine, Tsukuba-shi, Ibaraki-ken 305-0052
Tel: 029-853-8671
Fax: 029-853-8735
E-mail: nakazawa@mri-jra.go.jp

Mr. Keiichi Ohtani
Project-Director, Project of 3-D Full-Scale Earthquake Testing Facility
National Research Institute for Earth Science and Disaster Prevention
3-1 Tennodai, Tsukuba-shi, Ibaraki-ken 305-0006
Tel: 029-856-6234
Fax: 029-852-8512
E-mail: ohtani@bosai.go.jp

Dr. Nobuyuki Ogawa
Deputy Project Director, Special Project on the 3-D Full-Scale Earthquake Testing Facility
Disaster Prevention Research Group
National Research Institute for Earth Science and Disaster Prevention
3-1 Tennodai, Tsukuba-shi, Ibaraki-ken 305-0006
Tel: 029-851-1611
Fax: 029-852-8512
E-mail: ogawa@bosai.go.jp

Dr. Hisashi Okada
Director, Department of Structural Engineering
Building Research Institute
1 Tachihara, Tsukuba-shi, Ibaraki-ken 305-0802
Tel: 029-864-6633
Fax: 029-864-6773
E-mail: okada@kenken.go.jp

Dr. Yasuo Okuda

Chief Research Engineer, Department of Structural Engineering
Building Research Institute
1 Tachihara, Tsukuba-shi, Ibaraki-ken 305-0802
Tel: 029-864-6618
Fax: 029-864-6773
E-mail: y_okuda@kenken.go.jp

Mr. Yoshiyuki Saito
Head, Research Planning Office
Civil Engineering Research Institute of Hokkaido
1-3 Hiragishi, Toyohira-ku, Sapporo-shi Hokkaido 062-0931
Tel: 011-841-1119
Fax: 011-824-1226
E-mail: 90117@ceri.go.jp

Dr. Hiroshi Sato
Director, Structures Research Group
Public Works Research Institute
1-6 Minamihara, Tsukuba-shi, Ibaraki-ken 305-8516
Tel: 029-879-6726
Fax: 029-879-6739
E-mail: hsato@pwri.go.jp

Dr. Keiichi Tamura
Team Leader, Ground Vibration Research Team
Earthquake Disaster Prevention Research Group
Public Works Research Institute
1-6 Minamihara, Tsukuba-shi, Ibaraki-ken 305-8516
Tel: 029-879-6770
Fax: 029-879-6735
E-mail: tamura@pwri.go.jp

Dr. Masaomi Teshigawara
Chief Research Engineer, Department of Structural Engineering
Building Research Institute
1 Tachihara, Tsukuba-shi, Ibaraki-ken 305-0802
Tel: 029-864-6753
Fax: 029-864-6773
E-mail: teshi@kenken.go.jp

Mr. Ken-ichi Tokida
Director, Earthquake Disaster Prevention Research Group
Public Works Research Institute
1-6 Minamihara, Tsukuba-shi, Ibaraki-ken 305-8516
Tel: 029-879-6700
Fax: 029-879-6736
E-mail: tokida@pwri.go.jp

Dr. Takashi Tomita
Head, Storm Surge and Tsunami Division
Marine Environment Engineering Department
Port and Airport Research Institute
3-1-1 Nagase, Yokosuka-shi, Kanagawa-ken 239-0826
Tel: 0468-44-5052
Fax: 0468-44-1274
E-mail: tomita@pari.go.jp

Dr. Shigeki Unjoh
Team Leader, Earthquake Engineering Research Team
Earthquake Disaster Prevention Research Group
Public Works Research Institute
1-6 Minamihara, Tsukuba-shi, Ibaraki-ken 305-8516
Tel: 029-879-6773
Fax: 029-879-6736
E-mail: unjoh@pwri.go.jp

Dr. Yoshikazu Yamaguchi
Team Leader, Dam Structure Research Team
Hydraulic Engineering Research Group
Public Works Research Institute
1-6 Minamihara, Tsukuba-shi, Ibaraki-ken 305-8516
Tel: 029-879-6780
Fax: 029-879-6737
E-mail: yamaguti@pwri.go.jp

TEMPORARY MEMBERS

Mr. Koichiro Fumoto	Public Works Research Institute
Mr. Kenji Inagaki	National Institute for Land and Infrastructure Management
Mr. Hisaya Kamura	JFE R&D Corporation
Mr. Kenichi Kanenawa	Public Works Research Institute
Dr. Mitsumasa Midorikawa	Building Research Institute
Mt. Hiroaki Miyatake	Cabinet Office
Dr. Yoshifumi Sakumoto	Nippon Steel Corporation, Ltd.
Mr. Akihiro Sanada	National Institute for Land and Infrastructure Management

ASSOCIATE MEMBERS

Mr. Tomomitsu Fujii	Foundation of River Basin Integrated Communications
Dr. Minoru Fujiwara	Strait Crossing Highway Research Association
Dr. Masami Fukuoka	Manegement System Assessment Center
Prof. Masaya Hirosawa	Kogakuin University
Prof. Shiro Ibukiyama	Kogyokusha College of Technology
Dr. Kaoru Ichihara	Central Consultant Inc.
Dr. Ryuichi Iida	Japan Dam Engineering Center
Dr. Takashi Iijima	Kajimaroad Corporation, Ltd.
Mr. Yasutake Inoue	Fukuoka Kitakyushu Urban Expressway
Dr. Toshio Iwasaki	Civil Engineering Research Laboratory
Mr. Shunichiro Kamijo	Mitsui Construction Corporation
Mr. Kenji Kawakami	Kubota Corporation
Prof. Eiichi Kuribayashi	Professor Emeritus, Toyohashi University of Technology
Dr. Tatsuro Murota	Japan Housing and Wood Technology Center
Mr. Mitsuru Nagao	Japan Construction Mechanization Association
Prof. Kiyoshi Nakano	Tokyo Denki University
Dr. Kazuto Nakazawa	Public Works Research Center
Dr. Nobuyuki Narita	Public Works Research Center
Dr. Setsuo Noda	Mitsubishi Heavy Industries, Ltd.
Dr. Shin Okamoto	Japan Association of Representative General Contractors
Mr. Yoshijiro Sakagami	Japan Development Construction Corporation
Prof. Yasushi Sasaki	Hiroshima University
Dr. Yukihiko Sumiyoshi	Central Consultant Inc.
Mr. Jiro Taguchi	Construction Research Institute
Dr. Masateru Tominaga	Public Works Research Center
Dr. Hajime Tsuchida	Echo Corporation
Mr. Seizo Tsuji	Japan Utility Subway Company Inc.
Prof. Makoto Watabe	Formerly, Keio University
Prof. Koichi Yokoyama	Ibaraki University

TASK COMMITTEE MEMBERS

* denotes Task Committee Chair.

A. Geotechnical Engineering and Ground Motion

Mehmet K. Celebi*	USGS
Michael K. Sharp*	USACE-ERDC
David M. Boore	USGS
Roger D. Borcherdt	USGS
Harish Chander	DOE
Mary E. Hynes	USACE-ERDC
Joseph P. Koester	USACE-ERDC
Richard S. Olsen	USACE-ERDC
Erdal Safak	USGS
Donald E. Yule	USACE-ERDC
Osamu Matsuo*	National Institute for Land and Infrastructure Management
Takahiro Sugano*	Port and Airport Research Institute
Takaaki Kusakabe	National Institute for Land and Infrastructure Management
Keiichi Tamura	Public Works Research Institute
Jiro Fukui	Public Works Research Institute
Izuru Okawa	Building Research Institute
Hiroyuki Fujiwara	National Research Institute for Earth Science and Disaster Prevention
Chikahiro Minowa	National Research Institute for Earth Science and Disaster Prevention
Satoshi Nishimoto	Civil Engineering Research Institute of Hokkaido
Kazuhiko Fujihashi	NTT Access Network Service Systems Laboratories
Atsushi Nozu	Port and Airport Research Institute

B. Next-Generation Building and Infrastructure Systems

George C. Lee*	MCEER
Steven McCabe*	NSF
Fu-Kuo Chang	Stanford University
Mete A. Sozen	Purdue University
B. F. Spencer	University of Illinois
K. Thirumalai	DOT
Ming Wang	University of Illinois
Masaomi Teshigawara*	Building Research Institute
Keiichi Ohtani*	National Research Institute for Earth Science and Disaster Prevention
Toshifumi Fukuta	Building Research Institute
Takashi Kaminosono	National Institute for Land and Infrastructure Management
Chikahiro Minowa	National Research Institute for Earth Science and Disaster Prevention
Akira Wada	Tokyo Institute of Technology
Isao Nishiyama	Building Research Institute
Hiroshi Fukuyama	Building Research Institute
Akiyoshi Mukai	Building Research Institute
Michio Okahara	Public Works Research Institute
Shunsuke Otani	University of Chiba
Hitoshi Shiobara	University of Tokyo
Masayoshi Nakashima	Kyoto University
Toshimi Kabeyasawa	University of Tokyo
Shigeki Unjoh	Public Works Research Institute

C. Dams

Robert L. Hall*	USACE-ERDC
Enrique E. Matheu*	Louisiana State University
Anjuna Chudgar	USACE
Richard C. Dove	USACE-ERDC
Ziyad H. Duron	Harvey Mudd College
Larry K. Nuss	U.S. Bureau of Reclamation

Richard S. Olsen	USACE-ERDC
Rick Poeppelman	USACE
Donald E. Yule	USACE-ERDC
Yoshikazu Yamaguchi*	Public Works Research Institute
Yoshio Ohne	Aichi Institute of Technology
Tatsuo Ohmachi	Tokyo Institute of Technology
Josuke Kashiwai	Public Works Research Institute
Ken-ichi Kanenawa	Public Works Research Institute
Akira Nakamura	National Institute for Land and Infrastructure Management
Hideaki Kawasaki	National Institute for Land and Infrastructure Management
Takashi Sasaki	Public Works Research Institute
Hiroyuki Satoh	Public Works Research Institute
Isao Nagayama	Public Works Research Institute
Tsuyoshi Ueda	Japan Institute of Construction Engineering
Choshiro Tamura	Nihon University
Kaoru Niwa	Japan Dam Engineering Center
Shigeharu Jikan	Water Resources Development Public Corporation
Nobuteru Sato	Water Resources Development Public Corporation
Hiroyuki Watanabe	Saitama University

D. Wind Engineering

Joseph H. Golden*	NOAA
Nicholas P. Jones*	University of Illinois
Earl J. Baker	Florida State University
Bogusz Bienkiewicz	Colorado State University
Harold Bosch	FHWA
Donald Burgess	NOAA
Ahsan Kareem	University of Notre Dame
Steven McCabe	NSF
Mark D. Powell	NOAA
Liz Ritchie	University of New Mexico
Partha Sarkar	Iowa State University
Emil Simiu	NIST
Hisashi Okada*	Building Research Institute
Jun Murakoshi*	Public Works Research Institute
Yukio Tamura	Tokyo Institute of Polytechnics
Hiromasa Kawai	Kyoto University
Yasushi Uematsu	Tohoku University
Tetsuro Tamura	Tokyo Institute of Technology
Yasuo Okuda	Building Research Institute
Hitomitsu Kikitsu	Building Research Institute
Yukio Takemura	Meteorological Research Institute
Nobuyuki Kinoshita	Meteorological Research Institute
Hiroshi Sato	Public Works Research Institute
Koichiro Fumoto	Public Works Research Institute
Hitoshi Yamada	Yokohama National University
Hiroshi Katsuchi	Yokohama National University
Hiromichi Shirato	Kyoto University
Kichiro Kimura	Kyushu Institute of Technology
Kensaku Hata	Honshu-Shikoku Bridge Authority

F. Advanced Information and Communication Technology for Disaster Prevention and Public Health Evaluation

William E. Roper*	GWU
Josephine N. Malilay*	CDC
Andrew Bruzewicz	USACE
Jennifer Mesienberger	NIMA
Richard S. Olsen	USACE-ERDC
Daniel Shnyder	USGS
Kim Shoaf	UCLA
K. Thirumalai	DOT/RSPA

Akihiko Nunomura*	Cabinet Office
Takaaki Kusakabe*	National Institute for Land and Infrastructure Management
Hiromichi Maruyama	Geographical Survey Institute
Osamu Matsuo	National Institute for Land and Infrastructure Management
Hiroaki Miyatake	Cabinet Office
Takaaki Ohyama	National Institute of Infectious Diseases

G. Transportation Systems

W. Phillip Yen*	FHWA
Hamid Ghasemi	FHWA
Harold Bosch	FHWA
Michel Bruneau	MCEER
Nicholas P. Jones	University of Illinois
David H. Sanders	University of Nevada
Peter Chang	University of Maryland
Hiroshi Sato*	Public Works Research Institute
Koichi Yokoyama	Ibaraki University
Yozo Fujino	University of Tokyo
Kazuhiko Kawashima	Tokyo Institute of Technology
Syoichi Nakatani	National National Institute for Land and Infrastructure Management
Kenichi Tokida	Public Works Research Institute
Keiichi Tamura	Public Works Research Institute
Shigeki Unjoh	Public Works Research Institute
Jun Murakoshi	Public Works Research Institute
Jiro Fukui	Public Works Research Institute
Masuo Kondo	Public Works Research Institute
Junichi Hoshikuma	Public Works Research Institute
Koichiro Fumoto	Public Works Research Institute
Masahiro Ishida	Public Works Research Institute
Kenji Ikeda	Civil Engineering Research Institute of Hokkaido
Masataka Sumi	Japan Highway Public Corporation
Naoyuki Odagiri	Metropolitan Expressway Public Corporation
Toshihiko Naganuma	Hanshin Expressway Public Corporation
Kensaku Hata	Honshu-Shikoku Bridge Authority
Koji Kawaguchi	Honshu-Shikoku Bridge Authority
Motoki Kazama	Tohoku University
Kouji Ichii	Port and Airport Research Institute
Kazunobu Moroboshi	National Institute for Land and Infrastructure Management
Takahiro Sugano	Port and Airport Research Institute

RESOLUTIONS

RESOLUTIONS OF THE THIRTY-FIFTH JOINT MEETING U.S.-JAPAN PANEL ON WIND AND SEISMIC EFFECTS (UJNR)

National Institute for Land and Infrastructure Management, Tsukuba, Japan

12-14 May 2003

The following resolutions are hereby adopted:

1. The Thirty-fifth Joint Panel Meeting provided the forum to exchange valuable technical information that is beneficial to both countries. In view of the importance of cooperative programs on the subject of wind and seismic effects, the continuation of Joint Panel Meetings is considered essential. Both sides agreed to explore new ideas and areas to strengthen cooperative activities in support of the Panel's mission.

2. The following activities have been conducted since the Thirty-fourth Joint Meeting:

   a. Technology Exchanges. Technical experts, technical documents, and applications of the electronic media have been exchanged. These exchanges have contributed to the development of new research programs and enhanced ongoing research in both countries.

   b. Task Committee Workshops and Technical Coordinating Committee Meeting. The Panel held four workshops and one meeting:
      1. Task Committee (A), 6th U.S.-Japan Workshop on Geotechnical Earthquake Engineering, 27-28 February 2003, San Diego, CA, USA.
      2. Task Committee (B), 3rd U.S.-Japan Technical Coordinating Committee Meeting on Auto-Adaptive Media (Smart Structural Systems), 19 October 2002, Tsukuba, Japan.
      3. Task Committee (C), 3rd U.S.-Japan Workshop on Advanced Research on Earthquake Engineering for Dams, 22-23 June 2002, San Diego, CA, USA.
      4. Task Committee (D), 3rd U.S.-Japan Workshop on Design for Wind and Wind Hazard Mitigation, 2-5 October 2002, Seattle, WA, USA.
      5. Task Committee (G), 18th U.S.-Japan Bridge Engineering Workshop, 22-24 October 2002, Saint Louis, MO, USA.

3. The Panel approved the Task Committee reports presented during the Thirty-fifth Joint Panel Meeting. Each report included objectives, scope of work, accomplishments and future plans.

4. The Panel has successfully implemented the recommendations of the Strategic Plan, which was approved at its Thirty-third Joint Panel Meeting, and continues to work toward streamlining its structure and promoting the collaboration of researchers in both countries.

5. The Panel held the Strategic Planning Session, in which its activities were critically reviewed. The following are the highlights of those reviews.
   a. The Panel encourages Task Committees to conduct joint research. Various efforts such as Task Committee Workshops to coordinate joint research plans utilizing the NEES facilities in the U.S. and diverse laboratories in Japan, including E-Defense should be emphasized.
   b. The Panel has uploaded the technical programs, reports and manuscripts of the 31st-34th Joint Panel Meetings to its website, and will strengthen the website by including the Task Committee activities (http://www.pwri.go.jp/eng/ujnr/ujnr.htm).
   c. The current Task Committee structure works well. The Panel will explore further collaboration through the formation of new Task Committees on topics of mutual interest, e.g., lifelines, and storm surge and tsunami.
   d. The Panel will explore collaboration with other Panels, possibly through conducting a joint workshop or joint research.
   e. The Panel will consider appropriate metrics to evaluate the impact of its research on practice. The Panel will consider proposed metrics for adoption at the Thirty-sixth Joint Panel Meeting.

6. The Panel approved the new Task Committee F (Advanced Information and Communication Technology for Disaster Prevention and Public Health Evaluation) whose operating charter was submitted at the Thirty-fifth Joint Panel Meeting and met the criteria described in the Strategic Plan.

7. The Panel endorses the following four proposed Task Committee Workshops during the coming year:

   a. Task Committee (A), 3rd Workshop on Soil-Structure Interaction, 2004.
   b. Task Committee (B), Workshop on Future U.S.-Japan Collaborative Structural Research Utilizing Networked Large-Scale Test Facilities, October 2003.
   c. Task Committee (F), Workshop on Utilization of IT for Crisis Management and Disaster Mitigation (Tentative Title), May 2004.
   d. Task Committee (G), 19th U.S.-Japan Bridge Engineering Workshop, October 2003, Japan.

In the event that T/C co-chairs consider it essential to conduct a joint meeting or workshop that is not included in this Resolution, the T/C co-chairs will make such a request through their respective Secretary-General for approval by the U.S. and Japan Joint Panel Chairmen.

The U.S. and Japan-side Task Committee Chairs, with concurrence of the Joint Panel Chairmen, will develop and schedule their Workshops. Both sides' Secretaries-General will be kept informed of the planning, conduct, and results of workshops or committee meetings including resolutions and reports. Results of each activity conducted before the Thirty-sixth Joint Panel Meeting will be presented at the Thirty-sixth Joint Panel Meeting.

8. The Panel focused attention to the progressive collapse of buildings by featuring a special Technical Session theme to discuss this topic.

9. The Panel recognizes the importance of continuing its joint research programs on Soil Liquefaction and Countermeasures and on Auto-Adaptive Media (Smart Structural Systems).

10. The U.S.- and Japan-sides will encourage the conduct of joint investigations following earthquake and wind disasters in the U.S. and Japan.

11. The results of the Panel's work should be disseminated to improve the quality of life globally. The Panel will make use of the internet to the extent possible to disseminate information.

12. The Thirty-sixth Joint Panel Meeting of the UJNR Panel on Wind and Seismic Effects will be held by the U.S.-side Panel, in the U.S. in May 2004. The U.S.-side Secretariat will propose dates, program, location, and itinerary with the concurrence of the Japan-side Panel.

PAPERS

THEME 1

Geotechnical Engineering and Ground Motion

Status Report on Strong Motion Recording for Buildings in Japan

by

Izuru Okawa[1], Toshihide Kashima[2], Kuniaki Yamagishi[3] and Morimasa Watakabe[4]

ABSTRACT

In the first phase of the strong motion recordings in buildings, the number of instruments (recording channels) was quite small, There appeared single instrument on the basement or first floor. There was sometimes the case in which a pair of instruments were found in the bottom and the top of the buildings.
In this paper, the strong motion recording system for buildings in Japan was surveyed besides the BRI systems. The properties of those surveyed systems were summarized and the features of those systems currently on-going were reviewed with respect to the structural types, types of pile foundations, locations of recording instruments, etc.

KEYWORDS: Earthquake recording, Buildings, Instrumentation, Pile Foundation, Strong motion,

1. INTRODUCTION

The earthquake observations in and around ground have been increased after the Hyogo-ken Nambu earthquake in 1995. The National Research Institute of Earth Science and Disaster Prevention (NIED) had started to deploy a thousand strong motion seismometers nationwide. The Japan Meteorological Agency (JMA) and the local governments had also installed seismic intensity meters. In addition, the NIED had reinforced the earthquake observation instruments under ground.
On the other hand, the instrumentation for structures has been managed differently.
The earthquake observation for civil structures such as bridges, dams, port and harbor facilities, are maintained by the public organizations. Therefore, the management of recording system and data is not so difficult.
However, in the building engineering field, the situation is quite different.
Since building owners are mostly from private sectors, the instrumentation is so rare. Even if the owner installed the instrument, there is no guarantee that the data will be in the public domain.
This paper summarizes the current situation of the strong motion recordings of buildings in Japan. The strong motion recording system for buildings besides the BRI systems. in Japan was surveyed The properties of those surveyed systems were summarized and the features of those systems currently on-going were reviewed with respect to the structural types, types of pile foundations, locations of recording instruments, etc.

2. INSTRUMENTATION IN BUILDINGS

The strong motion recording of Japan started in 1953. The details can be found in the reference [1]. The first strong motion seismometer of Japan was installed in the Earthquake Research Institute, the University of Tokyo about 50 years ago. After that, many instruments were installed in various structures such as buildings, roadway bridges, dams, port and harbor facilities, etc.
The BRI played the leading role in developing the strong motion seismometers in Japan. Since then, the strong motion recordings in buildings have been continued for many purposes.
One is accumulating the strong motion records,

1 Senior Research Fellow, Department of Structural Engineering, Building Research Institute, Tsukuba, Ibaraki pref.
2. Senior Research Engineer, International Institute of Seismology and Earthquake Engineering, Building Research Institute, Tsukuba, Ibaraki pref.
3. Senior Research Engineer, Technical Research Institute, Sumitomo-Mitsui Construction Co. Ltd., Tochigi pref.
4 Deputy Manager, Structure Division, Techinical Research Institute, Toda Corporation, Tokyo

the other is for verifying the analytical methods used in seismic design and the effectiveness of the methodology. In 1968, the super high-rise building was constructed for the first time in Japan. About twenty years later, the base isolation devices such as rubber bearing and dampers were installed in buildings in 1990's. It was soon followed by the appearance of buildings with response control devices.
The 1995 Hyogo-ken Nambu earthquake prompted the adoption of base isolation system in the buildings.
In the building engineering field, the purposes of the instrumentations are for studies of the soil-structure interaction including the underground behavior of foundations especially piles and/or input mechanism from soil to building, for studies of new technologies such as the super high-rise buildings, the base isolation, and the response control. The instrumentation of BRI gave priority to the evaluation of effective input motion in SSI studies [2]. However, the general trend of the instrumentation field actually emphasizes the verification of the new technologies and the design method.

3. LITERATURE SURVEY RESULTS

The survey was conducted using the literature survey system of the Web site of the Architectural Institute of Japan (AIJ). The relevant literature was picked up with a keyword of 'earthquake recording or observation' among the published technical abstracts for the latest 10 years.
There are many organizations that install seismometers in their own buildings and make analyses using them. Each instrumentation is designed for its own purposes. The data will not be generally disclosed. These situations had not been improved to date. For these reasons, the publicized data had not been increased so quickly, but the accumulation of data is one of the most important tasks in view of the performance-based design trend in the future.

The instrumentation examples are listed in Table 1 (1) through (8). Most of the sites are in the densely populated area such as Tokyo, Yokohama, Chiba, Nagoya, Osaka, and Kobe. The survey results tends to emphasize the research aspect of the instrumentation because the survey was conducted using the abstracts of AIJ annual meetings. Therefore those installed for verifying the design properties such as the cases of high-rise buildings and base-isolated buildings that are mandated to be designed with dynamic analyses using the time history might not be included in the literature.
The authors believe that although there are many instrumentation examples besides the survey results, most of the examples of engineering significance are included in this survey results.

3.1 Structural types of instrumented buildings

The structural types of objective superstructure are classified mainly into several groups, i.e., reinforced concrete, steel and steel reinforced concrete structures in materials, frame or wall system as in structural system. The foundation types are also classified into mat foundation, pile foundation and under-reamed pile etc. These are as shown among the items in Table 1. Most of the buildings are used for offices. The building for personal use such as private housing was not found. Especially, the Japanese traditional wooden houses have never been instrumented and therefore there are no data on their behavior during earthquakes. It might be one of the big problems in that the major building type in Japan has never been instrumented and we do not have data of its behavior during earthquakes.
Buildings with base isolation devices are only exception for the instrumented housing..
The other types found in the instrumented buildings are those with response control devices, tall buildings, those densely instrumented for identifying the Soil-Structure Interaction effect in soft soil area.

3.2 Dimensions of the instrumented buildings

The number of stories and height of instrumented buildings vary. These are also shown in Table 1. The instrumented tall buildings took measures not only for earthquake but also wind. The highest instrumented building has 70 stories located in Yokohama.

3.3 Instrumentation of the buildings

The instrumentation is governed by the intention of the recording purpose. The purpose of the instrumentation in buildings with new technologies are mainly to verify the effectiveness of the devices. The layout of the instrumentation for the input mechanism in soil, foundation, and basement is rather complicated and generally densely installed. The instrumentation for spatial variation of input ground motion was found along the long layout plan.

4. CONCLUSIONS

The observation for effective input motion evaluation should be increased. For such observation, the conventional system with few seismometers is not enough, but dense instrumentation will be expected to clarify the complicated input mechanism among soil, foundation and superstructure. This will never be accomplished through the laboratory experiment. Whereas, the effectiveness of the devices can be evaluated through the basic experiment of the materials. In those cases, it in not likely to have new findings from earthquake observation but the verification of the performance will be the main target of the observation.

Effectiveness of new devices for earthquake force reduction and the investigation of input mechanism between soil and foundation are major targets of the current earthquake recordings in Japan

main target of the strong motion instrumentations.

(1) Evaluation of effective input motions

(2) Detailed database construction indicating Structural Performance

(3) Promoting the instrumentation in buildings

When we focus our attention on the strong motion property variations within the local area or even around one construction site, the aforementioned nationwide network does not necessarily give sufficient data for evaluating local site effect or effective input motions for specific building structures. The instrumentation density is still quite sparse except for specific large cities. However, it is not easy to increase the number of instrumentations only by appealing the necessity of the earthquake data for buildings. There should be incentives for promoting the instrumentations in buildings.

Meanwhile, the Building Standard Law of Japan has been recently revised in accordance with the performance-based-design oriented scheme. In the scheme, the structural designer is requested to quantitatively evaluate the structural performances for various types of external disturbances including earthquake motions. The developments of detailed evaluation techniques for structural performance should be done and it will become one of the most important tasks of the BRI. We need firstly identify that the earthquake recording gives a reliable tool for evaluating the seismic performance of buildings. The earthquake recording is generally still costly. If earthquake recording is to be utilized for detecting the vibratory characteristics of building as one of the crucial performance indices, a cost reduction of instrumentation will be secondly an important issue for wide use. When such situation is realized, more dense locations of instrumentation sites will be become possible.

The result shows the current status of the respective recording systems. That does not necessarily means the obtained data will be released to the open public.

The newly instrumented buildings are mostly equipped with a kind of new device. These are new technologies such as tall buildings, base-isolated buildings and those with response control devices, and to clarify the input mechanism of seismic waves through soil, foundation and structures by measuring the deformation or forces arising in the piles.

5. REFERENCES

1. Tanaka, T., "Development of Strong Motion Accelerometers and the Early Instrumentation in Japan", ORI report 4-02, 1994
2. Okawa, I., et al., "Earthquake Recording In Buildings As A Tool For The Comprehensive Structural Performance Evaluation", The Proceedings of the 34th UJNR Joint Panel for Wind and Seismic Effect, NIST, 2002
3. Okawa, I., et.al., "Dense Instrumentation in

BRI Building and Surrounding Ground", Proceedings UJNR Workshop on Soil-Structure Interaction, Menlo Park, California, September 22-23, 1998

4. Okawa, I., "Earthquake Recording for SSI Study by BRI", The Proceedings of the 2nd U.S.-Japan Workshop on Soil-Structure Interaction, March 6-8, Tsukuba, Japan, 2001

ACKNOWLEDGEMENT

The survey result presented herein is a cooperative work in the Special Study Group of the Building Research Institute Community (BRIC). The authors express their sincere thanks to the members of the study group for their contributions.

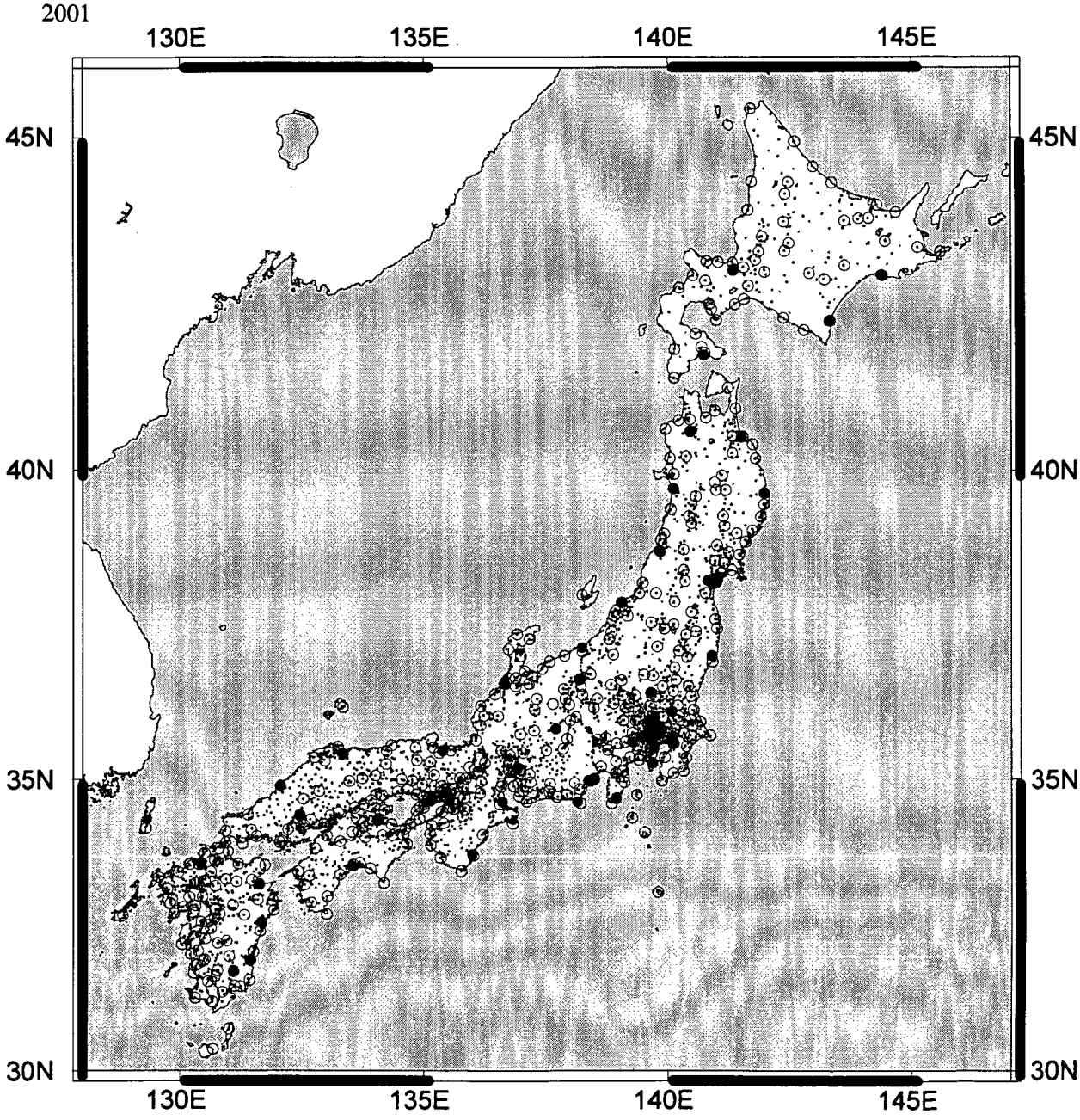


Figure 1 Nationwide Distribution of Major Strong Motion Recording Sites
The red circles indicate the stations maintained by BRI. The green dots indicate the stations of K-net maintained by NIED, MEXT. The open circles indicate the JMA sites for Seismic Intensity Evaluation.

Real-Time Seismic Monitoring Needs of a Building Owner and the Solution

by

M. Çelebi[1], A. Sanli[1], M. Sinclair[2], S. Gallant[2] and D. Radulescu[3]

ABSTRACT

A recently implemented advanced seismic monitoring system for a 24-story building facilitates recording of accelerations and computing displacements and drift ratios in near real-time to measure the earthquake performance of the building. The drift ratio is related to the damage condition of the specific building. This system meets the owner's needs for rapid quantitative input to assessments and decisions on post-earthquake occupancy. The system is now successfully working and, in absence of strong shaking to date, is producing low-amplitude data in real-time for routine analyses and assessment. Studies of such data to date indicate that the configured monitoring system with its building specific software can be a useful tool in rapid assessment of buildings and other structures following an earthquake. Such systems can be used as a health monitoring tool, as a method to assess performance based design and analyses procedures, long-term assessment of structural characteristics of a building, and as a possible long-term damage detection tool.

Keywords: real-time monitoring, seismic event, damage, acceleration, accelerometer, displacement, drift ratio, spectrum, steel moment resisting frame.

[1] Earthquake Hazards Team, USGS (MS977), 345 Middlefield Rd., Menlo Park; Ca, 94025
[2] Degenkolb Engineers, San Francisco, Ca.
[3] Digitexx, Pasadena, Ca.

1. INTRODUCTION

In all seismic areas, local and state officials and prudent property owners, establish procedures to assess the functionality of buildings and other important structures such as lifelines following a significant seismic event. Immediately following such an event, the decisions of functionality and occupancy of a building in most cases are based on visual inspections of possible damage to the structure. If the structure appears damaged, it is necessary to further examine and assess as to whether the damage condition of the structure presents an unsafe environment for the occupants or users of that structure. Therefore, to have instrumental measurements of shaking of a building or even a nearby ground site provides valuable information to decision makers.

In general, a system for seismic monitoring of structures must fulfill a stated need – that is, during and after a strong-shaking event, the monitoring system should yield data that serves the specific purposes for which it has been planned. Each user of the structural response data may have a different objective. In general, from the viewpoint of an owner, the objective could be to use such data obtained by monitoring to increase the likelihood that the building will be permitted to remain functional during and following an event. In practical terms, this means whether, immediately after occurrence of an event, a building will be tagged as "green = no restriction on use or occupancy", "yellow = limited entry, entry is permitted only by the owner for emergency purposes, at his or her

own risk", or "red = unsafe, the structure poses an obvious safety hazard" (ATC-20, 1989).

When seismic monitoring has been considered and implemented, in general, the principal objective has been the quantitative measurement of structural response to strong and possibly damaging ground motions for purposes of improving design and construction practices. Thus, it is expected that, an instrumented structure should provide enough information to (a) reconstruct the response of the structure in enough detail to compare with the response predicted by mathematical models and those observed in laboratories, the goal being to improve the models, and (b) make it possible to explain the reasons for any damage to the structure. The nearby free-field and ground-level time history should be known in order to quantify the interaction of soil and structure.

Therefore, the main objective to date has been to facilitate response studies in order to improve our understanding of the behavior and potential for damage of structures under the dynamic loads of earthquakes. As a result of this understanding, design and construction practices can be modified so that future earthquake damage is minimized. Up to now, it has not been the objective of instrumentation programs to create a health monitoring capability for structures.

However, structural engineers increasingly want the measurement of displacements in order to assess drift ratios during strong shaking events. In order to achieve these, the approach used in this paper is a suitable and technologically feasible way for real-time assessment and alarm system based on computation of drift ratios from double-integrated acceleration measurements. This approach can also be used for performance evaluation of structures. The described system is considered as a building health-monitoring system.

The objective of this paper is to describe a specific case whereby the owner of a building, in collaboration with a federal agency with expertise in seismic monitoring of buildings, private consulting engineers and a supplier, facilitated development and implementation of a state-of-the-art seismic monitoring system for a 24-story steel frame building in San Francisco, California. The objectives and implemented characteristics of the system meet the specific needs of the owner. This case illustrates that building-specific monitoring systems can be developed to meet the needs of owners of other buildings and structures.

2. BUILDING AND CHARACTERISTICS

The building was designed according to the 1979 UBC and its construction was completed in 1982. The ground floor (plaza level) with a height of 50 ft. (15.2 m.) appears as two nominal floors of the 284 ft. (86.6 m.) tall building. The building has a 70ftx90 ft (21.3m x 27.4m) square plan.

Perimeter steel moment resisting frames with welded connections are continuous from grade to roof level. The columns and beams are steel wide flange and box sections. Reinforced concrete on metal deck floors function as rigid diaphragms and transfer lateral loads to the perimeter moment frames. The perimeter moment frame beams are typically not composite with the metal deck floor system. The moment frames are expected to behave as strong-column weak-beam frames resulting in development of hinges at the beams. The building structure is therefore considered as a "pre-Northridge" perimeter welded steel moment frame. The steel columns typically terminate at just below

grade. The foundation of the building consists of 12" (0.305 m) square, reinforced, precast piles driven to approximately a 60 ft. (18.3 m.) depth. The reinforced concrete pile caps are interconnected by a grid of reinforced concrete grade beams.

A general three-dimensional schematic of the building with its overall dimensions is provided in Figure 1.

3.0 DISCUSSION OF NEEDS

The building owners are in need of reliable and timely expert advice on whether or not to occupy the building following an event. Furthermore, information gathered from the building during strong-shaking events will help the building owner to further assess technical issues as related to possible post-earthquake connection inspection, retrofit and repair of the building. For this reason, the following decisions have been made.

1.The building has been designated as part of the Building Occupancy Resumption Program (BORP, 2001). "This award-winning program (BORP) of the San Francisco Department of Building Inspection, developed in cooperation with SEAONC (Structural Engineers Association of Northern California), BOMA (Building Owners and Management Association), and AIA (American Institute of Architects) allows building owners to pre-certify private post-earthquake inspection of their buildings by qualified licensed engineers" (BORP, 2001). The owner's engineers post red/yellow/green placards, in accordance with ATC-20 Guidelines (ATC, 1989) in lieu of the city authorized inspectors who would typically be unfamiliar with the building and may not be available for several days following the earthquake. The owners and the consultants have agreed that general building-related evaluation work will commence in the building by cognizant personnel to reach decisions on the suitability of re-occupying the building following any one of the following events, or exceedence of thresholds that may be cause of possible damage in the building:

i. a state of emergency in the City or County of San Francisco has been declared,

ii. a M≥6.0 earthquake on the San Andreas or Hayward faults,
iii. a M≥6.0 earthquake on the Rodgers Creek fault, or

iv. the building experiences a peak acceleration greater than 0.25 g (this intended as free-field motion and adopted from Table 3-1, FEMA352[2000]).

Damage in steel moment frame structures presents itself as yielding or fracture of the welded connections. The damage is frequently not immediately visible due to the presence of building finishes and fireproofing. In the absence of visible damage to the building frame, most steel moment frame buildings will be tagged based on visual indications of building deformation, such as damage to partitions or glazing. Lack of certainty regarding the actual deformations that the building experienced will typically lead the inspector toward a relatively conservative tag – e.g. yellow tag instead of green.

The City of San Francisco has yet to adopt or develop criteria for post earthquake inspection and assessment of pre-Northridge welded moment frame structures beyond the ATC 20 (1989) tagging requirements. Similar to the process that occurred in Los Angeles following the 1994 Northridge earthquake, the City of San Francisco will likely require detailed inspections of the welded connections in high rise steel moment frame structures in

the area of strong ground shaking. It is reasonable to expect that these will be based on the most sophisticated set of requirements developed to date, FEMA 352: Recommended Post-earthquake Evaluation and Repair Criteria for Welded Steel Moment-Frame Buildings (2000).

Application of the FEMA 352 requirements for the subject building would result in inspection of 10% to 15% of the connections in the building. The building owner and engineers anticipate using the data provided by the system to justify a reduced inspection program than that which would otherwise be required by the City of San Francisco for a similar non-instrumented building in the same area. Depending on the deformation pattern observed in the building, it would also be possible to direct the initial inspections toward locations in the building that experienced peak drifts during the earthquake.

These objectives are best accomplished by deploying accelerometers at specific locations in the building to facilitate measurement of the actual structural response, which may indicate occurrence of damage and lead to making consequential decisions in a timely way. For this reason, in addition to measurement of ground level input motions, measurement of structural response is needed to compute parameters that will relate to the damage status of the structure.

The most relevant parameter in this case is the measurement or computation of actual or average story drift ratios. Specifically, the drift ratios can be related to the performance-based force-deformation curve hypothetically represented in Figure 2 modified from Figure C2-3 of FEMA Report 274 (1997). When drift ratios, as computed from relative displacements between consecutive floors that are determined from measured responses of the building, the performance and as such "damage state" of the building can be estimated as in Figure 2.

Therefore, the problem and the challenge are clear: to compute displacements from recorded acceleration responses in real-time or near real-time. Measuring displacements directly is very difficult and, except for tests conducted in a laboratory (e.g. using displacement transducers), has not yet been feasibly achieved for a variety of real-life structures. For long-period structures such as tall buildings and long-span bridges, displacement measurements using Global Positioning Systems (GPS) are possible (Çelebi and Sanli, 2002) but limited in application (*e.g.* GPS technology is limited to sampling rates of 10-20 Hz and, for buildings, measurement of displacement only at the roof is possible).

4.0 GENERAL DESCRIPTION OF REQUISITE MONITORING SYSTEM

The unique aspects of the requisite monitoring system that will facilitate the needs of the particular owner are generally described as follows:

- The monitoring system must facilitate rapid assessment of the building integrity following an earthquake;
- The monitoring system must provide data in a form that is easy to correlate with known and building specific engineering parameters (e.g. drift ratio), which in turn must relate to the expected damage condition of the building; and
- The monitoring system must deliver the data within a relatively short time (few minutes if not in seconds), if not in real-time, to facilitate informed decision making regarding post-earthquake building occupancy.

5.0 CAPABILITIES OF RECORDING SYSTEMS

We have assembled a monitoring system that provides the three basics requirements above. As defined, developed and implemented by the project team, the PC-based monitoring system does the following:

- The system has the standard recording capability (of acceleration data) at the site server PC. The system continuously streams, in real-time, acceleration response data at the site. Recording starts when pre-assigned thresholds of acceleration are exceeded at selected locations (where accelerometers are deployed as seen in Figure 1) in the building. This is similar to the standard way such recording is initiated with most current systems. As in most newer recording systems, this new system also can trigger at thresholds defined at ten locations. Data stored at the server can be retrieved manually at the site, retrieved remotely or transferred automatically to a pre-defined location.
- The system is (high-speed) internet-connected.
- Users are able to connect to the server via the internet and are able to view or record the data remotely. Users are provided with specific software (called "Client Software" herein) that will acquire streamed real-time acceleration data from the server and perform computations of velocity and displacement.
- Specific filter options are built into the client software for processing of the acceleration data before the integration process.
- Specific to the building being monitored, and programmed into the client software, is the capability to calculate a select number of drift ratios. While acceleration data from all of the channels are received continuously, due to time required to process and compute velocities, displacements, and ultimately the story drift ratios, only twelve channels of streamed data (as selected by the user) are visually displayed in real-time. However, once an event is recorded, it can be played back for analyses of the data from all of the channels.
- Corresponding to each drift ratio, there are 4 stages of colored indicators. When only the "green" color indicator is activated, it indicates that the computed drift ratio is below the first of the three specific threshold. As drift ratios exceed the designated three thresholds, as depicted in Figure 2, additional indicators are activated with a different color.
- The drift ratios are calculated using data from any pair of accelerometer channels oriented in the same direction. However, the expectation is that they will typically be used with drifts monitored over one story level intervals as shown in Figure 1. The threshold drift ratios are computed and decided by structural engineers using structural information. The performance-based theme, as illustrated in Figure 2, is compatible with Figure C2-3 of FEMA Report 274 (1997).
- The thresholds for the present installation are based on performance limits of the welded beam-column connections, established using FEMA352 Steel Moment Frames: Evaluation and Upgrade Criteria for Existing Buildings (2000). This allows the various drift ratio

thresholds to be matched to a probability of connection fractures in different areas of the building.

- At present, the first stage threshold corresponds to one quarter of the computed building yield level, approximately 0.2% drift. At this level of drift no connection fractures are anticipated although movement of the building should be detectable by the occupants. The second stage threshold correspond to the building yield level, approximately 0.8% drift, which is the lower bound drift for anticipated connection fractures. The third stage threshold correspond to drifts at which the beam rotation demands equal the strength degradation value determined in accordance with FEMA352 (2000). The third stage threshold varies between 1.4% and 2.2% drift depending on the location being examined in the building. At this level of drift, FEMA 352 predicts that approximately 50% of the connections will have fractured. The drift limits vary at different locations in the building due to the different frame member lengths and sectional properties.

A general schematic of the data management, communication and transmittal set-up is shown in Figure 3.

6.0 ACCELEROMETERS IN THE BUILDING

As seen in Figure 1, thirty accelerometers are now deployed throughout the building. This number of accelerometers is within the current norm that is recommended (COSMOS, 2001). Deploying accelerometers on every floor would have been too costly both from the point of added hardware and cabling required, and also the additional demands on digitizing of analog signals, recording, data streaming and transmission capabilities.

A tri-axial accelerometer is on the ground floor to provide requisite reference input motions to the building. Then at each of nine levels (at elevation 25' [7.6 m.], 6th , 7th, 12th, 14th , 17th, 18th, 23rd floors, and the roof), three uniaxial accelerometers are deployed. It is noted herein that, in the building, there is no 13th floor designation. At each of these levels, two parallel accelerometers are deployed, in the nominal EW direction, one at the north end and the other at the south end. The third accelerometer is deployed in the nominal NS direction. The configuration is the optimal distribution of accelerometers.

The purpose of this deployment scheme is to facilitate the computation of either actual drift ratios at several pairs of consecutive floors, or average drift ratios over various combinations of non-adjacent floors.

7.0 DATA RECORDING AND REAL-TIME ISSUES

7.1. Recording at the Server/Recorder at the Site

The server/recorder at the site is controlled by specific software that is multi-threaded. The system digitizer, an analog to digital [A/D] converter, within the server/recorder, processes the analog signals from all of the 30 sensors.

The raw data thread acquires data from the system digitizer at 1000 samples per second (sps), scales it to cm/s/s using sensitivity information of each channel, digitally low-pass filters the data, decimates to 200 sps, and

sends it continuously to the triggering thread and to the broadcasting thread. Continuously streamed data are not saved at the server/recorder unless trigger conditions are met.

The triggering thread of the software continuously monitors the trigger conditions by comparing the amplitude level on any ten (user selected) channels with the pre-determined trigger thresholds. In detail, the trigger thread takes the data from the raw data thread, filters the data with a band-pass filter, and compares the peak amplitude of each selected trigger channel with its corresponding threshold. When the exceedance criteria (e.g. 0.3% g) is met, the system will start recording raw data in an event file. In this specific case, the ten channels selected are at upper floors so that when the earthquake shaking of the ground floor at the particular site is ending, it will be possible to continue to capture the continued shaking response of the structure. Recording capability with pre-trigger (commonly referred to as pre-event) memory of 20 seconds (or suitable choice of duration), assures recording of the start of the shaking at the ground or basement level. To avoid false triggers, choice of level of shaking triggers (e.g. 0.3 % g), must be carefully selected to assure that triggering occurs during earthquake-generated motions originating at close or far distances.

The recording thread records raw data based on the trigger threshold exceedance. When one or more channels exceed their assigned trigger threshold (based on the trigger exceedance algorithm), acceleration data are recorded by the server as "raw data".

The broadcasting thread broadcasts data to multiple clients continuously via the internet, and only when at least one client is connected.

The posting thread sends the recorded raw data to pre-addressed users using FTP. Alternatively, events recorded at the site can be retrieved at the site or remotely via internet.

7.2 The Client Scheme

An interesting aspect of the system is that the response data are continuously streamed at the site recorder/server but they can also be streamed to a remote location using client software. Furthermore, the response data can be continuously retrieved in real-time remotely by the client software, which currently can handle visual streaming of only 12 channels due to time consumption required for computations described earlier, and to real-time graphic display limitations. To repeat, the computational load includes in real-time computation of 12 channels of velocity and displacement time-histories, drift ratios for 6 pairs of channels, and amplitude and response spectrum of a particular selected channel. Therefore, at each client location, by selecting appropriate channels from the configuration shown in Figure 1, and with the known story-heights and computed relative displacements, it is possible to compute six different story drift ratios in real-time. The decisions related to exceedence of pre-determined drift ratios as illustrated in Figure 2 are based on these computed and streamed drift ratios. The basis of judgment of the health of the building is done with the use of drift ratio computations in real-time.

Whenever recording is activated using the client software, raw acceleration data from all of the channels are recorded (at designated location of the client PC). The recording is activated upon exceedence of a threshold or manually if the user needs to record data remotely. Any recorded data can be played back by the client software or can be processed by additional other software.

Figure 4 shows a PC screen snapshot of the client software display. The upper left frame shows 12 channels of streaming acceleration time series. Each paired set of acceleration response streams is displayed with a different color. The upper right shows amplitude spectra for one of the channels and is selectable by the user. It is noted that several frequencies are clearly identifiable (as discussed later in the paper). In the lower left, time series of drift ratios are shown for 6 locations, each color corresponding to the same pair of data from the window above. In order to get the drift ratios, real-time double integration of filtered acceleration data are computed. For this, story heights, as shown in Figure 5, need to be manually entered. Figure 5 also shows the computed pairs of displacements that are used to compute the drift ratios. The thresholds of drift ratios for selected pairs of data must also be manually entered in the boxes in Figure 5. The figure hypothetically shows that the first level of threshold is exceeded, and the client software is recording data as indicated by the illuminated red button.

8.0 SAMPLE RECORDED DATA AND ANALYSES

Sample data obtained via the client software are shown in Figure 6. The data are from the two parallel channels (CH12 and CH21) and their difference as well as the orthogonal channel (CH30) at the roof recorded on February 12, 2003. The intent of the differential accelerations of parallel channels (CH12-CH21) is to identify the strong presence of torsion. The recorded peak accelerations are about 0.1-0.2 gals (~0.1-0.2 cm/s/s). The computed amplitude spectra clearly indicate a peak frequency for the fundamental translational mode (in both directions) at ~0.4 Hz (~2.5 second period) for all channels and at ~0.6 Hz (~1.67 s) for the torsional motion. Furthermore, the signals are good enough to identify the second translational mode at ~ 1.2HZ (~0.83 s). Similarly, the second torsional mode is at ~ 1.8 Hz (0.56 s). The identified translational frequency is typical of a framed building that is 24 stories high. The identified modes and frequencies are further supported with the cross-spectrum, coherency, and phase angle plots in Figures 7 and 8. The cross-spectrum, coherency, and phase angle plots of the motions recorded by CH12 and CH21 (the two parallel accelerometers at the roof level) are shown in Figure 7. The cross-spectrum actually exhibits all of the significant frequencies identified in Figure 6 with very high coherency (~1). At 0.4 and 1.2 Hz, the phase angles between the parallel motions are both 0 degrees which indicate that they are in phase and therefore belong to translational modes. At 0.6 Hz and 1.8 Hz, the phase angles are ~180 degrees which indicate that they are out of phase and belong to torsional modes. The strong torsional presense are further illustrated through Figure 8 that exhibits cross-spectrum, coherency, and phase angle plots of the motions recorded by differences of motions recorded by parallel channels (CH12-CH21) at the roof and (CH10-CH19) at the 18th floor. Again, at ~ 0.6 Hz, these torsional motions exhibit significant cross-spectral amplitude with very high coherency (~1) and 0 degree phase angle. Therefore, 0.6 Hz belongs to the first torsional mode.

At the level of low amplitude acceleration response recorded and exhibited in this set of sample data, the signal-to-noise ratio is quite high and satisfactory to indicate several modal frequencies. It is expected that the coherency of motions between such pairs of channels will further improve when the signal-to-noise ratio is even higher during strong-shaking events. Further detailed analyses of strong

shaking data will be carried out when recorded in the future.

9.0 CONCLUSIONS AND BENEFITS

Capitalizing on advances in computational and data transmission technology, it is now possible, as described in this paper, to configure and implement a seismic monitoring system for a specific building with the objective of rapidly obtaining sufficient response data during a strong shaking event in order to help make informed decisions regarding the health and occupancy of that specific building.

To meet such an objective and needs of a building owner, a seismic monitoring system for a 24-story steel moment frame building has recently been implemented. The system records accelerations and computes displacements (and drift ratios) in near real-time. The variable drift ratio is related to the damage and safe occupancy criteria of the specific building. Data can be streamed and recorded both at the server within the building and remotely by client software specifically configured for this building to meet the needs of the owner. The client software is capable of retrieving and recording real-time acceleration response data, and computing, in near real-time, velocity, displacements, and amplitude and response spectra of the streaming accelerations from selected accelerometers. Furthermore, the software can compute drift ratios using the near real-time computed displacements, and specific building data such as story heights. Alarms are related to thresholds of drift ratios computed for pairs of floors. The drift ratios are related to building performance and therefore are key in making occupancy and other decisions.

The monitoring system is now successfully working and, in absence of strong shaking to date, is producing useful low-amplitude data in real-time for analyses and assessment. This approach can be used for performance evaluation of structures, long-term assessments of structural characteristics, long-term damage detection, and health monitoring for buildings and other structures.

10.0 REFERENCES

ATC-20, 1989, Procedures for Post-Earthquake Safety Evaluation of Buildings, Applied Technology Council, Redwood City, CA.

BORP (Building Occupancy Resumption Program), 2001, City and County of San Francisco, Department of Building Inspection, Emergency Operation Plan, (Rev. 2001). [www.seaonc.org/member/committees/des_build.html)

Çelebi, M. and Sanli, A., 2002, GPS in Pioneering Dynamic Monitoring of Long-Period Structures, *Earthquake Spectra*, Journal of Earthquake Engineering Research Institute,Volume 18, No. 1, pages 47–61, February 2002.

COSMOS, 2001, Proceedings of Invited Workshop on Strong-Motion Instrumentation of Buildings, Publication No. CP-2002/04.

FEMA 274, 1997, NEHRP Commentary on the Guidelines for the Seismic Rehabilitation of Buildings, October 1997.

FEMA 352, 2000, Recommended Post-earthquake Evaluation and Repair Criteria for Welded Steel Moment-Frame Buildings, July 2000.

Uniform Building Code (1979), International Conference of Building Officials, Whittier, CA.

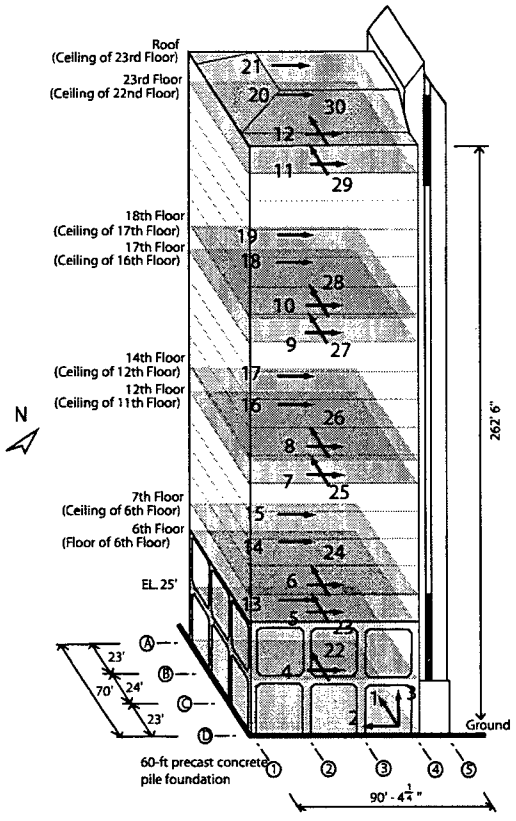


Figure 1. General three-dimensional schematic of the building. Also shown are the 30 accelerometers (heavy arrows) deployed throughout the building.

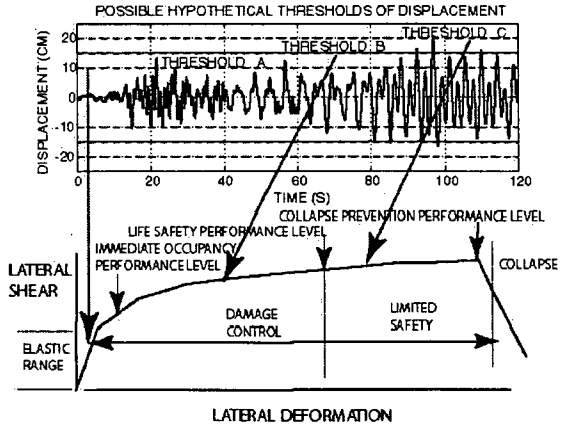


Figure 2. Hypothetical displacement time-history as related to FEMA 274.

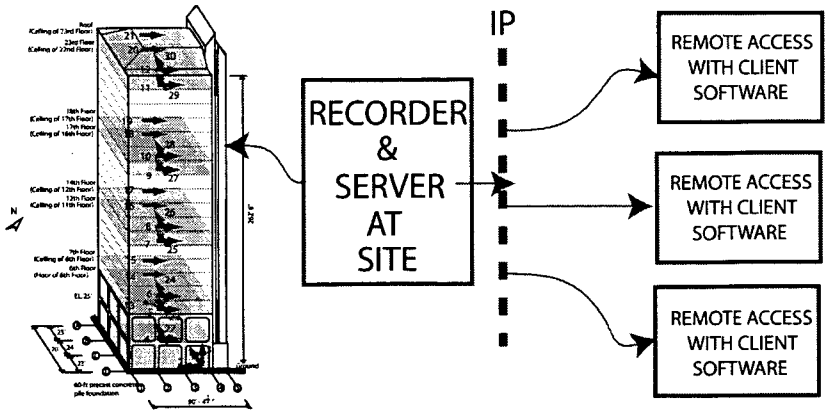


Figure 3. General schematic of data acquisition and transmittal for seismic monitoring of the building.

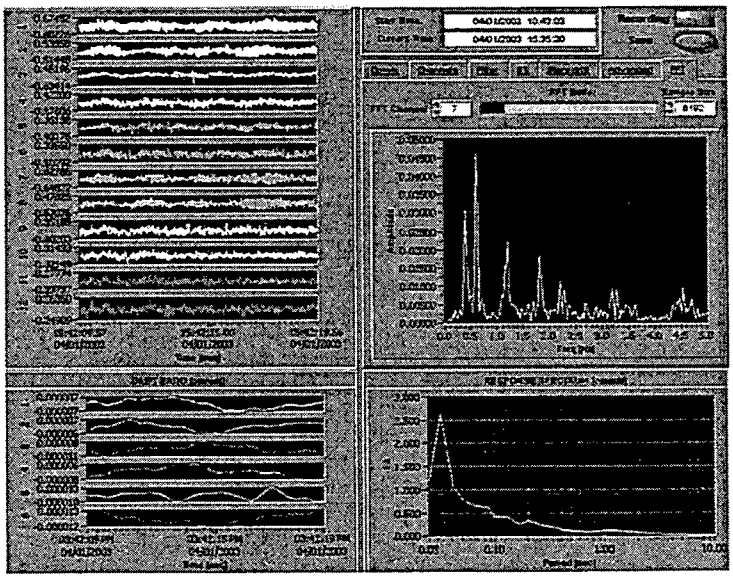


Figure 4. Screen snap-shot of client software display showing acceleration streams and computed amplitude and response spectra.

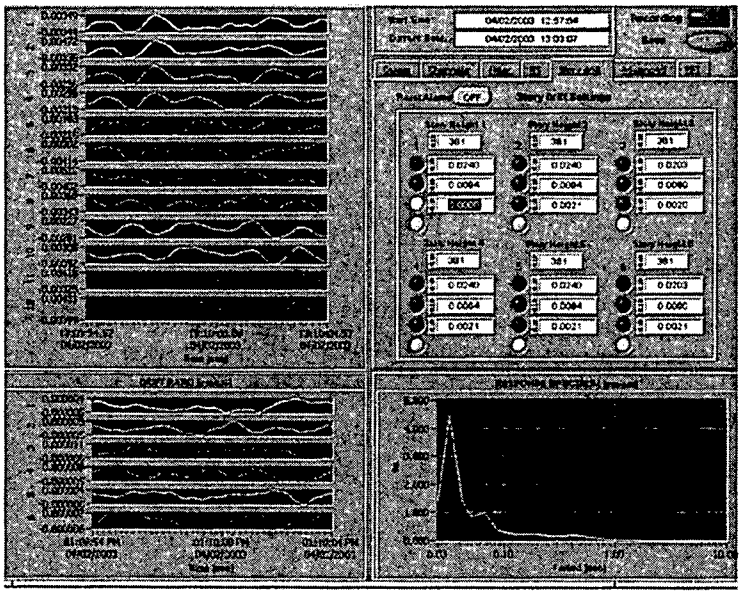


Figure 5. Screen snap-shot of client software display showing 12-channel (6 pairs with each pair a different color) displacement and corresponding 6-drift ratio (each corresponding to the same color displacement) streams. Also shown to the upper right are alarm systems corresponding to thresholds that must be manually input. The first threshold for the first drift ratio is hypothetically exceeded to indicate the starting of the recording and change in the color of the alarm from green to yellow.

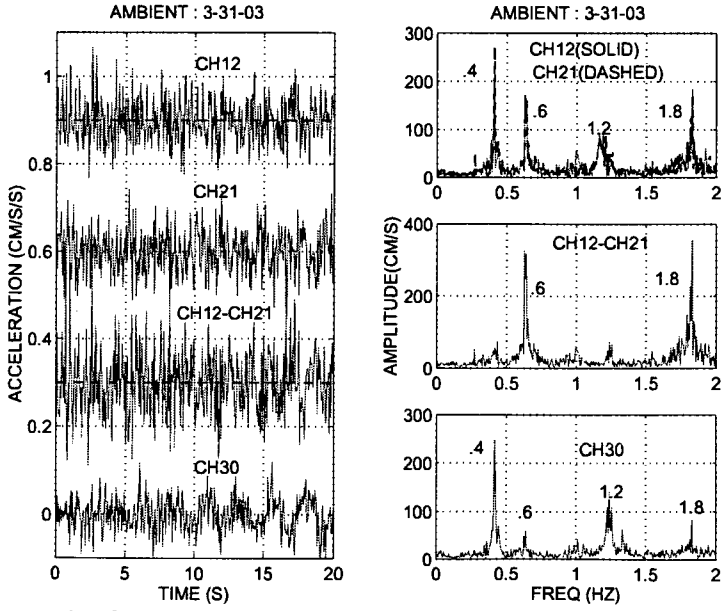


Figure 6. Twenty seconds of ambient acceleration response data obtained at the roof from parallel channels (CH12 & CH21), their difference (CH12-CH21), and from CH30, orthogonal to CH12 and CH21 (left) and corresponding amplitude spectra (right).

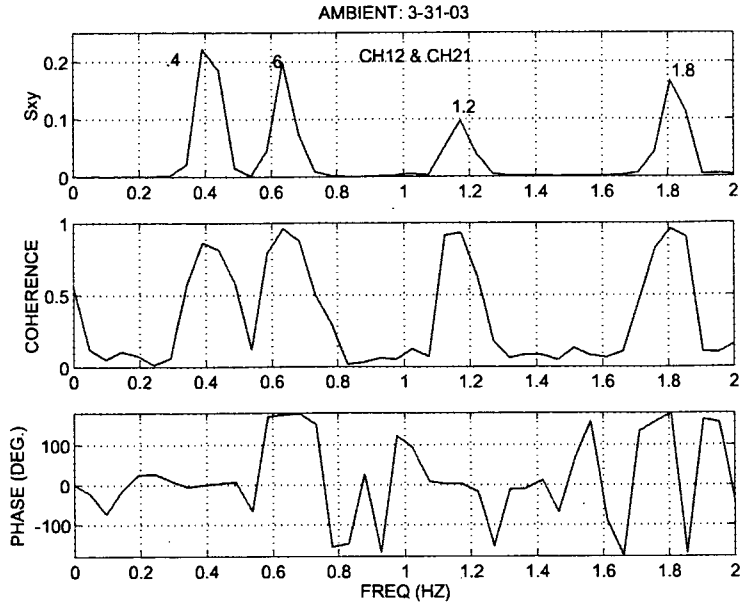


Figure 7. Cross-spectrum, coherency, and phase angle plots of ambient acceleration response data obtained from parallel channels (CH12 and CH21) at the roof.

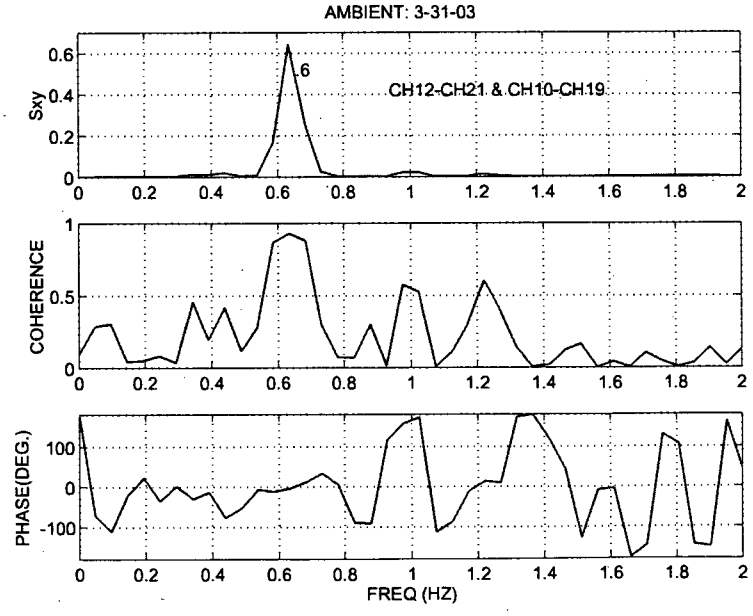


Figure 8. Cross-spectrum, coherency, and phase angle plots of ambient acceleration response data obtained from differences of parallel channels, CH12 - CH21 at the roof and CH10-CH19 at the 18th floor.

Study of Full-Scale / Big-Scale Experiment
(Report of theUS-Japan Symposium on the Seismic Performance of Urban, Reclaimed and Port Areas - Full-Scale Experiment at Tokachi Port -)

by

Takahiro Sugano[1] and Eiji Kohama[2]

ABSTRACT

The US-Japan Symposium on the Seismic Performance of Urban, Reclaimed and Port Areas –Full-Scale Experiment at Tokachi Port- was held under the sponsorship of the University of California, San Diego (UCSD), the Pacific Earthquake Engineering Research Center (PEER) and the Port and Airport Research Institute cooperated with the UJNR Task Committee A (Geotechnical Engineering and Ground Motion) at UCSD on February 27-28, 2003.

In past earthquakes, liquefaction-induced lateral spreading caused damages to under ground structures such as foundations, which in lead to the damages of superstructures that they were supporting. This includes the damages in port facilities, buildings, bridges, and lifelines.

Most of liquefaction and lateral spreading researches have focused on laboratory tests, centrifuge studies, 1G shake table tests, and case histories.

For the numerical simulation of liquefaction and lateral spreading phenomena, stress-strain relationships including excess pore water pressure generation and soil-structure interactions have to be considered.

These approaches mentioned above, however, cannot account for global translations of the liquefaction/lateral spreading soil-structure interaction. In light of this, full-scale/big-scale instrumented experiments are required.

KEYWORDS: liquefaction; lateral spread; earthquake; full-scale experiment.

1. SITUATION

As shown in Fig.1,

a) Actual damage investigation
b) Full/Big-scale experiments
c) Model tests, and
d) Numerical simulations

are connected by 'complement' or/and 'verification'.

1.1 Actual damage investigation

The data we can obtain are as following;

1) Before an earthquake, design documents, sounding data, boring log, etc.
2) During an earthquake, fortunately strong motion records
3) After an earthquake, damage investigation data, etc.

The lack of data during an earthquake is serious.

1.2 Model tests

In order to study the soil-structures interactions, serious problem is 'similitude' relationships between a model and a prototype, even in the case of centrifuge tests. Then, how do we evaluate the accuracy of the model test results? However, model tests have an advantage in obtaining 'dynamic behavior data' during an earthquake.

The disadvantages are it is rather expensive and takes relatively long time to conduct.

1.3 Numerical simulations.

Generally, a constitutive law is based on laboratory soil test data, such as a triaxial compression test, and hollow cylindrical shear test. Problems of finite element modeling in 1D-2D-3D and arrangements of input parameters exist. How do we evaluate the accuracy of the numerical simulations? However, we can obtain useful information such as element stress condition including excess pore water pressure time history. The disadvantages are, it cost rather expensive and it needs skilled operator.

[1] Head, Structural Dynamics Division, Port and Airport Research Institute, Yokosuka, Japan
[2] Researcher, Structural Dynamics Division, Port and Airport Research Institute, Yokosuka, Japan

1.4 Full/Big-scale experiments

To improve the model test techniques, similitude law, the numerical analysis technique and the accuracy, a full/big-scale instrumented experiments are needed. A Full/Big-scale experiment is often difficult to conduct, because it is extraordinary expensive and takes long time.

2. RECENT TREND

2.1 E-defense (Table 1)

The National Research Institute for Earth Science and Disaster Prevention (NIED) has been constructing the 3-D Full Scale Earthquake Testing Facilities.
(http://www.bosai.go.jp/sougou/sanjigen/3De/index.htm)

2.2 Outdoor shake table (Table 1)

The UCSD has been constructing the Large High Performance (LHP) Outdoor Shake Table.
(http://www.nees.org/EQ/sites/p2_ucsd.html)

2.3 Actual quay wall observatory

Hokkaido regional Development Bureau constructed –5.5m design depth caisson type quay walls with about 180ch of instruments such as seismograph, pore water pressure gauges, accelerometers, velocity sensors, and large earth pressure gauges (1m by 1m), etc. in Kushiro Port. The five years observation project started on April 1, 2002.

2.4 Full-scale experiment using controlled blast

In order to assess the seismic performance of structures, the US-JAPAN joint research project of 'Seismic performance of Urban, Reclaimed and Port Areas, -Full-scale Experiment at Tokachi Port- was conducted by 14 organizations.

3. COMMENTS

In case of a joint research of full/big-scale experiment, it is necessary to consider following matters,

1) Contract of joint research,
2) Fiscal year,
3) Budget handling,
4) Insurance,
5) In advance conference between researchers and construction workers,
6) Safety control of construction work and instrumentation work,
7) Synchronize data acquisitions,
8) Data handling, i.e. protocol and format, and
9) Publication.

Table 1 Specification of Shake Table

	NIED		UCSD
Payload	12MN		20MN
Size	20m*15m		7.6m*12.2m
Shaking Direction	Horizontal	Vertical	Horizontal
Maximum Velocity	200cm/s	70cm/s	180cm/s
Maximum Displacement	+-100cm	+-50cm	+-75cm
Maximum Allowable Moment	150MN-m	40MN-m	50MN-m

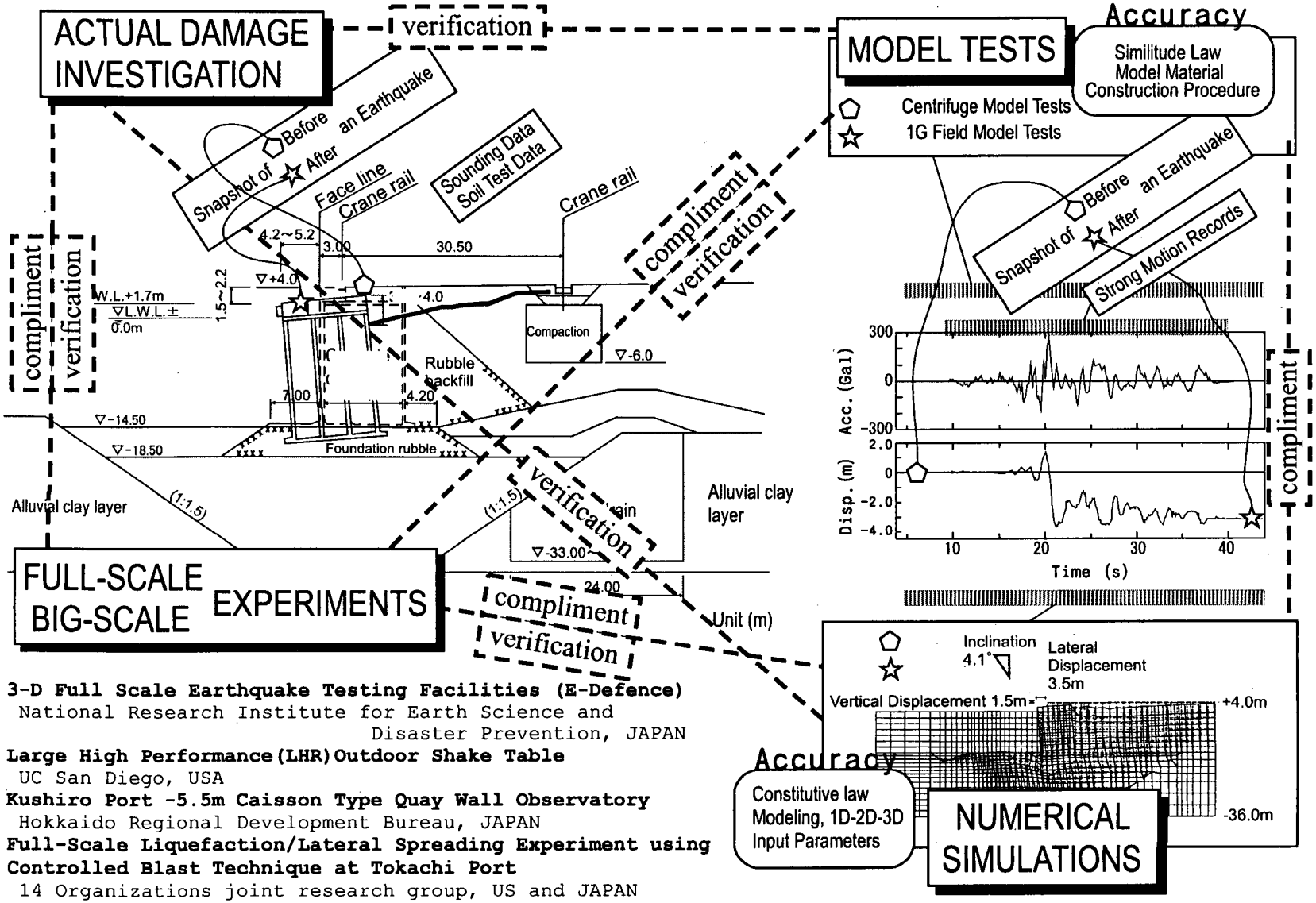


Fig.1 Situation of Full/Big-scale Experiments

3-D Full Scale Earthquake Testing Facilities (E-Defence)
National Research Institute for Earth Science and Disaster Prevention, JAPAN

Large High Performance(LHR)Outdoor Shake Table
UC San Diego, USA

Kushiro Port -5.5m Caisson Type Quay Wall Observatory
Hokkaido Regional Development Bureau, JAPAN

Full-Scale Liquefaction/Lateral Spreading Experiment using Controlled Blast Technique at Tokachi Port
14 Organizations joint research group, US and JAPAN

Seismic Response of Earth Dams on Liquefiable Foundations and Compaction Remediation

by

Michael K. Sharp, Ph.D., P.E.[1] and Korhan Adalier, Ph.D.[2]

ABSTRACT

Earthquake induced liquefaction is a major concern for earth dam safety in seismically active regions of the world. Many liquefaction induced embankment failures or near-failures have been reported around the world during various earthquakes. Such embankment damages were particularly destructive when the underlying saturated granular soils liquefied.

Through a series of twelve separate geotechnical centrifuge modeling tests, seismic behavior of a zoned earth dam with saturated sandy soil foundation was studied under moderate earthquake conditions. Soil response during and after shaking was monitored by many miniature accelerometers, pore pressure transducers, and displacement gauges placed throughout the soil model. The effect on the seismic behavior of the dam of different parameters such as the thickness, location, and depth of liquefiable layer is studied. This paper describes some of these tests and briefly presents the preliminary results. Valuable insights into the dynamic behavior of the employed embankment-foundation systems are provided. Currently, such testing results offer a valuable alternative to actual full-scale dynamic response, which is virtually non-existent.

KEYWORDS: Compaction; dams; liquefaction; remediation; seismic response

1. INTRODUCTION

The U.S. Army Corps of Engineers (COE) has responsibility for over 600 dams with a large number, over 1/3, being embankment dams with most of these lying in highly seismic areas of the country. The vast majority was constructed in the 1940's and 1950's when earthquake engineering was in its infancy and seismic hazards were neither recognized nor understood, leaving some inadequate for a seismic event. It is estimated that there are many other such seismically inadequate embankment dams around U.S. under the responsibility of federal, state and local governments, as well as the private sector.

Some of these embankments are founded on liquefiable soils, in many cases, necessitate-ing the development of appropriate remediation countermeasures (Marcuson et al. 1996). However, it is not feasible to remediate all of these structures due to the considerable cost involved. A determination of how much damage such structures could tolerate and still be able to perform their primary function could alleviate the need to remediate many dams. In cases that require remediation, understanding the deformations and dynamic response mechanisms of such dam/foundation systems would enhance our ability to design remedial procedures in a more effective and economical way. The potential for economic savings through better understanding of the involved mechanisms can be enormous considering the high cost of remedial treatment and the volume of dams that may require treatments in the coming years. Foundation remedial projects of Sardis Dam in Northern

Mississippi and Mormon Island Dam north of Sacramento, California both owned by the COE are only two recent cases, each of them costing over $30 million. Casitas Dam, Ventura-California owned by U.S. Bureau of Reclamation is another earth dam that is currently receiving a remedial treatment

[1]Director, Centrifuge Research Center, Engineer Research and Development Center, Vicksburg, MS 39180.
[2] Visiting Assistant Professor, Dept. of Civil and Env. Eng., Rensselaer Polytechnic Institute, Troy, NY 12180.

against foundation liquefaction with a cost of over $20 million. A similar $15 million upgrade is under way at the Bureaus' Bradbury Dam in the Santa Barbara-California area. Many other dams are currently under evaluation for liquefaction-induced hazards mainly by several federal and state governmental agencies.

It has been shown that the centrifuge dynamic model testing technique can play a major role in understanding the dynamic behavior of various earth structure-soil systems including earth dams (Arulanandan and Scott 1993; Adalier et al. 1998). Centrifuge testing is the most practical, most economical, and the only method for properly investigating and verifying earthquake induced equivalent-prototype behavior in soil, which behaves non-linearly and is stress-state dependent. Moreover, this centrifuge experimental model response also provides a basis for calibration of design and computational modeling procedures currently being performed by the ERDC.

In a series of 12 separate highly instrumented centrifuge model tests, seismic behavior of a zoned earth dam with saturated sandy soil foundation (Fig. 1) was studied under moderate earthquake conditions. The effect on the seismic behavior of the dam of different parameters such as the thickness, width, and depth of liquefiable layer is studied. This paper describes some of these tests and briefly presents the preliminary results. Valuable insights into the dynamic behavior of the employed embankment-foundation systems are provided. In addition to the pore pressure, acceleration, and model surface displacement measurements that are commonly done in most centrifuge tests, very detailed and extensive deformation mapping was performed based on pre- and post-shake meshes of markers throughout the body of the models. Such earthquake-induced deformations and damage is the key to making well-informed seismic safety and remediation decisions for embankment dams. Practice has demonstrated that remediation measures based on displacement criteria are much more cost-effective than those based on the factor of safety approach (Finn 2000). This study is believed to significantly expand and enhance our earthquake case history database regarding the earth dam on liquefiable foundation problem with more completely known and defined conditions and earthquake responses. Such an earthquake response database will provide: (1) a basis for modification and improvement of current methodology and assumptions, (2) realistic data for validation and improvement of numerical procedures (a current ongoing research), and (3) definitions of the physical processes and mechanisms involved in the liquefaction process and resultant effects on soil-embankment behavior.

2. CENTRIFUGE MODELING EQUIPMENT

The tests were done using the RPI's 100g-ton geotechnical centrifuge. It has an in-flight radius of 3.0 m and can test a payload up to 1 ton at 100g or 0.5 ton at 200g (i.e., 100 g-ton). More details about this centrifuge can be found on the WEB at http://www.rpi.edu/~dobryr/centrifuge/.

The main principle in centrifuge modeling is that a 1/N scale model subject to a gravitational acceleration of Ng (g is acceleration of gravity) will feel the same stress as the prototype. Then, stress-strain relationships at all equivalent points in the model and prototype will be the same if the same soil is employed and the behavior of the model will mimic the behavior of the prototype. Consequently, with the help of scaling laws (Schofield 1981) measurements in centrifuge tests under closely controlled conditions can be related directly to an equivalent full-scale prototype. The centrifuge modeling technique allows soil liquefaction tests to be performed at a conveniently reduced scale, and provides data applicable to full-scale problems.

In all tests, an in-flight shaker was employed to impart the model base shaking. Designed and built at Rensselaer, the centrifuge shaker is an electro-hydraulic, servo-controlled device with dual actuators (Laak et al. 1998). Total maximum force capability of the simulator is 80 kN. Input motion is imparted (in-flight) in a direction parallel to the centrifuge axis of the RPI shaker.

Special miniature accelerometers, pore pressure transducers, and displacement gages were used as sensors. A PC-based data acquisition system was used to register the data coming from the sensors. During flight, three closed-circuit television cameras monitor the centrifuge, the soil model plan, and the soil model side through a window in the model container's wall. A rigid model container with inner dimensions of 0.88 (l) x 0.37 (w) x 0.36 (h) meters was used. A transparent side window allowed for observation of the side of the model. More detailed information about the geotechnical centrifuge modeling instrumentation used in RPI is given by Adalier (1996).

3. MODEL CONSTRUCTION AND TESTING PROCEDURE

Nevada-120 sand was used in all tests. This is a fine (d_{50} = 0.15mm), uniform, sub-round, clean sand. Extensive data about the monotonic and cyclic response characteristics of this soil has been documented by Arulmoli et al. (1992) and available on the WEB at http://geoinfo.usc.edu/gees/velacs/. The embankment core was made out of kaolin clay compacted at around 32% water content (2% to wet side of optimum). It had a dry unit weight of 13.8 kN/m^3 and unconfined shear strength (Su) of 18-20 kPa. Soil model was build by air pluviation (Adalier 1996). Pluviation was interrupted periodically to place instrumentation. Thin bands of colored Nevada sand were placed at the interface of each horizontal foundation layer. Thin spaghetti sticks were then inserted vertically (driven in a steel tube casing), at predetermined positions. When softened by the pore fluid these sticks acted as inclinometers and made it possible to measure the internal deformations during model dissection. The models were saturated under vacuum. Metulose solution of 50 times water viscosity was used as the foundation soil pore fluid. Considering the fact that the tests were conducted at a 100g gravitational acceleration field, and in view of the scaling laws applicable to centrifuge experiments, about a two times more permeable foundation sand (relative to 1-g water permeability) was simulated (still a fine sand permeability). Embankment shells and reservoir fluid was water rather than a viscous fluid to simulate a coarser embankment material (as mainly found in field cases).

The tests were conducted in a 100g gravitational field. The centrifuge was brought to 100g very gradually so as to allow pore pressures to buildup almost statically without causing any potential instability problems. Self-weight compression of the model was monitored in each test and found to be insignificant compared to those dynamically-induced during the subsequent shaking events. All models were subjected to the same sinusoidal base horizontal acceleration of 30-cycles, 0.2g magnitude, and 1.5 Hz dominant frequency (prototype).

After the test was complete, the specimen was dissected carefully, digital photographs were taken, and a detailed visual observation was conducted of the deformation of each model. The profiles of the models at dissected sections were mapped very carefully (transformed on a thin plexiglass plate) and then digitized into computer graphics. By this method, very detailed pre- and post-test mid-section profile meshes of each model was obtained.

4. TESTING PROGRAM

A total of 12 dynamic tests were performed on 12 different soil models. At a 100g gravitational acceleration field, the models

depicted in Fig. 1 (a setup of a typical model) simulated a prototype earth dam of 10 m in height, 39.5 m in width, sitting on 9 m thick fine sand foundation deposit. Table 1 gives the summary of the conducted centrifuge tests. As seen in Table 1, mainly the effects of liquefiable layer I) thickness, ii) depth, and iii) location on the dynamic performance of the dam-foundation system were studied. In Series IV, the effects of longer earthquake shaking (40 cycles) and of a clay interlayer at 2.5-3.5 m depth on both downstream and upstream sides of the dam was evaluated. Full sets of horizontal accelerations, pore pressures, and deformations at different locations throughout the foundation-dam model were obtained for further analysis and interpretation. Additionally, these data are being studied numerically and used as a database for calibration and verification of several different FE codes or numerical schemes. Due to space limitation, only selected response records of Series I tests will be presented in the following sections and preliminary results will be briefly discussed. All of the test results are presented and discussed in prototype units, unless otherwise stated.

5. SERIES-I TESTS RESULTS - EFFECT OF LIQUEFIABLE LAYER THICKNESS

5.1 Model 1: LLL-LLL: Entire Foundation at $D_r = 35\%$

Figure 2 depicts model response at selected transducer locations and post-test deformed shape of the model mid-cross-section (after dissection). The simulated earthquake caused very large deformations both in embankment and in the foundation. A huge embankment crest settlement of 2.4 m was measured. Most of this settlement took place uniformly during the course of the base excitation. Both sides of the embankment slumped and moved laterally away from the centerline on the excess pore pressure (EPP) softened foundation. The migration of underlying foundation soil towards the free field was largely responsible for the observed embankment slump. Movements as large as 4 m were observed near the toe areas. In general, the deformations on the downstream side were somewhat bigger than those of upstream side. This is mainly attributed to the higher initial static shear stresses in the downstream foundation. The lateral deformation in the foundation soil was found to attain its maximum near ground surface, and to decrease with depth. This deformation may be associated with an average accumulated normal lateral tensile strain of about 20% along the embankment base. Indeed, this tensile strain was clearly manifested in the form of stretching and slumping of the embankment body.

At the upstream toe-foundation, the acceleration response gradually decreased within 3-4 cycles of base excitation, reflecting the associated loss of soil stiffness and strength due to induced high EPP. However, after a few initial cycles, a very peculiar behavior of large asymmetric acceleration spikes started to appear. This asymmetric spiky acceleration response is associated with cyclic-mobility down-slope shear deformations (Elgamal et al. 1996). Notice that the direction of these spikes are in opposite directions in upstream (a3) and downstream (a10) sides, as the lateral movement, and the initial static lateral shear stresses, are actually in opposite directions. It is noteworthy that the core/crest accelerations were significantly attenuated relative to the base input. As will be discussed later, the crest motions were largely affected by the embankment and foundation sandy soil state of strength during shaking event.
At P3 and P12, the soil built up EPP corresponding to initial liquefaction. The buildup at the upstream side was somewhat faster. Due to very large shear strains induced in the foundation and associated dilation effect the foundation EPP (P6) did not reach initial liquefaction values. The estimated excess pore pressure ratio at P6 is around 0.7.

5.2 Model 2: LLD-LLD: Top 3m Densified Foundation

In this model the top 3 m of the entire foundation layer was densified to D_r= 70%. In practice, various ground treatment strategies can be used to mitigate the liquefaction hazards. The most common improvement techniques have been densification, soil replacement, and cementation. Among these, compaction or densification has been the most popular method for embankment foundation remediation projects. This model may be considered simulating a case where top 3 m of the foundation soil densified as a countermeasure or this kind of layering exist in nature.

Figure 3 depicts model response at selected transducer locations and the post-test deformed shape. Both the embankment and the foundation deformations were much reduced when compared with the previous model. Embankment crest settlement was 1.3 m (i.e., about half of that of Model 1). The pattern of deformations was considerably different than that observed in the first model, as the maximum shear deformations were shifted downwards to the 6-m loose layer. From the deformed mesh one may infer that the 3-m top dense soil plus the embankment basically translated sideways (without internally going into significant shear deformations) on the EPP softened 6-m loose underlying layer. As in the first model, the deformations on the downstream side were slightly bigger than those of upstream side. The average accumulated normal lateral tensile strain along the embankment base was about 6.5% (compared to 20% in the Model 1). The accelerations at foundation mid-depth (a3 and a10) were both somewhat attenuated relative to base input. Also the asymmetric spiky response phenomenon was much less significant (compared to Model 1) as the lateral deformations were reduced. Clay core crest accelerations, although attenuated relative to base input, were higher than those of Model 1. This is attributed to overall stiffer and stronger foundation material surrounding the core. Both P3 and P12 at the mid-depth (in loose layer) measured EPP corresponding to initial liquefaction. P6 under the embankment also measured EPP values corresponding to initial liquefaction. Contrary to the Model 1 case, reduced overall lateral spreading and dilation effects helped the foundation soil to build up higher EPP.

5.3 Model 3: LDD-LDD: Top 6m Densified Foundation

In this model the top 6 m of the entire foundation layer was densified to D_r= 70%. Figure 4 depicts the Model 3 response at selected transducer locations and post-test deformed shape of the model cross-section. As seen, embankment crest settlement was a little less than the one measured in Model 2 at about 0.8 m. Likewise the embankment and foundation internal deformations were further reduced by the increase in densified layer thickness from 3 to 6 meters. The maximum shear deformations were observed in the base 3-m loose layer. As in the previous two cases, the downstream deformations were somewhat larger. The average accumulated normal lateral tensile strain along the embankment base was about 4.5% (compared to 20% in Model 1).

The acceleration response of a3 and a10 were significantly stronger than those observed in Model 1 and 2, as these transducers were in dense soil. Asymmetric acceleration behavior was less significant. Clay core crest accelerations were significantly larger than the ones measured during Model 1 and 2 tests. Despite the fact that P3 and P12 were located in the dense zone, they measured EPP corresponding to initial liquefaction. Their position being close to the underlying loose layer probably helped the EPP buildup at these zones.

5.4 Model 4: DDD-DDD: All Foundation Densified

In this model, the entire foundation layer had a D_r= 70%. It is noted that, in this case,

a calibration error resulted in an increase of about 20% in the peak input shaking accelerations. Yet, the embankment and foundation deformations were reduced drastically (Fig. 5). The pattern of internal deformations were somewhat different than those observed in Model 2 and 3 tests, as they were more uniformly distributed through the model height in this case. The crest settled about 0.8 m uniformly during shaking. The average accumulated normal lateral tensile strain along the embankment base was about 4.0%. The foundation deformations were largely lateral with essentially negligible vertical component, as the dense soil did not contract under cyclic shear.

The EPP buildup was overall somewhat slower; however the dissipations were faster (related to the smaller bulk modulus of the dense material) than those observed in the other model tests. Despite the high EPP, due to dilative characteristics of the initially dense soil, stiff response prevailed throughout the foundation (as suggested by the strong accelera-tions). It should be noted that dense sand, even liquefied, does not deform excessively like loose sand due to its high residual shear strength and dilative behavior arresting large strain increments. Dilative acceleration spikes were apparent at records a3 and a10, helped by the higher base input motion and higher soil density. The relatively high overall foundation sandy soil stiffness increased the effective confinement effect on the clay core resulting in relatively strong core-crest accelerations. It is interesting to note that, the densified foundation greatly reduced the earthquake induced deformations but at the same time increased the embankment accelerations (due to the ability of dense sand in transmitting shear stress through dilative behavior). In this respect, for the dams with sensitive appurtenant structures one may consider Model 3 countermeasure case as a viable option.

6. OVERALL RESPONSE

Figure 6 depicts the measured normalized (relative to Model 1) dam crest settlements, average dam base lateral tensile strains, maximum foundation settlements, and normalized (relative to base input motion) crest acceleration arias intensities for the four models. Densifications to all depths are all found to reduce the embankment and foundation deformations by a range of 50% to 90%. However, the gain in deformation parameters has diminished after 6 m deep densification. The biggest gain was achieved from 3 m densification. Deeper densifications (i.e., 6 and 9 m) further reduced the deformations however the improvement was at a diminishing rate. On the other hand, stiffer foundations (denser material) have resulted in stronger embankment accelerations. The variation of dam settlement and acceleration (for the cases that the crest accelerations may be important, e.g., dams with various superstructures or auxiliary systems) with densification depth (Fig. 6) suggest it may be necessary to optimize the treatment depth to reduce the dam settlement and lateral spread to an acceptable level while at the same time ensuring that the dam accelerations are tolerable.

7. SUMMARY AND CONCLUSIONS

Through a series of highly instrumented dynamic centrifuge tests the effects of loose foundation layer i) thickness, ii) location, and iii) depth on the dynamic behavior of a zoned earth dam with liquefiable foundations were investigated. Results of some of these tests were briefly presented herein. The study provided many valuable insights into the dynamic behavior of earth dams sitting on alluvial soils subjected to moderate earthquake shaking. Moreover, these test results are providing a very valuable database for the calibration and verification of several numerical analysis codes and procedures modeling the dynamic behavior of liquefiable foundation-earth dam systems.

Test results suggest that there may be an optimum depth of densification treatment beneath an earth dam beyond which the reduction of the earthquake-induced deformations is relatively minor. The tests results also indicate that relatively small and isolated zones (e.g., at depth) of loose material within a densified volume of soil may not impair the overall effectiveness of treatment and do not necessarily result in damaging displacements. This suggests that the remedial designs should be based on displacement criteria rather than on the factor of safety against liquefaction. The difficulty in such cases, however, is in determining the acceptable size and distribution of such zones. Further centrifuge modeling and/or calibrated numerical parametric studies in this respect will be very useful. As shown by this program, the results of such tests would be extremely effective in the development of verified design guidelines, as well as in calibration of computational procedures.

8. ACKNOWLEDGEMENTS

The authors would like to acknowledge the Corps of Engineers, Headquarters for their support of this research.

9. REFERENCES

1. Adalier, K. (1996). "Mitigation of Earthquake Induced Liquefaction Hazards," Ph.D. Thesis, Dep. of Civil Eng., Rensselaer Polytechnic Institute, Troy, NY, USA, 659 pp.
2. Adalier, K., Elgamal, A.W., and Martin, G.R. (1998). "Foundation Liquefaction Countermeasures for Earth Embankments," J. Geotech. Geoenv. Eng., 124(6), 500-517.
3. Arulanandan, K. and Scott, R.F., eds. (1993). "Verification of Numerical Procedures for the Analysis of Soil Liquefaction Problems," Conference Proceedings, Davis, CA, Balkema.
4. Arulmoli, K., Muraleetharan, K.K., Hossain, M.M., and Fruth, L.S. (1992). "Verification of Liquefaction Analysis by Centrifuge Studies Laboratory Testing Program Soil Data," Technical Report by The Earth Technology Corp., Irvine, California, March, 404 pp.
5. Elgamal, A.W., Zeghal, M., Taboada, V., Dobry, R. (1996). "Analysis of Site Liquefaction and Lateral Spreading Using Centrifuge Testing Records," Soils and Foundations, 36(2), 111-121.
6. Finn, W.D.L. (2000). "State-of-the-Art of Geotechnical Earthquake Engineering Practice," Soil Dynamics and Earthquake Engineering, 20, 1-15.
7. Marcuson, W.F., Hadala, P.F., and Ledbetter, R.H. (1996). "Seismic Rehabilitation of Earth Dams," Journal of Geotechnical Engineering, ASCE, 122(1), 7-20.
8. Laak, P.V., Adalier, K., Dobry, R., and Elgamal, A.W. (1998). "RPI's Large Centrifuge Shaker," Proc., Int. Conf. Centrifuge'98, Tokyo, Japan, 105-110.
9. Schofield, A.N. (1981). "Dynamic and Earthquake Geotechnical Centrifuge Modeling," Proc., Int. Conf. on Recent Advances in Geotech. Earthq. Eng. & Soil Dynamics, Rolla, Mo., Vol. 3, 1081-1100.

Table 1. Centrifuge testing program.

Centrifuge Test Series	Model Configuration 1DS-2DS-3DS—1US-2US-3US D: 70% D_r; L: 35% D_r
Series I- Effect of liquefiable layer ***thickness***	L-L-L—L-L-L L-L-D—L-L-D L-D-D—L-D-D D-D-D—D-D-D
Series II- Effect of liquefiable layer ***depth***	D-D-L—D-D-L D-L-D—D-L-D L-D-D—L-D-D
Series III- Effect of liquefiable layer ***location***	D-D-L—D-D-D D-L-D—D-D-D D-D-D—D-D-L D-D-D—D-L-D
Series IV- Clay Interlayer and Large Earthquake	L-L-Clay-D—L-L-Clay-D D-L-D—D-L-D

D_r: Relative Density; DS : Downstream; US: Upstream

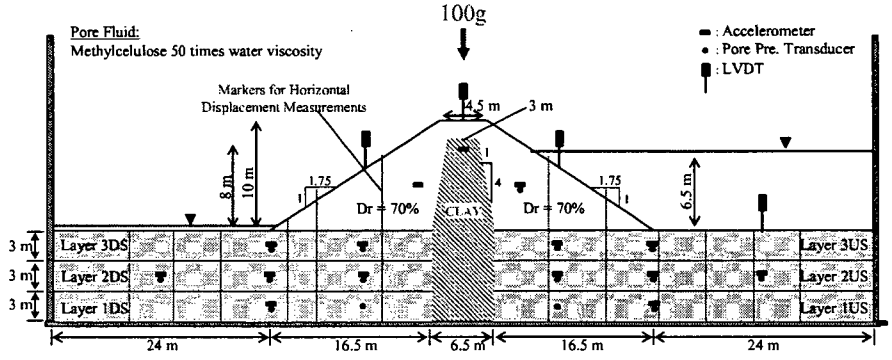


Fig.1 Schematic of a typical dam-foundation model.

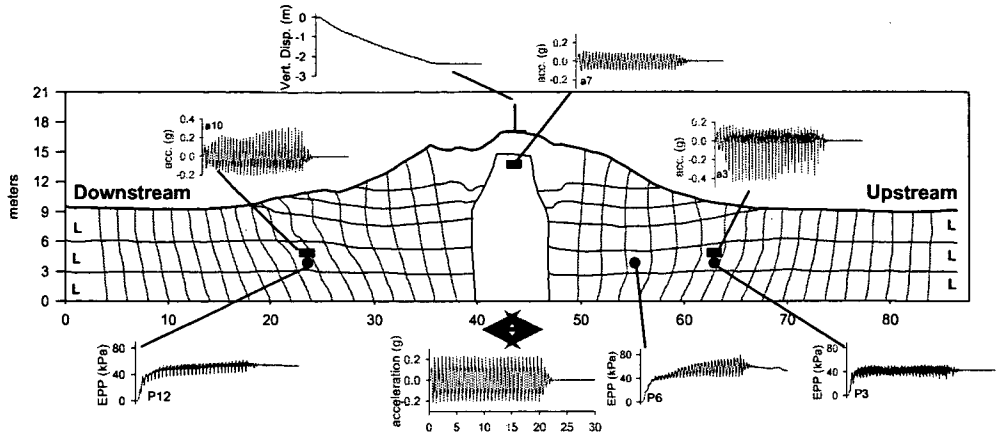


Figure 2. Model 1 selected transducer data and post-shake mid-cross-section.

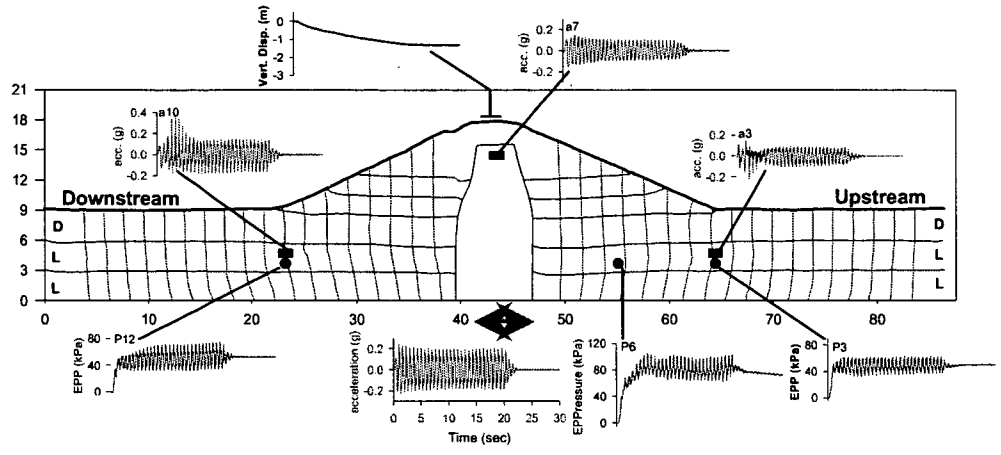


Figure 3. Model 2 selected transducer data and post-shake mid-cross-section.

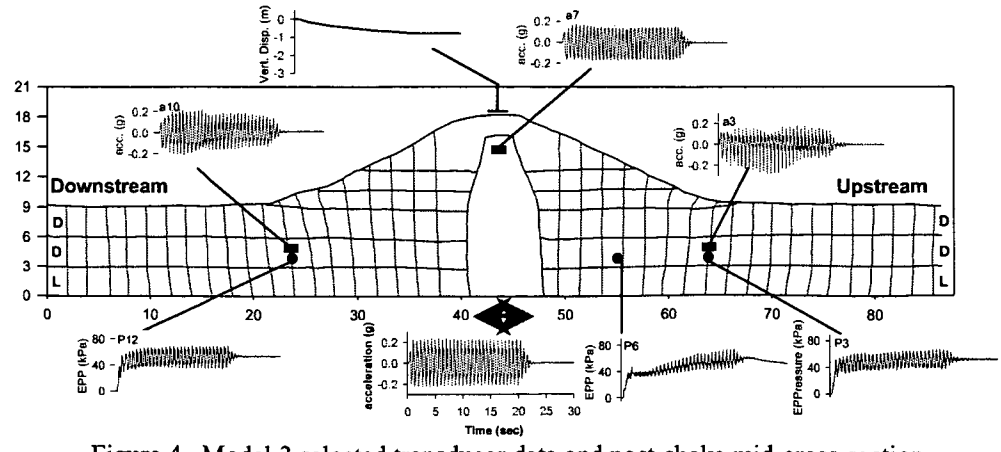


Figure 4. Model 3 selected transducer data and post-shake mid-cross-section.

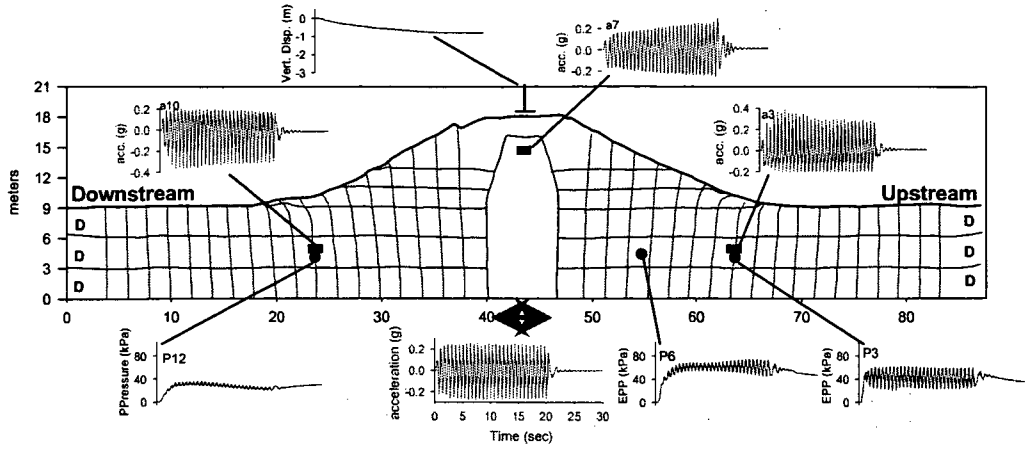


Figure 5. Model 4 selected transducer data and post-shake mid-cross-section.

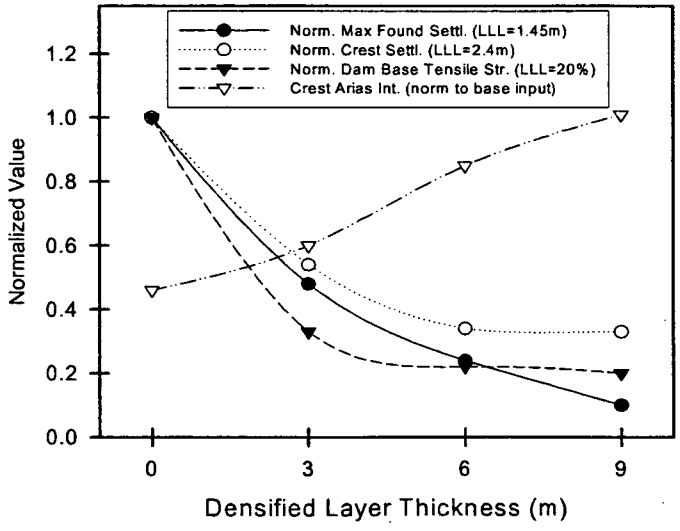


Figure 6. Some key dynamic performance parameters for the Models 1-4.

THEME 2

Dams

Current U.S. Army Corps of Engineers' Policy and Guidance for Seismic Design of Dams

by

Anjana Chudgar[1] and Enrique E. Matheu[2]

ABSTRACT

The seismic design of concrete hydraulic structures (concrete dams, locks, retaining walls, and other massive navigation or water control structures) constitutes a complex and time-consuming process that involves a variety of engineering disciplines. Procedures for seismic design or evaluation of these massive hydraulic structures need to account for the dynamic characteristics governing the response of the soil-structure-water system. Typically, this types of problems require a multidisciplinary team of structural, materials, geotechnical, and hydraulic engineers, engineering geologists, and seismologists to ensure the appropriate and successful completion of the design or evaluation process. This process, that typically requires extensive engineering judgment and experience, must be facilitated by a consistent framework of technical guidelines and recommendations. The purpose of this paper is to present a brief description of some of the most relevant guidance documents that provide the technical framework for seismic design or evaluation of dams under the responsibility of the U.S. Army Corps of Engineers.

KEYWORDS: Seismic Design and Evaluation; Embankment Dams; Concrete Dams; Gravity Dams; Intake Towers.

1. INTRODUCTION

The seismic design and evaluation of civil works projects under the responsibility of the U.S. Army Corps of Engineers (USACE) must be performed in accordance with the technical policy established in Engineer Regulation No. 1110-2-1806 (HQUSACE, 1995a). The purpose of this document is to provide general criteria for seismic design of new projects and seismic evaluation of existing projects. It applies to all projects which have the potential to malfunction or fail during major seismic events and cause hazardous conditions related to loss of human life, appreciable property damage, disruption of lifeline services, or unacceptable environmental consequences. According to this regulation, any seismic design and evaluation process should focus on assessing the ground motions, site characterization, structural response, functional consequences, and potential hazards within a consistent, well-integrated, and cost-effective framework. Furthermore, this regulation explicitly indicates that the overall analysis should be performed in various phases in order of increasing complexity, an approach that should provide higher degree of confidence in the resulting conclusions.

ER 1110-2-1806 also establishes the different ground motion levels to be considered in design and evaluation studies. The Maximum Design Earthquake (MDE) is defined as the maximum level of ground motion for which the structure is designed or analyzed. The structure should be able to withstand the MDE without catastrophic failure, although severe damage may be tolerated (i.e., the system may suffer serious damage but retain the project pool). The severity of the MDE selected for design or evaluation depends not only on the local seismic hazard but also on the "criticality" of the project. As established in ER 1110-2-1806, a critical project (or project feature) is that whose failure during or immediately after an earthquake could directly result in loss of life due to flooding. For design or analysis of projects deemed critical, the MDE must be set equal to the Maximum Credible Earthquake (MCE), which represents an estimation of the greatest earthquake that

[1] Headquarters, U.S. Army Corps of Engineers, Washington, DC 20314 (USA).
[2] Dept. of Civil and Environmental Engineering, Louisiana State University, Baton Rouge, LA 70803 (USA).

could be generated by a specific source. For other features (i.e., not linked to potential loss-of-life consequences), the MDE could be selected as a lesser earthquake than the MCE in order to provide a more economical design.

The MCE is determined by means of a deterministic seismic hazard analysis, and a common approach to define the corresponding earthquake loading at the site is based on the use of response spectral attenuation relationships. Using an attenuation relationship (appropriately selected for the corresponding site conditions and tectonic environment), it is possible to generate estimates of spectral ordinates based on the design earthquake magnitude and distance. These attenuation relationships are typically developed based on statistical regression analyses of relevant ground motion data, and the resulting spectral ordinates are associated to the corresponding parameters (mean value, variance, etc.) that define their statistical distribution. Therefore, the definition of the earthquake loading using this approach requires the selection of a specific spectral level (commonly defined as the mean spectrum, mean plus one standard deviation spectrum, etc). This constitutes an extremely important decision that significantly affects the design and evaluation of critical projects.

This document also addresses the sequence of analysis procedures to be followed during the design and evaluation process. In this regard, the recommendations provided in ER 1110-2-1806 are that the overall analysis should be performed in various phases in order of increasing complexity. This type of progressive analysis is summarized in Table 1, which shows that the recommended analysis progression is a function of the seismic hazard at the site and if the seismic response is controlling the design or evaluation.

2. EMBANKMENT DAMS

Technical guidelines for evaluating the seismic safety of existing embankment dams and foundations is provided in the USACE guidance document "Dam Safety Assurance Program," designated as Engineer Regulation 1110-2-1155 (HQUSACE, 1997). The stages of the evaluation process are designated as (1) Seismic Safety Review (SSR), (2) Phase I Special Study, (3) Phase II Special Study. The SSR is essentially a screening stage, using simple preliminary analysis with existing available data to determine whether seismic safety issues exist which require a Phase I Special Study. The Phase I study is to develop site specific ground motion, to perform site characterization with limited field investigations and laboratory studies, to evaluate liquefaction potential using 1-D analyses combined with simplified procedure for liquefaction evaluation, to assess post earthquake stability and post earthquake deformed shape. The Phase II study is detailed and sufficiently comprehensive such that the resulting conclusions should be definitive, and constitute the basis for detailed design and construction for project modifications or remediation. The Phase II study is to compute the site response using appropriate and validated dynamic finite element program with input ground motion time history developed in Phase I, to perform detailed field investigation and laboratory testing for defining the input parameters and the extent of potential problem zones, to perform post earthquake stability analysis, to estimate the deformation response of the embankment dam and the post earthquake shape using an appropriate 2-D and/or 3-D finite element program, to evaluate various remediation alternatives if remedial measures are recommended, and to develop detailed scope, cost, and schedule for pre-construction engineering and design. More detailed numerical procedures and tools used for seismic analysis in geotechnical engineering will be contained in the upcoming guidance document "Seismic Stability Evaluation of Embankment Dams," (EM 1110-2-6001) which is currently being reviewed.

3. GRAVITY DAMS

Recommendations for seismic design and evaluation of concrete gravity dams are provided in the USACE guidance document entitled "Gravity Dam Design" and designated as

Engineer Manual 1110-2-2200 (HQUSACE, 1995b). The purpose of this manual is to provide general criteria and guidance for the planning, design or evaluation of both conventional concrete and roller compacted concrete dams. Concrete gravity sections within an embankment dam should also be designed in accordance with these guidelines. Some of the specific topics covered include design considerations (Chapter 2), determination of concrete and foundation material properties, and definition of load conditions (Chapter 3), stability requirements (Chapter 4), static and dynamic stress analysis (Chapter 5), temperature control of mass concrete (Chapter 6), structural design considerations (Chapter 7), re-evaluation of existing dams (Chapter 8), and roller-compacted gravity sections (Chapter 9).

As an example of the information provided in these guidelines, the performance criteria for stability analysis are shown in Table 2. This table includes the criteria to be used for stability evaluation of concrete gravity dams using the seismic coefficient method. This method provides a simple and direct approach for stability evaluations. Depending on the loading scenario, different limit conditions have been established for sliding factor of safety and resultant location. In particular, for the extreme loading condition (seismic loads corresponding to the MCE level), the minimum sliding factor of safety is 1.3 and the resultant is required to be within the base.

It must be highlighted, however, that these sliding stability criteria has been mainly developed for evaluation of structures subject to moderate seismic forces. The factor of safety against sliding required by these conservative criteria may not be practically attainable for larger seismic forces representative of severe earthquake ground motions. Furthermore, it is necessary to take into account that even if consideration of the seismic actions results in a factor of safety of less than one (indicating the potential for sliding), this condition would be implicitly transient. Due to the oscillatory nature of the earthquake, instantaneous sliding may occur only during very short intervals, thus limiting the resulting displacement. An update/revision of the values specified for the corresponding factors of safety is currently under consideration, as indicated in a later section.

4. ARCH DAMS

Comprehensive information on design and evaluation criteria for arch dams is available in Engineer Manual 1110-2-2201, entitled "Arch Dam Design" (HQUSACE, 1994). The purpose and scope of this document is stated in its first chapter, which also provides a set of standard technical definitions. General design recommendations with special consideration of abutment and foundation conditions are addressed in Chapter 2, whereas technical aspects related to spillways (both attached and detached configurations), outlet works (intake structures, conduits, control house) and appurtenances (elevator tower, access bridges, galleries) are discussed in Chapter 3. Load definitions, loading combinations are presented in Chapter 4, which also discusses the problem of selection of load cases for each phase of the design process. Chapter 5 focuses on some specific aspects related to the design problem (initial geometric design, preliminary stress analyses, design optimization). The application of finite-element procedures for static stress analysis as well as recommendations for interpretation of the corresponding results are discussed in Chapter 6.

Details pertaining to dynamic stress analysis are presented in detail in Chapter 7. This chapter also discusses some of the modeling factors affecting the results from the dynamic response analysis. In particular, it is recommended that the analysis should be based on a 3-D idealization of the dam-water-foundation system which accounts for the interaction effects of the foundation rock and the impounded water. Arch dams are designed to resist most of the applied loads by transmitting them through arch action to the canyon walls. Consequently, the effects of foundation rock on the earthquake response of arch dams are expected to be significant. However, it is highlighted the fact that a

complete solution of the dam foundation interaction effects is very complicated and such procedures have not yet reach a development stage conducive to their wide application.
Issues related to temperature effects and determination of material properties are addressed in Chapters 8 and 9 of this document, respectively. The important topic of foundation investigations is discussed in Chapter 10. 10-1. Introduction. Foundation investigations for arch dams generally must be accomplished in more exacting detail than for other dam types because of the critical relationship of the dam to its foundation and to its abutments. The foundation investigation effort should be accomplished in phases with each leading to the succeeding one and building upon the previous one, and it is very important that the latest state-of-the-art techniques in geological and rock mechanics are employed in these investigations. Criteria for static and dynamic performance evaluation are proposed in Chapter 11. The final sections of the document (Chapters 12 and 13) address instrumentation and construction considerations.

5. OUTLET WORKS

Comprehensive information of design and evaluation for intake tower is available in Engineering Manual 1110-2-2400, entitled "Structural Design and Evaluation of Outlet Works" (HQUSACE, 2003a). The purpose and scope of the document is stated in its first chapter. Seismic criteria for design and evaluation are addressed in Chapter 4. The objectives of design and evaluation, structural stability analysis, seismic design and evaluation of intake towers and access bridges are included in this chapter. Also this chapter provides guidance on an alternative displacement-based analysis procedure for evaluation of existing rectangular and circular towers. Information on seismic analysis for preliminary design or screening evaluation of free standing intake tower are also provided in this document. The application of a two-mode approximate procedure is recommended to account for the dynamic characteristics of the tower structure. Additional guidance is provided to determine hydrodynamic added masses reflecting the influence of the water inside and outside the tower. This document also contains guidelines for investigating the rotational stability of intake towers.

6. RESPONSE-SPECTRUM ANALYSIS

Comprehensive technical guidelines regarding the application of response-spectrum procedures for seismic analysis of concrete hydraulic structures are presented in Engineer Manual 1110-2-6050, "Response Spectra and Seismic Analysis for Concrete Hydraulic Structures" (HQUSACE, 1999). This manual provides guidance regarding how earthquake ground motions are characterized as design response spectra and how they are then used in the process of seismic structural analysis and design. The manual is intended to be an introduction to the seismic analysis of concrete hydraulic structures. Chapter 1 provides an overview of the seismic assessment process for hydraulic structures and the responsibilities of the project team involved in the process, and also briefly summarizes the methodologies that are presented in Chapters 2 and 3. In Chapter 2, methodology for seismic analysis of hydraulic structures is discussed, including general concepts, design criteria, structural modeling, and analysis and interpretation of results. Chapter 3 describes methodology for developing the earthquake ground motion inputs for the seismic analysis of hydraulic structures. Emphasis is on developing response spectra of ground motions, but less detailed guidance is also provided for developing acceleration time-histories.

7. TIME-HISTORY ANALYSIS

Recommendations for seismic evaluation using time-history procedures are provided in the USACE guidance document entitled "Time-History Dynamic Analysis of Concrete Hydraulic Structures" (HQUSACE, 2000). This document is the final stages of review and it is currently designated as Engineer Circular 1110-2-6051. These guidelines describe general procedures for the linear-elastic time-history dynamic analysis of concrete hydraulic

structures. These structures present distinctive response characteristics when compared to other civil engineering structures, and the evaluation of their dynamic response is usually complicated by structure-foundation and structure-water interaction phenomena. The first chapter of this manual provides an overview of the seismic performance evaluation process for concrete hydraulic structures. Chapter 2 discusses the general methodology for their time-history dynamic analysis, including a general description of structural types, modeling aspects, water and foundation-rock interaction, energy absorption effects, and the ground acceleration time-histories required for each structural type. Chapter 3 focuses on the computational aspects regarding the solution of the equations of motion in both time and frequency domains. A general methodology for performance evaluation and qualitative estimation of the probable level of seismically induced damage is presented in Chapter 4, whereas Chapter 5 describes the procedures for development of earthquake input acceleration time-histories. The final chapter provides practical examples of time-history evaluation for major concrete hydraulic structures including a gravity dam, a concrete arch dam, an inclined intake tower, and a W-frame lock structure.

A main objective behind these guidelines was the development of a systematic methodology for seismic performance evaluation and qualitative damage estimation using the results from linear time-history analyses. A systematic interpretation of linear time-history results is presented in terms of local and global performance indices: demand-capacity ratio, cumulative inelastic duration, and spatial extent of overstressed regions. Several empirical performance criteria are defined in terms of these indices and they form the basis for the qualitative estimation of the level of damage. If the predicted performance falls within the specified limits, the seismically induced damage is expected to be minor or negligible and the results of the linear time-history analysis will be sufficient to characterize the performance. Otherwise, the structural damage is expected to be severe, and the accurate estimation of its extent and consequences should be carried out using an appropriate nonlinear model. As an example, Figure 1 shows the performance curve for concrete gravity dams. The USACE guidelines therefore provide the analyst with standard criteria that, along with the proper engineering judgment, allow him/her to ascertain whether a nonlinear dynamic analysis is needed.

8. STABILITY EVALUATION

Starting in 1997, USACE began to revise and consolidate their guidance on stability criteria with the goal of establishing standard criteria for use in the design and evaluation of the many various types of concrete structures common to Corps of Engineers civil works projects. This will achieved by a new guidance document "Stability Analysis of Concrete Structures", currently under technical review (HQUSACE, 2003b). In this context, "stability" refers to external global stability (sliding, overturning, and bearing).

This manual will consolidate and verify the types and combination of applied loads and the corresponding safety factors that will govern stability requirements for all concrete hydraulic structures. The process used to standardize factors of safety will be based on the premise that the traditional factors of safety specified for USACE concrete hydraulic structures, for the most part, provide adequate protection against stability failure. However, the standardization process will recognize that lower factors of safety can be assigned to those loads and loading conditions designated as unusual, or extreme because the probabilities of those loads and load conditions occurring during the life of the structure are significantly less than the probabilities for usual loading conditions. In addition, this guidance will incorporate the practice of assigning lower factors of safety to normal structures, as compared to those traditionally used for critical structures. The goal will be to generate a consistent set of safety factors that will account for loading probability, criticality of the structure, and availability of site information

In particular, this guidance document will recognize that evaluation of sliding stability represents a difficult aspect of the analysis, especially in those instances where the foundation is jointed, and where the strength properties vary throughout the foundation. The approach to evaluating sliding stability is based on the limit equilibrium method with the linear Mohr-Coulomb failure criterion as a basis for estimating maximum available shear strength. Because of the uncertainties associated with shear strength determination, uplift and ground motions a combination of experience and judgment is always necessary to appropriately determine the corresponding strength, drainage and seismic parameters.

As mentioned before, the analyses should be a performed in phases in accordance with requirements of ER 1110-2-1806. The seismic coefficient method, although it fails to account for the true dynamic characteristics of the structure-water-soil system, is convenient as the initial empirical method for estimating structural stability, and is often used as a tool to decide if dynamic analyses should be undertaken. Structures that meet stability requirements when evaluated by the seismic coefficient method are considered safe and no additional seismic stability analyses are required. Structures that fail to meet stability requirements when evaluated using this empirical procedure should not be necessarily regarded as unsafe or in need of stability retrofit. The failure to meet these requirements should justify the need for other dynamic analyses to realistically assess the demands placed on the structure and foundation during a major earthquake. From these advanced analyses, engineers can determine if the displacements and stresses experienced by the structure and foundation will place the structure at risk of a stability failure. In many instances, it is acceptable for sliding and rocking to occur at the base of the structure during extreme earthquake load conditions. Stability in such cases should be evaluated using dynamic analysis methods, and performance is ensured by limiting permanent displacements to acceptable levels.

9. ASSOCIATED R&D EFFORTS

In spite of continual major advances, serious gaps in the current knowledge base still exist in the areas of earthquake hazard estimation; site characterization; constitutive behavior and determination of material parameters for dynamic loads; behavior and strength characteristics of lift joints and dam-foundation interfaces. Improved procedures are also need to accomplish the appropriate calibration of fast advancing numerical methods based on actual field performance. These technical gaps might result in costly conservatism and less effective design and evaluation procedures. In order to address some of these issues, the recent update of USACE technical guidelines has been supported by the products from a multi-disciplinary research program. This research effort has also served to develop the in-house expertise required by the continuous advances in the field of dam earthquake engineering.

The accomplishments of the research program included the development of improved analysis procedures for the seismic evaluation of existing lightly reinforced concrete intake towers. A displacement-based procedure was developed that takes into account the characteristics of the main failure mode associated with these structures. The research involved extensive experimental efforts in the form of cyclic loading and shake-table tests performed on reduced-scale models of a typical intake tower. Other research efforts focused on the quantification of the available ductility in typical reinforced concrete hydraulic structures designed according to USACE guidance. These efforts also included experimental studies on reduced-scale models of structures such as a tainter gate pier and a typical retaining wall. The research work also focused on the development of numerical tools for the analysis and design of cantilever retaining walls based on Newmark analysis procedures.

Additional research studies were performed to generate benchmark experimental data to be used in calibration of numerical models

predicting the seismic response of concrete gravity dams. These studies included a series of shake-table experiments conducted on a 1/20-scale model of the Koyna Dam that highlighted the non-linear characteristics of the observed response. The research program also addressed the important problem of the characterization of the energy absorption phenomena that occur at the bottom of the reservoir. These interaction phenomena have a significant effect on the predicted behavior of concrete dams. The research included collaboration and participation in several experimental efforts in the US and China.

10. CONCLUSIONS

Current USACE policy and guidance documents for seismic design and analysis of dams are less than ten years old and subject to periodic review and update. A significant number of comprehensive documents have been developed that provide the necessary framework for the technical work carried out at the different USACE districts and divisions. The available technical guidelines address the different types of dams and appurtenant structures under USACE responsibility. Ongoing research and development efforts performed at the USACE research facilities provide the necessary input for guidance development and update and stay abreast with the state-of-the art in seismic design.

11. ACKNOWLEDGEMENTS

Preparation of this paper was sponsored by Headquarters, U.S. Army Corps of Engineers. This support is greatly appreciated. The authors also gratefully acknowledge the support of the Geotechnical and Structures Laboratory of the U.S. Army Engineer Research and Development Center, where the second author is currently a guest researcher. Permission to publish this paper was granted by the Chief of Engineers, U.S. Army Corps of Engineers.

12. REFERENCES

Headquarters, U.S. Army Corps of Engineers (1995a). "Earthquake Design and Evaluation for Civil Works Projects," Engineer Regulation 1110-2-1806, Washington, DC.

Headquarters, U.S. Army Corps of Engineers (1997). "Dam Safety Assurance Program," Engineer Regulation 1110-2-1155, Washington, DC.

Headquarters, U.S. Army Corps of Engineers (1995b). "Gravity Dam Design," Engineer Manual 1110-2-2200, Washington, DC.

Headquarters, U.S. Army Corps of Engineers (1994). "Arch Dam Design," Engineer Manual 1110-2-2201, Washington, DC.

Headquarters, U.S. Army Corps of Engineers (2003a). " Structural Design and Evaluation of Outlet Works," Engineer Manual 1110-2-2400, Washington, DC.

Headquarters, U.S. Army Corps of Engineers (1999). "Response Spectra and Seismic Analysis for Concrete Hydraulic Structures," Engineer Manual 1110-2-6050, Washington, DC.

Headquarters, U.S. Army Corps of Engineers (2000). "Time-History Dynamic Analysis of Concrete Hydraulic Structures," Engineer Circular 1110-2-6051, Washington, DC.

Headquarters, U.S. Army Corps of Engineers (2003b). "Stability Analysis of Concrete Structures," Engineer Circular 1110-2-2100 (Draft) Washington, DC.

Table 1. Recommended analysis progression

Table E-1
Seismic Analysis Progression

Zone	Project Stage				
	Reconnaissance		Feasibility		DM[1]
0 and 1	E	→	SCM	→	RS[2]
2A and 2B	E	→	SCM	→	RS
	SCM[2]	→	RS[2]	→	TH[3]
3 and 4	SCM	→	RS	→	TH
	SCM	→	RS	→	RS[4]
	RS[2]	→	TH[3]	→	TH[3]

Note:
E = Experience of the structural design engineer
SCM = Seismic coefficient method of analysis.
RS = Response spectrum analysis.
TH = Time-history analysis.

[1] If the project proceeds directly from feasibility to plans and specifications stage, a seismic design memorandum will be required for all projects in zones 3 and 4, and projects for which a TH analysis is required.
[2] Seismic loading condition controls design of an unprecedented structure, or unusual configuration or adverse foundation conditions.
[3] Seismic loading controls the design requiring linear or nonlinear time-history analysis.
[4] RS may be used in seismic zones 3 and 4 for the feasibility and design memorandum phases of project development only if it can be demonstrated that phenomena sensitive to frequency content (such as soil-structure interaction and structure-reservoir interaction) can be adequately modeled in an RS.

Table 2. Stability and stress criteria for concrete gravity dams

Table 4-1
Stability and stress criteria

Load Condition	Resultant Location at Base	Minimum Sliding FS	Foundation Bearing Pressure	Concrete Stress	
				Compressive	Tensile
Usual	Middle 1/3	2.0	≤ allowable	$0.3\ f'_c$	0
Unusual	Middle 1/2	1.7	≤ allowable	$0.5\ f'_c$	$0.6\ f'^{2/3}_c$
Extreme	Within base	1.3	≤ 1.33 × allowable	$0.9\ f'_c$	$1.5\ f'^{2/3}_c$

Note: f'_c is 1-year unconfined compressive strength of concrete. The sliding factors of safety (*FS*) are based on a comprehensive field investigation and testing program. Concrete allowable stresses are for static loading conditions.

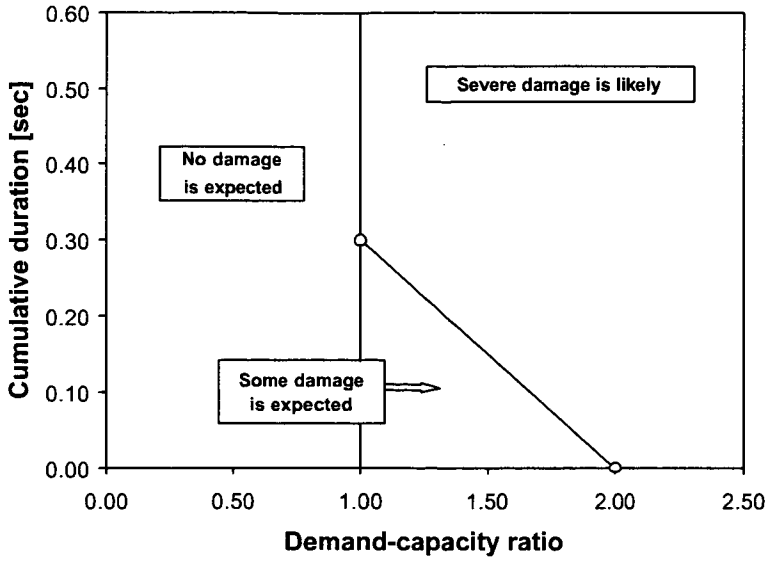


Figure 1. Performance curve for concrete gravity dams

Advanced Research Activities on Dynamic Analysis for Concrete Dams in Japan and an Study on Seismic Performance of Concrete Gravity Dams by Smeared Crack Model

by

Ken-ichi Kanenawa[1], Takashi Sasaki[2] and Yoshikazu Yamaguchi[3]

ABSTRACT

Several research activities about dynamic analysis to evaluate the seismic performances of dams have been conducted by the research institutes and agencies in Japan, and the effects of analytical conditions on the results by numerical analyses have been studied. The activities have speeded up since Hyogo-ken Nanbu Earthquake (the Kobe Earthquake). On the other hand, recent large earthquakes gave us the important acceleration data. Using these data, the efficiencies of developed numerical analysis methods have been verified.

In this report, we summary the recent research activities about dynamic analyses of concrete gravity dams in Japan, and introduce the examples of non-linear analysis results using the smeared crack model, one of advanced methods, by the PWRI.

KEYWORDS: Concrete Gravity Dam, Crack Development Analysis, Large Earthquake, Smeared Crack Model

1. INTRODUCTION

More than 2,600 dams with the height of 15m or higher have been constructed in Japan [1]. In Japan the earthquake-resistant design of dams is basically made by the seismic coefficient method [2] according to the Cabinet Order [3, 4], even though the more sophisticated methods can also be used. A lot of existing dams in Japan have experienced strong earthquake ground motions. However, no serious damage on these dams has been observed at large earthquake including the Kobe Earthquake [5]. The review of the earthquake-resistant design method, therefore, has not become an urgent issue. This situation is not similar to that for other public structures, e.g. bridges, levees. However, due to the recent rapid progress of computer's capabilities and numerical analysis techniques, it is possible to evaluate the dynamic performances of dams during an earthquake using the dynamic analysis method. Further, from a social viewpoint, accountability to general public about the safety of dams is quite important and necessary. Thus, to rationally evaluate the safety of dams during earthquakes is required by simulating dynamic behaviors of dams more realistically.

In this report, we introduce the recent research activities in Japan about the evaluation of dams with referring the report [6] prepared by the Subcommittee on Seismic Safety of Dams of the Technical Committee, Japan Commission on Large Dams, and present the results of non-linear dynamic analysis for concrete gravity dams using the smeared crack model by the PWRI.

2. ORIENTATION OF EVALUATION METHOD AND RESEACH ACTIVITIES ON DYNAMIC ANALYSIS

2.1 Proposal and Guideline for Seismic Design by the Japan Society of Civil Engineers

In view of the tremendous damage of public and private structures by the Kobe Earthquake, the Japan Society of Civil Engineer (JSCE) issued the Proposal on the earthquake-resistance design and criteria for civil engineering structures (the First Proposal) [7] in May 1995, the Second Proposal in January 1996 [8], and the Third Proposal in June 2000 [9]. The Subcommittee on Earthquake Resistant Design Standard of the

1) Researcher, Dam Structures Research Team, Hydraulic Engineering Research Group, Public Works Research Institute (PWRI), 1-6 Minamihara Tsukuba City, 305-8516, JAPAN
2) Senior Researcher, Dam Structures Research Team, Hydraulic Engineering Research Group, PWRI
3) Team Leader, Dam Structures Research Team, Hydraulic Engineering Research Group, PWRI

Earthquake Engineering Committee, the JSCE submitted a draft of Guideline for Earthquake-Resistant Design of Civil Engineering Structures [10] in 2001, based on these proposals.

The Guideline classified the strong ground motions to be used for structural design into the Level 1 earthquake motion and Level 2 earthquake motion as shown in Table 1. In addition, the lowest limit of the level 2 earthquake motions should be set as the earthquake ground motions caused by a magnitude 6.5 earthquake because of possibility of earthquakes by lurking faults.

The Guideline proposes the following 2 types of earthquake resistance performances from the viewpoint of the dam's basic function, that is, the water storage function.

Earthquake Resistance Performance I:
A concerned structure must not receive any structural damage.

Earthquake Resistance Performance II:
Even if a concerned structure is damaged structurally, the damage should be a repairable degree. A dam's water storage function must be maintained all the time.

The Guideline says that dams must have the Earthquake Resistance Performance I against Level 1 earthquake motions and the Earthquake Resistance Performance II against Level 2 earthquake motions. The evaluation of the Earthquake Resistance Performance II needs the consideration of the progress of structural damage to dam bodies and foundation rock during earthquakes. The practical Earthquake Resistance Performance II in the Guideline is shown in Table 2. That permits cracks in bodies of concrete dams and deformation of embankment dams that may be caused by Level 2 earthquake motions as long as the water storage function of dams is not affected. To confirm the Earthquake Resistant Performance II, the dynamic analysis method that can accurately evaluate the occurrence and progress of cracks in concrete dams is absolutely required.

As for embankment dams, the dynamic analysis method that can accurately evaluate the plastic deformation and residual deformation is necessary.

2.2 Research Activities on Numerical Analysis for Evaluation of Earthquake Resistance of Concrete Gravity Dams

Because any existing concrete dams in Japan have never been damaged severely during large earthquakes, it can be said that concrete dams have strong earthquake resistance performance. Generally speaking, the behavior of a concrete gravity dam body can be sufficiently simulated by the linear elastic analysis as long as the earthquake motion is relatively small and the may not cause cracks in the body.

There are several elastic analysis methods. The analysis using two-dimensional model of the dam body can sufficiently simulate the overall behavior of a dam during an earthquake. In addition, it may be possible to more accurately simulate the behavior of a dam during an earthquake by conducting an analysis combined with comprehensive foundation and reservoir model or by using the three-dimensional analysis method.

Besides, there are a few actual examples of crack occurrence into concrete dam body when the dam suffers strong earthquake motions [11].

In order to examine the earthquake resistance of a concrete dam against severe earthquake motions, it is necessary to conduct the non-linear analysis that takes into account its fracture mechanism. To conduct the non-linear analysis, it is necessary to determine whether or not the cracking of the dam body may occur, that is, to set up the dynamic physical characteristics of dam concrete. This is also important for the evaluation of linear analysis result. Studies on this aspect are being conducted mainly by experiments. As for the numerical analysis of a dam body, researchers have developed various numerical analysis codes to express its damage. They are gradually put in use.

The researches on linear analyses of concrete gravity dams, needless to say, have been conducted by many researchers. Recently, the accuracy evaluation of the results of numerical analysis has actively been conducted because the large acceleration records obtained at big earthquakes in Japan. Earthquake motions due to the Kobe Earthquake were observed at Hitokura Dam site, and its maximum acceleration value is the largest one among the acceleration records obtained at dam sites during the earthquake. Taguchi et al. [12] conducted the two-dimensional analysis of Hitokura Dam model using a dam model without the foundation and the reservoir, simulated its behavior and, as a result, confirmed the earthquake resistance of the dam. Shiojiri et al. [13] conducted the two-dimensional response analysis of the model of Hitokura Dam with the foundation and reservoir. By this analysis, the effects of the damping ratios of the dam body and foundation rock and the modulus of elasticity of the rock were examined. In addition to the above-mentioned two-dimensional analysis, Shiojiri et al. [14] conducted the three-dimensional model analysis of the dam body, foundation rock and reservoir water of the dam. A good result was obtained as compared with the actual dam's behavior by the three-dimensional analysis, and they concluded that the dam can be assumed to be behaved as a linear elastic body to simulate the dam behavior against the Kobe Earthquake. Ariga et al [15] conducted the two- and three-dimensional analyses of Tohira Dam model using the record of the 1993 Kushiro-oki Earthquake observed at the dam site. From these analyses, they estimated the damping ratios by separating material damping and added damping. As a result, it was concluded that larger damping ratios is needed for two-dimensional analysis in order to simulate the three-dimensional phenomena of a dam. At present, the three-dimensional analyses and the analysis with interaction model of a dam, a foundation and a reservoir are still in the process of development and there are various issues. It is considered that advanced skills of users are needed for these analysis methods.

When the vibration of a dam becomes large and the strain and the stress is beyond the range of linear elastic range, the non-linearity of dynamic characteristics of concrete, the effects of the occurrence and progress of cracks should be considered in the numerical analyses. Nagayama et al. [16] conducted studies on the dynamic tensile strength of concrete by conducting tensile tests under high speed loading. As a result, the relationships between the tensile strength and loading speed and that between the static tensile strength and the compression strength were found. To estimate not only the occurrence of cracks but also their progress, it is necessary to establish the stress-strain softening constitutive relation of concrete for dams. The Agency for Natural Resources and Energy and the Japan Electric Power Civil Engineering Association [17] conducted wedge inserting-type splitting tests of large specimens by setting the crack-opening speed and the maximum size of coarse aggregate as parameters. As a result, it was confirmed that the crack progress speed related to the amount of fracture energy and the bilinear strain-softening relations of concrete for dams were proposed. Ariga et al. [15] conducted the non-linear analyses of dam body and foundation by using the three-dimensional analysis. These analyses were made by the equivalent linearity method. The maximum tensile stress in dam body was $2.06N/mm^2$ for the PGA (Peak Ground Acceleration) 500gal earthquake and the dam's earthquake resistance was judged to be sufficient. The Agency for Natural Resources and Energy and the Japan Electric Power Civil Engineering Association [16, 18] analyzed the seismic cracking process of a 150m height model dam during a large earthquake. The seismic cracking process was analyzed based on the concept of the smeared crack model (crack-band model) using the above-mentioned strain-softening relation. As a result, they proposed the index to evaluate the stability of the earthquake resistance of a dam based on crack length ratio to the width of dam along the crack propagating plane. Ohmachi et al. [19] conducted the analysis of the seismic cracking of a dam body under intensive shaking by using a smeared crack model. This analysis was

conducted by using a 100m height model dam by taking into account the interaction of the dam body, foundation and reservoir. In this analysis a bilinear failure criterion based on the combination of the 1st principal stress and 3rd principal stress and the linear type of strain-softening relation was used. In the analysis, cracks were generated along the dam base and from the point where the upstream slope changes. From the results, the installation of local reinforcement with steel bars and the selection of dam body's cross sectional shape was considered to be one of effective possible measures to increase the earthquake resistance of dams.

In accordance with the development of comprehensive and complicated numerical analysis methods, many factors, such as the selection of physical characteristics of construction materials and foundation rock and the selection of boundary conditions will be involved in these analyses, and these factors often are unknown and to set proper values is difficult. It is, therefore, necessary to carefully recognize the purpose of an analysis to be conducted when selecting an appropriate analysis method for a concerned dam whether it should be simplified or complicated method. In the case of a non-linear analysis and seismic cracking analysis, more unknown factors will be involved than the case of a linear analysis. For these reasons, the effect of analytical conditions including concrete material properties and the modeling method of a reservoir and foundation should be carefully examined by the sensitivity analysis, and further studies on improvement of analysis techniques are necessary.

3. A STUDY ON DYNAMIC ANALYSIS CONSIDERING CRACK DEVELOPMENT IN CONCRETE GRAVITY DAM

3.1 Outline

The discrete model and the smeared crack model are major methods to consider the tensile fracture of concrete in the numerical analysis. The discrete model is necessary to beforehand set the elements that can describe cracks in proper locations where cracks may occur. But the smeared crack model doesn't need to determine the locations where the crack may occur in advance. Because it is difficult to estimate such locations in the dam body, we, the PWRI, have conducted researches on the crack development analysis of the concrete gravity dam using the smeared crack model and the safety evaluation method during the earthquake. The fracture progress of concrete material is decided by the characteristics of the fracture material characteristics of concrete material such as tensile strength, fracture energy and the tension-softening curve. Here, we report results of study on effects of the fracture material characteristics of concrete on the occurrence and the development of cracks in concrete gravity dam.

3.2 Analytical Condition

Figure 1 shows the FEM model of a concrete gravity dam with a height of 100m. Dead weight and hydrostatic pressure were considered as static loads. As physical properties of material are shown in Table 3, the tensile strength was set a value between 2.0 and 4.0MPa and the fracture energy was set a value between 100 and 500N/m in an analysis case. The damping coefficient was set as the Rayleigh type damping using the first and third natural frequency for the linear model without considering crack occurrence. The analyses were carried out using a tension-softening curve expressed by a simple straight line shown in Figure 2. The boundary condition of a bottom of a dam body was set as rigid and an effect of a reservoir was considered by added mass matrix obtained assuming water is incompressible fluid. The uplift pressure was not considered. As an input wave, we used the acceleration data observed at the lower inspection gallery of Hitokura Dam during the Kobe Earthquake. Only the amplitude of the acceleration data was enlarged, and it was inputted in the horizontal direction from the bottom of the dam body. Figure 3 shows the original time history data whose PGA is 183gal.

3.3 Result of Analysis

3.3.1 Location of Crack Occurrence

Figure 4 shows the location where cracks finally

occurred as the analytical result on condition that the PGA of the input wave was 300gal, the tensile strength was 2.5MPa, and the fracture energy was 300N/m. This shows all locations where the cracks were generated throughout analysis. Because the foundation was not modeled in this analysis and the stress concentration occurred at the bottom of the body, the development of the crack in such part stood out. The cracks are apt to occur in the bottom and near the slope changing point during the earthquake. According to the earthquake acceleration, the type of the seismic wave or the tensile strength of the concrete, the cracks may also occur on the downstream of the dam body like Figure 5.

3.3.2 Effect of PGA

Figure 6 shows the relationship between the PGA and the crack length (the distance from the dam surface to the crack's tip) for cracks at the slope changing point and the bottom of the dam body. The tensile strength is 2.5MPa, and the fracture energy is 300N/m. as seen in the figure, the larger the PGA is, the longer the crack length is, and the relationship between the crack length and the PGA is almost linear.

3.3.3 Effect of Tensile Strength

Figure 7 shows the relationship between the tensile strength and the crack length for the crack at the slope changing point and the bottom of the dam body. The PGA of the input wave is 300gal, and the fracture energy is 300N/m. From this figure, it is found that with the increase of the tensile strength, the crack length is shorter, and the relationship between the crack length and the tensile strength is almost linear.

3.3.4 Effect of Fracture Energy

Figure 8 shows the relationship between the fracture energy and the crack length about the slope changing point and the bottom of the dam body. The PGA of the input wave is 300gal, and the tensile strength is 2.5MPa. From the figure, it is found that with the increase of the fracture energy, the crack length decreases a little, but there is hardly any change for the crack at the bottom of the dam body.

3.3.5 Comparison of Effects of Tensile Strength and Fracture Energy

Figure 9 shows the relationship between ratio of crack and ratio of the tensile strength or the fracture energy. The ratio of crack was obtained from a crack length divided by the crack length on condition of the tensile strength 2.5MPa and the fracture energy 300N/m, and standards of the tensile strength and the fracture energy are, respectively, 2.5MPa and 300N/m. The PGA of the input wave is 300gal. As seen in this figure, it is found that the slope of the curve for the tensile strength is sharper than the fracture energy. From this result, the tensile strength must be set more appropriately set than the fracture energy when the material property is set.

3.4 Conclusions

The followings were found by this examination.

- The cracks tend to occur in the bottom of the dam body and near the slope changing point of the upstream face of the concrete gravity dam during the earthquake.
- The relationship between the crack length and the PGA of the input wave is almost linear.
- Because the tensile strength has larger effect on the crack development than the fracture energy, the definition of tensile strength is important for the crack propagation analysis of concrete gravity dam.

4. CONCLUSIONS

As mentioned at the beginning of this paper, the safety criteria for designing of dams in Japan are legislated, and the earthquake-resistant design using the seismic coefficient method is used in Japan. However, it is consider that not only the evaluation method of the earthquake resistance performances of existing dams but also the earthquake-resistant design method of the new dams should be improved to a more rational and accountable one from the engineering view point in the future. It is, therefore, necessary to continue the researches on the dynamic analysis method and evaluation ways of dam safety. On the other hand, advancing of further studies on the expectation method of large earthquake

motion for dynamic analysis is indispensable.

5. REFERENCES

1) Japan Commission on Large Dams, "Dam Yearbook 2000."
2) Mononobe, C., "Characteristics of Water Storage Gravity Dam and Its Rational Design Method." Journal of the Japan Society of Civil Engineers, Vol. 11, No. 5, 1925.
3) Ministry of Construction, "Cabinet Order Concerning Structural Standards for River Administration Facilities," July 1976.
4) Ministry of Construction, "Bylaw Concerning Structural Standards for River Administration Facilities (Revision)." October 1999.
5) Committee on the Evaluation of Earthquake Resistance of Dams, "Report of Committee on the Evaluation of Earthquake Resistance of Dams." November 1995.
6) The Subcommittee on Seismic Safety of Dams of the Technical Committee, Japan Commission on Large Dams, "Present Situations and Issues Regarding the Evaluation of the Earthquake Resistance of Existing Dams", Large Dams, Japan Commission on Large Dams, June 2002
7) Japan Society of Civil Engineers, "Proposal on Earthquake Resistance for Civil Engineering Structures (First Proposal)." May 1995.
8) Japan Society of Civil Engineers, "Proposal on Earthquake Resistance for Civil Engineering Structures (Second Proposal)." May 1996.
9) Japan Society of Civil Engineers, Special Committee on Earthquake Resistant Design of Civil Engineering Structures, "Proposal on Earthquake Resistance Civil Engineering Structures and Interpretation (Third Proposal)." June 2000.
10) Japan Society of Civil Engineers, Earthquake Engineering Committee, "Earthquake Resistant Design Standard for Civil Engineering Structures (Draft), A guide for the Preparation of Seismic Resistant Standards." Activity Report of the Divisional Committee on Seismic Resistant Standards, September 2001.
11) Chopra A.K. and Chakrabarti P.: The Koyna earthquake and the damage to Koyna Dam, Bull. Seism. Soc. Am., 63, pp.381-397, 1973
12) Taguchi, K., Sugimura, S. and Kido, K., "Dynamic Analysis of Hitokura Dam during Hyogo-ken Nangu Earthquake." Dam Engineering, No. 23, 1996.
13) Shiojiri, H. and Ueda, M., "Seismic Response Simulation Analysis of Hitokura Concrete Gravity Dam during Hyogo-ken Nanbu Earthquake by taking into Consideration the Combination of Dam, Bedrock and Reservoir." Dam Engineering, Vol. 8, No. 2, 1998.
14) Shiojiri, H. and Ueda, M., "Three Dimensional Seismic Response Simulation Analysis of Hitokura Concrete Gravity Dam during Hyogo-ken Nanbu Earthquake by taking into Consideration the Combination of Dam, Bedrock and Reservoir Water." Journal of the Japan Society of Civil Engineers, No. 640/I-50, 2000.
15) Ariga, Y., Sou, Z. and Watanabe, T., "Evaluation of Earthquake Resistance of Concrete Gravity Dams by taking into account of the Non-linearity during Strong Earthquakes." Large Dams, Japan Commission on Large Dams, No.175, 2001.
16) Nagayama, I., Sasaki, T., and Hatano, M., "Effects of Loading Speed on the Tensile Strength of Concrete." Dam Engineering, No. 148, 1999.
17) Ministry of Economy, Trade and Industry, Resources and Energy Bureau, and Japan Electric Powers Construction Engineering Association, "Study Report on the Improvement of the Earthquake-resistant Design of Dams." March 2001.
18) Masayuki Kashiwayanagi, et al.: Evaluation on Critical State of Concrete Gravity Dams based on Seismic Cracking Analysis, Proc. of Workshop [Modern Techniques for Dams – Financing, Consruction, Operation, Rsik Assesment], ICOLD, 2001.
19) Zhang, H. and Ohmachi, T., "Seismic Cracking and Strengthening of Concrete Gravity Dams." Dam Engineering, Vol. 8, No. 2, 1998.

Table 1 Definition of Level 1 and Level 2 Earthquake Motions [10]

Classification	Definition
Level 1 Earthquake Motions	Level 1 earthquake motions are those that are to be used for conventional design method, such as the allowable stress design method and so on.
Level 2 Earthquake Motions	Level 2 earthquake motions are those that are to be used for examining the safety of structures with taking account of damaging process if necessary. That motion should be the motion of the largest possible grade which may occur at a concerned site from the present to the future.

Table 2 Earthquake Resistance Performance II of Dams in order to secure Water Storage Functions [10]

Type of Dam	Requirement
Concrete Dam	• No falling down nor sliding • No through cracks in dam body nor foundation • No dam-body collapse
Embankment Dam	• No through cracks in impervious core zone • No overflowing of reservoir water • No dam-body collapse

Table 3 Physical Properties of Material

Elastic Modulus (MPa)	3.00E+04
Poisson Ratio	0.2
Tensile Strength (MPa)	2.0, 2.5, 3.0, 4.0
Fracture Energy (N/m)	100, 200, 300, 400, 500
Compressive Strength (MPa)	25
Unit Weight (kg/m^3)	2,300
Damping Coefficient (%)	10(Rayleigh)

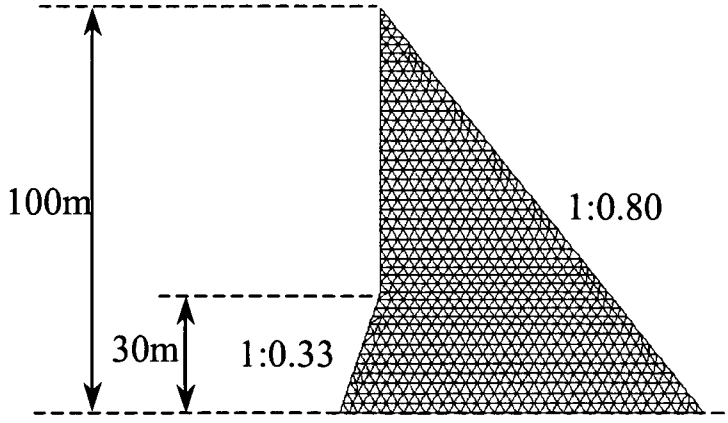


Figure 1 FEM Model

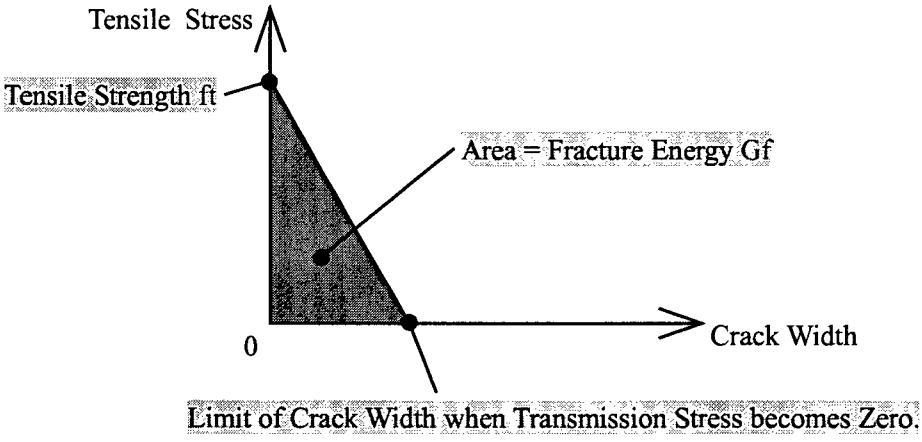


Figure 2 Tension-Softening Curve (Simple Straight Line Model)

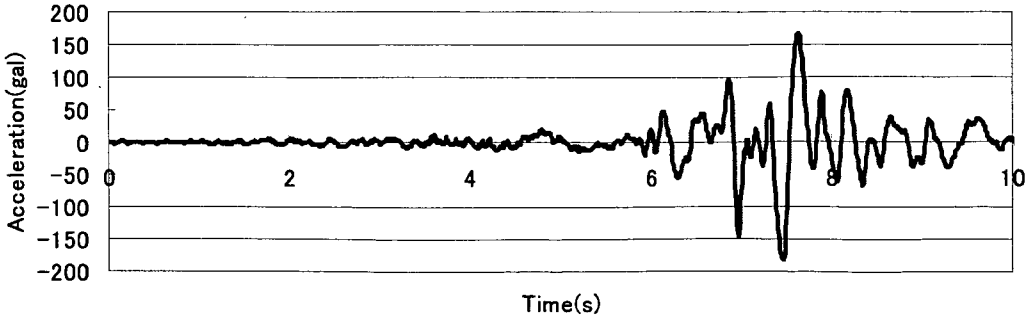


Figure 3 Input Wave (Original Wave was observed at Hitokura Dam.)

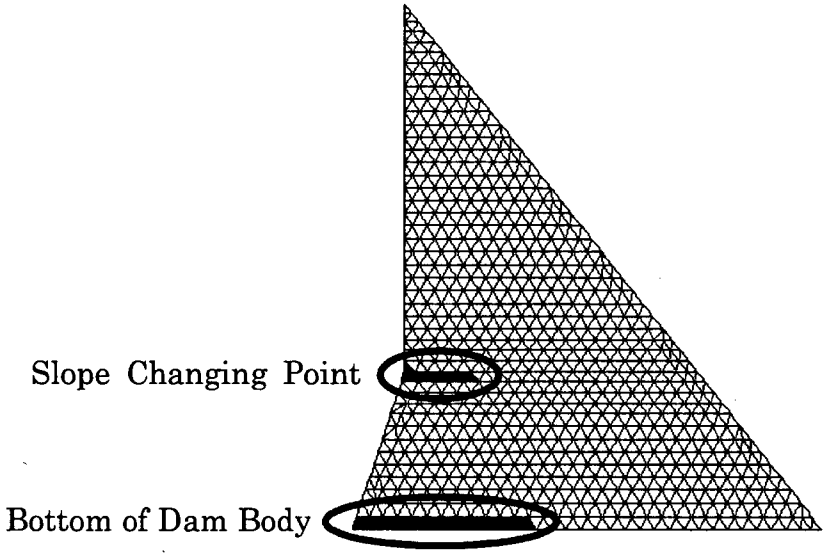


Figure 4 Position of Crack Generation (ft=2.5MPa, Gf=300N/m, PGA=300gal)

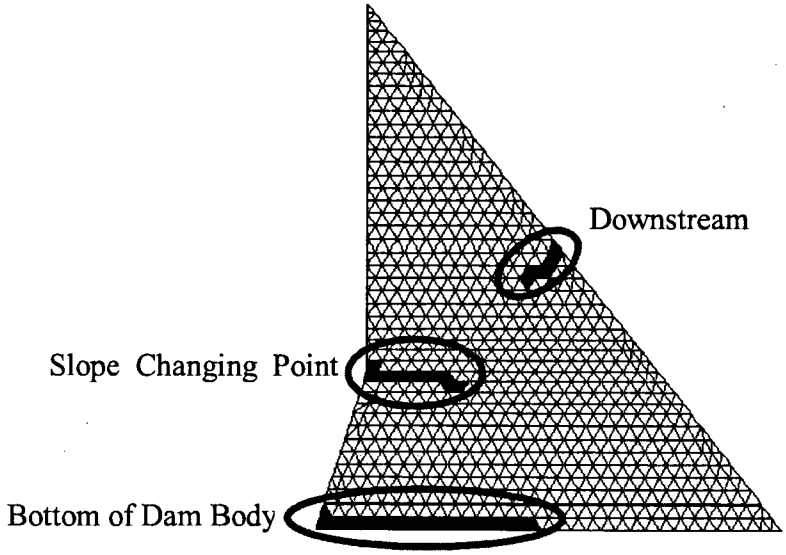


Figure 5 Position of Crack Generation (ft=2.5MPa, Gf=300N/m, PGA=400gal)

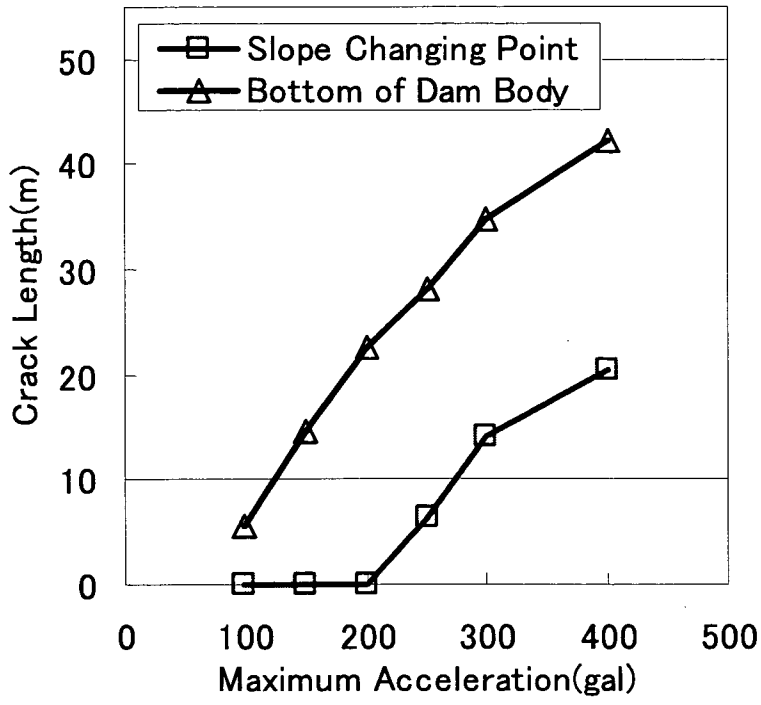


Figure 6 Relationship between Crack Length and PGA (ft=2.5MPa、Gf=300N/m)

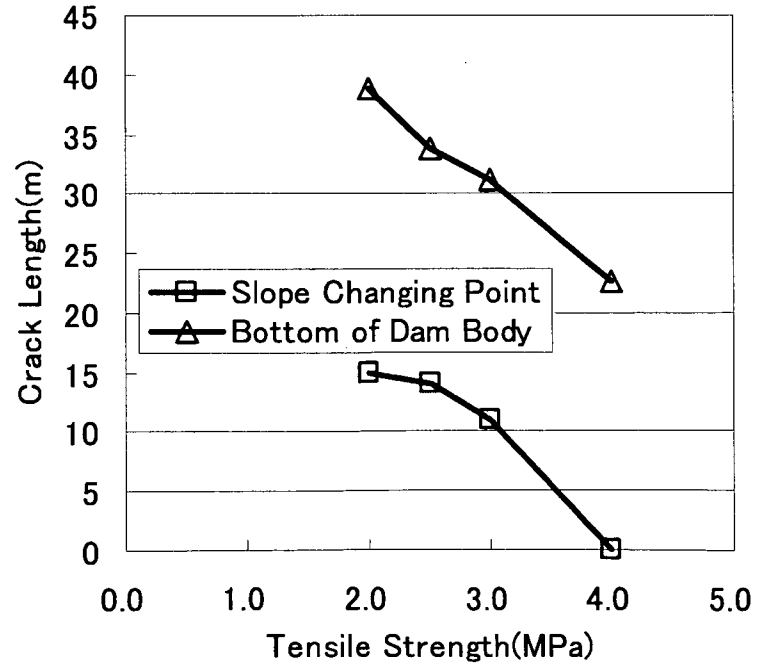


Figure 7 Relationship between Crack Length and Tensile Strength (Gf=300N/m, PGA=300gal)

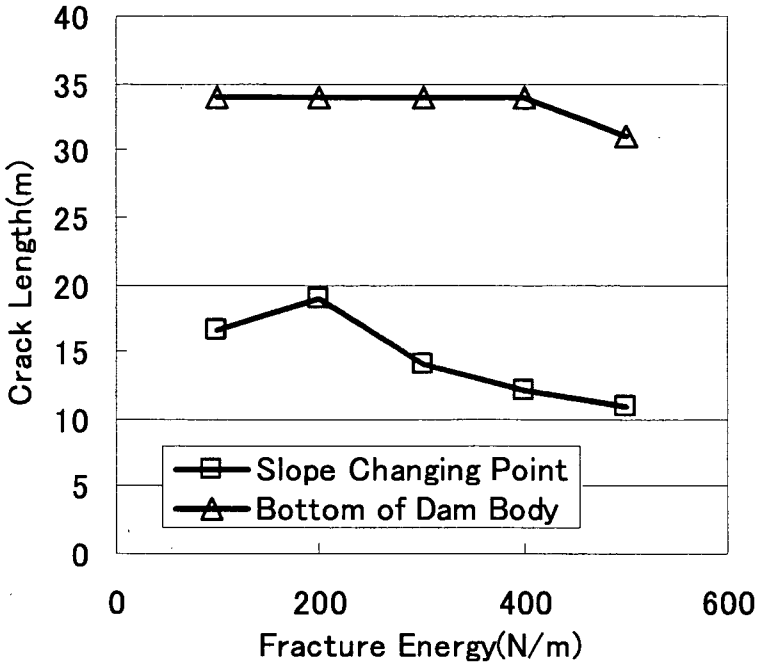
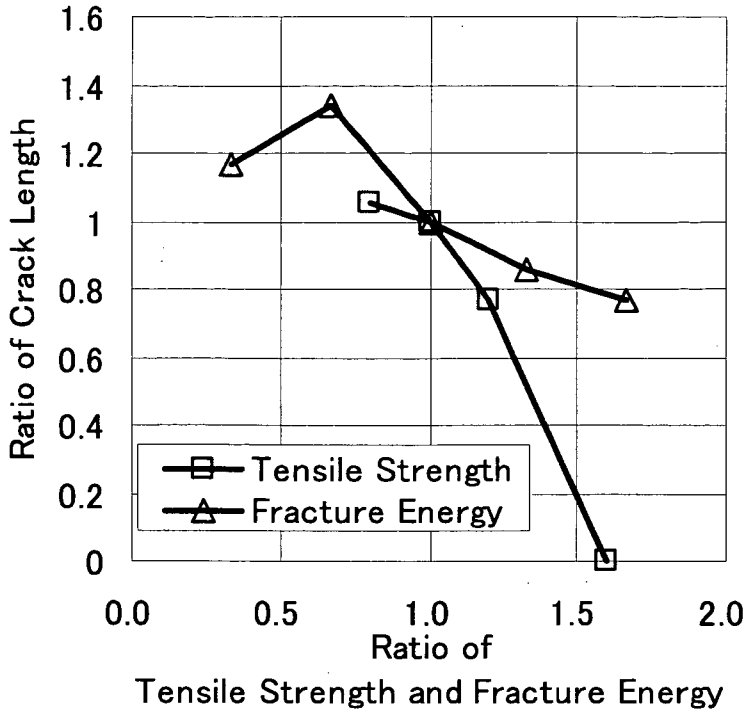
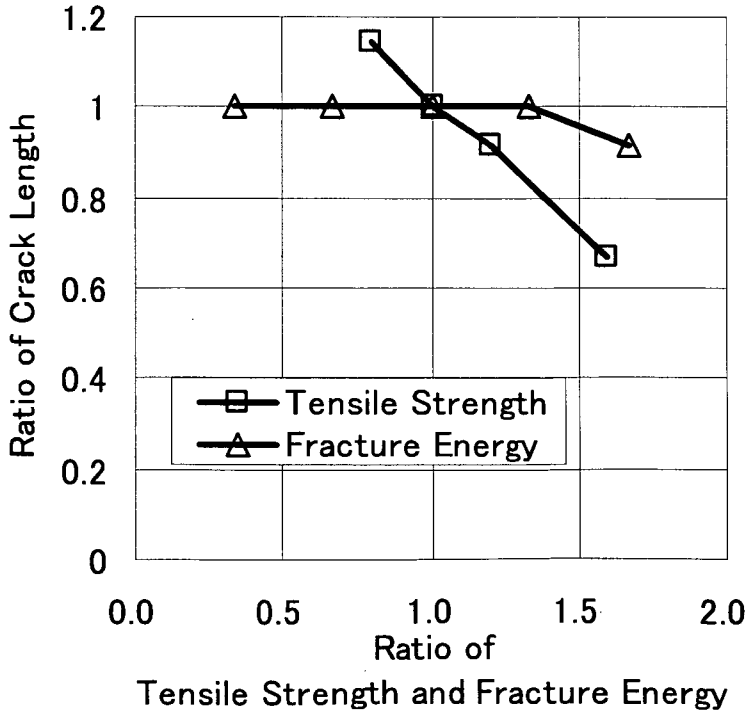


Figure 8 Relationship between Crack Length and Fracture Energy (ft=2.5MPa, PGA=300gal)



(a) Slope Changing Point



(b) Bottom of Dam Body

Figure 9 Relationship between Ratio of Crack and Ratio of Tensile Strength or Fracture Energy

The Value Added of Field Testing on Concrete Dams

by

Ziyad H. Duron[1], Enrique E. Matheu[2] and Robert L. Hall[3]

ABSTRACT

In general, field testing of concrete dams has not been widely embraced by dam owners and it is not typically regarded as an essential component in the process of evaluating the seismic performance of these massive structures. Over the years, proponents of field testing and the use of measured response behavior to validate numerical models have had difficulty convincing the broader consulting community of the added value associated with the costs of field testing. This is not to say, however, that the importance of field testing is not fully appreciated or understood. This paper is intended to present a current viewpoint associated with the state of field testing of concrete dams and the potential benefits derived from the availability of test data in evaluating seismic performance. A brief description of a recently completed seismic evaluation is discussed and presented as a case study to investigate the role played by the associated field testing and inspection program.

KEYWORDS: Field Testing; Seismic Evaluation; Concrete Dams.

1. INTRODUCTION

In 1990, a comprehensive report prepared with support of the National Research Council of the United States reviewed the state of practice on seismic design and evaluation of concrete dams and identified the corresponding research needs (NRC, 1990). This document also provided recommendations and improved criteria for evaluating the seismic performance of concrete dams. It was noted that as early as the 1950s, concrete dams were assumed essentially rigid systems even though the importance of their dynamic behavior was partially recognized. About a decade later, it was understood that amplifications large enough to cause damage could occur in concrete dams, but the analytical tools were not yet widely available for a proper consideration of these effects. With the introduction of analytical tools to evaluate effects of dam-foundation-reservoir interactions in the 1970s, improvements in the criteria to evaluate results from analytical studies were needed. For example, it was recognized that the numerical prediction of tensile stresses large enough to indicate initiation of cracking and/or compressive stresses larger than allowable working levels did not necessarily indicate instability. With the advent of advanced analytical techniques and computer technology, nonlinear analysis techniques and nonlinear material behavior of dams occupied much of the research focus in the 1980s and 1990s. Still, it is probably the case today that many consultants would prefer to avoid a full nonlinear analysis in-lieu of a linear elastic study supported by post-earthquake stability evaluation. Although inherently restricted by the linearity assumption, undoubtedly these types of studies still provide a great deal of information about the earthquake response that can be expected under realistic conditions.

An exhaustive review of experimental behavior and field-test data of concrete dams was presented by Hall (1988). This study examined available knowledge of the seismic behavior of concrete dams from observations made during actual earthquakes and from experiments conducted on prototype and model dams. Near the end of his review, Hall addressed the

[1] College of Engineering, Harvey Mudd College, Claremont, CA 91711 (USA).
[2] Dept. of Civil and Environmental Engineering, Louisiana State University, Baton Rouge, LA 70803 (USA).
[3] U.S. Army Engineer Research and Development Center, Vicksburg, MS 39180 (USA).

usefulness of testing techniques in the context of model validation. For example, a model's ability to reproduce field-test data acquired at varying water depths tests the model's distributed qualities in that comparisons are not only made at resonant peaks, but at frequencies between resonances as well. In addition, resonances predicted by models using material properties obtained from sample core testing can be compared against field-test findings. Furthermore, dynamic tests on dam models can be used to determine resonant frequencies and response shapes, and model testing can be most useful in the investigation of nonlinear dam response behavior.

Hall made a rather significant observation concerning water compressibility and model validation. Although a number of investigators had attempted to gather information on water compressibility, Hall reported that only one study had ever claimed the presence of significant water compressibility effects. Since his review, however, additional attempts at measuring compressibility effects have been made. Forced vibration tests were conducted on large concrete gravity dams in Canada during the 1990's in which measurements of acceleration and hydrodynamic pressure along the upstream dam face were used to evaluate dam-reservoir interaction effects (Proulx, 1994; Duron, 1995). Another series of experimental studies were conducted at Longyangxia Dam in China under the U.S.-China Protocol on Earthquake Studies (Ghanaat, 1999). The excitation for these field measurements was generated by the controlled detonation of explosive charges. In all these cases, the investigators were able to show probable compressibility effects associated with measured response behavior in the dam and in the reservoir. However, an exhaustive investigation regarding the significance of these effects in the context of a complete seismic evaluation has yet to be pursued.

Ventura and Horyna (1996) recently presented an updated literature review on vibration tests of large dams covering the period from 1975 to 1995. In general, these types of experimental studies are usually associated with a companion model validation effort. For example, the U.S. Bureau of Reclamation recently conducted a series of seismic safety evaluation studies of Morrow Point Dam using numerical models and available experimental measurements (Nuss and Chopra, 2001; Nuss et al., 2003). The objective of these studies was to adjust material properties and reservoir absorption coefficients to match measured behavior from the forced vibration tests on the dam. These studies attempted to characterize the sensitivities to various input parameters based on comparisons against measured field test results. Dramatic differences were found in the predicted maximum tensile stresses depending upon the analysis technique employed. For example, following a traditional analysis in which the foundation is considered as massless and incompressible added masses are used to represent the hydrodynamic effects, stresses as high as 9.9 MPa were obtained as compared to 2.3 MPa from an analysis with foundation mass and water compressibility interactions.

The availability of measured or observational evidence of how a dam system behaves can provide the analyst with a wealth of knowledge with which to critically evaluate analytical findings. In what follows, the authors will present a case study in which low level ambient field tests were instrumental in providing insight into the predicted seismic performance of a large concrete dam.

2. CASE STUDY: SEISMIC EVALUATION OF FLORENCE LAKE DAM

2.1 Description

Florence Lake Dam is located on the South Fork of the San Joaquin River, on the western slope of the Sierra Nevada, in Fresno County, California, approximately 93 km northeast of the city of Fresno. The dam and reservoir are owned and operated by Southern California Edison Company and is a 46-meter-high, reinforced concrete multiple-arch dam with a total crest length of 962 m. The dam, which was completed in 1926, consists of 58 arches (inclined 48

degrees to the vertical), each with a span of 15.2 m supported by counter forted buttresses. The dam consists of five tangent sections to take advantage of a rock ridge at the lower end of the reservoir basin. An aerial view is shown in Figure 1.

2.2 Analysis Approach

Florence Lake Dam had been the subject of various seismic evaluations since 1971 and the most recent study was commissioned in 1992 and completed in 2001. Complicating factors in the analysis of Florence Lake Dam stemmed from the complexity of the dam geometry, foundation stability concerns, and the acceptance of proposed analysis techniques for a multiple, thin arch reinforced concrete dam. While it is not the purpose of this paper to review the details associated with the Florence Lake Dam study, the study does serve as a great example to illustrate the value added of field investigations to improved understanding of predicted response behavior.

A diagram of the evaluation procedure followed for this study is shown in Figure 2. The numerical analyses performed for the seismic evaluation of Florence Lake Dam essentially consisted of two separate approaches. Each analysis, however, was motivated by different objectives. When the original analysis was conducted, it was determined that modeling the entire dam would be inefficient and unnecessary since a particular portion of the dam, namely the River Section, contained the 9 tallest arches and was considered to be the most critical portion for the evaluation. The engineers further determined that this section exhibited sufficient symmetry about the middle arch and that a symmetric analysis approach could be pursued. The numerical model (hereafter referred to as the symmetric model) for the symmetric analysis approach is shown in Figure 3. The finite element analysis of the symmetric dam-foundation-reservoir model was completed using the computer program EACD-3D.

Results from the symmetric analysis were presented to a Review Board in 1994 but did not meet with full acceptance over concern that a region of the River Section not contained in the symmetric model might not be accurately evaluated. The Board expressed additional reservations concerning the foundation material properties and stability at that time. Largely in response to the Board's concerns, a detailed 3-D numerical model of the full River Section (hereafter referred to as the full model) was developed and analyzed using commercially available software. The model is shown in Figure 4.

2.3 Conflicting Analysis Results

The decision to continue the seismic evaluation of Florence Lake Dam by pursuing a second analysis approach resulted in seemingly irreconcilable differences in the predicted stress and deformation characteristics of the River Section. Static stress levels (both tensile and compressive) based on the symmetric model were found to be within acceptable concrete strength limits. Corresponding stress results using the full model, however, predicted regions of comparatively high static tensile stress in the dam near the arch-haunch interface. Static tensile stresses approaching 5.52 MPa were predicted in these areas, suggesting that the arches would be cracked parallel and adjacent to the haunch. Dynamic stress results from the symmetric model indicated that dynamic tensile stresses of 5.1 MPa (earthquake only, not considering static loading) would occur near the top of the highest arches in the River Section during a large earthquake. Results from the full model predicted dynamic tensile stresses on the order of 6.90 MPa occurring at about the same location.

2.4 Model Validation Efforts

Model validation based on observable information could provide enhanced confidence to utilize model results in assessing the current and predicted behavior of a dam. In the case of Florence Lake Dam, the analysts performing the analysis felt the need to comparatively assess the accuracy of the full model using the results from a validated symmetric model of the dam to

perform their assessment. Upon validation, the symmetric model served to provide a context for the results obtained from the full model and aided the analysts in assessing relative conservatism in predicted stress levels in the dam.

Validation of a model is achieved if response characteristics derived from the analysis (e.g. resonant frequencies and response shapes) can be matched favorably against actual observed behavior. In the absence of actual dam response measurements due to earthquake excitation, dynamic testing of the complete river section using artificially applied excitation was considered. Available options for applying a known excitation to the dam included eccentric mass vibrators or low-level impact devices such as a calibrated hammer. Both options were discarded due to logistics associated with transporting heavy test equipment to the dam site and with safety concerns associated with the installation of large machinery onto the narrow crest at Florence Lake Dam.

Dynamic testing of the river section of Florence Lake dam was performed using the ambient testing technique. Ambient testing was particularly well suited at Florence Lake since no artificial excitation to the dam is required for an ambient test. In addition, ambient responses could be obtained with relative ease, with sufficiently high reliability and accuracy, and at low cost. The test procedure involves the monitoring of ambient acceleration responses over a sufficient length of time to ensure adequate signal quality and statistical confidence in identified response characteristics.

Acceleration responses were obtained using extremely sensitive servo force-balance accelerometers with micro-g sensitivity and flat frequency response characteristics. A triad (three accelerometers mounted in a small aluminum block) was used to acquire responses in the radial, tangential, and vertical directions at each measurement station along the arches. Figure 5 is a schematic of the measurement layout followed during the ambient tests. Two separate ambient surveys were completed at Florence Lake Dam in September 1995 and again in December 1995 under full and empty reservoir conditions, respectively. Testing under varying reservoir conditions presented a unique opportunity to investigate dam-foundation and dam-reservoir interaction effects as predicted by the results from the EACD-3D numerical model. Test procedures, instrumentation details, and measurement layouts were identical for each test. A total of 37 measurements along the crest (arches 52, 53, and 54) and 4 locations along the height of the tallest buttress between arches 52 and 53 were acquired. The location to the left of the center of arch 53 was selected as the reference for each test. Actual testing was completed by simply placing the triad block of accelerometers at each measurement station (two stations and the reference were monitored at a time) and time histories were acquired over a 6-minute period sampled at 200 samples per second. Signals were band-passed filtered and amplified prior to digitization.

Subsequent data analysis was performed using traditional fast Fourier transform (FFT) techniques in which spectral estimates of power spectral density (PSD), frequency response (FRF), and coherence functions were computed. Resonances in the dam were identified based on observed resonant peaks in the PSDs coincident with high coherence values (approaching unity). A comparison of the PSD (radial) reference response under both full and empty reservoir conditions is shown in Figure 6. Both curves indicate excellent data quality in terms of signal-to-noise ratios and identified resonances, typical throughout both series of tests. FRF information was combined over all measurement stations to produce response shapes for each identified resonance. Data from each ambient survey were used to validate the model as described below.

Ambient response shapes derived from the tests were easily characterized as either symmetric or antisymmetric, facilitating a direct comparison with computed symmetric and antisymmetric model characteristics. A first evaluation of whether the symmetric model and analysis approach could adequately represent the actual dam response behavior was based on comparisons of dam-foundation eigenvalues and

eigenvectors against resonances and response shapes identified from the empty reservoir ambient tests. A second comparison was performed using the computed complex frequency response of the generalized coordinates for the dam-foundation-reservoir system. The computed characteristics were then compared against those determined from the full reservoir ambient responses.

Results from the first comparison between the eigensolution of the dam-foundation sub-system and the empty reservoir ambient test results are described below. Table 1 lists computed eigenvalues and measured resonances below 10 Hz. The frequency comparisons provided a measure of confidence that the model response characteristics were in good agreement with observed behavior. A better understanding of the model response behavior, however, was obtained by comparing the measured response shapes with the eigenvectors.

The measured response shapes from the ambient tests are interpreted as linear combinations of the actual modal responses of the dam system. In as much as the measured power spectral density functions indicate well-spaced, lightly damped resonant responses, the measured shapes can be considered as mode shapes. Therefore, the comparison of eigenvectors associated with the dam-foundation sub-system against mode shapes from the empty reservoir ambient survey was considered appropriate. Shown in Figures 7 and 8 are comparisons of the fundamental symmetric and antisymmetric responses. A reasonable match in mode shape for each case is observed.

The second comparison was made between the computed frequency response behavior of the model against the measured characteristics from the full reservoir ambient survey results. Table 2 lists the computed system resonances along with measured resonances from the ambient (full reservoir) tests. The comparison in Table 2 is deemed quite favorable, and it provides additional evidence to support the analysis approach taken. The computed response shape at 3.5 Hz against the measured shape from the ambient (full reservoir) tests is shown in Figure 9. Computed resonances beyond 3.5 Hz are characterized by broader, more closely spaced peaks indicating some degree of modal coupling is present in these responses. Associated response shapes are more likely to contain contributions from higher frequency mode shapes.

Based on the comparison studies completed, and the results presented above, the response characteristics associated with the symmetric model appeared to be in good agreement with known response characteristics associated with the dam for both empty and full reservoir conditions. The validated symmetric model allowed the analysts to evaluate the degree of conservatism associated with the results from the full model. The validated model provided a sound baseline for the analyses using the full model and these comparisons increased the confidence in its application.

2.5 Consideration of Additional Field Data

In an attempt to correlate the analytical predictions of static stresses with probable cracked areas in the dam, a site inspection was conducted in 1998 under empty reservoir conditions. The detailed inspection included examination of every arch for signs of cracking consistent with analysis findings. The upstream arch faces, covered with 7.6 cm (nominal thickness) of shotcrete were observed to be in excellent condition. No significant cracking was observed in the shotcrete, at least any that could be attributed to the possible presence of cracks in the original or parent concrete. No cracking could be seen along the arch-haunch interface. Inspection of the downstream arch faces, however, did reveal the presence of cracks. The cracks, however, were not in the location suggested by the calculations, but were oriented vertically along the height of the arch (almost symmetrically placed about the crown) over each quarter point. It is interesting to note that the cracking observed is of the type discussed by Janas and Sawczuk (1964). These observed crack patterns at Florence Lake Dam were not consistent with the predicted regions of high static tensile stress from the full model analysis.

As a result, additional field evidence was sought that could reconcile the discrepancy between the predicted static behavior and the observed condition of the arches. Attention focused on the results from a previous analysis of the structural behavior of arch 21 in the dam (Bechtel, 1952). This study was based on data gathered at approximately forty locations along the downstream face of the arch. Based on the measured data, the maximum static deflection magnitude at the crown was estimated as 0.18 cm. The corresponding value predicted using the full model was 0.25 cm. In general, it was found that the static deflected shape predicted by the full model was in good agreement with the measured deflections demonstrating that tension could be developed in the arch under static loading at the crown and near the haunch.

The magnitude and pattern of the deflections observed in the 1952 study seemed to indicate the development of tensile stresses in the arch under full reservoir loading. However, the analyst rejected these measurements as unreliable based on the assumption of compressive arch behavior under static loading. This conclusion was probably correct, but not because the measured deflections were not real. Instead, the combined effects of different phenomena probably resulted in a redistribution of the load carrying capacity of the arch. Time variant conditions such as the cyclical loading and unloading associated with daily temperature variations and seasonal freezing and thawing cycles can affect the heterogeneous material composition of concrete. While creep can cause stress intensities to change, shrinkage stresses induce self-balancing stresses of unknown magnitude resulting in erratic, unpredictable crack patterns. Although finite element analysis may indicate that the arches could develop static tensile static stresses as high as 5.52 MPa, significant stress relief and redistribution in the arches is believed to have occurred over the dam's lifetime ensuring continued and adequate load carrying capability. Considering these factors, it is unlikely that the exact state of stress in the dam prior to an earthquake can be accurately known.

The predicted static stress state, therefore, if it ever existed in the dam, must have occurred during its early years (uncracked condition, prior to significant reservoir loading). At that time, cracking probably relieved excessive tensile stresses and subsequent loads were then carried by compressive, tensile, and shearing stresses in the remaining uncracked portions of the arch. In fact, much of the cracking observed in the arches must have occurred upon initial filling of the reservoir and was probably a result of the dam initially acting as an unreinforced or plain concrete structure. Therefore, any linear elastic representation of an actual dam in a cracked condition would tend to overestimate the current static stress state.

It is clear that the exact magnitudes of the dynamic stresses in the dam cannot be predicted accurately for reasons similar to those expressed earlier in the discussion of the static stress condition. However, the strong motion duration as long as 30 seconds (indicated in the stress time histories) and the large number of expected stress cycles suggested that tensile stresses in the dam would likely exceed the tensile strength of the concrete during the earthquake and lead to cracking. Therefore, an evaluation approach that considered the possible cracking scenarios would be needed to complete the study. This led to the development of a deformation-based evaluation approach for the final assessment of the expected seismic performance of the dam, as an attempt to resolve the discrepancies in stress results.

2.6 Deformation-Based Evaluation

Examination of the deformed shape of the dam during earthquake loading was used to provide understanding of the locations in the dam where cracking could be expected to occur. In particular, a review of the predicted animated dam response (using the full model) revealed excessive rotation at the haunch driven by cross-stream movements of the buttresses. Arches were squeezed when two adjacent buttresses moved toward each other, and were flattened when the buttresses moved away from each

other. The importance of the rotation at the haunch and its effect on the expected condition of the arches led to a series of parametric studies aimed at identifying the range of motions that the haunch could experience during strong motion. Parameters included concrete modulus and/or section properties in the arches, buttresses, and at the haunch interface. Results from these studies focused attention on the arch side of the haunch, while demonstrating that the buttress side of the haunch would experience low tensile stress levels during the earthquake.

Cracking associated with seismically induced deformations would not occur simultaneously on both faces of the arch, but would occur on one face during one cycle and then on the other face in the next cycle. As the earthquake progressed into its strong motion period, arch stiffness would be reduced in these cracked regions, leading to non-linear behavior. For a reinforced concrete structure such as Florence Lake Dam, evaluation of this non-linear response would be difficult to interpret and validate. Nonetheless, evaluating the consequences of this behavior was thought to be a critical component in the assessment of the dam. For this purpose, evaluation of cracked arch behavior was based on estimated arch deformation capacity compared to predicted deformation levels in the arches.

Therefore, the evaluation approach examined the deformation state in the dam, rather than the stress state during the earthquake. The evaluation approach effectively dealt with the somewhat differing linear stress results obtained from the symmetric and full river section analyses by assuming that the stress levels in the dam that would be present during the evaluation earthquake could reach concrete tensile limits. This assumption was conservative since the stress levels as predicted from the symmetric analyses indicated a lower overall stress state than the corresponding full model analyses.

Furthermore, the inability of either numerical model to include the effects of reinforcing steel present in the dam limited the confidence of each model to predict the stress state immediately after cracking of the concrete began. In lieu of conducting non-linear analyses using special finite elements that may incorporate reinforced characteristics, a series of linear analyses were conducted to obtain a range for the expected deformations of the dam during the evaluation earthquake. The deformations were estimated using the full model, and this was judged appropriate based on the agreement between measured and predicted static deflections for arch 21.

These deformations were the basis on which the evaluation of Florence Lake Dam was performed. The demand, in terms of expected seismic deformation, was compared to the capacity of the reinforced arches and buttresses of the dam. In this manner, a ratio of these quantities was used to indicate a safety margin and provide some indication of the expected behavior of the dam. An additional consideration in this evaluation was the confinement of the concrete necessary to resist or minimize loss of concrete that would significantly affect the dam's ability to impound the reservoir water during the earthquake.

In the buttresses, the coupled buttress-haunch motion produced small relative deformations indicating that any tensile stresses developed in the buttresses would be below concrete strength limits. For this reason, the buttresses were judged to perform adequately under the Maximum Credible Earthquake (MCE). The arches, however, driven by lateral buttress movements, required the review of two deformation states. The first one of these considers the effect on arch deformation resulting from buttresses moving toward each other, and the second is based on the buttresses moving away from each other. For each configuration, theoretical arch deflection formulas were combined with experimentally derived moment-curvature relationships for reinforced concrete sections in order to determine deformation capacity. These estimated deformation capacities were then compared to predicted values from the numerical model results. For the various stages of expected cracking in the arches, the ratio of

capacity to predicted deformation was always greater than 1.0.

3. CONCLUSIONS

A series of finite element analyses were completed for the seismic evaluation of Florence Lake Dam. Two separate analysis approaches provided comparative means for estimating both stress and deformation states that would be expected to occur in the dam during an extreme earthquake. Considering the age of the dam (over 70 years of service) and the limitations associated with using linear homogeneous material properties to represent composite (reinforced concrete) material behavior, calculated stress states were judged as inappropriate for the final evaluation of the dam. Furthermore, non-linear analyses were not pursued since model validation and interpretation of results would be difficult for this type of structure. In view of these limitations, a new evaluation approach was developed for Florence Lake Dam.

The availability of field data allowed the engineers to pursue a somewhat unorthodox approach to the seismic evaluation of Florence Lake Dam. These data were in the form of both historical and more recent field measurements of both static and dynamic response behavior. A field inspection was critical to placing predicted stress states in the context of the standing dam. The engineers were able to utilize a symmetric model validated in terms of linear elastic dynamic behavior to assess the relative conservatism of an analysis that employed a full model. The results form the validated symmetric model, although indicative of stable response behavior during the MCE, were not judged adequate by the review Board. Nonetheless, the successful validation of the symmetric model was very useful in assessing both the stress and deformations associated with the full model analysis. Based on the understanding gathered from the ambient vibration testing and other field data, the engineers were able to develop a deformation-based assessment of Florence Lake Dam that was met with acceptance by the Review Board.

4. ACKNOWLEDGEMENTS

Mr. Michael Knarr, Structural Engineer, Outten Engineering headed the seismic evaluations of Florence Lake Dam. His guidance and technical skills were essential in completing the study. The Southern California Edison Company funded the studies at Florence Lake Dam. Expert opinion on the Florence Lake Dam study was obtained from Prof. Mete Sozen at Purdue University and Prof. John F. Hall at Caltech. They contributed to the development of the deformation based criteria.

The field measurements acquired at Florence Lake Dam were processed and evaluated using ***iDAMS***, an internet based database for the analysis of measurements of large civil structures. Mr. Gene Lee and Mr. Daniel Sutoyo, De Pietro Fellows in Civil Engineering at Harvey Mudd College have developed the current version of this software through the generous support of the De Pietro Fellowship Program at Harvey Mudd College.

Development of ***iDAMS*** has been sponsored by the Direct-Allotted Civil Works Earthquake Engineering Research Program at the U.S. Army Engineer Research and Development Center (ERDC). This support is greatly appreciated. The authors also gratefully acknowledge the support of the ERDC Geotechnical and Structures Laboratory, where the second author is currently a guest researcher.

5. REFERENCES

National Research Council, "Earthquake Engineering for Concrete Dams: Design, Performance, and Research Needs," National Academy Press, Washington, DC 1990.

Hall, J. F., "The Dynamic and Earthquake Behavior of Concrete Dams: Review of Experimental Behavior and Observational Evidence," Soil Dynamics and Earthquake Engineering, Vol. 7, No. 2, pp 58-121, 1988.

Proulx, J., "Etude Experimentale Et Simulation Numerique De L'Interaction Barrage-Reservoir-

Foundation: Cas Du Barrage-Poid Outardes 3," PhD Thesis, University of Sherbrooke, Sherbrooke, Canada, March 1994.

Duron, Z., "Seven Mile Dam Vibration Testing: Results from the First and Second Series of Tests Performed February 20-27 1995 and August 14-20 1995," Final Report submitted to B.C. Hydro and Power Authority, Burnaby, B.C., Canada, May 1995.

Ghanaat, Y., "Field Measurements of Dynamic Interaction at Longyangxia Dam", 2nd U.S.-Japan Workshop on Advanced Research on Earthquake Engineering for Dams, Tokyo, 1999.

Ventura, C. E. and Horyna, T., "Vibration Tests of Large Dams – Literature Review," Earthquake Engineering Research Facility, Department of Civil Engineering, University of British Columbia, Vancouver, 1996.

Nuss, L. K. and Chopra, A. K., "Analyses using EACD3D96 for Morrow Point Dam", 3d U.S.-Japan Workshop on Advanced Research on Earthquake Engineering for Dams, San Diego, 2002.

Nuss, L. K., Chopra, A. K., and Hall, J. F., "Comparison of Vibration Generator Tests to Analyses Including Dam-Foundation- Reservoir Interaction for Morrow Point Dam," Presented at the Commission Internationale Des Grande Barrages, 20th Congress of Large Dams, Montreal, 2003.

Janas, M. and Sawczuk, A., "Some Aspects of the Load Carrying Capacities of Arch Dams," Theory of Arch Dams, Proceedings of April 1964 Symposium, Southampton University, Pegamon Press Ltd.

Bechtel Corporation, "Analysis of Structural Behavior of Arch 21 – Florence Lake Dam," Technical Report, August 12, 1952.

Table 1. Comparison of measured and computed resonances (empty reservoir).

Experimental (Hz)	Frequency Analysis (Hz)
3.0	3.3
3.4	3.6
5.5	5.9
6.2	6.5
6.6	6.8
7.3	7.5
7.7	7.9

Table 2. Comparison of measured and computed resonances (full reservoir).

Experimental (Hz)	Frequency Analysis (Hz)
3.5	3.5
6.3	6.4
6.8	7.3
9.9	9.5
11.7	11.8
14.3	14.0
16.8	16.8

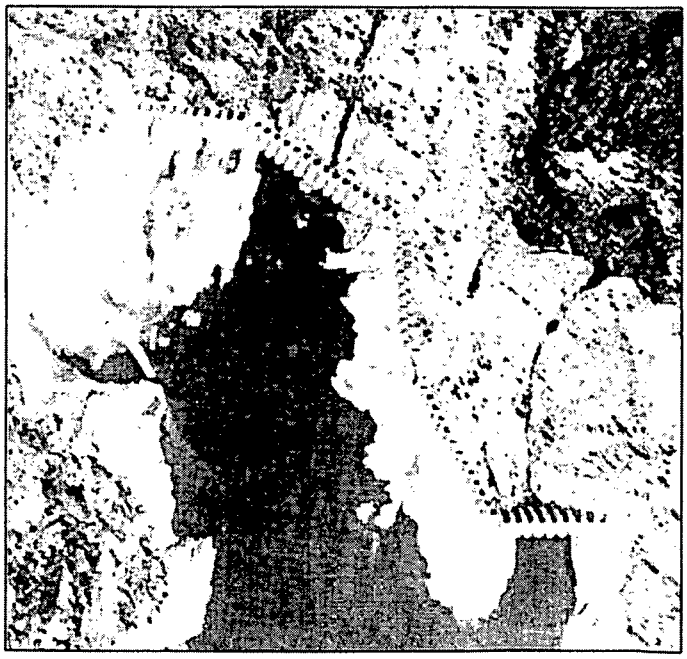


Figure 1. Aerial view of Florence Lake Dam.

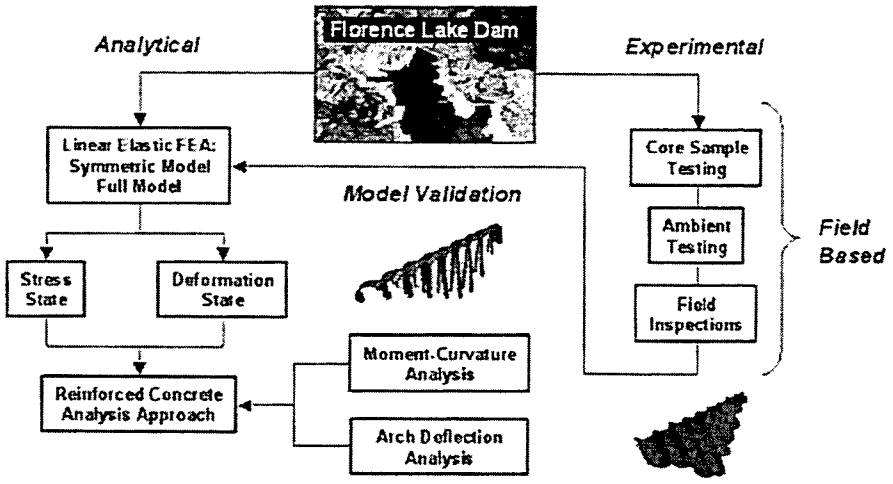


Figure 2. Overview of evaluation procedure.

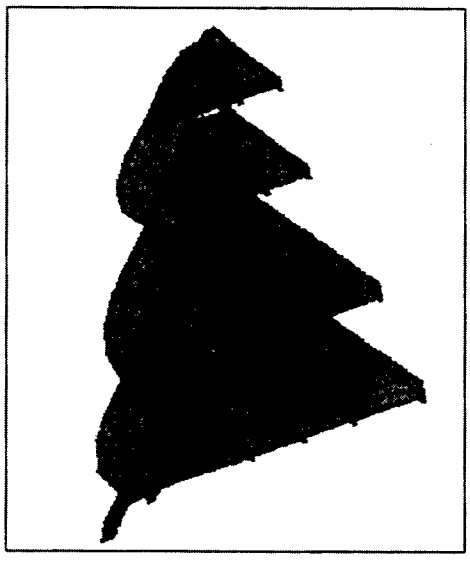


Figure 3. Symmetric numerical model of the River Section of Florence Lake Dam.

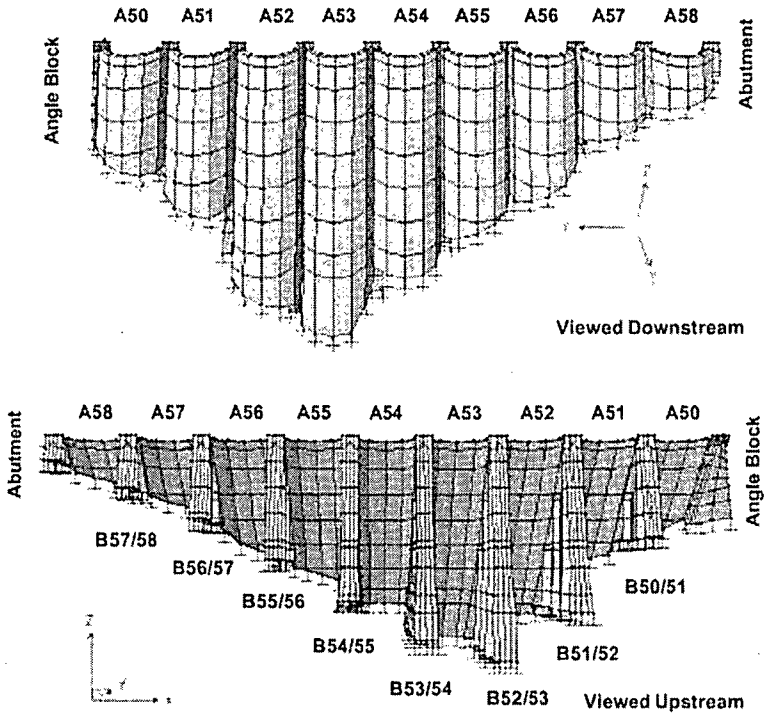


Figure 4. Full 3D numerical model of the River Section of Florence Lake Dam.

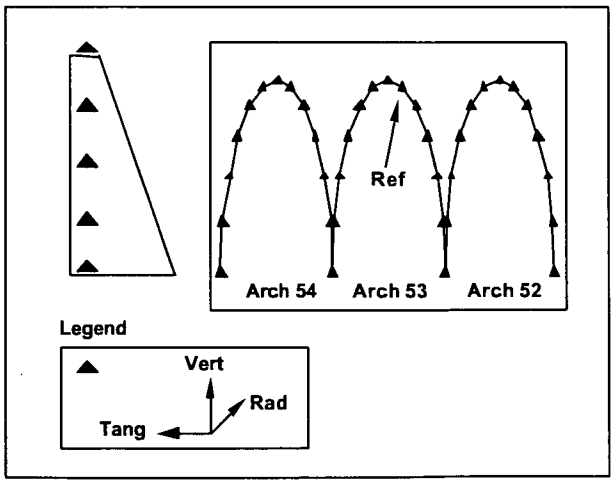


Figure 5. Measurement layout used during ambient testing at Florence Lake Dam.

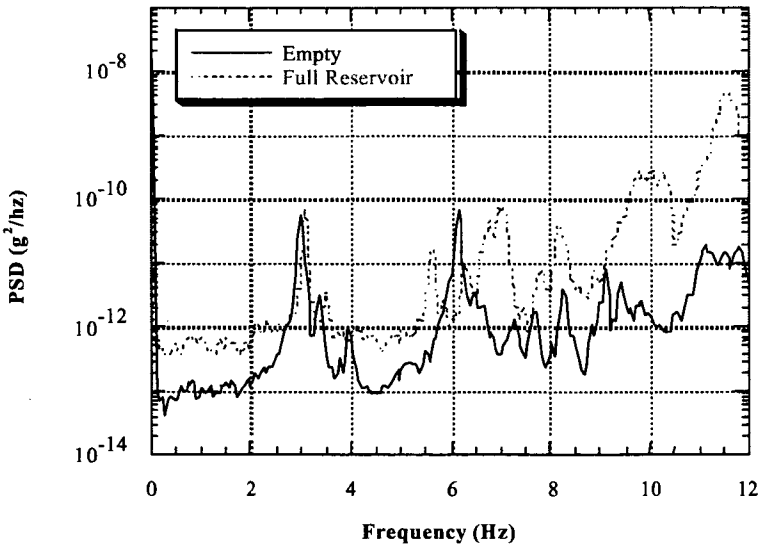


Figure 6. Measured power spectral density functions at Florence Lake Dam under empty and full reservoir conditions.

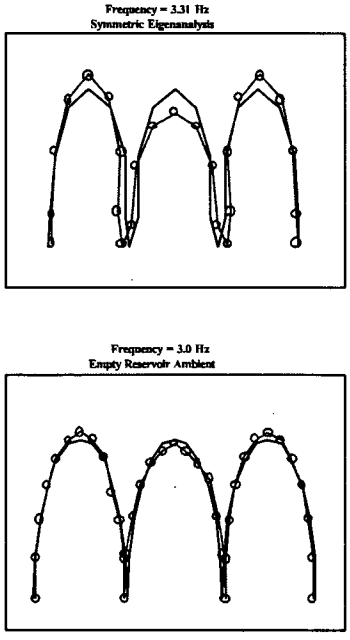


Figure 7. Comparison of predicted (top) and measured (bottom) fundamental symmetric response shapes at Florence Lake Dam under empty reservoir conditions.

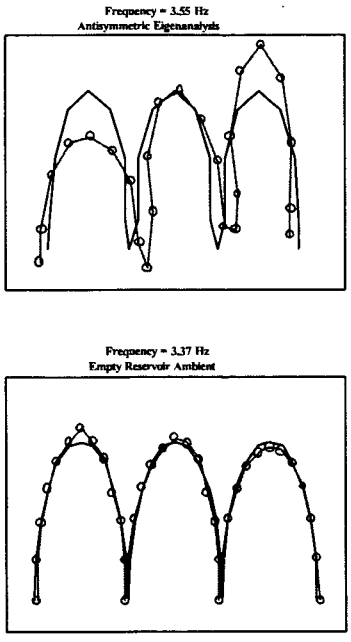


Figure 8. Comparison of predicted (top) and measured (bottom) fundamental antisymmetric response shapes at Florence Lake Dam under empty reservoir conditions.

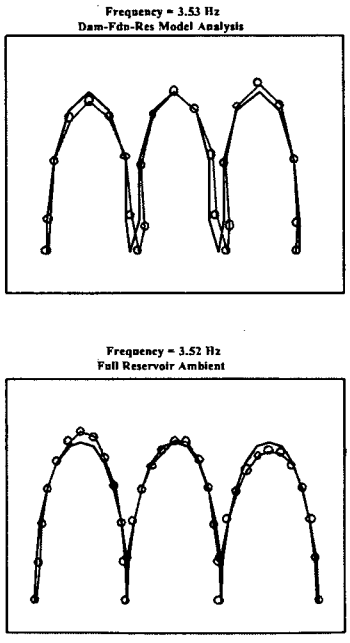


Figure 9. Comparison of predicted (top) and measured (bottom) fundamental symmetric response shapes at Florence Lake Dam under full reservoir conditions.

Characteristics of Seismic Vibrations on Rock Foundation of Dam Sites and Attenuation Relationships of Acceleration Response Spectra at Dam Foundations in Japan

by

Hideaki Kawasaki[1], Yoshikazu Yamaguchi [2], Takashi Sasaki[3] and Kenji Inagaki[4]

ABSTRACT

Japan has repeatedly experienced big earthquakes since ancient times. With the Kobe Earthquake as a turning point, the Ministry of Land, Infrastructure and Transport (MLIT) decided to install seismographs at all of jurisdictional dams for the intensification of the emergency management. The installation of seismographs was completed by the ends of the year 2000, the MLIT for 413 dams and it became possible to observe earthquake motions with high density at dam sites. Furthermore, the MLIT has been networking seismographs of dams and building the system, which can collect the information immediately after the occurrence of earthquake. In this paper, we introduce and discuss a vibration characteristic of dam foundation and a presumed attenuation equation of acceleration response spectra based on observed waveform records at dam sites.

KEY WORDS: Dam, Attenuation relationship, Characteristics of Seismic Vibration, Rock Foundation

1. INTRODUCTION

Japan is a country where many earthquakes occur, and has repeatedly experienced the big earthquakes in the past also in the world. Seismographs were installed at the Sarutani dam in 1957. It was the first case of seismograph instration among dams which the MLIT superintends, and the earthquake observation at the dam sites by the MLIT (former the Ministry of Construction) was started from that time. The Kobe Earthquake in 1995, Although the strong motion attacked many dams, some dams for power generation and city water uses near the earthquake fault had no seismographs, and earthquake data were not obtained. From such experience, the MLIT considers as the purpose of the emergency management in case of an earthquake and for the improvement of seismic design. After the Kobe Earthquake, new installation of seismographs to dams that had not got seismographs was started, and the renewal from analog-type seismographs to digital-type ones was speeded up. Installation to all 413 dams under the jurisdictional of the MLIT was completed by 2000.

Furthermore, The networking of seismographs of dams under the jurisdictional of the MLIT and Water Resources Development Public Corp. (WARDEC) has promoted, and construction of new system has been advanced for collecting of the information of dams immediately after an earthquake is occurs.
In 2001. the Public Works Research Institute

1) Head, Water Management and Dam Division, River Department, National Institute for Land and Infrastructure Management (NILIM), Ministry of Land, Infrastructure, and Transport (MLIT), 1 Asahi, Tsukuba-shi, 305-0804, JAPAN
2) Head, Dam Structures Research Team, Hydraulic Engineering Research Group (HRG), PWRI, 1-6, Minamihara, Tsukuba-shi, Ibaraki-ken, 305-8516 JAPAN
3) Senior Researcher, Dam Structures Research Team, HRG, PWRI
4) Researcher, Water Management and Dam Division, River Department, NILIM, MLIT

(PWRI) published two Technical Memorandums of PWRI about earthquake data collecting at dam sites. One [1] is about the information of seismograph installation and another [2] is about the observed data by March, 2000.

2. EARTHQUAKE MOTION CHARACTERISTICS OF ROCK FOUNDATION DAM SITES

2.1 The Range of Data

The data for analysis was acceleration data observed at the base of dam and free field near dam sites. Where, a dam base means the lowest gallery of a concrete dam, and the gallery beneath the impervious zone of a rock-fill dam. 143 sets (a horizontal direction 286, the vertical direction 143) of observation waveform records extracted from conditions of magnitude five or more, and epicentral distance to less than 200km. All waveform records were observed on the dam sites on rock foundation and the S-wave velocity of the foundation is considered to be faster than about 1000 m/s.

2.2 Analysis of Observation Waveform Records

Earthquakes were classified into three types (Inter-plate, Intra-palte, and Crustal) according to the locations of the earthquake focus. The Inter-plate earthquake is defined as the earthquake which epicenter is located in the ocean area and focus depth of is less than 60km, Iintra-plate type as the earthquake which occurs in inland area, and the Crustal type as the earthquake which occurs in the depths of 60km or more and epicenter is located in inland. Table 1 shows a list of number of earthquakes of 143 by three earthquake types.

Fig. 1 shows relationship of the magnitude, the hypocenter depth, and distance. Where, distance means the shortest distance to a fault line. The used data distributed in wide range. Although there are many earthquake records of Intra-plate type, mainly those are from the Western Tottori earthquake in 2000.

Fig. 2 shows relationship of the maximum acceleration of wave form records and distance. The presumed results from the distance attenuation relationship proposed by Fukushima et al. [3] are also shown. This distance attenuation relationship was drawn from the data recorded on firm ground. As compared with the presumed value by Fukushima et al., the acceleration at the dam site tends to be small, especially in the case of large magnitude.

Fig. 3 shows the relationship of the maximum acceleration of a horizontal direction and the vertical direction. The ratio is relatively low for the large horizontal acceleration. The effect of the earthquake types is not clear.

Fig.4 shows the correlation of the predominant period of the response spectra in the stream direction, and dam axis direction. From this figure, the predominant periods are not different for the stream direction and dam-axis direction, and are concentrated at around 0.2 seconds.

Fig.5 (a) shows the ratio of acceleration response spectrum of the stream direction and the dam-axis direction, Fig.5 (b) shows the ratio of average response spectrum of horizontal directions and response spectrum of the vertical direction. From Fig. 5 (a), the clear difference of the ratio about two horizontal components by three earthquake types isn't seen and the ratio seems to be constant over the all periods. From Fig. 5 (b), on the other hand, there is a tendency that the ratio about horizontal and vertical components is fluctuated over around 0.15 seconds

Fig.6 shows average acceleration response spectrum, and Fig.7 shows average acceleration response magnification spectrum by 3 magnitude ranges, that is, 5.5, 6.5 and 7.5, in the case of a intra-plate type. The data used

for these figures are about earthquakes of focus depth of 0-20km and distance of 0-40km. The larger the magnitude range is, the larger the period where the magnification spectrum meets the peak value is.

3 Attenuation Relationships of Acceleration Response Spectrum

For the seismic design of dams, it is important to regulate a design earthquake motion properly. Several attenuation equations of maximum acceleration or acceleration response spectra have been proposed [3][4][5][6] and utilized practically. But, those equations are for soil foundation or soft rock foundations. The new equation about attenuation relationship [7] of response spectrum presumption for rock foundation at dam was proposed recently using acceleration data accumulated in the NILIM. The equation was made based on the regression model proposed by Annaka et al. [5]. Equation (1) is a form of the regression model.

$$\log SA(T) = Cm(T)M + Ch(T)Hc - Cd(T)\log(R + 0.334\exp(0.653M)) + Co(T) \quad \cdots\cdot(1)$$

Where, T means periods, $SA(T)$ means average response spectrum of 2 horizontal directions, M means magnitude by definition of the Japan Meteorological Agency(JMA), Hc means the depth of center of fault plane, and R means the nearest distance to fault. The parameter of $0.334\exp(0.653M)$ expresses the saturation of $SA(T)$ when R approaches zero. Cm, Ch, Cd and Co are coefficients drawn by statistics processing from the acceleration waveform records observed at dam sites.

Fig.8(a) shows coefficients of Cm, Ch, Cd, Co in Equation (1) and Fig.8 (b) shows compensation factors for three earthquake types. Fig.9 shows the examples of presumed response spectrum $SA(T)$. The relationship between the presumed response spectrum $SA(T)$ and magnitude M is shown in Fig. 10(a) and the relationship between the presumed response spectrum $SA(T)$ and the distance R for specific periods, i.e. 0. 02, 0.2, 0.5, 1.0, 2.0, 4.0 sec.

4. CONCLUSION

The attenuation relationship of acceleration response spectrum for dam was introduced. The MLIT is planning revise the standard of an seismic design for dams. and presumed education introduced here is expected as one of technique to determine the design earthquake motion in seismic.We continue to collect earthquake data at dam sitesand set will improve the attenuation formula.

REFERENCES

[1] Y. Yamaguchi, T. Iwashita and J. Matsuura: Seismometers Installed in the Dams Under the Jurisdiction of the Ministry of Land, Infrastructure and Transport, Technical Memorandum of PWRI, No.3768, 2001. (in Japanese)

[2] Y. Yamaguchi and T. Iwashita: Earthquake Motion at Rock Foundation and Response of Embankment Dams by Acceleration Records at Dams in Japan, Technical Memorandum of PWRI, No.3780, 2001. (in Japanese)

[3] Fukushima et al.: Shimizu Tech. Res. Bull., Vol.10, 1-11, 1991. (in Japanese)

[4] Hongun SI and S.Midorikawa : New attenuation relationships for peak ground acceleration and velocity considering effect of fault type and site condition, J.Struct. Constr. Eng., AIJ, No. 523, pp.63-70,1999. (in Japanese)

[5] An-naka et al.: JSCE Earthquake Engineering Symposium, pp.161-164, 1997 .(in Japanese)

[6] Joyner, W.B. and D.M. Boore : Peak Horizontal Acceleration and Velocity from Strong-Motion Records Including Records from the 1979 Imperial Valley, California, Earthquake, Bull. Seism. Soc. Am., Vol.71, pp.2011-2038, 1981.

[7] Matsumoto et al.: Response Spectra of Earthquake Motions at Dam Foundations, ICOLD at Montreal, Q.83-R.35, 2003(inpress)

Table .1 Number of earthquakes clarified in 143 is classified for three earthquake type.

EQ Type	TOTAL
Intra-plate	88
Inter-plate	26
Crustal	29
TOTAL	143

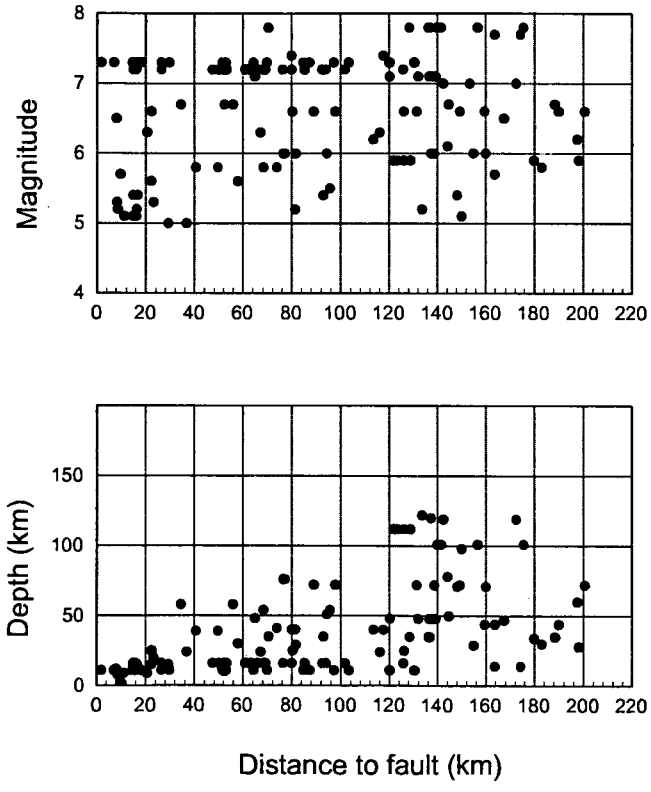


Fig.1 Relationship of magnitude, hypocenter depth with, and distance

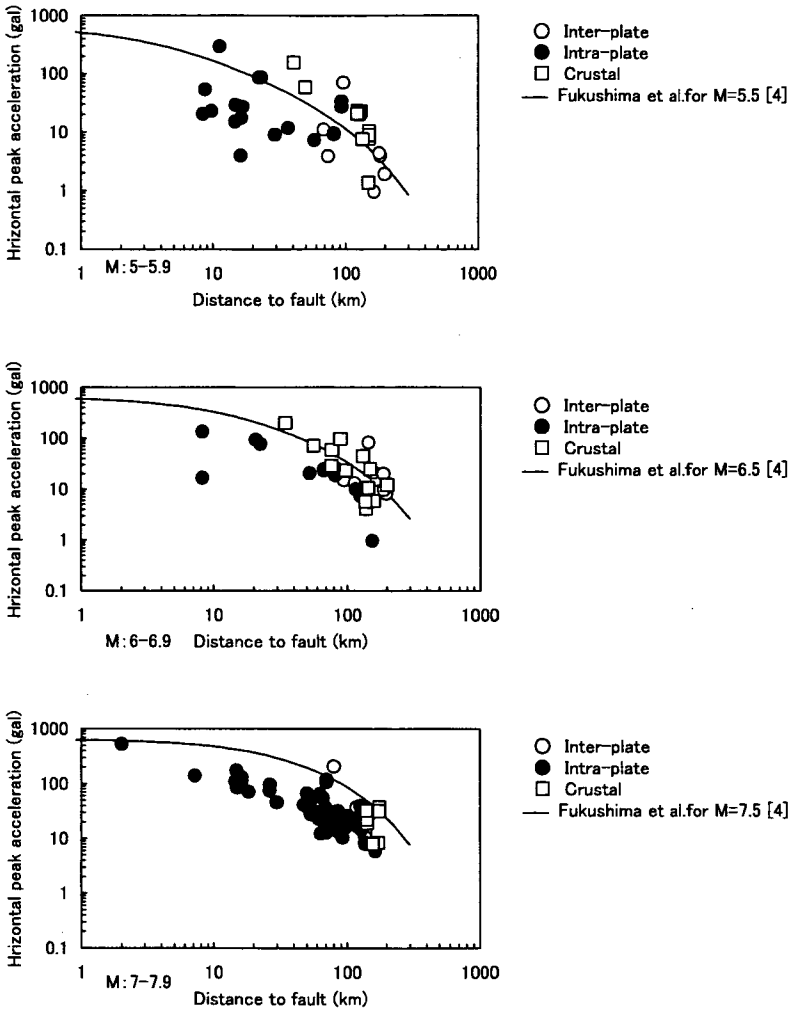


Fig .2 Relationship of maximum acceleration with distance for three magnitude ranges

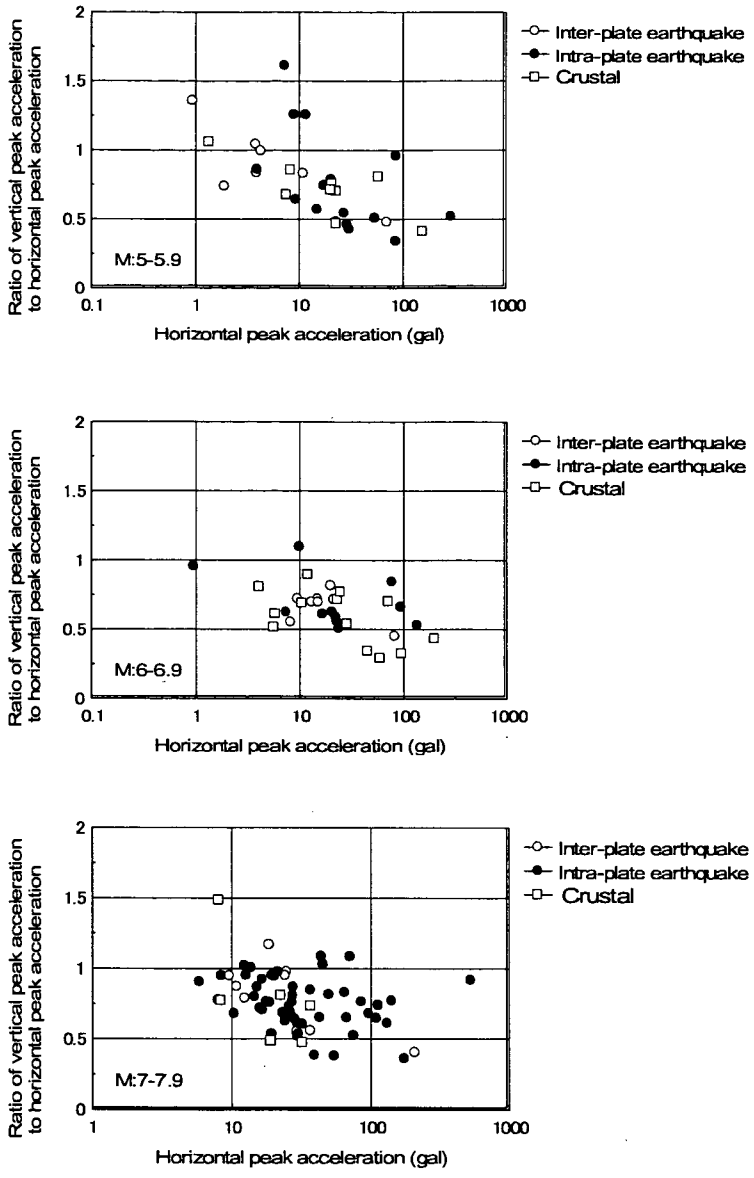


Fig .3 Relationship between maximum horizontal acceleration and ratio of maximum horizontal acceleration

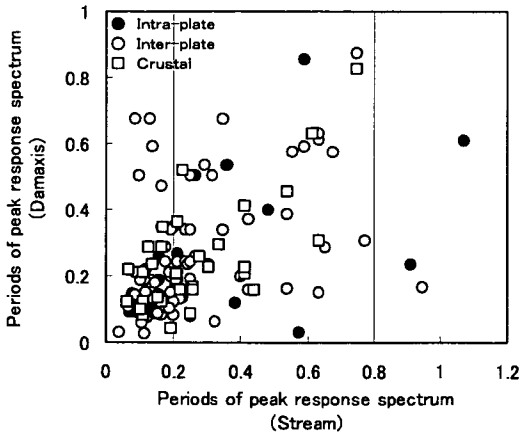
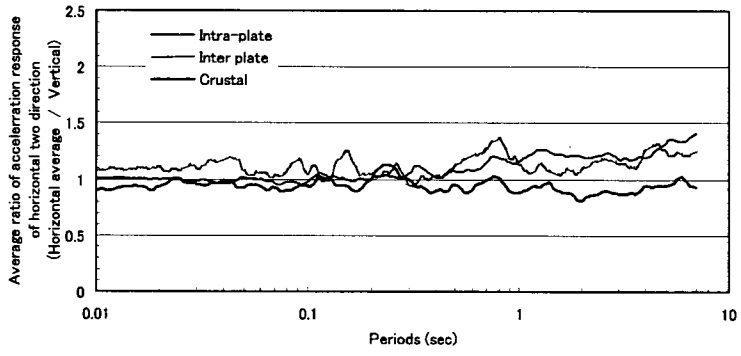
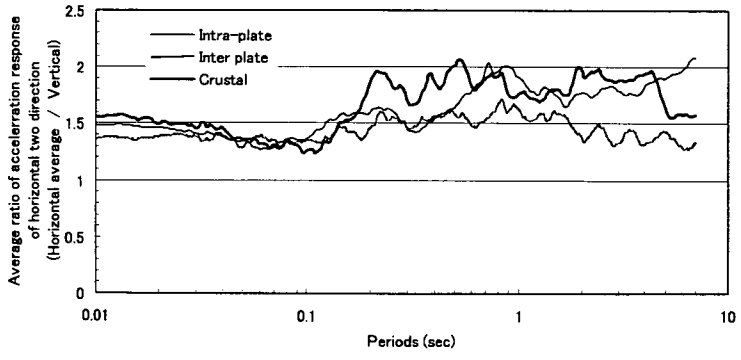


Fig.4 Correlation of predominant periods acceleration response for spectra for stream direction and dam-axis-direction



(a) Ratio of acceleration response of dam-axis direction and stream direction



(b) Ratio of acceleration response of horizontal direction and vertical direction

Fig.5 Ratio of acceleration response spectrum

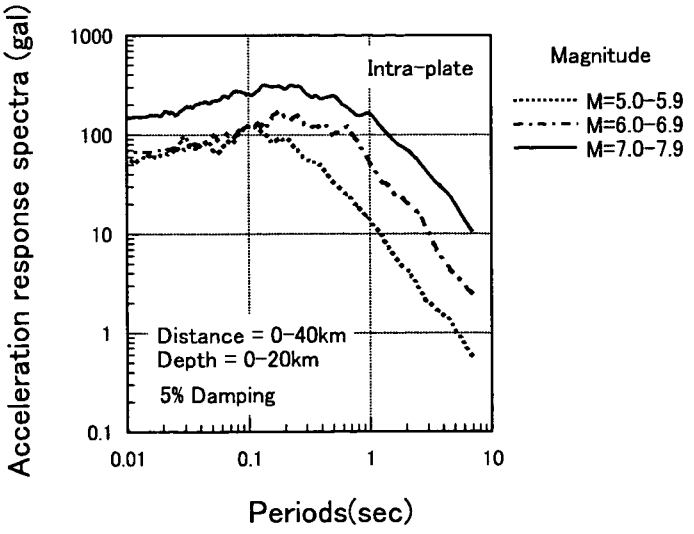


Fig 6 Relationship of average acceleration response spectrum by three magnitude ranges

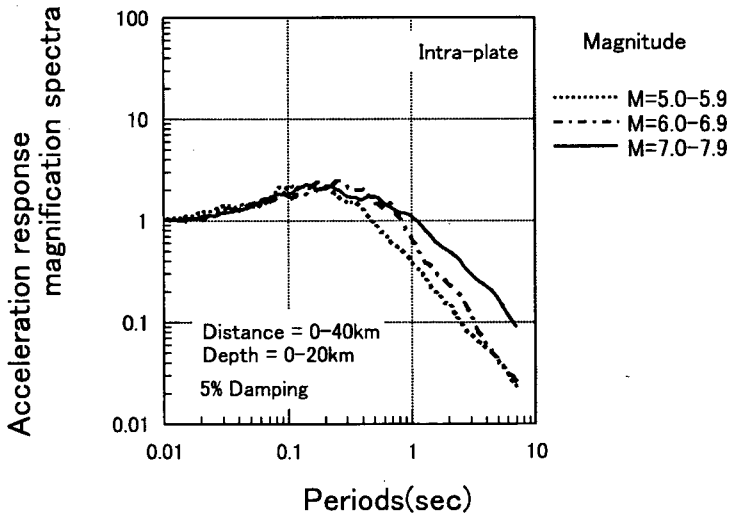
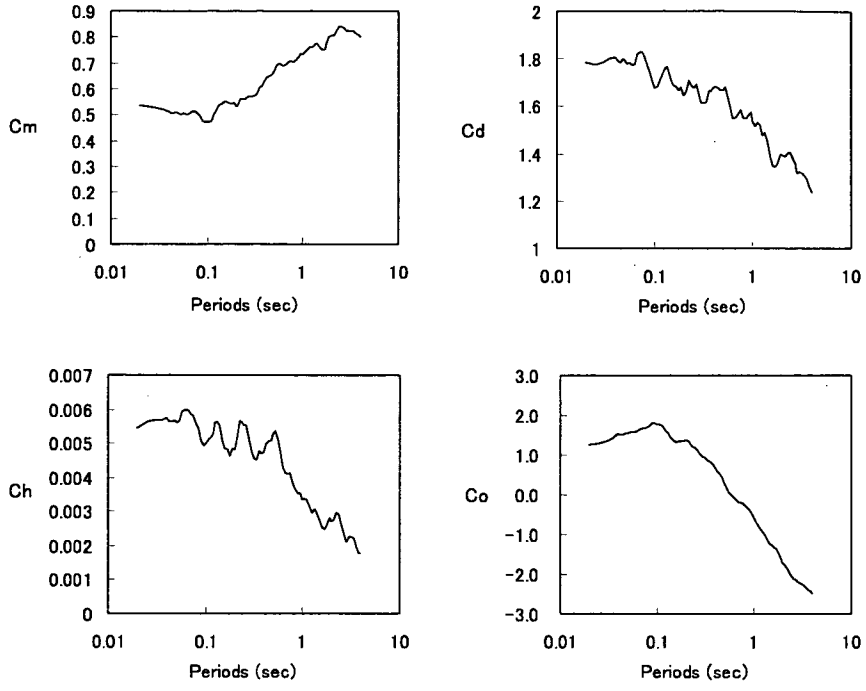
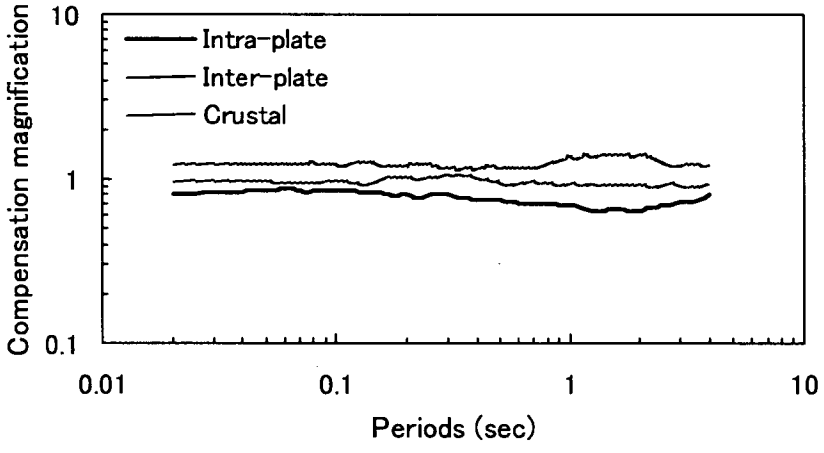


Fig 7 Relationship of average acceleration response magnification spectrum by three magnitude ranges



(a) Coefficients for attenuation equation



(b) Compensation magnification for three earthquake types

Fig 8 Coefficients for attenuation equation and compensation factors for three earthquake types

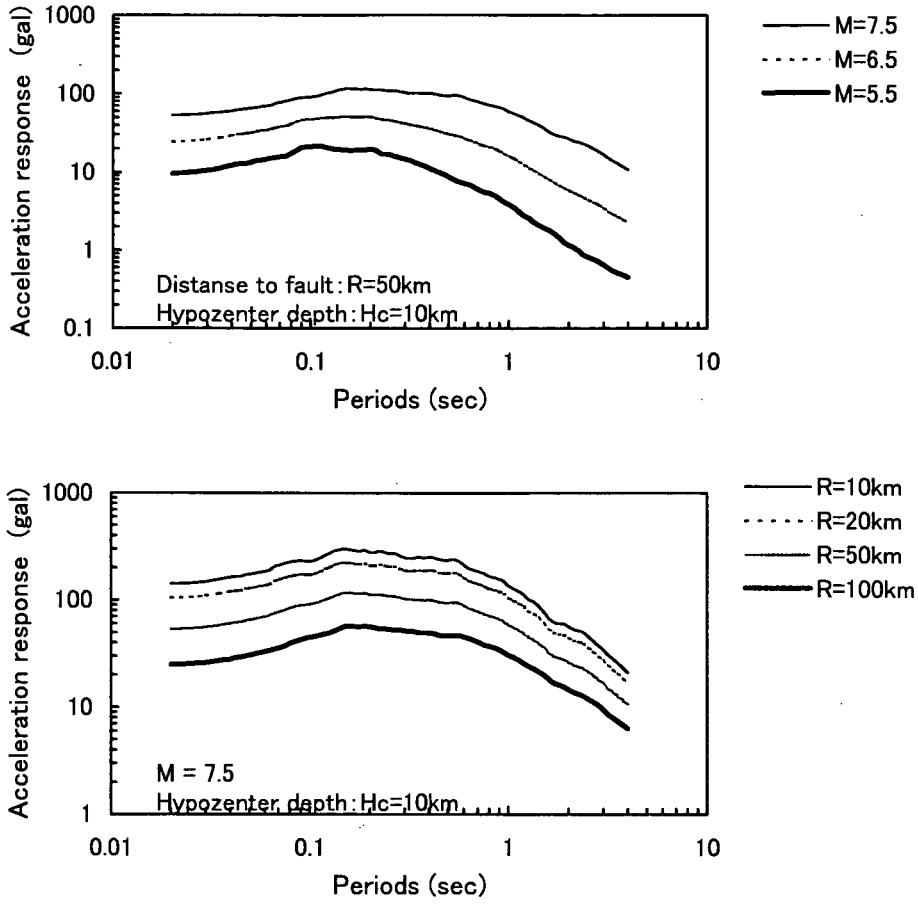
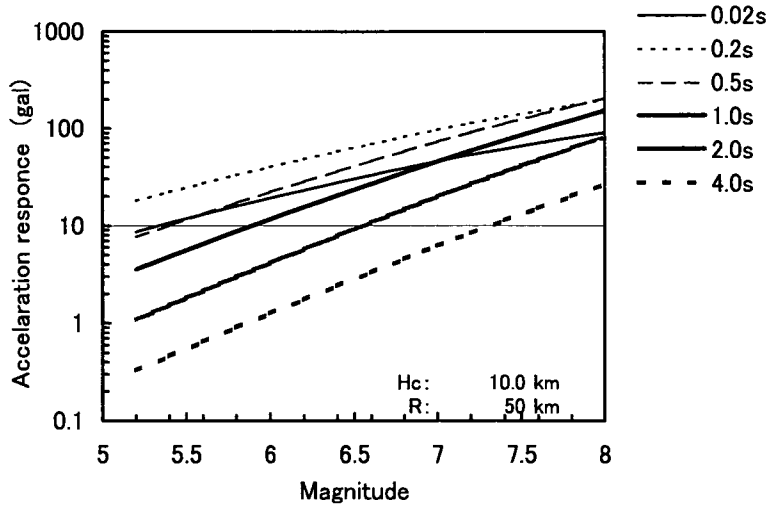
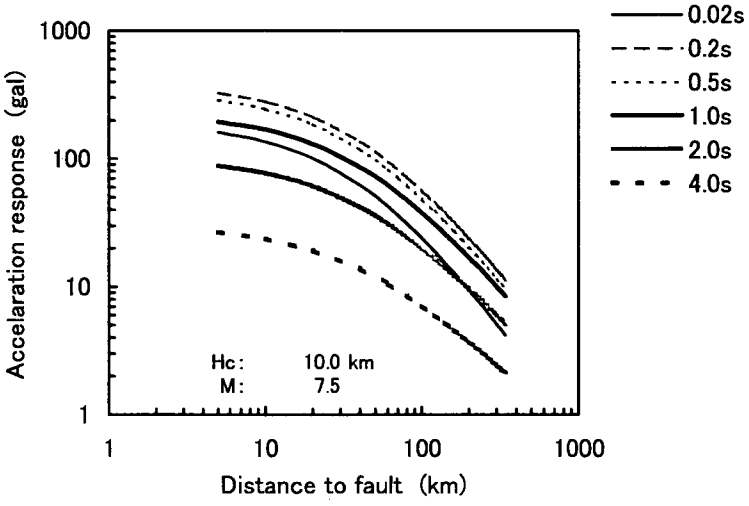


Fig 9 Presumed acceleration responses for dam foundation by attenuation equation in Ref. [7]



(a) Distance and acceleration response



(b) Magnutyude and acceleration response

Figure 10 Acceleration responses specified periods
(Depth :10km, Magnutude :7.5)

THEME 3

Next-Generation Building and Infrastructure Systems

Construction, Operation and Application of the George E. Brown, Jr. Network For Earthquake Engineering Simulation

by

Steven L. McCabe Ph.D., P.E.[1] and Joy M. Pauschke Ph.D., P.E.[2]

ABSTRACT

The George E. Brown, Jr. Network for Earthquake Engineering Simulation (NEES) recently funded by the National Science Foundation is described in this paper. Its origins, the current awards and the management of NEES is discussed. Plans for the usage of this system in large-scale research studies also are discussed.

1.0 INTRODUCTION

The George E. Brown, Jr. Network for Earthquake Engineering Simulation (NEES) is a major investment in the study of structural, geotechnical, hydraulic and infrastructure systems and their response to earthquake excitation. The NEES system is now in its final 18 months of construction and will be fully operational on October 1, 2004. Once operational, the NEES Laboratory will link researchers across the United States and the world, enabling collaboration on a scale not possible in the past.

This paper is a summary of the current status of the initiative and the plans for future use of this unique shared use system, a first of its kind in the United States.

2.0 THE INVESTMENT

NEES was developed by the National Science Foundation (NSF) based on input from the Community as to earthquake engineering experimental equipment needs as well as supportive Congressional testimony and support from the four NEHRP agencies (National Earthquake Hazards Reduction Program) that include FEMA (Federal Emergency Management Agency), NIST (National Institute for Standards and Technology), NSF, and USGS (US Geological Survey). A total of $82 million dollars (USD) was appropriated by the US Congress to fund the NEES initiative as part of a Major Research Equipment and Facilities Construction (MREFC) initiative. This is the first such large installation that has been funded by the NSF Engineering Directorate and was approved by the National Science Board in November 1998. The initial solicitation called for proposals to establish NEES equipment sites at universities within the United States as part of a Phase 1 effort. There also were solicitations for Phase 2 equipment sites, for a system developer to establish the information technology necessary to connect the sites with state-of-the-art Internet 2-based communications software and lastly for a consortium to manage the system.

The goals for NEES were to develop a system to integrate resources for research and education to serve the earthquake

[1] Program Director, Structural Systems and Hazards Mitigation, Division of Civil and Mechanical Systems, Directorate for Engineering, National Science Foundation, Arlington, VA

[2] Program Director, George E. Brown, Jr. Network for Earthquake Engineering Simulation, Division of Civil and Mechanical Systems, Directorate for Engineering, National Science Foundation, Arlington, VA

engineering community. The resources include shared use experimental facilities, data repository, simulation tools, collaborative/communication tools, leading edge computation, and model-based simulation capability.

The goals for NEES can be summarized by these items from the NEES.org website:

- Improve the seismic design and performance of our Nation's civil and mechanical infrastructure systems.
- Use advanced experimental and simulation capabilities to test and validate more complex and comprehensive analytical and computer numerical models.
- Provide end-to-end system connectivity to operate distributed experimental research equipment, including teleobservation and teleoperation, and to enable computation and distributed simulation for earthquake engineering experimentation.
- Provide researchers with remote access to a curated repository of databases, user-developed simulation software, and models for use in model-based simulation and visualization through access to a computational grid.
- Form an integrated network that facilitates interdisciplinary global collaboration among scientists and engineers.
- Enable participation from a broader earthquake engineering community, including educators, students, practitioners, and public sector organizations and individuals, who will have access to the equipment, data, models and software from NEES.

Proposals were sought by NSF from the research community in the following broad categories:

a. Shake table research equipment
b. Centrifuge research equipment
c. Tsunami/wave tank research equipment
d. Large-scale laboratory experimentation systems
e. Field experimentation and monitoring installations
f. System Integration

Proposals were reviewed and awards made. The system now is under contract with all sites actively working towards operational status. The sites that have been selected for awards are as follows:

Shake Table Research Equipment

- Award CMS-0217293
  "Large High Performance Outdoor Shake Table Facility"
  University of California, San Diego
  Frieder Seible, PI
  $5,890,000 NEES Project Web Camera:
  http://cecam.hpwren.ucsd.edu

- Award CMS-0086624
  "Development of a Biaxial Multiple Shake Table Research Facility"
  University of Nevada, Reno
  Ian Buckle, PI
  $4,398,450
  NEES project home page:
  http://bric.ce.unr.edu/nees/nees.htm
  Major equipment: Three (two upgraded) 4.3 m x 4.5 m biaxial (H-H) shake tables with two moveable, in-phase or uncorrelated motions, total specimen capacity of 1.35 MN.

- Award CMS-0086612
  "Versatile High Performance Shake Tables Facility towards Real-Time Hybrid Seismic Testing"
  State University of New York, University at Buffalo
  Michel Bruneau, PI
  $6,160,785
  NEES project home page:
  http://nees.buffalo.edu
  Major equipment: Two (one upgraded) 3.6 m x 3.6 m, 6 DOF shake tables (one moveable 50 metric ton, 100 Hz capacity), in-phase or uncorrelated motions, total specimen capacity of 100 metric tons.

Geotechnical Centrifuge Research Equipment

- Award CMS-0086566
  "A NEES Geotechnical Centrifuge Facility"
  University of California, Davis
  Bruce Kutter, PI
  $4,614,294
  NEES project home page:
  http://cgm.engr.ucdavis.edu/NEES
  Major equipment: Upgrades to existing centrifuge to enable operation up to 80 g, 2D H-V shaker, 4 DOF in-flight robot and MEMS accelerometers.

- Award CMS-0086555
  "Upgrading, Development and Integration of Next Generation Earthquake Engineering Experimental Capability at Rensselaer's 100 g-ton Geotechnical Centrifuge"
  Rensselaer Polytechnic Institute
  Ricardo Dobry, PI
  $2,380,579
  NEES project home page:
  http://www.ce.rpi.edu/centrifuge
  Major equipment: Upgrades to existing centrifuge with 2D H-H shaker, 4 DOF in-flight robot and MEMS accelerometers.

Tsunami Wave Basin

- Award CMS-0086571
  "Upgrading Oregon State's Multidirectional Wave Basin for Remote Tsunami Research"
  Oregon State University, Corvallis, Oregon
  Solomon Yim, PI
  $4,775,832
  NEES project home page:
  http://nees.orst.edu
  Major equipment: Upgrades existing wave basin to 3D tsunami testing facility, 48.8 m x 26.5 m x 2.0 m, wave maker, extensive sensors and imaging, comprehensive information architecture to support remote users, and tsunami experiment databank.

Large-Scale Laboratory Experimentation Systems

- Award CMS-0217366
  "Large Displacement Soil-Structure Interaction Facility for Lifeline Systems"
  Cornell University
  Harry Stewart, PI
  $2,072,716
  NEES project home page:
  http://nees.cornell.edu

- Award CMS-0217393
  "Real-time Multi-directional Testing Facility for Seismic Performance Simulation of Large-Scale Structural Systems"
  Lehigh University
  James Ricles, PI
  $2,593,317
  NEES project home page:
  http://nees.atlss.lehigh.edu

- Award CMS-0086611
"Large-Scale High Performance Testing Facility towards Real-Time Hybrid Seismic Testing"
State University of New York, University at Buffalo
Michel Bruneau, PI
$4,379,865
NEES project home page:
http://nees.buffalo.edu
Major equipment: Three 100-ton dynamic actuators, two 200-ton static actuators, hydraulic pumps, digital control system

- Award CMS-0086621
"Reconfigurable Reaction Wall-Based Earthquake Simulator Facility"
University of California at Berkeley
Jack Moehle, PI
$4,268,323
NEES project home page:
http://nees.berkeley.edu
Major equipment: Reconfigurable reaction wall blocks (14 - each 3.3m x 5.2 m), seven dynamic and static actuators, high performance digital control system. Equipment used to develop new hybrid testing methods.

- Award CMS-0086592
"Fast Hybrid Test Platform for the Seismic Performance Evaluation of Structural Systems"
University of Colorado, Boulder
P. Benson Shing, PI
$1,983,553
NEES project home page:
http://ceae.colorado.edu/nees
Major equipment: High speed actuator, 980 kN, +/- 120 mm stroke, 950-lpm servo valve with max. velocity of 120 mm/sec; upgrade two 490 kN actuators, +/- 120 mm stroke, with 950 lpm servo-valves to attain 450 mm/sec velocity; three channel digital controller; 32-channel data acquisition system

- Award CMS-0086602
"A System for Multi-Axial Subassemblage Testing (MAST)"
University of Minnesota-Twin Cities
Catherine French, PI
$6,472,049
NEES project home page:
http://www.ce.umn.edu/mast
Major equipment: MAST system consisting of cross heads (large steel weldments for the top and bottom reaction surfaces), digital controller with 6 DOF control system, and high performance actuators.

- Award CMS-0217325
"Multi-Axial Full-Scale Sub-Structuring Testing and Simulation Facility"
University of Illinois at Urbana-Champaign
Amr Elnashai, PI
$2,958,011
NEES Project Home Page:
http://cee.uiuc.edu/research/nees

Experimentation and Monitoring Installations

- Award CMS-0217421
"Permanently Instrumented Field Sites for Study of Soil-Foundation-Structure Interaction"
Brigham Young University
T. Leslie Youd, PI
$1,944,423
NEES Project Home Page:
http://nees.crustal.ucsb.edu/

- Award CMS-0086596
  "Field Testing and Monitoring of Structural Performance"
  University of California, Los Angeles
  John Wallace, PI
  $2,652,761
  NEES project home page:
  http://www.cee.ucla.edu
  Major equipment: One omni-directional and two uni-directional eccentric mass vibrators, one linear inertial shaker, cone penetration truck (seismic piezocone, 20-ton hydraulic push capacity, side augers, and in situ-soil vibration sensors)

- Award CMS-0086605
  "Large-Scale Mobile Shakers and Associated Instrumentation for Dynamic Field Studies of Geotechnical and Structural Systems"
  University of Texas at Austin
  Kenneth Stokoe II, PI
  $2,937,036
  NEES Project Home Page:
  http://www.geo.utexas.edu/nees
  Major equipment: One 3-D mobile shaker, 2 cubical stand alone 3D shakers, instrumentation van with field equipment and multi-channel data acquisition and processing system.

NSF 00-7, NEES: System Integration

- Award CMS-0117853
  "NEESgrid: A Distributed Virtual Laboratory for Advanced Earthquake Experimentation and Simulation"
  University of Illinois at Urbana-Champaign
  Daniel Reed, PI
  $10,000,000
  NEES Project Home Page:
  http://www.neesgrid.org.

- Award CMS-0004246
  "Earthquake Engineering Research Community Workshop"
  University of Illinois at Urbana-Champaign
  Thomas I. Prudhomme, PI
  $89,100
  Workshop Report:
  http://www.neesgrid.org

NSF 01-56, NEES: Consortium Development

- Award CMS-0126366
  "George E. Brown, Jr. Network for Earthquake Engineering Simulation (NEES) Consortium Development Project"
  Consortium of Universities for Research in Earthquake Engineering
  Robert Reitherman, PI
  $1,999, 907
  NEES project home page:
  http://www.nees.org

In addition to the awards listed above, additional funding is being provided by NSF to assist the NEES equipment sites in developing their local information technology infrastructure. This funding is in addition to the specific equipment and the overall system integration awards

Two studies have been awarded to provide NSF with input as to future usage of the NEES system:

Developing a Long-Term Research Agenda for the Network for Earthquake Engineering Simulation, Richard Little, PI, National Academy of Sciences, rlittle@nas.edu

The Earthquake Research Plan: Research Needs and Opportunities for Earthquake Engineering, Susan K. Tubbesing, PI, Earthquake Engineering Research Institute, skt@eeri.org

Results of the EERI study is available from EERI; the NAS study will be published

shortly. These studies will be utilized by NSF and by researchers in the development and selection of research topics for study using NEES.

It can be seen that there are three shake table facilities (UCSD, Reno and SUNY-Buffalo); one tsunami facility at Oregon State, three filed monitoring awards (UCLA, BYU and UT-Austin), two geotechnical centrifuge facilities (UC-Davis and Rensselaer), one award for system integration (Illinois) and seven large equipment sites (Colorado, Minnesota, UC-Berkeley, SUNY-Buffalo, Illinois, Lehigh and Cornell), Figs. 1-4. A total of 16 equipment awards at 15 different equipment sites, all at universities, plus awards for the overall system integrator and for NEES system management were made. At this time there are three sites that are operational, including the facilities at UN-Reno, Rensselaer and the tsunami facility at Oregon State.

In terms of the equipment, briefly the system provides the capability of examining performance of large systems-level problems. The three shake table facilities each have unique capabilities. UCSD is building an outside shake table facility that will have no headroom or crane limitations. Moreover, a soil pit is located adjacent to the table to enable studies of soil-foundation-structure interaction issues. The Reno and Buffalo facilities have the ability to input differential movements on the various tables (two at Buffalo and three at Reno). These movement permit study of motions exciting bridge piers and similar large structures where input motions are not identical at each support location.
The centrifuge facilities and tsunami tank provide abilities to study soil behavior and tsunami effects. The filed systems permit detailed monitoring of shaking and other attributes of soil or structural sites in real time. The large equipment sites provide servo-hydraulic actuator capabilities with advanced control features to impose motions, or forces, on structural elements.

The unique aspect of this overall system is that the telepresence and teleobservation features permit researchers to monitor testing conducted at another site in real time. Moreover, motions from one test can be imposed on another test specimen at another site. This permits large scale tests coupled with more detailed component tests of subsystems at other sites. The computational capabilities of the sites also permit researchers to substructure large systems so as to compute displacements and rotations of subassemblies and to impose these movements on test specimens at their or other sites. These capabilities are collectively referred to as NEESgrid and represent a significant advancement in distributed connectivity to permit real time data and audio and video communication. The system is schematically shown in Fig. 5.

3.0 NEES – A NEW APPROACH TO RESEARCH

The NEES Laboratory provides a large investment in state-of-the-art equipment for the various equipment sites. What is revolutionary is the collaboratory that also is set in place as part of NEES. With the IT system, the NEES equipment sites, as well as researchers worldwide are able to participate in research and to share and view results in real time. It will be possible for remote collaborators to participate actively in experiments in real time – to witness and even control testing as it occurs through telepresence features of NEES. Moreover, as part of the system, researchers are required to post results and to *share* data. This will permit greater usage of test results from those directly involved, as well as independent studies that may follow. All data will be placed in an archive to permit long-term storage and retrieval. Lastly, NEES will permit the use of secondary, or payload, experiments. Here tests will include nonstructural items such as sensors and transducers, mechanical systems and other important nonload carrying systems that may be tested as part of the overall structural testing. It is hoped that in this

way, next generation sensors and other new technologies may be developed and tested.

The NEES system will operate over the ten-year period from October 1, 2004 through September 30, 2014. Additional support will be provided by NSF during this ten year period to help the equipment sites operate and maintain this virtual laboratory. These funds will be separate from any research funding or other equipment awards from NSF.

A major part of the NEES system does not involve technology but people. The system provides a means for researchers anywhere in the world to actively participate in research. The integrated nature of the system and the NEESgrid infrastructure will permit researchers to truly collaborate with colleagues who may be located at other equipment sites, US universities or other institutions where there are no NEES awards, and with colleagues outside the United States. It becomes a truly universal laboratory that is not limited by the constraints of time or place.

Management issues with NEES also are significant. Figure 6 shows the NSF management team that is in place to manage this project. The team is located within the Civil and Mechanical Systems Division of NSF and draws on input from the various program directors within CMS. Research funding for NEES projects is being developed separate from the NEES project team but also within CMS, and draws on input from the NEES team. Figure 7 shows the overall NSF management plan during the 10 year operational period of NEES.

4.0 APPLICATION OF NEES IN RESEARCH

At the present time, NSF is preparing a major solicitation for research proposals to utilize the NEES System. This solicitation for NEES research will invite researchers to propose studies of three levels support: Individual Investigator Awards, Small Group Awards and Grand Challenge Awards. These awards range from small individual studies to larger systems investigations:

Individual Investigator Awards will be studies of a specific problem that will involve some level of experimental work at a NEES site. These projects are anticipated to be three years in duration. One or more principal investigators may be involved.

Small Group Awards will be made for larger projects that involve colleagues from more than one institution or organization. These problems will be of larger size and will involve usage of at least one NEES facility plus use of experimental facilities at other sites. More than one principal investigator will be involved. These awards will be of up to four years in duration.

Grand Challenge Awards will be made for large systems level projects that attack important problems that have not been studied previously. These projects will utilize the full capability of the NEES system and will involve many colleagues at a variety of institutions and will utilize testing facilities at NEES and other laboratories. Grand Challenge problems will be multidisciplinary in nature to examine *system* response. These large awards will be of up to five-year duration and will require a broad constituency to be involved. Colleagues from NEES and other facilities are required, as is representation from institutions from other geographical regions of the United States. Projects funded as Grand Challenge problems will be seminal in nature, that is, projects will be of a size and scope that a significant advance in the state of knowledge will be achieved. Incremental studies will not be funded as Grand Challenge problems.

In all of these awards, proposers are encouraged to involve underrepresented groups in the research teams. Colleagues from institutions not normally involved in earthquake engineering research are

encouraged to be included in these teams. Thus PI's from undergraduate, minority or from other schools that have not had a significant role in earthquake engineering research are strongly encouraged to be involved. These requirements are in addition to the typical goals of including colleagues from underrepresented groups that include racial, social and gender considerations.

In this way, NSF is attempting to put in place a system that will enable participants from across the United States to be involved. The technical limitations are being removed via the technology that is being employed. Social limitations are being removed by the proposal rules in place so that no one region, university system or NSF-sponsored engineering center will be permitted to solely submit proposals as Grand Challenge projects.

Funding levels for these projects are to be based on availability of funds. It is anticipated that significant new levels of funding will be required to sustain NEES-related research during the 10-year operation period overall and above current funding levels within CMS. The Grand Challenge projects are anticipated to be funded at levels up to $1.4 million per year over the five-year term. Support from the Community will be critical to ensure that the support for NEES research in terms of increased funding for earthquake engineering research will continue to be maintained during this 10 years of NEES operation.

One particular aspect of this new research tool is the role of international laboratories in NEES. Research. It is hoped that colleagues from institutions outside the United States will be interested in participating in NEES research. While NSF funding cannot directly go to support research in non-US locations, there is the strong interest within NSF and the Community to have colleagues from international locations actively participate via NEESgrid and related IT tools. Thus NEES becomes a truly international resource in which colleagues, no matter where they are located, can observe experiments, share data and fully participate in research at one or more of the NEES sites. International laboratories will have to opportunity to essentially become nodes on the NEESgrid so that geography will be eliminated and that the best possible research teams can be formed to tackle important research problems.

5.0 THE US-JAPAN JOINT PANEL AND NEES

The introduction of NEES as a research tool offers significant possibilities for future collaboration between institutions in Japan and the United States. One can easily foresee a series of connection points to NEES, or so-called "NEES nodes," that lay both inside and outside of the United States. While these international nodes will be funded by the appropriate "local" funding agency, the technical connection and interoperability of systems can be readily achieved. The possibility of having colleagues in the US work together with colleagues from other countries is an outcome of NEES that the Joint Panel should encourage. In particular, the strong cooperation of the research communities in Japan and the US over the years should serve both as a model and as a vehicle to empower this cooperation. The evaluation of different solutions developed in Japan and the US in response to common problems can be a very useful aspect of future research using NEES.

The role of Task Committee B in NEES also can be significant. The charge of the Committee is to promote the next generation of buildings and infrastructure technology. With the capability that NEES has, together with the focus of the upcoming NSF research solicitation, it is apparent that the goals of Task Committee B and of the NEES group within NSF are quite similar. Thus, it is important for Task Committee B to act as a mechanism to promote collaboration in

research among Japanese and American researchers. Moreover, Task Committee B – and the Joint Panel – can assist in helping to set the research agenda and to help identify the critical problems that the NEES System should be used to investigate.

6.0 CONCLUSION

The George E. Brown, Jr. Network for Earthquake Engineering Simulation (NEES) funded by the National Science Foundation will be operational on October 1, 2004. It is hoped that NEES will usher in a new era in truly collaborative research, involving the entire earthquake engineering community from across the US and across the world. The equipment that is being installed at the various sites will provide resources to study systems-level problems that have not been studied before due to facility limitations. During the 10-year operational period, it is hoped that knowledge of how large-scale systems, and their components, respond to earthquake excitation will be significantly increased. The goal is to greatly expand knowledge and to significantly impact the state of the art in design of systems to resist earthquake excitation.

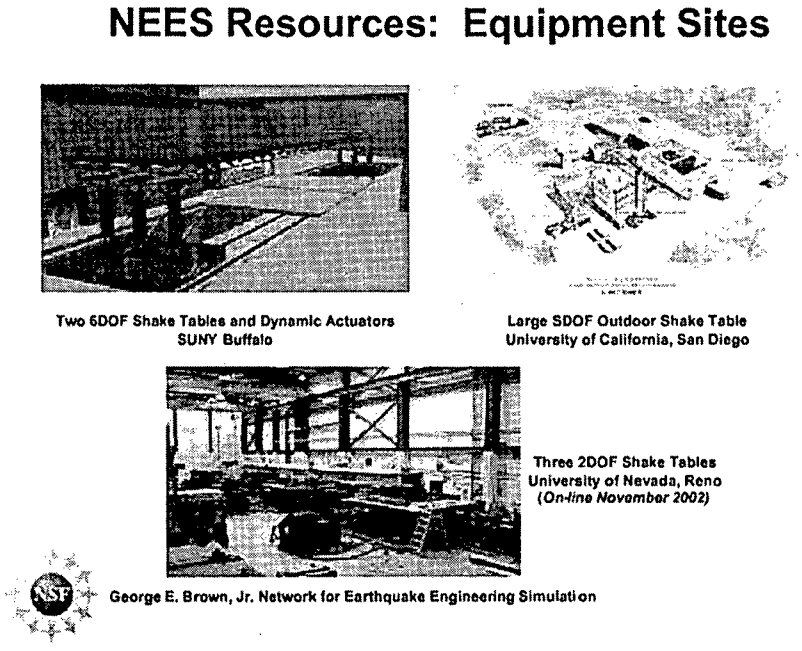


Figure 1. NEES Awards to SUNY Buffalo, UC San Diego and UN Reno

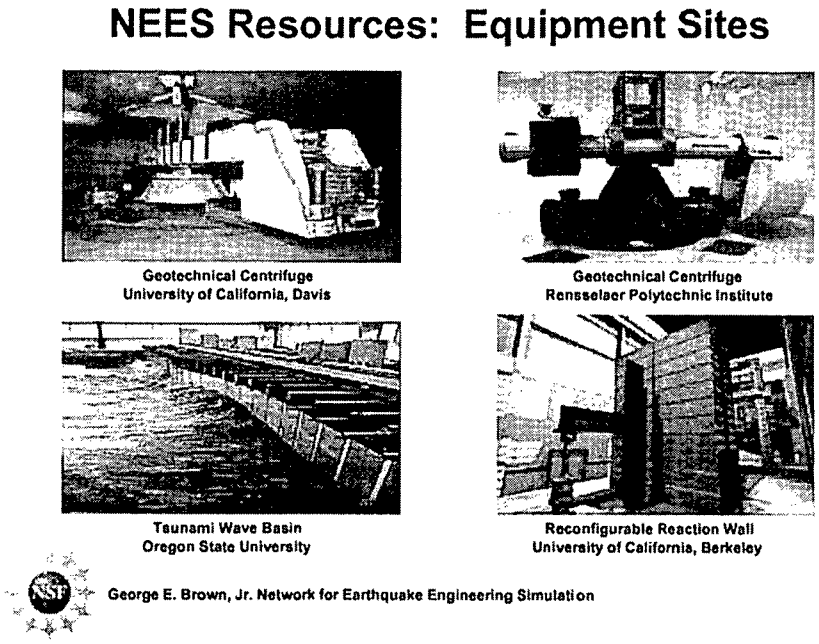


Figure 2. NEES Awards to UC Davis, Rensselaer, Oregon State and UC Berkeley

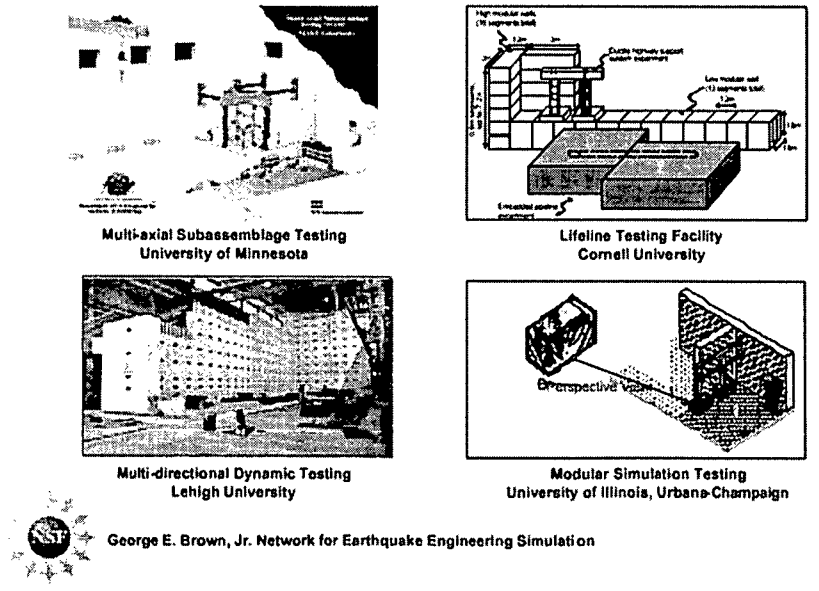


Figure 3. NEES Awards to Minnesota, Cornell, Lehigh and Illinois

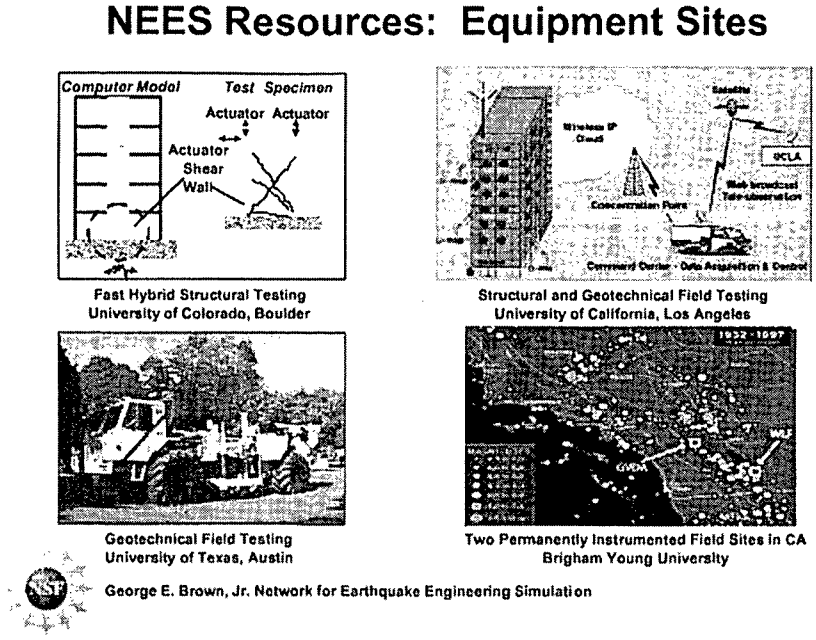


Figure 4. NEES Awards to Colorado, UCLA, UT Austin and BYU

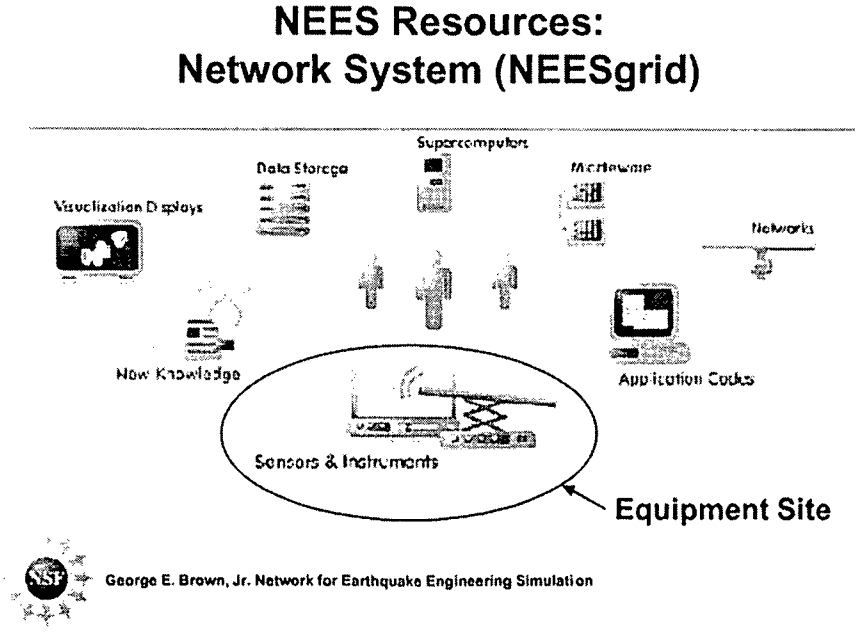


Figure 5. NEESgrid System

George E. Brown, Jr. Network for Earthquake Engineering Simulation
NEES Oversight during Construction Period: FY 2000 - FY 2004

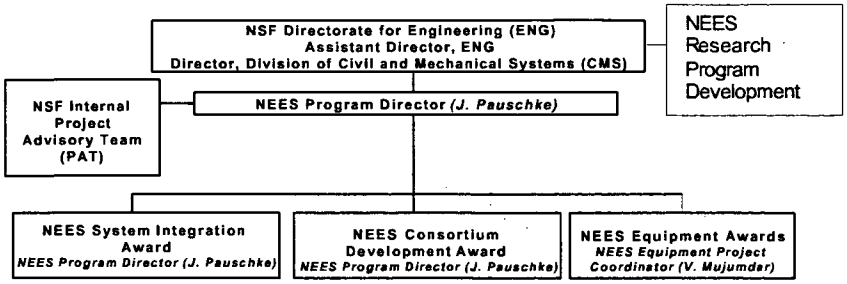


Figure 6. NSF Management Structure for NEES

George E. Brown, Jr. Network for Earthquake Engineering Simulation
NEES Oversight during Operational Period: FY 2005 - FY 2014

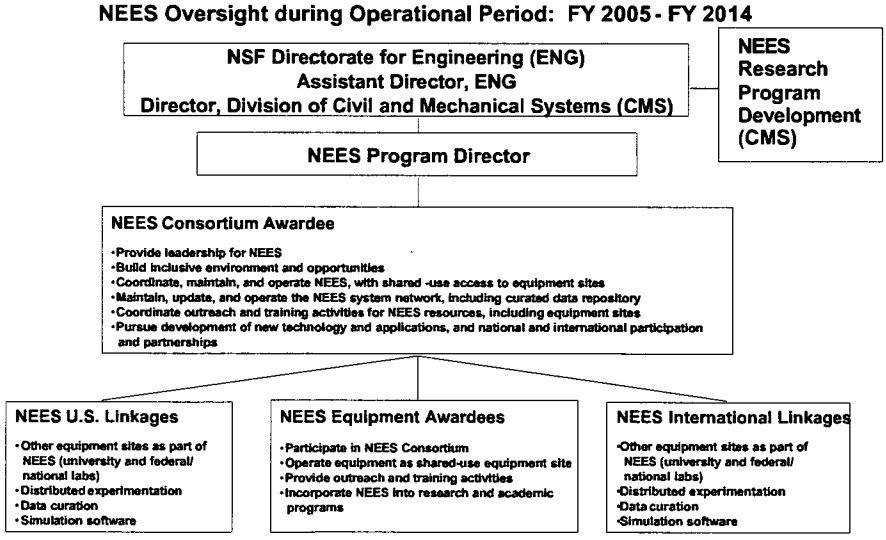


Figure 7. NEES Operation and Research Program

PROJECT ON 3-D FULL-SCALE EARTHQUAKE TESTING FACILITY (THE THIRD REPORT)

by

Keiichi OHTANI[1], Nobuyuki OGAWA[2], Tsuneo KATAYAMA[3], Heki SHIBATA[4]

ABSTRACT

Considering the lessons learnt from Hanshin-Awaji Earthquake, NIED plan to construct "E-Defense", which will be able to simulate the processes of destruction of structures under the condition of real strong earthquake motions. The basic performance of "E-Defense" are maximum lording capacity 1,200 tons, maximum velocity 200 cm/s and maximum displacement +/- 1 m for horizontal excitation and maximum velocity 70 cm/s, maximum displacement +/- 50 cm for vertical excitation to realize destructive ground motion. The construction work of "E-Defense" has been begun at early 2000, and will be completed at the beginning of 2005. We are conducting the construction works of the facility at the Miki-city, and the manufacturing of actuators, oil-pressure supply system and other major part of shaking table at the MHI. "E-Defense" is the very large scale and high performance testing facility in the world. "E-Defense" should be operated the international common use. For the international collaboration and the dissemination of research results, E-Defense Network ("ED-Net") will also construct until the completion of "E-Defense". We hope that "E-Defense" and ED-Net will be situated to one of the cooperative research organization for the earthquake disaster mitigation in the world.

KEY WORDS:

Failure mechanism of structures
Full Scale Testing
International Common Use
3-D Shaking Table
Network of Earthquake Research

1. INTRODUCTION

The Hanshin-Awaji Earthquake (Hyogoken-Nanbu Earthquake, January 17, 1995) clearly demonstrated that the occurrence of very strong ground motion in the area near to the seismic fault is capable of causing severe structural damage beyond general estimation. The destructive earthquake occurred in the worldwide in the recent years, such as Northridge earthquake (1994), Umbria-Marche earthquake (1997), Kocaeli earthquake (1999), Ji-ji earthquake (1999), El Salvador earthquake (2000), Gujarat earthquake (2001) and so on.

In order to reduce the hazards associated with large earthquakes, it is essential to improve the reliability of earthquake resistance estimations and reinforcement methods in the construction of urban and major structures. For this purpose, failure mechanisms and collapse processes of various kinds of full-scale structures must be investigated. Many types of experimental apparatus have been used for such investigations, and some of them have as large a size as possible to alleviate any difficulties arising from limitation

1) Project Director, 3-D Full-Scale Earthquake Testing Facility (E-Defense), National Research Institute for Earth Science and Disaster Prevention (NIED), Tsukuba, Japan

2) Project Sub-Director, E-Defense, NIRD, Japan

3) President, NIED, Japan

4) Visiting Research Fellow, NIED, Japan

of the model. Considering the lessons learnt from recent earthquake disasters, the National Research Institute for Earth Science and Disaster Prevention (NIED) planned to build a new three-dimensional, full-scale, earthquake testing facility, which can carry large-size soil and structure models and reproduce the processes of structural failure. This facility is expected to become a powerful tool for international collaboration in earthquake engineering research. It also requires international cooperation to successfully complete the facility and to use it effectively for engineering purposes.

Following the technical developments and surveys in earthquake engineering and related fields, the NIED began the design and construction of this new facility in the Japanese fiscal year of 1998.

We already reported twice for the Joint Meeting of Wind and Seismic Effects, UJNR. In the first report (30UJNR), we described the introduction of project on E-Defense. In the second report (34UJNR), we summarized the construction plan and Earthquake Engineering Network (EE-Net), which is the tool for ensure of the international collaboration and the dissemination of research results. The name of EE-Net was changed to E-Defense Network (ED-Net), because new name can explain more suitable to our network.

This paper is the progress report of our project, such as construction and installation works, control and measurement systems and management mechanism.

2. E-DEFENSE (3-D FULL-SCALE EARTHQUAKE TESTING FACILITY)

Based on the lessons learnt from Hanshin-Awaji earthquake, the Minister of State for Science and Technology was inquired to the Council for Aeronautics, Electronics and Other Advanced Technology, which is the one inquire organization of the Minister, for the discussion of the effective arrangement of research bases for earthquake disaster mitigation at March 29,1996. The Council was reported to the Minister at September 3, 1997.

The report was clearly pointed out the arrangement of large-scale three-dimensional earthquake simulator facility as the core facility of research bases for earthquake disaster mitigation.

NIED initiated the project on the large-scale three-dimensional earthquake simulator facility just after the occurrence of Hanshin-Awaji earthquake. The research and development for core technology for this facility (E-Defense) was started on 1995. The fundamental concepts of this project based on the report by the council.

The E-Defense will construct as the core facility of the research bases for earthquake disaster mitigation. Therefore, we need to clear the positions of the E-Defense.

1) Position of earthquake simulator for the main element of development of the "Time-Space Domain Simulation System for Earthquake Disaster.)
2) Position of the clearly understanding of failure mechanism of structures.
3) Position of the response mechanism for the request from major subject of earthquake engineering.

The importance of promoting the strengthening and rationalization of earthquake-proof structural design is just one of the lessons from Hanshin-Awaji earthquake. Because earthquake vibrations involve three-dimensional movement, it is necessary to set up a three-dimensional earthquake simulator facility to accurately reproduce earthquake motions. To perform tests on real-size objects or large-scale models of test structures and foundations, it is desirable to have the large-scale three-dimensional shaking table. If large-scale 3-dimensional shaking table is available, tests could be performed to shed new light on the mechanism of dynamic failure using real-size structures. If a stage reached whereby

design based on such discovery can be performed, this will contribute immensely to reducing earthquake disaster.

The main specification of E-Defense is shown in Table 1. The actuator performance for horizontal and vertical axes is shown in Fig. 1.

Table 1. Main Specification of E-Defense

Payload	12MN(1200tonf)	
Size	20m × 15m	
Driving Type	Accumulator Charge Electro-Hydraulic Servo Control	
Shaking Direction	X・Y – Horizontal	Z–Vertical
Maximum Acceleration (at Maximum Loading)	>900cm/s²	>1,500cm/s²
Maximum Velocity	200cm/s	70cm/s
Maximum Displacement	±100cm	±50cm
Maximum Allowable Moment	Overturning Momnet	Yawing Moment
	150MN・m	40MN・m

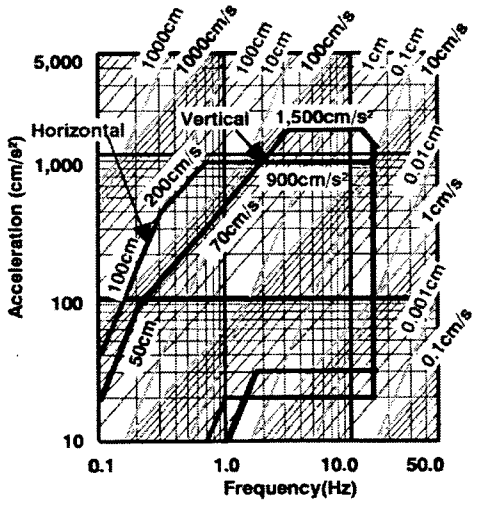


Fig. 1. Limit Performance of E-Defense

3. CONSTRUCTION AND MANUFACTURING OF E-DEFENSE

NIED have commenced the development work of shaking mechanism with very large size of hydraulic actuators in fiscal year 1995 and completed performance tests successfully in 1998. Following the above technical development and surveys in earthquake engineering and related fields, NIED have began the design and construction of E-Defense in 1998.

The construction work has been begun in 1998 and will be completed at the beginning of 2005. The new facility will start to operate at the 10 years after the Hanshin-Awaji earthquake. The E-Defense is constructed in "Miki Earthquake Disaster Memorial Park (tentative name)", which is being constructed in Miki city, on the north of Kobe city. The construction of shaking table foundation was started at the construction site in January 2000.

The manufacturing of testing equipments, such as actuators, 3-dimensional link joint, oil power pump unit, accumulator unit and so on, were started in 1998.

We will construct several buildings, such as Experimental Building, Operation Building, Hydraulic Unit Building, Preparation Building and so on. The 3-dimensional shaking table will be installed in the experimental building. Hydraulic oil will be supplied to shaking table by pipelines via underground culvert. The reaction foundation (shaking table foundation) has weight of about 2 GN (200,000 tonf) and set to the bedrock directly.

Following the construction of shaking table foundation, we construct the experimental building and other buildings. The experimental building is 60 m X 85 m in plan and 45 m height and has tow sets of 400 tons crane. For the construction of large space frame, we developed and applied new construction methods, such as the sliding construction method for roof members using permanent traveling crane structure, and the large panel method of external wall by steel frame and sandwiches panel. Fig. 2 and 3 show the construction views of sliding construction method and large panel method, respectively.

For the construction of hydraulic unit building, we also developed and applied new method, which is the robot painting method of external wall. Fig. 4 shows the robot painting method.

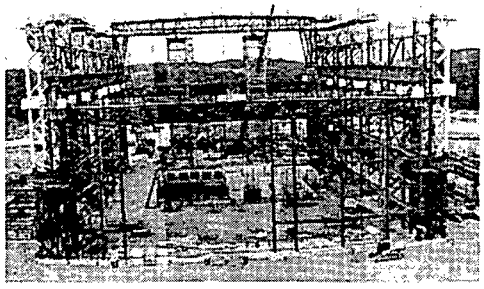


Fig. 2 Sliding Construction Method

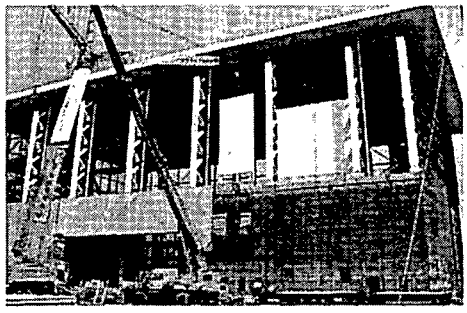


Fig. 3 Large Panel Method

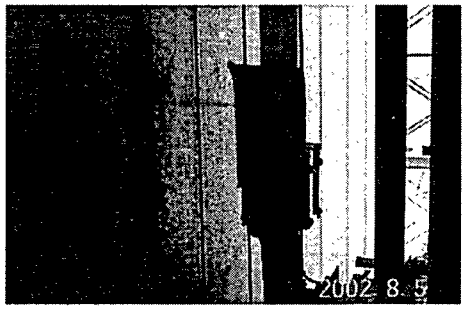


Fig. 4 Robot Painting Method

The manufacturing of the testing equipment, such as actuators, 3-dimensional link joint, oil power pump unit, accumulator unit and so on, were also started in 1998. By the condition of construction site, where is located at the hill area, the weight and length of manufactured unit are limited some size by the condition of transportation. The set-up working was done at the site.

The installation of piping system, actuators, pumping units and accumulator units were started in 2000. Figs. 5 – 8 are shown the installed condition of actuators, pumping units, accumulator units and the recent construction condition of buildings, respectively.

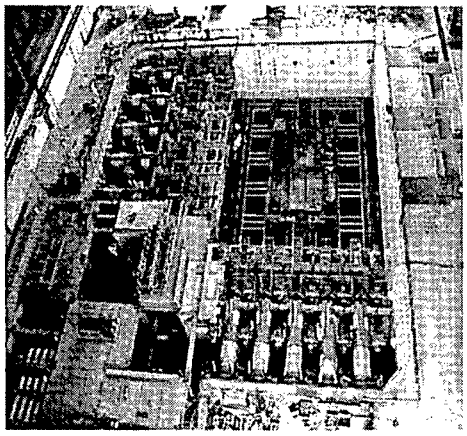


Fig. 5 Installation of Actuators

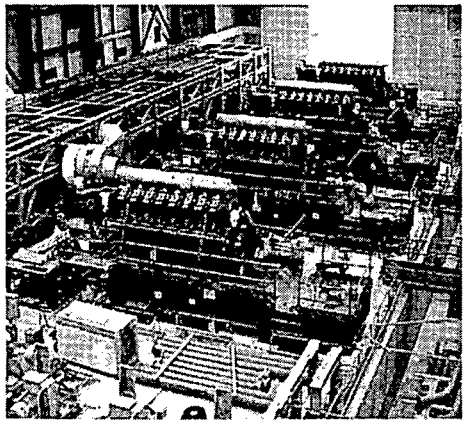


Fig. 6 Main Hydraulic Pump Units

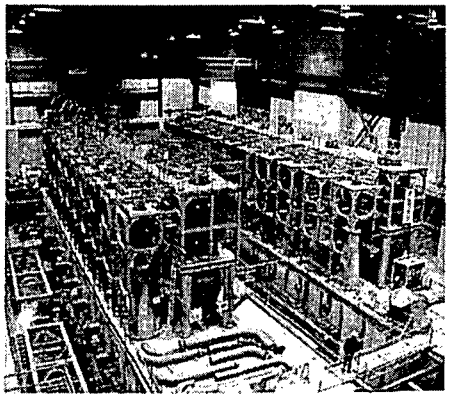


Fig. 7 Main Accumulator Units

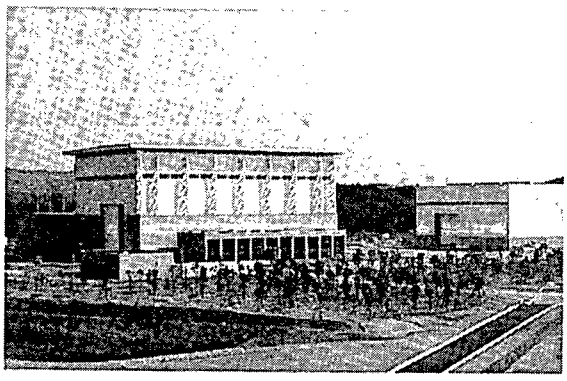


Fig. 8 Recent Construction Condition

4. CONTROL AND MEASURING SYSTEMS

The control system of shaking table and measuring system are key functions of the facility. We are currently arranging these systems.

The control model is composed 2 step systems, basic control system and Application control system. The basic control system is used for the safety control of shaking table, which is composed TVC (Three Variable Control) technique. Application control system is used for the more accuracy control of shaking table. The researcher can insert the own control technique to the control system. Fig. 9 shows the block diagram of control system.

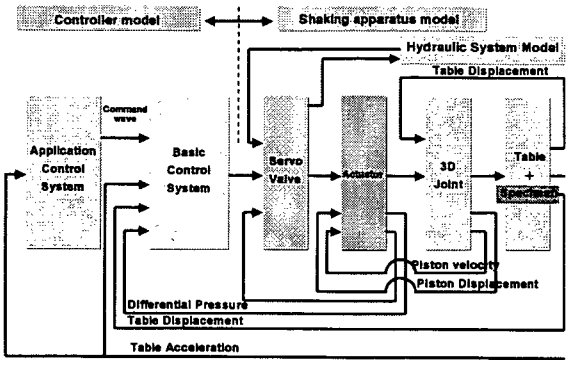


Fig. 9 Block Diagram of Control System

The E-Defense is the large scale testing facility, therefore, the researcher, who use this facility, want get a lot of data during test. We will install 960 measuring channels. We have 440 channels of the sensor for control signal. The 64 channels within these 440 channels are able to record the measuring system. The 896 channels of the sensor for measurement are installed for the research purpose. Fig. 10 shows the block diagram of measuring system.

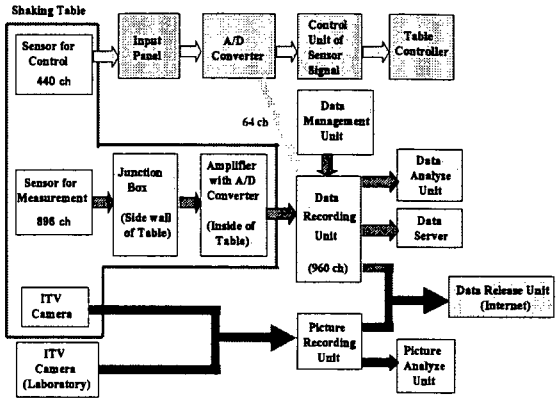


Fig. 10 Measuring System

5. MANAGEMENT MECHANIZM

For the management of E-Defense, we are thinking about following management mechanism. We will establish the Hyogo branch (tentative name) for the operation of facility and conducting the research works. But, by the limitation of number of regular staffs, we will establish the Supporting Consortium, such as outsourcing mechanism. This Supporting Consortium is functioned to conduct the smoothly operation of facility cooperate with the staffs of Hyogo branch. We established one council and one committee for more effective management and operation of facility.

The Management Council is organized by the representatives from government, academic and private sectors. Dr. S. Ito, President, Research Institute for Urban Disaster Mitigation, is chaired the Council. 18 members were nominated. This council will discuss the medium and long term management plan and more effective management of facility.

The Utilization Committee is organized by the active researchers from various fields of earthquake engineering. Prof. K. Kawashima, Tokyo Institute of Technology is chaired this committee. 19 members were nominated. This committee will discuss the research plan and research results by using this facility.
Fig. 11 shows the Management mechanism.

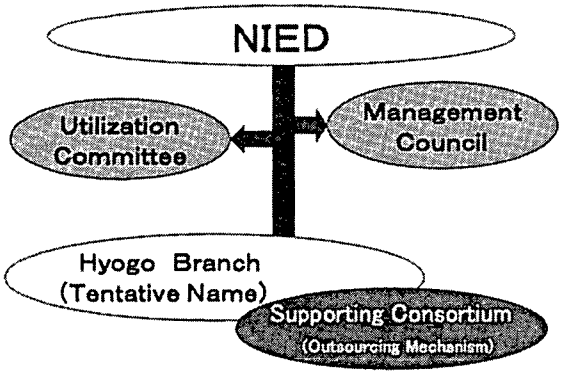


Fig. 11 Management Mechanism

6. EARTHQUAKE ENGINEERING COLLABORATION

E-Defense should be operated the international common use. To ensure the international common use and disseminate the test results, we will construct and install the E-Defense Network (ED-Net).
The ED-Net has tow major functions: The one is the connection tool between E-Defense in Miki and the Super Computer in Tsukuba. The other one is the connection tool between NIED and the other organization, such as research institute, university, private sector and so on. This function is not only limited to domestic, but also international manner.
We will install the tele-observation and tele-discussion capabilities, but not install the tele-operation function. Because, conducting of shaking table test, especially failure test, has very delicate and dangerous factors. Therefore, the operation of shaking table will limit by the shaking table administrator, who is the specialist of operation. Figure 12 shows the schematic image of ED-Net.

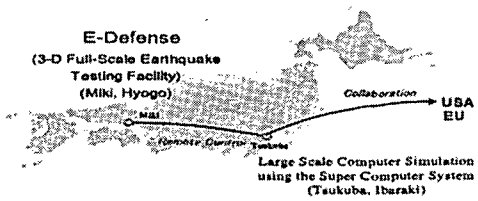


Fig. 12 Schematic Image of ED-Net

7. CONCLUDING REMARKS

Based on the lessons learnt from Hanshin-Awaji earthquake, we, NIED, need more research to understand the failure mechanism of different kind of structures during earthquake. For this research needs, we began the construction project of E-Defense (3-D Full-Scale Earthquake Testing Facility) and ED-Net (E-Defense Network). After completion, these tools will be perfectly opened to international use.
We strongly hope that these tools are contributed to the dramatic progress of the earthquake engineering research, especially the understanding of structural failure mechanism, the progress of the earthquake resistant design of structures and the evaluation/reevaluation of structural performance during earthquake, by the coordination and collaboration research works in the worldwide bases.

ACKOWLEGEMNTS

For the progress of Project "E-Defense", NIED established the Technical Advisory Committee (Chairman: Prof. H. Sato, University of Chuo, Committee members: 10 Professors). The authors acknowledge the Committee members for the support and kindly advice.

REFERNCES

Ohtani, K, Katayama, T, Shibata, H. (1998) "Project on

3-D Full-Scale Earthquake Testing Facility – First Report-", *30UJNR*

Ohtani, K, Katayama, T, Shibata, H. (2002) "Project on 3-D Full-Scale Earthquake Testing Facility – The Second Report-", *34UJNR*

Ogawa, N, Ohtani, K, Katayama, T, Shibata, H. (1999) "World's Largest Shaking Table Takes Shapes in Japan – A Summary of Construction Plan and Technical Development-", *SmiRT 15*

Ohtani, K, Ogawa, N, Katayama, T, Shibata, H, Nakagawa, O, Ohtomo, T. (2001) "World's Largest Shaking Table Takes Shapes in Japan (The 2nd Report)", *SmiRT 16*

Ohtani, K. (2001) "Tools for Seismic Safety Evaluation of Structures", *NEA/CSNI/R(2001)13/VOL3*

Ohtani, K, Ogawa, N, Katayama, T, Shibata, H. (2002) "3-D Full-Scale Earthquake Testing Facility and Earthquake Engineering Network", *3WCSC*

Ohtani, K, Ogawa, N, Katayama, T, Shibata, H, "Project "E-Defense" –Introduction of E-Defense-", *2003PCEE*

Harada, T, Koike, A, Uchida, M, Ohtani, K, Ogawa, N, "Project "E-Defense" –Technical Development of Mechanical Components-", *2003PCEE*

Rood, O.E, Ohtani, K, Yoshida, E, "Project "E=Defense" –Control System Architecture-, *2003PCEE*

MCEER Advanced Technology Research for Next Generation Seismic Resilient Buildings

by

Gary F. Dargush[1] and George C. Lee[2]

ABSTRACT

Over the last two decades, significant research effort has been directed toward the application of advanced technologies to improve the seismic performance of civil infrastructure. MCEER has played a role in that development. In this paper, we present an overview of the integrated MCEER research program aimed at the development of a new generation of seismic resilient buildings. While MCEER research has a broad scope, here we concentrate specifically on aspects relating to the further development of structural control devices and systems. Three new passive elements are examined, including scissor jack dampers, light-gauge steel shear panels and polymer matrix composite infill walls, along with a novel hybrid control system. Although these research projects are at different stages of development, all four have significant application potential. Naturally, the MCEER research program must also address the overall system level performance. Along these lines, we examine a new retrofit strategy involving strength reduction combined with damping enhancement. With this approach, the resulting retrofit structure can exhibit reductions in both displacements and base shear forces. Two distinct automated design approaches, involving heuristic and evolutionary methodologies, also are presented in some detail. Initial investigations indicate that these approaches are quite promising. All of the work presented here leads us to the conclusion that the integrated MCEER research approach can contribute substantially to the development of next generation seismic resilient buildings.

KEYWORDS: earthquake engineering, seismic design, structural control

1.0 INTRODUCTION

One of the fundamental long-term goals of earthquake engineering research in general and the Multidisciplinary Center for Earthquake Engineering Research (MCEER) in particular is to enable the evolution of disaster resilient communities. The development of innovative engineering technologies is an important component in this overall program. In the present paper, we provide overviews of a few of the recent MCEER research projects that focus on the development of advanced technologies for application to a new generation of seismic resilient buildings.

Our presentation is organized as follows. Research relating to the development of three new types of passive control elements and one semi-active control system is discussed in Section 2. Then, in Section 3, we summarize some recent work on a novel structural control strategy that combines an intentional structural weakening along with the introduction of passive elements. Afterwards, two new approaches are presented in Sections 4 and 5 for automated design of next generation building structures that incorporate protective systems. Somewhat more detail is included for these two on-going projects since the coauthors are actively involved in this research. Finally, Section 5 provides some concluding remarks.

2.0 STRUCTURAL CONTROL ELEMENTS

MCEER, along with its predecessor NCEER, has a long history of research accomplishments associated

[1] Professor, Dept. of Civil, Structural & Environmental Engineering, University at Buffalo, Amherst, NY 14260, USA

[2] Samuel P. Capen Professor, Dept. of Civil, Structural & Environmental Engineering, and Director, Multidisciplinary Center for Earthquake Engineering Research, University at Buffalo, Amherst, NY 14260, USA

with the development of protective systems. Much of the early work, supported under NCEER, is summarized in Constantinou et al. (1998) and Soong and Dargush (1997), where complete reference to the original literature is provided. Here we present brief overviews of some of the more recent control element development sponsored by MCEER. Initially, the emphasis is on passive energy dissipation components suitable for application to building structures. Included are scissor jack fluid dampers, metallic dissipating shear panels and polymer matrix composite infill wall systems. The final section describes a new combined RSPM and passive damping hybrid control system.

2.1 Scissor Jack Damper

In the usual arrangement, supplemental passive devices are incorporated into the structural system through the use of either diagonal or chevron bracing. With this configuration, the magnitude of the displacement across the passive device is at most equal to the interstory drift. Consequently, large dampers may be required, particularly for stiff structures. One remedy is to introduce a damping amplification. Kani et al. (1992) were perhaps the first to utilize the level principle to amplify the damping effect. Two fluid-filled dampers were employed in each frame bay along with an inverted T-shaped lever to achieve the amplification. More recently, Constantinou et al. (2001) developed toggle-brace-damper system configurations to significantly enhance the performance of high-energy dissipation density viscous fluid dampers. The analytical and experimental studies indicate that displacement magnification factors in the range from two to five are quite practical.

One difficulty that remains with all of these supplemental damper configurations pertains to the negative impact of bracing on the architectural aspects of design. Open bays are often much preferred. In order to address this issue, while achieving device amplification, Sigaher and Constantinou (2003) developed the scissor-jack-damper energy dissipation system, under support from MCEER.

A schematic of the scissor-jack-damper system is provided in Figure 1. Under the assumptions of small deformation theory with rigid frame and bracing elements, Sigaher and Constantinou (2003) characterize the performance of the system in terms of the two angles $?$ and $?$, along with the viscous damping coefficient C_0 for the fluid dampers. As a result, the displacement magnification factor κ can be written simply as $\kappa = cos\psi / tan\theta$.

Sigaher and Constantinou (2003) conducted an experimental program involving half-scale steel frame structures with a variety of beam-column connections. Both sinusoidal strong floor tests and numerous earthquake simulator experiments were used to verify the performance of the scissor jack system and to validate the numerical models. Excellent performance and correlations were obtained indicating that practical scissor jack systems can be designed with magnification factors in the range $2 \le \kappa \le 5$. Connection details must be given careful attention to ensure full magnification and proper load transfer.

2.2 Light-gauge Steel Shear Panels

Metallic passive devices, in the form of X-shaped or triangular plates and unbonded braces, have seen numerous applications for supplemental damping. Recent MCEER funded work has focused on the development of steel plate shear walls (SPSW). While significant effort since the mid-1980s has been directed toward the use of relatively thick hot rolled steel plates (Timler et al., 1998), the on-going MCEER research by Bruneau and co-workers employs light-gauge cold-formed steel infill panels. These new systems have the potential for a substantial increase in energy dissipation with minimal impact on exiting framing members. In order to examine the performance of these infill panels, Berman and Bruneau (2002) conducted a preliminary series of quasi-static, cyclic displacement-controlled loading tests. Both flat 1mm plate specimens and 0.75mm corrugated specimens were considered. For the experiments, the infill panel specimens were secured to the bounding frame with either welded or epoxy connections. Results from these preliminary tests indicate that the light-gauge cold-formed steel infill panels can enhance seismic performance through energy dissipation associated with tension field yielding. Further research is needed concerning connection details,

modeling approaches and seismic testing.

2.3 Polymer Matrix Composite Panels

Besides steel infill panels, one may also consider the use of non-traditional structural engineering materials. Early examples include viscoelastic infill panels (Gasparini et al., 1981) and viscous damping walls (Arima et al., 1988). Within MCEER, work is underway toward the development of a polymer matrix composite (PMC) infill wall system for seismic applications.

A schematic of the initial PMC system proposed by Aref and Jung (2003) is provided in Figure 2. The system consists of an inner panel sandwich construction with a fiber-reinforced polymer (FRP) laminate shell and a vinyl foam core. FRP laminates are also used to form the outer shell. For the initial version of the infill walls, viscoelastic honeycomb interface layers are used to transfer the shear forces between the inner panel and outer shells. This is intended to provide stiffness and energy dissipation.

The development of these new infill panels is based upon a combined experimental and numerical modeling approach, as described in Aref and Jung (2003). In particular, finite element models of the composite panels were employed to help guide the design in terms of geometric configuration and FRP lay-up selection. For the physical experiments, both monotonic and cyclic testing of a large-scale steel frame was conducted with and without the PMC panels. Significant increases in both the stiffness and strength of the frame were observed when the PMC panels were included. Energy dissipation also increased substantially with the panels, suggesting that the concept has potential. Additional work is needed to reduce local damage to the panel at high drift ratios and to improve the energy dissipation. With regard to the latter issue, Jung and Aref (2003) have investigated the combined use of the polymeric honeycomb and a solid viscoelastic material for the interface layer. Small-scale material tests indicate that this approach ultimately may allow the designer to tune the stiffness and damping characteristics of the proposed PMC panels.

2.4 Combined RSPM and Passive Damping Hybrid Control System

Real-time Structural Parameter Modification (RSPM) system is a semi-active nonlinear control system for reducing structural seismic responses (Liang, et al., 1999a,b; Lee et al., 1997). This semi-active nonlinear system can effectively reduce seismic responses, especially when the objective is to reduce displacement or story drift. A combined RSPM and passive damping control approach can achieve better seismic reduction than the passive damping alone. The combined system can reduce the acceleration response very effectively because of the added damping. Figure 3 shows this hybrid system that consists of a passive damper and a controlled stiffness unit. The passive damper is always engaged to dissipate energy. The stiffness unit is engaged when the deformation reaches a threshold value—termed as the open distance. If the relative displacement magnitude is larger than the open distance, the stiffness unit will contribute to reduce the response. If, at any instant, the displacement magnitude is smaller than the threshold, the RSPM nonlinear stiffness is disengaged. The stiffness is engaged again only when the displacement exceeds the threshold, and the RSPM control mechanism is activated only when the stiffness is engaged. The devices are combined in pairs of tension and compression units working as a push-and-pull set.

This hybrid control system has been studied and designed for two adjacent existing buildings in LA, as described in Lee et al. (2002). The weaker building is a seven story steel structure with full moment resisting connections. The seismic retrofit problem is to avoid collision of this building with the much stiffer adjacent buildings. A combined RSPM and passive damping system is considered between the two buildings at the roof level. A secondary requirement of this retrofit project is to reduce the acceleration response level, for which pure damping device can be effectively used. The combined RSPM and damping approach therefore is developed to take advantage of their respective strengths.

3.0 RETROFIT STRATEGIES

Many non-traditional retrofit strategies have been proposed in recent years, including a number of approaches involving passive, semi-active, active and hybrid control. Passive dampers, for example, are

often very effective for reducing the displacement response, but may tend to elevate base shears and accelerations due to the increase in strength and/or stiffness. This may be problematic, particularly when critical non-structural components must be protected.

An interesting new approach developed by Reinhorn, Whittaker and co-workers, within the MCEER Acute Care Facility research thrust, relies on an intentional structural weakening combined with added damping. The main ideas of this retrofit strategy can be found in Viti et al. (2002). The first step in this approach involves weakening of the existing structure, which may be accomplished, for example, by modifying connection details. The structural response is altered, as indicated by the schematic in Figure 4. This tends to reduce the base shear (and accelerations), but increase the deformations. Subsequently, in Step 2, supplemental dampers are introduced into this weakened structure. This has the potential to substantially reduce displacements, while causing modest increases in base shears. Consequently, the overall result may be quite good, depending of course on the specific details of the retrofit.

Viti et al. (2002) studied the application of this retrofit strategy to a five-story steel frame hospital in Los Angeles. The goal was to significantly reduce accelerations in order to better protect the non-structural components. In Step 1, hinges were introduced at the beam-column joints for a series of interior bays. Then viscous fluid dampers were added to those bays to increase the effective damping ratio to approximately 16% for a highly damped case. Both spectral analysis and nonlinear dynamic analysis indicated that base shears could be decreased significantly from the original structure, with only a slight increase in interstory drift. Consequently, this new approach provides interesting possibilities in the seismic retrofit of acute care facilities, as well as for more general building structures.

4.0 HEURISTIC DESIGN

Although passive energy dissipation has been used as a viable strategy for seismic protection of buildings for many years, the current design codes do not provide guidelines for optimizing damper configurations. However, a number of researchers have proposed computational design approaches to optimize passive device sizing and placement. Examples include the work by Zhang and Soong (1992) using a sequential placement strategy for rate-dependent dampers, by Gluck et al. (1996) with an optimal control theory approach, and by Singh and Moreschi (2001) via a gradient projection method.

Under sponsorship from MCEER, Liu et al. (2002) developed a heuristic approach to optimize the damper configuration based upon building performance objectives. This method combines the evolutionary approach and engineering knowledge to minimize different performance indices of response, such as interstory drift or acceleration.

The proposed optimization methodology combines the efficiency of a heuristic approach and the effectiveness of an evolutionary approach to search for the optimal solution based on improving through generations. The heuristic knowledge for improvement comes from modal analysis of the structure.

Since the added passive devices may contribute nonproportional damping to the structural system, the standard modal analysis approach cannot be used. However, the total response can be solved using the linear combination of contributions from all modes using a state-space technique. In general, each mode contributes to the total response. The relative magnitude of each modal contribution depends on its modal response, mode shape, and earthquake frequency content. It also depends on the performance requirement of the structure, since the high frequency modes generally contribute more to the acceleration response than to the displacement response.

Among all the modes that contribute to the total structural response, some modes will dominate and some will have negligible contribution. If we can capture the dominant modes and reduce their contribution, then the total response can be reduced. Consequently, the primary objective of the present heuristic approach is to reduce the contribution from the dominant modes by increasing their modal damping ratios.

Consider the case of linear viscous supplemental dampers added to a linear structural system. Then,

the following heuristic approach is adopted. To increase the modal damping of the dominant modes, the contribution from each possible device location is ranked. The devices are moved from the least effective location to the most effective location. Since this heuristic is not guaranteed to reduce the structural response under earthquake conditions, the powerful evolutionary approach is also used. The optimization problem of device configuration iterates through generations, and each generation is an improvement from the previous generations. With the heuristic included in the search, the iteration is expected to converge faster. Thus, the optimization results can be expected in a reasonable amount of time.

The procedure can be summarized as follows:

1. Select a performance index according to the building performance objective
2. Select an initial damper configuration
3. Analyze the structural modal composition and find the dominant modes
4. Find the effectiveness of each device location
5. Redistribute the devices iteratively

Further details on the methodology can be found in Liu (2003). Here we present results from that work for an illustrative example concerning a uniform ten-story building.

Let k and m represent the stiffness and mass for each of the ten stories, with $k = 4.5 \times 10^8$ N/m and $m = 2.5 \times 10^5$ kg. Then the first two natural frequencies are 1Hz and 3Hz. We assume that 50 purely viscous dampers are available for the design, each having a damping coefficient $c = 3.5 \times 10^6$ N-s/m. Meanwhile, the seismic environment is characterized by three ground motions. These represent frequency-adjusted versions of El Centro, Kobe and Northridge records.

Rows number one and two in Table 1 provide the maximum response quantities for the cases with no dampers and for a uniform damper distribution, respectively. The response is greatly reduced with the addition of dampers. Notice that the effective first mode damping-ratio is also provided in the table. This increases from 3% to more than 15% with the passive dampers.

The heuristic optimization algorithm is then used to more effectively distribute the supplemental dampers. Rows three and four in Table 1 present the results for cases in which the performance index is interstory drift and story acceleration, respectively. Notice that when interstory drift is optimized, an improvement of 24% from the maximum drifts of 13.92mm to 10.51mm is obtained. The corresponding optimal damper distribution is detailed in Table 2. Considerable damping is added to the lower stories.

On the other hand, when story acceleration is optimized, only modest reductions in maximum acceleration can be obtained in this example, as indicated in Table 1, and in fact the optimal damper distribution presented in Table 2 is nearly uniform.

As a final case, drift limits are set and damper cost is minimized. From Table 1, we find that drift levels comparable to the uniform design can be achieved with slightly less than half the number of dampers. Story accelerations are somewhat higher than with the uniform damper design configuration, but still well below the levels obtained in the bare frame. In conclusion, we find that for this and a series of additional examples (Liu, 2003), the heuristic algorithm provides a computationally efficient approach for optimal design of passively damped linear structures. The method can also be used to gain insight into the behavior of structures with supplemental damping.

5.0 EVOLUTIONARY DESIGN

Additional research is needed to extend the heuristic design approach of Section 4 to structural systems that respond in a nonlinear fashion under seismic excitation. As an alternative approach, purely evolutionary methodologies can be employed.

5.1 Complex Adaptive Systems and Methodologies

Over the past two decades, there has been increasing interest in the concept of complex adaptive systems, originally formulated by Holland (1975). These systems typically involve the complicated nonlinear interaction of many components or agents, which aggregate in a hierarchical manner in response to an uncertain or changing environment. As a result, complex adaptive systems evolve over time through

self-organization and ultimately acquire collective properties not exhibited by the components or agents acting alone. Classical examples are the human central nervous system, the local economy or a rain forest. Notice, however, that many of these same characteristics are essential for the development of disaster-resilient communities. This suggests that computational approaches suitable for studying complex adaptive systems may be quite appropriate for use in multidisciplinary seismic decision support.

By bringing ideas from biological evolution to bear on the problem, Holland (1962, 1975) also developed a unified theory of adaptation in both natural and artificial systems. Besides providing a general formalism for studying adaptive systems, this led to the development of a variety of evolutionary methodologies, including genetic algorithms. These computational approaches have enjoyed considerable success in recent years over a wide range of applications in science and engineering (Goldberg, 1989; Mitchell, 1996). These are essentially naturally parallel non-calculus based optimization procedures that can readily accommodate a disparate collection of models. Genetic algorithms are particularly effective for finding robust solutions to combinatorial problems in the presence of environmental uncertainties. Consequently, evolutionary methods hold significant promise as a possible framework for the development of a new class of decision support tools toward earthquake hazard mitigation. In the following section, an initial application of this approach for seismic retrofit of building structures with passive energy dissipation devices is considered.

5.2 Evolutionary Aseismic Design and Retrofit

In this section, we provide a brief overview of the proposed computational framework for aseismic design and retrofit. The primary objective is to develop an automated system that can evolve robust designs under uncertain seismic environments. As indicated in Figure 5, this evolutionary design process involves a sequence of generations. In each generation, a population of individual structures is defined and evaluated in response to ground motions that are realized in association with the geophysical environment. Cost and performance are used to evaluate the fitness of each structure in the population. These fitness values, along with random genetic operators modeling selection, crossover and mutation processes, define the makeup of the next generation of structures. In the current work, performance is judged by conducting nonlinear transient dynamic analysis using an explicit state-space transient dynamics code (tda). Alternatively, the finite element code abaqus may be utilized. The implementation of the genetic algorithm controlling the design evolution is accomplished within a modified version of Sugal (Hunter, 1995).

In the area of seismic passive energy dissipation systems, Singh and Moreschi (1999, 2000, 2002) developed the first genetic algorithm applications. Meanwhile further information on several different aspects of the present evolutionary aseismic design approach can be found in Dargush and Sant (2000, 2002), Dargush et al. (2002) and Dargush and Green (2002).

For illustrative purposes, we will now consider an example of a twelve-story steel frame retrofit with passive energy dissipators (e.g., Soong and Dargush, 1997). Three different types of dampers are available: metallic plate dampers, linear viscous dampers, and viscoelastic dampers. For each type, four different sizes are possible. Consequently, a four-bit genetic code is used to represent the devices used in each floor and a 48-bit chromosome is employed to completely specify the dampers present in any particular structure. Then for this problem, the set of attainable structures contains roughly 10^{14} members. Exhaustive search of the decision space is clearly not possible.

Currently, a two-surface cyclic plasticity model is applied for the primary structural system and metallic plate dampers, while a coupled thermoviscoelastic model with inelastic heat generation is used for the viscoelastic dampers. The mathematical models employed for these elements are defined in Dargush and Soong (1995) and Dargush and Sant (2002). In addition, the viscous dampers are strictly linear Newtonian devices. All of the bracing elements associated with the passive dampers are assumed to be perfectly rigid. In order to establish acceptable performance, limits are

imposed on both interstory drift and acceleration for each story.

For this twelve-story structure, let W_i and k_i represent the i th story weight and elastic stiffness, respectively. The frame model has story weights, $W_1 = \ldots = W_6 = W$, $W_7 = W_8 = 3W/4$, and $W_9 = \ldots = W_{12} = W/2$. Meanwhile, the story stiffnesses can be written as $k_1 = \ldots = k_6 = k$ and $k_7 = \ldots = k_{12} = k/4$. Notice that there is a strong discontinuity at the seventh story. After selecting the parameters W and k, the first two natural frequencies are 0.50Hz and 1.10Hz. Additionally, the story yield forces are also specified as follows: $F_1^{yL} = \ldots = F_6^{yL} = W/5, F_7^{yL} = \ldots = F_{12}^{yL} = W/20$.

We employ the USGS Gutenberg-Richter seismicity database for eastern North America (Frankel, 1995; Frankel et al., 1996) to model the seismic environment. The entire geographical region is subdivided into bins, with each bin representing 0.1 degrees of longitude and latitude. The USGS database then provides Gutenberg-Richter parameters a and b for each bin such that the number N of earthquakes per year of magnitude greater than or equal to M can be written as $\log N = a - bM$. We simulate the seismic environment by running Poisson processes in each bin to determine significant events that may occur during the intended life cycle of the structure. Whenever a significant event occurs, the ground motion generation algorithm defined by Papageorgiou (2000) is used to produce an appropriate synthetic accelerogram for the specified magnitude and epicentral distance.

Let us now assume that this steel structure is located on firm ground near Memphis, TN. The base structure without dampers survives less than 30% of the significant earthquakes. In our retrofit options, we permit all three damper types: triangular plate metallic dampers (tpea), viscous dampers (visc), as well as, viscoelastic dampers (ve). In order to restrict the search to more practical designs, we introduce a recessive gene concept in the genetic algorithm to prohibit structures with more than two different damper types. Hypothetical device cost data for various size dampers are set with each increment in damper size corresponding roughly to a doubling of the damping capacity. There is, of course, considerable subjectivity introduced in setting the relative cost-performance relations for the different damper types. However, we should emphasize that this is primarily a model problem intended to illustrate the methodology.

Figure 6 presents a snapshot of the overall graphical system. Included is a map that locates the generated seismic events, a database of candidate structures, and reliability plots of robust designs that have evolved through the automated design process. In particular, the upper left diagram provides a detailed view of the earthquakes generated throughout the New Madrid fault zone surrounding Memphis within a portion of one simulation. The variation of mean fitness of the population versus generation number is shown in Figure 7 for four separate simulations. As the system evolves, the population becomes enriched with robust structures. However, the mean fitness does not increase in a monotonic fashion due to the inherent uncertainty of the seismic environment and the continual search for better structures. Several robust designs that evolved over 256 generations are shown in Figure 8. Shading indicates the damper type, while the radius of the ring corresponds to damper size. Notice that each of these designs experienced over four hundred earthquakes with survival rates well above 90%. Interestingly, all three of these robust designs attempt to compensate for the structural discontinuity at the seventh story by introducing large viscoelastic dampers that provide increased damping and stiffness.

Results for this and a range of other structures suggest that the proposed evolutionary methodology is capable of identifying robust design alternatives while explicitly accounting for the uncertainty in the environment. Furthermore, this approach can be readily extended to other retrofit options, including those associated with secondary systems. Current work focuses on the development of efficient versions of the code for massively parallel computer architectures, on the incorporation of a knowledge base to help guide the evolutionary process and on the enhancement of the graphical user interface. Additionally, the evolutionary methodology is being extended to include macro-models for the newly developed passive elements described in Section 2

and to address problems of sociotechnical decision support.

6.0 CONCLUDING REMARKS

The long-term vision of MCEER is to assist in the development of seismically resilient communities. In the present paper, we have focused on the integrated research effort that specifically addresses enhanced structural performance of buildings through the development of advanced structural control technologies. Three promising new passive elements have been reviewed, including scissor jack dampers, light-gauge steel shear panels and polymer matrix composite infill walls. A novel combined RSPM and passive damping hybrid control system has also been presented. Furthermore, several new structural system level developments have been presented. These include a novel retrofit strategy involving the combination of intentional weakening and enhanced damping, along with two distinct automated design procedures. The latter developments, which were presented in some detail, can lead to the systematic design of efficient passively damped structures. Additionally, these computational approaches can provide new insight into overall structural system behavior under seismic excitation.

Finally, we should remark that the research developments summarized in this paper would not be possible within a traditional individual investigator environment. An integrated team approach is necessary to make substantial contributions toward the development of next generation seismic resilient buildings.

7.0 ACKNOWLEDGEMENTS

Support for the work described in this paper was provided in part by the Multidisciplinary Center for Earthquake Engineering Research under a cooperative agreement from the U.S. National Science Foundation (Grant EEC-9701471). The authors gratefully acknowledge this support.

Research within the MCEER community depends upon the collaborative effort of many individuals. The authors wish to acknowledge our MCEER colleagues at the University at Buffalo, whose work is highlighted in this summary paper. This includes Professors Aref, Bruneau, Constantinou, Green, Liang, Papageorgiou, Reinhorn, Soong, Tong and Whittaker.

8.0 REFERENCES

Aref, A.J. and Jung, W.-Y. (2003). Energy-Dissipating Polymer Matrix Composite Infill Wall System for Seismic Retrofitting, *J. Struct. Engrg.*, 129, 440-448.

Arima, F., Miyazaki, M., Tanaka, H. and Yamazaki, Y. (1988). A Study on Buildings with Large Damping Using Viscous Damping Walls, *Ninth World Conf. Earthquake Engrg.*, Tokyo, V-821-826.

Berman, J.W. and Bruneau, M. (2002). Experimental Investigation of Light-Gauge Steel Plate Shear Walls, *KEERC-MCEER Joint Seminar on Contributions to Earthquake Engineering*, Buffalo, NY.

Constantinou, M.C., Soong, T.T. and Dargush, G.F. (1998). *Passive Energy Dissipation for Seismic/Wind Design and Retrofit*, Multidisciplinary Center for Earthquake Engineering Research (MCEER) Monograph Series, University at Buffalo, Buffalo, NY.

Constantinou, M.C., Tsopelas, P., Hammel, W. and Sigaher, A.N. (2001). Toggle-Brace-Damper Seismic Energy Dissipation Systems, *J. Struct. Engrg.*, ASCE, 127, 105-112.

Dargush, G.F. and Sant, R.S. (2000). Computational Aseismic Design and Retrofit: Application to Passively Damped Structures, *Mitigation of Earthquake Disaster by Advanced Technologies-2*, MCEER, Las Vegas, NV, MCEER-01-0002, 175-185.

Dargush, G.F. and Sant, R.S. (2002). Computational Aseismic Design and Retrofit with Application to Passively Damped Structures, *Seventh U.S. Nat. Conf. Earthquake Engrg.*, EERI, Boston, MA.

Dargush, G.F., Green, M.L. and Zhao, X. (2002). Evolutionary Aseismic Design of Passively Damped Structural Systems, *International Conference on Advances and New Challenges in Earthquake Engineering Research*, Harbin, China.

Dargush, G.F. and Soong, T.T. (1995). Behavior of Metallic Plate Dampers in Seismic Passive Energy Dissipation Systems, *Earthquake Spectra*, 11, 545-568.

Dargush, G.F. and Green, M.L. (2002). Evolutionary Aseismic Design and Retrofit, *KEERC-MCEER Joint Seminar*, Buffalo, NY.

Frankel, A. (1995). Mapping Seismic Hazard in the Central and Eastern United States, *Seism. Res. Lett.*, 66, 8-21.

Frankel, A., Mueller, C., Barnhard, T., Perkins, D., Leyendecker, E.V., Dickman, N., Hanson, S. and Hopper, M. (1996). *National Seismic-Hazard Maps: Documentation*, U.S. Geological Survey, Open-File Report 96-532, 110pp.

Gasparini, D.A., Curry, L.W. and Debchaudhury, A. (1981). Damping of Frames with Viscoelastic Infill Panels, *J. Struct. Div.*, ASCE, 107, 889-905.

Gluck, N, Reinhorn, A.M., Gluck, J. and Levy, R. (1996). Design of Supplemental Dampers for Control of Structures, *J. Struct. Engrg.*, ASCE, 122, 1394-1399.

Goldberg, D.E. (1989). *Genetic Algorithms in Search, Optimization and Machine Learning*, Addison-Wesley, Reading, MA.

Holland, J.H. (1962). Outline for a Logical Theory of Adaptive Systems, *J. Assoc. Comp. Mach.*, 3, 297-314.

Holland, J.H. (1975). *Adaptation in Natural and Artificial Systems*, MIT Press, Cambridge, MA, 2nd Edition 1992.

Hunter, A. (1995). *Sugal Programming Manual*, Version 2.1, University of Sunderland, England.

Jung, W.-Y. and Aref, A.J. (2003). A Combined Honeycomb and Solid Viscoelastic Material for Structural Damping Applications, *Mech. Mater.*, in press.

Kani, N., Ogura, K., Tsujita, O., Hosozawa, O. and Shinozaki, Y. (1992). A Design Method and Development of Damping Amplifier System for Passive Response-controlled Structure, *Tenth World Conf. Earthquake Engrg.*, Madrid, A.A. Balkema, 4165-4170.

Lee, G.C., Tong, M., Wu, Y. H., Hwang, S. and Hart, G. (2002). Application of a Semi-Active Seismic Protective System in an Existing Building in Los Angeles, *Proc. 7NCEE*, Boston, MA.

Lee, G.C., Tong, M., Liang, Z., Houston, B., Taylor, S. Clinard, R.L., Tomita, K. and Gottwald, W. (1997). Structural Vibration Reduction with ISMIS Control Technology, *Proceedings of the 68th Shock and Vibration Symposium.*

Liang, Z., Tong, M. and Lee, G.C. (1999a). A Real-time Structural Parameter Modification (RSPM) Approach for Random Vibration Reduction: Part I – Principle, *J. Probabilistic Engrg.*, 14, 349-362.

Liang, Z., Tong, M. and Lee, G.C. (1999b). A Real-time Structural Parameter Modification (RSPM) Approach for Random Vibration Reduction: Part II - Experimental Verification, *J. Probabilistic Engrg.*, 14, 362-385.

Liu, W., Tong, M. and Lee, G.C. (2002). Optimization Strategy for Damper Configuration Based on Building Performance Indices, *KEERC-MCEER Joint Seminar on Contributions to Earthquake Engineering*, Buffalo, NY.

Liu, W. (2003). Optimization Strategy for Damper Configurations of Buildings Based on Performance Indices, Ph.D. Dissertation, University at Buffalo, Buffalo, NY.

Mitchell, M. (1996). *An Introduction to Genetic Algorithms*, MIT Press, Cambridge, MA.

Papageorgiou, A. (2000). Ground Motion Prediction Methodologies for Eastern North America, *Research Progress and Accomplishments, 1999-2000*, Multidisciplinary Center for Earthquake Engineering Research, University at Buffalo.

Sigaher, A.N. and Constantinou, M.C. (2003). Scissor-Jack-Damper Energy Dissipation System, *Earthquake Spectra*, 19, 133-158.

Singh, M.P. and Moreschi, L.M. (1999). Genetic Algorithm-based Control of Structures for Dynamic Loads, *Proc. IA-99*, Osaka University, Japan.

Singh, M.P. and Moreschi, L.M. (2000). Optimal Seismic Design of Building Structures with Friction Dampers, *Proc. US-China Millennium Symposium Earthquake Engrg.*, Beijing, China.

Singh, M.P. and Moreschi, L.M. (2001). Optimal Seismic Response Control with Dampers, *Earthquake Engrg. Struct. Dyn.*, 30, 553-572.

Singh, M.P. and Moreschi, L.M. (2002). Optimal Placement of Dampers for Passive Response Control, *Earthquake Engrg. Struct. Dyn.*, 31, 955-976.

Soong, T.T. and Dargush, G.F. (1997). *Passive Energy Dissipation Systems in Structural Engineering*, Wiley, London and New York.

Timler, P., Venture, C.E., Prion, H. and Anjam, R. (1998). Experimental and Analytical Studies of Steel Plate Shear Walls as Applied to the Design of Tall Buildings, *Struct. Design Tall Buildings*, 7, 233-249.

Viti, S., Reinhorn, A.M. and Whittaker, A.S. (2002). Retrofit of Structures: Strength Reduction with Damping Enhancement, *KEERC-MCEER Joint Seminar on Contributions to Earthquake Engineering*, Buffalo, NY.

Zhang, R.H. and Soong, T.T. (1992). Seismic Design of Viscoelastic Dampers for Structural Applications, *J. Struct. Engrg.*, ASCE, 118, 1375-1392.

Table 1: Heuristic Design – Ten Story Building (Liu, 2003)

	Number of Dampers	1st Mode Damping Ratio (%)	Drift (mm)	Acceleration (mm/s^2)	Velocity (mm/s)
No dampers	0	3.0	26.08	10207	1289
Uniform	50	15.3	13.92	4580	652
Optimal drift	50	22.8	10.51	5286	604
Optimal acceleration	50	17.5	12.69	4509	618
Optimal cost	24	13.3	13.56	6311	718

Table2: Heuristic Design – Ten Story Building Optimal Damper Configurations (Liu, 2003)

Story	Uniform	Optimal drift	Optimal acceleration	Optimal cost
10	5	0	2	0
9	5	0	3	0
8	5	0	4	0
7	5	0	4	0
6	5	2	5	0
5	5	5	6	0
4	5	8	6	3
3	5	10	6	6
2	5	12	6	7
1	5	13	8	8

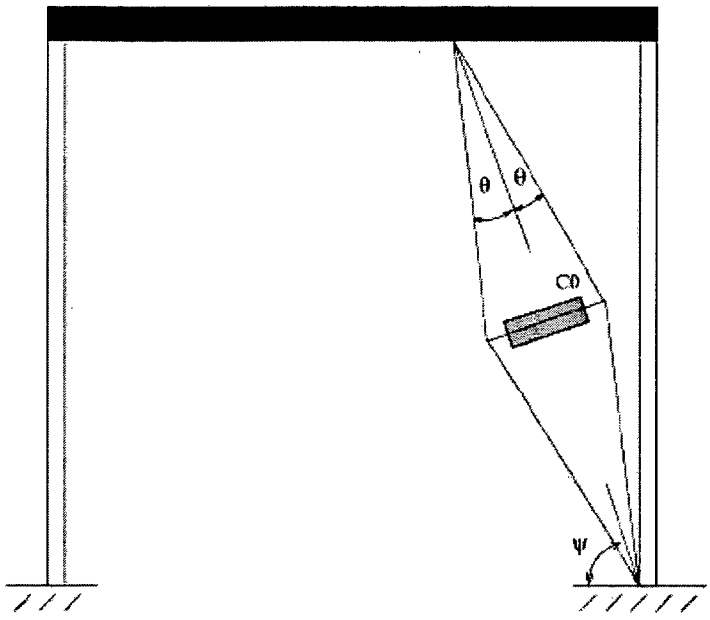


Figure 1: Scissor-Jack-Damper (Sigaher and Constantinou, 2003)

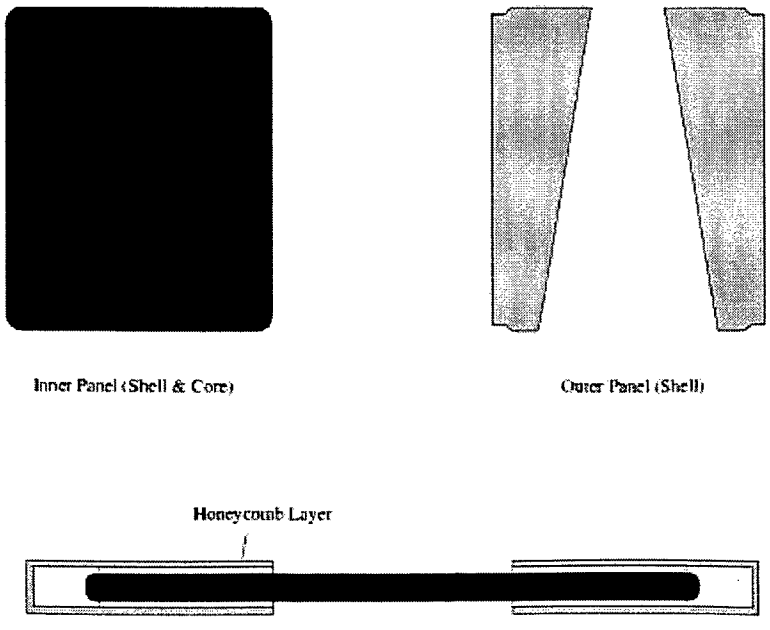


Figure 2: Polymer Matrix Composite Infill Panel (Aref and Jung, 2003)

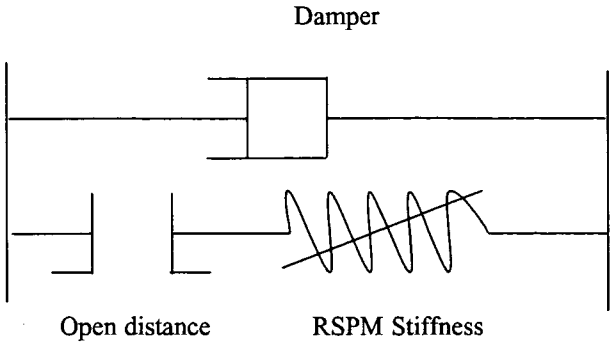


Figure 3: Combined RSPM and Passive Damping Hybrid Control System

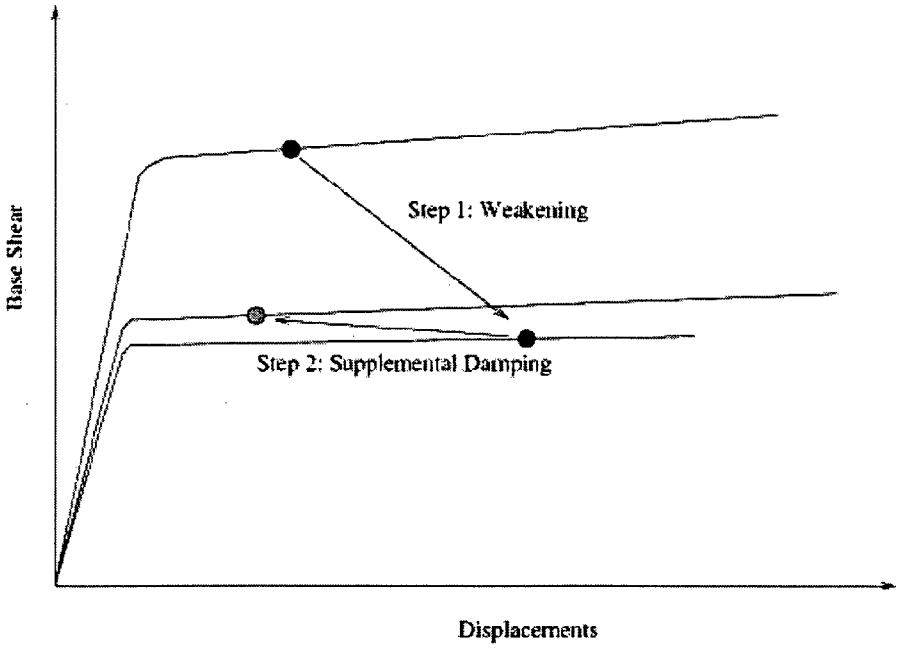


Figure 4: Strength Reduction with Damping Enhancement (Viti et al., 2002)

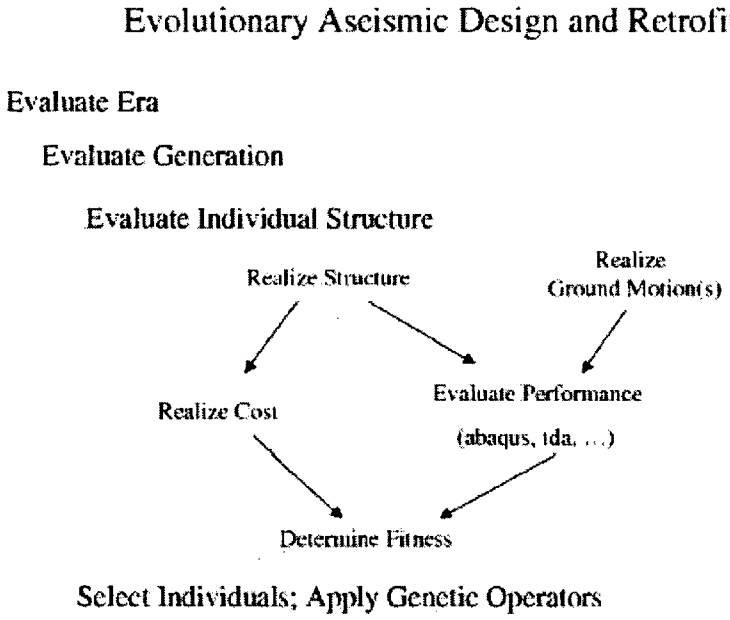


Figure 5: Evolutionary Aseismic Design and Retrofit - Overall Framework

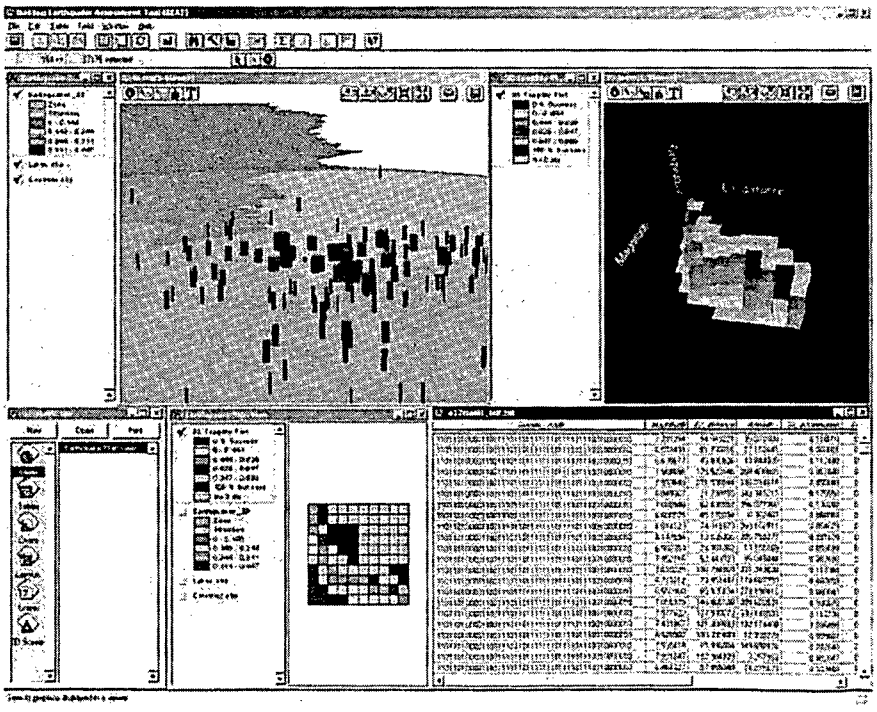


Figure 6: Evolutionary Aseismic Design and Retrofit - Graphical Interface

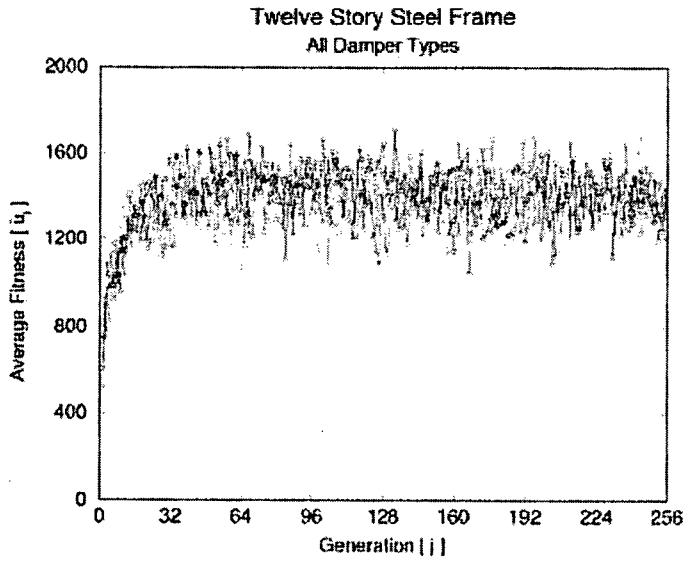


Figure 7: Evolutionary Aseismic Design and Retrofit – Average Fitness Variation for Twelve Story Steel Frame

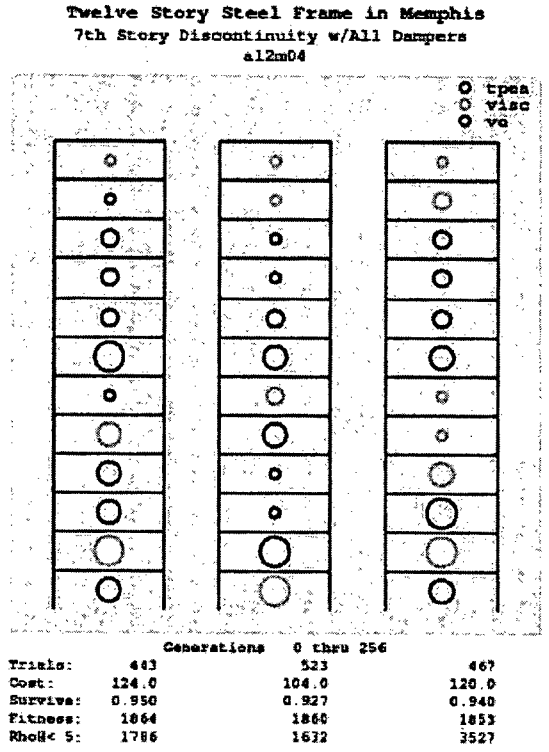


Figure 8: Evolutionary Aseismic Design and Retrofit – Robust Design Configurations for Twelve Story Steel Frame

Research and Development in the U.S.-Japan Cooperative Structural Testing Research Program on Smart Structural Systems

by

Shunsuke Otani[1], Akira Wada[2], Yoshikazu Kitagawa[3], Takafumi Fujita[4], Mitsumasa Midorikawa[5] and Masaomi Teshigawara[6]

ABSTRACT

Building Research Institute conducted a 5-year research and development project of "Smart Materials and Structural Systems" in 1998 as a part of U.S.-Japan cooperative research efforts. U.S. Counterpart is National Science Foundation. Smart Structural Systems (also called as Auto-adaptive Media) are defined as systems that can automatically adjust structural characteristics, in response to the change in external disturbance and environments, toward structural safety and serviceability as well as the elongation of structural service life. The research and development of (1) Concept and performance evaluation method of smart structure system, (2) Sensing of structure performance, and (3) Development and evaluation of structural elements using smart materials were conducted.

KEYOWORDS: Auto-adaptive, Engineered Cemetitious Composites(ECC), Induced Strain Actuators(ISA), Magneto-Rheological(MR), Monitoring, Shape Memory Alloy(SMA), Smart, Structure, System

1. INTRODUCTION

A conventional structural system is designed to achieve a set of intended functions under pre-selected loads and forces. Such a conventional system can not successfully develop its ability against unexpected loads and forces unless a large safety factor is provided for safety limit states to take into account various uncertainties in load and force amplitudes and structural response. Furthermore, since seismic design requirements have been improved after each bitter lessons learned through past earthquake disasters, the safety level of old buildings are always inferior to new buildings as evidenced in many past earthquake disasters, e.g., the 1995 Kobe earthquake disaster. Strengthening or removal of those old buildings becomes necessary to protect societal welfare.

Smart Structural Systems are defined as structural systems with a certain-level of autonomy relying on the embedded functions of sensors, actuators and processors, that can automatically adjust structural characteristics, in response to the change in external disturbance and environments, toward structural safety and serviceability as well as the elongation of structural service life [1.1].

1 Professor, Chiba University, Chiba-shi, Chiba-ken, 263-8522 Japan
2 Professor, Tokyo Institute of Technology, Yokohama-shi, Kanagawa-ken, 226-8503 Japan
3 Professor, Keio University, Yokohama-shi, Kanagawa-ken, 223-8521 Japan
4 Professor, Institute of Industrial Science, Department of Information and System, University of Tokyo, Tokyo 153-8505 Japan
5 Research Coordinator of Building Technology, Building Research Institute, Tsukuba-shi, Ibaraki-ken, 305-0802 Japan
6 Chief Researcher & Research Coordinator, Department of Structural Engineering, ditto

2. TARGET ISSUES AND RESEARCH ORGANAIZATION

The research and development are conducted focusing on the following issues.

1. Concept and performance evaluation: A series of auto-adaptive and high-performance systems are developed, and methods of performance evaluation are investigated.
2. Sensing of structure performance: Damage detection methods utilizing smart materials as sensors, such as Optical Fiber, Carbon Fiber, Shape Memory Alloy (SMA), and a Piezoelectric Ceramic (PZT) in addition to existing sensors are investigated, and methods for system identification associated with damage detection are studied.
3. Development and evaluation of smart structural elements: Devices utilizing the auto-adaptive material such as SMA, PZT, Magneto-Rheological (MR) and Electro-Rheological (ER) Fluids, high tensile strength and ductility concrete, self-repairing material are developed.

To achieve the three research objectives, following three sub-committees have been formed under Technical Coordinating Committee of the project, chaired by Prof. S. Otani, University of Tokyo:

"Sub-committee on structural system" chaired by Prof. A. Wada of Tokyo Institute of Technology,

"Sub-committee on sensing and monitoring technology" chaired by Prof. Y. Kitagawa of Hiroshima University,

"Sub-committee on effector technology" chaired by Prof. T. Fujita of Institute of Industrial Science, University of Tokyo.

The research organization is illustrated in Figure 1. The Building Contractors Society, the Housing and Urban Development Cooperation, the Building Center of Japan, and several materials and sensors makers participate in this R/D project.

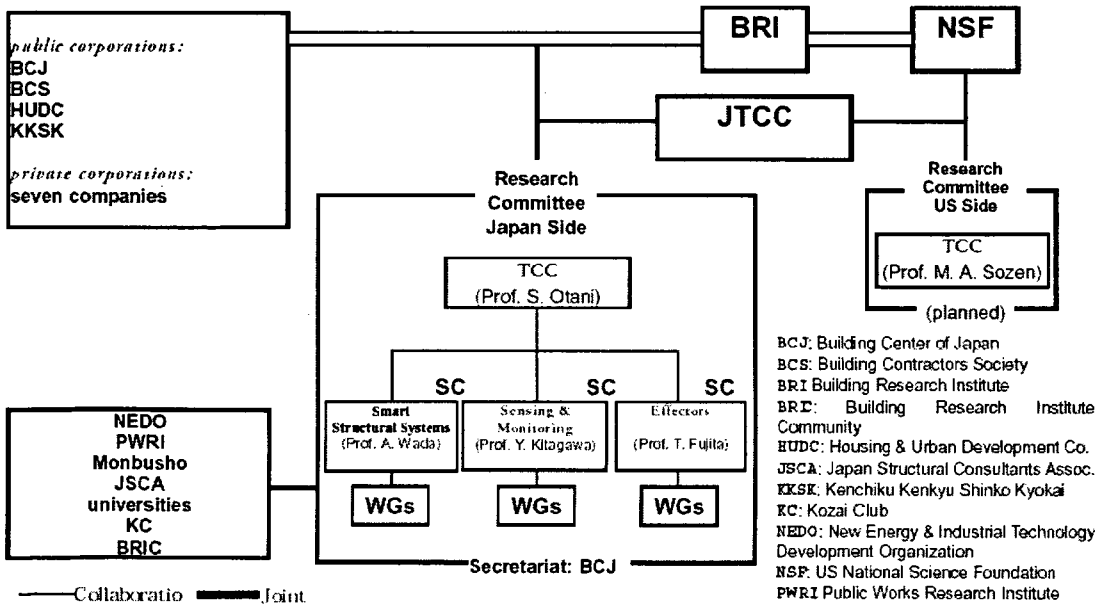


Fig.1 The Research Organization on Smart Structure

Table1 Research Time Table

	1998	1999	2000	2001	2002
System	Concept of Structure				
		Proposal of SSS		Large Scale Test	
				SSS Evaluation GLs	
Sensor	Survey of Sensors		R/D of Smart Sensors		
	Survey and R/D of Monitoring			Large Scale Test	
				Sensor & Monitoring GLs	
Effectors	Survey of Smart Materials				
		Application to Buildings		Large Scale Test	
				Smart Materials GLs	

This research program started at 1998 for 5 years. The research and development of (1) Concept and performance evaluation method of smart structure system, (2) Sensing of structure performance, and (3) Development and evaluation of structural elements using smart materials were conducted according to the timetable tabulated in Table-1. And these accomplishments were summarized to smart structure system evaluation guidelines, sensor and monitoring guidelines, and application guidelines of smart materials, through the large-scale test for performance verification.

In this research periods, US-Japan Joint Technical Coordinating Committee (JTCC) were held at Tsukuba[2.1] and Hawaii[2.2] in 2000, and at Tsukuba[2.3] in 2002. Last JTCC was accompanied with workshop on smart structural system [2.3]

3. SMART STRUCTURAL SYSTEMS

3.1. Outline

The performance level required of building structures becomes higher and wider in these days. It is considered that the smart structural systems are one of solutions to realize such performance of building structures. The concept of smart structural systems was initially proposed in the field of aerospace engineering. In this research and development project, we try to apply the concept of smart structural systems to building structures. Based on this concept, some smart structural systems are developed. Their performance is examined by numerical analyses and/or dynamic tests. Finally, the performance evaluation guideline for smart structural systems is proposed.

3.2. Concept of Smart Structures for Buildings

The concept of smart structural systems was initially proposed in the field of aerospace engineering, where the smart structural system was defined as "a system that can detect damage, restrain damage propagation, control the response from external disturbance actively, and adapt its configuration to optimum state for the environment." The objectives and needs of a smart structural system for buildings are different from those of aerospace engineering as shown in Table 3.1. Thus we need to revise the concept of smart structural systems when applying it to buildings. In this project, the smart structural system for building structures is defined as "a structural system with a certain level of autonomy relying on the embedded functions of sensors, actuators and/or processors, that can automatically adjust structural characteristics, in response to the change in external disturbances and environment, toward structural safety and serviceability as well as the elongation of structural service life" [3.1]. Based on this concept, we develop three types of

smart structural systems, which are auto-adaptive structural systems, reinforced concrete (RC) structural systems with damage fuses and innovative life safety systems. The research organization for these systems is shown in Fig.3.1.

3.3 Development of Smart Structural Systems

3.3.1 Auto-adaptive Structural System

Auto-adaptive structural systems have auto-adaptive features using smart materials and/or smart methods. These systems are expected to possess higher performances relying on the embedded functions of sensors, actuators or processors than the conventional structural systems. Two examples of these systems are shown in Fig.3.2. One is a hybrid system with semi-active vibration control dampers made with smart material for super-structure and base isolation. This system can reduce seismic response acceleration as well as displacement. The other is a rocking structural system with yielding base plates. This system has yielding base plates at the bottom of each steel column at the first story. When the base plates yield during a strong earthquake, the building causes rocking vibration automatically to reduce its seismic response. Although the rocking system has neither specific smart materials nor computer control systems, it satisfies the concept of smart structural systems. Two series of shaking table tests were carried out to examine the seismic response of the rocking structural system with yielding base plates. Two types of test frames are shown in Photo.3.1. Two types of base plates are also shown in Photo.3.2. From the results, it has been concluded that the base plate yielding systems reduce effectively the seismic response of building structures [3.2][3.3][3.4].

3.3.2 RC Structural Systems with Damage Fuses

The example of RC structural systems with damage fuses is shown in Fig.3.3 and photo.3.3. To realize this system, the damping effect of damage fuses such as dampers was studied. The seismic performance evaluation method considering the damping effect has been developed. This evaluation method is based on the capacity spectrum method [3.5], the energy input rate spectrum method and so on.

3.3.3 Innovative Life Safety Systems

Simple and effective methods to reinforce low-rise inferior structures were studied. First of all, we conducted a questionnaire survey to academics, graduate students and structural engineers. They have presented us with new plans of smart elements and/or systems for reinforcement or life safety. The ideas collected were summarized into the following methods; 1) uplift of structures, 2) support for structures, 3) isolation systems, 4) adaptive structures, and 5) connecting systems. With considering the survey results, we proposed new innovative life safety systems easy to set up, which use loose linking elements. The concept of the system is illustrated in Fig.3.4. The seismic response of this system was examined by numerical analyses and shaking table tests. Test specimen is shown in Photo.3.4 and Fig.3.5. From the results, the relation between the setup of the systems and its reinforcement effects has been cleared [3.6].

3.4. Performance Evaluation Guide Line

The contents of performance evaluation guideline for smart structural systems are as follows;

Chapter 1 Introduction
Chapter 2 Target performance
Chapter 3 Performance evaluation against seismic motions and wind forces
Chapter 4 Maintenance
Chapter 5 Safety
Chapter 6 Reparability
Chapter 7 Health monitoring after construction

According to this guideline, structural engineers are required to explain the target performance of a building to its owner or user using performance matrices. And the performance of the building

must be generally evaluated by the time history analysis. The reparability of the building is examined by analyzing the life cycle cost of it. The performance evaluation guideline will be published this year.

3.5. Conclusions

1) The concept of smart structural systems for building engineering was proposed.

2) Based on the concept of smart structural systems, new structural systems were proposed and developed.

3) The performance of proposed smart structural systems was examined. Especially, superior performances of rocking structural systems with yielding base plates and retrofit systems using loose linking elements were shown successfully by shaking table tests.

4) The performance evaluation guideline was proposed.

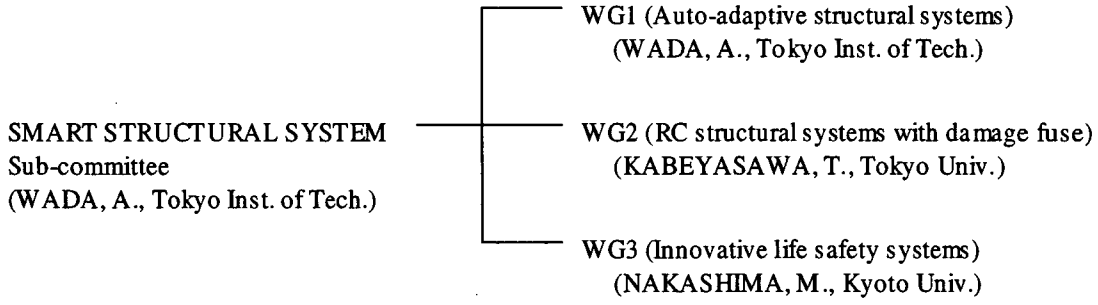
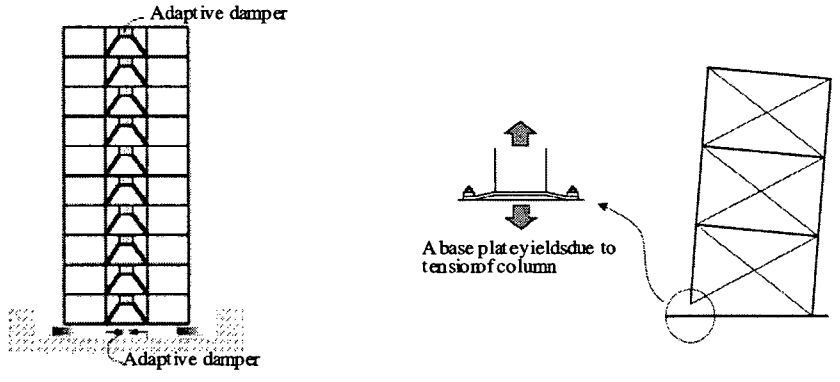


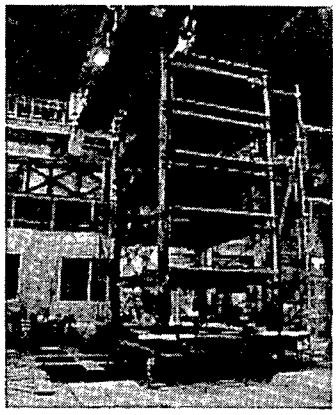
Fig.3.1 Research organization for smart structural systems



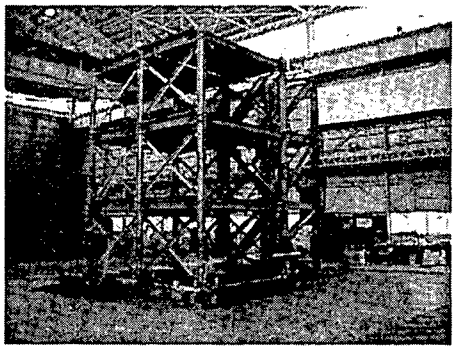
(a) Hybrid system with semi-active vibration control

(b) Rocking structural system with yielding base plates

Fig.3.2 Two examples of auto-adaptive structural



(a) Five-story test frame

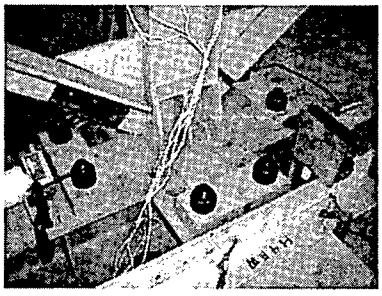


(b) Three-story test frame

Photo.3.1 Two types of test frames for shaking table tests



(a) Base plate with two wings for five-story test frame



(b) Base plate with four wings for three-story test frame

Photo.3.2 Two types of base plates

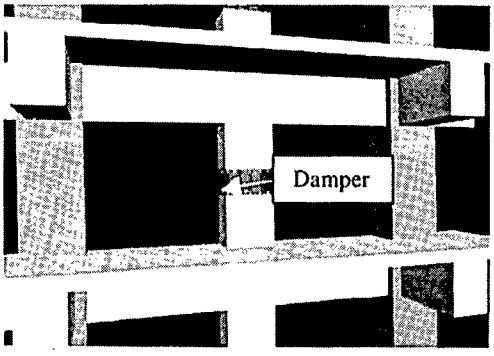


Fig.3.3 RC frame with damage fuses (dampers)

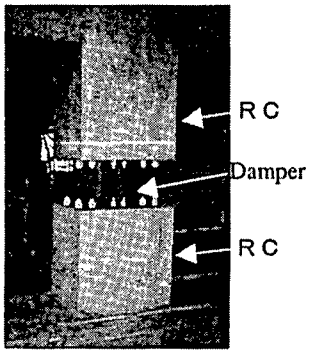


Photo.3.3 Example of dampers

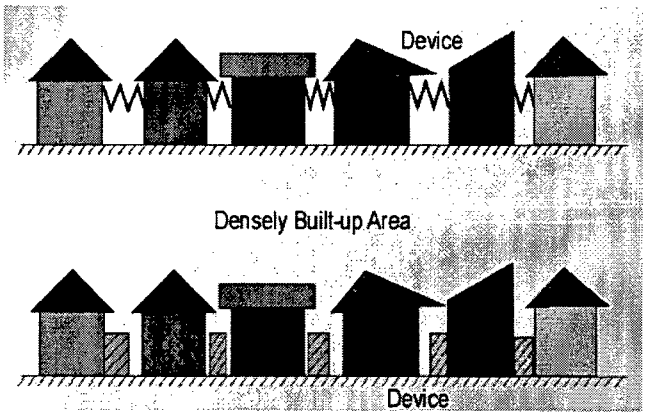


Fig.3.4 Retrofit system using loose linking elements

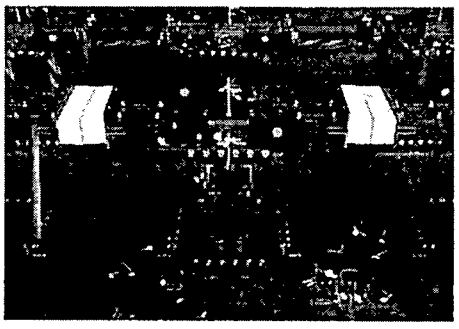


Photo.3.4 Test specimen for the retrofit system using loose linking elements

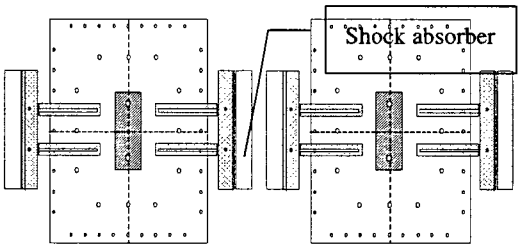


Fig.3.5 Plan of test specimen

4. SENSING AND MONITORING TECHNOLOGY

4.1 Outline of Sensing and Monitoring Technology

Objectives of sub-committee of "Sensing and Monitoring Technologies" are

1) To research and develop on systems that are provided with sensors and processor or with sensors with its own processor

2) To research and develop on smart sensors

Actual targets of research and development as shown below are defined after having discussed among members of sub-committee and working groups have been organized in accordance with these targets. Research organization is shown as Fig.4.1

Procedures of health monitoring are shown as Fig. 4.2. Inside of dash line in Fig 4.2, we tried something in this project. That is, from measuring data, we can evaluate physical parameters. But how to evaluate structural

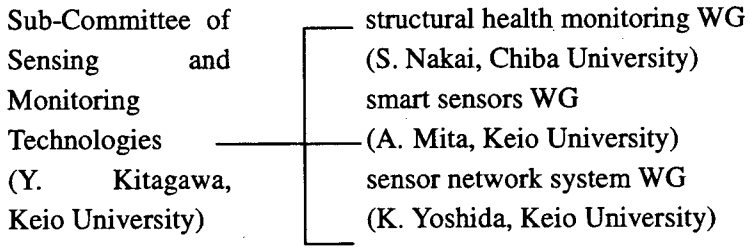


Fig.4.1 Organization of Sub-Committee of Sensing and Monitoring Technologies

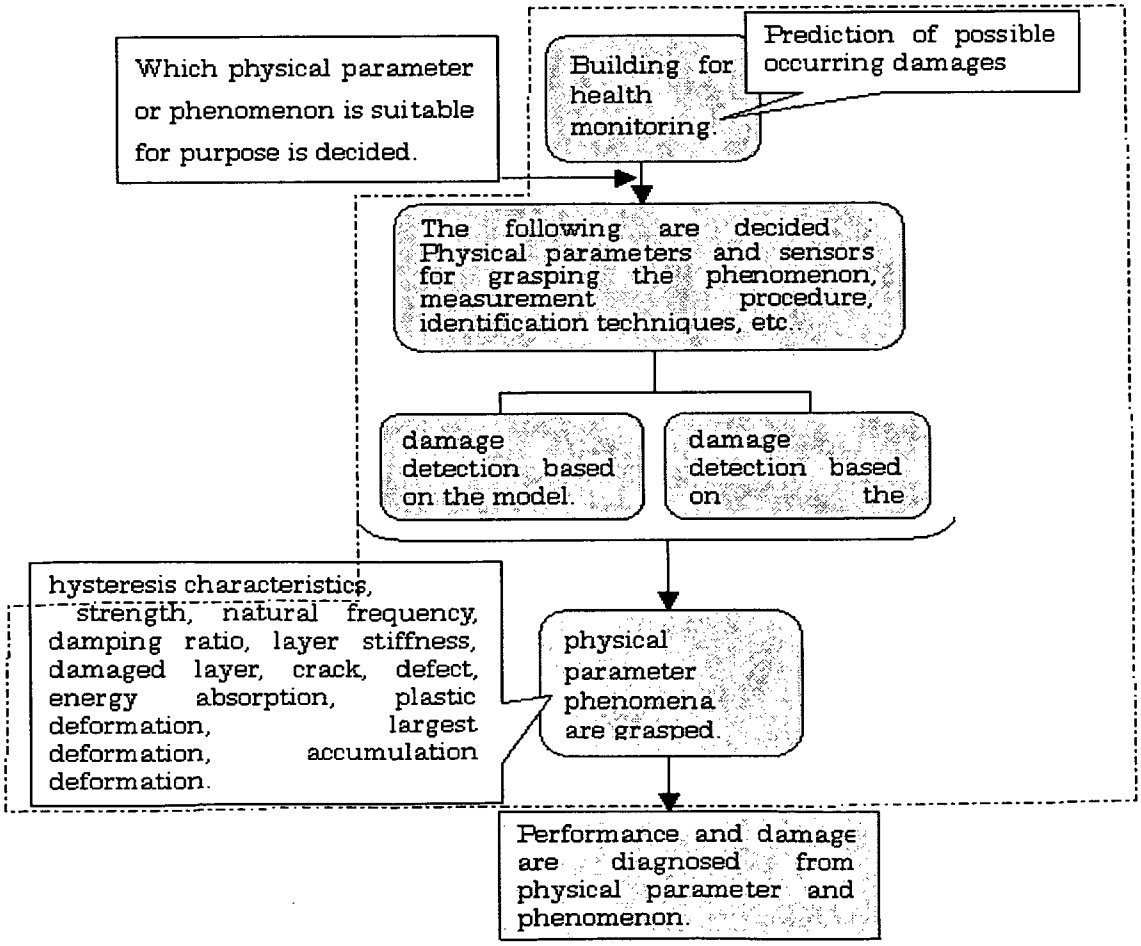


Fig. 4.2 Procedure of health monitoring

performance is not discussed in this guideline.

4.2 Structural Health Monitoring Technologies

4.2.1 Damage Detection Tests of Five-story Steel Frame

Damage detection tests of five-story steel frame with simulated damages are carried out. Test frame is five-story steel structure shown as Fig. 4.3. Fiber brag grating (FBG) sensors, accelerometers, strain gauges and laser displacement meters are installed in this test frame. We assume damages by removing studs from only one story, loosening bolts of beams, cutting part of beams and extracting braces from only one story. We apply flexibility method which is one of a damage identification methods using modal properties. We apply this method to experiments. In some cases we can estimate which story is damaged, and in other cases we cannot. If 1st story studs are removed, 1st story damage indicator is large as Fig.4.4. We also applied a method using multiple natural frequency shifts. Making use of the change in five natural frequencies due to damage, the location of damaged stories can be pinpointed. In both methods, we cannot identify damaged story in some cases. Some methods other than methods using modal properties have to be tried to apply in such cases.

4.2.2 Damage Detection Test Using Large Scale Test Frame

Shaking table test using a three-story large-scale steel structure with cementitious devices are carried out. The test frame is a three-story steel structure shown as Fig. 4.5. The test frame floor height is 1.8m, total height is 5.4m, floor plan is 4mx3m and there are two spans in excitation orthogonal direction. Shaking table test is carried out at large-scale earthquake simulator facility of the National Research Institute for Earth Science and Disaster Prevention. Cementitious devices

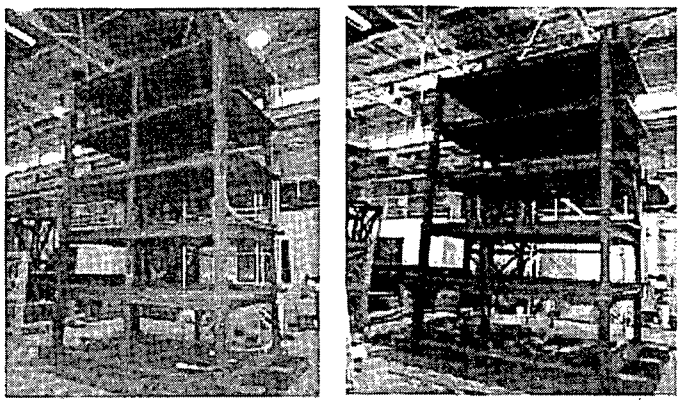


Fig. 4.3 Exterior of Test Frame

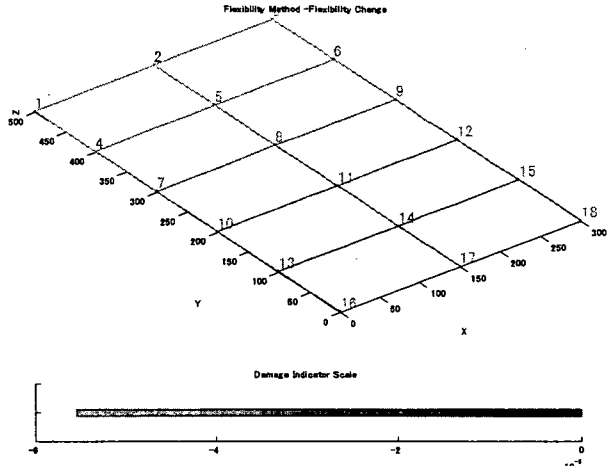


Fig. 4.4: Flexibility changes for no studs at 1st story

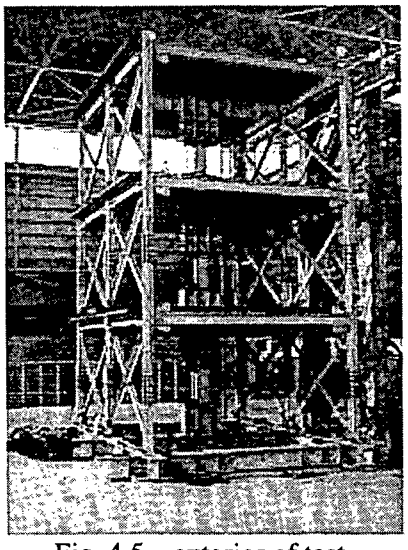


Fig. 4.5 exterior of test

are installed in the center frame of tested structure and devices are actually damaged during the shaking. We carry out damage

detection test by damaging devices and we measure the process of damaging devices. We apply damage identification methods to these phenomena. Two types of identification are tried. One is a) identification using the data under excitation and the other is b) identification using the data of before and after of the excitation. In both cases, we use identification method by ARX model. From identified results, natural frequency decreases, damping ratio increases and story stiffness decreases as experienced amplitude increases or input amplitude increases. Story stiffness results are shown as Fig. 4.6. Almost all characteristics by microtremor can be estimated to be same as those by white noise. A model using stick-slip elements is proposed. Natural frequency, damping ratio and story stiffness described by this model are consistent with experimental results.

4.3 Smart Sensor Technologies

4.3.1 Objective and Targets

The objective of this working group (WG) is to research and develop on smart sensors that measure and identify the state and phenomena of building structures and members. And finally This WG will propose guidelines for application of smart sensors for the health monitoring of building structures.

4.3.2 Sensors

This WG has surveyed materials, equipment, and systems that have possibility to use as sensors, and has studied on utilization and application of the sensors that have higher feasibility for the smart sensor. Following sensors were discussed.

1) Optical fiber sensors for displacement. deformation, strain, heat, and water

2) Carbon Fiber sensor in concrete for crack, strain, and deterioration of concrete

3) Radio-Frequency Identification (RFID) Tag sensor for crack on concrete

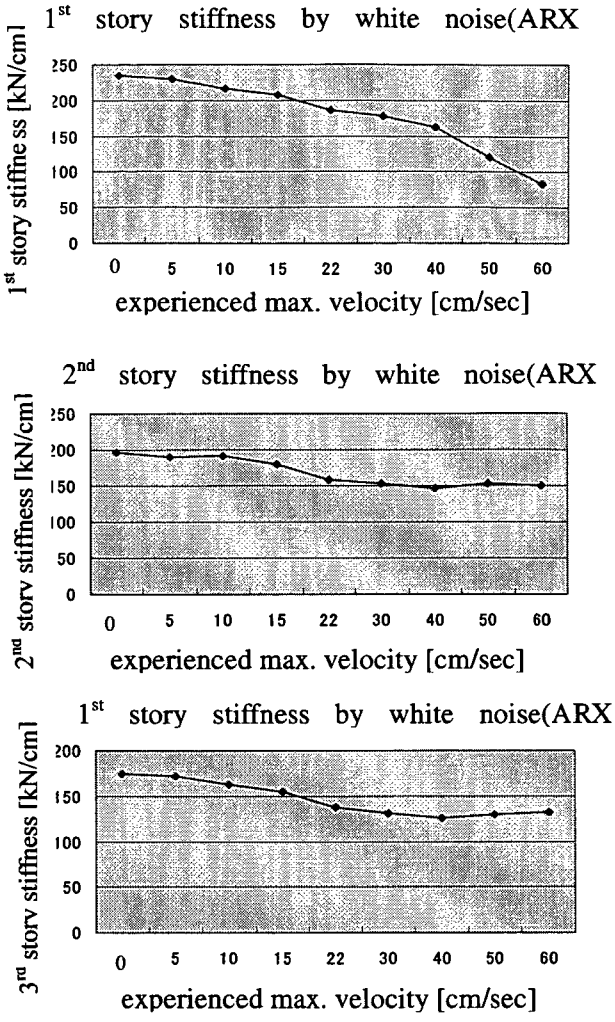


Fig. 4.6 : Stiffness change according to experienced max. velocity

4) Wave sensors for deterioration of concrete

5) Temperature sensor for plastic deformation of steel

6) Maximum value memory sensor for displacement

7) Two-wire sensing system with processor-built-in sensors

4.3.3 Radio-Frequency Identification (RFID)Tag sensor

The original concept of this sensor was proposed by Prof. Wood. This sensor consists of a IC tip with a tag number and an antenna which wire is elongated by additional wire, tape and carbon wire, as shown in Photo 4.1 and Fig.4.7. When a big crack occurs in the structural member,

the aluminum tape will be broken and the RF Transmit and Receiver cannot detect the RFID Tag sensor.

Only one RFID Tag sensor detected the crack occurred at the bottom of the RC member and the other sensors could not detected cracks, because almost cracks are less then 0.04 mm in width and the aluminum tapes have large ductility for crack detection. Therefore other wire materials such as small copper wires and carbon strings should be checked for detection of cracks.

4.3.4 Two-wire Sensing System with Processor-built-in Sensors

Outline of composition of the two-wire sensing system for the three-story steel frame test is shown in Fig.4.8. The system consists of 1) Processor-built-in sensors, 2) Two wires, 3)

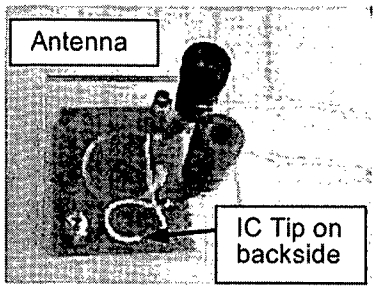


Photo 4.1 RFID Tag

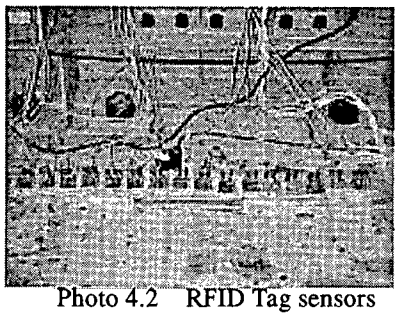


Photo 4.2 RFID Tag sensors

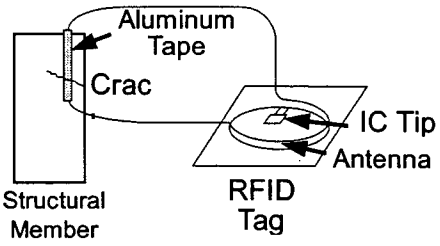


Fig.4.7 Schematic view of application of RFID Tag sensor to the structural members

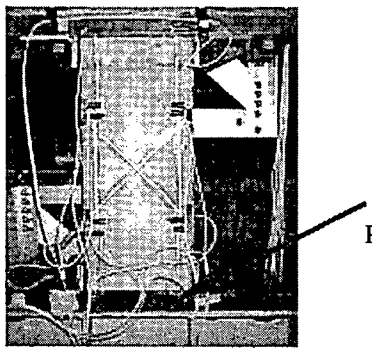


Photo.4.3 Aluminum tape for RFID

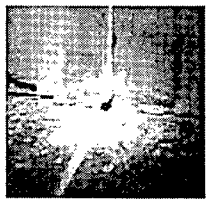


Photo4.4 Broken aluminum tape at the bottom of the RC member

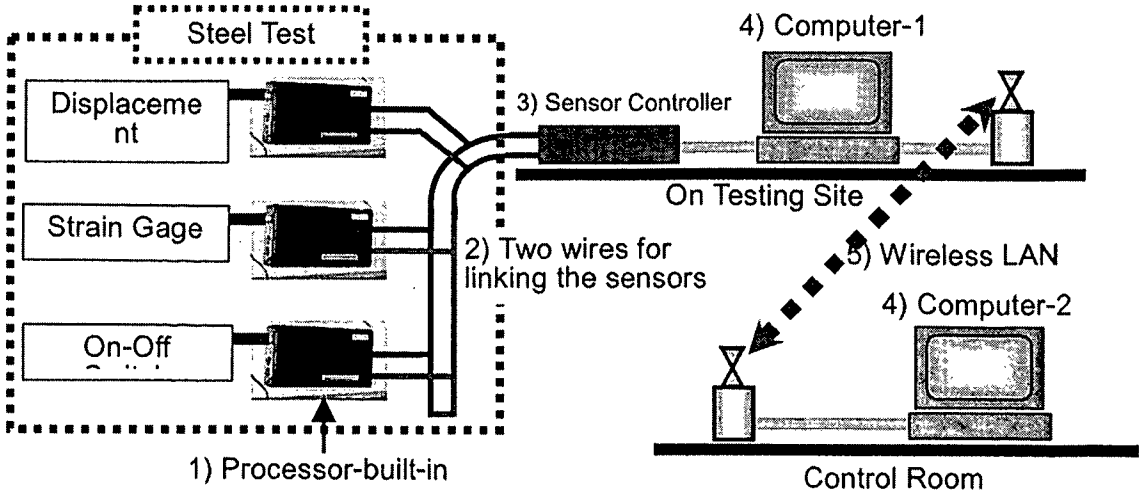


Fig.4.8 Outline of composition of wire-saving sensor system for the three-story steel frame test

Sensor controller, 4) Two computers, and 5) Wireless LAN system.

The processor-built-in sensor has a IC tip for strain measuring and a IC tip for A/D conversion and communication. Specifications of the processor-built-in sensors are as follows.

1) 1 channel for voltage and strain input for displacement transducers and strain gages

2) 4 channels for on-off switch for crack detection

3) 8 bits accuracy of A/D conversion

4) 10 msec interval of A/D conversion

5) 64 words for memory

6) Memory for maximum and minimum values

7) Memory for the local peak values (Fig.4.9)

8) Two-wire link for electric power supply and communication with controller

Fig.4.10 shows the comparison between peak values obtained from the wiring-saving sensor system and those from simulation using the measured data by dynamic measuring system. The peak values are in good correspondence. But this sensor has no time information now, so we cannot gat the time history but we can get

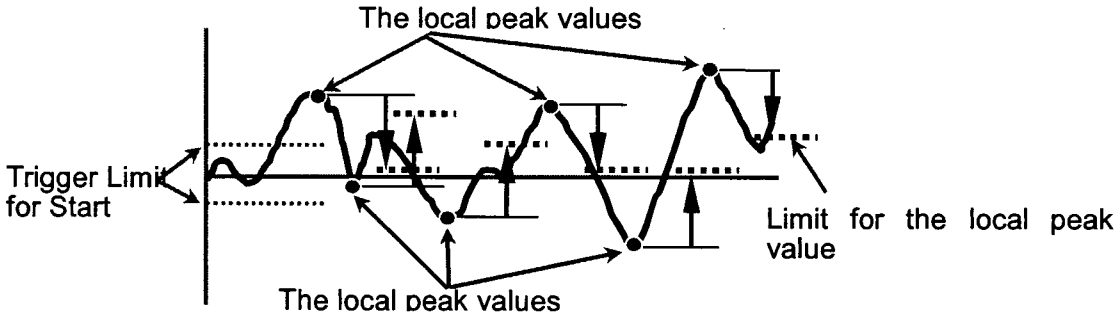


Fig.4.9 The local maximum and the local minimum values

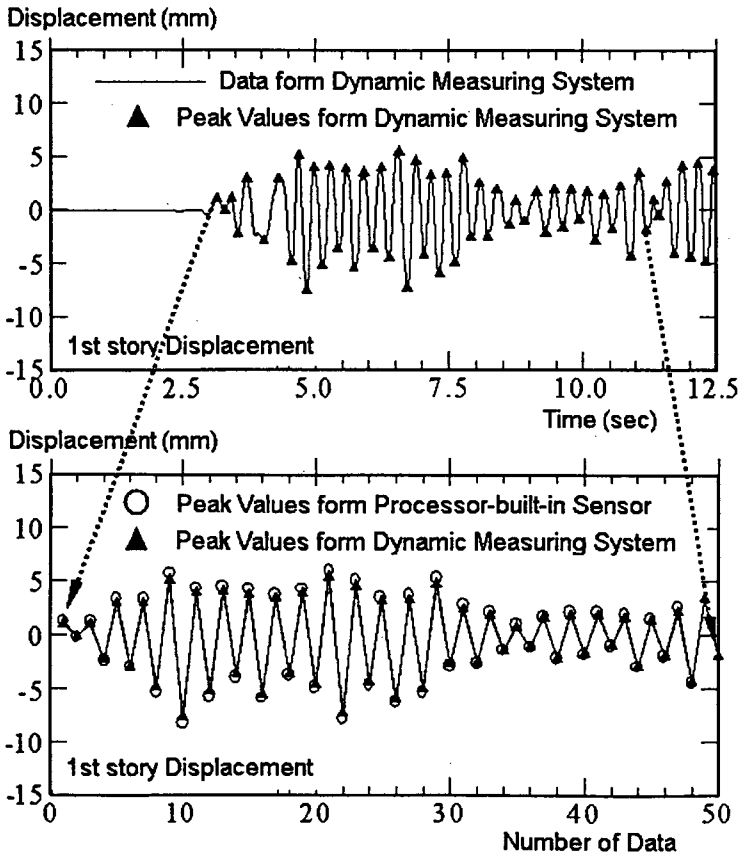


Fig.4.10 Comparison of peak date obtained from the dynamic measuring system and the wiring-saving sensor system

maximum and minimum values, each peak values and the accumulated value of data history.

4.4 Sensor Network System with RT-Linux

4.4.1 Introduction

As for the health monitoring which monitors the seismic performance of structure, it is needed to collect the data from various sensors installed in structure members and analyze them. And the collecting data system is needed.

This paper describes the "Sensor Network" which connects the installed sensors and provides health monitoring system of structures. The reference [1] showed the fundamental required items for this "Sensor Network" and this paper shows a health monitoring method of specimen which uses the "Sensor Network".

The main items are as follows (Fig.4.11);

(1) Networked Sensor System
(2) Simultaneous Measurement
(3) Real-Time Communication Mechanism
(4) Utilization of Existing Infrastructure
:Local Area Network
(5) Necessity of Real-Time Identification and Diagnosis

4.4.2 Sensor Network

In these years, after the information technology made much progress, buildings are prepared by Local Area Network (LAN) and connected each others. The Sensor Network in this paper is a measurement system of sensors installed at a part of this LAN of these buildings.

The most important point in the Sensor Network is to have a real time accuracy between the measuring of sensors. The real time accuracy means the limited time between the start time of a measuring and the end time of it. The Sensor Network is needed to guarantee the same start time of a measuring in all sensors and the same sampling time. That is why the Sensor Network uses the RT-Linux which is an operating system (OS) with the function of the real time process. Fig.4.12 shows the structure of RT-Linux. RT-Linux has an added function to deal with the real time process in the high level priority among the kernel executed in OS.

The communication system of this Sensor Network uses the RT-Messenger[2] which is the new real time application that can work under the RT-Linux.

In order to decrease the process for communication as less as possible and to escape from the

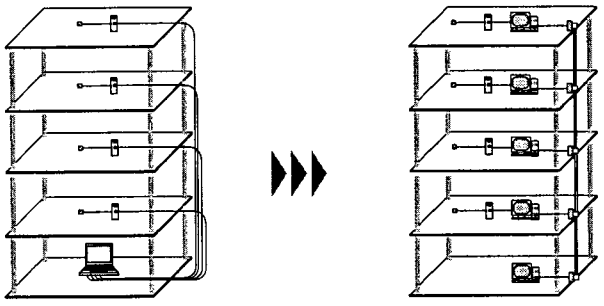


Fig.4.11 Utilization of LAN instead of Wiring

accidental late process by buffering, RT-Messenger is installed in the data-link-layer without TCP/IP (Transmission Control Protocol / Internet Protocol). RT-Message is defined as a packet type of RT-Messenger for receiving data of RT-Messenger from the data link layer.

4.4.3 Preliminary Experiment

The system of Sensor Network is shown in

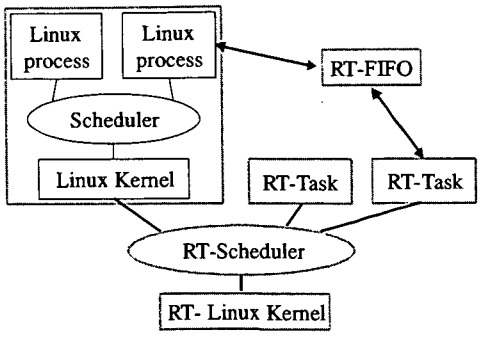


Fig.4.12 Structure of RT-Linux

Fig.4.13. RT-Messenger is installed in the 3 personal computers. The Network is 1 PC as a server, and 2 PCs as slaves for receivers. The PC properties are CPU: Pentium II 300, 400 [MHz], Kernel version of Linux: 2.2.14, RT-Linux version: 2.2.

In order to test the real time accuracy of the Sensor Network, RT-Messages are served in the time interval of 1 milli-second from the server and the late times of serving in the server and the late time of receiving in the Client-A and Client-B are measured. As a result, the late time of serve is 1.3 micro seconds in the maximum, and the late time of receive is 10.1 micro second in the maximum. After the transmit command in the interval of 1 milli-second, the time interval of serve and receive is exactly measured in 1 milli-second. It means that the late time of serve and receive is enough short to the time interval. That is why this Sensor Network has the enough real time accuracy.

And in order to verify the effects of RT-Messenger, the comparison between the system with RT-Messenger and the system without it are made. The comparison method is that 1 PC serves a packet in the time interval of 1 milli-second from RT-Task and the other PC receives the packet on RT-Task. Fig.4.14 shows the measuring results of the system with RT-Messenger.

In the system without RT-Messenger, an the side of serve, the ratio which the time interval is 1 milli-second is about 10%, and the tolerance is large. At the side of receive, the ratio which the time interval is 1 milli-second is lower than 5%, and the tolerance is large.

That is because the process interval times by the scheduler installed in Linux are guaranteed at most 10 milli-second. The RT-Linux is installed by the communication application called as RT-FIFO, but it works for the communications between the RT-Task and the user process of Linux in 1 computer, and RT-Linux does not permit to communicate RT-Task between the 2 computers directly. On the other hand, RT-Messenger permits to communicate RT-Task between 2 computers directly.

Finally, RT-Messenger is necessary for the "Sensor Network" which requires the real time accuracy.

4.4.4 Experiments

This Sensor Network is applied to the shaking test and the large-scale test.

In the shaking test, the comparison was made about natural frequencies in modes between this Sensor Network and FFT analyzer.

In the large-scale test, the comparison was made about the time history of data between this Sensor Network with the resolution of 12 bit and the high technology measurement device with the resolution of 24 bit.

According to these applications to tests, the

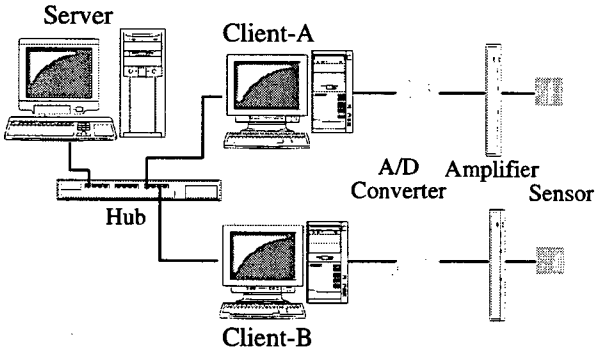


Fig.4.13 System of Sensor Network

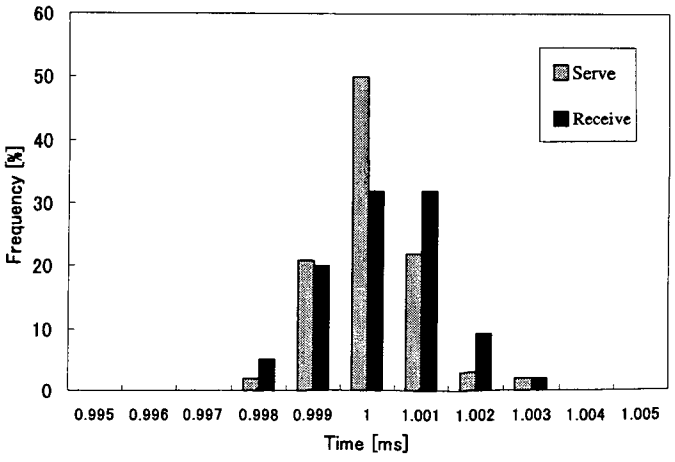


Fig.4.14 Time intervals with RT-Messenger

proposed Sensor Network has enough real time accuracy.

5. EFFECTOR TECHNOLOGY

5.1 Outline of Effector Technology

5.1.1 Research items

Purposes of researches in the " effector technology sub-committee " is to investigate characteristics of several "smart materials" and the applicability of "smart materials" or "smart members" to building structures. Due to requests to be made lighter materials and to be more effective and more reliable for control techniques, the smart materials are applied to systems in aerospace fields. On the other hands, the application of the smart materials to building use has not been popular because of necessity for a large amount of capacity and cost.

In the effector technologies sub-committee of the project " Development of Smart Structural Systems" , the smart materials, which will be applicable to the building structures in the very near future, were selected, and their characteristics and their applicability will be discussed.

The word "Effector" is defined materials and/or systems whose characteristics will be adaptive, that is, changing through external situation or external signals. These materials and systems will exert forces to structures more effectively than materials and systems will do in the passive situation. In addition, the materials are included which will make the structural performance higher during earthquake. Following items are being conducted.

i)Material characteristics and applications of the materials through summarizing results in published references.

ii)Material characteristics will be clarified through fundamental tests.

iii)Devices and systems will be produced and tested for verification as smart materials.

As materials which will be applicable in near future, following materials are selected.

a)Shape memory alloys

b)Electrorheological and magnetorheological fluids

c)Induced strain materials

d)High performance fiber reinforced cementitious composites

Research results are summarized in guidelines for characteristics of materials and devices, and applicable examples for buildings.

5.1.2 Research organization

Under the effector technology sub-committee, the research is being conducted in working groups for each materials as shown in Fig.5.1

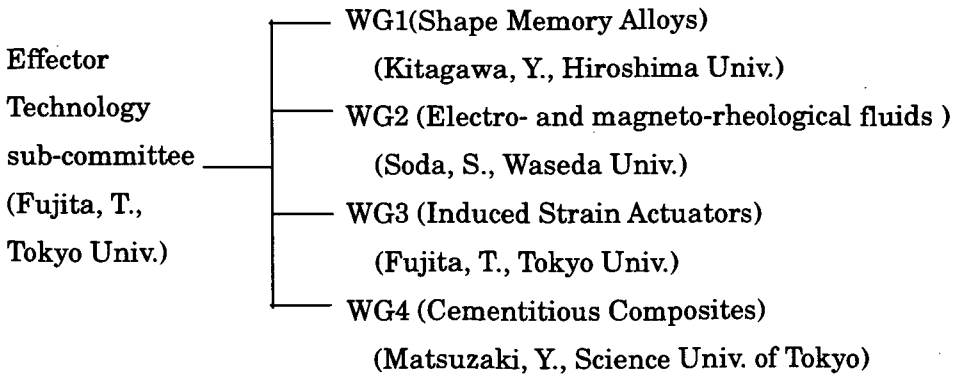


Fig.5.1 Organization of Effector Technology Sub-committee

5.2 Shape Memory Alloy

5.2.1 Research Objectives

The shape memory alloys(SMAs) shows two properties, that is, superelasticity and shape memory. These characteristics are dependent on a temperature in which the SMAs are used, as shown in Fig.5.2

This project focused on the superelastic properties of titanium-nickel alloy, currently the easiest shape memory alloy to obtain, to study its material properties as well as ways of using these material properties in building structures. In products, the alloy demonstrates stable material properties; in wire form, approximately 110 kNs of titanium-nickel alloy is used each year to manufacture antennas for mobile phones, and it is also used to make eyeglass frames. In building construction, the material has been used in the form of tensile braces for seismic reinforcement of a historical building. All of these applications have used the superelastic properties of the alloy. In wire form, the material is not only stable but has already demonstrated comparatively high performance in terms of energy absorption from cyclic loading. In this project, wires and bars were studied to determine the material properties of the alloy, with the aim of using it in building structures. And it was examined to determine the potential of their superelastic properties to control structural response of buildings.

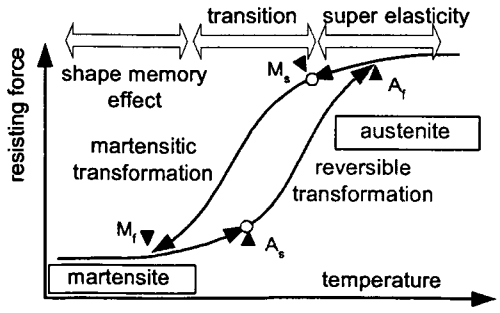


Fig.5.2 Material Phase-Property-Temperature Relation of SMA

5.2.2 Research Results

The following results were obtained, in particular from the material tests of bar prototypes(see, Figs.5.3 to 5.5).

1) In tensile tests, the material demonstrated clear superelasticity, with deformation of around 5% or less.

2) When the amount of energy absorption from cyclic loading is compared using the equivalent damping factor, the value for bars was lower than that for wires.

3) In compression tests, the material did not demonstrate perfect superelasticity; residual deformation was produced after unloading.

4) The stress-strain properties were different for tension and compression.

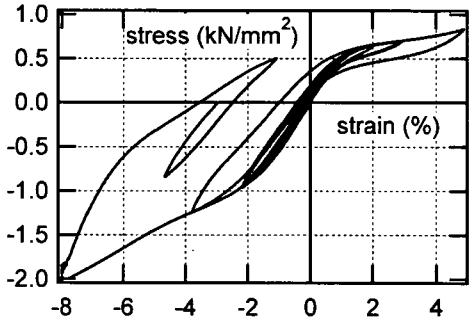


Fig.5.3 Stress-strain Relation of SMA-bar

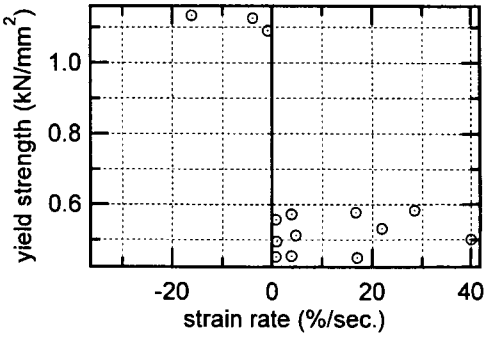


Fig.5.4 Yield Strength vs. Strain Rate

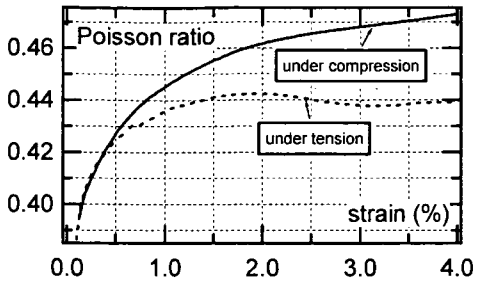
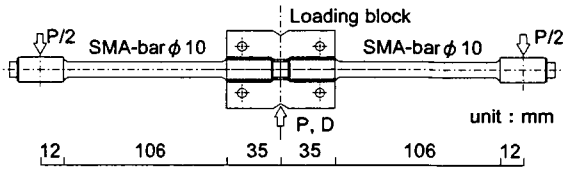


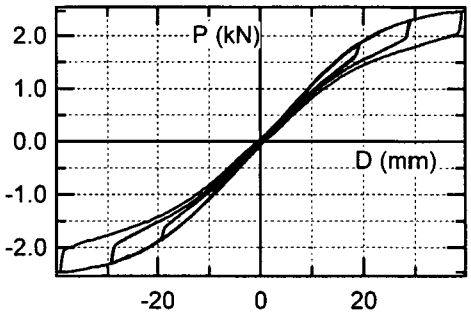
Fig.5.5 Poisson Ratio of SMA

Bars of the alloy were used to form tensile braces, bending members(see Fig.5.6), anchor bolts for column bases, and bolts for beam-column joints. Wires were used as longitudinal reinforcements for concrete members(see Fig.5.7) and tendons for prestressing members. These test specimens were studied to determine the potential of their superelastic properties to restore structural deformation to its original state (in other words, to determine their repair or restoration performance). The results of these tests show that the members demonstrated repair performance matching their material properties, and if the materials are used in a manner appropriate for the type, scale etc. of the structure, they have the potential to demonstrate both restoration performance and energy absorption. However, it was also learned that, even with the same alloy composition and method of manufacture, bars had a lower degree of energy absorption from cyclic loading under superelastic conditions. It was also learned that, in some cases, bars fractured brittlely under cyclic loading.

If one assumes that shape memory alloys will be used for response control of building structures, a member with large restoring force capacity will be needed. Accordingly, for the verification tests in this project, bars were considered to be one of the possible solutions, and so bars were used for tension members and bending members. Even with a bar form that has a large cross-sectional area, improvement of the manufacturing process is desirable to enable great energy absorption from cyclic loading to be obtained and to ensure that the material will not fracture in the early stages. In addition, the application of these bars must be designed to ensure suitable control over the range of the applied stress and deflection.

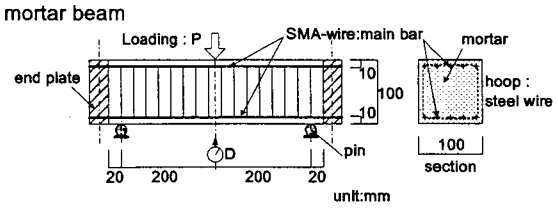


a) Test Specimen

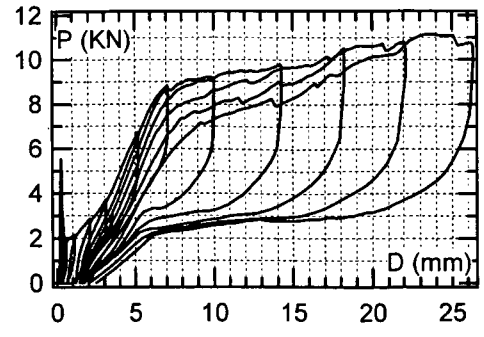


b) Force-displacement Relation

Fig. 5.6 Bending Test on SMA-bar



a) Test Specimen



b) Force-displacement Relation

Fig. 5.7 Bending Test on Mortar Beam

5.2.3 Conclusions

In this project, research focused on the superelasticity of shape memory alloys to determine their material properties and behavior when used for vibration control, etc. in building structures, and the potential for the use of these materials in building construction was discussed. Although shape memory alloys are a single material, they have two different material properties, as shown by the fact that they have not only superelasticity but a temperature domain with a shape memory effect. These two properties make shape memory alloys "smart" materials that can provide multiple functions, and thus they are both attractive and intriguing as metal materials.

It is thought that limited objectives for application, careful scrutiny of the performance needed to achieve these objectives, and effective use of the properties of these materials will enable optimal design for building structures. These materials are expected to find use in structures of various types.

5.3 Magnetorheological Fluid

5.3.1 Research Objectives

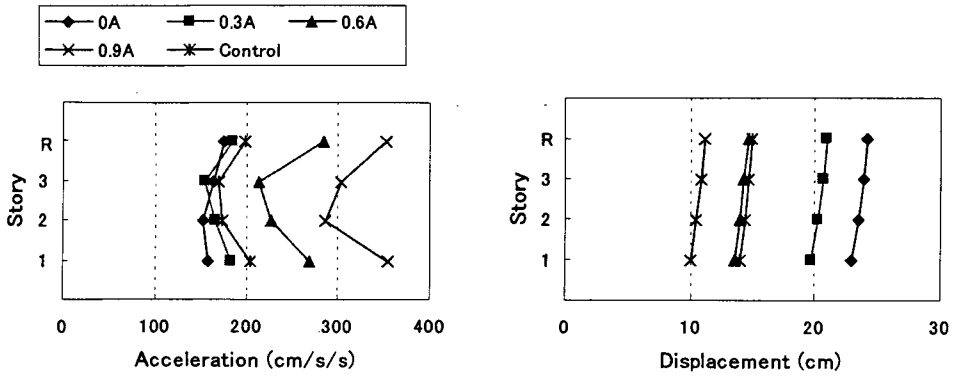
Magneto-rheological (MR) fluids have essential characteristics that change from free-flowing, linear viscous fluid, to a semisolid with a controllable yield strength when exposed to a magnetic field. This fluid is effective material for development of controllable devices. It is intended to develop a structure that changes its damping characteristic to behave adaptively against earthquake or wind forces and achieve safety and function by using MR devices with less Energy.

Some researches on application technology of MR fluid by Spencer et al. were conducted at the beginning of this project. They developed a 200kN MR damper[5.1] and proposed structural control strategies in case of base-isolated[5.2] and fixed base[5.3] building structures.

5.3.2 Researches and Development of MR Fluids and MR Dampers

Magnetorheological (MR) fluid is a dispersion of fine magnetizable particles in a liquid medium. In order to improve the stability, BRI and research group developed MR fluid *"#230"* with enhanced stability[5.4].

BRI and research group developed some MR dampers. At first, a simple MR damper (Photo 5.1) was developed in order to verify the performance of MR damper, for example, force-displacement relationship, force-velocity relationship, influence of temperature and



(a) Absolute acceleration (b) Relative displacement

Fig. 5.8 Average Values of Response of Each Story of Positive Side and Negative Side (El Centro 1940 NS, Maximum velocity is 50cm/sec)

response speed of MR damper[5.5]. Then a 200kN MR damper was developed in order to verify the same items in case that the electromagnet is attached at the bypass flow portion, which is connected to the cylinder[5.6].

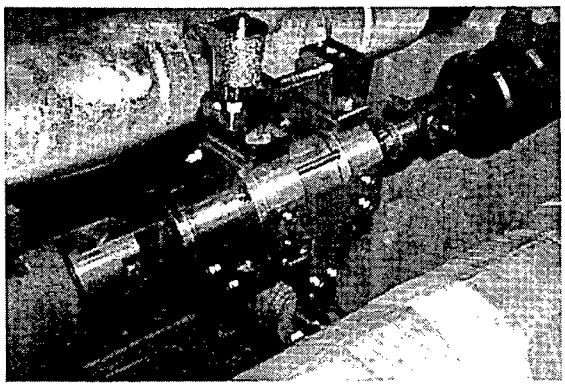


Photo 5.1 20kN MR Damper

Next, a long stroke MR damper (Photo 5.2: +/-295mm)) was developed for base-isolated structural model. The MR damper was used for a large scale shaking table test.

5.3.3 Verification by Large-scale Test

Semi-active control reduces both response displacements and accelerations. MR damper generates damping force, which does not depend on the piston speed so much. The target of this subject is to improve the safety and functionality and habitability by controlling the response displacements and accelerations by using MR dampers. For this purpose, a series of shaking table tests was conducted[5.7].

Figure 5.8 shows one of the test results. The controlled accelerations are reduced the same as one of 0.3A, and the controlled displacements are reduced the same as 0.6 A. This shows that semi-active control by the MR damper can reduce the response displacements while reducing the response acceleration[5.8].

5.3.4 Application to An Actual Base-isolated Building

A 400kN MR damper for an actual base-isolated building was developed and its dynamic

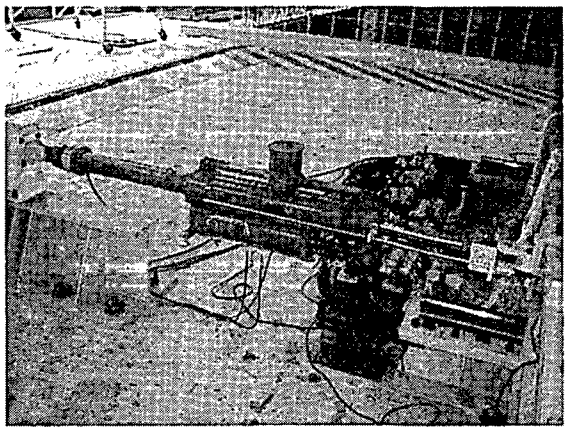


Photo 5.2 Long Stroke MR Damper

characteristics verified by experimental tests. The MR damper has 950mm (+/-475mm) stroke and by-pass flow potion. To verify the dynamic characteristics of the MR damper, a series of experimental tests were conducted by using dynamic actuator. Figure 5.9 shows the force-displacement relationship. The yield force of the MR damper increases with the rise of the electric current, and it was verified that the maximum damping force was controllable by adjusting the magnetic field[5.4].

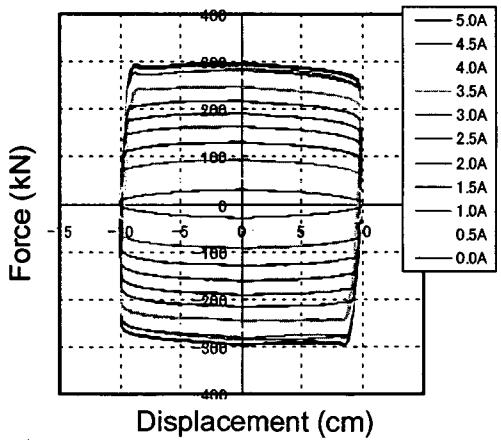


Fig. 5.9 Force-displacement Relationship of 400kN MR Damper

5.3.5 Conclusuions

Several kinds of MR dampers are developed. The damper with 20kN-capacity was developed to verify the performance. The 200kN and 400kN dampers were developed, which have the bypass flow piston. And the long stroke damper was developed for the base isolation building. The

semi-active control by the MR damper is effective to reduce both displacement and acceleration responses through the large scale test model.

As results of this research, some future tasks are summarized.

1) Development of evaluation method of stability and durability of MR fluid.
2) Development of structure of MR damper for the effective use of MR fluid
3) Development of semi-active control strategy for the effective use of MR damper

5.4 Strain Induced Actuator

5.4.1 Research Objectives

Induced Strain Actuators (ISA) can change their own shapes according to external electric/magnetic fields, and vice versa. Recently these materials have been widely used for the small/precision machines because of some advantages from viewpoint of small sizes, rapid reaction, high power, high accuracy etc. The objectives in this study are to develop smart members for building and to realize the smart, comfortable and safe structures. The research items are as follows:

1) Semi-active isolation of structures using piezoelectric actuator
2) Using ISA as sensor materials
3) Improvement of Acoustic Environment

We will show some examples of application of ISA in this study.

5.4.2 Semi-active Isolation of Structures Using Piezoelectric Actuator

Using passive base-isolation technique, response acceleration of the superstructure is sufficiently reduced but large horizontal displacement between the ground and superstructure is needed. So to keep the margin space is necessary, but it becomes useless space when earthquakes do not attach the structure. In Japan, land prices are very expensive, so it is desired to make margin space smaller. In this study, semi-active base-isolation technique, which can reduce the acceleration of the structure and keep the margin space small, is adopted. Furthermore, semi-active system cannot supply energy to structure, so it is very safe system.

In this study, semi-active base isolation system with controllable friction damper using piezoelectric actuators is proposed. Two types of friction damper are proposed, one is holding type and the other is releasing type. (Figs. 5.10 and 5.11)It is better to use releasing type if we consider fail safe effect. By simulation study, it could be realized to reduce response displacement of the structure to 50% of values of the passive isolation.

5.4.3 Application of Piezoceramic Actuator to Active Noise Control

In order to improve the noise transmission loss of walls and windows, the conventional method of noise control often fails to reduce noise at low frequencies in particular. We experimentally confirm the practicability of the PZT to utilize for the secondary sources of the active noise control system.

As shown in Fig. 5.12, a loudspeaker is located inside the enclosure as a noise source and the opening was closed by an aluminum plate of 0.5mm thickness. PZT actuator is stuck on the middle of the aluminum plate. As a noise signal, a broad band noise of from 100 to 1kHz is radiated from the loudspeaker inside the enclosure. The deficiency of the transmission loss at around 125Hz is improved about 10dB by the active noise control.

5.4.4 Application of PVDF as A New Strain Gauge for Membrane

A key in membrane structure control is how to sense the stress state in the membrane. Measuring strain in membrane requires special technique since membrane has low stiffness. Ordinary wire strain gauges are generally too stiff and they

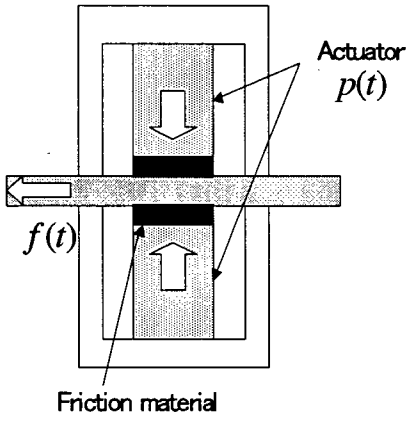


Fig. 5.10 Controllable Friction Damper (Holding Type)

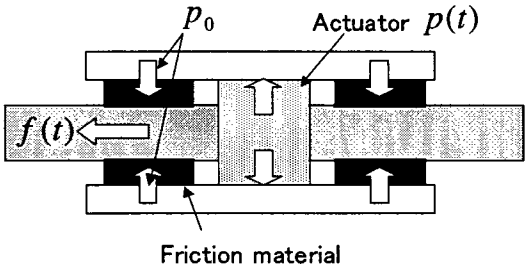


Fig. 5.11 Controllable Friction Damper (Releasing Type)

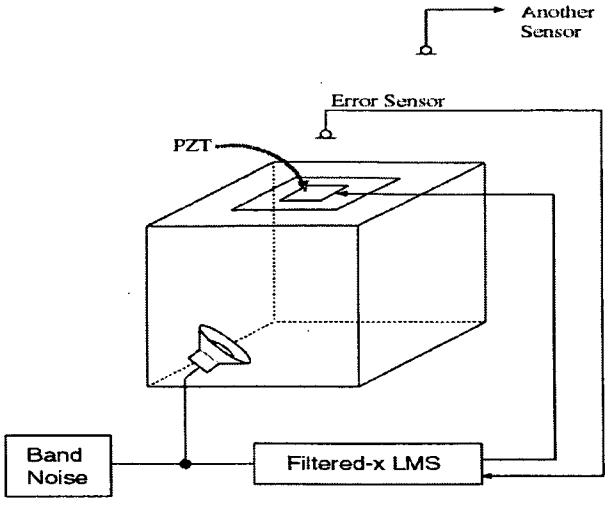


Fig. 5.12 Experimental Setup for Active Noise Control

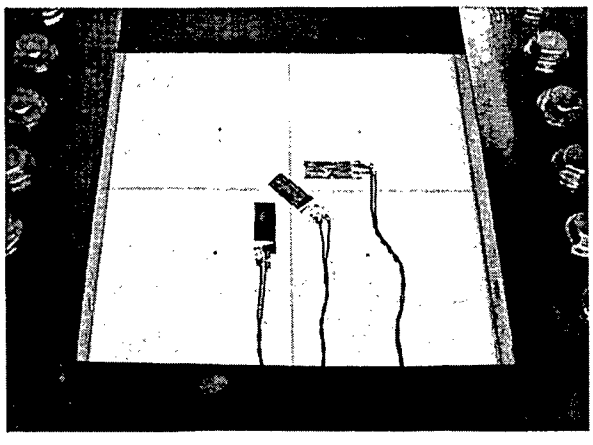


Fig.5.13 PVDF sensors for Membrane Specimen

violate the natural deformation state of the membrane.

In this paper we report the results of a series of tests aiming to develop a new flexible, low-stiffness, strain gauge for membrane using PVDF. Figure 5.13 shows experimental set up and the location of the sensors. Square grids were drawn on the membrane for the electric slide caliper. The strain rate was 6～8 me/sec, quasi static. For static strain sensor, slower static deformation process should be measured with same accuracy. For membrane strain sensor glue and gluing scheme which transmit the deformation of the membrane to PVDF without any reduction should be developed.

5.4.4 Conclusions

Research results are summarized as follows;

a) Semi-active isolation

As one of the methods to execute semi-active isolation of structures by smart structure, friction controllable damper using piezoelectric actuator was proposed in this study. Simulation study was carried out, and this damper is very effective to reduce response.

b) Active noise control

In this study, we indicate that PZT actuator can be used as the secondary source of the active noise control even for the broad band noise.

c) PVDF sensor

Low stiffness strain sensor for membrane, using PVDF, was proposed and two methods, open circuit and closed circuit, were examined.

5.5 High Performance Cementitious Composites

1.5.1 Research Objectives

The objective of this research is to develop high performance cementitious structural elements, which have highly energy dissipation and damage tolerant properties utilizing High Performance Fiber Reinforced Cementitious Composites (HPFRCC), to achieve a damage tolerant structural system as a smart structural system. Feasibility study will be conducted for the other types of cementitious smart materials, elements and systems. The self-repairable material is one of the research items. Guidelines for utilization of HPFRCC are final target of the research program.

5.5.2 What Is HPFRCC?

Figure 5.14 is an example of the flexural test of un-reinforced HPFRCC plate. HPFRCC is chopped fiber reinforced cementitious composites (mortar/concrete), which exhibits strain-hardening with superior strain capacity, shear ductility, and extreme damage tolerant mechanical behavior. The ultra ductile behavior of HPFRCC, combined with its flexible processing requirements, isotropic properties, and moderate fiber volume fraction (typically less than 2% depending on fiber type and interface and matrix characteristics) make it especially suitable for critical elements in seismic applications where high performance such as energy absorption, steel/concrete deformation compatibility, spall resistance and damage tolerance are required. Applications to both new structures and in retrofitting of existing R/C structures to withstand future earthquakes are considered.

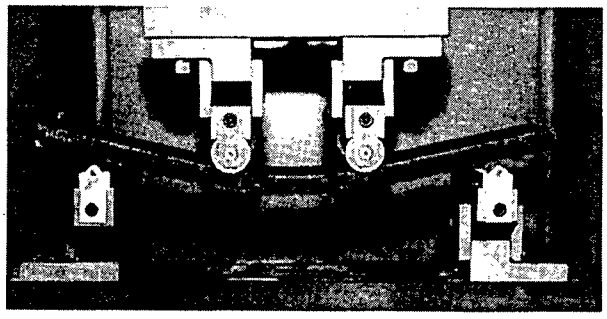


Fig. 5.14 Flexural Test of
Un-reinforced HPFRCC Plate

5.5.3 Merit of Smart Structural System with HPFRCC

HPFRCC elements are expected to decrease the response and damage of building structures under external disturbances to achieve a high level of building performance requirements. Those requirements are not only structural safety but also reparability, serviceability, and durability of

buildings after external disturbances.

The strength and ductility of the HPFRCC elements can be controlled easily by its dimensions and types of material used. Then it is expected to develop the suitable energy dissipation and damage tolerant elements for concrete structures with higher stiffness than the other types of structures. Since the HPFRCC elements will be able to dissipate the input energy by external disturbances even in the small deflection state of the buildings, response and damage of building will be decreased.

5.5.4 Research items and Results

Following research items have been investigated.

1) Development of HPFRCC materials, material design methods and clarification of its properties; There is an example of the tension properties of the developed HPFRCC, as shown in Fig. 5.15.
2) Development of the construction methods for HPFRCC elements
3) Development of HPFRCC constitutive model for FEM
4) Relationships between HPFRCC material properties and structural performance
   Influence of tension properties of HPFRCC to the elemental performance
   Influence of compression properties of HPFRCC to the elemental performance
   Application into the HPFRCC damper for structural control is shown in the Figs. 5.16 and 5.17.
5) FEM analysis to investigate the relationships between material properties and structural performance
6) Feasibility study on the application example as HPFRCC damper, CES columns and self-repairing HPFRCC

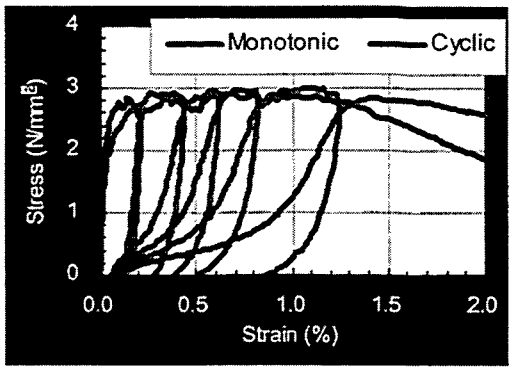


Fig. 5.15 Material Properties of Developed HPFRCC

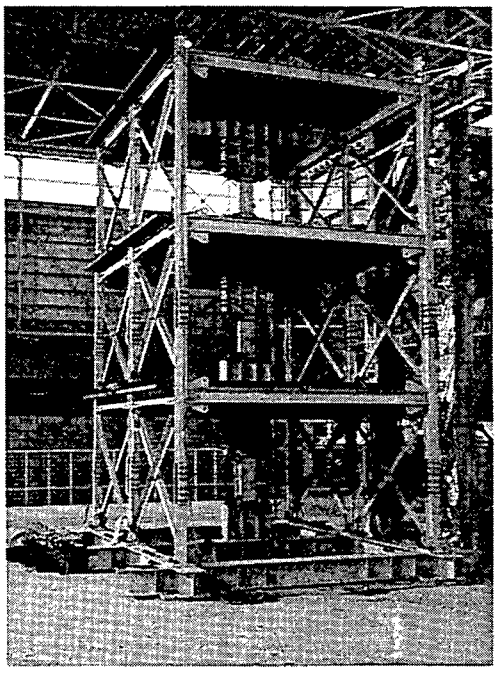


Figure 5.16 Application example - HPFRCC damper for structural control

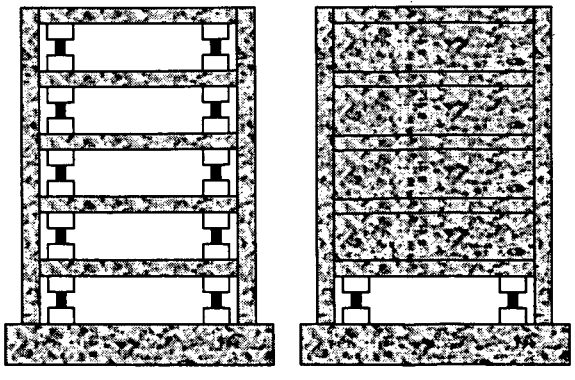


Fig. 5.17 Application examples of HPFRCC damper for R/C structures

5.5.5 Conclusions

The research results are summarized as follows;

1)The HPFRCC has high performance (very ductile) against tensile force through the material tests.

2)The strength and ductility of the HPFRCC elements can be controlled easily by its dimensions and types of material used.

3)The HPFRCC elements have highly energy absorbing characteristics

Actual application of the HPFRCC is highly expected to meet the variety of social requirements. The building regulation should be modified to support the development of the new technologies like HPFRCC materials and smart structural system with HPFRCC.

6 CONCLUDING REMARKS

Building Research Institute and the National Science Foundation, U.S.A. initiated the research and development of "Smart Structural Systems" in 1998 as a 5-year research project. The results of research are :

1) The concept of smart structural systems for building engineering was proposed.

2) Based on the concept of smart structural systems, new structural systems were proposed and developed.

3) The performance of proposed smart structural systems was examined. Especially, superior performances of rocking structural systems with yielding base plates and retrofit systems using loose linking elements were shown successfully by shaking table tests.

4) The performance evaluation guideline was proposed.

5) Some methods of system identification were tried and story damages and stiffness were detected.

6) Some newly developed sensors are tried to detect damages and some cracks or energy absorption were detected.

7) Sensor Network with RT-Linux is very useful for the monitoring system which requires the real time accuracy.

8) As materials which will be applicable in near future, following materials are selected;

+Shape memory alloys

+Electrorheological and magnetorheological fluids

+Induced strain materials

+High performance fiber reinforced cementitious composites

Characteristics of materials and these members and the applicability of these materials to building structures are investigated.

The MR dampers and Induced strain materials be applicable to response control through the semi-active control of buildings during earthquakes.

9) The MR dampers are effective to reduce the seismic response under an appropriate control.

10) The application of piezoceramic actuators to not only structural response control during earthquake but also Noise control for comfortable livings will be probable.

11) The HPFRCC will be applicable to damage control members of buildings.

12) The application of SMA to structural members in buildings will provide buildings will possess a self-restoration function.

Results of this program are summarized in annual report [6.1]~[6.5] of smart structural system published from BRI, BCJ, and et.al.. Report of 3 JTCCs and proceedings of workshop were summarized in references[2.1]~[2.3]. Forty-three papers in English are submitted as listed in Appendix.

This research and development project aims to apply advanced technologies, such as new materials and new structural systems, to develop smart structural systems. It is expected that the

project can improve the performance

7 ACKNOWLEDGEMENT

This work has been carried out under the US-Japan cooperative structural research project on Smart Structure Systems. The authors would like to acknowledge all members of the project for their useful advice and suggestions.

8 REFERENCES

1.1 Otani S, 1999

2.1 Proceedings of "US-Japan Workshop on Smart Structural Systems –the first JTCC of US-Japan cooperative researdh project" 2000

2.2 Proceedings of "The Second Joint Technical Coordinating Committee Meeting –US-Japan Cooperative Research on Auto-Adaptive Media (Smart Structural Systems)-" 2000

2.3 Proceedings of "Workshop on Smart Structural Systems organized for U.S.-Japan Cooperative Research Programs on Smart Structural Systems (Auto-adaptive Media) and Urban Earthquake Disaster Mitigation" 2002

3.1 Otani, S., Hiraishi, H., Midorikawa, M. and Teshigawara, M., "Research and development of smart structural systems", Proc., 12th World Conference on Earthquake Engineering, Paper ID 2307, 2000.2.

3.2 Azuhata, T., Midorikawa, M., Ishihara, T. and Wada, A., "Shaking Table Tests on Rocking Structural Systems with Base Plate Yielding", Proc. of SEWC2002, T2-7-a-2, 2002.10.

3.3 Midorikawa, M., Azuhata, T., Ishihara, T., Matsuba, Y. and Wada, A., "Shaking table tests on earthquake response reduction effects of rocking structural systems", SPIE's 10th Annual International Symposium on Smart Structures and Materials, 2003.3.

3.4 Midorikawa, M., Azuhata, T., Ishihara, T. and Wada, A., "Shaking table tests on rocking structural systems installed yielding base plates in steel frames", Proc. of STESSA 2003, 2003. 6.

3.5 Kuramoto, H., et al., "U.S-Japan Cooperative Research Project on Smart Structure System, Dynamic Response Behavior of Reinforced Concrete Buildings with Damping Devices (Part.1-3)", Summaries of Technical Papers of Annual Meetings, AIJ, pp.943-948, 2002.8. (In Japanese)

3.6 Nakashima, M., et al., "Earthquake Responses of a Cluster of Building Structures Connected with Loose Linking Elements", Proc. of Workshop on Smart Structural Systems Organized for U.S.-Japan Cooperative Research Programs on Smart Structural Systems (Auto-adaptive Media and Urban Earthquake Disaster Mitigation), pp.451-463.

4.1 Mizuo INUKAI, Kazuo YOSHIDA, "U.S.-Japan Cooperative Research Project on Smart Structure System. (Part:11) Research Plan of Sub-WG about Networking, in Subcommittee on Sensoring Techniques", Summary of technical papers of annual meeting (Tohoku), vol.B-2, September 2000, Architectural Institute of Japan. (in Japanese)

4.2 Hideo SATOH, Takahiro YAKOH, "Real time application for strict time control multimedia", Transaction Journal of Information Processing Society of Japan, vol., 42, No. 2, (2001) (in Japanese)

5.1 B. F. Spencer Jr., G. Yang, M. K. Sain and J. D. Carlson:"Samrt" Dampers for Seismic Protection of Structures:A Full-Scale Study, Proc. of 2WCSC, 1998.6-7, pp.417-426.

5.2 E. A. Johnson, J. C. Ramallo, B. F. Spencer Jr. and M. K. Sain:Intelligent Base Isolation Systems, Proc. of 2WCSC, 1998.6-7, pp.367-376.

5.3 F. Yi, S. J. Dyke, S. Frech and J. D. Carlson:Investigation of Magnetorheological Dampers for Earthquake Hazard Mitigation, Proc. of 2WCSC, 1998.6-7, pp.349-358.

5.4 Hideo FUJITANI, Hiroshi SODEYAMA, Takuya TOMURA, Takeshi HIWATASHI, Yoichi SHIOZAKI, magnetorheological damper for a real base-isolated building, SPIE's 10th Annual International Symposium on Smart Structures

and Materials, 5052-31, 2003.3
5.5 Katsuaki Sunakoda, Hiroshi Sodeyama, Norio Iwata, Hideo Fujitani and Satsuya Soda:Dynamic Charac- teristics of Magneto-Rheological Fluid Damper, Proc. of SPIE Vol. 3988, SPIE's 7th Annual International Symposium on Smart Structures and Materials, Newport Beach, California, pp.194-203, 2000.3.
5.6 Fujitani H., Shiozaki Y., Hiwatashi T., Hata K., Tomura T., Sodeyama H. and Soda S. : RESEARCH AND DEVELOPMENT OF SMART BUILDING STRUCTURES BY MAGNETO-RHEOLOGICAL DAMPER, Proceedings of International Conference on Advances in Building Technologies, 2002.12.
5.7 Takeshi HIWATASHI, Yoichi SHIOZAKI, Hideo FUJITANI, Masanori IIBA, Takuya TOMURA, Hiroshi SODEYAMA and Satsuya SODA : Semi-active control of large-scale test frame by Magneto-Rheological Damper, Proc. of 3WCSC, 2002.4.
5.8 Fujitani H., Azuhata T., Morita K., Hiwatashi T., Shiozaki Y., Hata K., Sunakoda K., Soda S. and Minowa C. : LARGE-SCALE TESTS ON SMART STRUCTURES AND SEMI-ACTIVE CONTROL BY MR DAMPER, International Conference on Advances and New Challenges in Earthquake Engineering Research, 2002.8.
6.1 Annual report on US-Japan cooperative structural research project on Smart Structure Systems (in Japanese), 1998
6.2 Annual report on US-Japan cooperative structural research project on Smart Structure Systems (in Japanese), 1999
6.3 Annual report on US-Japan cooperative structural research project on Smart Structure Systems (in Japanese), 2000
6.4 Annual report on US-Japan cooperative structural research project on Smart Structure Systems (in Japanese), 2001
6.5 Annual report on US-Japan cooperative structural research project on Smart Structure Systems (in Japanese), 2002

APPENDIX

List of publication in English

1) Otani, S., Hiraishi, H., Midorikawa, M., and Teshigawara, M.: Research and Development of Smart Structural Systems, Proc. of the 12th World Conference on Earthquake Engineering, New Zealand, Paper ID 2307, 2000.1-2

2) Otani, S., Hiraishi, H., Midorikawa, M., Teshigawara, M., Saito, T., and Fujitani, H.: Development of Smart Systems for Building Structures, Proc. of SPIE Vol. 3988, SPIE's 7th Annual International Symposium on Smart Structures and Materials, Paper 3988-01, Newport Beach, California, 2000.3

3) Katsuaki Sunakoda, Hiroshi Sodeyama, Norio Iwata, Hideo Fujitani andSatsuya Soda:Dynamic Characteristics of Magneto-Rheological Fluid Damper, Proc. of SPIE Vol. 3988, SPIE's 7th Annual International Symposium on Smart Structures and Materials, Paper 3989-20, Newport Beach, California,

4) Hiroshi Sodeyama, Katsuaki Sunakoda, Hideo Fujitani, Satsuya Soda and Norio Iwata : Development of A Magneto-rheological fluid damper for Semi-active Vibration Control Systems of Real Building Structure, Proceedings of Fifth International Conference on MOTION and VIBRATIONCONTROL '2000, Sydney, December 4-8, 2000.

5) Hideo Fujitani, Hiroshi Sodeyama, Katsuhiko Hata, Norio Iwata, Yutaka Komatsu, Katsuaki Sunakoda and Satsuya Soda : Dynamic Performance Evaluation of Magneto-Rheological Damper, Proceedings of Advances in Structural Dynamics 2000, Hong Kong, 13-15 December, 2000.

6) Koichi Morita, Masaomi Teshigawara, Hiroshi Isoda, Takuji Hamamoto, Akira Mita : Damage Identification Tests of Five-story Steel Frame with Simulated Damages, SPIE 6th Annual International Symposium on NDE for Health Monitoring and Diagnostics, 4335-18, 2001.3

7) Masaomi Teshigawara, Hiroshi Isoda, Toshihide Kashima, Tadashi Ishihara : Modeling and Measurement for Health Monitoring of an Existing SRC 8-story Building, SPIE 8th Annual International Symposium on Smart Structures and Materials, 4330-11, 2001.3

8) Satsuya Soda, Norio Iwata, Katuaki Sunakoda, Hiroshi Sodeyama, Hideo Fujitani : Experimental and analytical methods for predicting mechanical properties of MRF damper, SPIE 8th Annual International Symposium on Smart Structures and Materials, 4330-24, 2001.3

9) Koichi Morita, Takafumi Fujita, Shiro Ise, Ken'ichi Kawaguchi, Takayoshi Kamada, Hideo Fujitani, Development and Application of Induced Strain Actuators for Building Structures, SPIE 8th Annual International Symposium on Smart Structures and Materials, 4330-51, 2001.3

10) Mitsumasa Midorikawa, Tatsuya Azuhata, Yutaka Matsuba, Yoshiyuki Matsushima and Tadashi Ishihara : Rocking Structural Systems to Reduce Earthquake Responses of Buildings, EERI Annual Meeting (Poster Session), 2001.2

11) Hideo Fujitani, Satsuya Soda, Norio Iwata, Hiroshi Sodeyama, Katsuhiko Hata, Katsuaki Sunakoda and Yutaka Komatsu : Dynamic Performance Evaluation of Magneto-rhelogical Damper by Experimantal and Analytical Method, Proc. of the US-Japan Workshop on Smart Sructures for Improved seismic Performance in Urban Regions, August 14, 2001, pp.237-248.

12) Mitsumasa Midorikawa, Tatsuya Azuhata, Tadashi Ishihara, Yutaka Matsuba Yoshiyuki Matsushima and Akira Wada:Earthquake Response Reduction of Buildings by Rocking Structural Systems, SPIE's 9th Annual International Symposium on Smart Structures and Materials, vol.4696, pp.265-272, 2002.3

13) Norio Iwata, Katsuhiko Hata, Hiroshi Sodeyama, Katsuaki Sunakoda, Hideo Fujitani, Takeshi Hiwatashi, Yoihi Shiozaki and Satsuya Soda : Application of MR damper to base-isolated structures, SPIE 9th Annual International Symposium on Smart Structures

and Materials, 4696-45, 2002.3
14) Toshibumi FUKUTA, Masanori IIBA, Yoshikazu KITAGAWA, Yoshirou SHUGO : Experimental results on stress-strain relation of Ni-Ti shape memory alloy bars and their application to seismic control of buildings, proceedings of 3rd World Conference on Structural Control, 2002.4
15) Hideo FUJITANI, Mitsumasa MIDORIKAWA, Masaomi TESHIGAWARA, Masanori IIBA, Koichi MORITA, Tatsuya AZUHATA, Hiroshi FUKUYAMA, Akiyoshi FUKUDA, Yoichi SHIOZAKI, Takeshi HIWATASHI and Chikahiro MINOWA : Large-scale Tests on Smart Structures for Their Performance Verification, Proc. of 3WCSC, 2002.4.
16) Yoichi SHIOZAKI, Takeshi HIWATASHI, Hideo FUJITANI, Katsuhiko HATA, Katsuaki SUNAKODA and Satsuya SODA : Study of Response Control by MR Damper for base-isolated buildings, Proc. of 3WCSC, 2002.4.
17) Takeshi HIWATASHI, Yoichi SHIOZAKI, Hideo FUJITANI, Masanori IIBA, Takuya TOMURA, Hiroshi SODEYAMA and Satsuya SODA : Semi-active control of large-scale test frame by Magneto-Rheological Damper, Proc. of 3WCSC, 2002.4.
18)Fujitani H., Azuhata T., Morita K., Hiwatashi T., Shiozaki Y., Hata K., Sunakoda K., Soda S. and Minowa C. : LARGE-SCALE TESTS ON SMART STRUCTURES AND SEMI-ACTIVE CONTROL BY MR DAMPER, International Conference on Advances and New Challenges in Earthquake Engineering Research, 2002.8.
19) Hiroshi FUKUYAMA, Haruhiko SUWADA and Yang IISEUNG: HPFRCC Composite Damper for Structural Control, Workshop on Smart Structural Systems organized for U.S.-Japan Cooperative Research Programs on Smart Structural Systems (Auto-adaptive Media) and Urban Earthquake Disaster Mitigation, Building Research Institute, Tsukuba, Japan, October 18, 2002, pp.1-12.
20) Hiroshi KURAMOTO, Tomohiro ADACHI and Kiyohiko KAWASAKI: Behavior of Concrete Encased Steel Composite Columns Using FRC, Workshop on Smart Structural Systems organized for U.S.-Japan Cooperative Research Programs on Smart Structural Systems (Auto-adaptive Media) and Urban Earthquake Disaster Mitigation, Building Research Institute, Tsukuba, Japan, October 18, 2002, pp.13-26.
21) Takuya Tomura, Katsuhiko Hata, Hideo Fujitani and Shin Morishita : MAGNETORHEOLOGICAL FLUIDS WITH IMPROVED STABILITY, Workshop on Smart Structural Systems organized for U.S.-Japan Cooperative Research Programs on Smart Structural Systems (Auto-adaptive Media) and Urban Earthquake Disaster Mitigation, Building Research Institute, Tsukuba, Japan, October 18, 2002, pp.87-93.
22) Hiroshi Sodeyama, Hideo Fujitani, Satsuya Soda and Katsuaki Sunakoda : DEVELOPMENT OF MR DAMPERS FOR TESTS WITH LARGE SCALE STRUCTURE MODEL, Workshop on Smart Structural Systems organized for U.S.-Japan Cooperative Research Programs on Smart Structural Systems (Auto-adaptive Media) and Urban Earthquake Disaster Mitigation, Building Research Institute, Tsukuba, Japan, October 18, 2002, pp.95-107.
23) Satsuya SODA, Norio IWATA, Hideo FUJITANI, Yoichi SHIOZAKI, Takeshi HIWATASHI and Chikahiro MINOWA : Semi-Active Seismic Response Control of Base-isolated Building with MR Damper, Workshop on Smart Structural Systems organized for U.S.-Japan Cooperative Research Programs on Smart Structural Systems (Auto-adaptive Media) and Urban Earthquake Disaster Mitigation, Building Research Institute, Tsukuba, Japan, October 18, 2002, pp.109-116.
24) Toshifumi FUKUTA, Yoshikazu KITAGAWA, Masanori IIBA and Yuji SAKAI :

Loading Tests on Mortar-beam Reinforced by Shape Memory Alloy with Super-elastic Property, Workshop on Smart Structural Systems organized for U.S.-Japan Cooperative Research Programs on Smart Structural Systems (Auto-adaptive Media) and Urban Earthquake Disaster Mitigation, Building Research Institute, Tsukuba, Japan, October 18, 2002, pp.181-192.

25) Koichi MORITA and Masaomi TESHIGAWARA: Damage Detection Test Using Large Scale Test Frame, Workshop on Smart Structural Systems organized for U.S.-Japan Cooperative Research Programs on Smart Structural Systems (Auto-adaptive Media) and Urban Earthquake Disaster Mitigation, Building Research Institute, Tsukuba, Japan, October 18, 2002, pp.207-220.

26) Takuji HAMAMOTO, Koichi MORITA and Masaomi TESHIGAWARA: Story Damage Detection of Multistory Buildings Using Natural Frequency Shifts of Multiple Modes, Workshop on Smart Structural Systems organized for U.S.-Japan Cooperative Research Programs on Smart Structural Systems (Auto-adaptive Media) and Urban Earthquake Disaster Mitigation, Building Research Institute, Tsukuba, Japan, October 18, 2002, pp.221-234.

27) Masaomi TESHIGAWARA and Hiroshi ISODA: Development of Health Monitoring System for an Existing Building, Workshop on Smart Structural Systems organized for U.S.-Japan Cooperative Research Programs on Smart Structural Systems (Auto-adaptive Media) and Urban Earthquake Disaster Mitigation, Building Research Institute, Tsukuba, Japan, October 18, 2002, pp.247-258

28) Kazuo YOSHIDA, Mizuo INUKAI, Yoichi AOKI and Hirofumi OGAKI: Development of Sensor Network with RT-Linux, Workshop on Smart Structural Systems organized for U.S.-Japan Cooperative Research Programs on Smart Structural Systems (Auto-adaptive Media) and Urban Earthquake Disaster Mitigation, Building Research Institute, Tsukuba, Japan, October 18, 2002, pp.369-374

29) Tatsuya AZUHATA, Mitsumasa MIDORIKAWA, Y. MATSUBA and Akira WADA: Shaking Table Tests on Rocking Structural Systems for Their Performance Verification, Workshop on Smart Structural Systems organized for U.S.-Japan Cooperative Research Programs on Smart Structural Systems (Auto-adaptive Media) and Urban Earthquake Disaster Mitigation, Building Research Institute, Tsukuba, Japan, October 18, 2002, pp.375-382

30) Masayoshi NAKASHIMA, Tatsumi SHINOHARA, Shigehiro MOROOKA, Maho KOBAYASHI, Noriaki MISAWA, Toru NAKAGAWA, Mitsumasa MIDORIKAWA and Tadashi ISHIHARA: Earthquake Responses of a Cluster of Building Structures Connected with Loose Linking Elements, Workshop on Smart Structural Systems organized for U.S.-Japan Cooperative Research Programs on Smart Structural Systems (Auto-adaptive Media) and Urban Earthquake Disaster Mitigation, Building Research Institute, Tsukuba, Japan, October 18, 2002, pp.451

31)Tatsuya Azuhata, Mitsumasa Midorikawa, Tadashi Ishihara and Akira Wada: Shaking Table Tests on Rocking Structural Systems with Base Plate Yielding, Proc. of SEWC2002, T2-7-a-2, 2002.10.

32) Hiroyuki TAMAI, Yoshikazu KITAGAWA : Pseudoelastic Behavior of Shape Memory Alloy Wire anad its Application to Seismic Resistance Member for Building, Computational Materials Science, Vol.25, pp.218-227, 2002.9

33)Norio Iwata, Hiroshi Sodeyama, Katsuaki Sunakoda, Katsuhiko Hata, Takeshi Hiwatashi, Yoichi Shiozaki, HIdeo Fujitani, Satsuya Soda, Experimental study on the effectiveness of a simple semi-active control algorithm for base-isolated structures, 11th Japan Earthquake Engineering Symposium, No.326, 2002.11.

34)Hideo Fujitani, Yoichi Shiozaki, Takeshi

Hiwatashi, Katsuhiko Hata, Takuya Tomura, Hiroshi Sodeyama, Satsuya Soda, A Research and Development of Smart Building Structures by Magneto-rheological damper, Proceedings of Advances in Building Technology, Vol.1, pp.473-480, 2002.12.
35) Hiroshi Sodeyama, Hideo Fujitani, Katsuaki Sunakoda, Satsuya Soda and Norio Iwata :Dynamic tests and Simulation of Magneto-rheological Damper, Journal of Computer-aided Civil and Infrastructure Engineering 18 (2003), pp.45-57.
36)Satusya Soda, Haruhide Kusumoto, Ryosuke Chatani, Norio Iwata, Hideo Fujitani, Yoichi Shiozaki, Takeshi Hiwatashi, Semi-active seismic response control of base-isolated building with MR damper, Proceedings of the SPIE's 10th Annual Int., Symposium on Smart Structures and Materials, No.5052-56, 2003.3.
37)Hideo Fujitani, Hiroshi Sodeyama, Takuya Tomura, Takeshi Hiwatashi, Yoichi Shiozaki, Katsuaki Sunakoda, Shin Morishita, Satsuya Soda, Development of 400kN magnetorheological damper for a real base-isolated building, Proceedings of the SPIE's 10th Annual Int., Symposium on Smart Structures and Materials, No.5052-31, 2003.3.
38) Takeshi Hiwatashi, Yoichi Shiozaki, Hideo Fujitani, Chikahiro Minowa, Satsuya Soda, Shaking table tests on Semi-active base-isolation system by Magnetorheological Fluid damper, Proceedings of the SPIE's 10th Annual Int., Symposium on Smart Structures and Materials, No.5056-50, 2003.3.
39) Mitsumasa Midorikawa, Tatsuya Azuhata, Tadashi Ishihara, Yutaka Matsuba and Akira Wada: Shaking table tests on earthquake response reduction effects of rocking structural systems, SPIE's 10th Annual International Symposium on Smart Structures and Materials, 2003.3.
40) Tatsuya Azuhata, Mitsumasa Midorikawa and Akira Wada: Study on applicability of rocking structural systems to building structures, SPIE's 10th Annual International Symposium on Smart Structures and Materials, 2003.3.
41) Y. Sakai, Y. Kitagawa, T. Fukuta, M. Iiba : Experimental Study on Enhancement of Self-restoration of Concrete Beams using SMA Wire, SPIE 10th Annual International Symposium on Smart and Materals, March 2003
42) Hiroyuki TAMAI, Kenji MIURA, Yoshikazu KITAGAWA, Toshifumi FUKUTA : Application of SMA Rod to Exposed-type Column Base in Smart Structural System, SPIE 10th Annual International Symposium on Smart and Materals, March 2003
43) Mitsumasa Midorikawa, Tatsuya Azuhata, Tadashi Ishihara and Akira Wada: Shaking table tests on rocking structural systems installed yielding base plates in steel frames, proc. of STESSA, 2003. 6.

Potential of Satellite and Aerial Remote Sensing Technologies for Earthquake Disaster Management

by

K. Thirumalai[1]

ABSTRACT

The paper focuses on potential payoffs and the importance of exploring innovative technology applications using remote sensing capabilities for earthquake hazard and disaster management. New tools are presented for potential application to earthquake disaster management from the result of a national program on remote sensing and spatial information technology application to transportation, a joint program with the National Aeronautics and Space Administration (NASA) managed by the Research and Special Programs Administration (RSPA) of the U.S. Department Of Transportation. The paper discusses the potential application of remote sensing technologies for disaster management in the following critical areas:

1) Application of Synthetic Aperture Radar (SAR) technology for detection and measurement of ground strains in large land masses associated with strain energy accumulation and releases leading to earthquakes.

2) Remotely sensed imagery analysis for assessment of critical infrastructure vulnerability to transportation service disruptions and for community planning of emergency preparedness.

3) Development of new sensing platforms for near real time and readily deployable imagery capability using Unmanned Airborne Vehicles (UAVs) for applications to emergency management of transportation, after an earthquake event.

[1]Chief Engineer, Research and Special Programs Administration, Department of Transportation, Washington, DC 20590-0001

KEYWORDS: remote sensing technology, synthetic aperture radars, transportation network vulnerability, disaster management, Unmanned Airborne Vehicles (UAVs).

1.0 INTRODUCTION

During the past three decades, earthquake hazard mitigation research in the U.S. and Japan, has made significant advances in technical understanding and analysis of earthquake mechanisms and predicting damage to structures. Viable tools for measuring precise ground movements in large land mass structures generated by strain energy accumulation that lead to earthquakes are not currently available. This limitation presents a barrier for achieving responsive earthquake pre-event recognition and disaster mitigation processes. Space or aerial based sensing and measurement of ground strain in large land areas associated with earthquake energy accumulations would have the potential for recognizing earthquake events before their occurrence and provide new tools for disaster management. The advances in satellite and aerial based sensing, information and communication technologies offer a range of potential 'leap frog' technologies for application to earthquake event recognition and disaster management. During the next decades, earthquake R&D programs for hazard mitigation should focus on exploring the potential application of these remote sensing technologies and concepts to predict earthquake events and plan for the safety and evacuation of communities in regions prone to earthquakes.

2.0 SYNTHETIC APERTURE RADAR APPLICATION FOR LAND MASS STRAIN DETECTION

Synthetic Aperture Radar (SAR) is a new space geodetic imaging technology that has the potential for enabling precise measurement of changes in the Earth's surface and surface deformation over large land masses before, during, and after earthquakes. Fundamentally, SAR measures the range of reflected radar signals to determine ground alterations and strains from an observing satellite using advanced processing of the reflected signal's amplitude and phase. The sensing range is determined by measuring the time between transmission of a pulse to receiving the echo from a target .

An airborne radar could collect data while flying long distances and then process the data as if it came from a long antenna. SAR measurement is similar to holography in that two SAR images are differenced, revealing changes in the Earth's surface with a resolution of fractions of the radar wavelength. Modern SAR satellites can precisely measure and map hundreds of square miles of land areas in a very short time. Civilian exploration of SAR technology application to infrastructure planning and construction will increase during this decade , because lower cost electronics are just beginning to make SAR technology economical for smaller scale uses.

SAR has the potential to accurately image millimeter level changes in the Earth's surface in response to changes in stress and strain energy accumulation within the Earth's crust. SAR can measure slow accumulation of strain changes in the Earth's surface and provide views of micro changes in land mass surface at resolutions adequate for performing ground strain measurements leading to earthquakes. The analysis of imageries using SAR has the potential to lead to revolutionary change in our understanding of the strain build up and forces leading to earthquake events.

Sequences of SAR images could detect the land mass changes and weakness in the overburden as an early sign of incipient ground failure. Recent technological advances in space born radar interferometry permit observation of mm-level surface deformation. The National Research Council, National Science Foundation, NASA and the United States Geological Survey have identified SAR as an essential tool in developing and extending our ability to warn of impending natural hazards and disasters.

3.0 APPLICATION OF REMOTE SENSING IMAGERIES FOR ASSESSEMENT OF TRANSPORTATION NETWORKS AND PLANNING FOR EARTHQUAKE EMERGENCIES

Remote sensing technologies enhance the decision process on critical transportation infrastructure service condition for emergencies by providing a visual perspective of critical links to highway networks such as highway bridges, rail lines and critical intersections. Custom software and analysis methods are now available for augmenting existing centralized national databases such as National Highway Planning Network (NHPN) and Highway Performance Monitoring System (HPMS) that 'tracks down' highway bridges and critical links from remotely sensed imagery and facilitates information on condition and serviceability in transportation networks after an earthquake event.

Figure 1 shows an example of an illustration of the working one of the custom software developed in a DOT study (2) for damage and vulnerability assessment of critical transportation infrastructure network using SPOT imagery. The imageries reveal structural characteristics that simplify the

interpretation of serviceability for emergency response, following a disaster. Comparison of the imageries taken before the event with 'After' event images using a centralized geospatial information system provides comparative damage assessment and serviceability evaluation for evacuation. The serviceability condition of critical networks and the extent of disruption are immediately ingested into a network-modeling program to generate critical intelligence for emergency managers on serviceability status of traffic networks for emergency planning and evacuation.

Evacuation of communities during unplanned and unexpected disaster events place a congestion burden on existing transportation networks. Transportation network vulnerability event analysis is an important first step for ensuring that the communities in earthquake prone regions have open transportation network systems for emergency evacuation. Congestion evaluation , in the event of a disaster, helps public policymakers and planners in building transportation systems that are robust in the event of unplanned disruption to critical transportation links. The dynamic flow model developed in a U.S. DOT project (3) captures system-wide impacts on congestion and its propagation over space and time.

Residential development in disaster prone regions is occurring at an unprecedented rate. Many threatened areas do not have an evacuation plan. In order to illustrate potential application of remote sensing technology for emergency preparedness decision process, a hazard example is taken from a study completed by U.S. DOT project team in a sample community east of Salt Lake City, Utah , a region highly prone to high fire recurrence levels (3) . Satellite imagery and data from the developer were merged to identify the road network and location of homes in the subdivision. This information was used with traffic simulation software to design and test neighborhood evacuation plans. The method allows an analyst to map the sub-neighborhood variation in household evacuation travel-times and potential transportation bottlenecks during a disaster. It also identifies the location of the bottleneck. Figure 2 depicts the mean household evacuation times for a relatively urgent evacuation where an average of 2.5 vehicles departed each household and the mean departure time following notification of the entire neighborhood was 10 minutes. The Figure also shows the effect of reducing the evacuation time by providing a second exit for this community. It demonstrated to the residents and planners that the new road significantly alleviates traffic problems during an evacuation and supported the decision by the County to build a second exit road.

4.0 NEAR REAL-TIME REMOTE SENSING DURING EARTHQUAKE DISASTER EVENTS USING UNMANNED AIRBORNE VEHICLES (UAVs).

A capability to deploy remote sensing operations immediately after a disaster event is important for an immediate assessment of the damage and serviceability of transportation infrastructure and critical transportation networks in the proximity of earthquake disaster locations . The operations should permit analysis of the impact of events immediately following a disaster event in near real-time.

The technology for unmanned vehicles are advancing at a rapid pace adding new capabilities for remote sensing . The U.S. DOT project teams (4, 5)conducted pioneering demonstrations on using UAVs for remote sensing of transportation systems and for obtaining imageries of transportation networks and performing near real-time analysis of results for application. UAVs can be

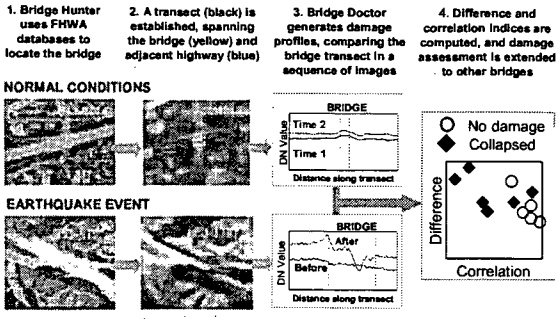
programmed off-line and controlled in real-time to navigate and to collect imageries for transportation network surveillance immediately following a disaster. Small UAVs for transportation application can range in weights from 10 to 60 pounds and can carry a variety of multiple and interchangeable imaging devices, including day and night real-time video, multispectral and hyperspectral sensors, thermal, synthetic aperture radars, moving target indication radar, laser scanners, and chemical, biological and radiological sensors. Figure 3 shows a micro UAV and an Airborne Data Acquisition Systems (ADAS) tested for transportation application in DOT projects. UAVs have been successfully tested for tracking urban and rural transportation networks and multimodal operations and can be deployed for application to emergency management in the event of an earthquake disaster.

5.0 REFERENCES

The following references cited in the paper are from preliminary results from ongoing research by several investigators in a U.S. DOT Joint program with NASA. Copies of the project reports can be obtained by writing to the author at U.S. DOT/RSPA, 400 Seventh Street SW, Suite 7110, Washington, D.C. 20590

1. US DOT and NASA team discussions on SAR technologies for disaster application (RS Work Group of SDR)
2. Disaster damage and emergency response by ImageCat. Inc (Ron Eguchi)
3. Community evacuation Community planning using RS technologies by University of Utah (George Hepner and Tom Cova)
4. Micro UAV Applications to Transit Management by Bridgewater State College (Lawrence J. Harman)
5. Airborne Data Acquisition System by GeoData Systems (Ernest Carrol)

Figure 1. Remote Sensing Imagery Application For Damage And Vulnerability Assessment of Critical Transportation Bridges For Emergency Transportation after an Earthquake (U.S. DOT Project Results by Imagecat Inc)



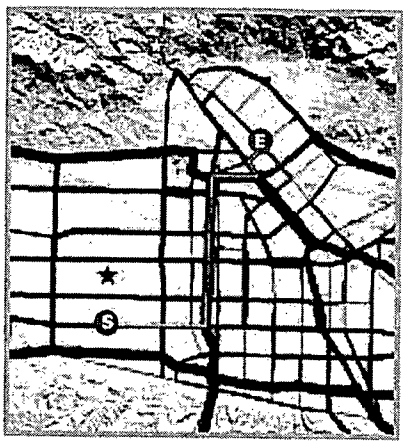
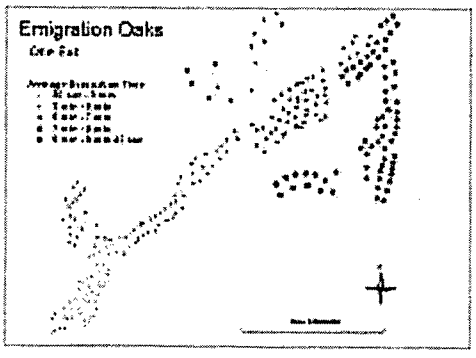


Figure 2. Modeling Emergency Evacuation in Community Planning (U.S. DOT Project Results by University of Utah)



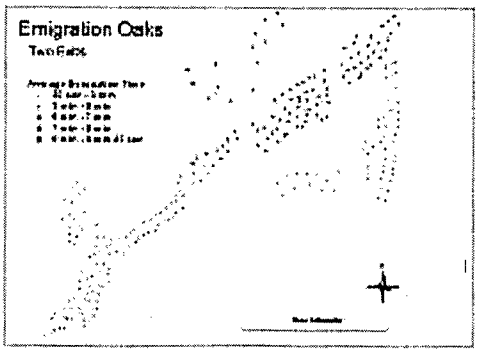
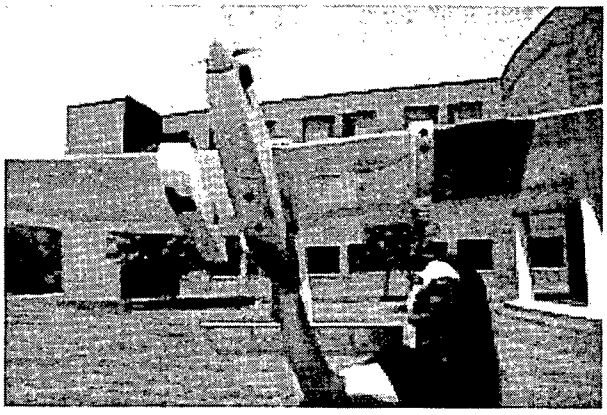
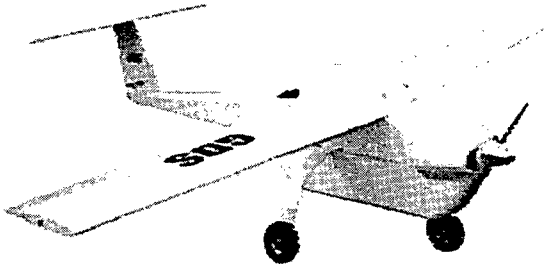
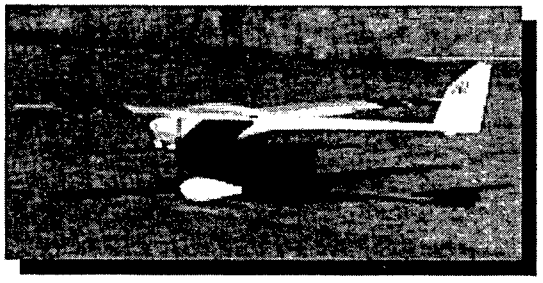


Figure 3. Micro UAVs For Urban Transportation Management (U.S. DOT Project Results by Moakley Center-Bridgewater State College) and Airborne Data Acquisition System (ADAS) for Traffic Management (U.S.DOT Project Results by Geodata Systems Inc.)







THEME 4

Transportation Systems

SEISMIC PERFORMANCE OF RC BRIDGE COLUMNS SUBJECTED TO BILATERAL EXCITATION

by

Kazuhiko Kawashima[1], Gakuho Watanabe[2] and Ryoji Hayakawa[3]

ABSTRACT

This paper represents a series of cyclic loading test and a fiber element analysis to clarify the effect of bilateral loading of reinforced concrete bridge columns. Four loading orbits (diagonal, square, circular and ellipsis) were used in the test in addition to the unilateral loading. It was found that an extensive deterioration of flexural strength and displacement ductility capacity occurs under the bilateral loading, and that the fiber element analysis provides an accurate simulation for the test results.

KEYWORDS: Bridges, Seismic Design, Reinforced Concrete Structures, Flexural Capacity, Ductility

1. INTRODUCTION

The combination of two lateral components of seismic effect has been a major concern in seismic design of bridges. It is obvious that during an earthquake a bridge is subjected to a set of three components of ground motions in two lateral and the vertical directions. Since the effect of vertical component is a unique problem, we have to consider a rational combination of two lateral components of seismic effect by appropriately taking account of the effect of vertical component.

In practice, it is general to size a bridge column assuming that it is subjected to two lateral components of a ground motion in the weak and strong axes independently. Flexural strength and ductility capacity of a column are generally determined based on the experimental data of cyclic loading test under unilateral direction. Since it has been revealed that flexural strength and ductility capacity under bilateral excitation are less than those under unilateral excitation, it is likely that the current design values for flexural strength and ductility capacities are overestimated

It was important to simplify design procedure when an analytical tool was poor. However, an improvement of design tools has made it possible to take account of the bilateral excitation effects in design. This is particularly important to non-standard bridges in which bilateral excitation effect is significant. It is required to properly include the effect of bilateral excitation effect in seismic design of bridges.

This paper presents a cyclic loading test for 5 reinforced concrete specimens with the same structural properties to clarify the effect of bilateral excitation. Accuracy of a fiber element analysis which includes a new empirical stress vs. strain relation of confined concrete is verified based on the test data.

2. EXPERIMENTAL SETUP

2.1 Experimental Models

Five reinforced concrete specimens with the same structural properties as shown in Fig. 1 were constructed. They are 1,750 mm tall and the effective column height is 1,350 mm. They were designed in accordance with the Japanese 1996 Design Specifications of Highway Bridges using the Type-I (middle-field) and Type-II (near-field) ground motions. Moderate ground condition (Type-II Ground Condition) was assumed. Axial stress at the plastic hinge region of the columns resulted from the dead weight of a superstructure was assumed 1 MPa.

[1] Professor, Department of Civil Engineering, Tokyo Institute of Technology, O-Okayama, Meguro, Tokyo, Japan 152-8552

[2] Research Associate, ditto

[3] Graduate Student, ditto

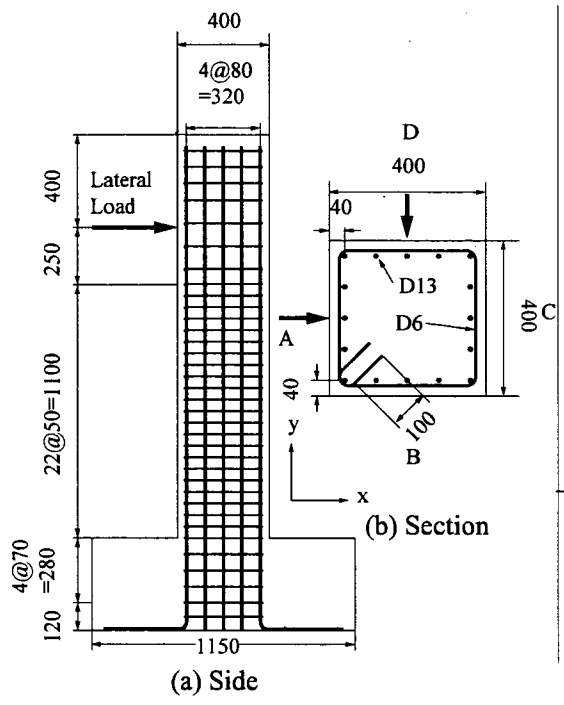


Fig.1 Models

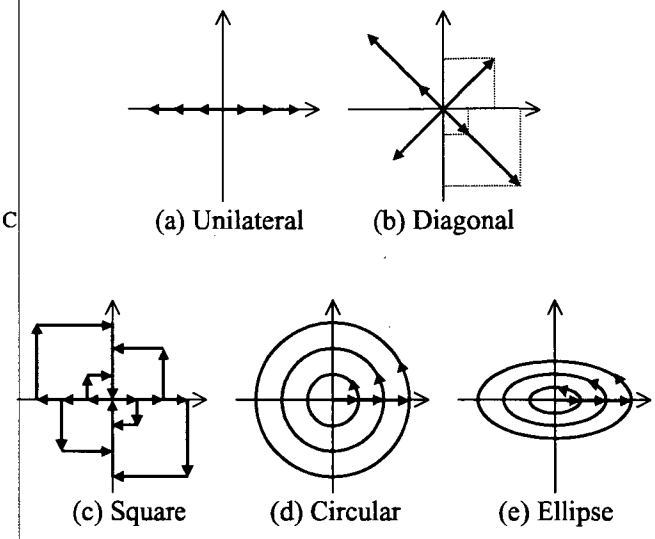


Fig. 2 Bilateral Orbits

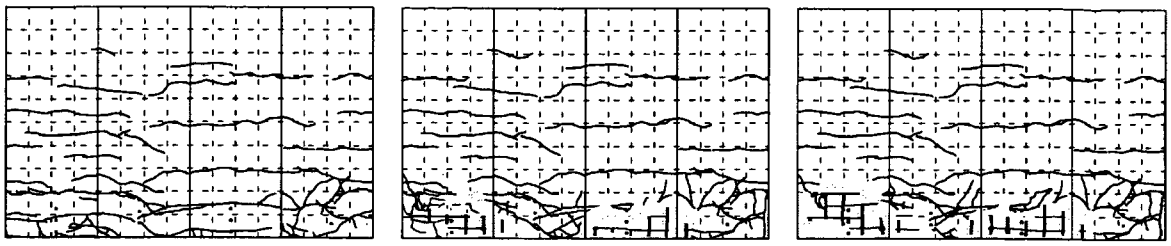
Sixteen 13 mm diameter deformed bars with a nominal strength of 295 MPa (SD295A) were provided for longitudinal reinforcements, and 6 mm diameter deformed bars (SD295A) were provided every 500 mm interval for ties. The tie bars were anchored using 135 degree bent hooks with a development length of 100 mm. Longitudinal reinforcement ratio is 1.27 % and the tie volumetric reinforcement ratio is 0.79 %. Concrete strength ranged from 26.2 to 31.3 MPa.

2.2 Loadings

Cyclic loading test was conducted at the Tokyo Institute of Technology. Three dynamic actuators were used to provide bilateral loading under a constant vertical load of 160 kN. The vertical load resulted in an axial stress of 1 MPa at the plastic hinge region. In the following, the surfaces perpendicular to x axis are called A and C, while the surfaces perpendicular to y axis are called B and D, as shown in Fig. 1.

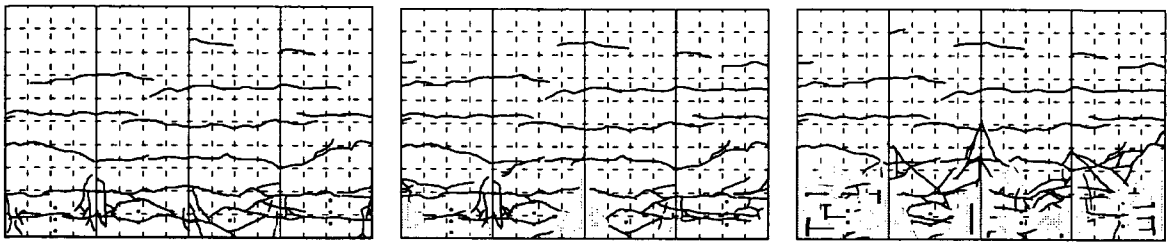
Four orbits as shown in Fig. 2 were used for the bilateral loading. In the diagonal loading, a column was first loaded three times in the diagonal direction in the 1st and 3rd quadrants with a displacement of u equivalent to 0.5 % drift. Then it was loaded three times in the diagonal direction in the 2nd and 4th quadrants with a displacement u equivalent to 1 % drift. This set of loading was repeated until failure. The loading displacement was step wisely increased from 0.5 % drift with an increment of 0.5 % drift. Since 1 % drift is 13.5 mm, it corresponds to approximately 3 times the yielding displacement u_y. Due to limitation of space, the loading test using the ellipsis orbit is not presented here.

In the square orbit loading, a column was first loaded in the x direction, and then in the y direction with a displacement of 0.5% drift keeping the displacement in the x direction. Then, the column was unloaded in the x direction first followed by unloading in the y direction to return to the rest position. This completes a loading with 0.5% drift in the 1st quadrant. The same loading was repeated in the 3rd quadrant. This loading in the 1st and 3rd quadrants were repeated three times. Then this set of loading was conducted in the 2nd and 4th quadrants by increasing the loading



(a) Drift3.5% (b) Drift 4.0% (c) Drift 4.5%

(1) Unilateral (P-1)



(a) Drift 2.0% (b) Drift 2.5% (c) Drift 3.5%

(2) Diagonal (P-2)

Fig. 3 Progress of Failure of Columns subjected to Unilateral and Diagonal Orbit Loadings

displacement to 1 % drift. Thus, loading was repeated alternatively in the 1st and 3rd quadrants and 2nd and 4th quadrants by increasing the loading displacement with an increment of 0.5 % drift.

In the circular orbit loading, a column was first loaded in the x direction until the displacement reaches 0.5% drift. From this point the column was loaded three times by circular orbit. Finally the column was unloaded in the x direction to the rest position. This set of loading was repeated until failure with an increment of loading displacement of 0.5 % drift.

For comparison, a column was loaded in the unilateral direction. Loading was repeated three times each and the loading displacement was step wisely increased from 0.5 % drift with an increment of 0.5 % drift.

3. PERFORMANCE OF COOLUMNS

3.1 Unilateral and Diagonal Loadings

Fig. 3 shows the progress of failure under the unilateral and diagonal orbit loadings. Under the unilateral loading, compression failure started to occur in the covering concrete in the plastic hinge zone at 3 % drift at A surface. At 4 % drift, the covering concrete started to spall off and longitudinal and tie bars were exposed. Some longitudinal bars buckled. The damage further progressed at 5 % drift.

Fig. 4 shows the lateral force vs. lateral displacement hysteresis under the unilateral loading. Hystereses under the diagonal loading which will be described latter are presented here for comparison. The hysteresis under the unilateral loading reaches at its maximum strength of 119.8 kN at 3 % drift, and is stable until 3.5 % drift. At 4 % drift, strength starts to deteriorate resulted from compression failure of the concrete and buckling of longitudinal bars. The strength deteriorates from its maximum strength by 37 % and 52 % at drift 4.5 % and 5 %, respectively.

On the other hand, the column subjected to the diagonal loading started to suffer damage at corners. For example, the column suffered damage at the corner of A and D surfaces (referred hereinafter A-D corner) and the corner of B and C surfaces (referred B-C corner) at 2.5 % drift, since the column was subjected to a diagonal loading in the direction of A-D and

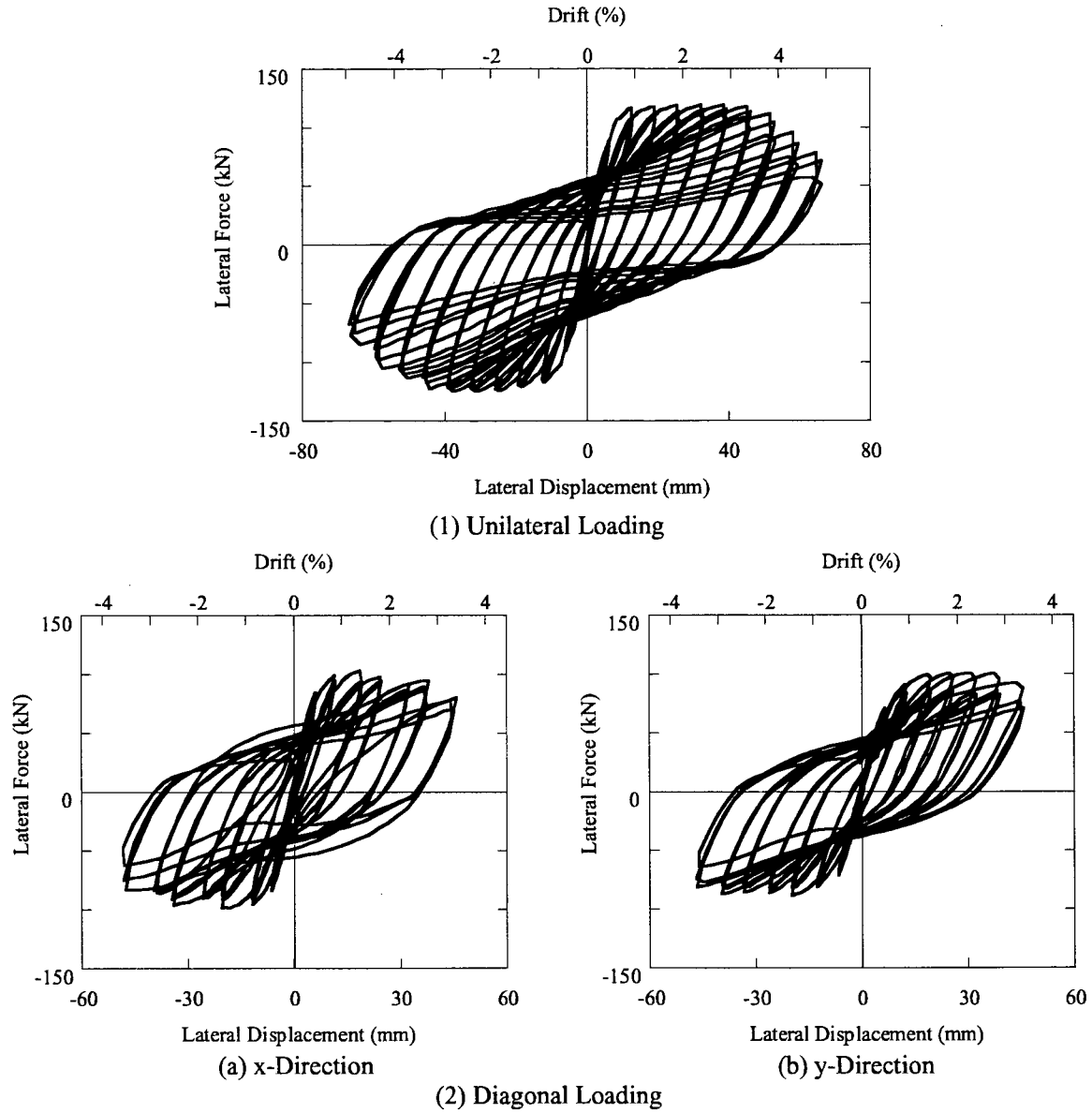
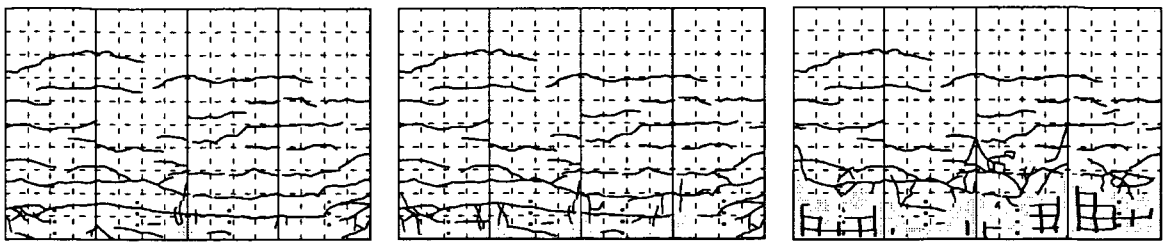


Fig. 4 Lateral Force vs. Lateral Displacement Hystereses of Columns subjected to Unilateral and Diagonal Loadings

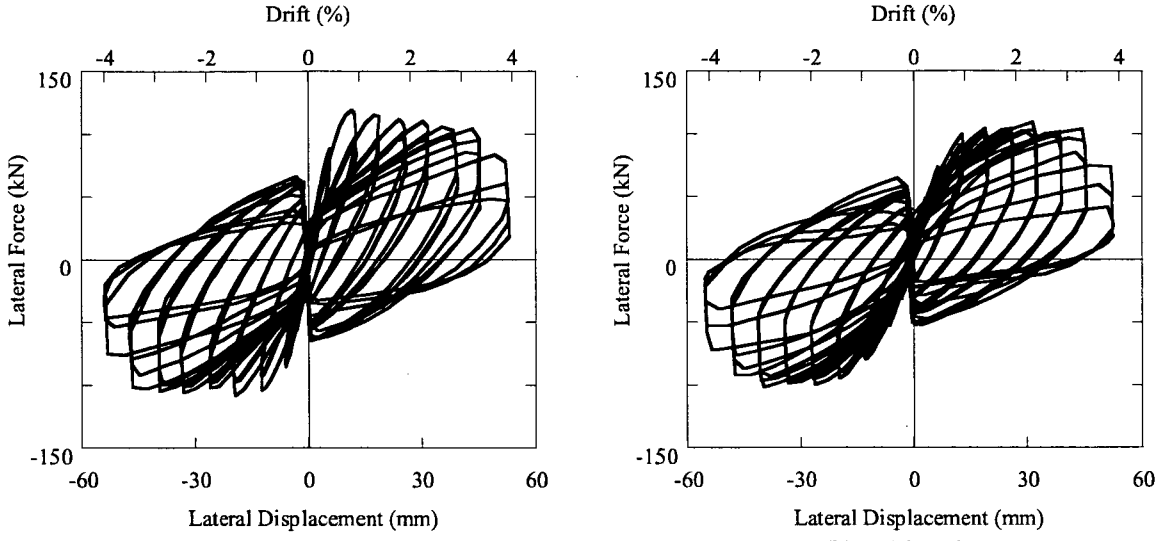
B-C corners in this loading step. Similarly at 3 % drift, damage occurred at A-B and C-D corners since the column was loaded in this direction. Failure at the corners progressed to four surfaces, and the covering concrete spalled off all around the surfaces at 3.5 % drift. A couple of longitudinal bars buckled. The damage of the column under the diagonal loading is more extensive than that under the unilateral loading.

Fig. 4 (2) shows the lateral force vs. lateral displacement hystereses of the column subjected to the diagonal loading. The column reached its maximum strength of 103 kN at 1.5 % drift in the x direction, while it reaches its maximum strength of 100.6 kN at 2 % drift in the y direction. The strength deteriorated to 80 % of the maximum at 1st and 2nd excursion of 3.5 % drift loading in the x and y directions, respectively.



(a) Drift 2.0% (b) Drift 2.5% (c) Drift 3.5%

Fig. 5 Progress of Failure of a Column subjected to Square Orbit Loading



(a) x-Direction (b) y-Direction

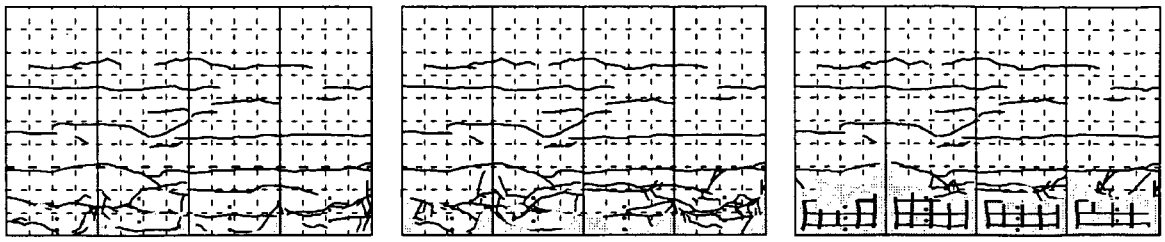
Fig. 6 Lateral Force vs. Lateral Displacement Hystereses of Columns subjected to Square Orbit Loading

3.2 Square Orbit Loading

Fig. 5 shows progress of failure of the column subjected to the square orbit loading. Damage of the column under the square orbit loading was more extensive than the damage under the unilateral loading. Extensive failure occurred at A-B corner and C-D corner at 2.5 % drift. Longitudinal bars were partly exposed. At 3.5 % drift, not only the spalling off of the covering concrete at surfaces A, C and D in the range of 200-300 mm from the bottom, the core concrete suffered extensive damage. Longitudinal and tie bars were exposed. At 4 % drift, lateral confinement was lost, and longitudinal bars buckled at several heights in various directions.

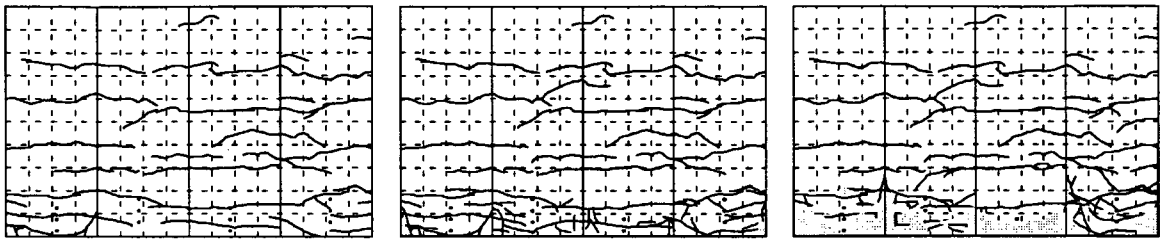
Fig. 6 shows the lateral force vs. lateral displacement hystereses in x and y directions. The hystereses are unique because they are pinched near zero displacement. Taking the hysteresis in x direction as an example, this occurs because an unloading of the column in y direction (to the rest position) following an unloaded in x direction (refer to Fig. 2) results in a deterioration of restoring force in x direction. In other words, a deterioration of restoring force in one direction occurs as a consequence of an unloading in the perpendicular direction. This represents an effect of the interaction of restoring force of a column.

In Fig. 6, the hysteresis in the x direction reaches its maximum strength of 120 kN at 1 % drift. The strength in this direction subsequently deteriorates until 3 % drift, where a sudden decrease of the restoring force to 80 % of its maximum strength occurs. At 3.5 % drift, the restoring force significantly decreases at 2nd and 3rd loading excursions. On the other hand, in the y direction, the restoring force reaches its



(a) Drift 2.0% (b) Drift 2.5% (c) Drift 3.5%

(1) Circular Loading (P-4)



(a) Drift 2.0% (b) Drift 2.5% (c) Drift 3.5%

(2) Ellipse Loading (P-5)

Fig. 7 Progress of Failure of a Column subjected to Circular Orbit Loading

maximum strength of 109 kN at 2.5 drift. At 3.5 % drift, a sudden deterioration of the restoring force to 80 % of its maximum strength occurs.

3.3 Circular Orbit Loading

Fig. 7 shows progress of failure of the columns subjected to the circular orbit loading. Extensive damage similar to the damage under the square orbit loading occurs. Damage starts to occur at corners, and progressed to four surfaces at 2.5 drift. At 3.5 % drift, covering concrete completely spalled off up to about 200 mm from the bottom, and longitudinal and ties bars were exposed.

Fig. 8 shows hystereses of the columns under the circular orbit loading. The loading and unloading hystereses are round near the peak displacements. This results from the interaction of restoring force in two directions. Dislike the square orbit loading, the interaction of restoring occurs successively in the circular orbit loading. It is noted in Fig. 8 that only the hystereses at the first excursions in each loading step have a feature similar to that under the unilateral loading. This is because under the circular orbit loading the column was first loaded only in the x direction in the first excursions at each loading step (refer to Fig. 2).

4 EFFECT OF LOADING ORBITS

Table 1 summarizes the maximum strengths and ultimate displacements. The ultimate displacements are defined here as the displacement where the strengths deteriorate to less than 80% of the maximum strengths. It is apparent that the strengths under the diagonal, square and circular orbit loadings are 10-20% smaller than those under the unilateral loading. The ultimate displacements under the diagonal, square and circular orbit loadings are 18-24% smaller than those under the unilateral loading.

Figs. 9, 10 and 11 compare the hystereses under the unilateral loading and those under the diagonal, square and circular orbit loadings. Since the hystereses under the diagonal, square and circular orbit loadings are similar between x and y directions, only the hystereses in the x-direction are presented here. The deterioration of strength, the pinching near zero displacements and the round corners near the peak displacements of the columns subjected to the diagonal, square and circular orbit loadings, respectively, are well predicted by the analysis.

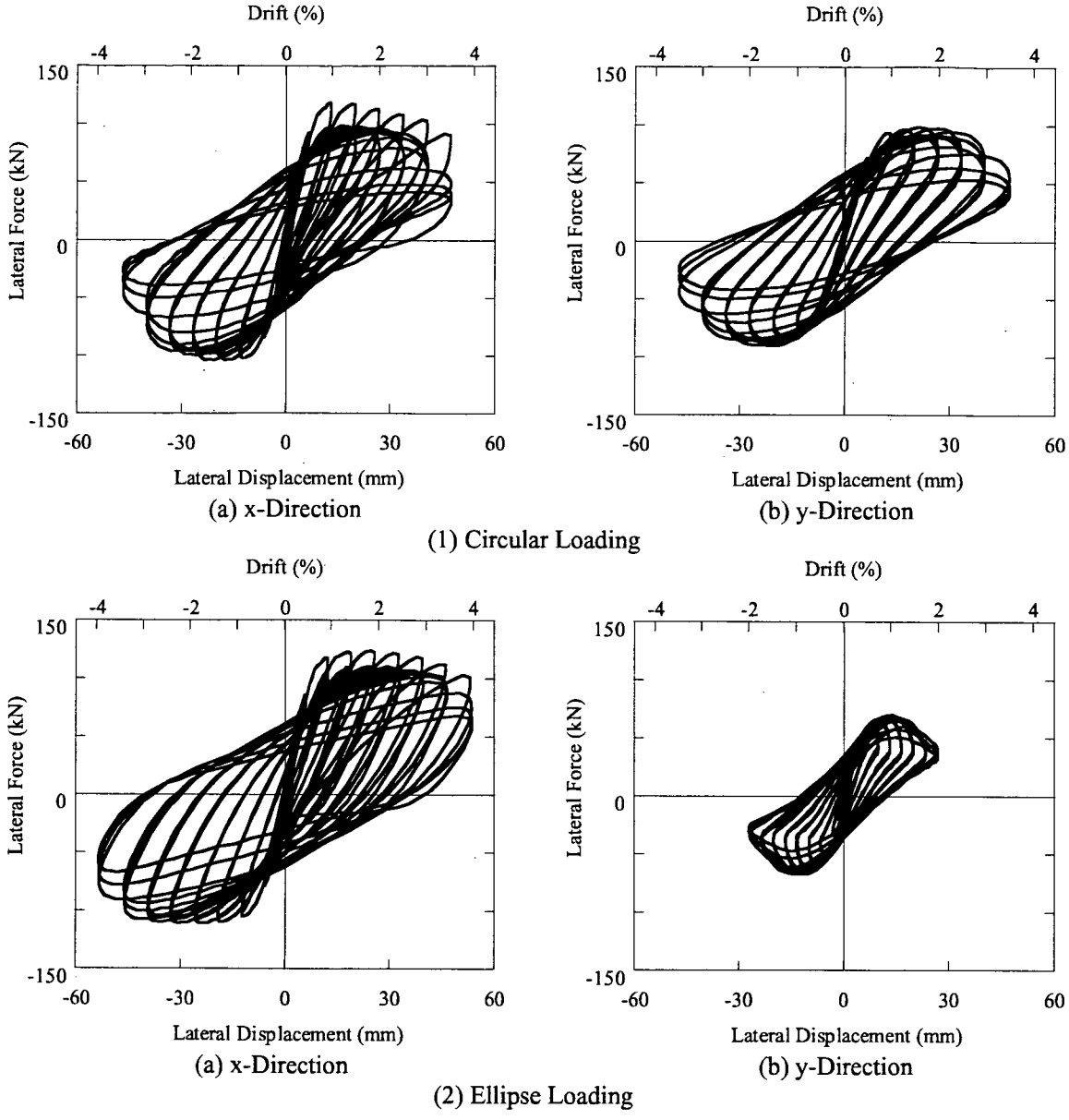


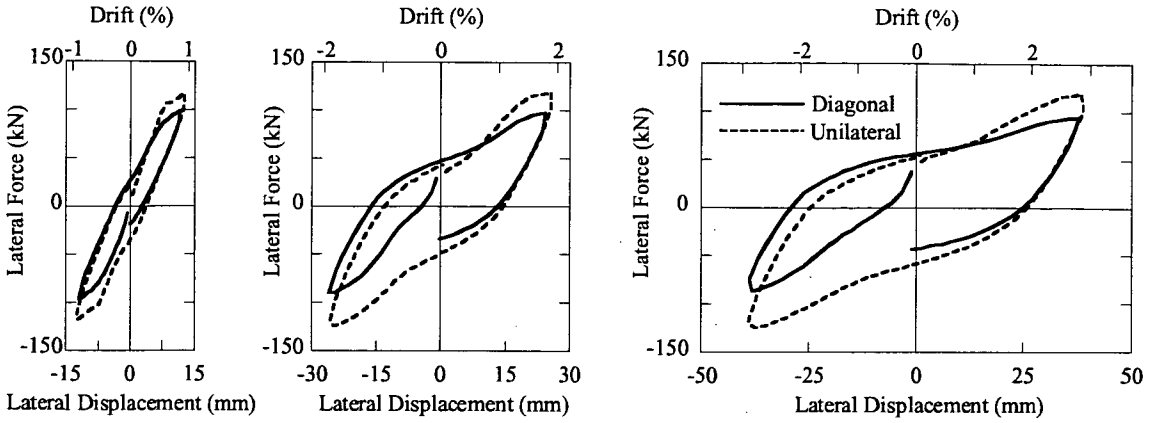
Fig. 8 Lateral Force vs. Lateral Displacement Hystereses of Columns subjected to Circular Orbit Loading

5 FIBER ELEMENT ANALYSIS

5.1 Analytical Model

The columns were modeled as shown in Fig. 12. The plastic hinge zone was idealized by a fiber element. The effect of deformation of longitudinal bars in the footing was represented by a rotational szpring at the bottom of the columns. The stress σ_c vs. strain ε_c relation of the confined concrete was assumed based on Hoshikuma et al [1] as

$$\sigma_c = \begin{cases} E_c\varepsilon_c\left\{1-\frac{1}{n}\left(\frac{\varepsilon_c}{\varepsilon_{cc}}\right)^{n-1}\right\} & \cdots \quad 0 \le \varepsilon_c \le \varepsilon_{cc} \\ \sigma_{cc} - E_{des}(\varepsilon_c - \varepsilon_{cc}) & \cdots \quad \varepsilon_{cc} < \varepsilon_c < \varepsilon_{cu} \\ 0.2\sigma_{cc} & \cdots \quad \varepsilon_{cu} < \varepsilon_c \end{cases} \tag{1}$$



(a) Drift 1% (b) Drift 2% (c) Drift 3%

Fig. 9 Comparison of Hystereses between Columns subjected to Unilateral and Diagonal Orbit Loadings

Table.1 Effect of Bilateral Excitation

(a) Ultimate Strength

Loading Orbits	Maximum Flexural Strength (kN)						
	x-Direction			y-Direction			Average of (1) and (2)
	+	-	(1) Average	+	-	(2) Average	
Unilateral	119.8	124.5	122.2 (100%)	-	-	122.2 (100%)	122.2 (100%)
Diagonal	103.1	98.7	100.9 (83%)	100.6	88.3	94.5 (77%)	97.7 (80%)
Square	119.5	108.3	113.9 (93%)	109.3	101.6	105.5 (86%)	109.7 (90%)
Circular	118.8	103.5	111.2 (91%)	98.1	90.0	94.1 (77%)	103.2 (84%)
Ellipse	124.4	111.0	117.7 (96%)	-	-	-	-

(b) Ultimate Displacement

Loading Orbits	Ultimate Displacement (Drift)						
	x-Direction			y-Direction			Average of (3) and (4)
	+	-	(3) Average	+	-	(4) Average	
Unilateral	4.0	4.5	4.25 (100%)	-	-	4.25 (100%)	4.25 (100%)
Diagonal	3.5	3.5	3.5 (82%)	3.5	3.5	3.5 (82%)	3.5 (82%)
Square	3.0	3.5	3.25 (77%)	3.5	3.5	3.5 (82%)	3.38 (80%)
Circular	3.5	3.0	3.25 (77%)	3.5	3.0	3.25 (76%)	3.25 (76%)
Ellipse	4.0	4.0	4.0 (94%)	-	-	-	-

where, n: coefficient representing the shape of ascending branch, σ_{cc} and ε_{cc} : maximum strength of confined concrete and the strain corresponding to σ_{cc} , E_{des} : stiffness of confined concrete at the descending branch, ε_{cu} : ultimate strain, and they are represented as

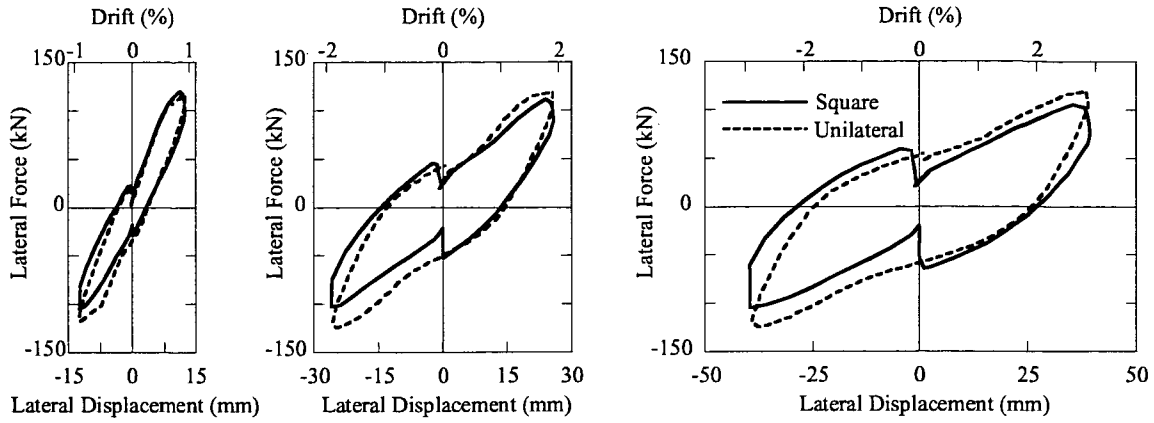
$$n = \frac{E_c \varepsilon_{cc}}{E_c \varepsilon_{cc} - \sigma_{cc}} \tag{2}$$

$$\sigma_{cc} = \sigma_{ck} + 0.76 \rho_s \sigma_{sy} \tag{3}$$

$$\varepsilon_{cc} = 0.002 + 0.0132 \frac{\rho_s \sigma_{sy}}{\sigma_{ck}} \tag{4}$$

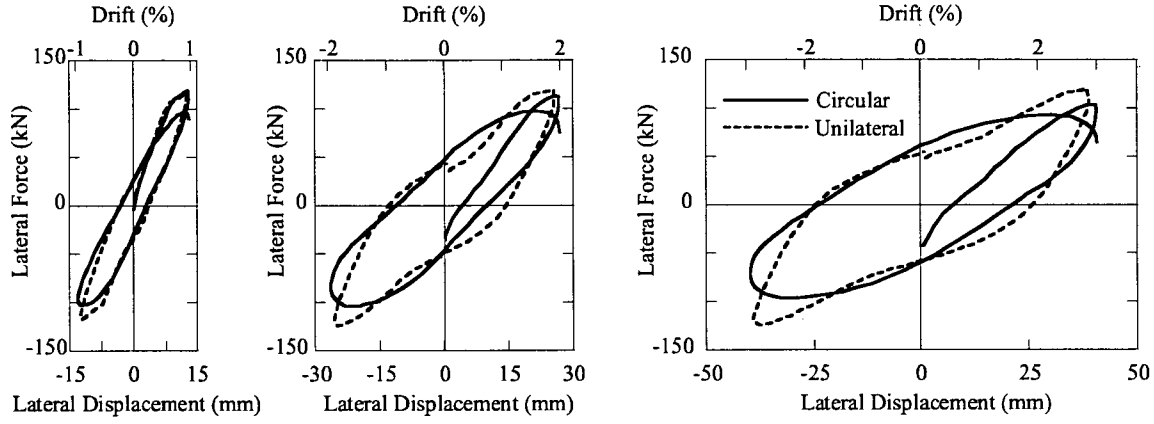
$$E_{des} = 11.2 \frac{\sigma_{ck}^{\,2}}{\rho_s \sigma_{sy}} \tag{5}$$

$$\varepsilon_{cu} = \varepsilon_{cc} + \frac{0.8 \sigma_{cc}}{E_{des}} \tag{6}$$



(a) Drift 1% (b) Drift 2% (c) Drift 3%

Fig. 10 Comparison of Hystereses between Columns subjected to Unilateral and Square Orbit Loadings



(a) Drift 1% (b) Drift 2% (c) Drift 3%

Fig. 11 Comparison of Hystereses between Columns subjected to Unilateral and Circular Orbit Loadings

where, σ_{ck} : strength of concrete, σ_{sy} : strength of tie bars, ρ_s : volumetric tie reinforcements ratio.

On the other hand, the stress σ_c vs. strain ε_c relation of the covering concrete was assumed as

$$\sigma_c = \begin{cases} E_c\varepsilon_c\left\{1-\frac{1}{n}\left(\frac{\varepsilon_c}{0.002}\right)^{n-1}\right\} & \cdots 0 \le \varepsilon_c \le \varepsilon_{cc} \\ \frac{\sigma_{cc}}{0.005}(0.007-\varepsilon_c) & \cdots\cdots \varepsilon_{cc} < \varepsilon_c \le \varepsilon_{cu} \\ 0 & \cdots\cdots \varepsilon_{cu} < \varepsilon_c \end{cases} \quad (7)$$

Unloading and reloading hystereses were idealized based on a model by Sakai, and Kawashima [2]. In this model, hystereses are provided for a set of 1) full unloading, 2) full reloading, 3) partial unloading and 4) partial reloading. For example, if a full unloading occurs from a point with strain ε_{ul} (unloading strain) on a skeleton curve, the strain reduces to $\varepsilon_{pl.1}$ at zero stress as shown in Fig. 13. This $\varepsilon_{pl.1}$ is called 1st plastic strain. Let $\sigma_{ul.1}$ represent the stress at ε_{ul} at the first unloading (1st unloading stress). If the concrete is reloaded from $\varepsilon_{pl.1}$ until the strain reaches the unloading strain ε_{ul}, the stress at this strain

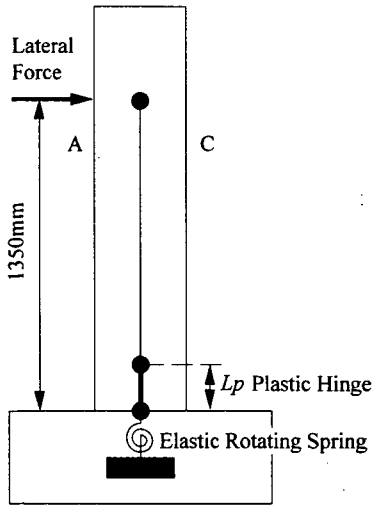


Fig. 12 Analytical Model

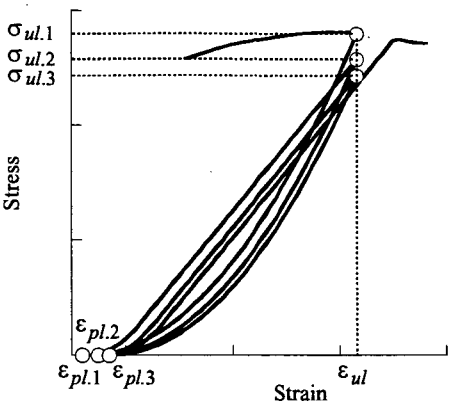


Fig. 13 Unloading and Reloading model of Confined Concrete

$\sigma_{ul.2}$ (2nd unloading stress) may be smaller than $\sigma_{ul.1}$. Thus, if we repeat a full unloading and a full reloading n times, the n-th unloading stress becomes $\sigma_{ul.n}$, and n-th plastic strain becomes $\varepsilon_{pl.n}$. The stress vs. strain relation of confined concrete subjected to n times full unloading and full reloading are represented as

$$\sigma_c = \sigma_{ul.n}\left(\frac{\varepsilon_c - \varepsilon_{pl.n}}{\varepsilon_{ul} - \varepsilon_{pl.n}}\right)^2 \qquad (8)$$

$$\sigma_c = \begin{cases} 2.5\sigma_{ul.n}\left(\dfrac{\varepsilon_c - \varepsilon_{pl.n}}{\varepsilon_{ul} - \varepsilon_{pl.n}}\right)^2 & \cdots 0 \le \tilde{\varepsilon}_c < 0.2 \\ E_{rl}(\varepsilon_c - \varepsilon_{ul}) + \sigma_{ul.n+1} & \cdots 0.2 \le \tilde{\varepsilon}_c \le 1 \end{cases} \qquad (9)$$

where, $\tilde{\sigma}_c$ and $\tilde{\varepsilon}_c$ are normalized stress and strain defined by

$$\tilde{\sigma}_c = \frac{\sigma_c}{\sigma_{ul.n}} \;;\; \tilde{\varepsilon}_c = \frac{\varepsilon_c - \varepsilon_{pl.n}}{\varepsilon_{ul} - \varepsilon_{pl.n}} \qquad (10)$$

and E_{rl} represents the averaged stiffness in the reloading path between $0.2 \le \tilde{\varepsilon}_c \le 1$ defined by

$$E_{rl} = \frac{\sigma_{ul.n+1} - 0.1\sigma_{ul.n}}{0.8(\varepsilon_{ul} - \varepsilon_{pl.n})} \qquad (11)$$

Representing the deterioration rate of $\sigma_{ul.n}$ and the increasing rate of $\varepsilon_{pl.n}$ by two parameters as

$$\beta_n = \frac{\sigma_{ul.n+1}}{\sigma_{ul.n}} \;;\; \gamma_n = \frac{\varepsilon_{ul} - \varepsilon_{pl.n}}{\varepsilon_{ul} - \varepsilon_{pl.n-1}} \qquad (12)$$

β_n and γ_n are given as

For $n = 1,2$

$$\beta_n = \begin{cases} 1 & \cdots 0 \le \varepsilon_{ul} \le 0.001 \\ 1 - (10n + 22)(\varepsilon_{ul} - 0.001) & \cdots 0.001 < \varepsilon_{ul} < 0.0035 \\ 0.92 + 0.025(n-1) & \cdots 0.0035 \le \varepsilon_{ul} \le 0.03 \end{cases}$$

For $n \ge 3$

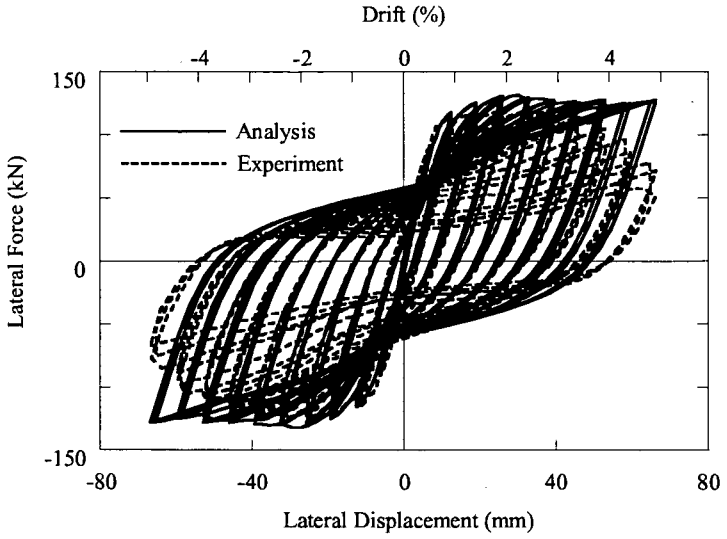


Fig. 14 Computed Lateral Force vs. Lateral Displacement Hystereses of a Column subjected to Unilateral Loading

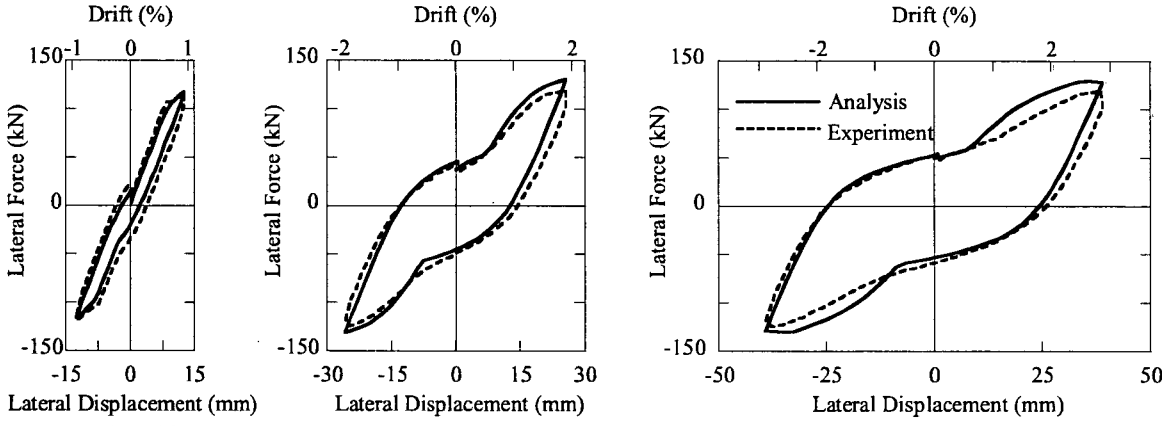


Fig. 15 Comparison of Analytical and Experimental Hystereses at 1%, 2% and 3% Drifts (Unilateral Loading)

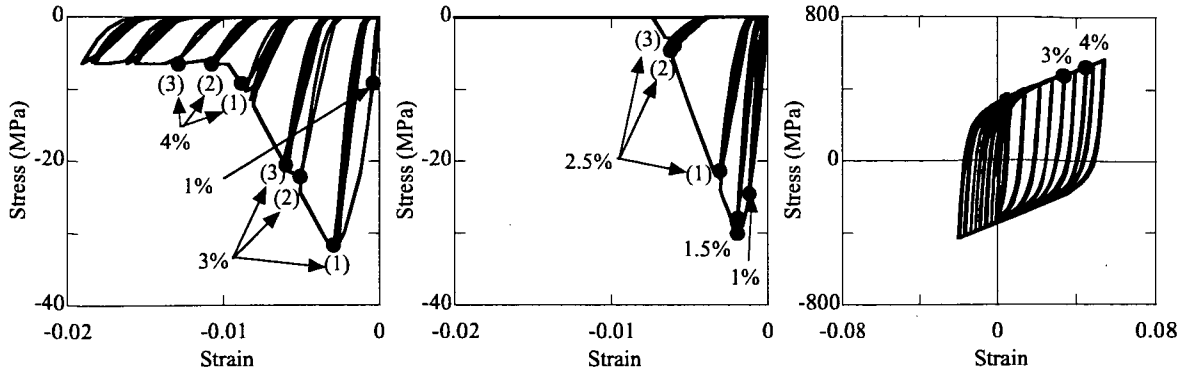
$$\beta_n = \begin{cases} 1 & \cdots\cdots 0 \le \varepsilon_{ul} \le 0.001 \\ 1-(2n+8)(\varepsilon_{ul}-0.001) & \cdots\cdots 0.001 < \varepsilon_{ul} < 0.0035 \\ 0.965+0.005(n-3) & \cdots\cdots 0.0035 \le \varepsilon_{ul} \le 0.03 \end{cases} \quad (13)$$

$$\gamma_n = \begin{cases} 0.945 & \cdots n = 2 \\ 0.965+0.005(n-3) & \cdots n \ge 3 \end{cases} \quad (14)$$

On the other hand, the Menegotto-Pinto model was used to idealize the stress vs. strain hysteresis of the axial bars [3].

5.2 Analysis for Unilateral Loading

Fig. 14 compares the computed lateral force vs. lateral displacement hysteresis with the experimental result. Fig. 15 compares the hystereses in the first loading excursion of 1%, 2% and 3% drifts. The computed hystereses by the fiber element method are very close to the experimental results. Since the effect of local buckling and rupture of longitudinal bars is not



(a) Core Concrete (Extreme Fiber at A-Surface)

(b) Covering Concrete (Extreme Fiber at A-Surface)

(c) Longitudinal Bar (Center of A-Surface)

Fig. 16 Computed Stress vs. Strain Hystereses of a Column subjected to Unilateral Loading

included in the fiber element analysis, the hystereses after 3.5% drift are not accurately predicted.

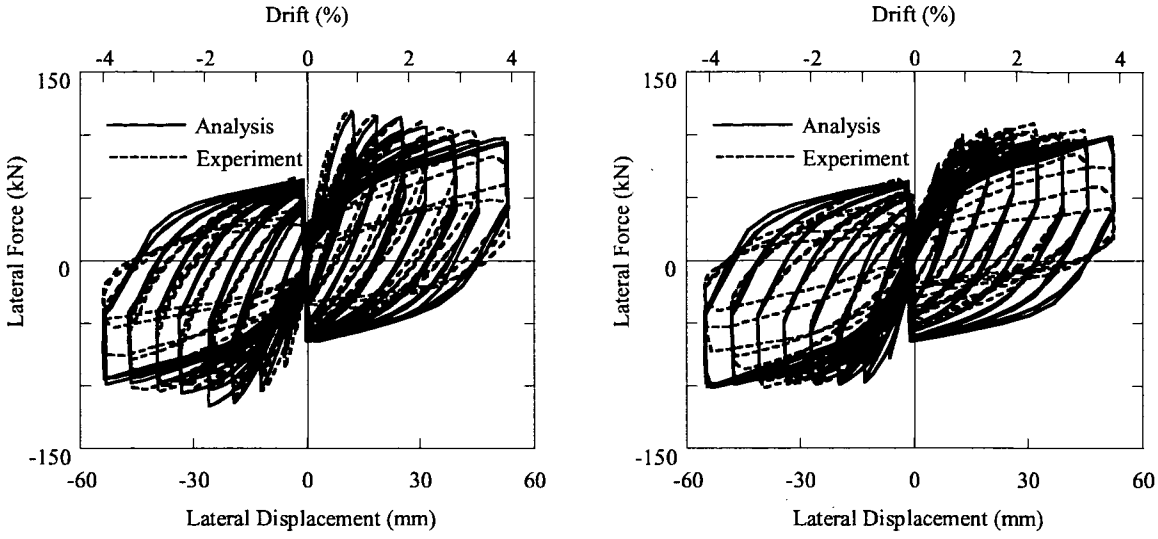
Fig. 16 shows the computed stress vs. strain hystereses of the core concrete and the covering concrete at the extreme fibers and a longitudinal bar at the center of A surface (refer to Fig. 1). The stress of core concrete at the extreme fiber reaches the maximum strength σ_{cc} at the first loading excursion of 3% drift, and deteriorates to 20% of σ_{cc} at 4% drift. Because the covering concrete is not confined, stress of the covering concrete reaches the maximum strength σ_{cc} at 1.5 % drift, and becomes almost zero at the second excursion of 2.5% drift. Strain of the longitudinal bar becomes 0.033 at 3% drift and 0.045 at 4% drift.

The computed stress and strain of the core and the covering concrete and the longitudinal bar well represents the failure mode of the model column under the unilateral loading. The covering concrete started to spall off at 3% drift in the test. As described above, at this 3% drift it is predicted that the stress of covering concrete deteriorates to almost zero. Extensive failure of core concrete started to occur at 4% drift with the longitudinal bars and the ties being exposed in the test. At the 4% drift, it is predicted that the stress of the core concrete deteriorates to 20% of the maximum strength σ_{cc} in the analysis.

5.3 Analysis for Square Orbit Loading

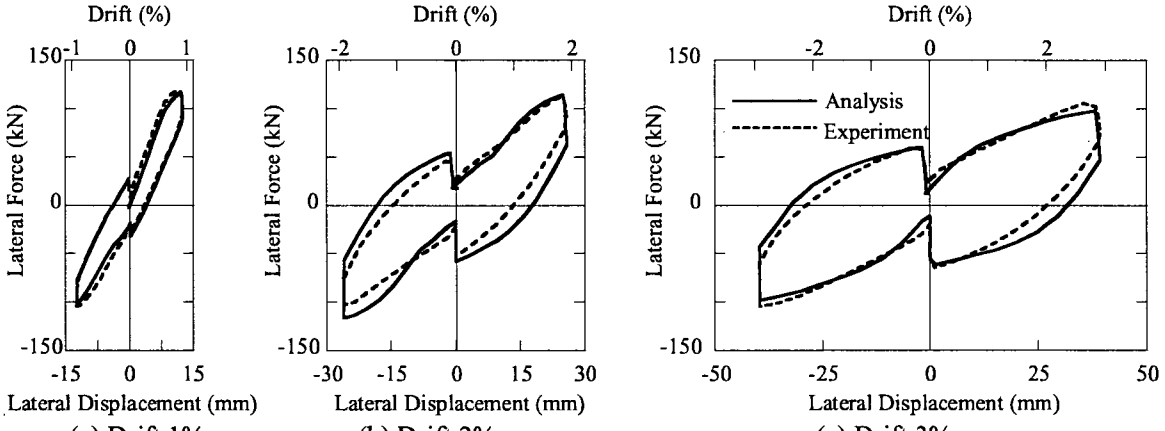
Fig. 17 compares the lateral force vs. lateral displacement hystereses between the experiment and the analysis for x and y directions. The computed hystereses agree well with the experimental results until 3.5% drift. Over the 3.5% drift, the strength started to deteriorate significantly resulted from failure of not only the covering concrete but also the core concrete at all 4 surfaces in the test. Fig. 18 shows a comparison of the hystereses of the first excursion at 1%, 2% and 3% drifts between the test and the analysis. The sharp deterioration of the strength at the maximum and zero displacements are well predicted by the analysis.

Fig. 19 shows the computed stress vs. strain hystereses of the core and covering concrete at the extreme fibers and longitudinal bars at the center of the surfaces A and B (refer to Fig. 1). The hystereses at the A surface are similar to those at the B surface. At the extreme fiber of core concrete the stress reaches σ_{cc} at the 1st excursion of 2% drift, but it sharply deteriorates at the 3rd excursion. This shows that the core concrete starts to deteriorate extensively at 2% drift. At the extreme fiber of covering concrete the stress reaches σ_{cc} at 1.5% drift, and deteriorates to zero at the 3rd loading excursion of 2% drift. At the longitudinal bar at the center strain becomes 0.029 at 3% drift.



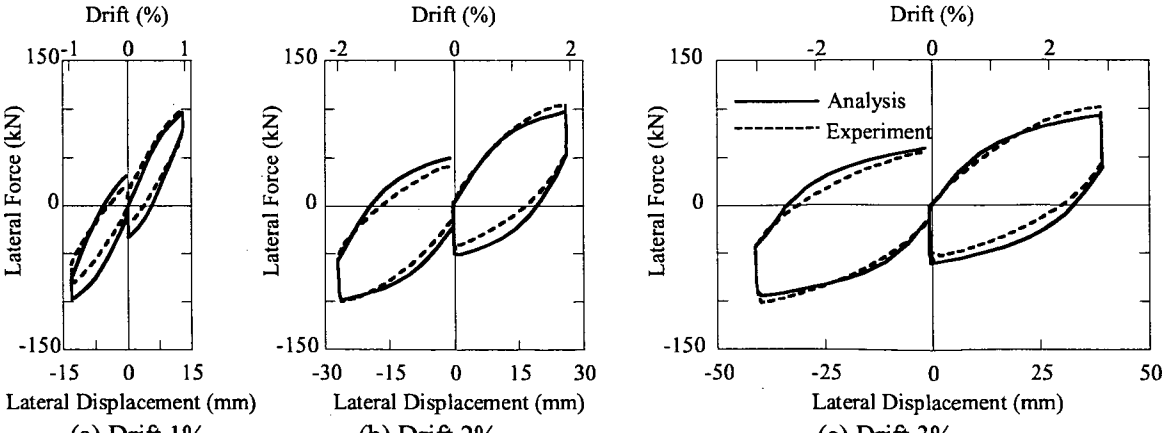
(a) x-Direction (b) y-Direction

Fig. 17 Computed Lateral Force vs. Lateral Displacement Hystereses of a Column subjected to Square Orbit Loading



(a) Drift 1% (b) Drift 2% (c) Drift 3%

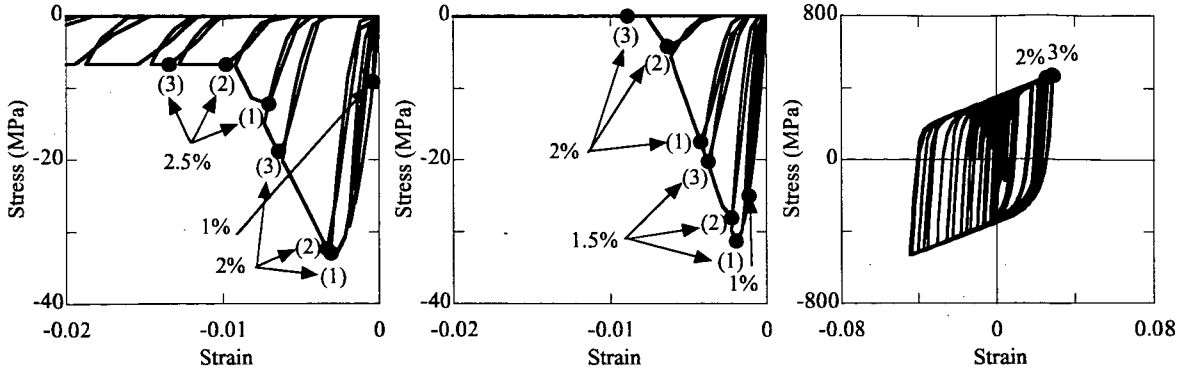
(1) x-Direction



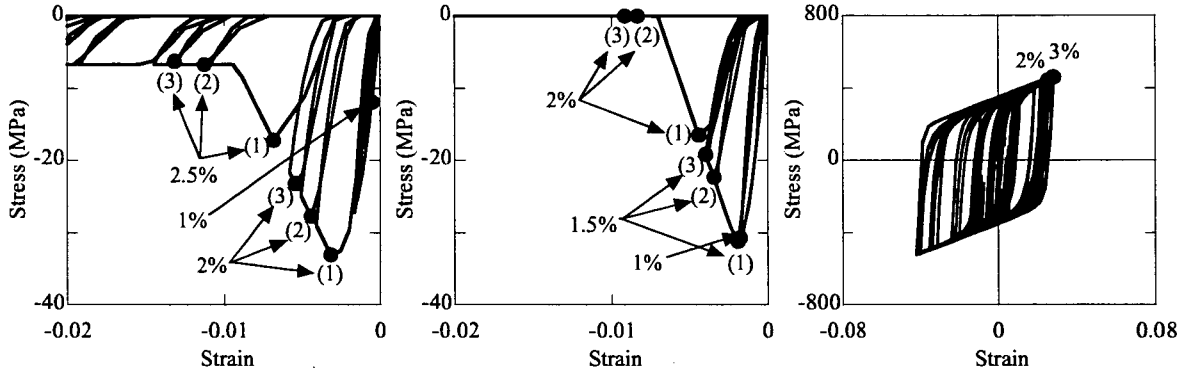
(a) Drift 1% (b) Drift 2% (c) Drift 3%

(2) y-Direction

Fig. 18 Comparison of Analytical and Experimental Hystereses at 1%, 2% and 3% Drifts (Square Orbit Loading)

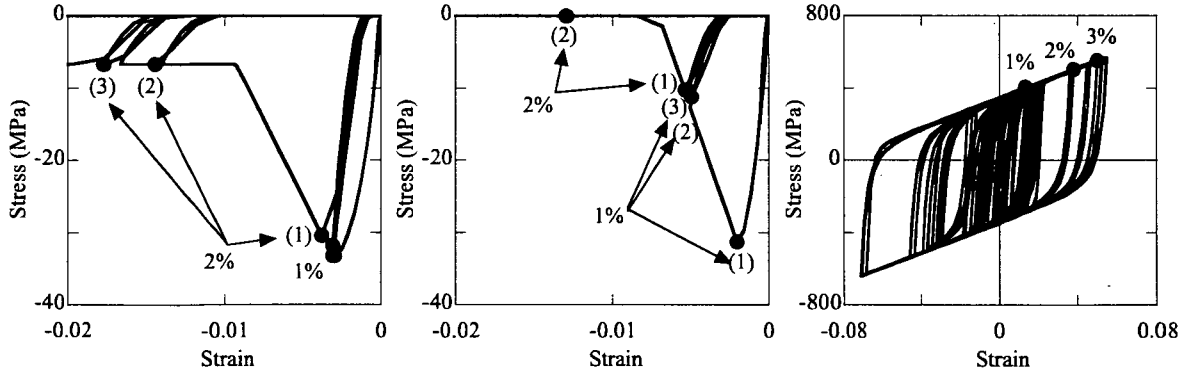


(a) Core Concrete (Extreme Fiber at A-Surface) (b) Covering Concrete (Extreme Fiber at A-Surface) (c) Longitudinal Bar (Center of A-Surface)



(a) Core Concrete (Extreme Fiber at B-Surface) (b) Covering Concrete (Extreme Fiber at B-Surface) (c) Longitudinal Bar (Center of B-Surface)

Fig. 19 Computed Stress vs. Strain Hystereses of a Column subjected to Square Orbit Loading (numbers in parentheses represent the number of loading excursions)



(a) Core Concrete (b) Covering Concrete (c) Longitudinal Bar

Fig. 20 Computed Stress vs. Strain Hystereses at the A-D Corner of a Column subjected to Square Orbit Loading

At the corners larger deterioration occurs resulted from the combination of bilateral excitation. Fig. 20 shows the computed stress vs. strain hystereses of the core and the covering concrete and the longitudinal bar at the A-D corner. It should be noted here that compressions of bilateral loading are coupled at 1%, 2% and 3% drifts at the A-D corner, but

they are not coupled here at 1.5%, 2.5% and 3.5% drifts. Due to the coupling of bilateral loading, the stress of core concrete reaches σ_{cc} at the first loading excursion of 1% drift. Although it is still 91% of σ_{cc} at the first loading of 2% drift, it sharply deteriorates to 20% of σ_{cc} at the second loading excursion of the 2% drift. The strain of the corner longitudinal bar is 0.05 at 3% drift, which is 72% larger than the strain of a longitudinal bar at the center of surface A. It is thus well explained that the corners are subjected to larger inelastic deformation. This, in turn, explains that the failure started to occur from the corners in the test.

6. CONCLUSIONS

A series of cyclic loading tests and a fiber element analysis were conducted to clarify the effect of bilateral loading of square reinforced concrete bridge columns. Based on the test and analysis presented herein, the following conclusions may be deduced.

1) Bilateral loading results in larger deterioration of flexural strength and ductility capacity of columns than that under the unilateral loading. In particular, this effect is significant under the square and circular orbit loadings.
2) Although failure started to occur at the surfaces in the plastic hinge zone subjected to alternative compression and tension under the unilateral loading, it started to occur from the corners under the bilateral loadings.
3) Fiber element analysis which takes account of deterioration of confined concrete predicts the test result with a good accuracy. The failure mode and progress of failure of the columns can be well explained based on the fiber element analysis.

7. ACKNOWLEDGEMENTS

The authors express their sincere appreciation to Dr. Yabe, M., Chodai Consultant, for design of the model columns, and Dr. Sakai, J., University of California, Berkeley, for use of the confined model of concrete. Extensive support was provided by Messrs. Uehara, K., Hatada, S., Yamagishi, M., Shimoyamada, E., Nakazawa, N., Nagata, S., Matsukawa, R., Wan, K. and Nakamura, G. for constructing and executing the cyclic loading test.

8. REFERENCES

1. Hoshikuma, J., Kawashima, K., Nagaya, K. and Taylor, A. W.: Stress-Strain Model for Confined Reinforced Concrete in Bridge Piers, Journal of Structural Engineering, ASCE, 123(5), 624-633, 1997
2. Sakai, J. and Kawashima, J.: An Unloading and Reloading Stress-Strain Model for Concrete Confined by Tie Reinforcements, Proc. 12th World Conference on Earthquake Engineering, CD-ROM No. 1432, Auckland, New Zealand, 2000.
3. Menegotto, M.and Pinto, P.E.: Method of Analysis for Cyclically Loaded R.C. Plane Frames Including Changes in Geometry and Non-Elastic Behavior of Elements under Combined Normal Force and Bending, *Proc. of IABSE Symposium on Resistance and Ultimate Deformability of Structures Acted on by Well Defined Repeated Loads*, pp.15-22, 1973

Multi Hazard Dynamic Testing for Bridge Piers

by

W. Phillip Yen, Ph.D., P.E [1] and Kornel Kerenyi, Ph.D. [2]

ABSTRACT

The goal of this research is to test various combinations of hazards such as wind, flood, scour and dynamic loadings (e.g., earthquakes and vessel impacts) for impacts to bridge pier structural stability. Most equations and design criteria currently in use treat these hazards separately, although they can occur concurrently. A study that combines all hazards and dynamic loadings would be very complicated. Therefore the initial research is designed and fabricated to study only flow (flood), soil (sediment particle size and river bed geometry) and dynamic loading (harmonic, random and impulsive loads). A rigid mass, single degree of freedom (SDOF) oscillator represents the simplified bridge pier. A specially designed flume, which is 3000 mm long and 400 mm wide, allows for the investigation of different soil conditions and various flow velocities. The oscillating pier is mounted elastically on a structure over the test section of the flume. Two synchronous linear drive motors apply the dynamic loads. The oscillating bridge pier, neglecting flow and soil conditions, represents a perfect linear spring-damper system. In combination with flow and soil the system is highly nonlinear. The goal of this initial research is to replace the soil and flow effects with an equivalent spring-damper system. Additional goals are to detect the nonlinear spring and damping characteristics and to determine an equation of motion.

KEYWORDS: fluid soil structure interaction, multi hazard impacts on bridge piers.

1.0 INTRODUCTION

This study is concerned with the safety of bridges subjected to different natural hazard events. The events of interest are earthquakes, scour, hurricanes and vessel impact. Several bridge foundations are under water, so the structural response during an earthquake under these combined conditions is very complicated. Research at the Federal Highway Administration (FHWA) Turner Fairbanks Highway Research Center (TFHRC) Seismic Hazard Mitigation has focused on developing an experimental set-up to investigate a simple model where flow, scour (soil) and earthquakes (dynamic forces) interact with a bridge pier structure.

The experimental set-up is designed to study the fluid-soil interaction of a rigid single degree of freedom (SDOF) oscillator using a forced oscillation experiment. The linear SDOF oscillator acts as a reference system to investigate the nonlinear behavior of the system when it interacts with fluid and soil. The identification procedure to determine the additional fluid and soil forces based on a forced oscillation test are similar used to identify fluid dynamic damping and stiffness. Staubli (1983) and Deniz (1997) used forced oscillation tests in a tow-tank to determine force coefficients and phase angle to describe the fluid dynamic system. Scruton (1963) and Bardowicks (1976) proposed a description of flow-induced load in the form of components in phase with body displacement and velocity. They use controlled vibration experiments in a wind tunnel.

2.0 EXPERIMENTAL SET-UP

The experimental set-up consists of two major subsystems: a flume to simulate various flow and

[1] Research Structural Engineer, Seismic Hazard Mitigation (HRDI-07), Federal Highway Administration, 6300 Georgetown Pike, McLean, Virginia 22101; PH (202) 493-3056; FAX (202) 493-3442; email: wen-huei.yen@fhwa.dot.gov

[2] Hydraulic Research Engineer, GKY and Associates, Inc., 5411-E Backlick Road, Springfield, Virginia 22151; PH (703) 642-5080; FAX (703) 642-5367; email: kornel.kerenyi@fhwa.dot.gov

riverbed conditions and the shaking device to apply different dynamic loadings.

2.1 Flume

The flume consists of a 1300 mm long inlet and a 2000 mm straight channel (Figure 1). The upstream flow conditioning is achieved using filter mats, a honeycomb flow straightener, and a carefully designed trumpet-shaped inlet. The flume is designed to have a uniform flow distribution over the width and to have fully developed turbulent flow (following Prandtl's velocity distribution) at the test section. The recess at the test section is 400 mm x 300 mm (length x width) and 80 mm deep, and can be filled with sand particles of various sizes. The roughness of the fixed bed upstream of the recess can be varied according to the sand particles used in the recess. A 25 l/s pump provides the flume with water, which is stored under the flume in a water tank. A flow meter measures the discharge and an ultra sonic flow depth meter determines the flow depth. A laser distance meter, which is mounted on a portal robot, can scan scour holes during test runs. The flow velocity is measured with an electro magnetic velocity probe.

2.2 Shaking device

The shaking device is mounted above the flume on a rigid frame at the test section. The rigid frame with shaker can be turned 90 degrees and is portable. Two synchronous linear drive motors apply dynamic forces up to 12 Hz. Band limited random noise can be used to simulate earthquake-loading. A ridged model bridge pier is fixed to a platform with linear bearings, which is attached to a linear guide system and mounted elastically to the drive platform. The natural frequency can be varied by using different coil springs for the elastical support. The mechanical (structural) subsystem represents a linear SDOF system, which is lightly damped to study a significant peak resonant response. The damping ratio is determined by the Half-Power (Band-Width) method. The other end of the vertical rigid model pier is mounted in soil to interact with the soil subsystem. The body response displacement is measured with a laser distance meter and the response acceleration with accelerometers. The response velocity is determined by integrating the response acceleration. Two load cells measure the applied dynamic loading.

3.0 MATHEMATICAL BACKGROUND

The objective of this research is to replace flow and soil with an equivalent spring damper system and to determine the non-linear behavior of the additional spring and damping coefficients (Figure 3).

3.1 Identification Procedure

The identification procedure is based on the idea of a forced oscillation experiments used to determine fluid dynamic stiffness and damping. Additional damping and stiffness coefficients can model the fluid dynamic and the soil subsystem (equation 1), which are functions of several parameters (e.g., amplitude and frequency)

$$\begin{aligned} & m\,\ddot{v}(t) + c\,\dot{v}(t) + k\,v(t) + \\ & + c_e(a,\overline{\omega})\,\dot{v}(t) + k_e(a,\overline{\omega})\,v(t) \\ & = p_o \exp(\mathrm{i}\,\overline{\omega} t) \end{aligned} \qquad (1)$$

For the tests described here only the exciting frequency $\overline{\omega}$ and the amplitude ρ will be varied by keeping scour depth s, pier depth d, flow depth h and flow velocity V_{FLUID} constant.
The identification concept is based on the balance of forces acting on the linear mass oscillator (Figure 4) under steady state harmonic condition whereby the total response is:

$$v(t) = \rho \exp[\mathrm{i}(\overline{\omega} t - \theta)]\,. \qquad (2)$$

Force equilibrium requires that the sum of the inertial $f_I(t)$, damping $f_D(t)$ and spring forces $f_S(t)$ equal the applied load.

$$p(t) = p_o \exp(\mathrm{i}\overline{\omega} t)\,. \qquad (3)$$

These forces are:

$$f_I(t) = m\,\ddot{v}(t) = m\,\overline{\omega}\,\rho \exp[i(\overline{\omega} t - \theta)] \qquad (4)$$

$$f_D(t) = c\,\dot{v}(t) = i\,c\,\overline{\omega}\,\rho \exp[i(\overline{\omega} t - \theta)] \qquad (5)$$

$$f_S(t) = k\,v(t) = k\,\rho \exp[i(\overline{\omega} t - \theta)] \qquad (6)$$

These forces, along with the applied loading, are shown as vectors in the complex plane (Figure 5) also shown is the closed polygon of forces required for equilibrium in accordance with equation (7)

$$f_I + f_D + f_S = p(t). \qquad (7)$$

Inertial, damping, and spring forces as given in equation (4) are in phase with the acceleration, velocity, and displacement motions, respectively. If the linear mass oscillator interacts with flow and soil additional damping and stiffness forces are required for equilibrium (Figure 6). These forces are frequency and amplitude dependent as shown in equations (8) and (9).

$$f_{S-FSI}(t) = k_e(\rho, \overline{\omega})\, v(t) = k_e(\rho, \overline{\omega})\, \rho \qquad (8)$$

$$f_{D-FSI} = c(\rho, \overline{\omega})\, \dot{v}(t) = i\, c(\rho, \overline{\omega})\, \overline{\omega}\rho = i\, c(\rho, \overline{\omega}) \qquad (9)$$

To determine these additional forces cross power spectrum is used to compute the phase angle θ between body response displacement amplitude ρ and applied dynamic force amplitude p_o. The forces can be expressed by equilibrating the dynamic force components

$$f_{S-FSI} = p(t)\cos\theta - f_S + f_I \qquad (10)$$

$$f_{D-FSI} = p(t)\sin\theta - f_D \qquad (11)$$

Substituting equations (4) to (6) and equations (8) and (9) into equation (10) and (11), one obtains the fluid-soil coefficient functions

$$k_e(\rho, \overline{\omega}) = \frac{p_o \cos\theta - k\rho + m\ddot{\rho}}{\rho} \qquad (12)$$

$$c_e(\rho, \overline{\omega}) = \frac{p_o \sin\theta - c\dot{\rho}}{\dot{\rho}} \qquad (13)$$

Where $\dot{\rho}$ and $\ddot{\rho}$ represent the response velocity and response acceleration amplitude, respectively.

4.0 REFERENCES

Deniz S., Staubli T., (1997), Oscillating rectangular and octagonal profiles: Interaction of leading- and trailing-edge vortex formation, Journal of Fluids and Structures, Vol. 11, p. 3-31.

Barowicks, H., (1976), Effects of cross-sectional shape and amplitude on aeroelastic vibrations of sharp-edged prismatic bodies, Doctoral Dissertation, Techn. Universitaet Hannover, Germany.

Staubli, T., (1983), Investigation of oscillating forces on a vibrating cylinder in cross-flow, Doctoral Dissertation, ETH Zuerich, Switzerland

Scruton, C., (1963),. On the wind-excited oscillations of stacks, towers and masts, 1st Conference wind effects on buildings and structures, Teddington, UK, Paper 16

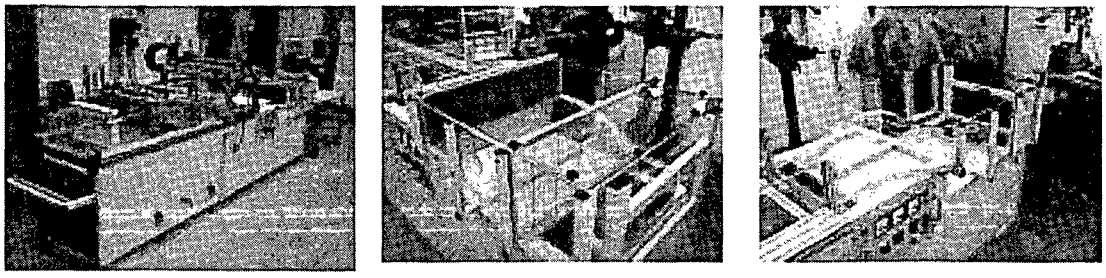


Figure 1. Test flume and trumpet shaped inlet

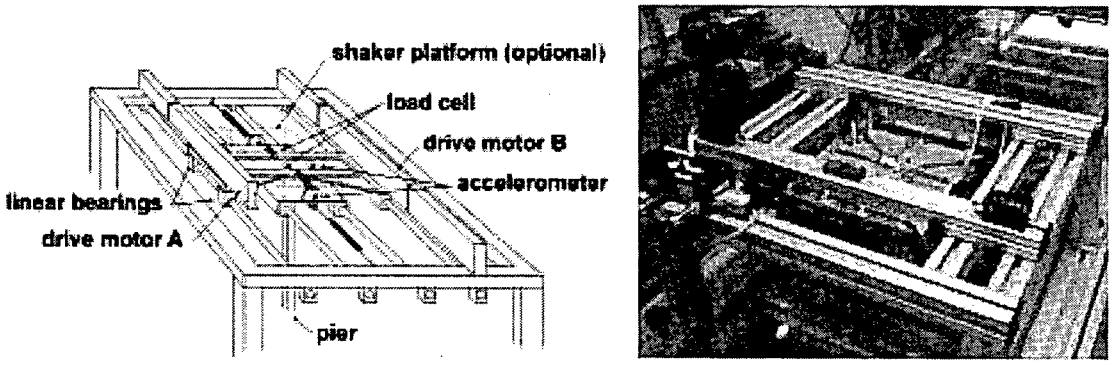


Figure 2: Shaking device

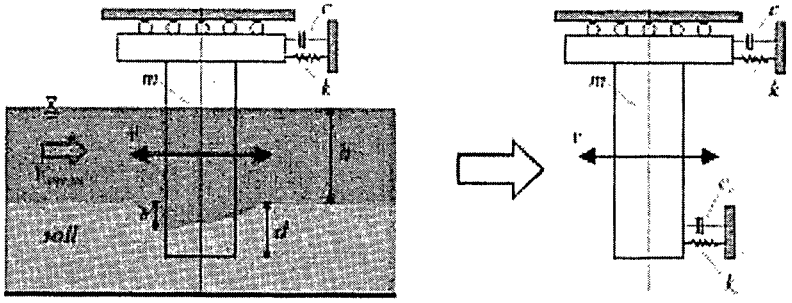


Figure 3: Equivalent fluid-soil spring-damper system

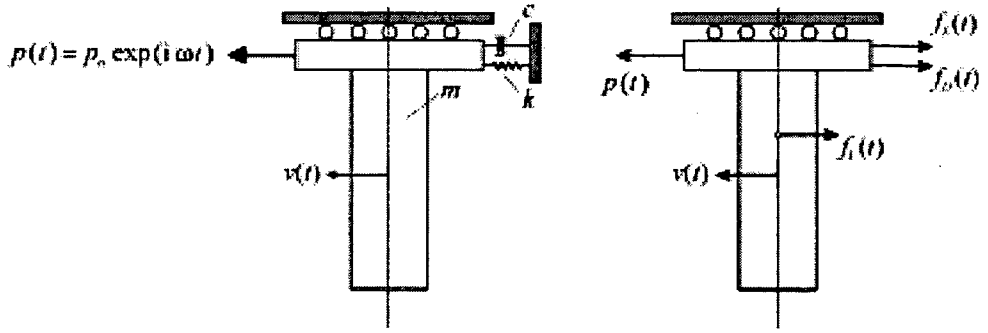


Figure 4: Linear SDOF system with basic components and forces in equilibrium

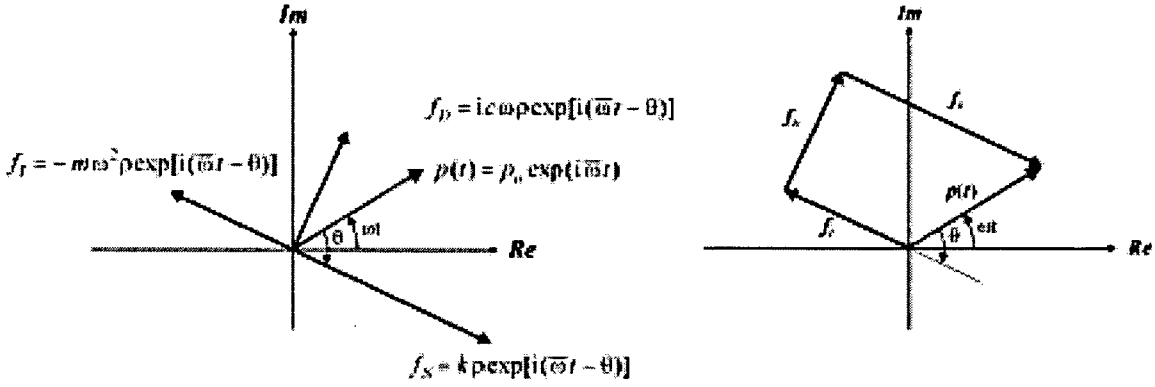


Figure 5: Steady state harmonic forces using viscous damping in a complex plane representation and closed force polygon representation

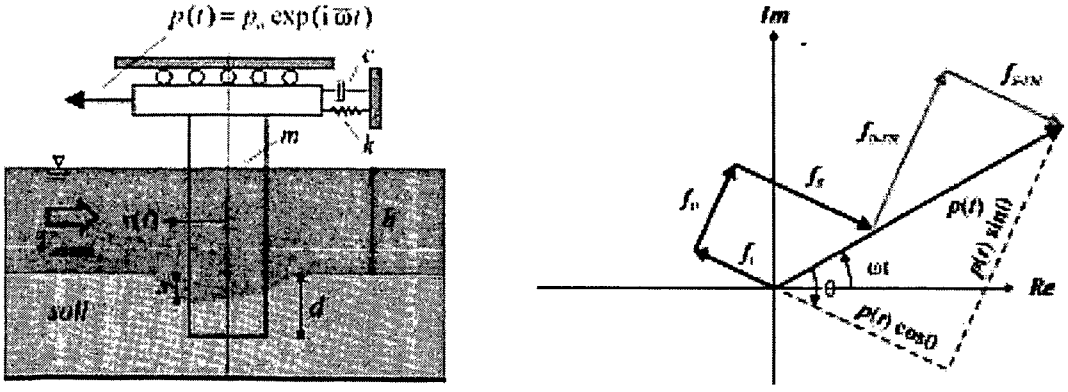


Figure 6.: SDOF system interacting with fluid and soil and closed polygon representation including additional nonlinear damping and stiffness forces

SITE-SPECIFIC DESIGN EARTHQUAKE GROUND MOTION AND SEISMIC DESIGN TECHNOLOGY IN NEXT GENERATION

by

Shigeki UNJOH[1], Takaaki KUSAKABE[2], Sho-ichi NAKATANI[3], Takeshi OHSHITA[4], Yasuhiko WAKIZAKA[5], Kei-ichi TAMURA[6] and Jiro FUKUI[7]

ABSTRACT

This paper briefly describes the outcome of the earthquake engineering R&D in the 5-years R&D program for developing the road technology and the implementations conducted by the Road Bureau of the Ministry of Land, Infrastructure and Transport (MLIT), National Institute for Land and Infrastructure Management (NILIM), MLIT, and the Public Works Research Institute (PWRI). The 5-years program was initiated in November 1998 and concluded in the end of March 2003. The comprehensive R&D issues for the road technology including road environment, safety and security of roads, efficiency of road traffic, and accountability of public works were raised. In total, 13 projects were given high priority and had been conducted in the program.

The earthquake engineering R&D, titled as "Site-Specific Design Ground Motion and Seismic Design Technology in Next Generation," was selected as one of the 13 projects. R&D on the evaluation technology of site-specific active fault and the fault-induced earthquake ground motion, and the rational seismic design technology to assure the safety and economical efficiency had been conducted.

KEYWORDS: 5-year R&D Program
Road Technology
Earthquake Engineering R&D
Road Structures
Fault-induced Ground Motion
Rational Seismic Design

1. 5-YEARS R&D PROGRAM FOR ROAD TECHNOLOGY

For the purpose to create and improve a better social environment in 21st century, the road construction and improvement projects have been expected to play an important role in stimulation of the economy. The Road Bureau of the Ministry of Land, Infrastructure and Transport (MLIT), National Institute for Land and Infrastructure Management (NILIM), MLIT, and the Public Works Research Institute (PWRI) developed the 5 years program for road technology initiated in

1) Leader, Earthquake Engineering Team, Earthquake Disaster Prevention Research Group, Public Works Research Institute (PWRI), Tsukuba-shi, Ibaraki-ken, 305-8516 Japan

2) Head, Earthquake Disaster Prevention Division, Research Center for Disaster Risk Management, National Institute for Land and Infrastructure Management (NILIM), Ministry of Land, Infrastructure and Transport (MLIT), Tsukuba-shi, Ibaraki-ken, 305-0804 Japan

3) Head, Bridge Division, Road Department, NILIM, MLIT

4) Leader, Construction Technology Team, Construction Technology Research Department, PWRI

5) Director, Daidogawa Dam Construction Office, Kinki Construction Bureau, MLIT (Former Leader, Geology Team, Material and Geotechnical Engineering Research Group, PWRI)

6) Leader, Ground Vibration Team, Earthquake Disaster Prevention Research Group, PWRI

7) Leader, Foundation Engineering Team, Structures Research Group, PWRI

November 1998 [1]. The comprehensive R&D issues on road technology including "Road Environment," "Safety and Security of Roads," "Efficiency of Road Traffic," and "Accountability of Public Works" were pointed out.

Based on these concepts, the following 13 projects were given high priority to be conducted in 5 years.

(1) Improving the Road Environment

1) Technology for improving the roadside environment and the source of atmospheric, noise and vibration pollution
2) Technology for preserving and rehabilitating the natural environment

(2) Improving the Safety and Security of Roads and Living

1) Development of the AHS (Advanced Cruse Assist Highway System) which aims to prevent accidents through the provision of driver information and driving assistance
2) Evaluation of earthquake ground motion taking into account the regional characteristics, and development of the earthquake resistance engineering for next generation
3) Risk management technology for bedrocks and landslides

(3) Improving the Efficiency of Road Traffic

1) Technology for reinforcing bridges and pavements, and enlargement the diameter of tunnels to accommodate large vehicles
2) Development of distribution systems that strengthen inter-urban and intra-city transportation linkages
3) Technology for realizing the TDM (Traffic Demand Management) policy
4) Environmentally friendly technology for setting countermeasures against extremely snowy and cold road conditions by utilizing unused energy

(4) Improving the Accountability of Public Works

1) Management technology for increasing the life span of pavements and bridges, and minimizing the LCC (Life Cycle Cost)
2) Efficient road planning and design technology that takes into account regional features
3) Technology for construction of new transportation link that promotes regional cooperation and consolidation

2. EARTHQUAKE ENGINNRING R&D

The earthquake engineering related R&D was one of the 13 projects with high priority. The title of the research is "Site-specific Earthquake Ground Motion and Seismic Design Technology in Next Generation." Project team was established from the seven teams and divisions in total from the NILIM including the Earthquake Disaster Prevention Division and the Bridge Division, and the PWRI including the Construction Technology Team, the Geology Team, the Earthquake Engineering Team, the Ground Vibration Team and the Foundation Engineering Team.

2.1 Background and Objective of R&D

Japan is one of the most earthquake prone countries in the world and has a history of numerous devastating earthquakes. During the Hyogo-ken-nanbu Earthquake in 1995, over 6,000 people died, and the damage of houses was about 513,000 in which about 249,000 were near collapse. The social and economic loss due to damage caused by the earthquake was immeasurable. Loss of the GDP was estimated as Reduced Ratio of 0.1～0.45. Direct damage to roads, ports, railways were estimated as 2,200 billion Yen. Collapse of highway was caused on 27 routes and the close of highways was caused at 36 points.

Main causes of serious damage was the strong earthquake ground motion with a wide natural period range caused by the inland active fault just under the urban area, and the serious damage to structures were caused mainly at the structures with smaller ductility capacity.

Based on the past experience of earthquake

disasters, road networks that are reliable and less impacted by disasters is necessary to be constructed. In the recommendations submitted by the Construction Technology Development Council (1997), and the Comprehensive National Land Development Plan titled, "Ground Design for the National Land Development in the 21st Century (1998)," "improving safety throughout Japan" and "ensuring safety and security" were placed as two most important technology for revising the seismic design standards. Development of evaluation method of active faults and prediction method of earthquake ground motions were required. They are the basis for ensuring the safety of infrastructures in the event of earthquakes.

On the other hand, from the perspective of reducing the construction cost and promoting the efficient investment of social infrastructures, technology for securing both earthquake safety and economical efficiency is required.

The fundamental target of the earthquake engineering R&D was that no serious effect on the people lives against large inland earthquakes and large inter-plate type earthquakes. Since the roads have important functions as emergency routes and to support social and economical activities, higher performance for road networks are required. Therefore, it was needed to develop the earthquake engineering for next generation to achieve the higher level of the seismic performance and to reduce the construction cost under the difficult economic and financial conditions.

2.2 Earthquake Engineering R&D

To improve the earthquake safety and the reliability of road networks and society, and to promote the efficient development of social infrastructures with reasonably reduced costs, the following research was conducted. The target of the R&D was to develop the technology and to reflect the outcomes to the practical implementations including the development and revise of design codes/guidelines/manuals.

(1) Development of Evaluation Method of Design Earthquake Ground Motion considering the Effect of Active Faults

1) Risk Evaluation Technology and Hazard Mapping Technology of Anticipated Earthquake Effect considering Historical Earthquake Record and Active Fault Information

2) Evaluation Technology of Active Faults and the Structures of Deep Soil Layers, and Prediction Method of Site-Specific Near-Field Earthquake Ground Motions for the Seismic Design

(2) Development of Rational Seismic Design Methods for Infrastructures

1) Rational Seismic Design Methods and Seismic Retrofit Methods for Highway Bridges
   a) Development of Performance-based Seismic Design Concept for Highway Bridges
   b) Improvement of Evaluation/Verification Methods of Seismic Performance of Highway Bridges
   c) Development of Rational Seismic Retrofit Methods of Highway Bridges

2) Seismic Design Methods for Underground Structures and Soil Structures based on the Deformation Evaluation

3. OUTCOMES OF EARTHQUAKE ENGINEERING R&D

The wide ranged outcomes had been produced from the project. The main outcomes are introduced in the following.

3.1 Risk Evaluation Technology and Hazard Mapping Technology

Currently used earthquake hazard map in Japan

was developed based on the measured earthquake record data for about past 100 years and the historical earthquake information for about past a thousand and several hundreds years. These information is not enough to evaluate more accurate earthquake hazard considering the earthquakes induced from active faults with the return period of over a few thousands years. Also, large scale earthquakes known as repeatedly occurred at specific active faults and inter-plates were not considered in detail in the current hazard map and the effect of the earthquakes in the near-fault area was not accurately evaluated.

In the project, the hazard mapping technology was developed considering both the past earthquake occurrence information and the information on the large scale earthquakes known as repeatedly occurred at the specific active faults and the inter-plates which has been recently accumulated. The developed mapping method was verified using the JMA Intensity information from 1926. **Fig.1** shows a model hazard map computed for throughout the Japan. These results are expected to be contributed in the next revision of design codes for the rational seismic design considering the regional earthquake information.

3.2 Evaluation Technology of Active Faults and the Structures of Deep Soil Layers

To estimate the ground motion induced from specific active faults, it is necessary to evaluate the parameters including size, segmentation, directions, and so on, of each active fault. In the project, to accurately evaluate the place and size of active faults, the evaluation technology by reading the aerial photographs was studied. The relation between the active fault tracing and active fault landform, and the reliability and activity was studied. The results were compiled as an investigation manual for the evaluation of active faults.

Regarding the length of the active faults, the segmentation of active faults which moved at the same time was studied, and the pattern of the activity of fault segment according to the branch pattern was proposed.

To evaluate more accurate earthquake ground motion transmitted from the earthquake source, it is necessary to know the effect of deep soil layers which characteristics is surveyed by the soil search. The effects of the deep soil structures and the shallow soil layer over the stiff soil layer were analytically studied. The earthquake ground motion was found to be significantly affected by the bedrock depth and the form of the deep soil structure as well as the depth of stiff soil layer of shallow soil layer. These results were compiled as the attention points to be considered in the development of soil layer model.

3.3 Prediction Method of Site-Specific Earthquake Ground Motions

The evaluation technology of the earthquake ground motion induced from specific active faults using an empirical green function has been currently applied for the estimation of fault-specific earthquake ground motion. The method can estimate the ground motion of larger scale earthquake by superimposing the earthquake records of small earthquake according to the active fault modeling. The limitation of the method is that the appropriate earthquake records during small earthquakes is necessary at the point at which the earthquake ground motion is evaluated. Because of lack of the earthquake records, the accuracy and applicability of the method is limited.

To compensate the limitation of the above method, the method using a statistical green function is proposed. In this method, the earthquake records of small earthquakes are artificially produced based on the statistical analyses of a number of small earthquake records. The proposed method was compared with the strong motion observation data and the statistical attenuation equations, and the good

correspondence was verified. **Fig. 2** shows the demonstration example to estimate the peak ground acceleration distribution caused by the 1923 Kanto Earthquake. The peak acceleration is varied site by site and the effect of the failure mechanisms of the faults is considered. This proposed method has been applied to evaluate the design earthquake ground motions of the several actual projects of long span bridges.

Other than the above outcomes, the evaluation method of surface fault displacement induced from active faults, and the application method of nonlinear acceleration design spectrum were also studied.

3.4 Performance-based Seismic Design Concept for Highway Bridges

The Japan Road Association (JRA) Design Specifications for Highway Bridges were revised based on the Performance-based design code concept for the purpose to respond the international harmonization of design codes and the flexible employment of new structures and new construction methods. The performance-based design code concept is that the necessary performance requirements and the verification policies are clearly specified. The JRA specifications employed the style to specify both the requirements and the acceptable solutions including the detailed performance verification methods which were based on the existing design specifications including the design methods and the design details. For example, the analysis method to evaluate the response against the loads was placed as one of the verification methods or acceptable solutions. Therefore, designer can propose the new ideas or select other design methods with the necessary verification.

The most important issue of the performance-based design code concept is the clear specifications of the requirements, which the designers are not allowed to select other methods, and the acceptable solutions, which the designers can select other methods with the necessary verification. In the JRA Specifications, they were clearly specified including the detailed expressions. In future, the acceptable solutions will be increased and widened with the increase of the verification of new ideas on the materials, structures and constructions methods.

The code structure of the Part V: Seismic Design is as shown in **Fig. 3**. The static and dynamic verification methods of the seismic performance as well as the evaluation methods of the strength and ductility capacity of the bridge members are placed as the verification methods and the acceptable solutions, which can be modified by the designers with the necessary verifications.

In addition to the above outcomes, the following outcomes were produced.

1) Performance matrices considering Input-Output-Cost Curve
2) Selection method of seismic performance considering cost-benefit efficiency
3) Limit state concept for bridge structures
4) Analysis method of partial safety factors for seismic design of highway bridges based on reliability analysis
5) Testing methodology of reinforced concrete columns (**Photo 1**)
6) Improved ductility evaluation methods of reinforced concrete and steel columns and the ductility improvement technology
7) Design method of abutment based on ductility design concept
8) Improved evaluation method of soil resistance in foundation design considering the effect of liquefaction
9) Improved evaluation method of soil bearing capacity and a dynamic nonlinear modeling of foundations (**Photo 2**)

3.5 Rational Seismic Retrofit Methods of for Existing Foundations

There are existing infrastructures with weak

resistant capacity against large scale earthquakes. Seismic retrofit works for such structures including bridges have been conducted after the 1995 Hyogo-ken-nanbu Earthquake. However, the seismic retrofit works are restricted and affected by the conditions of sites such as the limitation of construction space. The seismic retrofit methods under the restricted construction conditions had been developed. The micro pile retrofit method, as shown in **Fig.4**, is one of the effective retrofit methods for the foundations. Five types of micro pile retrofit methods were developed and the effectiveness was verified. The design and construction manual was complied and the test constructions were made at 9 sites. **Photo 3** shows one example of actual implementations.

3.6 Seismic Design Methods of Underground and Soil Structures based on the Deformation Evaluation

Underground structures including highway tunnels and common utility ducts have relatively safer seismic performance than structures on the ground like buildings and bridges. To evaluate the seismic performance of underground structures against the large scale earthquake, the analysis method of soil-structure interaction, evaluation method of shear deformation of structures, standard design earthquake ground motion which is to be used as input motion on the base of surface layer, and the design method against floating effects due to soil liquefaction (**Photo 4**) were proposed.

For the soil structures, the stability was currently evaluated by the equilibrium of forces applied to the structures. The method can evaluate the safe or not, but cannot evaluate the seismic performance in detail. Therefore, the deformation characteristics of soil structures subjected to large scale earthquakes and the evaluation method was proposed.

3.7 Practical Applications/Implementations of the Research Outcomes

From the research project, the following outcomes and practical applications have been made.

(1) Design Earthquake Ground Motion considering the Effect of Active Faults

1) Evaluation Methods of Site-specific Level 2 Design Earthquake Ground Motions, to be published by NILIM
2) Development Method of Earthquake Hazard Map, to be published by NILIM
3) Manual for Evaluation of Active Faults from Landform, Cooperative Research Report of PWRI, No.284, March 2003

(2) Rational Seismic Design Methods for Infrastructures

1) Specifications of Highway Bridges, Part V: Seismic Design, JRA, March 2002
2) Manual for Earthquake Countermeasure Methods (Pre-earthquake and Post-earthquake measures), JRA, April, 2002
3) Data Book for Seismic Retrofit and Repair of Seismic Damage of Highway Bridges considering the Lessons learned from 1995 Hyogo-ken-nanbu Earthquake, Cooperative Research Report of PWRI, No.272, March 2001
4) Manual for Design and Construction of Micro-pile Retrofit Methods for foundations, Cooperative Research Report of PWRI, No.282, September 2002

(Micro Pile Retrofit methods have been implemented at 9 bridges.)

7. CONCLUDING REMARKS

This paper briefly presented the outcome of the earthquake engineering R&D in the 5-years R&D program for developing the road technology and the implementations conducted by the Road Bureau of MLIT, NILIM, and PWRI.

The outcomes of the project have already been

reflected to some of the seismic design codes/manuals as well as the practical applications. It is expected that the outcomes will be contributed in the wide area of applications and that the improvement and development will be continuously conducted to achieve the construction of safer, more durable and more cost-effective infrastructures against earthquakes in the future.

ACKNOWLEDGMENTS

The outcomes of the earthquake engineering R&D were evaluated by the "Evaluation Committee for Earthquake Engineering R&D (Chairman: Prof. Kazuhiko Kawashima, Tokyo Institute of Technology; Members: Prof. Koichi Maekawa, University of Tokyo, and Mr. Tomoyasu Hamada, Kajima Corporation)" and will be reviewed by the "Committee for New R&D for Road Technology (Chairman: Prof. Hideo Nakamura, Professor Emeritus of University of Tokyo)." The authors would like to express our appreciation to Chairmen and all members of the evaluation committee.

The Earthquake Engineering R&D project had been conducted and worked with the following several committees and groups. The Authors greatly thank all the members of committees and groups for their contribution to the projects.

1) Research Committee on the development of Evaluation Methods of Level 2 Earthquake Ground Motion (Chairman: Prof. Tatsuo OHMACHI, Tokyo Institute of Technology)
2) Japan Road Association, Bridge Committee (Chairman: Dr. Shoichi Saeki, PWRC), Subcommittees on the Seismic Design for Highway Bridges and the Foundation Design
3) Cooperative Research on Development of Evaluation Methods of the Place and Size of Active Fault (PWRI and 13 Private Companies)
4) Cooperative Research Project on Investigation, Repair and Seismic Retrofit of Highway Bridges (PWRI, JH, MEX, HE)
5) Cooperative Research Project on Retrofit of Foundation using Micro-Piles (PWRI, ACTEC, 12 Private Companies)

REFERENCES

1) Road Bureau of the Ministry of Land, Infrastructure and Transport, National Institute for Land and Infrastructure Management, and Public Works Research Institute: New Five-year Program for Road Technology in Japan, November, 1998
2) Japan Road Association: Design Specifications of Highway Bridges, Part I Common Part, Part II Steel Bridges, Part III Concrete Bridges, Part IV Foundations, and Part V Seismic Design, 2002
3) Ministry of Construction: Report on the Damage of Highway Bridges by the Hyogo-ken-nanbu Earthquake, Committee for Investigation on the Damage of Highway Bridges Caused by the Hyogo-ken-nanbu Earthquake, 1995
4) Kazuhiko Kawashima, et. al.: 1996 Design Specifications for Highway Bridges, 29th UJNR Joint Panel Meeting, May 1996
5) Shigeki Unjoh, et. al.: 2002 Design Specifications for Highway Bridges, 34th UJNR Joint Panel Meeting, May 2002

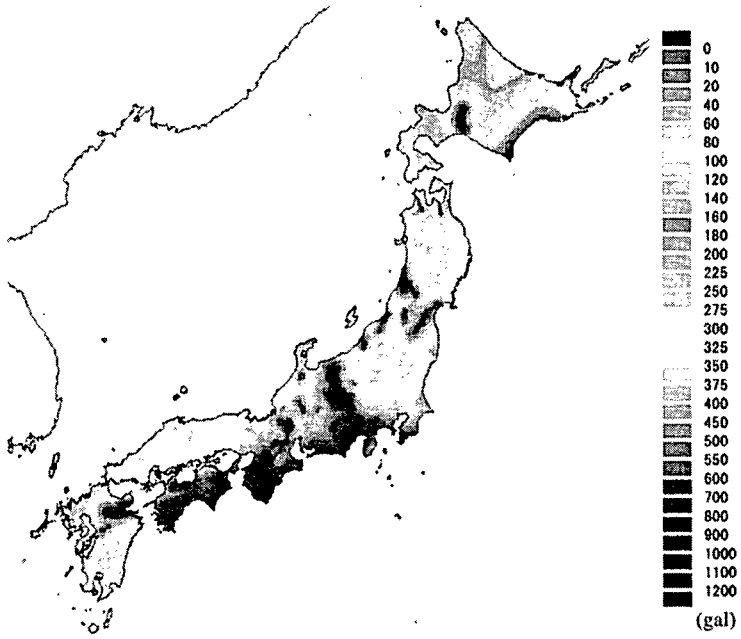


Fig.1 A Computed Model Map of Earthquake Hazard (Maximum Ground Acceleration with 5% exceeding probability in 100 years from January 1, 2001)

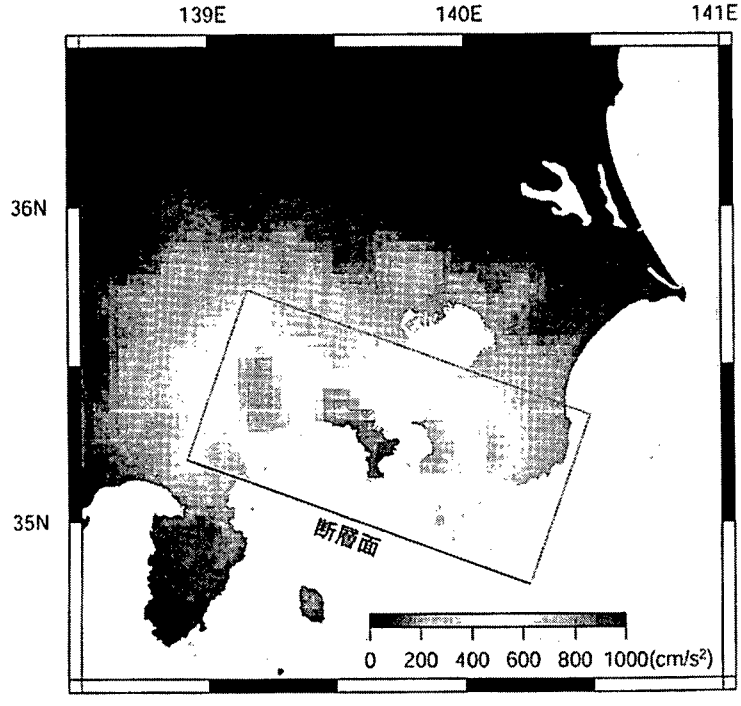


Fig.2 Evaluation of Peak Ground Acceleration on Stiff Bed Soil Layer caused by the 1923 Kanto Earthquake

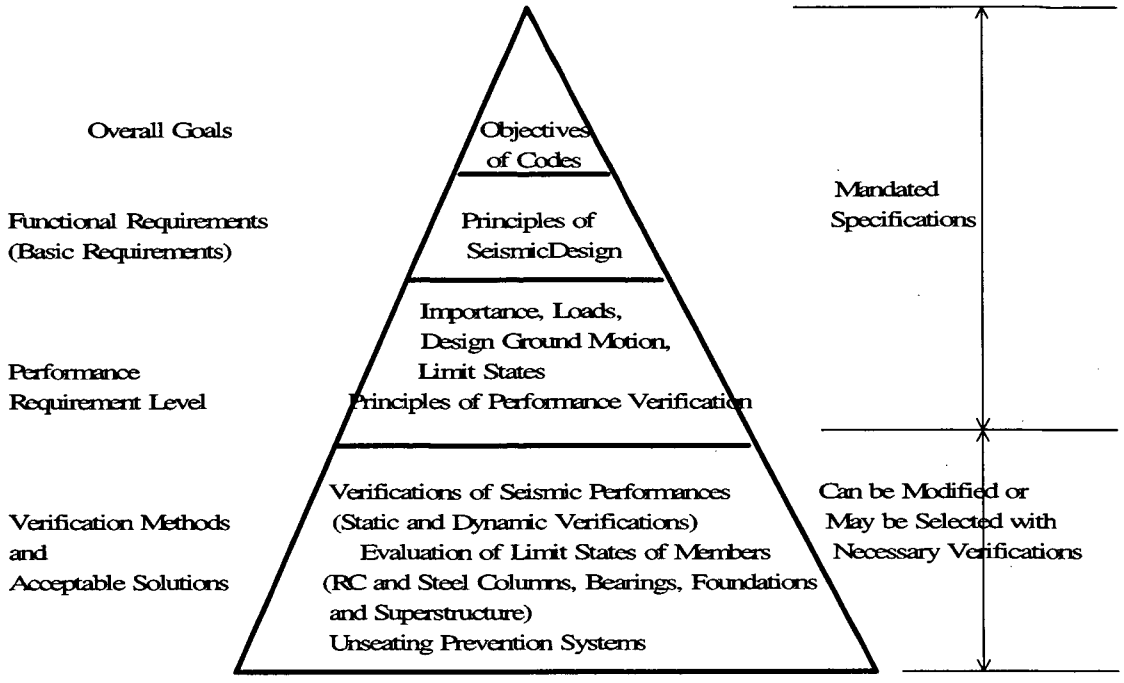


Fig. 3 Code Structure of JRA Design Specifications, Part V: Seismic Design

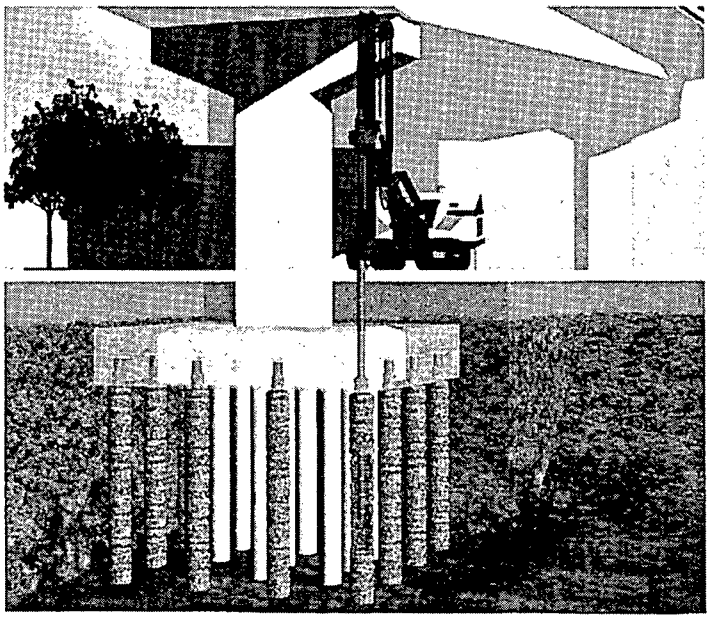
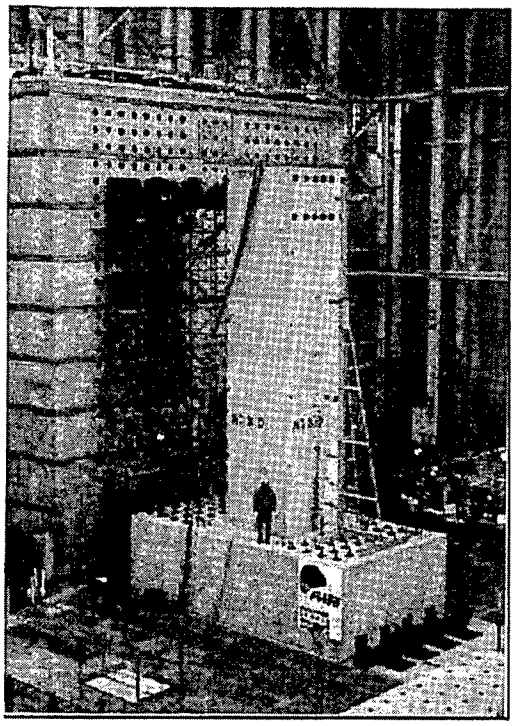
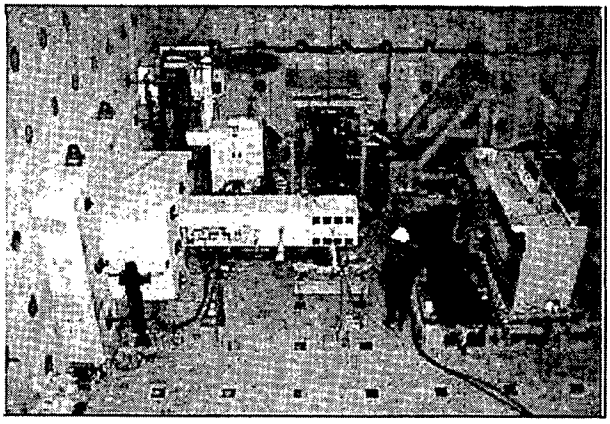


Fig.4 Micro Pile Retrofit Methods



(a) Real Size Testing



(b) Scaled Size Testing

Photo 1 Large Scale Testing for Verification of Seismic Performance of Reinforced Concrete Columns

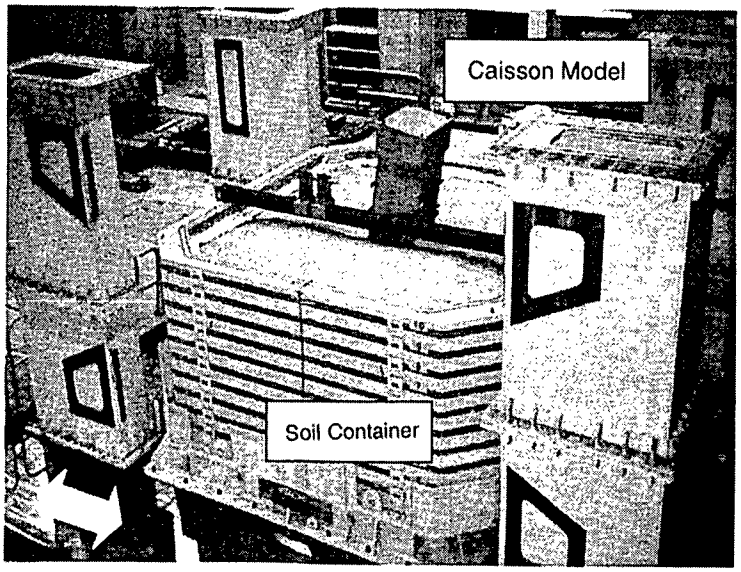


Photo 2 Shake Table Test of Caisson Foundations to investigate Dynamic Behavior of Foundations

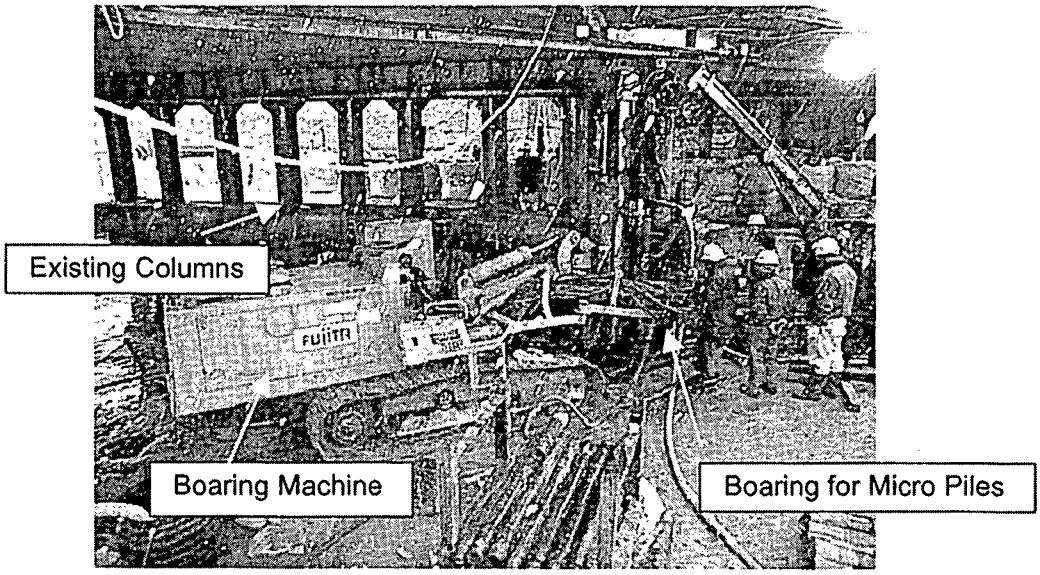
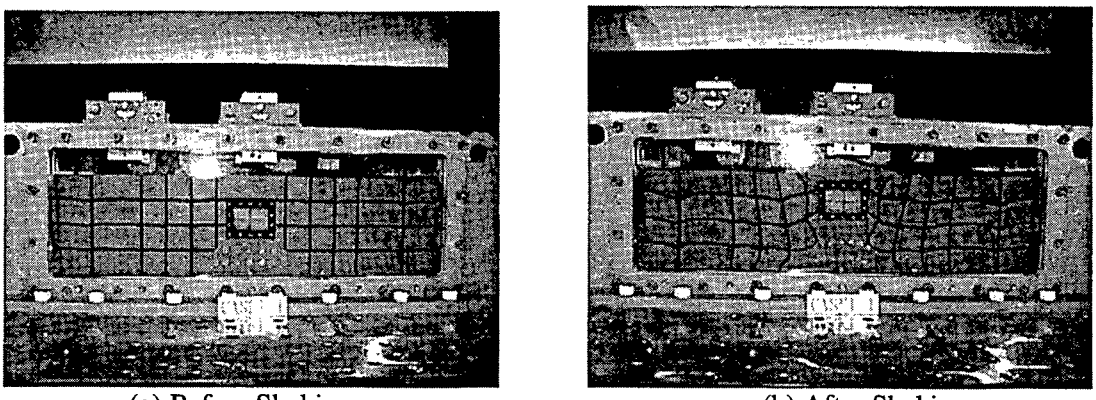


Photo 3 Practical Implementation of Micro Pile Retrofit Methods



(a) Before Shaking (b) After Shaking

Photo 4 Centrifuge Tests on Floating Effect of Underground Structures in Liquefiable Soil Layers

Seismic Analysis and Design of Flared Bridge Columns

by

Hisham Nada[1], David Sanders[2], and M. Saiid Saiidi[3]

ABSTRACT

Past earthquakes have shown that flared columns are susceptible to premature shear failures. In the 1994 Northridge Earthquake, shear failures were caused by a plastic hinge forming at the base of the flare and a subsequent increase in the level of column shear demand above design levels. This paper presents an experimental and analytical study that is examining new details for flared columns and joints. The primary feature is a gap at the top of the column and the amount of transverse flare reinforcement. Two two-column bents were tested on the shake table to examine dynamic effects as well as column and beam interaction. The test specimens had different amounts of confining reinforcement in the flare. The details had an overall displacement ductility that was well above 6. Test also showed that gap started to close at a displacement ductility level below 6.

KEYWORDS: bent; bridge; flared columns; seismic; shake-table

1.0 INTRODUCTION

Design of flared columns to resist earthquake loading is a complicated issue due to the changing cross section along the column length. Past earthquakes have shown that flared columns could have poor behavior due to the large increase of column flexural capacity at the top of the column. The increased capacity can cause the plastic hinge region to shift away from the column-beam interface into the column. This causes the column to behave like a much shorter column and therefore have increased shear demand. The shifting of the hinge and the larger shear demand was not included in many previous designs and has led to brittle shear column failures. Brittle shear behavior may lead to significant damage and/or complete collapse of the bridge.

It was believed that if the flares had low longitudinal and transverse reinforcement ratios, they would spall during earthquakes. Therefore, the column core would be the element remaining to resist the earthquake. Experiments and past experience proved that even lightly reinforced flares contribute to increasing the column's flexural capacity (Sanchez et al 1997). To solve this problem, the California Department of Transportation (Caltrans) has developed new details attempting to separate the flared portion of the column from the overall flexural stiffness and capacity of the column. This is achieved by separating the flare from the bent cap using a gap between the top of the flare and the beam bottom surface, see Fig. 1. Caltrans' recommendations came as a result of single column slow-cyclic tests (Sanchez et al 1997) and not on system bent tests. The purpose in conducting shake-table bent tests is to study the effectiveness of the flare detail and to examine the behavior within the joint region as well as the overall system response. Four bents will be tested as part of the overall study. Two bents will be flexurally dominated while two will have shorter column heights to cause higher column shear demand. The columns are pinned at the base with a two-way hinge. Within each bent of similar height, the amount of flare transverse

[1] Principal Engineer, Alrabiah-Cowi Consulting Engineers, Dammam, KSA
[2] Associate Professor, Dept. of Civil Engineering, University of Nevada, Reno, Nevada, 89557
[3] Professor, Dept. of Civil Engineering, University of Nevada, Reno, Nevada, 89557

reinforcement will be varied. In one case the amount of transverse reinforcement in the flare will be in accordance with current Caltrans' guidelines while in the second case, the amount of reinforcement will be reduced in accordance to a proposed Caltrans detail. This document will focus on the tall bents tested (LFCD1 & LFCD2), which are flexurally dominated. The experiments were conducted at the Large-Scale Structures Laboratory at the University of Nevada, Reno.

2.0 MODEL DESIGN

2.1 Column Design

A survey was made of existing bridges in California to develop a prototype. Because the model will be used for new bridge detailing, only bridges that were designed according to the latest code provisions were considered in the survey. Based on these details and the 445 kN vertical load capacity of a single shake table, a 1/5-scale model was developed. The vertical axial load acting on each column was based on 10% of $f'_c A_g$ where A_g is the gross column cross section and f'_c is the concrete compressive strength

The 10% level was set as a typical upper range for the majority of new columns in regular bridges. This level resulted in a total axial load of 451.5 KN. In order to distribute this load along the length of the bent, lead buckets in combination with small rams were used. The other key details for the columns are given in Table 1 and shown in Fig. 2. All reinforcement is Grade 60 (414 MPa) to conform to current design. Some dimensions that cannot be scaled due to practical issues, like concrete cover, are kept within the minimum range that allows for practical use. The flexurally-dominated tall columns had a clear height of 1,625.6 mm while the shorter columns had a height of 939.8 mm. The bents described in this paper had the taller columns.

2.2 Flare Design

Flare reinforcement layout was calculated by scaling the prototype dimensions. Current Caltrans recommendations state the following (Caltrans Seismic Design Criteria):

- The gap width is calculated based on the estimated rotation at the top of column so as to prevent gap closure. The minimum height of the gap is 50 mm.
- The longitudinal flare reinforcement is nominal. Spacing between longitudinal flare reinforcement shall not exceed 450 mm and not less than 150 mm.
- The transverse flare reinforcement ratio (ρ_h) in the upper 1/3 of the flare height is equal to 0.45%±0.05 while that ratio for the lower 2/3 of the flare height is equal to 0.075%±0.025.

Where;

$\rho_h = 2 A_b / S D$
S = Spiral pitch
D = Column diameter
A_b = Area of spirals

To investigate these provisions and their effectiveness, two flare details were developed. The first one had a flare lateral reinforcement ratio that complied with the above-motioned provisions. The second detail had constant lateral flare reinforcement ratio along the total height of the flare. This was set to the lowest value of ρ_h=0.075%.

2.3 Bent Cap Design

To match the prototype, the center-to-center span of the bent should have been 2,286 mm. Since it was decided to use lead to apply the axial load, there was insufficient spacing between the columns to accommodate all of the lead. For this reason, the span was increased to 2,718 mm. The beam's depth was also increased in order to have the same relative flexural stiffness between the columns and the beam as

in the prototype. The bent cap was designed according to Caltrans' recommendations, which states that the beam capacity should be 1.2 times the capacity of the plastic hinge in the column. This is done to assure that a plastic hinge would form in the columns rather than the beam.

3.0 TESTING

3.1 Test Setup

The specimens were constructed at the University of Nevada, Reno. A total of 110 strain gauges were attached to reinforcement in the columns, flares and the beam-column connections. Material properties for the specimens are summarized in Tables 2 and 3.

The footing was tied to the shake table using prestressed steel bars to prevent any uplift during the test. The axial load was applied using steel buckets filled with lead blocks. The maximum vertical load capacity the shake table can sustain limited the weight of the specimen plus lead to 445 KN. The specimen weight was about 133.4 KN including the footing. The total axial load for both columns was 451.4 KN. In order to reduce the weight on the table, 178 KN of axial load was modeled using self-equilibrating rams in combination with the mass rig, see Fig. 3. The mass rig is a steel structure supported by frictionless pins so that it allows the system to move laterally without restraining it. The four rams were mounted over the two column and the mass rig was connected to the specimen with a rigid link and a load cell.

Beside the strain gauges, 34 transducers were used to measure the curvature along the column height and along the beam, beam-column connection in-plane displacements, out-of-plane displacements and horizontal movement of the bent and the column base. Accelerometers were mounted on the table, on top of the specimen and the lead, on the mass rig and in the transverse direction.

3.2 Runs and Observations

The loading procedure for the specimen consisted of a series of earthquake runs. This loading sequence was chosen so that it would capture the important points like cracking, yield and ultimate. The specimens were excited with scaled versions of the Sylmar record (Northridge Earthquake, 1994). The acceleration of the original record was multiplied by a factor. The following numbers are the factors used for the series of earthquake records: 0.15, 0.5, 0.75, 1.0, 1.25, 1.5, 1.75, 2.0, 2.125, 1.75, and 1.75 times Sylmar. During the test of LFCD1, it was observed that after 2.125 Sylmar the frequency of the specimen dropped dramatically from an initial value of 3.2 Hz. to 1.0 Hz. Because of this large drop it was decided not to increase the motion but to repeat lower motions to characterize the system. The 1.75 Sylmar record was repeated twice for LFCD1 and once for LFCD2. Fig. 4 shows final crack patterns for LFCD1 while Fig. 5 shows final crack patterns for LFCD2. Observations during the test and maximum strain level reached are summarized in Tables 4 and 5.

The relative rotation between the beam and the column increased dramatically after yielding of the reinforcement in the gap region causing the gap to be closed for both specimens. The curvature trend along the flare height proportionally increased with elevation for LFCD2 while this is not the case for LFCD1, see Figs. 6 and 7. LFCD1 had increased curvature at the base of the flare caused by increased confinement in the flare. The accumulative load-deflection curves of the two specimens for all runs are shown in Fig. 8.

Fig. 9 shows the envelope curve for the two specimens. The graph shows a kink in the load-deflection envelope at approximately 70 mm for LFCD1 and LFCD2 followed by a large increase in the overall stiffness. This behavior was due to the gap closure that caused an increase in the load carrying capacity that was predicted to be 160.1 KN. The difference of gap closure effect on the load-displacement envelope of the two specimens was because of concrete crushing of LFCD2 at the top portion of the flare. This behavior reduced the capability of the flare to transfer force to the beam.

The experiments were stopped due to concerns about the overall stability of the specimen. Since the reinforcement at the top of the columns was near the strain-hardening region, bar fracture could cause the top of the column to quickly lose moment capacity. It was also observed that while the last two runs had smaller input accelerations, the displacement histories were the same as 2.125 Sylmar. Increased moment capacity did lead to shear cracking in the middle portion of the flare and a shear crack in the beam as well as concrete crushing in the middle of the flare (see Figs. 4c and 5c).

LFCD2 shows wider and longer shear crack plus many small shear and flexural cracks spread over the beam span. Another important observation is that the shear crack appearing in LFCD1 started after a distance of about d/2 from the end of the flare. In LFCD2, this distance of d/2 is measured from the column core. This shows that the extensive concrete spalling shifted the primary load path to the core of the column in LFCD2.

4.0 POST-TEST ANALYSIS

4.1 Finite Element Analysis

After extracting the results from the data obtained from the tests, a finite element analysis was done using a program called DIANA. The test specimens were modeled as 2-D plane stress elements with the reinforcement modeled as 2D truss elements (see Fig. 10). Drucker-Prager failure envelope was used for concrete accompanied with a tension cut-off to model the brittle tensile strength of the concrete. The strain-rate effect was taken into consideration by increasing the concrete compressive strength and the yield stress of the steel reinforcement. For the concrete, the test cylinder strength was multiplied by 0.85 to convert from the uniaxial test strength to the specimen strength and then by 1.2 to account for the strain rate effect. This resulted in a net factor of 1.02. The reinforcement yield strength was multiplied by 1.2 to account for strain rate effects. The ultimate stress properties were not modified.

Contact elements were used in the form of non-linear springs at the location of gap closure. These elements stiffness was specified to be zero until gap closure occurred where their stiffness jumped to transfer the loads through the regions in contact. The frames were loaded vertically with distributed loads equivalent to the lead weight. The lateral load was specified as a single load from one side of the beam. The loading was performed in one direction until the failure of the system. The analysis was repeated by applying the lateral load in the opposite direction of the system to compare the analysis with the complete load-displacement curve envelopes from the experiments.

The results are shown in the Figs. 11 and 12. The curves show very good correlation with the tested specimens. Table 6 summarizes the obtained results compared to the experimental ones. This analysis was used as the base for analytical parametric study that will be published in subsequent papers.

4.2 Strut-and-Tie Model

The above FE analysis was used to construct a Strut-and-Tie Model (STM) for the disturbed-regions (D-regions) that existed in the system. The need for the STM was raised as a result of the fact that simple analysis based on section analysis did not succeed in estimating the maximum capacity of the system. Also, the STM helps to understand the stress flow and can be used as a powerful design tool. The system's D-regions are shown in Fig. 13 based on Saint Venant's principle: the base hinge region, the flare region and the beam-column connection region. With the principal stress trajectories and the cracking patterns were obtained from the FE analysis and the experimental results, a STM for each portion of the structure was constructed. A detailed description about the STM will be published in subsequent papers.

The above analysis led to the construction of the models shown in Fig. 14 for the columns. The experimental data showed the yielding of the columns longitudinal reinforcement, the

premature yielding of the base hinge dowels and the yielding of the flare hoops as well. The yielding of the flare hoops was caused by a spreading of the forces into the flare. Limiting this reinforcement would limit the spreading of forces into the flare. The results were used in calculating the system capacity by evaluating the forces in the ties that represent the base hinge dowels, the flare hoops and the column longitudinal bars at the gap region. Having the lateral force as the unknown, the system is statically determinate. The above procedure resulted in the values shown in Table 7. The model was able to predict the maximum capacity efficiently.

5.0 CONCLUSIONS

- Both of the Caltrans details are well above the target displacement ductility limit of 6 that is recommended by Caltrans.
- While the ductility level is adequate, the closure of the gap increased the capacity at the top of the column that led to shear cracks in the columns. This behavior is undesirable for it might lead to brittle shear failure the columns.
- The gap closure affected the plastic hinge formation at the top of the column, and hence, transferred higher loads to the bent cap that resulted in shear cracks in the bent cap.
- An analysis or design based on only the column core stiffness did not accurately model the observed behavior. Analysis that is more representative using Strut-and-Tie model of the system was able to predict the capacity of the system. It was also able to model the behavior in the joint region.
- While the flare gap closure did cause damage in the beam, it also provided for increase strength at a point in the load-displacement history where the load was beginning to decrease. If the beam and column were designed for gap closure, gap closure could be used as a way to increase overall displacement capacity.

6.0 ACKNOWLEDGEMENTS

The authors would like to express their appreciation to design engineers that assisted greatly in this joint effort between Caltrans and the University of Nevada, Reno. Saad El-Azazy from Caltrans was the lead in this cooperative effort. Caltrans is also acknowledged for their financial support. The authors would like to thank Patrick Laplace and Paul Lucas for their work in the Large-Scale Structures Laboratory at the University of Nevada, Reno. The opinion expressed in this paper are those of the authors and do not necessarily represent the opinions of the sponsor.

7.0 REFERENCES

Anthony V. Sanchez, Frieder Seible, and M.J. Nigel Priestley (1997). Seismic Performance of Flared Bridge Columns, *Report No. SSRP-97/06*, The University of California, San Diego.

Caltrans Seismic Design Criteria, Version 1.1 (July 1999). Caltrans, Sacramento, CA

DIANA User's Manuals, TNO Building and Construction Research Inc., Netherlands, 1999.

Nada, Hisham, David Sanders, M. Saiid Saiidi (2003). Seismic Performance of RC Bridge Frames with Architectural Flared Columns. CCEER#03-01, University of Nevada, Reno, Department of Civil Engineering, pp 476.

Table 1: Summary of model and prototype dimensions.

Description	Prototype	Model	Factor
Column Diameter (mm)	1,524	304.8	0.2
Flare Width (mm)	3,175	635	0.2
Column Reinforcement	30 # 44 mm	14 # 13 mm	1
Column Reinforcement Ratio	2.39	2.4	1
Column Spirals	19 mm @ 101.6	4.88 mm @ 31.75	N/A
Spiral Volume Ratio ($2A_b/SD$)	0.0037	0.0039	1
Column Height (mm)	8,128	1,626	0.2
	LFCD1	**LFCD2**	
Transverse Reinforcement at top 1/3 of the flare	4.88 Dia. @ 27.9 mm	3.76 Dia. @ 96.5 mm	
Transverse Ratio	0.439 %	0.075 %	
Transverse reinforcement at remaining 2/3 of flare height	3.76 Dia. @ 96.5 mm	3.76 Dia. @ 96.5 mm	
Transverse Ratio	0.075 %	0.075 %	
Vertical Flare Reinforcement	6 Wires – 3.76 mm Dia.	6 Wires - 3.76 mm Dia.	

Table 2: Reinforcement yield stress

Reinforcement Diameter	Yield Point (MPa)
15.9 mm	482
12.7 mm	427
9.5 mm	448
Dia. 4.88 mm	418
Dia. 3.73 mm	491

Table 3: Concrete compressive strength on testing day (MPa)

Member	LFCD1	LFCD2
Footing	35.2	47.4
Columns	37.4	43.6
Girder	38.4	36.2

Table 4: Summary of test observations

Factor	LFCD1 Observations	LFCD2 Observations
0.15 - 0.5	Minor cracking in the beam-column connection and the column.	Minor cracking appears in beam-column connection and in flare region.
0.75 & 1.0	Cracks increased in the beam-column connection and initial cracks in the flare region.	A significant increase of cracking in the beam-column connection occurred. Flare cracks increased in length and new cracks started to form.
1.25	A significant increase of cracking in the beam-column connection occurred	Minor crack development in beam-column connection. Shear and flexural cracks appeared in flare region. Concrete cover spalling in the top of the flare.
1.5 & 1.75	Cracks formation in the beam-column connection drops while the number and extension of diagonal cracks in the flares increases	Crack formation stopped in beam-column connection while flexural and shear cracks increased in the flare and in the bottom of the column.
2.0 & 2.125	Flare cracks increased and widened. Concrete spalling was observed in the middle third of the column and at the top of the flare	Flare cracks increased and widened. Shear cracks along the column height. Extensive concrete spalling occurred in top portion of the flare region.
Last two 1.75	Extensive shear cracking extends along the column height. Displacement was equivalent to 2.125 Sylmar	Flare cracks increased extensively and widened. Concrete spalling in top portion of the flare region. Second 1.75 Sylmar is not included
After bucket removal	Many wide shear cracks were found in the beam and extensive flexural cracks in the middle of the span.	Shear cracks were found in the beam and few flexural cracks in the middle of the span.
Yield Displacement (experimentally calculated)	12.7 mm	12.7 mm
Yield Force	93.4 KN	93.4 KN
Maximum Achieved Displacement	184 mm	184 mm
Maximum Force	282.5 KN	266.9 KN
Ductility Ratio (Includes base slip)	14.5	14.5
Displacement at Gap Closure	69.9 mm	69.9 mm
Ductility at Gap Closure	5.5	5.5

Table 5: Summary of maximum strain

Factor	LFCD2				LFCD2			
	Column		Flare		Column		Flare	
	Long. Steel	Spiral	Long. Steel	Hoops	Long. Steel	Spiral	Long. Steel	Hoops
0.15 & 0.5	0.0029	0.00067	0.0401	0.0145	0.0016	0.002	0.009	0.0037
0.75 & 1	0.013	0.0016	0.0402	0.0145	0.011	0.0028	0.012	0.0053
1.25	0.0144	0.004	0.014	0.017	0.013	0.009	0.014	0.0013
1.5 & 1.75	0.016	0.0037	0.017	0.0145	0.017	0.004	0.013	0.0023
2 & 2.125	0.018	0.002	0.0402	0.0145	0.026	0.007	0.024	0.0033
1.75	0.05	0.0019	0.0403	0.014	N/A	0.0085	0.039	0.0033
1.75	0.05	0.003	0.0403	0.014	N/A	N/A	N/A	N/A

Table 6: Analytical and Experimental results for LFCD1 & LFCD2

	LFCD1	Measured	% of Measured	LFCD2	Measured	% of Measured
Yield force [KN]	228.2	210.3	108%	220.2	203.3	108.3%
Max. Force [KN]	314.4	284.2	N/A	298.0	268.6	N/A
Max. Disp. [mm]	182.9	165.1	N/A	185.2	165.2	N/A
Effective Disp. [mm]	20.8	23.4	89%	24.4	23.9	102%
Displacement Ductility	8.78	7.07	124%	7.59	6.9	110%
Disp. at West Flare Gap Closure [mm]	74.9	67.3	111%	74.7	64.8	115.3%
Disp. at East Flare Gap Closure [mm]	76.2	N/A	N/A	74.7	N/A	N/A
Disp. at West Base Hinge Gap Closure [mm]	109.2	N/A	N/A	110.5	N/A	N/A
Disp. at East Base Hinge Gap Closure [mm]	144.8	N/A	N/A	144.8	N/A	N/A

Table 7: STM results versus experimental results

Specimen	First yield plateau (KN)			Maximum load (KN)		
	Measured	STM	% of Measured	Measured	STM	% of Measured
LFCD1	205.9	197.7	96%	284.2	274.0	96%
LFCD2	203.6	197.7	97%	268.6	274.0	102%

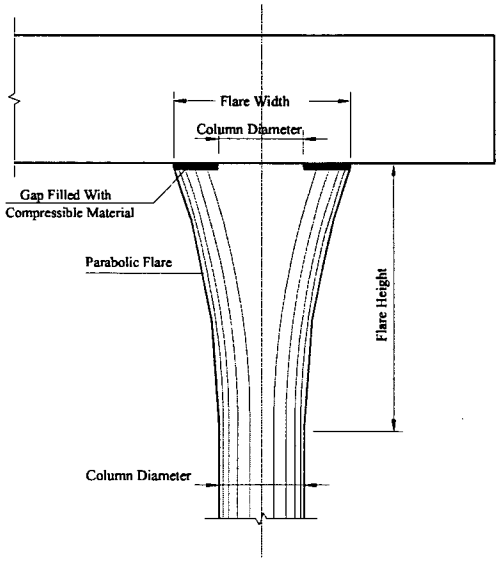


Figure 1: Layout of the proposed detail

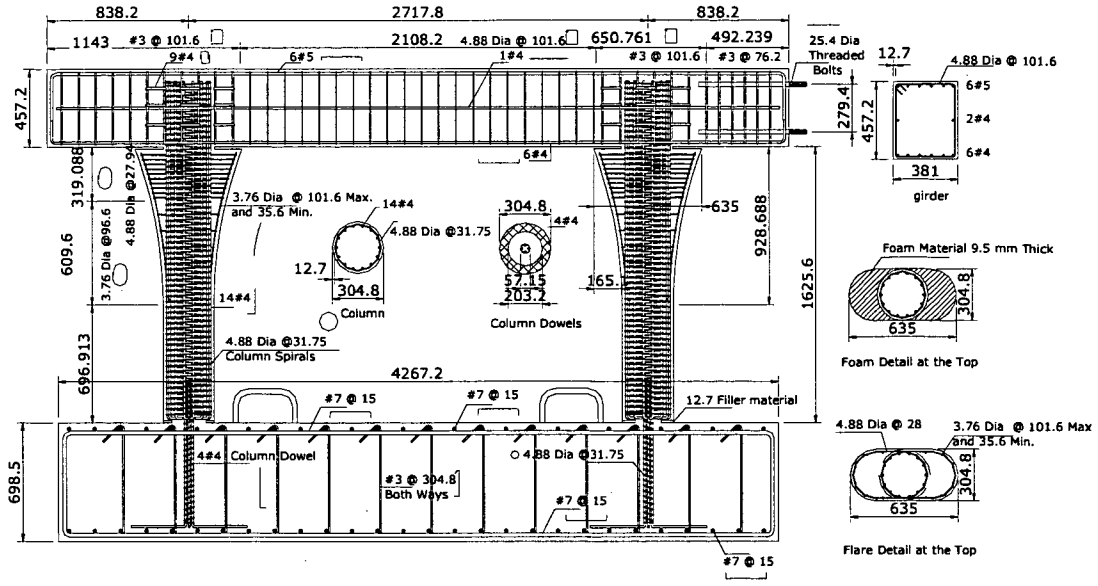


Figure 2: Specimen LFCD1 layout and reinforcement detailing

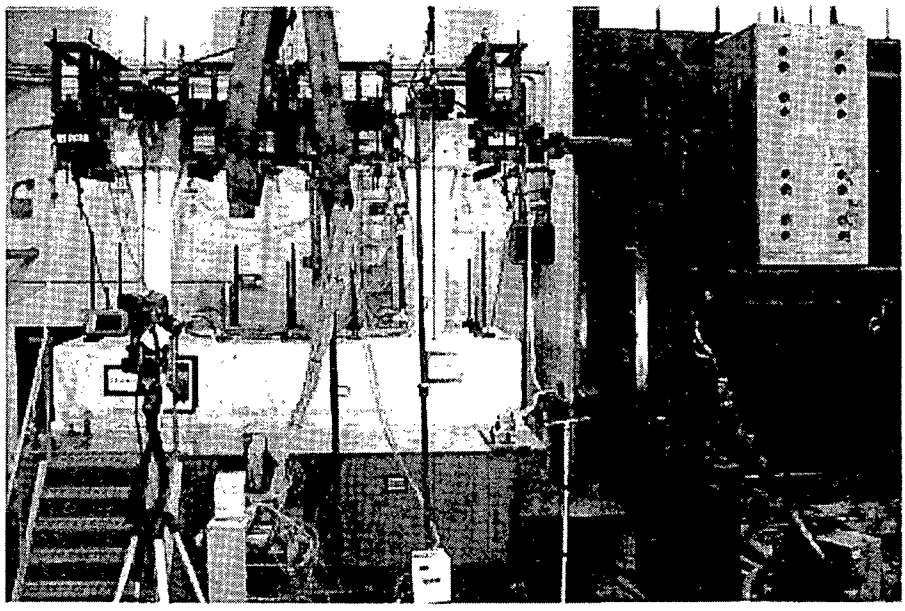
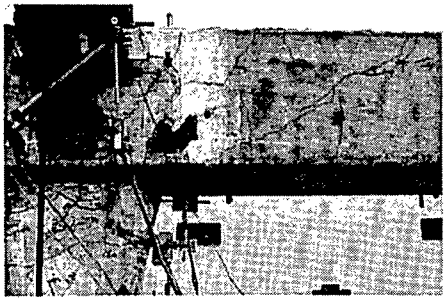
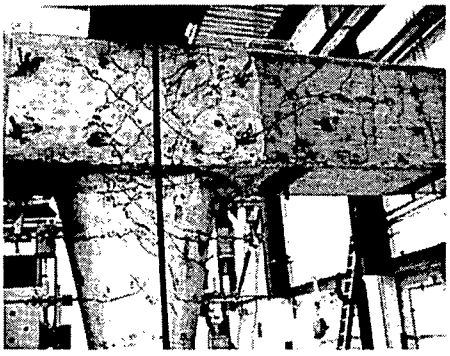


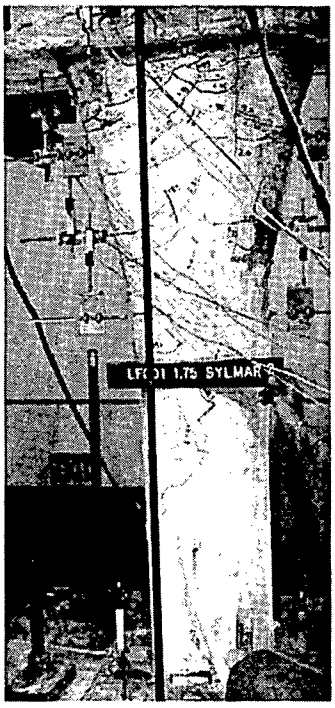
Figure 3: Test setup



(a)



(b)

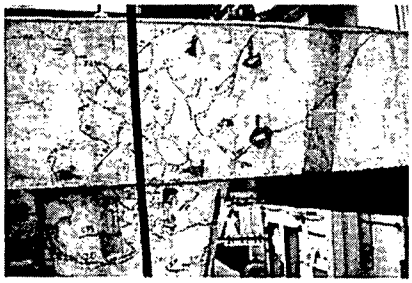


(c)

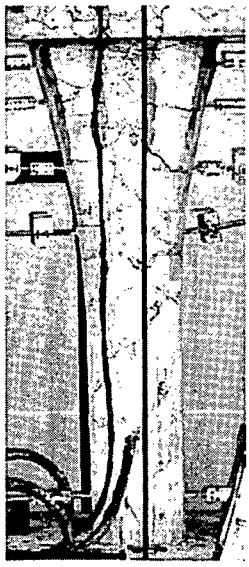
Figure 4: LFCD1 crack patterns, (a) shear cracks in the beam, (b) beam column connection cracks, (c) column cracks



(a)

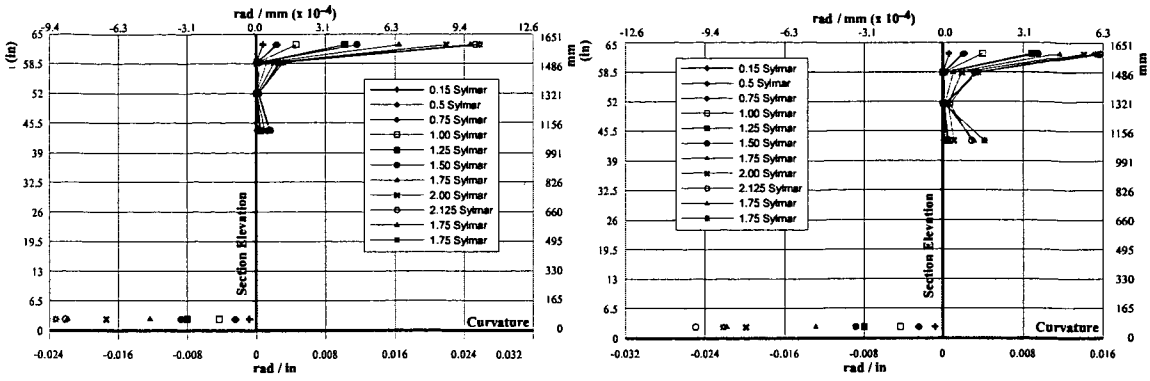


(b)



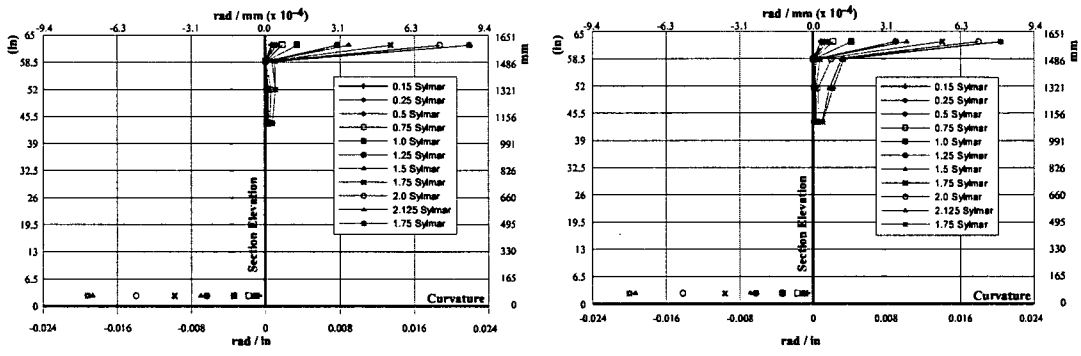
(c)

Figure 5: LFCD2 crack patterns, (a) shear cracks in the beam, (b) beam column connection cracks, (c) column cracks



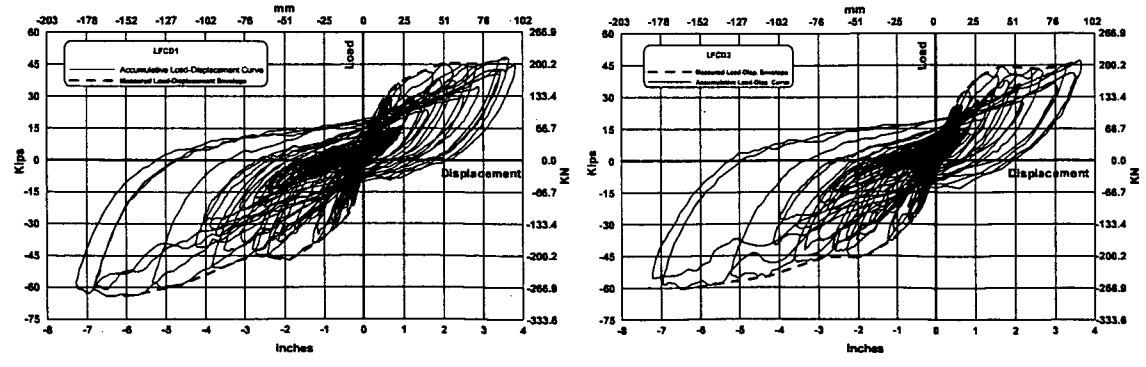
(a) (b)

Figure 6: Curvature along flare height for LFCD1 (a) Left Column (b) Right Column



(a) (b)

Figure 7: Curvature along flare height for LFCD2 (a) Left Column (b) Right Column



(a) (b)

Figure 8: Accumulative load-displacement curve, (a) LFCD1, (b) LFCD2

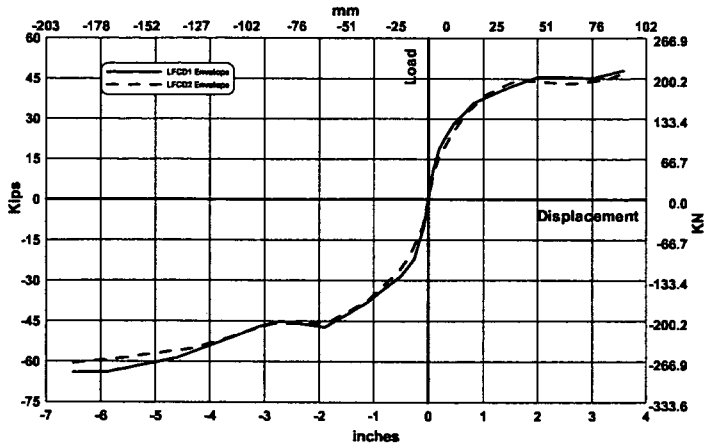


Figure 9: Load-displacement envelope curve

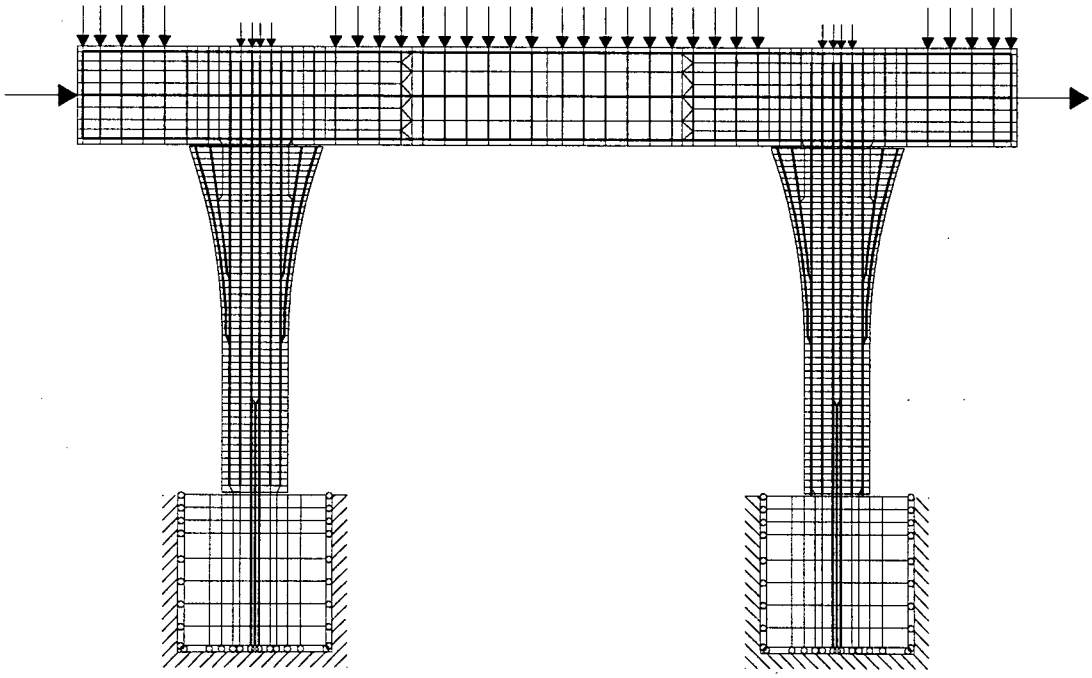


Figure 10: Finite element model

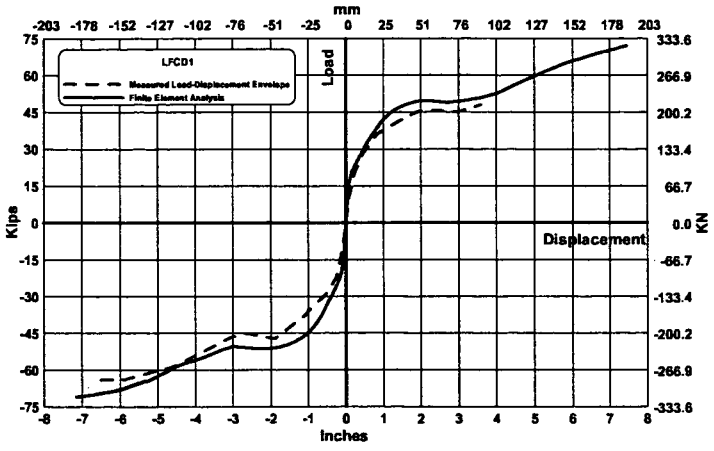


Figure 11: Analytical Results versus Experimental Results for LFCD1

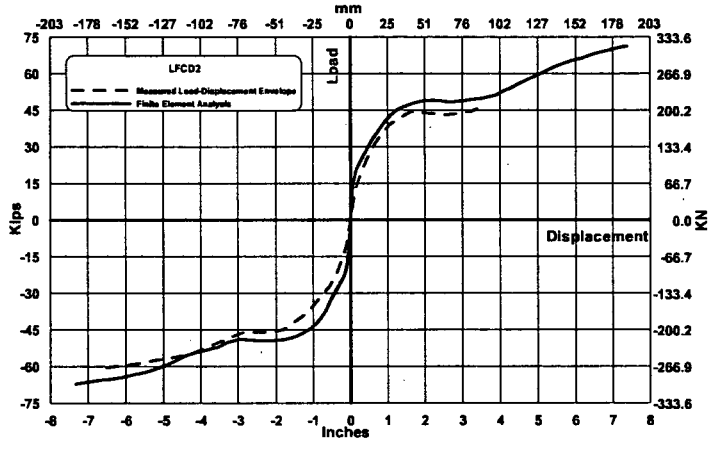


Figure 12: Analytical Results versus Experimental Results for LFCD2

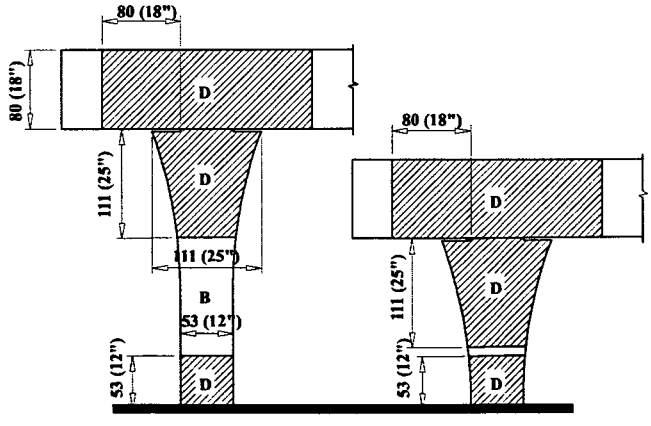


Figure 13: D-Regions and B-Regions for flared columns with a gap

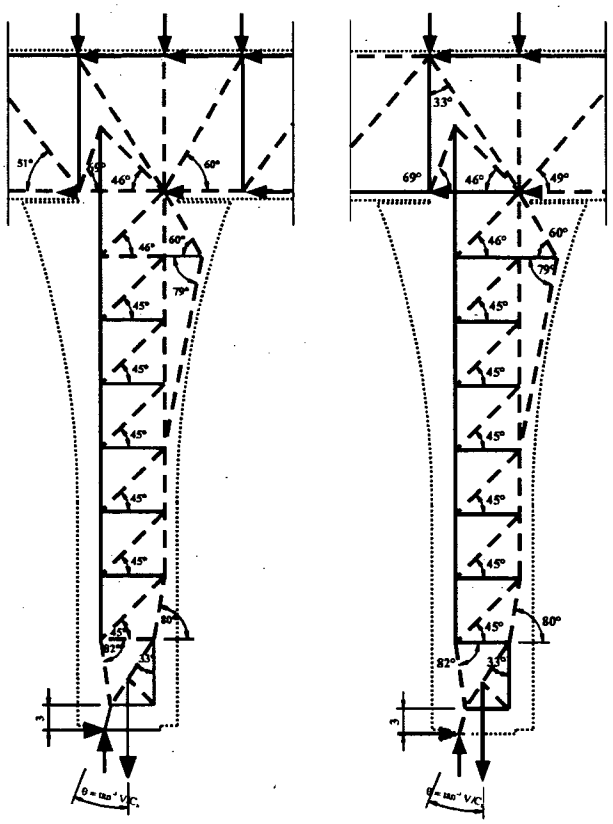


Figure 14: Strut-and-tie model for left and right columns

THEME 5

Advanced Information and Communication Technology for Disaster Prevention and Public Health Evaluation

General overviews and future perspectives of disaster information systems in Japan

by

Hiroaki Miyatake[1], Akihiko Nunomura[2]

ABSTRACT:

After the Hanshin/Awaji Earthquake, Japanese government enforced improvement of disaster information management systems. Because the lack and shortage of the disaster information and communications among the ministries, agencies and public became obstructs for quick response and recovery from the disaster. For 8 years after the earthquake, each ministries and agencies developed information systems in its system and it makes possible to collect and transform information quickly. In these days, there occur new problems in government, especially; the lack of information exchange between the systems that constructed by different organizations is one of the large problems. The Central Disaster Prevention Council determined "the Basic Policies for Improvement of Disaster Information Systems" in March 2003. This Basic policy consist of the following five discrete policies; (1) Assuring information coverage - in both time and area, (2) Establishing mechanisms for better use of information, (3) Sharing and utilizing information during usual times to assist in emergency measures, (4) Building the e-government for disaster management, and (5) Establishing an organization responsible for promoting implementation of disaster information systems. Japanese government will establish the e-government for disaster management in three years.

KEYWORDS: Information system, Information sharing, the e-government for disaster management

1. ISSUES FOR DISASTER INFORMATION SYSTEMS IN JAPAN

1.1 Assuring Information Coverage - in Both Time and Geographical Area

The Great Hanshin/Awaji Earthquake that hit Japan in 1995 posed several major issues for disaster information systems in Japan. Prompt and effective rescue activities presuppose accurate and immediate identification of the scale of the disaster and allocation of appropriate supplies and human resources across a large area. The larger the scale of the disaster is, and the greater the area

[1] Deputy Director for volcanic and earthquake disaster management, Disaster Prevention Bureau, Cabinet Office, Chiyoda-ku, Tokyo, 100-8969 Japan

[2] Director for volcanic and earthquake disaster management, Disaster Prevention Bureau, Cabinet Office, Chiyoda-ku, Tokyo, 100-8969 Japan

affected is, more and more information is required to facilitate such activities; however, exactly the opposite may happen - the amount of information which can be gathered may be limited in major disasters, and the time it takes tends to be long. This is because the information systems available may be directly impaired by the disaster, such as disruption of communication network, inability to dispatch human resources due to breakdown of transportation networks, and system failure due to power outage. Such circumstances create information void; void in terms of time, meaning no information at all may be available immediately after the disaster struck, and void in terms of area, meaning no information may be available particularly concerning the most heavily hit area due to impaired information gathering activities.

Fig.1 graphically shows the relationship between the casualty count and the number of missing people in the Great Hanshin/Awaji Earthquake, shown against time elapsed since the quake struck. Casualty and missing count data is one of the most crucial indicators to identify the totality of a natural disaster. As this quake was a major one affecting a large geographical area, it greatly impaired the information collection activities immediately after the quake. The graph shows that it took almost three days until the government reached the final count of dead and missing people. It is notable that at eight-thirty, almost three hours after the quake hit at 5:46, only 27 dead and missing were reported; it is obvious that there was information void in time during this time.

In Hokudan-cho, the most heavily hit area in Awaji Island across from Kobe, there was delay in the identification of the extent of the damage compared to the surrounding area, which suffered limited damages, and this town was the last to call for help to the prefecture government. By the time Hokudan-cho was able to reach the prefecture government, supporting personnel had already been dispatched to other towns, and no help could be provided to this town. Such information void, this time in terms of area coverage, becomes an obstacle for taking effective rescue actions. Thus we need to eliminate such information void in terms of time and space.

1.2 Facilitating Better Use of Information

In disasters affecting a large geographical area, different disaster-related organizations need to closely and flexibly liaise with one another when taking actions. In the case of the Great Hanshin/Awaji Earthquake, there was insufficient interaction and collaboration among the various disaster-related institutions involved. Since then, those institutions have been striving to establish multitudes of disaster information systems to help with prompt information collection and communications. However, it must be noted that each of those systems was built independently of others, meaning that each is effective in promptly communicating accurate disaster-related information to the upper-level unit within the same line organization. At the same time, municipal government bodies close to the area

suffering from disasters, including city, town, village as well as prefecture governments, are required to send the same information to different upper-level institutions in different formats as required by such entities, and such procedure can cause considerable delay in initiating immediate disaster recovery/prevention activities. Furthermore, even though there may be systems to send individual pieces of information gathered by the regional branch office of national disaster-prevention institutions or by the city/town/village or prefecture government bodies to their respective upper-level institutions, where they are compiled to identify the total view of the disaster, there is no appropriate mechanism to provide feedback to the originating municipal bodies. Because of this lack of feedback mechanisms, there may be no information sharing across the different branch institutions taking rescue actions at the disaster site; there is insufficient collaboration among such institutions; or information on a disaster that happened in one town may not be available to the head of that town except through mass media. There is a need to establish mechanism to help with better and full use of information, as well as improving collection and communication of disaster-related information.

1.3 Good Practice of Sharing and Utilizing Disaster Information during Usual times

Since the Great Hanshin/Awaji Earthquake, different disaster-related governmental bodies and institutions have established various disaster information systems. Such information systems are equipped with functions assuming use during emergencies of course, but the more complex and equipped with more functions those systems are, the rarer they are used, particularly during usual times. Therefore, in the midst of confusion during emergency, the emergency personnel may be unable to operate the system effectively, and even worse, the systems themselves may fail to function because they are left unattended during usual times.

One example is that of communication lines. Disaster-related governmental bodies were ready with priority communication lines in preparation for emergencies. However, during usual times, they used the lines with LCR (Least Cost Routing) device, which selects the lowest cost phone carrier, for cost consideration. So it happened even during the Hanshin/Awaji Earthquake the phone equipment selected lines other than the priority line, leading to communication disruption, just as other phone lines for the general public, because of the heavy traffic.

Recent IT developments have led to extensive functions of communication tools such as mobile phones, and they may become useful as tools to provide information to the general public. However, some of the population, including senior citizens, are not used to using such mobile terminals including phones, therefore may not be in the habit of carrying one on themselves at all times, and they may not be able to operate the mobile to access the information.

In the case of the Mt. Usu eruption in 2000, the

local residents and the municipal government bodies had, well in advance of the eruption, prepared hazard maps, and there had already been established a close collaboration on emergency actions between relevant institutions and the residents. When the eruption hit, the communication to the residents on evacuation and other actions went very smoothly and adequately, because it was an extension of the already existing close cooperation, therefore, there was not even one casualty. As this example shows, there is a need to maintain a practice of sharing and utilizing disaster-related information during usual times, and also to assure that the population and the governmental bodies are familiar with the use of information tools.

1.4 Building an e-Government Focused on Disaster Management

Advances in information technology enabled the various disaster prevention authorities to exchange large volume data, including obtaining visual image data of the disaster site to help them understand the exact situation; the volume of information handled by such authorities and relevant institutions has gone through a dramatic increase. However, different formats used for communicating information may hinder smooth and adequate information collection, communication, or storage. For example, disaster information system and the GIS system used by individual prefectures are not compatible with one another. This can create problems in cases of disasters affecting a multiple of municipal government districts, such as inability to compile statistics, including damage estimate, or to arrange for supply shipments across the prefecture borders. Introducing systems from other prefectures would require the municipal governments to install multiple computer terminals. In order to establish a "community of collaboration prepared for emergency," consisting not only of "public support" provided by national, regional/municipal governmental bodies and other relevant authorities in times of disasters, but also of "self support" where the residents themselves strive to protect their own lives and assets, and "mutual support" where residents and other parties including NPO's act together to protect one another's lives and assets, all functioning with a good balance, all parties involved in disaster/emergency support activities, including disaster-related governmental bodies, residents, NPO's for disaster rescue activities, and private sector businesses, need to work together to establish an IT-enabled disaster information systems and mechanisms, that help all parities to efficiently share and make full use of disaster information through advanced IT.

2. Looking back on programs to date in Japan

Disaster information systems in Japan have shown rapid progress, particularly since the Great Hanshin/Awaji Earthquake. The following are examples of programs and efforts undertaken by the Cabinet Office.

2.1 Assuring information coverage - in both time

and area

Cabinet Office is in the process of establishing DIS, Disaster Information System, to eliminate the information void, in time and area, at the very initial stage after the occurrence of a disaster. DIS, as shown in Fig. 2, aims to resolve the dilemma between the limited information available at the time of a disaster affecting a large area, and the need for greater volume of information to provide better support. In order to realize this, DIS uses central disaster radio network to connect between different disaster-related authorities and governmental bodies to help with better information sharing, as well as complimenting the limited volume of information with estimates. EES, a sub-system of DIS, combines seismic intensity measured at the designated observation points, which is provided on-line from the Japan Meteorological Agency, with pre-entered data on ground, structures/buildings, and population, and is capable of estimating, within 30 minutes of the quake, personal injuries due to destruction of buildings. The output is provided on-line to relevant authorities. EMS, another sub-system of DIS, is capable of combining and overlaying various types of disaster information on one same terminal to extract useful information, thus different institutions can utilize such information for taking emergency rescue actions. Information provided by EMS includes data on various disaster-related authorities, discontinuation of critical "lifeline" utilities such as electricity and gas, and information on damages to infrastructure such as roads. In addition, Cabinet Office is in the process of developing a system utilizing artificial satellite image technology as a new tool to gather information and to identify the extent of damages. This system compares, and detects the differences in, the artificial satellite image taken after the disaster from the one taken before the event to help identify the extent of damages across a large area. The information detected by this system will be that on distribution of damages across geographical areas and that on damages to selected and pre-registered major structures and buildings. All this information can be shared among relevant authorities via DIS. Currently DIS connects 15 governmental agencies and institutions and 4 other designated institutions, with plans for expansion (Fig. 3).

2.2 Establishing the Disaster Prevention Radio Communications System (Fig.4)

In order to assure collection and communication of information between Cabinet Office (responsible for disaster prevention/rescue) and relevant disaster-related authorities, and to facilitate emergency activities, Cabinet Office, in fiscal year 1978, launched on a project to establish a fixed line communication network connecting disaster-related institutions and bodies including designated administrative bodies in Central Tokyo and other designated public entities. Subsequently, starting in fiscal year 1991, the project extended to digitize the equipment in their replacement cycle, and this changeover was

almost fully completed within fiscal year 2000. Also, the following projects were undertaken with great urgency since the Great Hanshin/Awaji Earthquake.

2.2.1 To be prepared for possible damages in the Metropolitan area incurred by natural disasters such as earthquakes with seismic center right below Southern Kanto area, a fixed line communication network connecting nine disaster prevention institutions located in Tachikawa Wide Area Disaster Prevention & Relief Base.

2.2.2 To secure a hot line communication in case of emergency between 47 prefectures and central governmental agencies and ministries including the Prime Minister's Public Residence and Emergency/Disaster Countermeasure Headquarters, an emergency line via line of Ministry of Land, Infrastructure & Transport was established.

2.2.3 Because of the criticality of visual information for adequate initial actions in large scale disasters, visual data communication pathways have been established between ministries that are capable of collecting visual data via helicopters (namely Defense Agency, National Police Agency, Fire & Disaster Management Agency, Japan Coast Guard, and Ministry of Land, Infrastructure & Transport), Prime Minister's Public Residence and Cabinet Office (responsible for disaster prevention), as well as relevant bodies located inside the Tachikawa Wide Area Disaster Prevention & Relief Base. Further efforts are being made to expand the scope of such visual data transmission network to include other designated administrative bodies.

2.2.4 A project is underway to establish a ground station for satellite communication network, which will connect entities for which disaster recovery is urgent, including regional utility companies, as well as designated public institutions including Japan Railway and NTT.

2.2.5 In order to be prepared for the situation where a major earthquake occurs right below Tokyo, which may destroy buildings and thus disable existing public communication network and central disaster prevention radio network, a project is underway to establish a ground station for satellite communication, that can be used independently thus provides the minimum means of communication for the government.

3. For the Future

3.1 Basic Policies for Improvement of Disaster Information Systems

So far, each of the disaster information systems of governmental bodies that are involved in disaster prevention tended to be built independently by the respective body. As a result, communication of information within one body has greatly improved in accuracy and speed, but some issues remain, such as insufficient sharing of information across multiple

organizations. Recent IT developments brought disaster information systems to a higher level, creating the need for formulating basic policies common to all relevant governmental bodies, so that they can work closely together to build a disaster prevention information systems and to share such information. The "Central Disaster Prevention Council" of the national government has established a "Specialist Investigation Committee on Sharing of Information for Disaster Prevention," and has had discussions on how disaster-related information should be shared in national and municipal government bodies, among residents, among/in private sector businesses, and NPO, and how scientific disaster prevention information should be provided. Based on these discussions, "Basic Policies for Improvement of Disaster Information Systems" were formulated, and were adopted by the Central Disaster Prevention Council as the national government's basic policies.

Basic policies consist of the following five discrete policies:

(1) Assuring information coverage - in both time and area,

(2) Establishing mechanisms for better use of information,

(3) Sharing and utilizing information during usual times to assist in emergency measures,

(4) Building the e-government for disaster management,

and

(5) Establishing an organization responsible for promoting implementation of disaster information systems.

It was also determined that the organization responsible for promoting implementing disaster information systems should formulate action plans and promote system implementation with a three-year target time frame, and that a conference for promoting sharing of disaster-related information should be established to help in any follow-up as required and overall coordination for the progress status.

The specifics of the measures proposed under the basic policies shall be described in the following section.

3.2 Specifics Measures - Overview

3.2.1 Combine actual damages and estimated information to facilitate identification of the total damages incurred (Fig.5)

Cabinet Office, as described earlier, uses EES to estimate the damages in order to eliminate any information void, both in time and area coverage, immediately after the disaster hits. At the same time, artificial satellites and aircrafts will be utilized to identify the distribution of actual damages across the geographical area. In addition, "lifeline" entities including some of the utility and gas companies will be connected with DIS, so that facility control information, such as power outage and gas supply stoppage, can be collected on-line. Gathering different types of information from varied sources provides the

relevant authorities with mutually complementary information, and helps to assure full time and area coverage of information. Sending such comprehensive information to all parties involved, including Prime Minister's Public Residence, national government's disaster prevention related agencies & ministries, municipal governmental bodies including prefectures, as well as lifeline utility providers and residents, not to mention the on-site emergency support center and medical institutions, will contribute to more effective emergency activities. Next step will be to gather information from extended sources, such as regional residents and taxi or truck drivers; this is expected to provide more detailed information and help to fill any part missing from fully understanding the extent of the disaster.

3.2.2 Emergency communication through shared use of communication networks

Each of the governmental institutions involved in disaster prevention has its own information communication network suited to its own needs. Each of those systems has its own purpose for existence and intended use, and its use for other purposes is in principle not allowed. It is permitted however to use such networks among governmental bodies for non-designated purposes in case of emergencies, such as a network failure due to damage by disaster; yet the specific procedures for use and the detailed rules have not been determined. Also, while it is desirable that communication of disaster or disaster prevention-related information is maintained continually during usual times, instead of limited to the time of actual emergencies, there may be some institutional restrictions on shared use of information networks during usual times. Building specific and practical mechanisms toward shared use during emergencies, and a study on mechanisms allowing shared use in times other than emergencies, are required.

3.2.3 Integrating disaster-related information through the use of GIS (Geographical Information System) (Fig.6)

Disaster information systems established by various institutions vary in the information contained and format used. If the systems are connected among various institutions as they are currently, there may be some practical problems; different institutions may need to install separate terminals, or they may be unable to compare similar data from different sources due to format differences. Disaster-related information held in different systems need to be standardized in their contents and format to facilitate better use. In particular, GIS (Geographical Information System) is an effective tool for information sharing, and its use needs to be promoted. For example, in case of a disaster, different types of information, including traffic information such as congestion and roadblocks, disaster prevention information such as rescue and support activities, and geographical information on heliports, villages, and hospitals, can be combined and overlaid on GIS. This will help to identify the extent of damages to houses, and will form the

basis for making different types of decisions required, such as selecting the route for transporting emergency patients.

3.2.4 Establishing a common platform for disaster prevention information

The flow of information in case of emergencies is, in principle, as follows: information collected by the local branch offices of national governmental organizations is sent to their respective upper-level organization, and ultimately it reaches the Prime Minister's Public Residence and Cabinet Secretariat, where it is compiled together. As the information flows only within each relevant organization, information required by each institution is communicated very promptly and accurately. However, cross-functional collaboration is insufficient, and prefecture government bodies are said to be required to send out collected information to over 200 locations in over 100 different formats. Building a common platform for sharing disaster-related information will, without losing the advantages of the current information flow, help to assure cross-organizational sharing of information, and will also reduce the workload for the regional governmental bodies to prepare reports.

3.3 Issues for the future

Since the Great Hanshin/Awaji Earthquake, which caused an unprecedented degree of damages, disaster prevention information systems by administrative bodies have gone through major progress. However, it cannot be denied that, precisely because its progress was quick, such systems were built without sufficient sense of collaboration among governmental bodies. For the future, based on a comprehensive blueprint for all relevant authorities, coordinated efforts need to be made to bring a common system into reality. So far, the basic policies, i. e., the comprehensive blueprint, have been formulated; yet the government has yet to formulate action plans prescribing the roles and schedule for each of the relevant authorities, and proceed to the next stage of actual system implementation, with coordination efforts made as needed.

Furthermore, in order to build a community of collaboration for disaster prevention, with well-balanced combination among self-support, mutual support, and public support, the administration needs to support self-support and mutual support through provision of crucial information. Yet, there has not been enough study made on how information should be communicated between governmental bodies and other parties such as residents. For the future, with Central Disaster Prevention Council's "Specialist Investigation Committee on Sharing of Disaster Prevention Information" taking the initiative, there needs to be more progress seen on formulation of basic policies of the government, formulation of specific actions plans and their implementation.

4 REFERENCES

" Basic Policies for Improvement Disaster

Information Systems" March 2003, Central Disaster Prevention Council

"Compilation of Information and Learning from the Great Hanshin/Awaji Earthquake" March 2000, Disaster Prevention Agency, National Land Agency, Urban Disaster Prevention Research Institute

"Report on Studies Made on Future Disaster Information Communication Systems" March 1996, Ministry of Construction, Construction & Electrical Technology Association

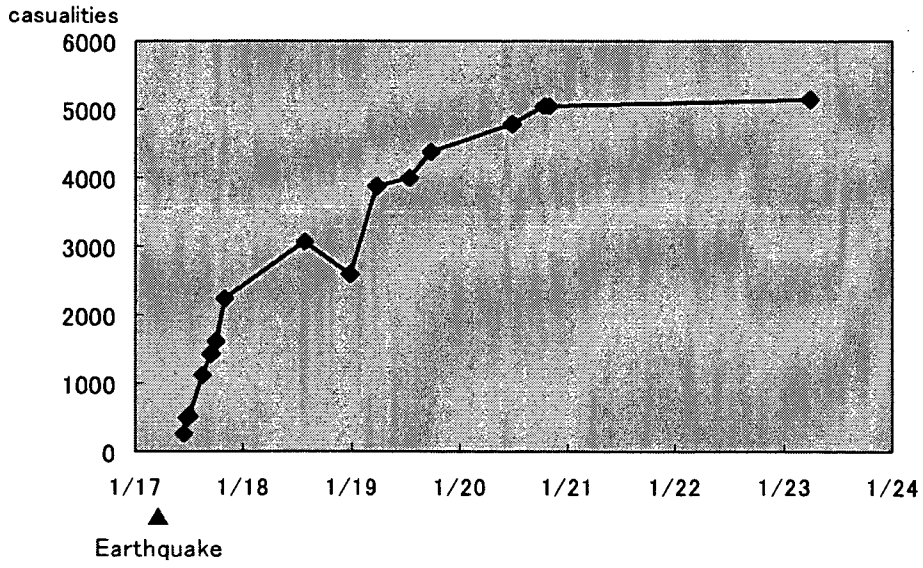


Fig.1 Time transition for Determining dead/missing in the Great Hanshin/Awaji Earthquake

阪神・淡路大震災における死者／行方不明者把握状況の推移

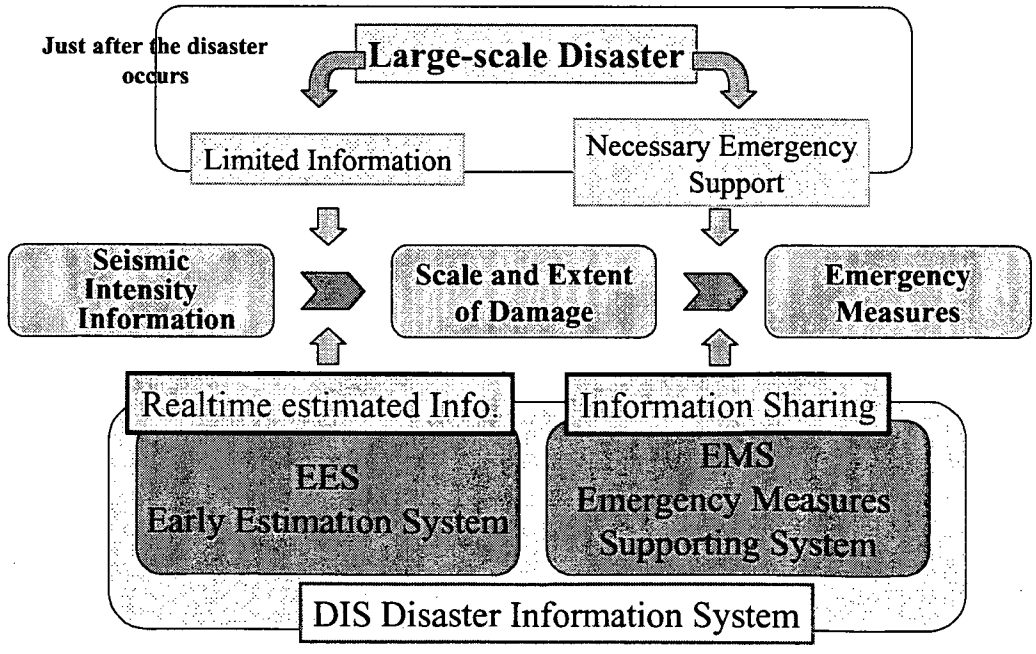


Fig.2 The Aim of the DIS

地震被害早期評価システムの狙い

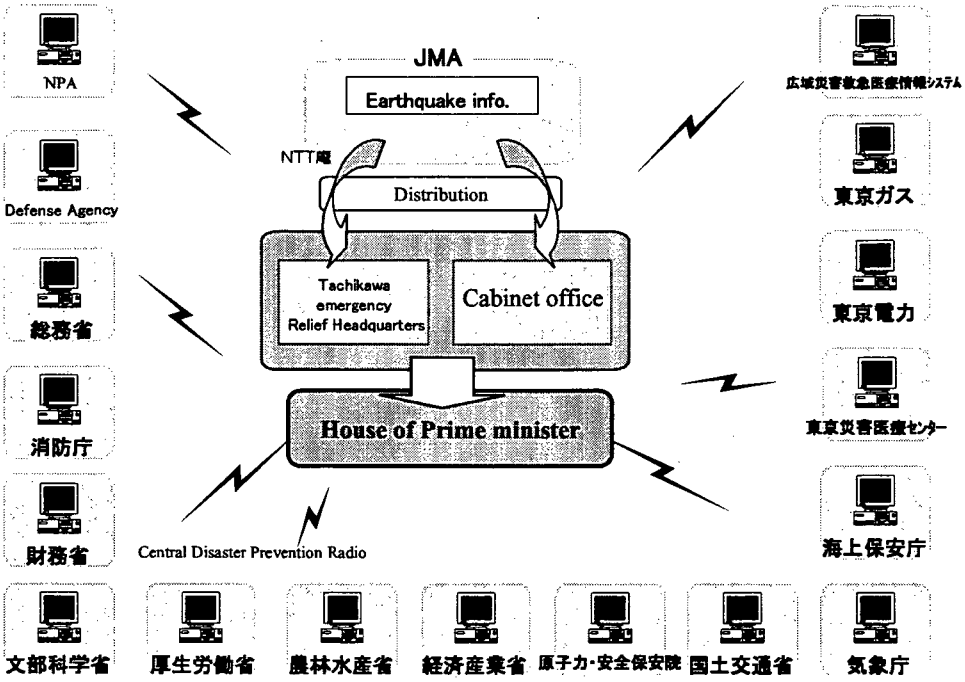


Fig.3 Overview of Central Disaster Prevention Radio Network

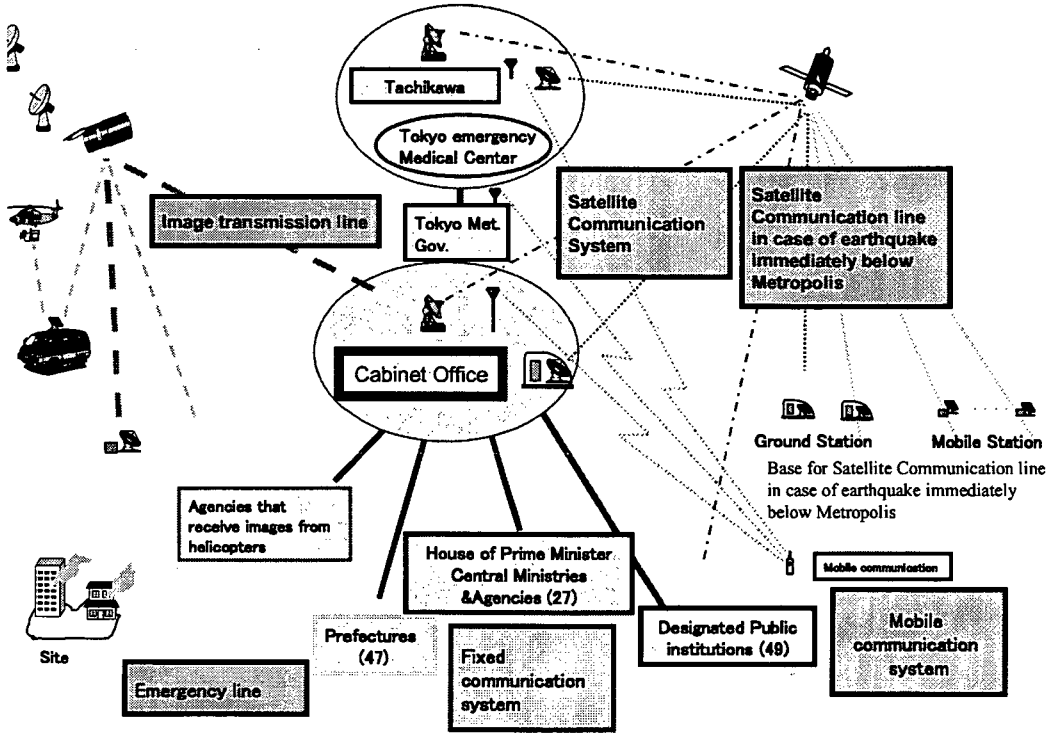


Fig.5 Network of Governmental Bodies involved in Disaster Prevention & Relief

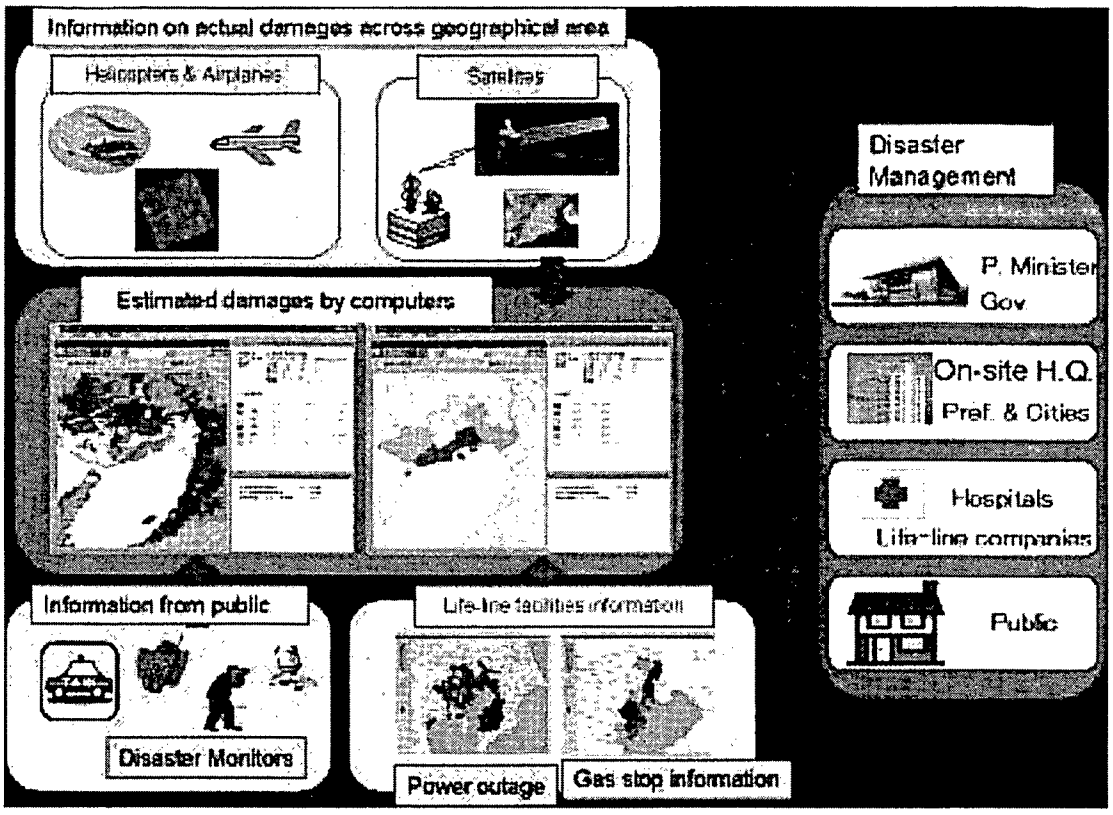


Fig.5 Combine actual damages and estimated information to facilitate identification of the total damages incurred

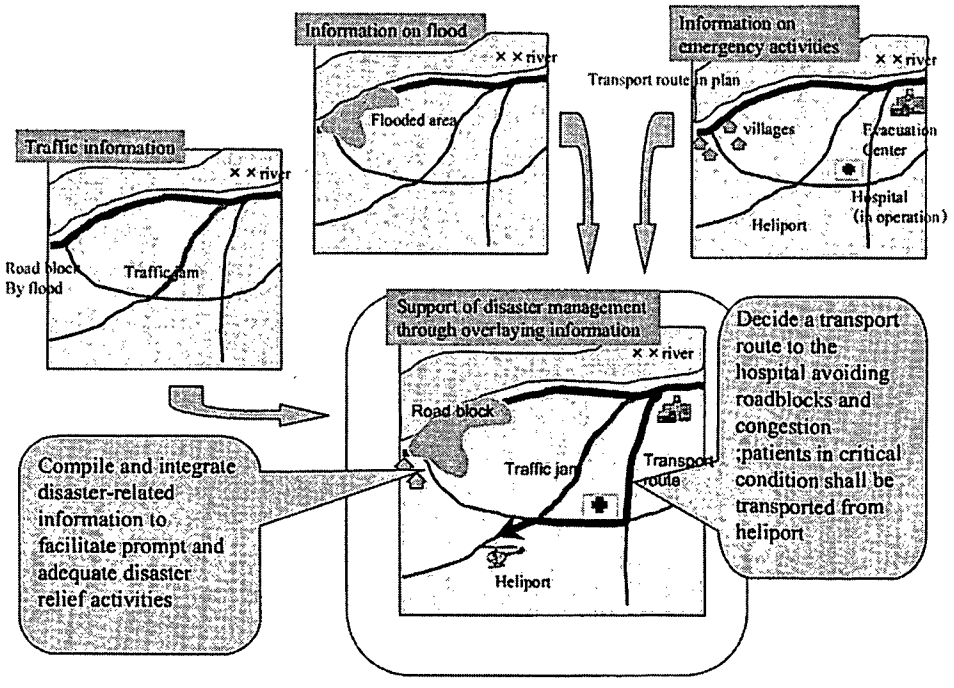


Fig.6 Integrating disaster-related information through the use of GIS

Mortality during Landslides, Chuuk, Federated States of Micronesia, 2002

by

Carlos Sanchez[1], Stacy Young[1], Nachsa Siren[2], Tzesan Lee[1], Dahna Batts-Osborne[1], Josephine Malilay[1]

ABSTRACT

Landslides often accompany hydro-meteorological events, such as floods and tropical cyclones, where deaths have been characterized at length. However, little is known about the role of landslides in contributing to resulting mortality. The event of Tropical Storm Chata'an in Chuuk State, Federated States of Micronesia on 2 July 2002 precipitated massive landslides, leading to deaths among islanders long accustomed to the seasonal onslaught of storms. We conducted an epidemiologic investigation to identify preventable risk factors for mortality and formulate public health strategies for future events. Of 43 deaths occurring from twelve landslides on six islands, almost 90% (36/40) died immediately, 56% (24/43) were female, and over half (22/43) were children <15 years of age. Though the landslides occurred over a 12-hour period, nearly 74% (67/91) were unaware of other landslides before being affected. Nearly 83% (76/92) did not know that landslides could accompany tropical storms. Location of the home and building material were not significant. Targeting preparedness to include children and improving communications between and within islands are viable strategies for risk reduction.

KEYWORDS: disasters, natural disasters, landslides, mortality, Micronesia

1.0 INTRODUCTION

Landslides represent a significant geologic hazard worldwide, affecting an estimated 2.1 million people and resulting in approximately 9,500 deaths in the past ten years (IFRCRCS, 2001). Landslides are caused by disturbances in the natural slope stability, have been associated with variations in soil porosity, and can accompany heavy rains or follow drought (Iverson et al., 2000). Although they commonly occur with other major natural disasters such as floods and earthquakes, little is known about the role of landslides in overall mortality, particularly when precipitated by hydrometeorological events.

On July 2, 2002, Tropical Storm Chata'an struck the islands of Chuuk with almost 20 inches of rainfall in a 24-hour period. Of 265 various landslides attributed to the storm, at least 62 massive landslides occurred on July 2 and resulted in 43 deaths and hundreds of injuries on six islands. This event was unique because it occurred in a population long accustomed to the seasonal onslaught of tropical storms and typhoons, but had not experienced landslides in more than two decades. We present descriptive results from an investigation of deaths caused by landslides in Chuuk during Tropical Storm Chata'an to characterize mortality and formulate preventive strategies. For this report, we focused on factors related to the geology of landslides, rainfall, structural characteristics, and behavioral response of case- and comparison subjects.

[1] National Center for Environmental Health, Centers for Disease Control and Prevention, Atlanta, GA 30333 USA

[2] Department of Health, Chuuk State, Federated States of Micronesia

2.0 METHODS

We reviewed death certificates from deaths categorized as "landslide-related" by the Chuuk State Hospital to collect demographic information on the decedents. We calculated mortality rates using age-specific population data from the 1994 census of the Federated States of Micronesia (FSM, 1994).

We conducted a descriptive cross-sectional study to identify specific risk factors during landslide events. We administered a questionnaire to study participants to assess knowledge of warning systems, behavioral response, access to medical care, construction material, and possible predisposing conditions such as physical disabilities and alcohol consumption. We defined a case subject as a person who died as a result of suffocation or trauma due to the landslides occurring on July 2, 2002. Family members or individuals familiar with the circumstances of the decedent at the time of the landslide were eligible to be case proxies. We identified a comparison group consisting of injured and non-injured persons who were present at the site of the landslide at the time of the slide. Neighborhood comparison subjects were identified at the site of the landslide and at sites where displaced people were known to have relocated. We compared cases with a comparison group to ascertain risks.

We collected rainfall records from the Weno Weather Station to compare the quantity of rain fallen over a given time with the approximate times when the deaths occurred.

3.0 RESULTS

Forty-three deaths related to the landslides occurred on six islands (Table 1). The first fatality was reported at 2:30 am. Within twelve hours, forty people were killed, and three additional people died from their injuries within the next three days (Figure 1). The overall mortality rate for this event was 1.47 deaths per 1,000 habitants. Almost 90% (36/40) of the decedents were reported to have died immediately during the landslides. Suffocation (burial) was reported to be the cause of death for 93% (40/43) of the decedents.

3.1 Demographics

More than one-half (24/43) of the fatalities were female. The median age of the decedents was 14 years, with ages ranging from 3 months to 84 years. Children less than 15 years of age accounted for over one-half (22/43) of the fatalities in this event.

The relative risk for children under 15 years of age was 1.32. Compared with crude death rates for the landslides by age groups to estimates from all causes for previous years, mortality increased slightly among the 5-14 age group, not noted in previous years (Figure 2).

3.2 Knowledge and Awareness of Landslides

Almost 70% (36/52) of the comparison group reported knowing about the incoming tropical storm at least one day in advance, mostly by radio, but only 4% (2/52) reported knowing about the landslides by radio. Retrospectively, 85% (44/52) of the comparison group reported not knowing that landslides could accompany heavy rain, and 75% (33/44) of these also reported that they had not considered landslides a hazard.

Although the landslides occurred over a 12-hour period, almost 70% (35/51) of the comparison group reported being unaware of other landslides in Chuuk that day and less than 10% (5/51) reported knowing about occurring landslides more than an hour before being affected. Of those who faced the landslide with little anticipation (35/52), only 31% (11/35) reported noticing natural warning signs such as rushing water and rumbling earth.

3.3 Location and Activities during the Landslide

The proportion of subjects reporting being inside a structure at the time of the landslide was higher among case subjects [59% (23/39)] than among

injured comparison subjects [36% (14/39)], and similar to that among non-injured comparison subjects [62% (8/13)]. Among those who were not aware of the possibility of landslides, the proportion of decedents inside a structure during the landslide [56% (18/32)] is similar to that of injured subjects [58% (15/26)] and both are lower than the proportion for non-injured [67% (6/9)].

Only 17% (3/17) of the case subjects who were outside during the landslides were in the midst of preparations for a possible typhoon. Most (10/17) were performing activities such as walking on the road, picking breadfruit and bananas, or bringing down laundry.

3.4 Structural Characteristics

Among the fatalities reporting being inside a structure (23/39) when the landslide occurred, 80% (18/23) occupied a structure located at the bottom of a slope or by the sea, and almost 70% (16/23) reported having concrete walls. Of those inside concrete structures, at least half (8/15) left their homes and sought shelter from the tropical storm.

3.5 Rainfall

During the last four decades, the islands of Chuuk received on average 7 to 14 inches of rainfall for any given month, with highest values recorded between May and October. The Weather Station on Weno Island documented a record monthly rainfall (34.34 inches or 858.5 mm) during July, 2002 (Personal communications, September 2002). Monthly pecipitation levels had not been that high since July, 1962 (32.99 inches or 824.75 mm).

On July 2nd, 2002, the islands received almost 20 inches (500 mm) of precipitation in 24 hours, with a peak reaching over 3 inches (75 mm) per hour, resulting in at least 265 landslides during the tropical storm. Although some landslides continued to occur the following days, most of the more massive landslides and all fatalities occurred on this day. (The last landslide reported in Chuuk occurred in 1976, when monthly precipitation levels peaked at 28.4 inches, or 709.75 mm.)

The hourly amounts of rainfall and the reported times of the fatal landslides appeared to peak on or about the same time (Figure 3). Rainfall data was available only for Weno, the capital and site of the only meteorological station in the state.

4.0 DISCUSSION

This investigation showed that although landslides struck during a 12-hour period, most people were unaware that deadly landslides also were occurring in different villages on the same island and on other islands throughout Chuuk. This highlights an immediate need to improve the state's infrastructure for communications and to sensitize warning systems in emergency situations within and between islands.

Although the affected community appeared to be prepared and knowledgeable about tropical storms and typhoons, few knew that even tropical storms could trigger deadly landslides. Thus, their choice of shelter was probably inappropriate for the hazards that they perceived. In this event, a typhoon watch was issued on Sunday, June 30 in anticipation that winds of 74 miles per hour (mph) or greater possibly would hit the area within the next 48 hours (Weno Weather Station, 2002; Pielke, Pielke, 1997). Two days later, at tropical storm status (maximum sustained winds of 60 mph), some people moved to storm shelters, usually concrete structures belonging to relatives, while continuing to prepare for the advancing typhoon. For example, all decedents in the landslide in Penia were siblings between 6 and 13 years of age who were left in a concrete storm shelter while their mother returned home to prepare food in advance of a typhoon.

According to the United States Geological Survey (USGS), slopes where debris flows have occurred in the past are likely to experience them in the future, and that people should be located away from steep slopes, streams and rivers, intermittent-stream channels, and the mouths of mountain channels USGS, 2000). In settings like

those of Chuuk, this may be difficult to accomplish because villages are often located on a coast at the base of a slope and near a source for fresh water.

Descriptive and consistent warning signs can assist in prompting appropriate behavioral response. In this event, preliminary rumbling and mud were reported as natural warning signs for incoming debris flow. In Meseiku, where the landslide occurred at approximately 2:30 a.m., the rumbling of the creek woke the parents of the only two fatalities in the village, and probably contributed in saving the other five children in this home. In Mwalitw at 7 a.m., the landslide also came down the course of a creek, and different reports agreed that water and mud came first, shortly followed by debris. In Nechap, the village with the greatest destruction and casualties, a wave described as a "wall of water" preceded the landslide. In Nepukos, people were unable to distinguish mud from landslide and reported them as simultaneous. The USGS cautions that a trickle of flowing or falling mud or debris may precede larger flows (USGS, 2000) and recommends that people near a stream or channel be alert for any sudden increase or decrease in water flow and for a change from clear to muddy water, which may indicate debris flow activity upstream.

One striking finding of this descriptive work was that children under 15 years of age were vulnerable in this landslide event. Among the study population, the increased mortality rate for those less than 15 years of age and those 35 years and over is consistent with previous reports on other natural disasters, where the risk of serious or fatal injury was found to be greatest among children and older adults (Glass et al., 1977; Osaki, Minowa, 2001).

Although construction material has been linked to a higher risk of death during earthquakes (Glass et al., 1977), our study found no association between the risk of becoming a fatality and the construction material of the house. Other factors might play a more important role than construction material, such as construction type and reinforcement, but these were not evaluated.

Structures at the base of steep slopes have been described to be at risk from landslides (Harp, Reid, 2002), but our investigation did not verify this. The volcanic formation of most islands in Chuuk results in the establishment of villages at the bases of slopes. Further, landslides are highly localized, and their size and speed depend on many factors in addition to the orography of the area.

Being outside a structure appeared to be protective against death and injury in this event. Most (15/22) of the case subjects were inside a structure with concrete floor and walls just before the landslide. The other seven case subjects were reported to be inside wooden walls, but five of these come from a single family in Kuchua, where the entire house was swept away by the landslide. The other two decedents inside were reported to be asleep at the time of the landslide.

Landslides, often regarded as secondary to major disaster events, can be naturally triggered by earthquakes, floods, volcanic eruptions, or hurricanes, and can result in more damage and life loss than the primary event. To date, the public health consequences of hurricanes and tropical storms result mainly from torrential rains and floods, rather than from high winds. The catastrophic death toll (10,000) after Hurricane Mitch in 1998 was primarily attributed to widespread flooding and thousands of landslides following heavy rainfall in Honduras, Nicaragua, and Guatemala, and became the most deadly hurricane in the Atlantic Ocean in 200 years (Crone et al., 2001). Floods and landslides in Venezuela during December 1999, considered one of the most severe disasters in the Americas this century, sustained precipitation levels that peaked at 410 mm and led to the deaths of over 300 people (Pan American Health Organization, 1999).

Human deforestation is also known to increase the probability of landslides in certain slopes. According to a report by the United Nations Disaster Assessment and Coordination Team that addressed landslide sites other than those with fatalities, many landslides occurred in gardens and plantation areas cultivated for taro, cassava, banana,

sweet potato and breadfruit above the villages (Higgins, Teleni, Jayaprakash, 2002.) Because our investigation concerned only twelve landslide sites with fatalities, we did not address deforestation as a contributor to mortality.

5.0 CONCLUSIONS

A greater proportion of people who died during landslides triggered by Tropical Storm Chata'an were unaware of the hazards of landslides and were children under 15 years. Viable risk reduction strategies should focus on 1) improving communication systems during tropical storms between and within the islands; 2) enhancing community knowledge and preparedness for landslides and other hazards; and 3) targeting health and disaster education to groups, especially children. Being outside or inside a structure during a landslide should be further evaluated for appropriate safety seeking behavior.

6.0 REFERENCES

Crone AJ, Baum RK, Lidke DJ et al. Landslides induced by Hurricane Mitch in El Salvador—an inventory and descriptions of selected features. United States Geological Survey, Denver, Colorado, 2001.

Federated States of Micronesia (FSM). 1994 FSM Census of Population and Housing.

International Federation of Red Cross and Red Crescent Societies (IFRCRCS). World Disasters Report. 2001.

Glass RI, Urrutia JJ, Sibony S et al. Earthquake injuries related to housing in a Guatemalan village. Science 1977;197:638-643.

Harp E, Reid ME. United States Geological Survey. Landslides triggered by Typhoon Chata'an in Chuuk State, Federated States of Micronesia. Provision landslide reconnaissance and hazard evaluation. August, 2002.

Higgins C, Teleni E, Jayaprakash VT. United Nations Disaster Assessment and Coordination (UNDAC) Team. Typhoon Chata'an Mission Report, July, 2002.

Iverson RM, Reid ME, Iverson NR, LaHusen RG, Logan M, Mann JE, Brien DL. Science. Acute sensitivity of landslide rates to initial soil porosity." Science 2000;290:513-516.

Osaki Y, Minowa M. Factors associated with earthquake deaths in the Great Hanshin-Awaji earthquake, 1995. Am J Epidemiol 2001;153:153-156.

Pan American Health Organization. Epidemiological Bulletin. December 1999, Vol. 20, No. 4.

Pielke RA Jr, Pielke RA Sr. Hurricanes: their nature and impacts on society. United Kingdom: John Wiley & Sons, 1997.

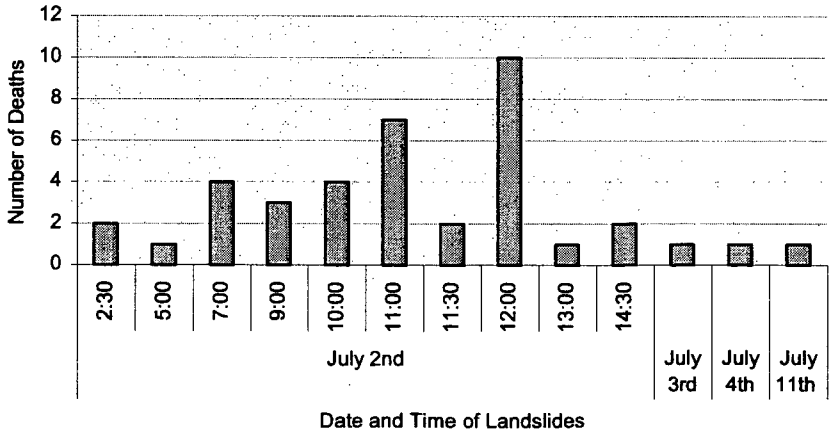
United States Geological Survey (USGS). Landslide hazards. USGS Fact Sheet. Landslide Fact Sheet FS-071-00, May 2000.

Weno Weather Station, Chuuk, Federated States of Micronesia. Personal communications, September 2002.

Table 1. Mortality by island, Chuuk, Federated States of Micronesia, July 2002

Island	Cases (%)	Cases not accounted for	Mortality rate (per 1,000)
Tonoas	21 (52.5)	3	6.08
Udot	5 (12.5)	0	3.13
Siis	1 (2.5)	0	2.10
Fefen	8 (20.0)	0	1.98
Uman	1 (2.5)	0	0.33
Weno	4 (10.0)	0	0.25
Total	40	3	1.37

Figure 1. Case subjects by reported time of death*, Chuuk, Federated States of Micronesia, 2002



* unknown time of death for 4 case-subjects

Figure 2. All cause crude death rates (1990-1993) and landslide-related death rates by age group, Chuuk, Federated States of Micronesia, 2002

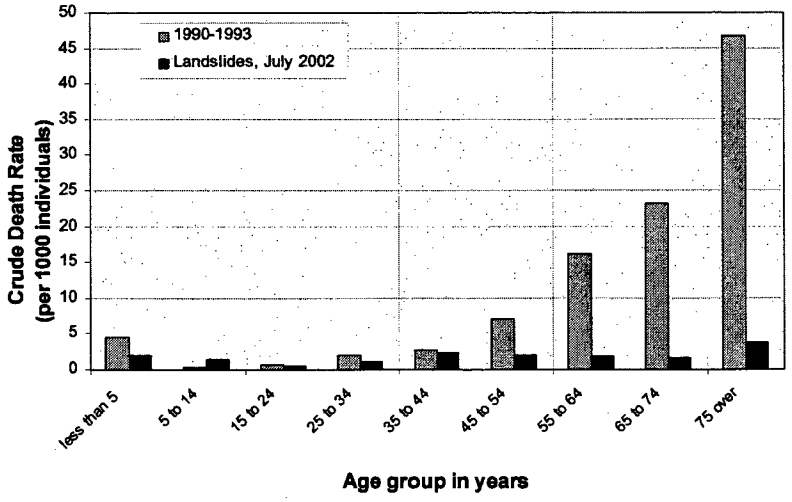
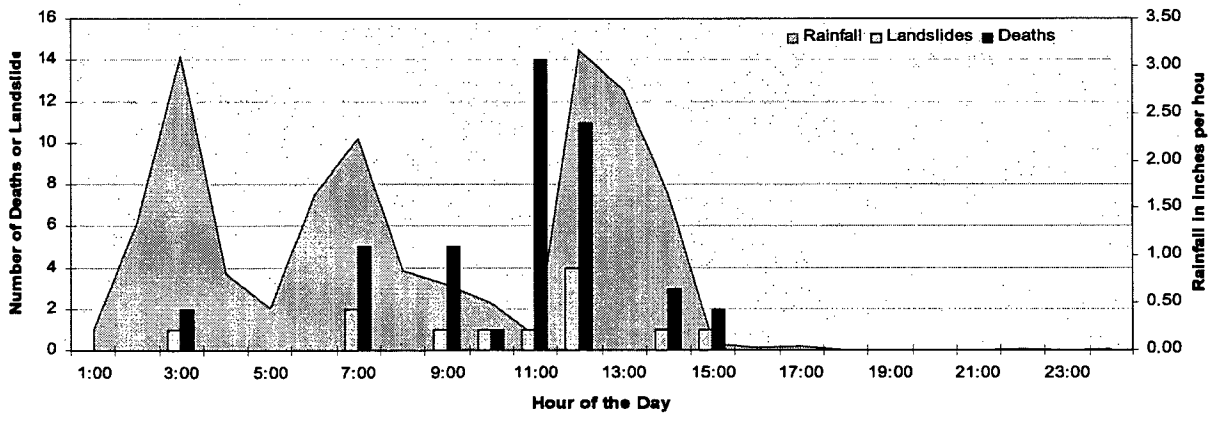


Figure 3. Total hourly rainfall, and total number of fatalities and landslides by time of landslide, Chuuk, Federated States of Micronesia, July 2, 2002



Application of Remote Sensing and Information & Communication Technologies for Disaster Response

by

Akihiro Sanada [1] and Takaaki Kusakabe [2]

ABSTRACT

At natural disasters, damage detection & urgent response is key issue to save lives, reduce damage influence and recover properly. This paper presents possibility and effectiveness to apply remote sensing and information & communication technologies to emergency response, mainly collection of information about facility damage and dissemination of information about disaster operation among field staffs and headquarter-level. The results indicate that 1) about 2m spatial resolution is required to detect damaged facilities by high-resolution satellite, 2)it is possible to detect facility damage by LIDAR. It is also recognized that introduction of palmtop for emergency response increases the efficiency of communication and information shearing between field-level and headquarter-level.

KEYWORDS: Communication, Damage Detection, High-resolution Satellite, LIDAR, Palmtop

1. INTRODUCTION

The bigger natural disaster becomes, the more rapid response should be executed. In reality, it is more difficult to collect, process, analyze and disseminate information including facility damage information at major disasters. At severe natural disaster, personnel in charge of emergency response and administrating infrastructure likely suffer from disaster damages. It causes shortage of staffs. Under such situations, remote sensing and information & communication technologies can support staffs in fields and headquarters. An example how such technologies can support emergency response is shown in Fig-1. Remote sensing technologies lead to rapid damage detection. Gathering, Processing and providing information real-time electronically can save the number of staff for communication about disaster operation.

This paper thus reports on studies 1) to apply high-resolution satellite and LIDAR for detection of facility damage and 2) to introduce palmtop for field staffs to send and acquire information to/from headquarters.

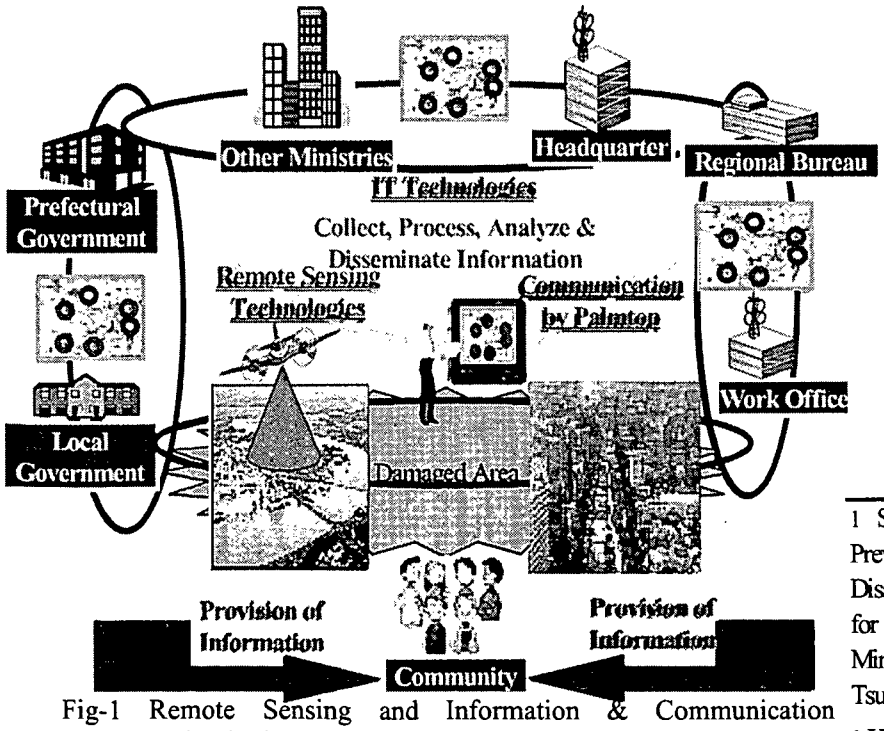


Fig-1 Remote Sensing and Information & Communication Technologies that can support disaster management

1 Senior Researcher, Earthquake Disaster Prevention Division, Research Center for Disaster Risk Management, National Institute for Land and InfrastructureManagement, Ministry of Land Infrastructure Transport, Tsukuba-shi, Ibaraki-ken 305-0804 Japan

2 Head, ditto

Table-1 Target Remote Sensing

Platform	Sensor
Artificial Satellite	Optical Sensor
Stratspheric Platform	SAR
Aircraft	(Synthetic Aperture Radar)
Helicopter	LIDAR
UAV	(Light Detection and Ranging)
(Unmanned Air Vehicle)	

2. DAMAGE DETECTION BY REMOTE SENSING

In 1995 Hyogo-ken Nanbu Earthquake, a lot of road facilities collapsed due to strong ground motion. Nevertheless, residents used cars for their evacuation. In result, very serious traffic congestion occurred. Personnel in charge of facility inspection always use vehicles to investigate their facilities. Naturally they were involved in traffic jam. This was one of reasons why damage detection was delayed at the earthquake. On the other hand, several high-resolution satellites are now operated. One of characteristics of remote sensing is that it can acquire data of wide ground surface at the same time. At a serious natural disaster, damaged area is widely spread. Therefore, it is suitable to recognize the distribution of damaged facilities by remote sensing shown in Table-1. In this study, high-resolution satellite and airborne LIDAR are picked up from this table.

2.2 High-resolution satellite

The possibility to capture facility damage by images from optical sensors is discussed. Images are set with five different spatial resolutions. And by means of 1) watching raw images by staffs themselves and 2) applying image processing, relations between spatial resolution and visibility are investigated. In addition, applicability of image processing to various kinds of damage type is studied.

2.2.1 Sample images

Images are made by scanning aerial photos of damaged facilities, which are chosen from the 1995 Hyogo-ken Nanbu Earthquake as shown below;

1) Kobe-Hamate Bypass, National Highway #2 (Fig-2)

Girder shifted 1.5m in transverse direction to bridge axis.

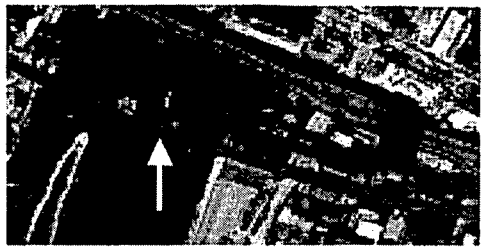


Fig-2 Shifted Girder at Kobe-Hamate Bypass (Simulated Image with 1m resolution)

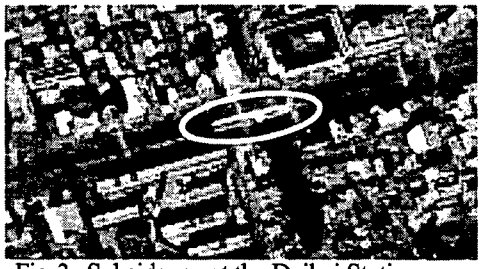
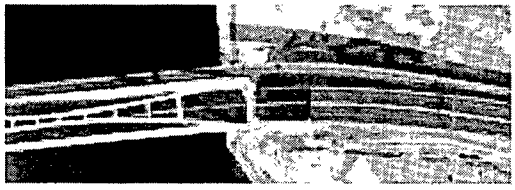
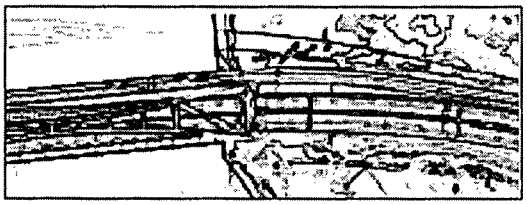


Fig-3 Subsidence at the Daikai Station (Simulated Image with 1m resolution)



(a) Simulated Raw Image with 1m resolution



(b) Result of Edge-enhancement

Fig-4 Approach Bridge that fell down at Nishinomiya Port Bridge



(a)Simulated Raw Image with 1m resolution (b)Result of Supervised Classification

Fig-5 Damaged bulkhead, outflowing sand and liquefaction at the Naka Tottei

Table-2 Possibility to extract Damaged Facilities

Facility	Damage	20cm Resolution		50cm Resolution		1m Resolution		2m Resolution		10m Resolution	
		Color Image	Monochrome Image	Color Image	Monochrome Image	Color Image	Monochrome Image	Color Image	Monochrome Image	Color Image	Monochrome Image
Kobe-Hamate Bypass	Shifted Girder	○	○	○	○	○	○	×	×	×	×
Daikai Station	Subsidence	○	○	○	○	△	×	×	×	×	×
Approach Bridge	Collapsed Bridge	○	○	○	○	○	○	○	○	×	×
Naka tottei	Liquefaction	○	○	○	○	○	○	○	○	×	×
	Outflowing Sand	○	○	○	○	○	○	○	○	○	×
	Collapsed Bulkhead	○	○	○	○	○	○	○	○	×	×

○:Easy to extract △:Possible to extract ×:Impossible to extract

2) Daikai Station of Kobe Rapid Transit Line (Fig-3)

The center pillars in Daikai station, which was located in underground, collapsed. This resulted in subsidence at the surface, National highway #28, for 90m long and 28m wide. Depth is maximum 2.5m.

3) Approach bridge of Nishinomiya Port Bridge, at Bay Shore Route of Hanshin Expressway (Fig-4(a))

Approach bridge, 52m span and 6 lanes, fell down about 25m.

4)NakaTottei Pier in Kobe Port (Fig-5(a))

Bulkhead was damaged for 190m long and sand were outflowing. Additionally, liquefaction occurred in Nakatottei area.

2.2.2 Possibility to detect damage by watching raw images

In this experiment, civil engineers who have no information about locations of damaged facilities check the images. And it is judged whether they can find damaged facilities or not. Each image is size of 30cm×20cm and covers a spatial area of several hundreds meter around including damage facilities. How clearly damages are found is classified into three categories as following;

1) It is easy to extract damages from images.
2) It is possible to extract them.
3) It is impossible to extract them.

Most influenced factor in extraction is spatial resolution of images. Therefore, 5 different resolutions,i.e.10m, 2m, 1m, 0.5m and 0.2m, were examined in this experiment. The result is shown on Table-2.

1) Resolution 0.2m to 0.5m

In the case of Daikai Station, it is possible to detect cracks but difficult to understand caving down. Except subsidence at the Daikai Station, it is easy to find out damages of facilities.

2) Resolution 1m to 2m

It becomes difficult to detect girder shift at Kobe-Hamate Bypass and subsidence in Daikai Station.

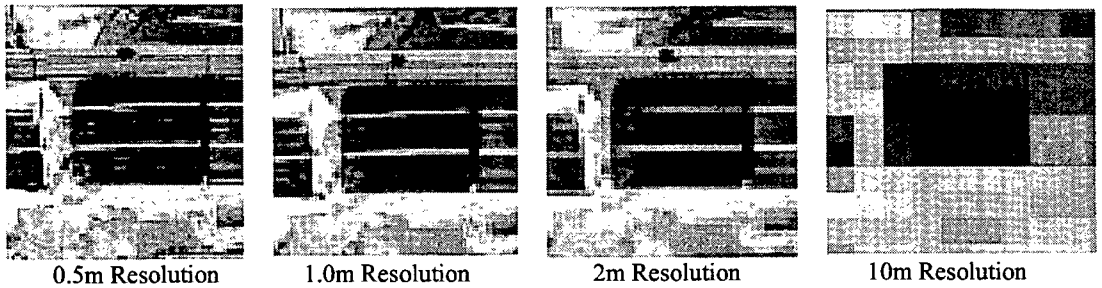
3) Resolution 10m

There is no damage that can be detected easily except outflowing sands in Nakatottei Pier.

Thus, it is understood that the minimum of 2m resolution is required to detect facilities damages, even though widely spread damages like liquefaction and land slide can be extracted from 10m resolution images.

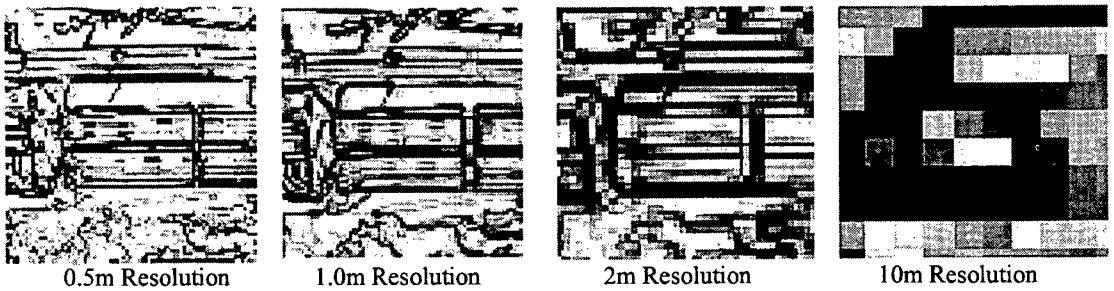
2.2.3 Application of image processing

In this experiment, two kinds of image processing, which are edge-enhancement and supervised classification, are applied to the two images: approach bridge of Nishinomiya Port Bridge and Nakatottei Pier. After image processing, possibility to extract damages from the images is estimated on each resolution. Fig –4(b) shows the result of application of edge-enhancement. This indicates that enhanced edges at road side and road center becomes discontinuous in the collapsed parts. In other parts, enhanced edge is continuous and looks clear. Fig-6 shows the result of applying edge-enhancement in 5 different resolutions. It is possible to detect collapsed part in the case of 2m or better resolution images, but impossible in the case of 10m resolution. In addition, results on the application of edge-enhancement to Nakatottei Pier indicate that edge-enhancement is suitable to detect damages of line-shaped facilities and difficult to detect damages which spread widely (Fig-5(b)). Widely spread damage should be detected by classification. In this study, supervised classification is applied. The result is shown in Fig-7. In classification, as training data, three sample pixels inside the liquefaction and outflowing area are chosen and pixels which has similar color with training data are judged as damaged area. The result indicates



0.5m Resolution 1.0m Resolution 2m Resolution 10m Resolution

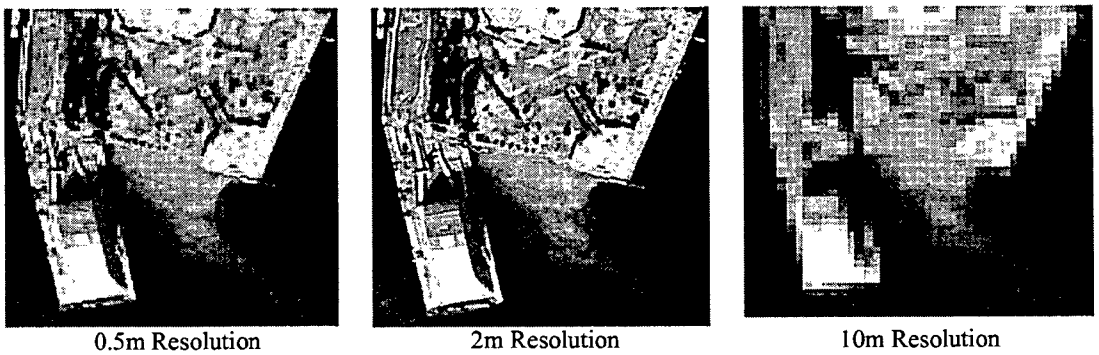
(a) Raw Images



0.5m Resolution 1.0m Resolution 2m Resolution 10m Resolution

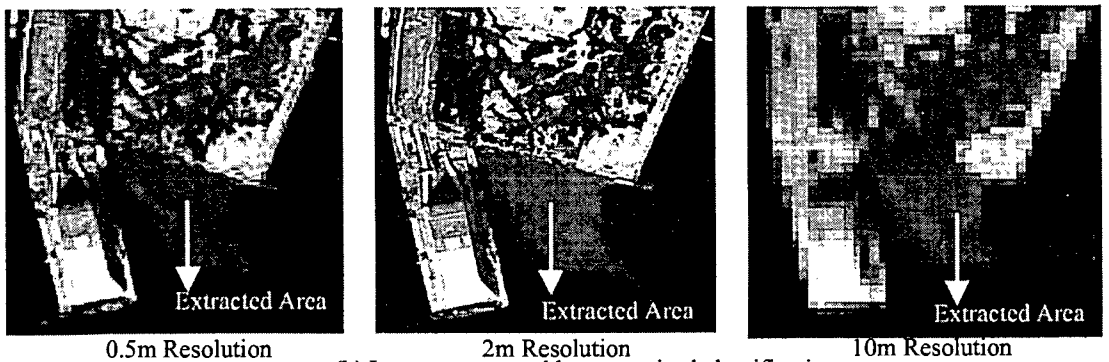
(b) Images processed by edge-enhancement

Fig-6 Approach Bridge of Nishinomiya Port Bridge



0.5m Resolution 2m Resolution 10m Resolution

(a) Raw Images



0.5m Resolution 2m Resolution 10m Resolution

(b) Images processed by supervised classification

Fig-7 Naka Tottei Pier in Kobe Port

that the image of 2m or better resolution is good to specify the spread of liquefaction area.

Thus, suitable matching between damage type and image processing exists. In addition, same as extraction by human, in information extraction by computer, 2m or better resolution is necessary.

Table-3 Specification of Measurement by LIDAR

Laser repitition rate	15000Hz
Scan frecuency	25.2times/sec
Scan angle	8°
Swath width	136.4m
Horizontal accuracy	0.3m,1σ
Vertical accuracy	0.15m,1σ
Operating altitude	975m
Ground speed	185km/hr(51m/sec)

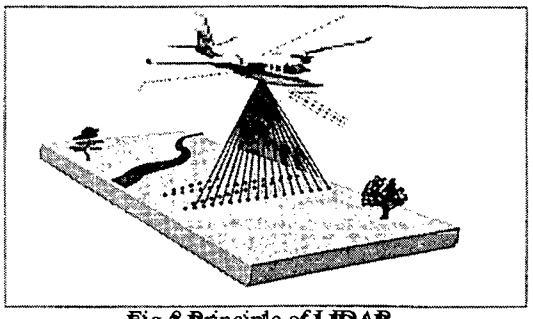


Fig-8 Principle of LIDAR

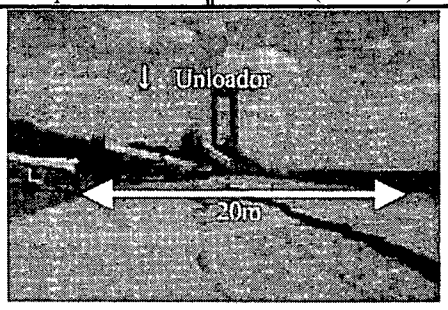
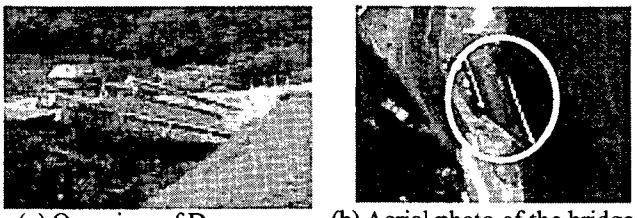


Fig-9 Damaged Quaywall in Sakai Port



(a) Overview of Damage (b) Aerial photo of the bridge

Fig-10 Collapsed Bridge in Saihaku-cho

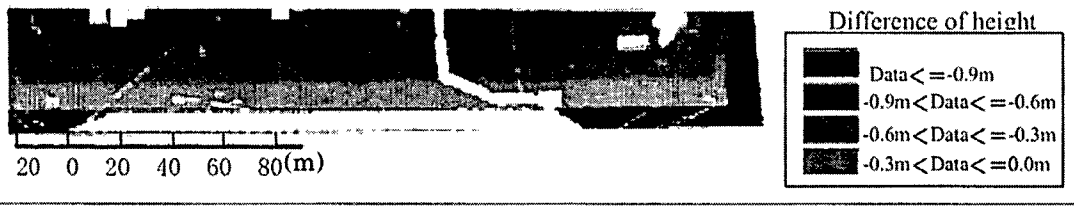


Fig-11 Level difference from the average height of face line of the quaywall

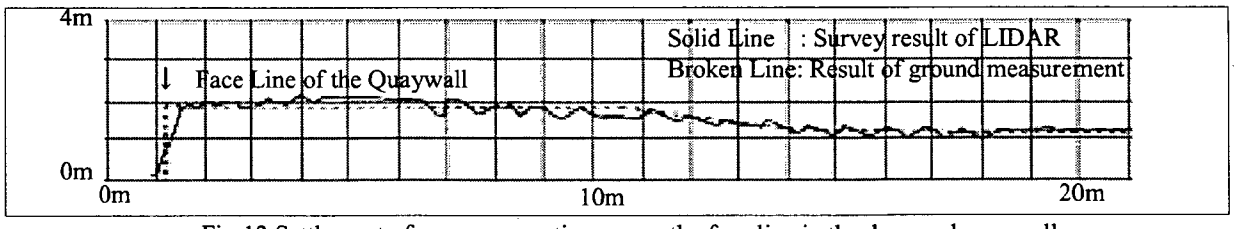


Fig-12 Settlement of one cross section across the face line in the damaged quaywall

2.3 LIDAR

Using LIDAR makes it easier to get ground elevation data. Because a lot of kinds of damage due to earthquakes are expressed by changing elevation represents , it is examined to capture damages based on LIDAR data in this study. Specification of measurement is in Table-3.

The principle of LIDAR is shown in Fig-8. Using the time taken for beams of light to return to the sensor after firing to the ground, elevation is calculated.

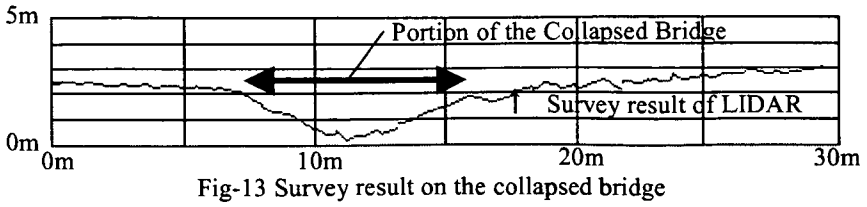


Fig-13 Survey result on the collapsed bridge

2.3.1 Target damaged facilities

In this study, damaged facilities at the 2000

Tottori-ken Seibu Earthquake, in Oct. 2000 were measured by means of LIDAR. Target damages are shown below.

1) −13m Quaywall in Sakai Port

Cracks and settlement occurred behind caisson along the face line. Difference in level was 60cm(Fig-9).

2) One span bridge in Saihaku-cho

The bridge,7m long and 4m wide, fell down because of damage in abutment(Fig-10).

2.3.3 Result of measurement

Fig-11 is the map of level difference from average height of face line of quaywall. White areas in Fig-11 are ship coming alongside the quaywall and the unloador shown in Fig-9. At the approximately 10m inside from the face line, color changes in Fig-11. This indicates that damage in quaywall can be captured by LIDAR. Fig-12 shows settlement of one cross section across the face line of the quaywall. The solid line is the survey result of LIDAR and broken line is the result of ground measurement. In points of the location and width of inclination, and the volume of height-difference, result measured by LIDAR is in good agreement with ground measurement.

Fig-13 shows the survey result of LIDAR on the collapsed bridge. Because elevation at pre-earthquake in this bridge is not obtained, precise comparison is difficult. However, LIDAR data in the portion of collapsed bridge decline. It indicates that LIDAR can capture a damaged bridge.

Based on these two examples, elevation data captured by LIDAR may have provided a useful indication of existence of damaged facilities.

3. EFFICIENT INFORMATION SHEARING by IT(INFORMATION TECHNOLOGIES)

At disaster risk management, various kinds of information are sheared among related entities. Personnel in charge of sending and receiving information to/from other division likely make mistakes such as forgetting to provide data. Even inside one division, it becomes difficult to revise data and shear them at sever disasters. Headquarter always enforces lower level to gather and send information immediately. This increases confusion of lower level organization at disaster response.

Introduction of information & Communication technologies to disaster risk management is studied to improve these serious situations. In this paper, application of palmtop devices for staffs in fields is reported.

3.1 Present Difficulties

3.1.1 Staffs in fields

1) They always bring paper-based maintenance data to fields during inspections of facilities. This data is bulky, heavy, big and inconvenient.
2) They mainly use cell phone in communication with headquarter. In serious disaster, normal communication system is overloaded and easily becomes unavailable.
3) Most of information is only from field staffs to headquarter. In result, field inspectors can recognize only what they watch by themselves.

3.1.2 Staffs in Headquarter

1) They want to know road closure due to disaster immediately. In reality, it takes long time to inspect facilities to make it clear where road is closed. Because progress of field inspection cannot be informed to them for long time, staffs in office cannot judge situations of each portions in road network whether no road closures are reported in result of inspection or road closures are not reported because staffs can not reach them.
2) In the case of closure, additionally, they want to know the reason why the part is closed, difficulty level of recovery and time to re-open.

   Sometimes oral reports are difficult for staffs in office to recognize situations.
3) Information is sent from various sources and it is difficult to make them in time line. In result, they cannot understand what are latest situations.
4) Information on supplies and equipments for restoration and recovery is now conveyed by telephone. It is difficult to send them orally.

3.2 Application of palmtop

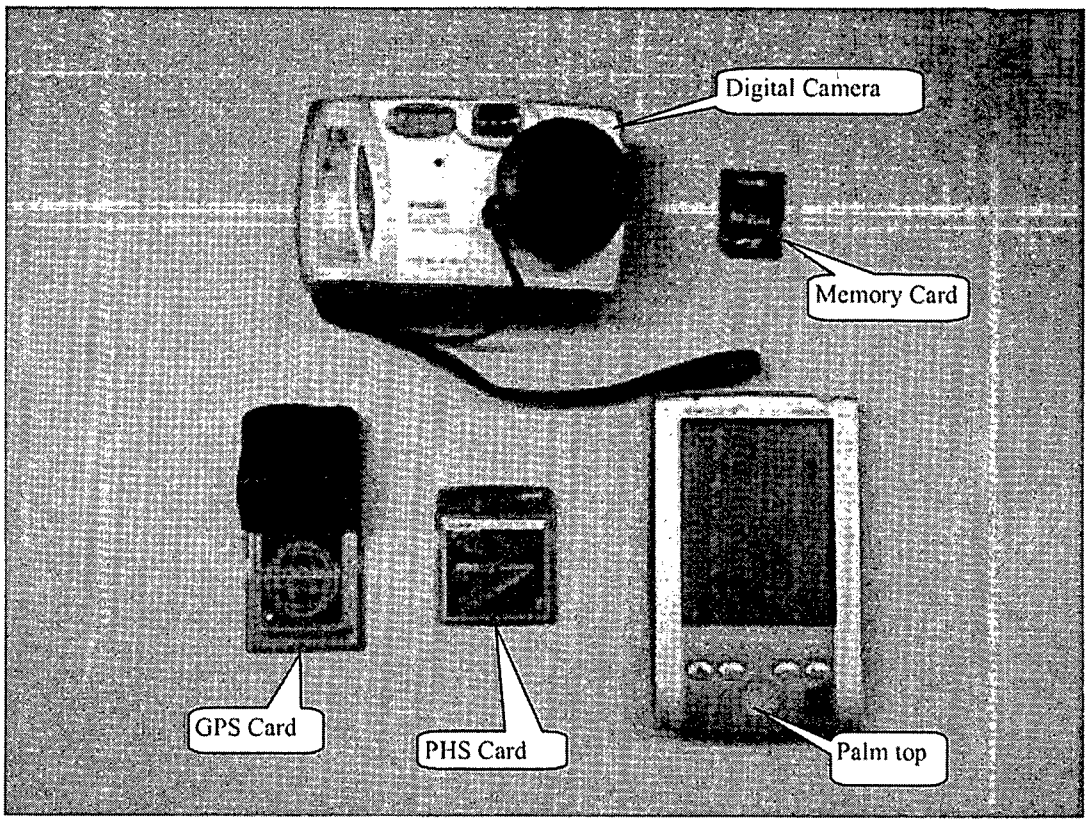


Fig-14 Palmtop and other devices used in the experiment

To solve these problems listed in 3.1, application of palmtop is studied. Based on preset problem, first, functions with which palmtop should be equipped are discussed.

3.2.1 Functions of palmtop for headquarters

1) Function of recording time and date
   Data that are input to palmtop should have the attribute of time and date. It becomes easy to make data in time line. Accessing to the newest data is easily executed.
2) Function to deal with images
   Not only text data but also image data can be sent to headquarters. Personnel in headquarters can easily recognize situation including damages in fields. Judging damage level objectively is difficult. However, by sending images, field staffs do not need to judge damage level and personnel in headquarter can judge it by their own criteria.
3) Function of GPS
   Locations in which field staffs are working are recorded in real-time. This data is sent to headquarters. In result, headquarters can know at any time where they are. They also can know which facility is already inspected.

3.2.2 Functions of palmtop for field staffs

1) Function of indicating seismic ground motion level.
   Data observed by seismographs are announced on palmtop. Staffs can easily recognize distribution of ground motion and size of an earthquake.
2) Function of indicating estimated damage
   Before/during field inspection, staffs can refer to estimated facilities damage.
3) Function to deal with images
   Situation in field can easily and precisely reported to headquarter.
4) Memory Function
   Facility management data can be stocked in palmtop and provided for field inspectors through palmtop. They do not need to bring paper-based data. In addition, in reporting facility damage, such data is attached to the report. Headquarters can realize damaged facility detail easily.

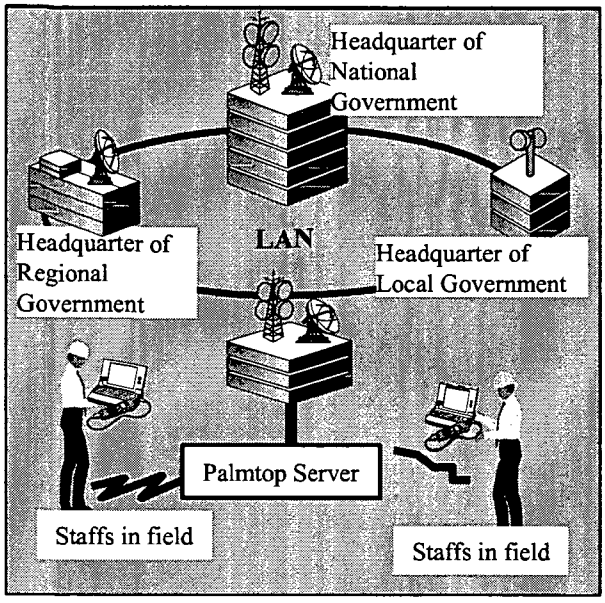


Fig-15 Structure of network in this experiment

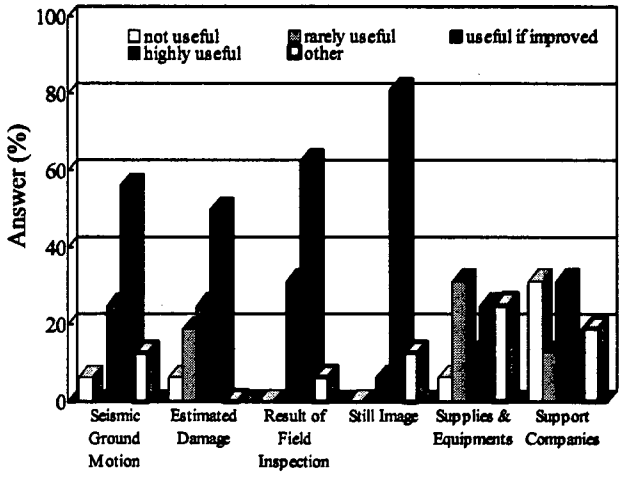


Fig-16 Usefulness of each information

3.3 Field experiment

Based on the discussion in 3.2, these new functions are equipped in palmtop and the availability and efficiency of those functions are checked by the field experiment. The palmtop and related devices used for this experiment are shown in Fig-14.

3.3.1 Scenario

In the field experiment, under the assumption of earthquake occurrence, personnel in charge of maintenance facilities execute field inspection. During the inspection, they report their result and facility damage condition to headquarters using palmtop. At the same time, field inspectors get several kinds of information from other field inspectors, headquarter and facility management database. Personnel working for headquarters acquired the facilities damage level through palmtop by text data and still images.

3.3.2 Information that are dealt with on palmtop

(1) Seismic ground motion

(2) Estimated damage

Estimated damages are gotten from SATURN[1](Seismic Assessment Tool for Urgent Response and Notification).

(3)Information about support companies

Locations of support companies' offices are shown on the map in palmtop by icon. Companies' attributes (name of company, telephone number, contact person's name) are on palmtop when the icon is clicked.

(4) Information concerning supplies and equipments for recovery

Locations of storages of supplies and equipments for recovery are shown on the map in palmtop. And list of stocked supplies and equipments come out on the screen of palmtop when the icons are clicked.

(5) Function to read and send digital camera shots

In addition to these data, by networking palmtop server and servers of local (municipal), regional (prefectural), and national headquarters, information shearing can be done among not only headquarters but also staffs in fields. Fig-15 indicates the structure of networking in this experiment.

3.3.3 Result of field experiment

After the experiment, opinions of participants are obtained through questionnaires to evaluate the effect of palmtop.

The usefulness of each data in 3.3.2 is shown in Fig-16. This result indicates that information about 1) seismic ground motion, 2) estimated damage, 3) report of field inspection results to headquarter through palmtop, 4) report of situations in field with images, 5) acquiring information from headquarter and other staffs in

fields is efficient for field staffs. On the other hand, it is understood that information about 1) supplies and equipments for recovery and 2) support companies are not effective. Participants as field staffs in the experiment have opinions that it is difficult to input data by pen and voice input or selection from pull-down menu are useful.

Participants as staffs in headquarters have opinions that information shearing using network means incorrect data and uncertain data are also sheared in an instant. Once such data are conveyed, it is more difficult to modify them. Therefore, in such cases, data should be transferred with the attribute of level of precision (i.e. uncertain data/certain data).

At the introduction of palmtop to disaster response, it is pointed out by the experiment that palmtop for only disaster response use is not good from the point of cost performance. Functions for disaster risk management and usual facility management should be in one palmtop. In the field of road management, palmtop for roadway patrol has been already introduced. Therefore, in this study, it is now ongoing to add functions for disaster response to the palmtop for roadway patrol.

4. CONCLUSIONS

Detection of damaged facilities due to earthquake by high-resolution satellite and LIDAR was demonstrated. In the case of high-resolution satellite, 2m or better resolution is needed. And palmtop demonstrated its potential for improving field staffs' activities at disaster response. More works such as standardization of data format are necessary by utilizing other information & communication technologies in order to realize smooth and efficient disaster management.

5. REFERENCES

1. Sugita, H. and Hamada, T. : Development of Real-time Earthquake Damage Estimation System for Road Facilities, *Proc. 7th U.S.-Japan Workshop on Earthquake Disaster Prevention for Lifeline System*, 1997.

Spatial Data Fusion for Infrastructure Condition Assessment

by

William E. Roper[1]

ABSTRACT

Information systems and their application to infrastructure management and protection with particular focus on transportation infrastructure are addressed in this paper. The opportunities for information systems leveraging geospatial and other data sources are presented. Remote sensing imaging and non-imaging sources of information are explored. Coordination and sharing of in information is explored to improve the ability of multiple organizations to more effectively manage and respond to disasters and infrastructure condition assessment issues. These include 3-D visualization, thermal infrared imagery, LIDAR data systems, IKONOS one-meter panchromatic imagery, SPOT imagery and the use of digital aerial imagery. The general area of disaster response management is also addressed and the findings of various studies in this area are summarized. Recommendations for the use of information systems and geospatial sensors and products in the future for transportation infrastructure condition assessment and protection are presented.

Keywords: Information systems, Transportation infrastructure protection, Infrastructure condition assessment, Geospatial information, IKONOS satellite data, Digital imagery, Data management, Disaster management, LIDAR, Infrared remote sensing, GIS mapping, Global Positioning System

[1] Professor and Chair, Civil and Environmental Engineering Department, George Washington University, Washington, DC 20052
wroper@seas.gwu.edu

1.0 INTRODUCTION

Infrastructure managers at all levels face unprecedented challenges today. Increasing demands are being placed on agencies to preserve the existing infrastructure system and to take on new missions of improved system safety and security management. A variety of advanced technologies are available to enhance planning, designing, managing, operating, and maintaining all aspects of the nations public and private facilities. The national transportation system is one example of a major part of our infrastructure system and a critical asset for national growth and development. Aerial and satellite remote sensing represents one area of rapid development that can be leveraged to address these challenges. These technologies have significant and unique potential for application to a number of cross cutting transportation security and infrastructure condition assessment issues.

2.0 INFORMATION SYTEMS CONSIDERATIONS FOR INFRASTRUCTURE CONDITION ASSESSMENT

It is clear that despite excellent efforts by many groups the approach to providing information for disaster management is not often effectively utilizing a wealth of data that resides, with various organizations. This existing information and technology could provide disaster mangers important information products that could save lives, reduce damage to property, and lessen the environmental impacts of disasters. The current situation is characterized by numerous shortcomings that inhibit optimal decision making for disaster management. The inability to access information and the lack of standardization, coordination, and communication are all obstacles that need to be overcome.

2.1 Information Management Goals

Considerable effort has been expended throughout the Disaster Management community to articulate issues and to characterize the dynamics and the inter-relationships that needs to be accommodated in a viable information management strategy. An important guide for this effort is found in the recommendations made by the Board On Natural Disasters (BOND) in their report to the National Research Council. The BOND's primary goals as articulated in its charter were to:

1. Improve decision making for emergencies through better access to quality data and information
2. Identify users and their needs
3. Provide information products specifically designed to meet users' need
4. Promote efficiency and cost effectiveness
5. Stimulate and facilitate mitigation

These are important components in any workable framework for comprehensive disaster management. However, the focus here is directed towards derived products, procedure and protocol. It is important that the process develops baseline products and implement solutions that reflect the complex fabric of the disaster management community. This work is done at a lower, more formative level in the information management life cycle and in fact forms the basis for the production of the products referred to by the BOND. As noted above the assessment process will work to identify the constituent components associated with specific disaster events and scenarios. The constituent components will then become the basis for technology specifications and the delivery of capabilities that encompass the products identified by the BOND.[1]

2.2 Data Management Considerations

This section provides assumptions based on information and conclusions that have emerged from recent studies in disaster management community itself. These assumptions certainly do not constitute and exhaustive set of parameters. Rather, they provide a point of departure and a set of "operating hypotheses" that can be used to help frame discussion and consideration of needs and requirements. Available Information and capacity is not uniform, consistent and standardized for disaster managers. Large cities may have invested millions of dollars in their information systems, while smaller municipalities may be operating with one personal computer. Disasters will constantly crosscut established boundaries. A fundamental problem in dealing with disasters is that they do not respect boundaries that include organizational, political, geographic, professional, topical, or sociological consideration.[2]

Disasters will often overwhelm mechanisms for coordination and communication. In addition, the mechanisms to bring data and information to decision makers are uncoordinated. Information is often produced from disparate sources and transmitted in whatever format the provider prefers, requiring significant effort to compile it into a form that provides a coherent picture or even thwarting integration altogether. Data standards are often inconsistent, and, even more dangerous; users are sometimes unaware of the limitations and uncertainties in data or are presented with conflicting interpretations of data without the means to assess the reliability of the sources. All of these issues reduce the efficacy of the decision-making process. The problem is compounded because information delivery systems in many cases become overloaded during crises. For instance, in 1996 a moderate (magnitude 4.7) earthquake in San Jose, California, led to more than a million attempted hits in less than one day on the U.S. Geological Survey's World Wide Web earthquake information server.[3] Most of those attempts were unsuccessful, including those by emergency managers trying to access data and information to aid in the formulation of a response plan.

3.0 INFORMATION MANAGEMENT PROCESS ISSUES

Disaster management is an exercise in logistics and information processing and distribution. To effectively undertake these tasks requires a good understanding of disaster information requirements and the characteristics associated with disaster events knowing that each event is uniquely different. Disasters come in different sizes, have different behavior and can be categorized on the basis of their impact on natural resources, agriculture, communities etc. They can also be discriminated and classified along a number of dimensions including impact, severity, duration, geographic setting and advance warning (NAPA 1998). In order to develop the Information Technology architecture for case scenarios application it is essential to understand the disaster event from the perspective of those responsible for assimilating the data. The effective use of this information for producing operational plans to deal with the disaster event and its aftermath is critical.

3.1 Consideration of Infrastructure Information Phase Management

For instance, it is important to appreciate that the four basic phases of disaster management may actually manifest themselves in different ways depending on the nature of the disaster. The mitigation phase is essentially a continuous process of preparation, analysis of performance and subsequent modification and refinement. As a result it will likely exhibit the smallest amount of variance. However, the other phases (preparedness, response and recovery) will likely have significantly different attributes depending on the nature of the event. For example consider the difference in the preparedness phase that would be associated with major seasonal flooding along the Mississippi or the Missouri Rivers, the Chaparral fires along the Pacific Coast, a Tsunami that impacts much of the Pacific Rim and an earthquake such as Northridge or Loma Prieta. In each case the geographic coverage and the amount of time for planning and staging is very different. As a result, many of the other systemic aspects of the disaster management initiative will be different as well.

An event warning which impacts the manner in which the preparedness phase is managed also has implications and consequences for the recovery phase (e.g. In the case of the Loma Prieta earthquake the emergency response resources were directed to the bay area despite the fact that Santa Cruz and Watsonville had more significant damage). Partially as a result of this California is building the Tri-Net seismic sensing network to measure shake and model damage in order to make more informed decisions regarding staging recovery resources.

3.2 Infrastructure Disaster Management Communities

The disaster management is extremely heterogeneous. In order to develop effective systemic solutions to the needs of this community any framework must address the need to effectively and efficiently share information across institutional boundaries within and between the groups that make up this community. In essence an interface must be specified at each boundary that separates levels in an agency or at the juncture between different agencies or between different sectors. These interfaces each have at least three components: 1) technical, 2) institutional and 3) institutional administrative. The importance of these interfaces is also proportional to the difficulty of implementing them in an automated context. For instance, the lightest weight interfaces should be between levels within the same entity within a single sector. In contrast the heaviest interfaces would be those that attempt to span sectors.[4]

A number of these communities have made significant institutional investments in the

construction of foundation data products that feed modeling, analysis and decision support in a range of contexts. Not surprisingly the situation in the disaster management community in regard to data parallels spatial data issues across the federal government and throughout state and local government and the private sector. The BOND also addressed the issue of data sharing by the disaster management community. Their findings recognized that despite the importance of significant databases, their utility is impaired by a host of problems deriving from incompatible formats, inconsistent geographic reference systems, conflicting standards, and other human-caused factors. Many of these problems could be resolved and the value and utility of the databases for disaster decision making greatly enhanced through improved organizational and technological coordination with only an incremental increase in cost.[5] This is clearly in the public interest to accomplish this.

Disaster management scales for international agencies and governments to the individual. However, a very significant level of responsibility is vested at the local level. For instance, it is the on the ground officials, many of whom are local, that ultimately play the role of first responders (e.g. police, fire, medical and public works) and who also manage many of the recovery operations. To be effective in this context protocols must define communications, database structure, data formatting, hardware and software requirements, networking, quality control, and other issues needed to assure the linkage will improve decision making before, during, and after emergencies through improved access to quality information. In addition, such a linkage will provide information products that are specifically designed to meet the needs of users

3.3 Common Characteristics of Disasters

Disaster management is not a linear process that can be documented easily in a flow chart with a readily apparent beginning and absolute end point. Rather, it is a cyclical process of approximation, response and re-calibration that involves many different actors whose roles in relation to one another are likely to change based on circumstances and the stage in the process. The one constant evident in the process is the chaos that drives the system. Another absolute is that the effective, efficient application of information technologies and products has the capacity to improve the system in a number of ways that will combine to save lives, mitigate overall damage, conserve resources and ameliorate human suffering.

To develop effective architectures and technologies that meet the needs of the disaster management community there must be a precise understanding of the disaster management life-cycle (Mitigation, Preparedness, Response and Recovery), the Information Communities that combine to define the disaster management community and the information processing requirements associated with the cycle of data development, dissemination, analysis and review. In addition, and perhaps more importantly, there must be a precise understanding of the dynamics between these components and the "interfaces" that these dynamics imply. Only with such an understanding can we effectively model the process and derive technology solutions that map well into the business model of disaster management.[6]

3.4 Data and Information Processing Requirements

Data needs, the characteristics of data and the ability of data to contribute to analysis, response and recovery is well understood. The basic attributes of information that are considered most important by this community include:

1. Timeliness: delivery of data and information in time to drive decision-making

2. Consistency: delivery of data and information in a consistent, uniform manner
3. Understandability: delivery of data and information in a manner that is appropriate and understandable to the target community
4. Accuracy: precision in measurement and observation
5. Flexibility: adaptability to multiple situations

These information attributes have evolved over time within the disaster management community representing the viewpoint of a range of providers, users and consumers scaled from the local to national level. In this regard the communities involved transcend boundaries between recognized sectors at each of these levels (private, public, not-for-profit, NGO etc.).

4.0 TRANSPORTATION INFRASTRUCTURE INFORMATION SYSTEMS

The nation's transportation networks function as the lifelines of commerce, security, and recreation. They are also vulnerable to attack and severe disruption. As officials have discovered since September 11, protecting and preserving the extensive U.S. transportation networks against terrorist attacks remains a daunting task. Fortunately, today's powerful geospatial tools, especially remote sensing, positioning, navigation, and timing (PNT), and geographic information systems (GIS), can assist in this crucial effort.

4.1 Overview of America's Transportation Infrastructure

America's transportation infrastructure is a reflection of the nation's economic vitality, which in turn is predicated on maintaining stable economic, political, and social environments. Under most circumstances the nation's transportation system works smoothly and efficiently; but, as President Eisenhower recognized in authorizing the Interstate Highway system during the Cold War 1950s, it is vulnerable to attack from unexpected quarters. Although the U.S. public had become accustomed to peaceful stability within U.S. borders, the appalling events of September 11, 2001, require a shift in thinking. While the transportation system cannot be re-engineered in its entirety to cope with this new operational environment, a variety of coping strategies can aid in protecting its many modalities and components. Among these is a higher use of aerial and satellite imagery (and collateral sensor data from non-imaging systems), to obtain intelligence for situations that develop rapidly and which demand real-time decision-making.

The transportation system is extensive, complex and critical to maintaining the U.S. economy (see table 1). The Administration's report, *Securing the Homeland, Strengthening the Nation*[7], underscores the urgency in strengthening. transportation security. The proposed 2003 White House budget includes not only the establishment of a Transportation Security Administration within the Department of Transportation, but requests $4.8 billion "...to fulfill the mandates established by the [Aviation and Transportation Security Act of 2001]."

4.2 Potential of Image & Sensor Data for Improving Lifeline Security

Remote sensing technologies, together with other geospatial technologies such as GIS and PNT systems, have a significant role to play in the improvement of the Nation's transportation security and critical infrastructure condition assessment. Remote sensing from space combines a broad synoptic view with the ability to detect changes in surface features quickly and routinely. Remote sensing from aircraft provides the ability to examine areas in great detail from below the clouds, and ground-based systems make possible the close-in observation of events in real time. Each of these spheres of remote sensing technology hold benefits and drawbacks for use in

transportation, and in particular, for the security of the Nation's complex transportation networks.[8]

Examples of the use of remotely sensed data to support transportation security include the ability to:

1. Develop accurate digital terrain models and 3-D surface features as a means for modeling landforms along rights-of-way;
2. Visualize terrain from different perspectives, with the potential for developing threat cones and view sheds;
3. Classify vegetation types along transportation lifelines as a possible deterrent to concealment;
4. Detect, classify, and analyze temporal and spatial changes in surface features;
5. Identify facilities where topography or identifiable hazards (e.g., nuclear, chemical, fuel facilities), place communities at risk;
6. Analyze environmental factors quickly and effectively;
7. Merge real-time sensor output (video, bio-chemical sensors) with archived geospatial data;
8. Identify, characterize, and analyze a wide variety of risks to transportation networks through a gradual program of gathering image intelligence along rights-of-way;
9. Create detailed maps of an area that has suffered attack to assist in response.

The September 11 attacks have forced a reevaluation, not only of the security aspects of U.S. critical transportation infrastructure, but also of the nation's institutional policies toward access to and use of information. For example, current policies governing the collection, use, and sharing of critical geospatial information inhibit the most efficient use of these data in developing mitigation procedures and in responding to terrorist threats and actions. On the one hand, the potential for misuse of critical information has caused federal and state agencies to restrict access to information by removing it from the Internet and other public venues. On the other, combating the threat of terrorism and responding to future attacks will require more effective sharing and use of geospatial data and information. It will also necessitate within the geospatial community continued improvement of analytical geospatial methods and software directed at improving transportation security.

Accordingly, the nation needs new institutional policies to support coordinated efforts in support of improved transportation security and coordinated emergency response. The need for interoperability of communications systems is widely understood;[9] the need for interoperability of geospatial information is less well understood. Workshop participants recognized that meaningful progress toward preparing the nation to prevent and respond to attacks on elements of the nation's transportation networks required the coordinated effort of agencies across the federal government, among federal, state and local governments, as well as among government and private sector geospatial data providers and analysts. For example, it is little recognized by the general public that in addition to destroying two large buildings and killing nearly 3000 people, the attacks on the World Trade Center severely affected New York's transportation lifelines, making rapid response by emergency workers especially difficult. Throughout the cleanup process, transportation routings changed daily and even hourly, making timely map updates necessary. Although the agencies and individuals who responded to the challenges of saving lives and cleaning up after the attacks accomplished wonders despite having no advanced warning and working in extremely dangerous conditions, the lack of established coordination plans slowed their efforts. In effect the teams "made do" with what they could cobble together in terms of base data and imagery acquired by daily aircraft over flights, which

commenced on September 14, three full days after the attacks.[10] Fortunately, thanks to the many individuals and organizations willing to help, they were eventually able to provide coordinated mapping, GPS, and imagery information in a rapid fashion.[11] This coordination was more a reflection of individuals committed to dealing with a massive problem, than the result of prior planning by the responsible local, state, or federal agencies. These organizations could have put teams in place and worked more quickly and effectively if institutional policies of their various agencies had encouraged the sharing of information and responsibility for response.

The geospatial data and information developed for other uses can also support improvements in transportation security. One of the strengths of a geospatial information systems approach is that one comprehensive database for a region can support many different applications. For example, as several workshop participants noted, much of the information developed by state and local communities to support infrastructure planning can be used to mitigate the threat of terrorist attacks or to enhance the speed and effectiveness of emergency response teams in case of attack or natural disaster. However, to be fully useful in combating potential terrorist threats, the structure and content of geospatial databases, including remotely sensed imagery, will have to be reviewed for their applicability in improving transportation security. In some cases, the existing framework and transportation databases will need to be enhanced.

The need to improve critical infrastructure protection has created new requirements for remote sensing and GIS analysis. In order to reap the benefits of data and information from non-transportation sources, it will be necessary to develop analytical software designed especially for the security mission. Such software and methods need to be widely available to provide comparable analytical capabilities across the United States. New analytical methods in RS/GIS specifically devoted to the support of critical infrastructure protection could greatly strengthen the nation's ability to improve transportation security. Particular attention should be given to a significant, but limited number of critical transportation assets (e.g., pipelines, bridges, ports, inter-modal facilities), rather than attempting to develop functionalities that encompass everything.

Some remote sensing methods that have been developed for military applications may be transferable to civilian security use. However, civilian measures must consider economic, social, and legal aspects that are be less relevant in a purely military situation. The measures must be designed for high reliability. Needs include:

1. New methodologies and research to identify assess and monitor high value, highly vulnerable transportation facilities across the United States;

2. New methods of analysis and use of sensor and imagery assets to assess vulnerabilities, monitor assets, and aid in post-event recovery. For example, sensitive non-imaging sensors that can detect chemical, explosive, or radioactive plumes could help in monitoring container cargo ships from aircraft or bridges under which all ships in a port must pass.

Remote sensing technologies could be a major asset in identifying and mitigating transportation security weaknesses throughout the United States. In the past, security has not been a primary consideration in transportation planning. The U.S. transportation system as it now exists possesses many vulnerabilities that could have been avoided with careful advanced planning. For example, in some cases, critical infrastructure elements have by chance been co-located with high-value, vulnerable facilities, such as petroleum refineries or power plants. Such co-location

has been a matter of convenience or of a previous lack of concern about terrorist attack. Remote sensing technologies can in time assist in reducing some of these vulnerabilities. Over the longer term, the need for instituting extensive security measures can be reduced by preemptive planning of lifeline facilities to minimize the criticality of individual facilities to the network. The planning process should emphasize decentralization of facilities and redundancy of the functions of those facilities. In this way individual facilities, be they pipeline corridors or roadway conurbations, are reduced in their critical role in the network and their attractiveness as targets. Future planning and implementation of transportation lifeline facilities must have security as a primary consideration.

The United States needs to develop an accessible geospatial infrastructure corresponding to, and compatible with, the nation's transportation infrastructure. The resulting geospatial information should reflect all elements of the transportation infrastructure, and include detailed information on location, structure, condition, and other attributes. This information should be broadly accessible to transportation and security professionals. Improving the interoperability of transportation geospatial databases should be a high level priority in the attempt to enhance U.S. transportation security. Currently, in attempting to use transportation databases, users often experience limitations on availability, integration, and use of geospatial data and technologies for transportation security. Workshop participants pointed out that the information regarding the nation's information infrastructure is widely dispersed in a variety of databases, in a multiplicity of formats and software. Hence, many of these databases are not readily interoperable, making the task of using them especially difficult in times of crisis.

In particular, there is a lack of suitably interoperable technical standards, both for data sharing and for the operation of hardware and software. Although the Federal Geographic Data Committee (FGDC) has established federal standards for preparing and sharing geographic data, which have done much to improve interoperability of geospatial databases on the federal level, much more needs to be done on the state and local level to reap the benefits in times of crisis. State and local databases often lack sufficient interoperability in emergency situations, whether caused by natural disasters, human error, or deliberately by terrorists. Yet, most emergency situations involving transportation systems, either actively or passively, will involve state and local agencies and jurisdictions. The FGDC has recommended several actions that, if accomplished, would sharply improve the nation's security.[12] If extended to transportation, these recommendations would under gird the U.S. transportation security.

4.3 Value of Remote Sensing for Critical Infrastructure Condition Assessment

4.3.1 Imaging Sensors

Scalability: Literally hundreds of civil applications make use of remotely sensed imagery in a variety of analytical products. A multiplicity of image types has evolved to address specific applications, and many can also be used for transportation lifeline protection, if ingested and integrated into shareable databases. Imagery can be acquired across many scales and corrected geospatially to fit agency-specific map projections. For incident management, planners already have tools available to them for integrating coarse with fine resolution satellite views, and with more detailed high, medium, and low altitude aerial data sets from LiDAR and RADAR systems. The large number of demonstrated applications meeting industry and government standards should be systematically reviewed for their use in transportation lifeline security.

Spatial Relationships, Vulnerability, and Up-Dating: Urban planners have traditionally recognized the importance of tone, texture, size, shape, and spatial arrangement in analyzing landscape features. For transportation lifelines, most applications focused on right-of-way planning, engineering cut and fill measurements, feature identification, and land use classifications for map-making purposes. The imagery was generally archived or even destroyed after its immediate use was achieved. Where these archives can be retrieved, they represent a resource for measuring the rates and directions of lifeline infrastructure growth. These images also show the changing spatial relationships among urban features that might not be considered by planners until the post-recovery phase of an incident (for example, obstructions like fences between buildings and roads that would prevent rapid evacuations, or road designs that have changed from two-lanes to four-lanes with a median). Most important, time series imagery is scalable from the local level for which it was acquired, to smaller scales for which it will be required for incident management. In short, lifeline vulnerabilities develop over time and can only be efficiently catalogued, referenced, and assessed by examining the history of imagery of an area.

Data Mining & Visualization: For the more sophisticated needs of the 21st Century, transportation planners should recognize that time-series digital images represent a data archive that can be used to answer questions not yet posed. They are essential for responding quickly and efficiently to an emergency. Today's technology allows image archives (also called image pools) to be highly compressed for digital storage, and for them to be queried constantly for phenomena that are "out of the ordinary." Data mining algorithms can burrow through a set of chronologically arranged images (pixel-by-pixel if need be), and can be programmed to detect specific features, relationships, or trends that "trigger" an event or suggest locations where field personnel might visit. To take an example from the environmental realm, the ability to detect the future onset of El Nino episodes is enhanced by daily, seasonal, and annual data mining queries of sea surface temperatures in the equatorial Pacific. Future "episodes" of El Nino are being predicted on the basis of past occurrences melded with our growing understanding of the triggering mechanisms. Mathematical techniques such as rule-based systems and fuzzy logic help the data mining algorithms to interpret the intelligence contained in the images. We are, in effect, "teasing" information out of data in much the same way an accountant can find aberrant numbers in a column of numbers.

Visualization: Exciting opportunities abound for visualizing aspects of transportation lifelines. Visualization usually involves integrating digital elevation models (derived from either stereo photographs, LiDAR, or Synthetic Aperture Radar) with imagery and other geospatial data. Airport glide path obstructions, inter-modal facilities, underpasses, overpasses, flyovers, bridges, pipelines, international border crossings, port facilities, and railroad crossings are all candidates for 3-D visualizations and virtual reality, once the proper data structure and environment have been established. For several years, military pilots have trained for missions in new settings by "flying over" an area virtually using imagery gathered by satellite, draped over a digital elevation model of the area. For lifeline security planning, this capability alone may help thwart or mitigate incidents involving shipments of hazardous materials, or interdict possible terrorist activities, by showing swat teams the entire incident area before deploying human resources (for example, height of roadside embankments, locations and sizes of culverts, view sheds, and related incident attributes. Visualizations can, of course, be created without image backdrops, and for some

needs these may even be desirable; but for realistic, real-time, incident management, the actual ground area needs to be modeled. In the case of a hypothetical airport incident the use of high-resolution imagery could be used to provide overall situational awareness to supplement ground intelligence. Figure 1 illustrates the capability of the new quick bird II satellite system from Digital Globe that has a panchromatic resolution of 61 centimeters.

Detecting Subtle Landscape Changes: Change detection over time is one of the major advantages of remote sensing technology. Two change detection applications that have widespread appeal for lifeline safety and proven adaptability for incident management are detection of thermal patterns and subsidence zones. The former represents mature technology in use for the last 30 years or more, particularly in fire mapping. Hot spots at WTC ground zero were mapped in the days after September 11 and were used in recovery operations to direct ground crew operations. Figure 2 displays an image of these spots, collected by Earth Data International. These hot spots are detectable in the 3-5μm spectrum because they are much hotter than their surroundings. For detecting specific phenomena in the ambient landscape a sensor operating in the 8-14μm spectrum would be used (for such phenomena as ship wakes, contrails, cool spots left by parked vehicles), all of which represent intelligence for counter terrorism or illegal activities.

Detecting subsidence patterns is a less mature technology, but one having proven transportation lifeline safety applications that should adapt well to incident management and planning. Subsidence occurs frequently in areas where ground water withdrawals exceed recharge on a seasonal or annual cycle. Subsidence is also a characteristic of active earthquake zones. Interferograms produced from time series of synthetic aperture radar phase data are capable of detecting subsidence on the order of centimeters; enough to endanger pipelines, rail lines, and highways, and enough to damage bridges and make on- and off-ramp speeds unsafe. Figure 3 shows an area along the northern coast of California where seasonal subsidence occurs.

Monitoring Consequences of Incidents: Recovery from damaging incidents, natural or otherwise, is an ongoing element of security, public safety planning and infrastructure condition assessment. Relief and health officials need to know where the transportation lifelines have been disrupted, which avenues are still available for evacuation, which structures are safe, or where evacuees are beginning to congregate. Image analysis within GIS architecture can assist to develop this information. An example is the airborne imagery[14] shown in figure 4 of the condition of an interstate highway interchange following the North Ridge Earthquake in California. This data was used in the initial response phase and when integrated with other information was used as part of the recovery and reconstruction-planning phase. Digital imagery can also be used to directly assist the local condition in disaster recovery events such as the tornado damage characterization shown in figure 5. This is digital frame camera data that was used for damage assessment and emergency response following a tornado that occurred on June 1, 1998 in Mechanicsville, New York.

4.3.2 Non-Imaging Sensors

Detect Precise Object Locations at a Precise Time: The constellation of global positioning system (GPS) satellites is a well-known and widely used capability for pinpointing the locations of objects on Earth and for navigating between points. A companion capability develops data from an inertial measurement unit (IMU) to translate platform location to precise object locations on the ground. In day-to-day office environments, object locations can be adequately derived from using imagery analyzed by soft-copy photogrammetric

techniques and integrated with traditional GIS datasets; but incident management may require the determination of spot locations, or to the ability to follow objects moving along lifelines. These capabilities are possible and need to be incorporated into the stable of operational techniques employed at local and regional levels. Because the GPS satellites also broadcast precise time signals, they are also highly useful for recording the precise time of events, which may be critical in certain applications.

Detect Biological and Chemical Agents: Some remote sensors are designed to detect and analyze the chemical constituents of gases emanating from objects. Recently developed technologies also include techniques capable of detecting trace amounts of gases (in the parts per million range, and finer). These are non-imaging multi-spectral sensors that can be "tuned" to find specific chemical compounds in a complex atmosphere of numerous gases. Sometimes called "snifters," such devices could be deployed over multimodal transfer points and international border crossings to identify suspicious containers, railroad cars, or trucks. Harbor facilities might also monitor movements of ships and other watercraft by installing snifters on uninhabited aerial vehicles (UAVs) that can stay aloft for anywhere from a few hours to several days or weeks. Within territorial waters, these devices might also be mounted on helicopters for monitoring ships well before they enter harbor areas.

4.4 Transportation Infrastructure Threat Reduction

Transportation organizations at all levels face unprecedented challenges today. Increasing demands are being placed on agencies to preserve the existing transportation system and to take on new missions of improved system safety and security. A variety of advanced technologies are available to enhance planning, designing, managing, operating, and maintaining all modes of transportation. Aerial and satellite remote sensing represents one area of rapid development that can be leveraged to address these challenges. These technologies have significant and unique potential for application to a number of cross cutting transportation security issues.

Advances in geospatial sensors, data analysis methods and communication technology present new opportunities for users to increase productivity, reduce costs, facilitate innovation and create virtual collaborative environments for addressing the challenges of security improvement for all modes of transportation. Sensor developments include a new generation of high-resolution commercial satellites that will provide unique levels of accuracy in spatial, spectral and temporal attributes. An example is shown in figure 3 using data from the Digital Globe's commercial Quick Bird satellite to image a portion of Reagan National Airport at a spatial resolution of sixty-one centimeters. This provides a degree of detail not available previously to the civil transportation community from space based sources. In addition to the high resolution panchromatic imagery illustrated above there are a number of other commercial imagery products that are potentially applicable to transportation. They include air borne and satellite radar, LIDAR, multi-spectral, and hyper-spectral sensors. There is a range of spectral and spatial resolution capabilities for each of these sensor systems. Part of the challenge is matching the best sensor to the specific transportation related application.

Visualization and advanced data analysis methods are also important capabilities. Automated change detection within a defined sector is one example of analysis capability that will assist in detection of unauthorized intrusion events. A specific application of these techniques to transportation security is unauthorized right of way intrusion on pipeline systems. Pipelines often cover thousands of miles and are located in remote areas that are difficult

and expensive to monitor. Canada is experimenting with the use of satellite imagery to assist in monitoring of pipeline rights of way to detect unauthorized intrusion onto pipeline right-of-ways in a remote area.

These geospatial technologies and data analysis capabilities can also be applied to the evolution of other new methods and approaches for enhancing the safety and security of critical transportation systems and infrastructure. The geospatial area is a family of technologies that is in transition. The speed of geospatial product delivery will continue to get faster while the cost goes down. As the use of geospatial produces increases there will be an expansion in new software tool development. There will also be continued improvement in imagery resolution and the quality of derived products. There are a number of transportation related applications of geospatial technology. These include: site assessment and investigation, monitoring critical transportation corridors, designing security systems, monitoring critical infrastructure, rapid change detection over wide areas and security data and system integration.

There remain a number of challenges that may slow or impede the application of geospatial technologies to the transportation sector. These include the need for improved methods and authorities for better data sharing across institutional boundaries. The developed and user communities need to communicate better and overcome some significant disciplinary differences. There are also some very challenging technical issues in the multi-sensor data fusion area to be overcome. Finally, there is a need for a focused interdisciplinary effort for the development of geospatial transportation priorities and the identification of specific product requirements.

5.0 CONCLUSIONS

It is clear that despite excellent efforts by many groups the approach to providing information for infrastructure condition assessment in emergencies is not effectively utilizing a wealth of data that resides, with various organizations. This existing information and technology could provide mangers important decision support products that could save lives, reduce damage to property, and lessen environmental impacts. The current situation is characterized by numerous shortcomings that inhibit optimal decision making for emergency management. The inability to access information and the lack of standardization, coordination, and communication are all obstacles that need to be overcome. In addition there are tools in the geospatial information area that could contribute immensely to infrastructure management in emergencies and in more routine operational situations. One of the ways to accomplish these aims is to make more effective and timely use of aerial and satellite surveillance and monitoring technologies. The challenge is how to adapt the existing capabilities of image-derived intelligence in the short-term to fit new operating circumstances, and what new ways of doing business will we need in the long-term to develop an infrastructure that is resilient to various forms of attack.

Advances in Information systems, satellites imaging systems and improved software technologies have led to opportunities for a new level of information products from remote sensed data. The integration of these new products into existing disaster response systems can provide a wide range of analysis tools and information products that were not possible before. For example, with the higher resolution imagery change detection for building damage assessment can be conducted rapidly and accurately with these new data sources. Transportation infrastructure and system wide situational awareness over a broad area could also be addressed using remote sensing data sources. In the area of spectral sensing new hyper-spectral sensing systems will allow

detection and identification of specific surface materials, air and surface pollutants and ground vegetation types. All of these information products can be useful in the response, recovery, and rehabilitation phases of infrastructure management prepardness.

The strength of any paradigm shift is realized if new questions can be answered along with traditional ones. Using remote sensing technologies combined with information sharing will address many, if not most, traditional safety, hazards, and disaster issues facing infrastructure managers, as well as provide for those raised by deliberate acts of aggression. Despite technological advance, disaster risk continues to grow. Infrastructure emergency managers and others continue to be called on to make decisions during disaster events, as well as in the pre-and-post disaster phases, with incomplete information. In order to make optimal decisions to reduce the loss of life and property, stakeholders uniformly must be able to obtain the needed information in a format that is appropriate for their capabilities. There is also the need for parties at great distances from each other to be able to share information in a seamless fashion that also allows the shared information to be interactive with local data and be used to create new integrated products tailored to the situation.

6.0 REFERENCES

1. NRC Report, Information Infrastructure for Managing Natural Disasters, Board on Natural Disasters, National Academies Press, 1998

2. Tobin, Graham A., and Burrell E. Montz, *Natural Hazards: Explanation and Integration*, New York, NY: The Guilford Press, 1997

3. Burton, Ian, Robert W. Kates, and Gilbert F. White, *The Environment as Hazard, 2d Edition*, New York, NY: The Guilford Press, 1993

4. NRC Report, Information Infrastructure for Managing Natural Disasters, Board on Natural Disasters, National Academies Press, 1998

5. NAPA Report, *Geographic Information for the 21st Century: Building a Strategy for the Nation*, National Academy of Public Administration Press, 1998

6. Disaster Information Task Force Report, Harnessing Information and Technology for Disaster Management, Global Disaster Information Network, 1997

7. http://whitehouse.gov/homeland_security_book.html

8. Roper, William, *Geospatial Technology Support to the Nation's Navigation System*, Transportation Research Board, National Research Council, Washington, DC, January 1999

9. http://www.whitehouse.gov/homeland/

10. Statement of Bruce Baughman Office of National Preparedness, Federal Emergency Management Agency, before the Committee on Transportation and Infrastructure, Subcommittee on Economic Development, Public Buildings, and Emergency Management, U.S. House of Representatives, April 11, 2002.

11. Jerry Dobson, "How Will GIS Help Fight the War on Terrorism?" *GEOWorld: http://www.geoplace.com, November2001.*

12. Bruce Cahan and Matt Ball, "GIS Ground Zero: Spatial Technology Bolsters World Trade Center Response and Recovery," *GEOWorld: http://www.geoplace.com, January 2002.*

13. "Homeland Security and Geographic Information Systems,"

http://www.fgdc.gov/publications/homeland.html

14. Jensen, John, R. Remote Sensing of the Environment: An Earth Resource Perspective, Prentice-Hall, Inc. Upper Saddle River, NJ, pp 463-467, 2000

7.0 LIST OF TABLES AND FIGURES

Table 1: Estimated size of America's Transportation System (Source: DOT/RSPA

Figure 1: Digital Globe Satellite image of Regan National Airport at 61 cm spatial resolution

Figure 2: Image from the Multi-spectral Thermal Imaging Satellite of DOE, which was used to better understand hot spots during the World Trade Center recovery

Figure 3: Illustration of interferometry to identify subsidence risk areas along the coast of northern California

Figure 4: Imagery of bridge failures following the Northridge Earthquake in California, January 22, 1994

Figure 5: Imagery used in damage assessment and recovery planning following a tornado in Mechanicsville, NY

System	Infrastructure	Use
Highways	210 million vehicles 4 Million miles of road 500,000 bridges (1/3 of 127,00 urban bridges serve as major arterials	4 trillion passenger miles 920 billion freight ton miles
Rail	18 million railroad cars 250 inter-city Amtrak trains 150,000 track miles	20 million passenger miles 1.3 trillion ton-miles
Aviation	175,000 aircraft 5,500 public use airports	403 million passenger miles
Waterways	12 million watercraft 25,000 miles of waterways	600 billion ton-miles of oil Plus 958 billion ton-miles of other bulk commodities
Ports	Freighters, trucks, barges, rail cars	Million per year through major U.S. ports
Pipelines	1.6 million miles	19 trillion cu. ft. of gas

Table 1: Estimated size of America's Transportation System (Source: DOT/RSPA)

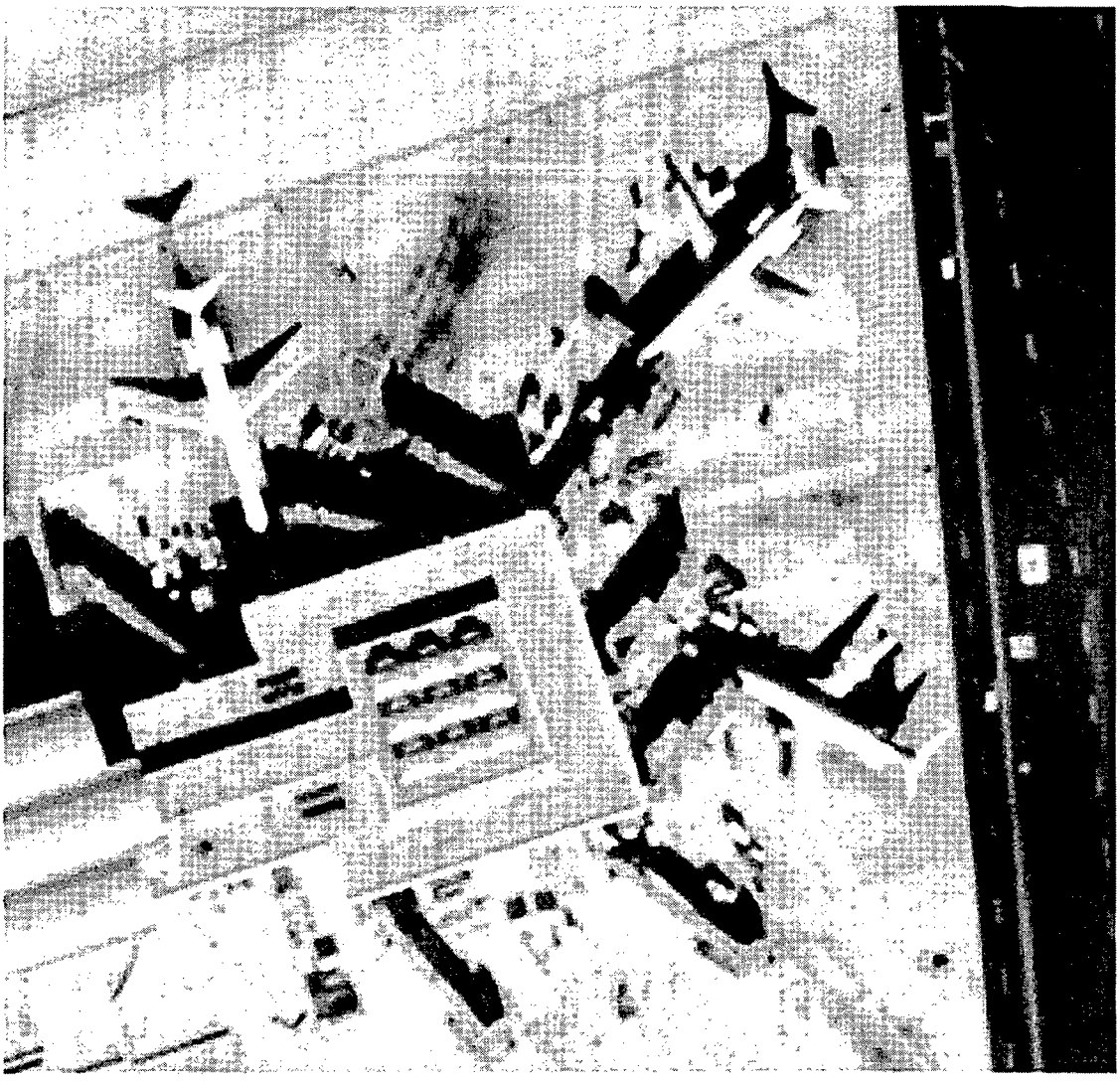


Figure 3: Digital Globe Satellite image of Regan National Airport at 61 cm spatial resolution

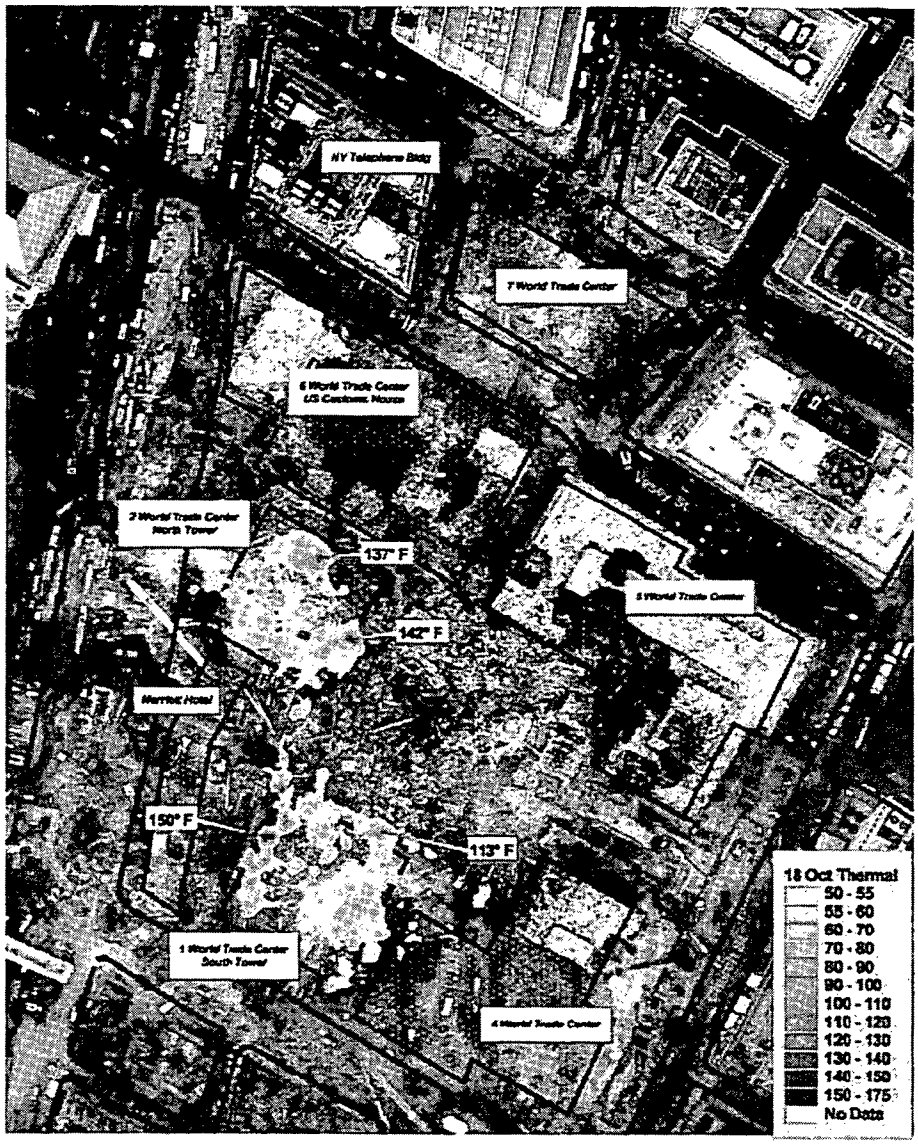


Figure 1: Image from the Multi-spectral Thermal Imaging Satellite of DOE, which was used to better understand hot spots during the World Trade Center recovery

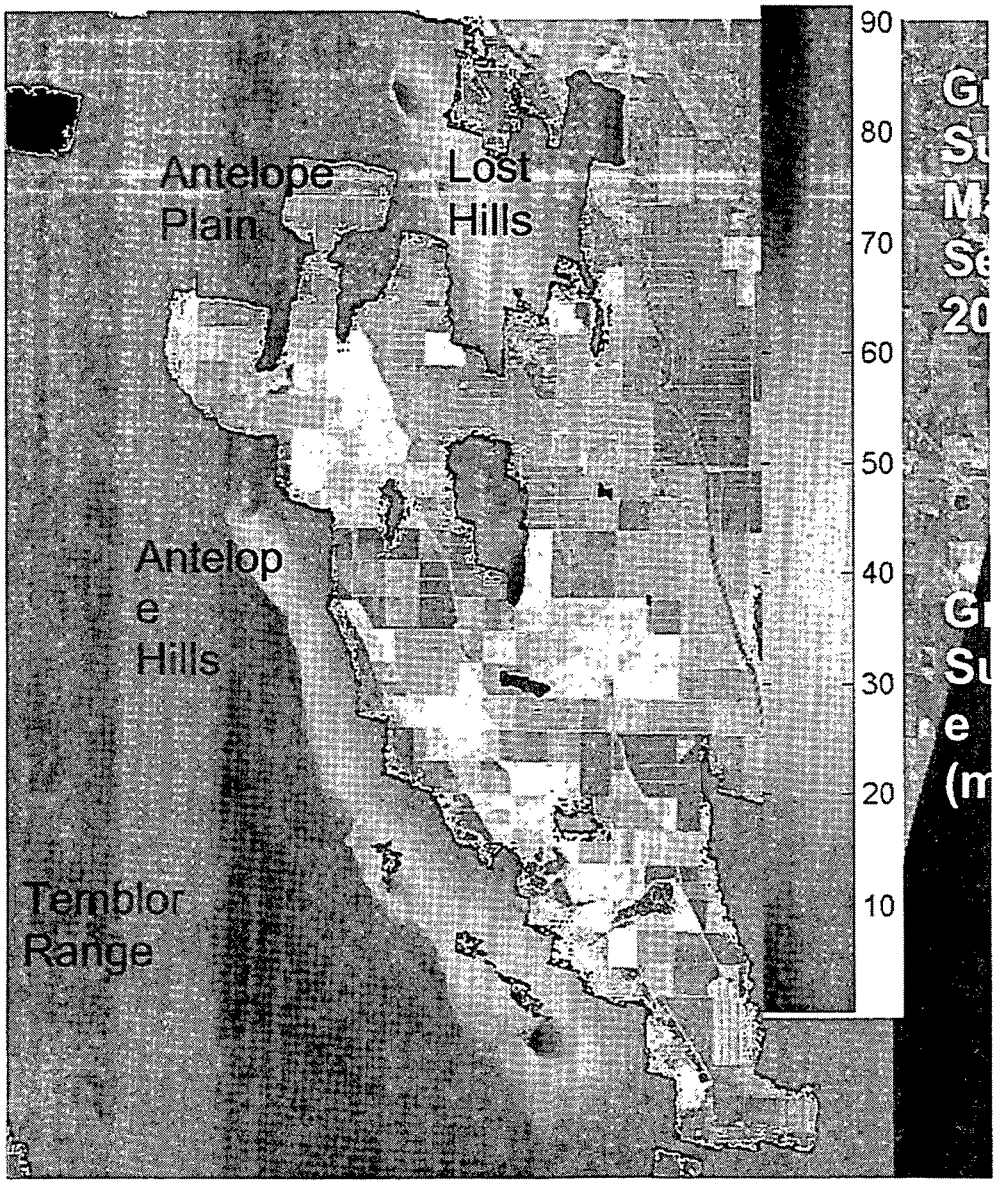


Figure 2: Illustration of interferometry to identify subsidence risk areas along the coast of northern California

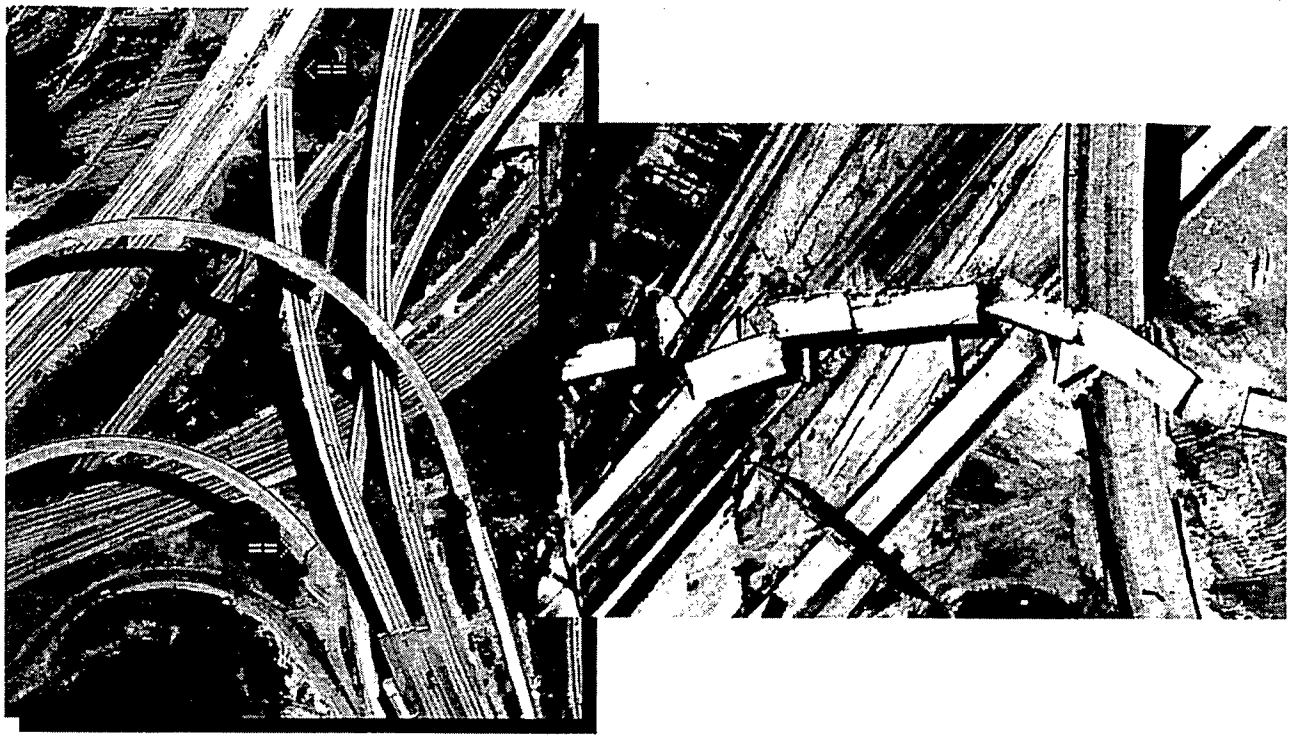


Figure 4: Imagery of bridge failures following the Northridge Earthquake in California, January 22, 1994



Figure 5: Imagery used in damage assessment and recovery planning following a tornado in Mechanicsville, NY

Geomorphologic Survey for Hazard Mapping and Real-Time GIS, Aided with LiDAR Technology

by

Sotoshi Nakata*, Seiji Ichikawa*, Koji Sango*, Masaharu Tsuzawa*,
Jun-ichi Kisanuki*, and Soichiro Sato*

ABSTRACT

This paper presents the current trend of Geomorphologic Survey for Hazard Mapping by Geographical Survey Institute. This survey has become a combined survey with land-condition survey for flood disasters, land condition survey of volcano for volcanic disasters, and basic mapping of volcano. For the demands of geographic data for real-time hazard mapping, GSI introduce airborne laser scanning and satellite imaging technology to improve thematic mapping..

KEY WORDS
Land-condition Map, Hazard Map, Airborne Laser Scanner, Digital Elevation Model, Digital Terrain Model, Digital Surface Model, Real-time

1. ORIGIN OF SURVEY

1.1 Thematic Mapping for Natural Disasters

On the day 26 September 1959, Typhoon No.15, named "Ise-wan Typhoon" as following disaster, rushed to the coast area of Ise Bay, and generate storm surge by its strong wind and low pressure. The highest tide of Nagoya Port was 3.89m during this event. Most of embankment along bay coast and river streams was overflowed or break, and southern part of Nobi Plain was inundated, 4624 lives were lost.

Just before this largest flood disaster of modern age in Japan, one thematic map sheet was compiled from the national committee of natural resource, organized by Japan's Government. After World War II, geomorphological study was expanded by free utilization of aerial photograph. The thematic map "Geomorphological Map of Nobi Plain for Flood Control" was the result of geomorphological survey by photo-interpretation. Just after the disaster, geomorphologist found obvious correlation between inundation area and detailed landform of plain (Fig.1). Since then, geomorphological survey became principal means for flood control works. Land-condition Map, product from Geographical Survey Institute, hereinafter "GSI", is the one of typical result of geomorphological survey for flood control. Recently, volcanic disaster also became one object of geomorphological survey.

1.2 Hazard Mapping depend on Law

On the day 11 September 2000, Typhoon No.14 generated humid south wind, which brought heavy rainfall to central Japan. River streams overflowed into built-up area of Nagoya City, this flood ruined many properties of the city (Fig. 2).

After that disaster, Flood-Fighting Law was altered to give each obligation on hazard mapping to local government and river improvement office. River improvement office has to publish the result of simulated inundation area and depth. Local government has to announce the inundation area with hazard map. Since then, hazard mapping became national administration matter. In response to this matter, GSI decides to produce geographic information for hazard mapping; one layer is the landform classification by geomorphologic survey for zoning of flood types, the other is detailed digital elevation model surveyed by Airborne Laser Scanner, hereinafter "LiDAR", for the simulation of inundation area.

* Geographical Survey Institute



Fig.1: Disaster Map of Ise-wan Typhoon.

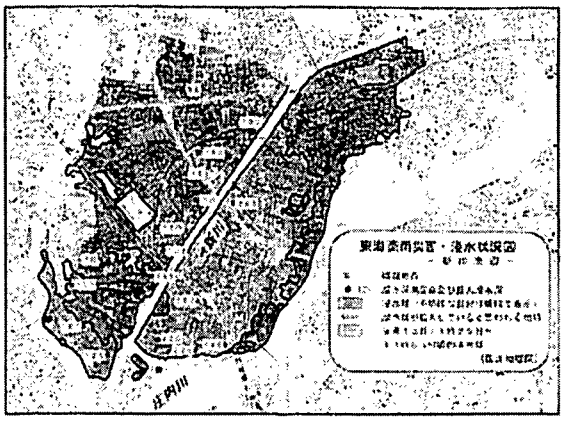


Fig.2: Disaster Map of the flood 2000 in Nagoya City

2. THEMATIC MAPS FOR DISASTERS

2.1 Land-condition Survey

GSI has been carrying out geomorphologic survey to produce thematic map series for disaster prevention, for half century. This map shows landform classification depends upon uniformed legend, and 1m-interval contour of detailed ground elevation of alluvial plane. Landform classification is from photo-interpretation and field survey. Ground elevation is surveyed from levelling and photogrammetry. Results of this survey are printed map-sheet, in scale 1:25,000,(Fig.3) or digital geographic data. Printed map-sheets are published from Japan Map Center.

2.2 Land-condition Map of Volcano

This thematic map series began in 1988. Each map shows landform classification of each volcano, which is reflected by development of eruption or erosion. Objective volcanoes are selected from the list of active volcanoes by the study plan of Working Group for Volcanic Eruption of Japan Science Academic Council.

Printed map-sheets of this series are published from Japan Map Center.

Every volcano has their each characteristic history of its activity, so that legend of landform classification is specialized for each volcano, as followings;

Mt. Bandai (Fukushima-pref.): During its development history, huge collapses and debris-avalanches occurred at least five times. Deposit of debris avalanche formed characteristic landform "Flow Mounds" on foot of the volcano. Land-condition Map shows detailed distribution of them and the relationship between multiple stage of volcanic bodies and debris avalanche (Fig.4).

Mt. Fuji (Yamanashi-pref., Shizuoka-pref.): This is the largest active volcano of Japan, however it has not been recognized as active by the majorities of Japanese nation, for the reason that there have been scarcely any activities without femoral for almost three centuries after huge eruption of 1707. In 2000, low-frequency earthquakes were observed frequently just below the summit crater. That brought new understanding of Mt. Fuji as active. Japanese government establishes Investigation Committee for Hazard Mapping of Mt. Fuji. GSI cooperates this committee by geomorphologic survey for land-condition map of volcano. At this survey, the legend of landform classification of Mt. Fuji emphasizes distributions of debris and corridors of slash-avalanche, which is the most characteristic event of disaster on slopes.

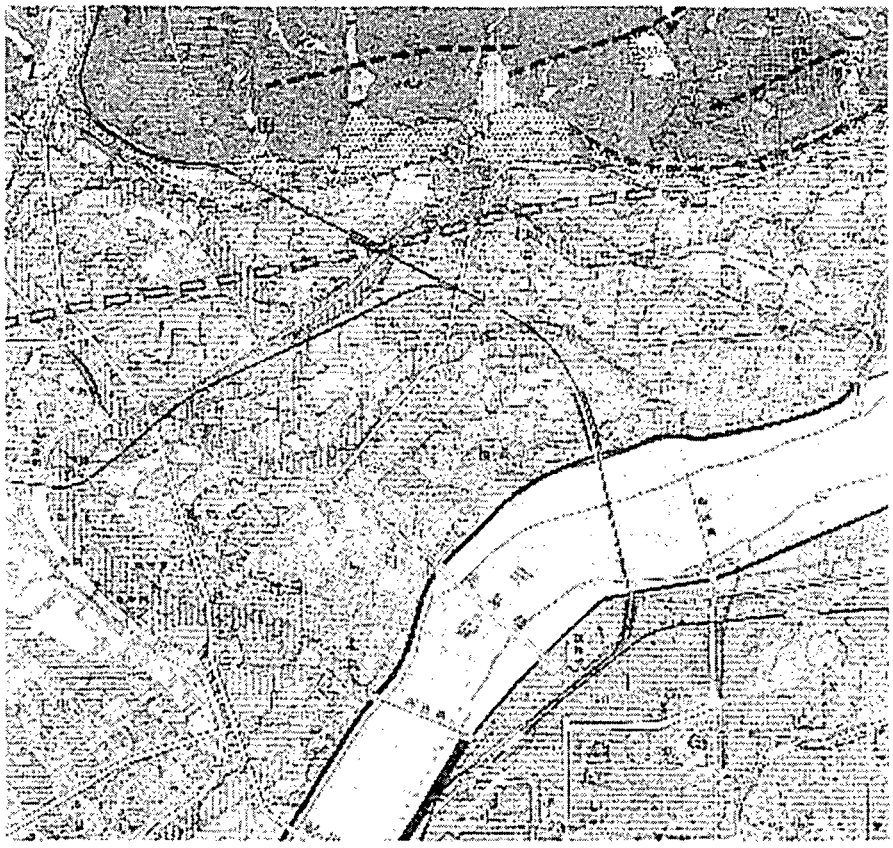


Fig.3: Land-condition Map (1:25,000) "Wakayama"



Fig.4: Land-condition Map of Volcano (1:30,000) "Mt. Bandai"

2.3 Volcanic Base Map

This is the kind of basic map series with specialized format for active volcano (Fig.5). Principal data of this series is 5m-interval contour of elevation, which is surveyed by photogrammetry. Printed map sheets are published from Japan Map Center.

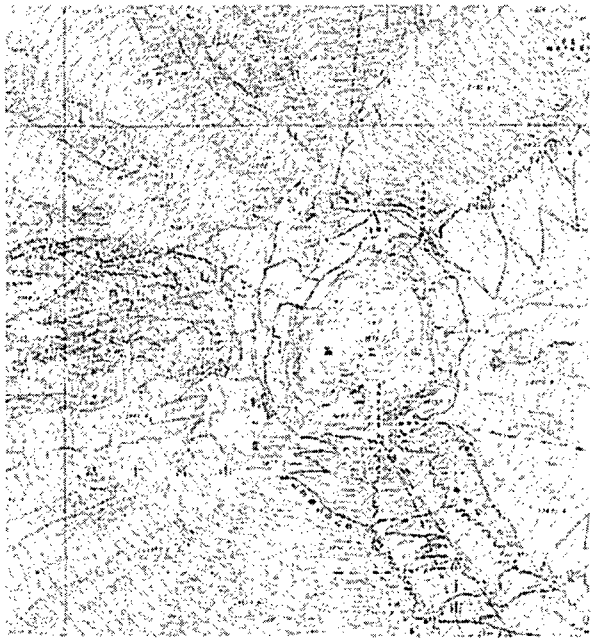


Fig.5: Volcanic Base Map "Summit of Mt. Fuji".

2.4 Digital Elevation Model 10m Grid

This digital elevation model is compiled from elevation contour of Volcanic Base Map (Fig.6). CD-ROM is published from Japan Map Center.

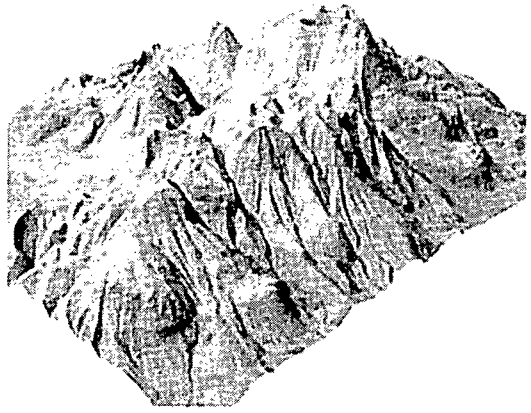


Fig.6: Bird's eye view, calculated from DEM

3. DTM BY LIDAR

3.1 Need for Flood Simulation

In 1975, Ministry of Construction published two types of disaster map; one was the observed inundation area map, the other was a estimation map of flood. This was the first hazard information map of flood, to citizens, as compared with Land-condition map, which was for professional use (Ichikawa, 2001). In 1994, Ministry construction established Guideline for Hazard Mapping for Flood Disaster. In 2001, Flood-Fighting Law was altered to give each obligation on hazard mapping to local government and river improvement office. River improvement office has to simulate inundation area and flood depth for publication.

Simulation of inundation area and flood depth is calculated at each estimated overflow point, by digital elevation model. Map of simulated inundation area shows every maximum depth of each grid (Akagiri, 2001). Standard grid size has been 500m, recently grid size is becoming to 250m.

3.2 Air-born Laser Survey

Principal instrument of this survey is Air-borne Laser Scanner, or LiDAR. Air-borne Laser Scanner is the combined technology with GPS, IMU, and Laser-pulse Profiler. This system enables us to get three-dimensional data in whole surveyed area (Fig.7). Each laser-pulse is reflected at plural points; surface of house or building, canopy of tree, and ground surface (Gig.8).

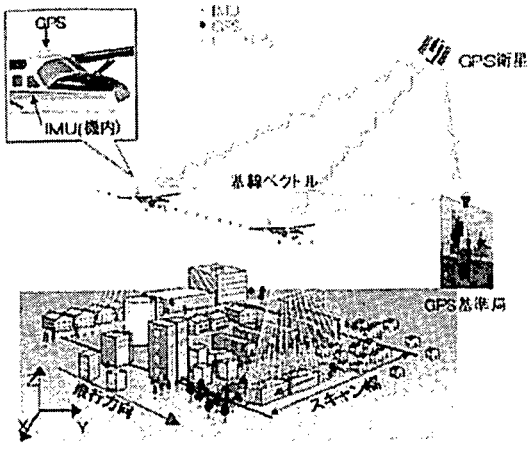


Fig.7: Air-borne Laser Scanning System

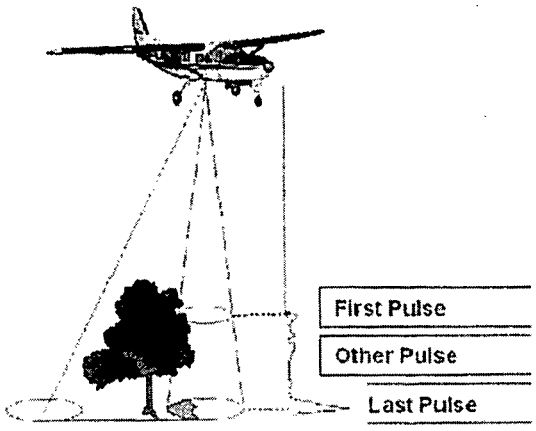


Fig.8: First Pulse, Other Pulse, and Last Pulse

3.3 Digital Terrain Model 5m Grid

This is a new series of digital map from GSI. Such high-density grid data could be obtained by air-born laser survey. Original scanned data is composed of several types of positioning points; surface of man-made structures, canopies of trees, and ground surface, in each grid. Digital Surface Model covers whole surface elevation with buildings and vegetation. Digital Terrain Model is filtered data for representation of ground elevation. Fig.8 shows shading figure of western part of Saitama City, calculated from Digital Terrain Model 5m Grid "Saitama South-East". Compared with Land-condition Map "Ohmiya", blue or green colored area is alluvial plane along Ara-kawa River. Detailed landforms, Natural Levee or Former River Channel could be recognized on both maps.

In case of the Digital Terrain Model 5m Grid "Saitama South-East", air-borne laser survey was done by cooperation between GSI and Ara-kawa River Lower Reaches Work Office. At this river improvement office, flood simulation shall be calculates from 50m mesh in immediate, and it is already possible to get more accuracy for the simulation.



Fig.9: Shading Image of Alluvial Plain along Ara-kawa River in Suburban area of Saitama City.

4. REAL-TIME HZARD MAPPING

4.1 Subject for Improvement of Geomorphologic Survey for Hazard Mapping

Publishing Data of the survey composed from Landform classification and detailed elevation.

The demands for such geographic data will increase rapidly, by two backgrounds. One is the obligation of hazard mapping by each local government, originated from Flood-fighting Law. The other is the mitigation of tsunami disasters along the coastal area. Latest reports of Central Disaster Mitigation Council warn that estimated Tokai, To-Nankai, and Nankai Earthquakes generate large tsunami. For more rapid survey, several new technologies must be use for practical.

Air-born laser survey shall relieve from levelling and photogrammetry for the production of detailed elevation data.

Advanced investigations realize that calculation of digital terrain model is effective for geomorphological analysis; extraction of detailed landform or knick lines (Kamiya et al.).

Advanced Land Observing Satellite (ALOS) is planning to be launched in 2004. Part of objectives of ALOS is as followings; providing maps for Japan and other countries, conducting disaster monitoring around the world. The sensor, Panchromatic Remote-sensing Instrument for Stereo Mapping (PRISM) produces wide range 2.5-meter spatial resolution with stereo pair, periodically. Printed image of resolution expects to be used as ordinary aerial-photograph, in practical. Especially, nadir view image becomes almost orthogonal projection, so that the results of interpretation could transport on basic cartographic data.

Table. Major Specifications of ALOS/PRISM

Observation Band	0.52 - 0.77μm (Forward-Nadir-Backward)
Base/Height ratio	1.0
S/N	70
Spatial Resolution (IFOV)	2.5m (3.57μrad)
MTF	0.20
Swath Width	35km
Pointing Angle	±1.5° (cross track)

4.2 Needs of Real Time Hazard Mapping

After the occurrence of natural disaster, it needs not only fixed information, but also real time renewal information by circumstantial condition, on GIS, for rescue, refuge, restoration, secondary warning, and reconstruction. GSI and National Institute for Land and Infrastructure Management participate the development project for integrated technology "Real Time Disaster Information".

Subjects by GSI are as followings; Real time analysis of crustal movement by GPS, Quick calculation of air-born laser scanning resolution, and standardize of geographic data for common use on GIS. Fig.10 shows the utilization model of Real Time Disaster Information System.

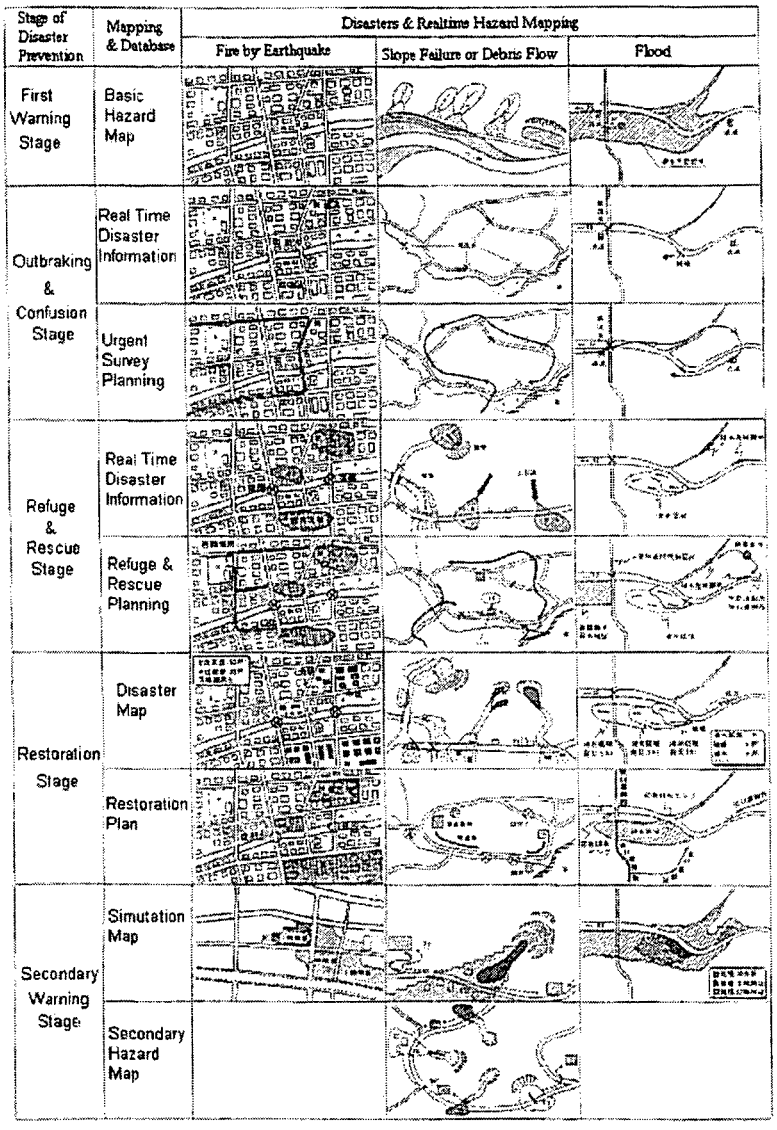


Fig.10: Connectional Timetable for Real Time Hazard Mapping (Tsuzawa, 1992)

Bibliography:

Akagiri, T. et al. (2001): Hazard Map for Flood Disaster – Current Status and Future – . Map Journal, 133, autumn, 16-23.

GSI (1972): "Land-condition Survey – Tokyo and its Surroundings – "

Ichikawa, S. (2001): Development of Hazard Mapping. The Journal of Survey, 52, 2, 41-46.

Kamiya, I. et al. (1999): Production of Slope Map and its Application. Geoinformation, 10, 2, 76-79

Kamiya, I. et al. (2000): Interpretation of Geomorphology and Geology using Slope Gradation Map

NASDA (2003): "Advanced Land Observing Satellite"

Oya, M. (1956): Geomorphological Map "Nobi Plain – Lower Reach of Kiso-gawa River", National Committee of Natural Resource.

Tsuzawa, M. (1992): Disaster Information System – Digital Mapping for Disaster Prevention. APA, 53, 1, 1-14.

THEME 6

Wind Engineering

Wind-Induced Vibration of Stay Cables: Summary of FHWA Study

by

Nicholas P. Jones[1] Thusitha Kumarasena[2], Peter Irwin[3], and Andreas Felber[4]

ABSTRACT

A study sponsored by the US Federal Highway Administration was recently completed in order to develop a set of consistent design guidelines for mitigation of excessive cable vibrations on cable-stayed bridges. In order to accomplish this goal, the Project Team started with a thorough review of existing literature to determine the state of knowledge and identify any gaps to be filled in order to enable the formation of a consistent set of design recommendations. This review indicated that while the rain/wind problem seemed to be known in sufficient detail, galloping of dry inclined cables was a critical wind-induced vibration mechanism in need of further experimental research. A series of wind-tunnel tests was performed to study this mechanism. Analytical and experimental research was performed to study mitigation methods, covering a range of linear and non-linear dampers and cross-ties. The study also included studies on live load induced vibrations and establishing driver/pedestrian comfort criteria.

Based on the above, design guidelines for mitigation of wind-induced vibrations of stay cables were developed. This paper summarizes the important findings from that study. Much of the text that follows is extracted in summary form from the report that was coauthored by all the project investigators listed above.

KEYWORDS: bridge engineering, long-span bridges, stay-cable vibration, wind engineering, wind-rain vibration.

1.0 INTRODUCTION

Cable-stayed bridges have become the structural form of choice for medium to long span bridges over the past several decades. With their increasingly widespread use, some cases of serviceability problems with large amplitude vibrations of stay cables due to environmental conditions have surfaced. A significant correlation had been observed between the occurrence of these large amplitude vibrations and occurrences of rain combined with wind, leading to the adoption of the term "rain/wind vibrations." However, a few instances of large amplitude vibrations have also been reported (in the literature) without rain.

In 1999, the Federal Highway Administration (FHWA) commissioned a study team led by HNTB Corporation and three subconsultants, Johns Hopkins University, Rowan Williams Davies & Irwin, Inc. (RWDI), and Buckland and Taylor, Ltd. to investigate wind-induced vibration of stay cables. The Project Team represented expertise in cable-stayed bridge design, academia, and wind engineering.

By this time, a substantial amount of research on this subject had already been conducted by researchers and cable suppliers in the U.S. and abroad. This work has established water rivulet formation and its interaction with the wind flow as the root cause of the rain/wind vibrations. With this understanding, various surface modifications had been proposed and tested with the aim of disrupting this water rivulet formation. Recently developed mitigation measures such as "double

[1] Professor and Head, Dept. of Civil and Environmental Engineering, University of Illinois at Urbana-Champaign, Urbana IL 61801, USA (formerly Johns Hopkins University.)
[2] HNTB Corporation, 75 State St., Boston, MA 02109 and 352 Seventh Ave., 6th Floor, New York, NY 10001-5012
[3] Rowan Williams Davies & Irwin, Inc., 650 Woodlawn Road West, Guelph, Ontario N1K 1B8
[4] Buckland and Taylor, Ltd., Suite 101, 788 Harborside Drive, North Vancouver, BC V7P3R7

helix" surface modifications as well as traditional measures such as external dampers and cable cross-ties have been provided to many of the newer bridges. However, the lack of a uniform criteria or a consensus in some of the other key areas such as large amplitude galloping of dry cables has made the practical and consistent application of the known mitigation methods difficult.

The objective of this FHWA sponsored study was to develop a set of uniform design guidelines for vibration mitigation for stay cables on cable-stayed bridges. The project was subdivided into the following distinct tasks:

- Task A: Develop electronic database of reference materials
- Task B: Develop electronic database of inventory of U.S. cable-stayed bridges
- Task C: Analysis, evaluation and testing
- Task D: Assessment of mitigation approaches
- Task E: Identification of research needs
- Task F: Project documentation

The initial phase of the study consisted of a collection of available literature on stay cable vibration. Due to the large volume of existing literature, the information was entered into two electronic databases. These databases were developed to be user friendly, have search capabilities, and also facilitate entering of new information as it becomes available. The databases have been turned over to FHWA for future maintenance. It is expected that these will be deployed over the internet for use by the engineering community.

The Project Team conducted a thorough review of the existing literature to determine the state of knowledge and identify any gaps that must be filled to enable the formation of a consistent set of design recommendations. This review indicated that while the rain/wind problem is known in sufficient detail, galloping of dry inclined cables was the most critical wind-induced vibration mechanism in need of further experimental research. A series of wind-tunnel tests was conducted at the University of Ottawa propulsion wind tunnel to study this mechanism.

The Project Team obtained additional funds from Canada's National Engineering and Sciences Research Council (NSERC) for the testing at the University of Ottawa, effectively doubling the original funding for the wind tunnel testing task. The Project Team also supplemented the study by incorporating work of its key team members on other ongoing, related projects.

Analytical research was also performed covering a wide spectrum of related issues, such as the behavior of linear and nonlinear dampers and cable cross-ties. The research also included brief studies on parametric excitation and establishing driver/pedestrian comfort criteria with respect to stay cable oscillation.

Based on the above investigations, design guidelines for mitigation of wind-induced vibrations of stay cables were developed. It must be noted that this is the first time such design guidelines have been proposed. They are meant to provide a level of satisfactory performance for stay cables with respect to recurring large amplitude stay oscillations due to common causes that have been identified to date, and are not intended to eliminate stay cable oscillations altogether (as this would be impractical).

It is expected that these guidelines can be suitably refined based on future observations on actual performance of stay cables in bridges around the world as well as developments in stay-cable technology. With the widespread recognition of the mitigation of stay cable vibration as an important design issue among long-span bridge designers, all new cable-stayed bridges are more than likely to incorporate some form of mitigation discussed in this document. This would provide ample future opportunity to measure real life performance of bridges against the design guidelines contained herein.

As a precautionary note, the state of the art in mitigation of stay cable vibration is not an exact science. These new guidelines are only intended for use by professionals with experience in cable-stayed bridge design, analysis, and wind engineering, and should only be applied with engineering judgment and due consideration of

special conditions surrounding each project.

2.0 COMPILATION OF EXISTING INFORMATION

2.1 Reference materials

An extensive literature survey was initially performed to form a baseline for the current study. An on-line database of references was created so that all members of the Project Team could add or extract information as necessary. The database had 198 references and includes the article titles, authors, reference information, and abstracts when attainable and has built-in search capabilities.

2.2 Inventory of U.S. cable-stayed bridges

An inventory of cable-stayed bridges in the United States was created to organize and share existing records with the entire Project Team. This database includes information on geometry, cable properties, cable anchorages, aerodynamic detailing, site conditions, and observed responses to wind for 26 cable-stayed bridges. The inventory is stored in Microsoft Access (Microsoft Office) database format, which allows for easy data entry and retrieval.

This electronic database of U.S. cable-stayed bridges, along with the reference database, has been turned over to FHWA. They are expected to be launched over the internet for use by the engineering community.

3.0 ANALYSIS, EVALUATION, AND TESTING

3.1 Mechanics of wind-induced vibrations

There are a number of mechanisms that can potentially lead to vibrations of stay cables. Some of these types of excitation are more critical or probable than others but all are listed here for completeness:

- Rain/wind induced vibrations of cables
- Galloping of single cables inclined to the wind
- Aerodynamic excitation of overall bridge modes of vibration involving cable motion
- Vortex excitation of an isolated cable or groups of cables
- Wake galloping of groups of cables
- Galloping of cables with ice accumulations
- Motions due to buffeting by wind turbulence
- Motion due to fluctuating cable tensions

The first three of these will be discussed briefly below, as they formed the focus of much of the investigation.

3.2 Rain/Wind induced vibrations

The combination of rain and moderate wind speeds can cause high amplitude cable vibrations at low frequencies. This phenomenon has been observed on many cable-stayed bridges and has been researched in detail.

Rain/wind induced vibrations were first identified by Hikami and Shiraishi (1987) on the Meiko-Nishi cable stayed bridge. Since then, these vibrations have been observed on other cable-stayed bridges, including the Fred Hartman Bridge in Texas, the Sidney Lanier Bridge in Georgia, the Cochrane Bridge in Alabama, the Talmadge Memorial Bridge in Georgia, the Faroe Bridge in Denmark, the Aratsu Bridge in Japan, the Tempohzan Bridge in Japan, the Erasmus Bridge in Holland, and the Nanpu and Yangpu Bridges in China. These vibrations occurred typically when there was rain and moderate wind speeds (18-34 mph, 8-15 m/s) in the direction angled 20° to 60° to the cable plane with the cable declined in the direction of the wind. The frequencies were low, typically less than 3 Hz. The peak amplitudes were very high, in the range of 10-in to 3-ft (0.25-m to 1.0-m), with violent movements resulting in clashing of adjacent cables observed in several cases.

Wind tunnel tests have shown that rivulets of water running down the upper and lower surfaces of the cable in rainy weather were the essential component of this aeroelastic instability (Hikami & Shiraishi, 1987; Matsumoto et al., 1989). The water rivulets changed the effective shape of the cable, and moved as the cable oscillated causing cyclical changes in the aerodynamic forces which led to the wind feeding energy into oscillations. The wind direction causing the excitation was

approximately 45° to the cable plane. The particular range of wind velocities that caused the oscillations appears to be that which maintained the upper rivulet within a critical zone on the upper surface of the cable.

It is noteworthy that some of the rain/wind vibrations that have been observed on cable-stayed bridges have occurred during construction when both the damping and mass of the cable system are likely to have been lower than in the completed state, resulting in a low Scruton number. For the Meiko-Nishi Bridge, the Scruton number was estimated at 1.7. The grouting of the cables adds both mass and damping, and often sleeves of visco-elastic material are added to the cable end regions which further raises the damping. The available circumstantial evidence indicates that the rain/wind type of vibration primarily arises as a result of some cables having exceptionally low damping, down in the $\zeta = 0.001$ range.

Since some bridges have been built without experiencing problems from rain/wind vibration of cables it appears probable that in some cases the level of damping naturally present is sufficient to avoid the problem. The rig test data of Saito et al. (1994), obtained using realistic cable mass and damping values, are useful in helping to define the boundary of instability for rain/wind oscillations. Based on their results it appears that rain wind oscillations can be reduced to a harmless level using the following criteria for the Scruton number (PTI, 2001):

$$\frac{m\zeta}{\rho D^2} > 10$$

This criterion can be used to specify the amount of damping that must be added to the cable to mitigate rain/wind vibrations.

Since the rain/wind oscillations are due to the formation of rivulets on the cable surface, it is probable that the instability is sensitive to the surface roughness. Several researchers have tried using small protrusions on the cable surface to solve the problem. Flamand (1994) has used helical fillets 1/16 inch (1.5 mm) high on the cables of the Normandie Bridge. This technique has proven successful, with a minimal increase in drag coefficient. This type of cable surface treatment is becoming a popular design feature for new cable-stayed bridges, including the Leonard P. Zakim Bunker Hill Bridge (MA), U.S. Grant Bridge (OH), Greenville Bridge (MS), William Natcher Bridge (KY), Maysville-Aberdeen Bridge (KY), and the Cape Girardeau Bridge (MO).

3.3 Galloping of dry inclined cables

Galloping of single dry, inclined cables is a theoretical possibility. Results from one experimental study (Saito et al., 1994) seem to suggest that this could be a concern for cable-stayed bridges. Theoretical formulations predict that this galloping may occur at high wind speeds with possible large-amplitude vibrations and that many existing cable-stayed bridges are susceptible, but there is no evidence of their occurrence in the field.

Single cables of circular cross-section do not gallop when they are aligned normal to the wind. However, when the wind velocity has a component that is not normal to the cable axis, an instability with the same characteristics as galloping has been observed. For a single inclined cable the wind acts on an elliptical cross-section of cable. An ellipticity of 2.5, corresponding to an angle of inclination of the cable of approximately 25°, can occur in the outer-most cables of long-span bridges. (Ellipticity is defined as the maximum width divided by the minimum width - e.g., a circle has an ellipticity of 1.0.) There is the potential for galloping instability if the level of structural damping in these cables is very low.

Saito et al. (1994) conducted a series of wind tunnel experiments on a section of bridge cable mounted on a spring suspension system. Their data suggest an instability criterion given approximately by the following:

$$(U/fD)_{CRIT} = 40\sqrt{S_c}$$

This data was for cases where the angle between the cable axis and wind direction was 30° to 60°. The above criterion is a difficult condition to satisfy, particularly for the longer cables of cable-

stayed bridges with a typical diameter of 6 to 8-in (150 to 200-mm). Further experimental research was necessary to confirm the results of Saito et al. (1994) and to extend the range of conditions studied. All of their experiments used low levels of damping, so it was important to investigate whether galloping of an inclined cable is possible at damping ratios of 0.005 and higher.

Based on existing information, it was apparent that galloping of dry inclined cables presented the biggest concern and biggest unknown for wind-induced vibration mitigation. The Project Team therefore focused the wind-tunnel test program on this subject.

The model was developed to be similar to that used in the test carried out by Saito et al. (1994). A 22-ft (6.7-m) long cable consisted of an inner steel pipe covered with a smooth polyethylene tube with an outside diameter of 6.3-in (160 mm). The effective mass per cable length was 40.9 lb/ft (60.8 kg/m). The end supports at the upwind end were maintained out of the wind flow above the wind tunnel, and at least 19.2-ft (5.9-m) of the 22-ft (6.7-m) length of the cable was directly exposed to the wind tunnel flow.

Testing was performed for various levels of structural damping, cable frequency ratios, surface roughness and at various angles of wind flow. The cable model orientation was changed against the mean wind flow direction for several configurations.

Limited-amplitude oscillations were observed under a variety of conditions. The limited-amplitude vibrations occurred within narrow wind speed ranges only, which is characteristic of vortex excitation of the high speed type described by Matsumoto (1998). For the typical cable diameters and wind speeds of concern on cable-stayed bridges the Reynolds number is in the critical range where large changes in the airflow patterns around the cables occur for relatively small changes in Reynolds number. The excitation mechanism is thus likely to be linked with these changes. The maximum amplitude of the response depended on the orientation angle of the cable. For wind blowing along the cable, for cables with a vertical inclination angle, the increase of surface roughness made the unstable range shift to lower wind speeds.

The results of this testing showed a deviation from the criterion described earlier. While significant oscillations of the cable occurred (double amplitudes up to 1D), it is not conclusive that this was dry inclined cable galloping. In fact, as indicated above they had similar characteristics to Matsumoto's (1998) high speed vortex excitation. Divergent oscillations only occurred for one test setup at very low damping, and the vibrations had to be suppressed since the setup only allowed for amplitudes of 1D. Large vibrations were only found at the lowest damping ratios ($\zeta<0.001$). Above a damping ratio of 0.003, no significant vibrations (> 0.4-in ; >10-mm) were observed.

This testing suggests that if even a low amount of structural damping is provided ($\zeta>0.003$), then vortex shedding and inclined cable galloping vibrations are not significant. This damping corresponds to a Scruton number of approximately 3, which is less than the minimum of 10 established for suppression of rain/wind vibrations. Therefore dry cable instability should be suppressed by default if enough damping is provided to mitigate rain/wind vibrations.

3.4 Deck-stay interaction due to wind

Measurements of both deck and stay movements have been taken at the Fred Hartman Bridge that suggests that in some instances the deck is driving the cable to vibrate with large amplitude in its fundamental mode. Vortex-induced vibration of the deck is thought to be the driving mechanism for this motion. Further studies are continuing to identify additional occurrences of this behavior for corroboration, and to better understand the underlying mechanisms their consequences. It is emphasized that this appears to be a relatively uncommon event.

4.0 MITIGATION APPROACHES

Space limitations preclude the full presentation of the various studies of mitigation undertaken. Presented here in summary form are some of the important results for dampers and cross ties.

Additional resources can be found in the references and bibliography.

4.1 Dampers

4.1.1 Linear viscous damper

Free vibrations of a taut cable with an attached linear viscous damper were investigated in detail. An analytical formulation of the complex eigenvalue problem was used to derive an equation for the eigenvalues that is independent of the damper coefficient. This "phase equation" reveals the attainable modal damping ratios ζ_i and corresponding oscillation frequencies for a given damper location ℓ_1/L, affording an improved understanding of the solution characteristics and revealing the important role of damper-induced frequency shifts in characterizing the response of the system.

When the damper-induced frequency shifts are small, an asymptotic approximate solution has been developed, relating the damping ratio ζ_i in each mode to the nondimensional damper coefficient, κ.

For damper locations resulting in small frequency shifts (e.g., dampers near the end of the stay), the expression can be written as:

$$\frac{\zeta_i}{(\ell_1/L)} \cong \frac{\pi^2\kappa}{(\pi^2\kappa)^2+1} \qquad (1)$$

where κ is a nondimensional parameter grouping defined as

$$\kappa \equiv \frac{c}{mL\omega_{o1}} i\frac{\ell_1}{L} = \frac{1}{\pi}\frac{c}{\sqrt{Tm}} i\frac{\ell_1}{L} \qquad (2)$$

Equation 1 gives the damping attainable in a particular mode of vibration i as a function of the damper coefficient c, mass per unit length m, cable length L and fundamental circular frequency ω_{o1} as well as normalized damper location ℓ_1/L.

In Figure 2, the normalized damping ratio $\zeta/(\ell_1/L)$ has been plotted against the nondimensional damping parameter, κ, for the first five modes for a damper location of ℓ_1/L=0.02, and it is evident that the five curves collapse very nearly onto a single curve in good agreement with the approximation of Equation 1. It is important to note that because the mode number is incorporated in the nondimensional damping parameter κ, the optimal damping ratio can be achieved in only one mode of vibration in the case of a linear damper. This is a potential limitation, because it is currently unclear how to specify, a priori, the mode in which optimal performance should be achieved for effective suppression of stay-cable vibration, and designing a damper for optimal performance in a particular mode may potentially leave the cable susceptible to vibrations in other modes.

When the damper is far from the end of the stay, different regimes of behavior can be observed, potentially significantly altering the performance of the damper. For such situations, the reader is referred to the publication Main and Jones (2002a).

4.1.2 Linear damper with a friction threshold

An asymptotic solution for the damping ratios in the case of a taut cable with a linear viscous damper was extended to the nonlinear case of a viscous damper with a friction threshold using an "equivalent viscous damper" formulation. Relevant nondimensional parameter groupings were identified, and the solution characteristics were explored. It is observed that this formulation does a poor job of estimating the amplitude at which the damper is completely locked due to friction, and the results of this analysis should only be considered accurate for relatively small values of the friction parameter μ,

$$\mu \equiv \left(\frac{F_o}{T}\right)\left(\frac{Ai}{L}\right)^{-1} \qquad (3)$$

for which the assumption of nearly sinusoidal oscillation is appropriate (F_0 is the friction threshold). The observed effect of the friction threshold is to reduce the optimal value of the viscous damping parameter κ and ultimately to reduce the attainable damping ratios from the values for a purely viscous damper. Figure 3 shows an example of this effect.

4.1.3 Power-law damper

Details of a power-law damper solution are omitted here and can be found in Main and Jones (2002b).

4.2 Cross ties

One of the methods that is sometimes adopted to counteract the undesired oscillations is to increase the in-plane stiffness of stays by connecting them together by means of a set of transverse cables, defined as cross-ties (or "aiguilles"). These cables are also used to reduce the cable sag variations among the stays of different length, ensuring a more uniform axial stiffness on the consecutive stays. From the dynamic perspective, the properties of the single cable, considered as a separate element, are modified by the presence of the lateral constraints that influence its oscillation characteristics. Similarly, a connection of simple suspended elements is transformed into a more complex cable network; a closed-form solution to the dynamic problem is more elusive.

The analysis method developed was applied to the study of a cable network that was modeled after the Fred Hartman Bridge, a twin-deck cable-stayed bridge over the Houston Ship channel, with central span of 380m and side spans of 147m.

The investigated system corresponds to the south-tower central-span portion, a set of twelve stays with a three-dimensional arrangement (Figure 4). Stay "24S" is assumed as reference element; all other stay quantities are normalized with respect to this element.

A careful study of the solution patterns showed two categories of roots (Figure 5). The first are associated with "global modes", in which the whole set of cables is involved in the oscillation and with a substantial increment in the generalized mass of the mode, with respect to the individual cable modes. The second category is one of "localized modes", in which the response of network is not global but the maximum amplitudes are located in the intermediate segments of specific cables only. Moreover the overall characteristics of these modal forms (both symmetric or antisymmetric) can be different from the solution for individual cables, and influenced by the presence and the location of the transverse connectors. The wavelength of these modes is essentially governed by the distance between two consecutive connectors (being almost coincident with the nodes of the modal shape). The high density of solutions is related to the fact that these modes are the components of high-order modes of the individual cables with different magnitude, for which the location of the connector on each cable represents a node of the individual mode shape. These modal patterns carry important implications for design.

More details can be found in Caracoglia and Jones (2002a-c)

5.0 DESIGN GUIDELINES

The preceding investigations and analyses led to the develop of a set of guidelines for mitigation against stay-cable vibration. These are divided into guidelines for new bridges, and for existing bridges in sections 4.1 and 4.2 below.

5.1 New cable-stayed bridges

1. General:
A sufficiently detailed cable vibration analysis (including modal analysis of the cable system) must be performed as part of the bridge design to identify the potential for cable vibration. The following factors must be examined: the dynamic properties of the cables, dynamics of the structural system, geometry of the cable layout, cable spacing, exposure conditions, and estimated Scruton Numbers (Sc).

2. Mitigation of rain/wind mechanism:
At a minimum, providing an effective surface treatment for cable pipes to mitigate rain/wind vibrations is highly recommended. One common method is the use of double-helical beads. The effectiveness of the surface treatment must be based on the tests applicable to the specific system, provided by the manufacturer.

3. Additional mitigation:
Depending on the outcome of the vibration study (Item 1), the provision of at least one of the following major cable vibration mitigation measures (in addition to surface treatment) is

recommended:

- Additional damping (using external dampers)
- Cable cross-ties

4. Minimum Scruton Number
Following are minimum desired Scruton Numbers (Sc):
$m\zeta/\rho D^2 > 10$ for regular cable arrangements

$m\zeta/\rho D^2 > 5$ for cable pipes with effective surface treatment suppressing rain/wind vibrations (see note below)

Note: Limited tests (Larose & Smitt, 1999) on cables with double-helix surface treatments have suggested that $m\zeta/\rho D^2 > 5$ may be acceptable. However, it is felt that such reductions should be made only for regularly spaced single cable arrangements. In general it is recommended to keep the Scruton Number as high as possible by providing external dampers and/or cross-ties. For unusual geometry or double stay arrangements where parallel stays are placed within close proximity to one another, careful case-by-case evaluation of these limits are recommended.

5. External dampers:
Manufacturer warranties should be provided for all damping devices. Most dampers used in bridges are proprietary items and design details should be provided by the manufacturer.

A damper can be tuned to yield optimal damping in any one selected mode. For other modes the level of damping will be less than this optimal value. Rain/wind vibrations occur predominantly in mode 2. Therefore, if a damper is to be tuned to a particular mode to mitigate rain/wind vibrations, it appears logical to select mode 2.
There are many types and designs of dampers, and linear dampers have been shown to be effective through their widespread use in the past. However, recent analytical studies show that non-linear dampers can be used to provide a more optimal condition than linear dampers, as these are effective over a larger range of modes. In particular, the damping performance of square-root dampers is independent of the mode number and is only affected by the amplitude of vibration.

With some dampers (such as dash-pot type), an initial static friction force must be overcome before engaging of the viscous element. Field experiments have shown the presence of this stick-move-stick-move behavior associated with such dampers. This may effectively provide a fixed node instead of the intended damping for the cable at low amplitude oscillations, and should be considered. The viscoelastic type dampers where an elastomeric element is permanently engaged between the cable and the supporting elements, theoretically, are free of such initial frictional thresholds. On the other hand, there are also damper designs that rely on friction as the energy dissipation mechanism and the static friction threshold for such dampers may be higher than for the other types.

Another factor needing consideration is the directionality of the damper. The cable vibrations observed in the field indicate both vertical and horizontal components of motion. Some damper designs are antisymmetric and provide damping against cable motion in any direction. Other dampers (e.g. dash-pot types) provide damping against motion only along the axis of the damper. It is possible to arrange two or more such dampers so that the combination is effective in all directions. As the majority of the observed motion due to rain/wind vibrations is in the vertical direction, it may be sufficient to provide damping against only the vertical motion. However, this has not been clearly established. It is recommended that damping be made effective against cable movement in any direction.

Damper mounting details may transfer lateral forces due to damper action onto components of the cable anchorage. Such forces must be considered in the design of the cable anchorages.

6. Cable cross ties:
If used, provide clear and mandatory specifications for cable cross-ties. Experience shows that cross-ties, when properly detailed and installed, can be an effective method for suppressing undesirable levels of cable vibrations. Reported failures of cross-ties have been generally traced to improper details and material selection.

The use of cross ties creates local modes, which must be considered in design. The frequency of the first plateau of local modes should be kept as high as possible. Symmetric configurations of the restrainers with respect to intermediate-length cables is preferred to increase the frequency interval (lower limit in particular) corresponding to local modes, since they minimize the longest segment length.

Cable cross-ties must be provided with initial tension sufficient to prevent slack of the cross-ties during design wind events. The level of tension depends on the dynamic properties of the cable system and the design wind event. The initial cross-tie tensions must be established based on rational engineering analysis. Also, the tie to cable connection must be carefully designed and detailed for the transfer of the design forces.

7. User tolerance limits:
A preliminary survey on sensitivity of bridge users to stay cable vibrations has indicated that the comfort criteria for cable displacement can be described using the following maxima (within 0.5 to 2.0 Hz range):

- 0.5 D (Preferred)
- 1.0 D (Recommended)
- 2.0 D (Not to Exceed)

While this aspect may need further study, the above can be used as a guide when such displacements can be computed and/or needed as input for design of such elements as dampers and cross-ties. The displacement limits need not be considered for extreme events.

5.2 Retrofit of existing bridges

If an existing bridge is found or suspected to exhibit episodes of excessive stay cable vibration, an initial field survey and inspection of the cable system should be performed to assemble the following information:

- Eye-witness accounts, video footage of episodes
- Condition of the stay cable anchorages and related components, noting any visible damage and/or loose, displaced components

A brief field instrumentation and measurement program can be used to obtain such parameters as the existing damping levels of the cables. Instrumentation of cables to record the vibration episodes, wind direction, wind velocity, and rain intensity during their occurrences could also provide some confirmation of the nature of cable vibrations.

The mitigation methods available for retrofit of existing bridges follow closely those provided for the new bridges. However, the application of surface treatment may be difficult, not practical, or cost prohibitive on existing structures. The addition of cross-ties and/or dampers is recommended.

A split-pipe with surface modifications can be installed over the existing cable pipe if this is found to be practical and cost effective. In many of the older bridges for cables using polyethylene (PE) pipes, ultraviolet (UV) protection to cable pipes is provided by wrapping the PE pipe with Tedlar tape. These cables require periodic re-wrapping as part of routine maintenance. The newer high-density polyethylene (HDPE) cable pipes are manufactured with a co-extruded outer shell that provides the needed UV resistance, thus providing a split-pipe as a secondary outer pipe has the added benefit of eliminating the need for future Tedlar taping for the UV protection.

In addition, any damaged cable anchorage hardware must be properly retrofitted or replaced. It is recommended that the original cable supplier be contacted to ensure the replacement of cable anchorage components and that the addition of mitigative devices are compatible with the original design of the stay anchorage area.

6.0 RECOMMENDATIONS FOR FUTURE RESEARCH AND DEVELOPMENT

The design guidelines provide a concise approach to suppress wind-induced vibrations in cable-stayed bridges, and are based on the existing knowledge base and further investigations performed through this project. While the design recommendations are empirical, the mitigation methods discussed (dampers, cable cross-ties, and surface

modification) are proven to be effective through both past experience and research. Future research in the following areas clarifying some of the remaining key issues would strengthen the design guidelines.

This is the first time a set of design guidelines have been proposed for the mitigation of stay cable vibration. It is expected that future adjustments based on actual cable performance and advances in cable technology may require further refinements to the design guidelines.

1. Additional wind-tunnel testing of dry inclined cables.

2. Further investigation of characteristics of deck-induced vibration of stay cables.

3. Development of mechanics-based model of rain/wind induced vibrations.

4. Develop a mechanics-based model for stay-cable vibration enabling the prediction of anticipated vibration characteristics.

5. Predict the performance of stay cables after mitigation using the model.

6. Perform a detailed quantitative assessment of various alternative mitigation strategies.

7. Develop improved understanding of inherent damping in stays and that provided by external devices.

8. Improved understanding of cross-tie solutions.

9. Refine recommendations for effective and economical design of stay-cable vibration mitigation strategies for future bridges.

7.0 CONCLUDING REMARKS

This project has been successful in producing a set of guidelines and recommendations for stay-cable vibration mitigation based on information available at the time of its conclusion. While this does include information based on a review of the literature and a significant amount of research on the characterization of field measurements and damper performance, the guidelines may be improved through the future research items proposed.

8.0 ACKNOWLEDGEMENTS

This research was supported through an FHWA-sponsored project (Harold Bosch technical contact) on stay-cable vibration awarded to a team of investigators including HNTB Corporation, New York, Johns Hopkins University, Baltimore, Maryland; Rowan Williams, Davies and Irwin, Ontario, Canada, and Buckland and Taylor of Vancouver, BC, Canada. The Fred Hartman and Veterans' Memorial Bridges project were funded by the Texas Department of Transportation (TxDoT) through Texas Tech University (TTU) and the University of Texas at Austin (UTA) in a project managed by Whitlock, Dalrymple Poston and Associates, Inc. (WDP) of Austin, Texas.

All components of the research team were assisted by various staff and other personnel. The first author would like in particular to acknowledge the significant contributions of the following graduate students and post-doctoral fellows: Joseph Main, Luca Carcoglia; Ender Ozkan; Delong Zuo.

9.0 REFERENCES

Flamand, O. (1994). Rain-wind induced vibration of cables. Proceedings of the International Conference on Cable-stayed and Suspension Bridges (AFPC), Deauville, France, Oct. 1994, 2, 523-531.

Hikami, Y. and Shiraishi, N. (1988). "Rain-wind induced vibrations of cables in cable stayed bridges", Journal of Wind Engineering and Industrial Aerodynamics, Vol. 29, p. 409-418

Matsumoto, M., Shiraishi, N., & Shirato, H. (1989). Inclined-cable aerodynamics: Structural design, analysis & testing proceedings. Proceedings of the ASCE Structures Congress, San Francisco.

Matsumoto, M. (1998). Observed behaviour of prototype cable vibration and its generation mechanism. Bridge Aerodynamics, Larsen &

Esdahl (eds), Balkema, Rotterdam, 189-211.

PTI Guide Specification (2001). Recommendations for stay cable design, testing and installation. Post-Tensioning Institute Committee on Cable-Stayed Bridges, 4th ed.

Saito, T.; Matsumoto, M.; and Kitazawa, M. (1994). "Rain-wind excitation of cables on cable-stayed Higashi-Kobe bridge and cable vibration control", Proceedings of Conference on Cable-Stayed and Suspension Bridges, p. 507-514

10.0 BIBLIOGRAPHY

Listed below is a partial list of publications that resulted from the research effort described herein.

Caracoglia, L. & Jones, N. P. (2002a) "Analytical method for the dynamic analysis of complex cable structures." Proceedings, ASCE Engineering Mechanics Division Conference. Columbia University, NY.

Caracoglia L., & Jones N. P. (2002b) "In-plane dynamic behavior of cable networks I: formulation and basic solutions." Journal of Sound and Vibration. (In review)

Caracoglia L., & Jones N. P. (2002c) "In-plane dynamic behavior of cable networks II: Prototype prediction and validation." Journal of Sound and Vibration. (In review)

Jones, N. P. & Zuo, D. (2002) "Measurement of Stay Damping - Sunshine Skyway Bridge, Tampa, FL" Report to Lendis Corporation and FHWA.

Jones, N. P. & Main, J. A. (2002) "Evaluation of Mitigation Strategies for Stay-Cable Vibration." Proc. Structures Congress. ASCE, Reston, VA.

Main, J. A. & Jones, N. P. (2002) "Analytical Investigation of the Performance of a Damper with a Friction Threshold for Stay-Cable Vibration Suppression." Proceedings, ASCE Engineering Mechanics Division Conference. Columbia University, NY.

Main, J. A. & Jones, N. P. (2001) "Analysis and design of linear and nonlinear dampers for stay cables." Proceedings Fourth International Symposium on Cable Dynamics, Montreal, Canada, AIM.

Main, J. A., & Jones N. P. (2002a) "Free Vibrations of a Taut Cable with Attached Damper. I: Linear Viscous Damper." Journal of Engineering Mechanics, ASCE, 128(10), 1062-1071.

Main, J. A., & Jones N. P. (2002b) "Free Vibrations of a Taut Cable with Attached Damper. II: Nonlinear Damper." Journal of Engineering Mechanics, ASCE, 128(10), 1072-1081.

Main, J. A., & Jones, N. P. (2001) "Measurement and mitigation of stay-cable vibration." Proceedings Asia-Pacific Conference of Wind Engineering. Kyoto University, October.

Main, J. A., & Jones, N. P. (2001) "Stay-cable vibration in cable-stayed bridges: Characterization from full-scale measurements and mitigating strategies." Journal of Bridge Engineering. ASCE, 6(6), 375-387.

Main, J. A., Jones, N. P. & Yamaguchi, H. (2001) "Characterization of rain/wind induced stay-cable vibrations from full-scale measurements." Proceedings Fourth International Symposium on Cable Dynamics. Montreal, Canada, AIM.

Ozkan, E. & Jones, N. P. (2001) "Investigation of cable-deck interaction using full-scale measurements on a cable-stayed bridge." Proceedings 1st Americas Conference of Wind Engineering. Clemson University, June.

Ozkan, E., Main, J. A. & Jones, N. P. (2001) "Full-scale measurements on the Fred Hartman Bridge." Proceedings Asia-Pacific Conference of Wind Engineering. Kyoto University, October.

Ozkan, E., Main, J. A. & Jones, N. P. (2001) "Long-term measurements on a cable-stayed bridge." Proceedings IMAC-XIX. Society for Experimental Mechanics.

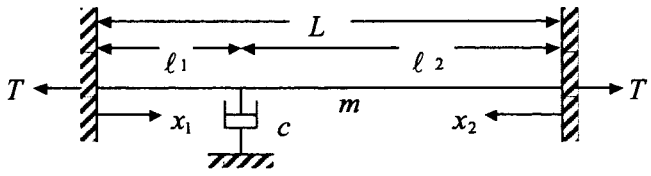


Figure 1: Taut cable with a linear damper.

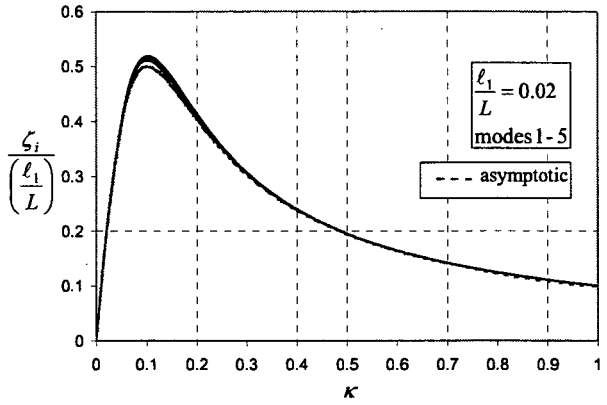


Figure 2: Normalized Damping Ratio versus Normalized Damper Coefficient.

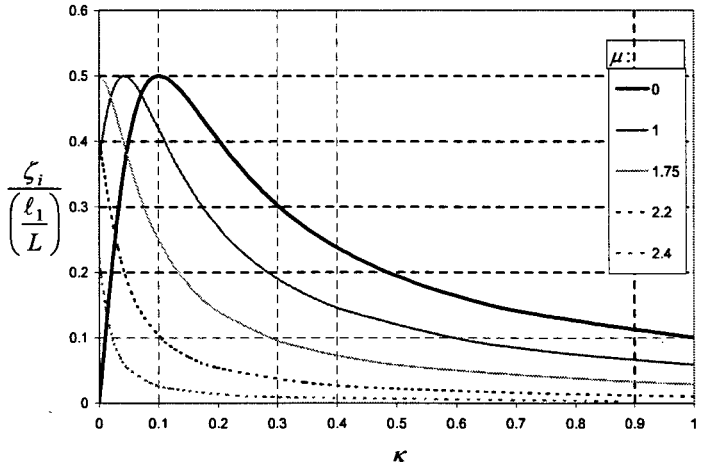


Figure 3: Normalized Damping Ratio vs. κ with varying μ.

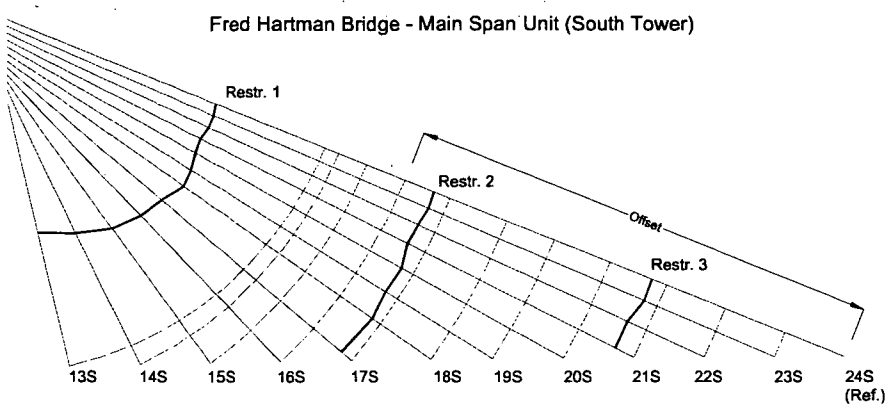


Figure 4: General problem formulation (original configuration).

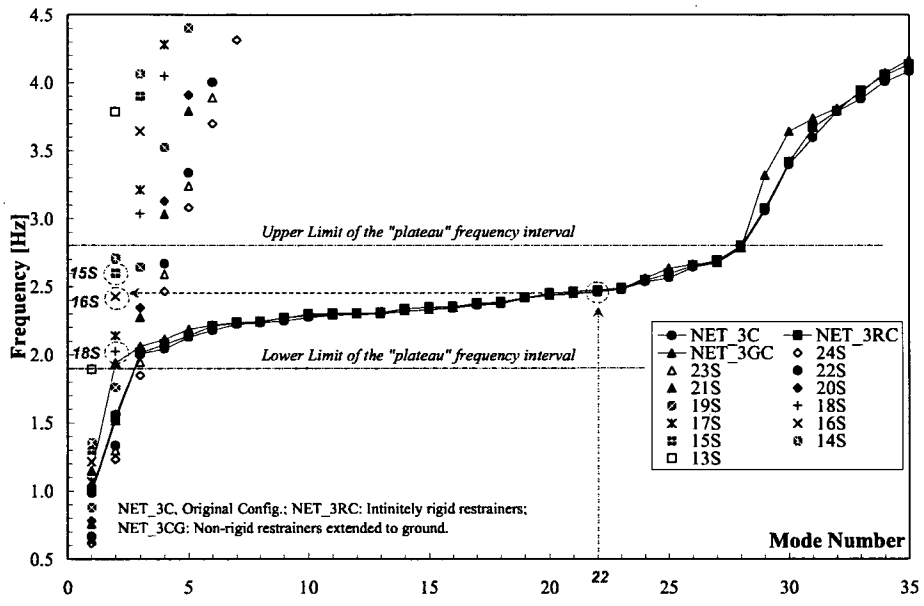


Figure 5: Comparative analysis of network vibration characteristics and individual-cable behavior; Fred Hartman Bridge; NET_3C, original configuration; NET_3RC, infinitely rigid restrainers; NET_3CG, spring connectors extended to ground (Restr. 2,3).

Utilization of Digital Surface Model in Urban Area for Wind Engineering

by

Yasuo Okuda[1], Hisashi Okada[1], Kikitsu Hitomitsu[1], Takaaki Kono[1],
Tetsuro Tamura[2], Shuyang Cao[2], Masamiki Ohashi[3],
Takahisa Kobayashi[4], Osamu Suzuki[4], Hiroshi Yamauchi[4] and Naoki Shirai[5]

ABSTRACT

This paper discusses utilization of digital surface model in urban area for wind engineering; for example, estimation of wind profiles in urban area, estimation of wind loads of tall buildings, and so on. Recent advancement for quality of digital surface model makes it possible to construct sophisticated numerical models for wind flows over roughened ground in urban areas. Urban areas are modeled mainly by the arrangement of buildings with actual shape on the ground surface. LES is carried out for different types of actual urban areas. The validity of the simulated results on wind profiles or wind pressure coefficients and greenery volume in urban area are also discussed.

Key Words: Digital Surface Model, Large Eddy Simulation, Urban Area, Wind Profile,

1. INTRODUCTION

It is very difficult to categorize the wind profile on building site for wind-resistant structural design according to the arrangement of surrounding buildings, houses and plants on the ground. However, there are several recommendations to indicate vertical distributions of mean and fluctuating wind velocities with regard to the surface roughness. These recommendations have been reflected in various international standards and codes, but their definition tends to be ambiguous by showing photos of several roughness examples and so on. Based on this background, we have the aims to deal with the characteristics of urban strong wind on the basis of numerical simulations. Large eddy simulation (LES) is carried out for the estimation of wind profile in the urban area. As for the information on the characteristics of the roughness terrain, we utilize digital surface model. Resent advancement for the quality of Digital surface model makes it possible to construct a sophisticated numerical model for the wind flow over urban areas by using the altitude data for ground surface with fine horizontal resolutions (ex. 2m). With these digital data, the urban area can be represented by the arrangement of buildings with almost actual shape on the ground surface.

In this paper, the validity of the simulation mentioned above is highlighted. First, we show the accuracy of the LES prediction through the comparison with the field measurement data, taking a center of Tokyo and a residential area as the examples of the urban area. Second, we analyze the wind loads on actual high-rise buildings in Tokyo metropolitan sub-center, considering physical mechanism of the behavior of the method of extracting greenery data in Tsukuba area are outlined, which is supposed to be regarded the separated shear

1 Building Research Institute
2 Tokyo Institute of Technology
3 National Institute of Land, Infrastructure and Management
4 Meteorological Research Institute
5 Kokusai Kougyo Co.

layer and the vortices in the wake. And third, the field measurement of wind profile and as the inlet conditions for the LES simulation. These studies are considered to contribute to development of "Numerical Simulator of Urban Wind".

2. ESTIMATION OF WIND PROFILE IN URBAN AREAS

In this section, the results of the LES computations of the boundary layer on the actual urban areas with digital surface model are shown in Figure 1 and its validity is discussed.

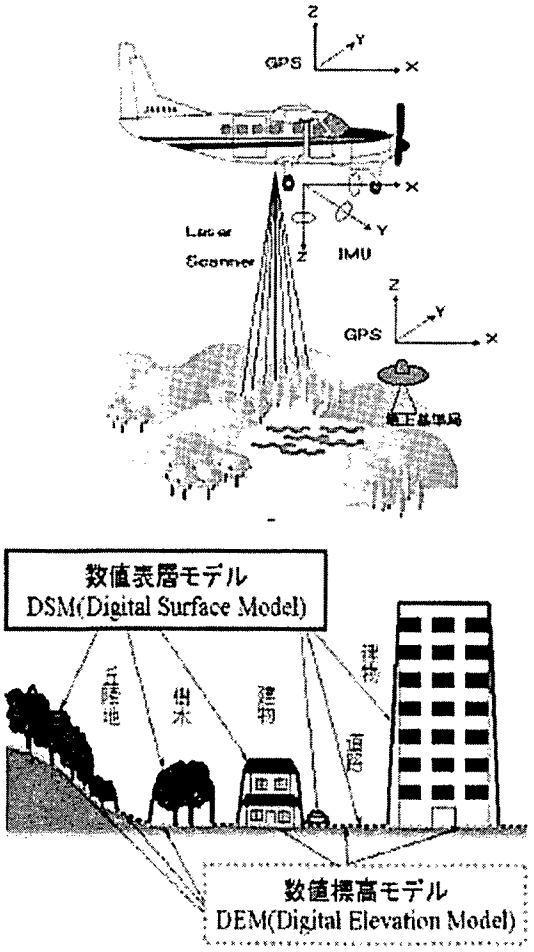
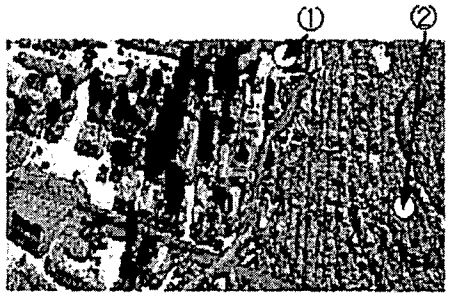


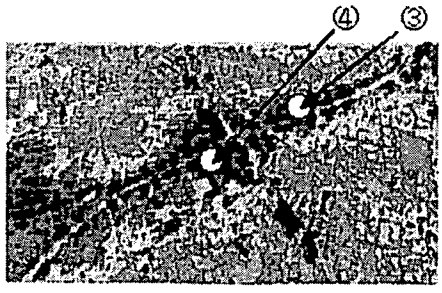
Figure 1 Digital surface model

2.1 Computed Wind Flows in Urban Areas

Figure 2 illustrates two types of urban areas, a center of Tokyo and the residential area. The surface geometries are visualized by digital surface model (RAMS-e, Kokusai Kougyo Co.)[1], whose resolution is potentially 2m, but represented here by 8m grid data. Even by this resolution, we can recognize that there are tall buildings densely arranged in central area, and that in residential area, a-few-storied houses or trees occupy but higher buildings are limited only along the main streets. The computational domain is 2048m in the stream-wise direction, 1024m in the transverse direction and 800m in the vertical direction. For the grid size for computation, 4m is given horizontally as a half of resolution for the surface geometry because of programming efficiency, and 4m is also given vertically in the limited region near the ground and stretched at higher region. As a result, the number of grid is 512 x 256 x 96. The wind direction for computation is given as left to right (south wind).



(a) Central area with densely arranged tall buildings



(b) Residential area

Figure 2 Numerical model visualized by digital surface model for urban area of Tokyo

Figure 3 shows the LES results of wind flows in the central area by instantaneous wind velocity contours. The complex structures of wind turbulence with various scales can be seen by contours of the instantaneous velocities close to the ground. It is recognized that the wind flow converges into the street canyon and there is a high wind speed region along the main street or the railway.

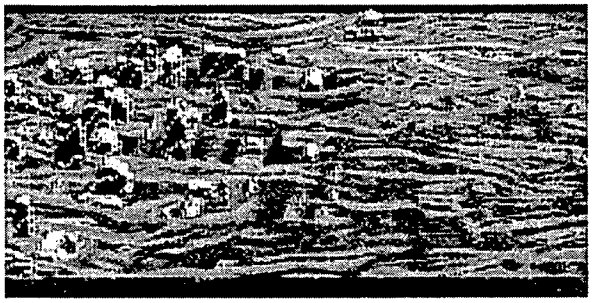


Figure 3 Near-ground instantaneous wind velocity contours in urban area

2.2 Comparison of Simulation Results with Observation Data during Typhoon

The typhoon attacked Tokyo area on September, 11, 2001. The record of wind velocity near ground was gathered at Points ①-④ in Figure 2. We also obtain the wind velocity vectors by analyzing the Doppler radar data at two locations in Kanto area, Narita International Airport and Haneda National Airport. Figure 4 shows the typhoon track represented by the wind velocity vectors. The movement of a typhoon eye is clearly recognized. Figure 5 shows the hourly time variations of the wind velocities and directions for observation data by anemometers and Doppler radars. As the typhoon was approaching and leaving, the velocity magnitude and the wind direction were reasonably changing. Figure 6 shows the comparison between wind profiles computed by LES and observation data. Both data show good agreement with each other.

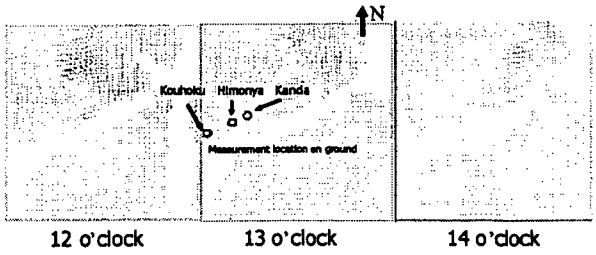


Figure 4 Time variation of wind velocity vectors measured by Doppler radar

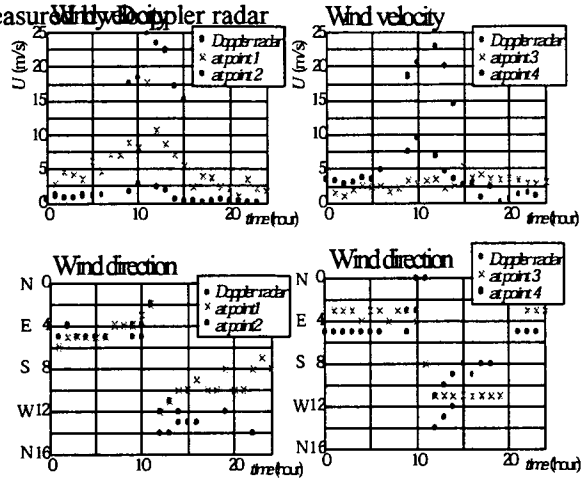


Figure 5 Observation data during Typhoon

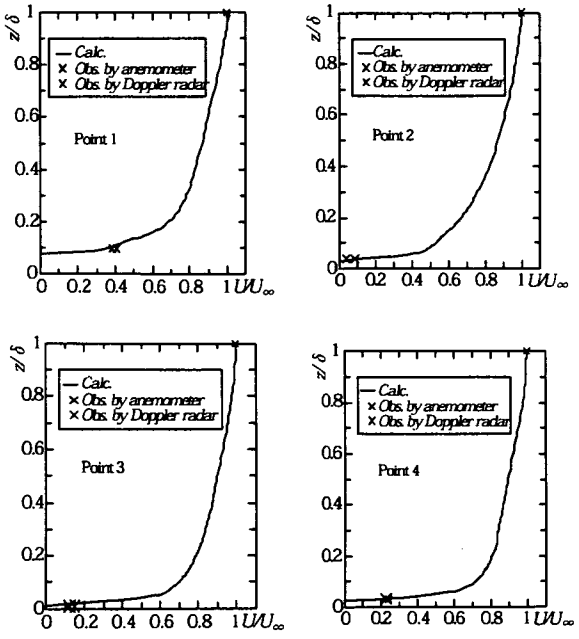


Figure 6 Comparison of simulation results with observation data

2.3 Estimation of Wind Profiles in Urban Areas

In this section, we examine detailed characteristics of the wind profiles in urban areas. Figure 7 shows vertical distribution of roughness parameters, the roughness density and the probability density function of building heights, estimated by Digital surface model. The reasonable results are obtained for both areas. The central urban area has a much higher value for vertical integral λ of roughness density than the residential area, but their maximum values for vertical profiles occur almost at same height very close to the ground. By using these roughness parameters, we can estimate the power law exponents of wind profiles based on the empirical rules by Raupach[2] and Counihan[3] (Table 1). For use of Raupach's curve of λ vs. z_0/h (z_0: roughness length), the roughness height h is determined by the mean value for the probability density function of building heights. The schematic for estimation procedure of the power law exponent is given in Figure 8. Also, we show the computed wind profiles by LES and the power law exponents estimated by these wind profiles in two types of urban areas (Figure 9). The power law exponents estimated by the empirical procedure, are 0.23 for the central area and 0.21 for the residential area, while 0.27 and 0.19 by wind profiles in the LES results. These differently estimated power law exponents are reasonably coincident with each other in the residential area. But in the central urban area the empirical estimation indicates a small value.

Table.1 Power law exponents of wind profile estimated by roughness parameters

	Central area	Residential area
Roughness density	0.305	0.111
Roughness height (m)	15.22	4.578
Raupach's Z_0 /h	0.053	0.089
Z_0	0.807	0.407
α	0.231	0.205

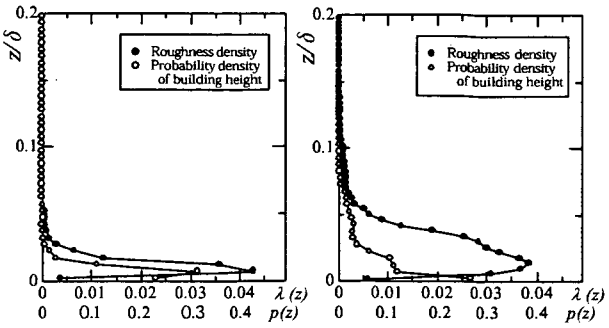


Figure 7 Vertical distributions of roughness parameters estimated by digital surface model

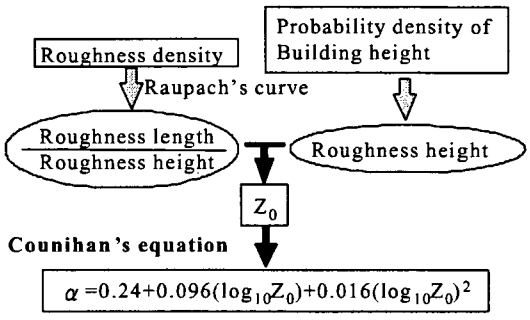


Figure 8 Schematic for estimation procedure of power law exponent

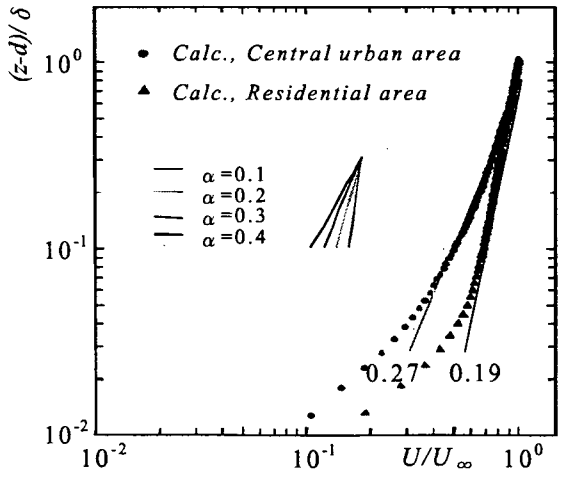


Figure 9 Power law exponents estimated by the wind profiles

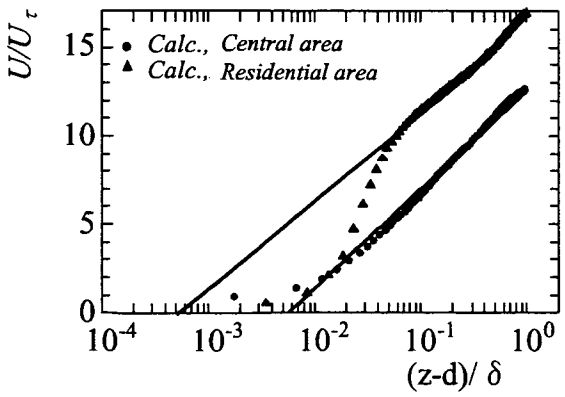


Figure 10 Computed velocity profiles fitted to the log law curves

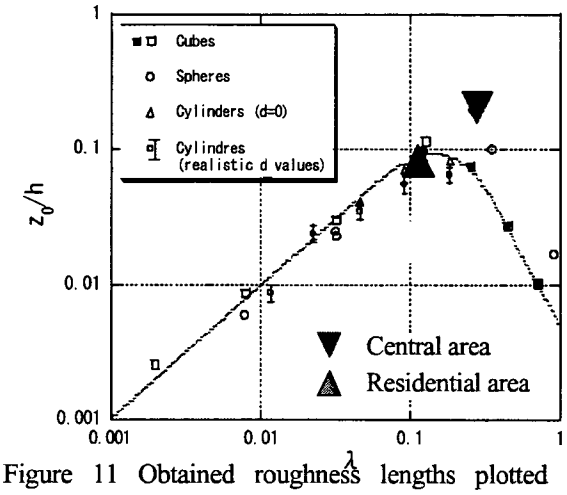


Figure 11 Obtained roughness lengths plotted in Raupach's curve

Next we try to obtain the roughness length z_0 by using the LES results. Figure 10 shows that the computed velocity profiles are fitted to the log law curves. The zero displacement d is determined based on the vertical profile of the computed Reynolds shear stress by Jackson's method[]. The obtained roughness lengths are plotted in the Raupach's figure (Figure 11). The data in the residential area are much coincident, but the computed data in the central area of the city is larger than the Raupach's curve. It causes that roughness length of blocks with various heights does not change to a decrease even as the roughness density much increases, while uniform roughness returns to a smooth-like state. Or, it can be considered as one of the reasons that the height of tall buildings is too high compared to the depth of the turbulent boundary layer, so the universality of roughness parameters comes un-appropriate.

3. ESTIMATION OF WIND LOADS ON TALL BUILDINGS IN URAN AREA

The objective of this section is to analyze the wind loads on actual tall buildings under limit grid resolution, considering physical mechanism of the behavior of the separated shear layer and the vortices in the wake. In this numerical simulation, Immersed Boundary Method, which uses boundary body forces that impose the boundary conditions on a given surface not coinciding with the computational grid, is utilized to reproduce the configuration of the given buildings.

3.1 Computational Model for Tall Buildings at Shinjuku Area

In order to get computational model for actual tall buildings in the urban area, we utilize data of the electronic mapping information at Shinjuku in Tokyo where tall buildings are densely built. The digital surface model represents the ground surface by height of surface roughness (RAMS-e, Kokusai Kogyo Co.) such as buildings and trees. Expression of surface shapes has a resolution of 2m in the horizontal directions. Figure 12 illustrates the perspective view of Shinjuku area with tall buildings, which is visualized by using digital surface model data. Discretization of the area is fine enough to represent the shape of each building or house. The data can be directly transferred to formulate the computational model represented by the Cartesian coordinates for simulating wind flows around actual tall buildings. First we carry out the LES computation for three tall buildings which are selected partly from buildings in Shinjuku area and closely placed with various wall-surface directions (Figure 12). The heights of these three buildings are

more than 200m: building (A) is 209m, (B) is 200m and (C) is 223m. At the present stage of LES computation, we only impose the uniform flow on inflow boundary. But at the next stage, we are planning to simulate the wind flow around tall buildings under the condition that the oncoming flow is set up in the spatially developed turbulent boundary layer.

In this analysis, north wind is assumed as inflow direction. The Reynolds number, based on the uniform flow at the inlet boundary, U, and the real scale length of 50m, L, is 1000. The computational domain is 18L in the stream-wise direction (x) and 20L in the lateral direction (y). 10L is given in the vertical direction (z) to 4.46L of the highest building (C). Three buildings are located at the center in width of the computational domain and 5L distant from the inflow boundary. A non-uniform Cartesian mesh is used and the total number of grid points is 274×268×234. Especially, 168×112×200 grid points are placed to form uniform resolution, L/40, in the vicinity of buildings, while the mesh size is increased with a distance from the buildings. For the boundary condition, free-slip condition is given at the side and top surfaces. No-slip condition is given at the bottom. The outflow boundary is convective outflow condition.

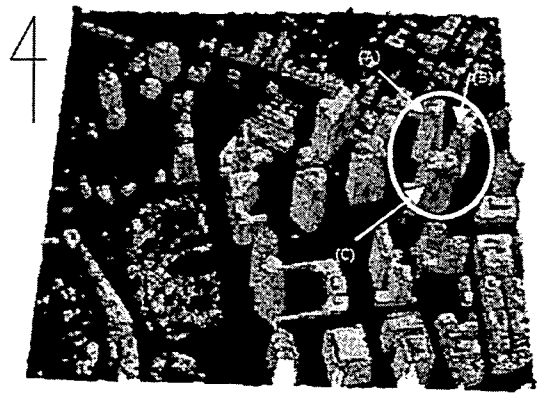
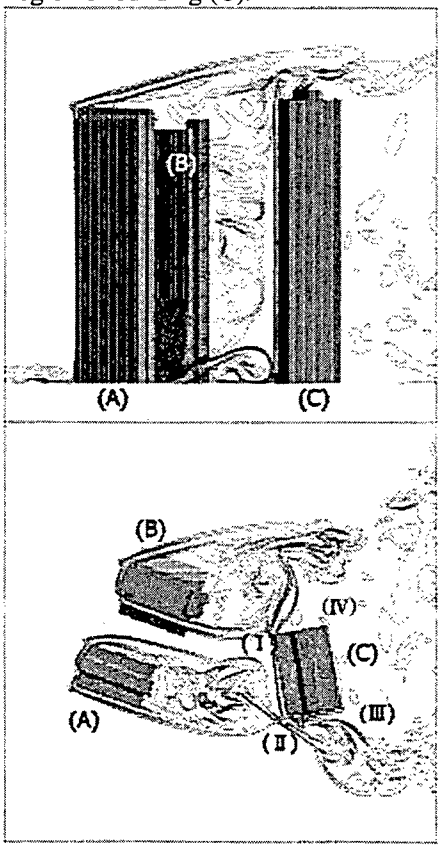


Figure 12 Buildings under consideration in Shinjuku area

3.2 Computed Wind Flow and Aerodynamic Characteristics of Tall Buildings

Figure 13 shows the instantaneous vorticity contours around three tall buildings. We can certainly recognize the vortex structures which are much deformed in the complicated arrangement of these tall buildings. It can be presumed that the wind flow, is coming between two upstream tall buildings, increases its velocity and impinges on the frontal surface of a downstream tall building. Also, strong horse shoe vortex can be seen at the bottom of the tall building in Figure 13(a). According to details of flow patterns in Figure 13(b), the separated shear layer from the upper corner of building (A) comes close to the building (A), affected by the wall of building (B). The wake flows of building (A) cover the frontal region of building (C).



(a) x-z plane

(b) x-y plane

Figure 13 Instantaneous vorticity contours around three tall buildings

As a result, the pressure distribution on the frontal surface of building (C) is largely deformed, as seen in Figure 14(a). In Figure 14(b) we also recognize an interaction of shear layers separated from lower corner of building (B) and upper corner of (C). Because the vorticity of these shear layers has an opposite sign, the vortices of the shear layers are made weaken each other, and eventually the shear layer of building (C) keeps away from the wall. The pressure distribution on the surface (Ⅳ)-(Ⅰ) of building (C), shown in Figure 14, indicates the slight recovery. Figure 14(b), also, shows that turbulence in the wake region of building (A) affects behavior of the lower shear layer from building (C). The shear layer increases the occurrence to reattach to the after-body of building (C), and the pressure distribution displays a slight reduction of C_p on the surface (Ⅱ)-(Ⅲ), in Figure 14. A strong horse shoe vortex at the bottom of the building (C) shown in Figure 13(b) has a much influence on surrounding wind environment. Wind load is also influenced by the adjacent buildings and the frontal pressure in lower region decreases compared to the case of a single building.

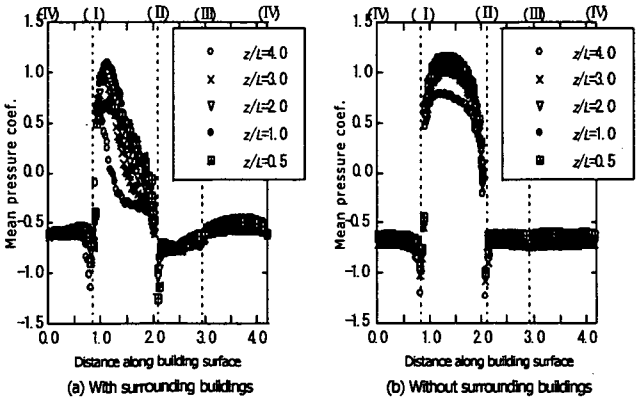


Figure 14 Time averaged wind pressure coefficient along the surface of the building (C)

4. ESTIMATION OF WIND PROFILE AND GREENERY VOLUME IN URBAN AREA

In this section, the field measurement of wind profile and the method of extracting greenery data in Tsukuba area are outlined. As for the field measurement, wind profiles are measuring at two different points, which makes it possible to evaluate the special structure of strong wind in the given region. And by the evaluation of the greenery volume, we can numerically discuss the degree of effect of trees on the urban roughness condition. Such information is applied in the numerical simulation on the wind environment in Tsukuba area.

4.1 Comparison of Characteristics on Wind Profiles in Tsukuba Area

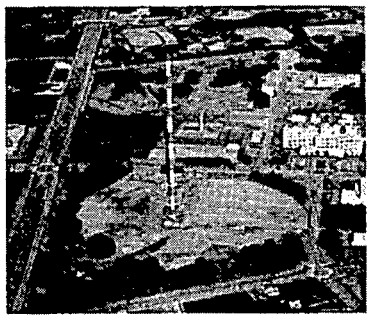
Authors have carried out the wind field measurement in Tsukuba area, where is supposed to be flat field with rare topographic ups and downs. As shown in Figure 15, Doppler Sodar installed in Building Research Institute (BRI) and super sonic anemometers at an observation tower, 213m high, in Meteorological Research Institute (MRI) are used for the wind measurement. MRI is located about 10km to the south from BRI. In this section, measurement results on March 3rd through 21st are outlined.

As for the wind velocity and direction between two places, it is confirmed that there is a certain correlation as shown in Figure 16. On the vertical profile of the wind velocity, averaged index of the power law in MRI is larger than that in BRI and depends on wind velocity as shown in Figure 17. The averaged values in MRI are 0.40 against northern wind and 0.33 against western wind, while those in BRI are 0.19 against northern wind and 0.21 against western wind, respectively. As for the index in MRI, the averaged index from northern wind is larger than that from western wind, which is probably because there is an urban area with middle-rise buildings to the north of MRI, where there is relatively rural distinct to the western of MRI. Cross-correlation coefficients obtained from every ten minutes' index of the power law of the each point are shown in Figure 18. They

result in getting maximum values at time lag of 10 through 20minutes, which means that it is useful to evaluate the profiles by considering wind with time scale of a few ten minutes. One example of the each profile is in Figure19.



(a)Monostatic Doppler Sodar (BRI)



(b)Obseravation tower (MRI) with anemometers

Figure 15 Wind measument systems

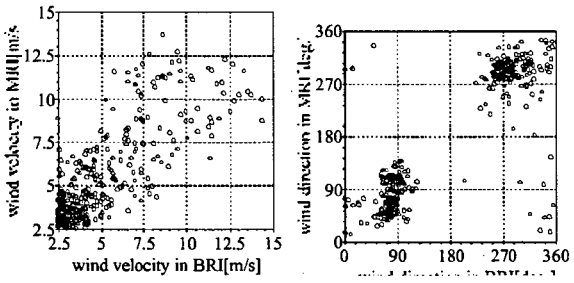
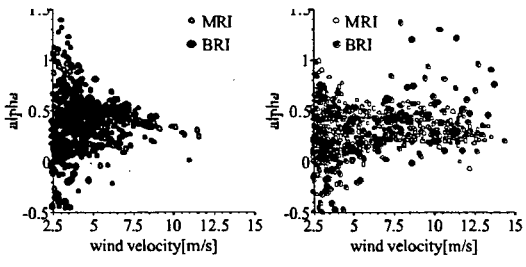


Figure16 10-min averaged wind velocity and direction by the Monostatic Doppler Sdar in BRI and super sonic anemometer in MRI



(a) NW– NE (b) SW – NW

Figure 17 Wind velocity and index of power law

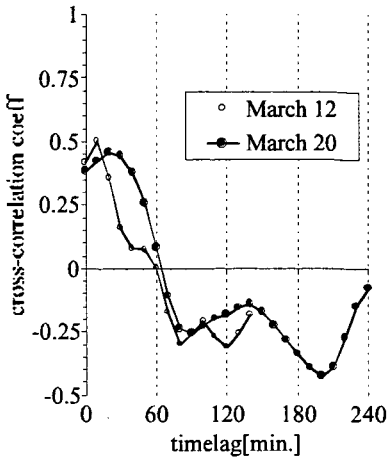


Figure 18 Cross-correlation coefficients of power law index in BRI and MRI

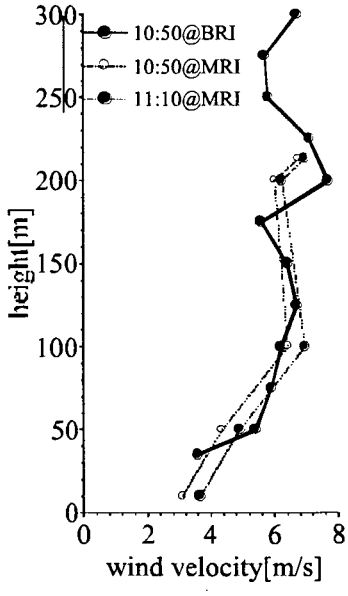


Fig.19 Example of wind profile in BRI and MRI at 10:50 and 11:10 on March 20th

4.2 Numerical Evaluation of Greenery Volume in Tsukuba Area

We use IKONOS satellite images superposed on digital surface model data in order to extract greenery volume in some urban areas. However, in this section we introduce another scheme of using only digital surface model data to analyze urban greenery coverage. Figure 20 shows small target region of

Tsukuba area, field size is 180m x 180m. The ground surface measure result of this place by airborne LIDAR is shown in Figure 21 as a same direction view of Figure 20, and top view of this region is shown in Figure 22. It shows the canopy of trees has a characteristic geometric pattern like a hedgehog. We extracted the greenery coverage area from digital surface model data using this feature. We have chosen Co-occurrence Matrix [4] for method of this study, on the analogy of image analysis. Co-occurrence Matrix can be obtains complexity information of target region. If accumulate concentrate to the near diagonal lines of this matrix then it meaning flat surface pattern like a building top else if distributed separate from the diagonal line then it have a complex pattern like a canopy of tree. Parameterized this matrix pattern used for extracting greenery coverage. The calculation parameters of Co-occurrence Matrix, displacement vector is d=1 used at all four directions (θ=0, 45, 90, 135°) and the number of height levels is L=10 (ground level to 50m height divided into 10 levels). The examine window size is 3 x 3 at each point. The results of the calculation are shown in Figure 23.

These results suggest will be useful to making it possible to calculating the greenery volume in urban area by digital surface model made from only airborne LIDAR data.

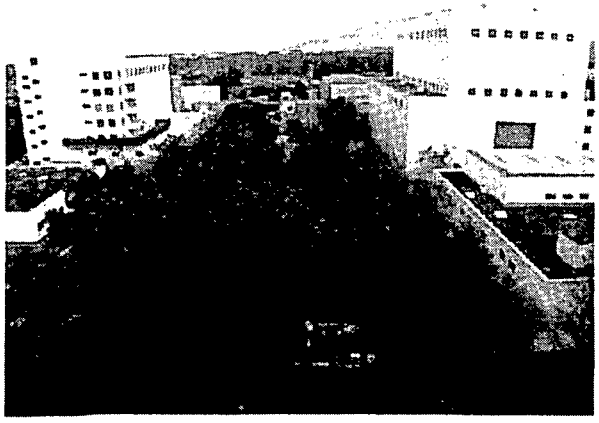


Figure 20 Target region (180m x 180m)

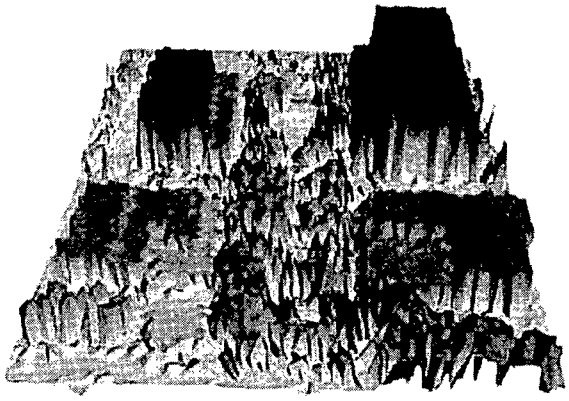


Figure 21 Digital surface model made by airborne LIDAR shown by TIN (Triangulated Irregular Network)

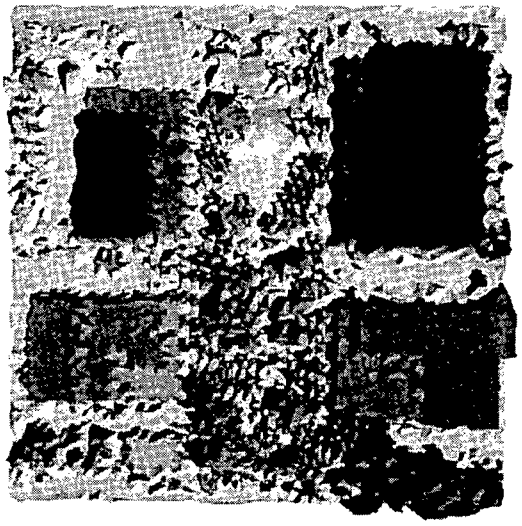


Figure 22 Top view (TIN)

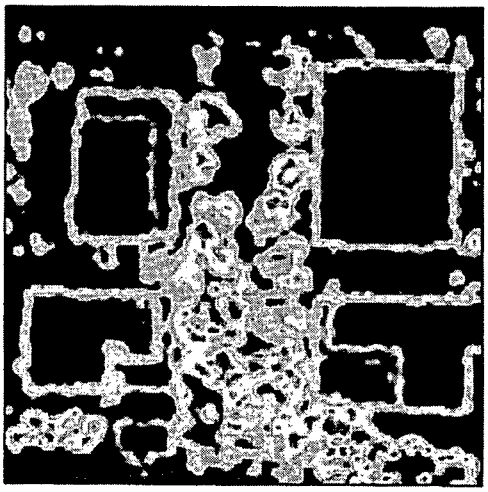


Figure 23 Greenery extractions(θ=0+45+90+135°)

3. CONCLUSIONS

In this paper, the evaluation of urban wind characteristics by numerical methods was introduced and their validity was discussed. The fundamental techniques in this paper will work for developing of "Numerical Simulator of Urban Wind".

REFERENCES

[1] Okuda Y., Okada H., Tamura T. et al., *Use of Digital Surface Model for Estimation of Surface Roughness in Urban Area*, Proc. of 17th National Symposium on Wind Engineering, pp.13-18, 2002.

[2] Raupach M.R. Antonia R.A. and Rajagopalan S. , *Rough-wall turbulent boundary layers*, Appl. Mech. Rev., Vol. 44, pp.1-25, 1991.

[3] Counihan, J., *Adiabatic Atmospheric Boundary Layers*, Atmos. Environ., Vol. 9, pp. 871-905, 1975.

[4] Haralick R. M., *Statistical and structural approaches to texture,* Proc. IEEE, Vol. 67, No. 5, pp. 786-803, 1979.

A Model to Predict Hurricanes Induced Losses for Residential Structures

by

Jean-Paul Pinelli[1], Chelakara. Subramanian[1], Liang Zhang[1] , Kurtis Gurley[2], Anne Cope[2], Emil Simiu[3], Sofia Diniz[3], and Shahid Hamid[4]

ABSTRACT

This paper presents a practical probabilistic model for the projection of annualized damage costs to residential structures due to hurricanes. The estimation of the damage is accomplished by first defining the basic damage modes for components of specific building types and their probabilities of occurrence as functions of estimated wind speeds. The damage modes are then combined in possible damage states, whose probabilities of occurrence are calculated from Monte Carlo simulations carried on engineering numerical models of typical houses. Once this is done it is possible to estimate repair/replacement costs associated with building damage induced by windstorms. The calculation of damage (repair/replacement costs) allows us to estimate building vulnerabilities. Finally, we discuss and illustrate the estimation of expected losses for groups of buildings, including regional expected annual losses, and expected losses induced by a hurricane event. The probabilistic input is based on statistical surveys of the Florida building population, laboratory studies, post-damage surveys, insurance claims data, engineering analyses and judgment, and Monte Carlo simulation methods.

KEYWORDS: Hurricane, Monte Carlo simulation, probability, residential structures, vulnerability, wind speeds.

1.0 INTRODUCTION

Within the U.S., windstorms are one of the costliest natural hazards, far outpacing earthquakes in total damage (Wind Engineering, 1997; Landsea et al, 1999). A recent analysis of windstorm damage for the U.S. East and Gulf coasts by Pielke et al. (1998) suggests that the average annual economic loss is about $5 billion. This agrees closely with National Oceanic and Atmospheric Administration (NOAA) estimates of 84 billion dollars in hurricane related damage since 1980. Over half of the hurricane-related damage in the U. S. occurs in the state of Florida, which has $1.5 trillion in existing building stock currently exposed to potential hurricane devastation. With approximately 85 % of the rapidly increasing population situated on or near the 1200 miles of coastline, Florida losses will continue to mount in proportion to coastal population density. It is therefore critical for the state of Florida, and the insurance industry operating in that state, to be able to estimate expected losses due to hurricanes and their measure of dispersion. For this reason the Florida Department of Insurance asked a group of researchers to develop a public hurricane loss projection model. This paper describes a model for the estimation of the damage to residential buildings due to hurricane or severe storms.

Although a number of commercial loss projection models have been developed, only a handful of

[1] Florida Institute of Technology, USA
[2] University of Florida USA
[3] National Institute of Standards and Technology, USA
[4] Florida International University, USA

studies are available in the public domain to predict damage for hurricane prone areas. Most studies use post-disaster investigations of available claim data to fit damage versus wind speed vulnerability curves. (e.g. Mitsuta et al. 1996; Huang et al., 2001). Although simple, this approach is highly dependent on the type of construction and construction practices common to the areas represented in the claim data. Recent changes in building codes or construction practices cannot be adequately reflected by vulnerability curve based on past data. In addition, damage curves obtained by regression from observed data can be misleading, because very often, as was the case for hurricane Andrew, few reliable wind speed data are available.

In contrast, a component approach explicitly accounts for both the resistance capacity of the various building components and the load effects produced by wind events to predict damage at various wind speeds. In the component approach the resistance capacity of a building can be broken down into the resistance capacity of its components and the connections between them. Damage to the structure occurs when the load effects from wind or flying debris are greater than the component's capacity to resist them. Once the strength capacities, load demands, and load path(s) are identified and modeled, the vulnerability of a structure at various wind speeds can be estimated. Estimates are affected by uncertainties regarding on one hand the behavior and strength of the various components and, on the other, the load effects produced by hurricane winds. A damage prediction model that incorporates elements of a component approach is being implemented for the HAZUS project (Minor and Schneider, 2001).

The purpose of this paper is to present and illustrate the principle of a probabilistic component approach to the prediction of wind-induced damage and of corresponding repair/replacement costs. Our approach makes use of probabilistic information on *basic damage modes.* This information is used to calculate probabilistic information on *combined damage states.* The latter consist of combinations of basic damage modes, determined by engineering judgment, post-disaster observations, and/or analysis.

The next section discusses basic damage modes and their probabilistic characterization. We then consider combined damage states and the derivation of their probabilistic characteristics. Once this is done it is possible to estimate repair/replacement costs associated with building damage induced by windstorms. Such costs are referred to as *wind-induced building damage*, or for short *damage.* Note that we will occasionally refer to some types of damage in a physical, as opposed to monetary sense. For example, we will refer to the physical damage of, say, tiles. We will omit the adjective "physical" and refer to physical damage more briefly as "damage" whenever the context is sufficiently clear that no confusion can result from this use. The calculation of damage (repair/replacement costs) allows the estimation of building vulnerabilities. In a wind engineering context we will define *vulnerability* as a measure of the susceptibility to damage, expressed as a function of the wind speed. Finally, we discuss and illustrate the estimation of expected damage for groups of buildings, including regional expected annual damage, and expected damage induced by a hurricane event. Uncertainties associated with such estimates will be dealt with in a subsequent paper. A companion team of researchers for this project is developing the wind field model that will provide this damage model with the probabilities of occurrence of various wind speeds, thus allowing the estimation of annualized insurable loss. Development of the wind field model is not a part of this paper, and will be the subject of a forthcoming separate document.

2.0 BASIC DAMAGE MODES

This research is currently focused on residential low-rise structures of different types that make up the overwhelming bulk of the Florida building stock. For purposes of illustration, the paper presents the approach for a building belonging to a specified type: an unreinforced masonry house with timber gable roof covered with tiles. Its most vulnerable types of components are shown in Fig. 1. They correspond to the following five significant basic damage modes: (1) breakage of openings (O); (2) loss of tiles (T); (3) loss of roof or gable end

sheathing (S); (4) roof to wall connection damage (C); and (5) masonry wall damage (W). For a specified wind speed v the building will either not experience damage, or experience several of these five basic damage modes. Some damage modes are independent of each other (e.g., loss of tiles and breakage of openings); others are not (e.g., given that the building has experienced window breakage, the probability of its losing sheathing increases)

The model is further refined by dividing each basic damage mode into several sub-damage modes (e.g., O_i, i =0,1,2,3) according to the degree of damage: no damage, light, moderate, or heavy damage. For example, we can define O_0 as zero loss of opening (no damage), O_1 as loss of less than 25% of openings (light), O_2 as loss of 25% to 50% of openings (moderate), and O_3 as loss of in excess of 50% of openings (heavy). Sub-damage modes can similarly be defined for the other basic damage modes, denoted by T_j, S_k, C_l,, W_m, (j,k,l,m =0,1,2,3). The sub-damage modes corresponding to a damage mode must be so defined that they are mutually exclusive. For example, the union of the sub-modes O_i (i = 1,2,3) is equal to the mode O, and the sum of their probabilities is equal to the probability of O.

A first step toward the estimation of wind-induced damage is the probabilistic characterization of the basic damage (or sub-damage) modes. This requires estimates of (1) probabilities that, under wind speeds contained in specified intervals defined by a speed v, a building of a specified type will experience damage (sub-damage) modes of various kinds, and (2) measures of statistical dependence between the events associated with those modes. The wind speeds v considered in the study are 3 sec average gust wind speeds at 10 m. For purposes of illustration, Table 1 lists assumed probabilities of occurrence of the sub-damage modes for the case of opening failures (see Figure 1), conditional on wind speeds belonging to 5m/s intervals centered on values of v varying from 45 to70 m/s. For example, the fifth column-second row cell states that for v in the interval 57.5m/s $< v \leq$ 62.5m/s, $P(O_2|v)$=35% is the probability that a building will experience moderate opening damage, and the fifth column- third row cell $P(O_3|v)$= 60% is the probability that the building will experience heavy opening damage. To simplify the notation we may omit the notation "$|v$" in all subsequent developments, that is, we will use the shorthand notation P(x) in lieu of P(x|v).

For each damage mode the event "no damage" (i=0) is unity minus the sum of the probabilities of the three sub-damage modes (i=1,2,3). For example, for v=55 m/s the probability of no opening damage is $P(O_0)=1-P(O)=1-[P(O_1)+P(O_2)+P(O_3)] = 100\%-5\%-40\%-40\%=15\%$.

The requisite probabilities of basic damage modes can in principle be obtained directly: (1) from laboratory tests (e.g., Baskaran and Dutt, 1995), after translating physical damage usually reported in laboratory tests into monetary terms; (2) from post-disaster observations of damage, duly accounting for the fact that reported damage includes damage due to effects other than wind (for example storm surge); (3) from numerical studies entailing simulations; and, (4) last but by no means least, from engineering judgment needed to supplement or interpolate between sparse data.

The choice of basic damage modes is in general determined by practical considerations such as the type of structure, the format of the requisite probabilistic information and the extent to which it is available, the need for keeping the model reasonably simple, and the requisite accuracy of the loss estimation. The methodology described in this paper is independent of the basic damage modes being considered in the calculations.

3.0 COMBINED DAMAGE STATES

When a windstorm causes damage to a structure, it will usually cause different damage modes to different components at the same time. We shall refer to these combinations of damage modes as combined damage states. Since the resulting combined damage states require not only set-theoretical but also architectural and structural engineering scrutiny, it is appropriate to use an engineering approach to their definition. The damage states being considered must satisfy the

following requirements:

- They must be combinations of the damage modes described previously
- They must be chosen with a view to enabling damage estimates to be made correctly, in the sense that no possible damage state is omitted, and no double or multiple counting of damage states occurs.
- They must make sense from an architectural and structural engineering point of view. For example, for a building covered by conventional sheathing, it may be assumed that wall damage will not occur without some loss of sheathing. Similarly, although tile and opening failures do not necessarily cause roof-to-wall connection damage, it is reasonable to assume that no roof to wall connection damage will occur without some tile loss and opening breakage.

The basic damage modes are represented in the diagram of Figure 2. The partial or total overlap of the basic damage modes is based on engineering judgment. Figure 2 is the point of departure in the process of defining combined damage states. Associated with the basic damage modes O, T, S, W and C are events -- combined damage states – whose union represents the total damage universe shown in Figure 2. Combined damage states can similarly be considered that involve sub-damage modes. We consider the events associated with the occurrence of the following combinations of sub-damage modes:

Event 1. O_0T_0 (no damage). See hatched area in Fig. 3a. Since it is assumed that all damage involves first some opening breakage and/or tile loss, the lack of both of these is equivalent to no damage.

Events 2, 3, 4. $O_i\ T_0$ – i=1, 2, 3 (opening failure and no tile loss). The hatched area in Fig. 3b represents the sum of events 2,3,4 or ($O\ T_0$). Recall that each area O_i is a subset of the set O; for convenience this is not shown in any of the graphs of Fig. 3.The probabilities of these sub-states will help to estimate the cost of repair of homes that have only opening failures.

Event 5, 6, 7. $O_0\ T_j\ S_0$–i=1, 2, 3 (tile failure and no opening or sheathing loss). The hatched area in Fig. 3c represents the sum of events 5,6,7 or ($O_0\ T\ S_0$). The probabilities of these sub-states will help to estimate the cost of repair of homes that have only roof cover failures (e.g., homes with effectively boarded openings and strong garage doors).

Events 8 through 16. $O_i\ T_j\ S_0$ – i,j=1,2,3 (opening and tile failure and no sheathing loss). The hatched area in Fig. 3d represents the sum of events 8 to 16 or ($O\ T\ S_0$).

Events 17 through 25. $O_0\ T_j\ S_k$ – j, k=1,2,3 (tile and sheathing failure and no opening failure). The hatched area in Fig. 3e represents the sum of events 17 to 25 or ($O_0\ T\ S$).

Events 26 though 52. $O_i\ T_j\ S_k\ W_0\ C_0$ (opening, tile and sheathing loss and no wall and connection failure) – i, j, k =1, 2, 3. The hatched area in Fig. 3f represents the sum of events 26 to 52 or ($O\ T\ S\ W_0\ C_0$).

Events 53 through 133. $O_i T_j\ S_k\ C_l W_0$ -i,j,k,l=1,2,3 (opening, tile, sheathing and connection failure and no wall failure). The hatched area in Fig. 3g represents the sum of events 53 to 133 or ($O\ T\ S\ C\ W_0$).

Events 134 through 214. $O_i\ T_j\ S_kW_m\ C_0$ - i,j,k,m=1,2,3.(opening, tile, sheathing and wall failure but no connection failure). The hatched area in Fig. 3h represents the sum of events 134 to 214 or ($O\ T\ S\ W\ C_0$).

Events 215 through 457. $O_i\ T_j\ S_k\ C_l\ W_m$ – i,j,k,l,m=1,2,3.(opening, tile, sheathing, wall, and connection failure). The hatched area in Fig. 3i represents the sum of events 215 to 457 or ($O\ T\ S\ W\ C$).

There are a total of 457 damage state events. However, not all of these events are of interest from a damage estimation point of view. Engineering considerations allow the elimination of a number of events. There are several scenarios:

When roof cover damage (T) and sheathing damage

(S) occur at the same time, the damaged area of the roof cover must be equal or larger than the damaged area of sheathing. We can therefore eliminate all the damage states which pertain to damaged area of roof cover smaller than the damaged area of sheathing, i.e. eliminate events that contain T_jS_k when $j<k$.

When roof cover damage (T) or sheathing damage (S) or opening damage (O) occur together with wall damage (W) or connection damage (C), the level of damage for T or S or O should be larger than for W or C. That is, there is only a small probability that a wall would suffer heavy damage while the roof cover has suffered light damage. Thus we can eliminate all the damage states which contain lower levels of roof covering damage and decking damage and opening damage than wall damage and connection damage. i.e. eliminate events containing O_i, S_k, T_j, W_m, and C_n when i, j, $k < m$, n. In particular, when severe wall damage and severe roof to wall connection damage occur together, the whole structure collapses. So if roof to wall connection and wall damage are both heavy (i.e., if W_3 and C_3 occur), the only significant damage event will be$O_3T_3S_3W_3C_3$, so that we can eliminate all events $O_iT_jS_kW_3C_3$ for which i, j, k =1,2.

These engineering considerations allow the elimination of 240 damage states, leaving 217 damage states. Note from Fig. 2 that, for any specified wind speed, any two distinct damage states are mutually exclusive. For example, a structure cannot experience both the state $O_i\,T_j\,S_k\,W_0\,C_0$ and the state $O_i\,T_j\,S_k\,W_0\,C_l$.

The implementation of this model is currently under way. The determination of values for the basic damage modes, and the combined damage state events rely upon the use of a component-based Monte Carlo simulation engine. The simulation relates estimated probabilistic strength capacities of building components to 3 sec average gust wind speeds through a detailed wind and structural engineering analysis that includes effects of wind-borne missiles. The component approach taken in the Monte-Carlo simulation explicitly accounts for both the uncertain resistance capacity of the various building components and the load effects produced by wind events to predict damage at various wind speeds. The resistance capacity of a building is broken down into the resistance capacity of its components and the connections between them. Damage to the structure occurs when the load effects from wind or flying debris are greater than the component's capacity to resist them. The probabilistic strength capacities, load paths, and load sharing between components are identified and modeled. The probable damage to a particular building class at a given wind speed is estimated through many simulations of the same structure at that wind speed, randomly sampling component capacities between each simulation. Each simulation represents an instance of a storm of same intensity. Changes in loading on components as a result of component /connection failure within a single simulation are accounted for. The wind speed is then increased to the next discrete value and the process repeated. The end result is a table describing the probability of combined damage levels to the components, conditioned upon peak wind speeds.

No duration effect is included in the model. It is assumed that the wind speed represents the highest 3 sec peak gust speed over the duration of a storm at a particular location, and when applied to the building model it produces the maximum loading for that storm. Since the component strengths are set, if they do not fail at the highest 3 second gust, they won't fail at all. Other average wind speeds could be considered for the simulation (e.g. 1 min or 10 min average wind speed), in which case, the pressure coefficients to compute the pressure distributions would be adjusted accordingly, resulting in the same maximum pressures. The wind speed – whatever form it is expressed in – thus serves as an index of the storm intensity; and the damage is independent of whether the index being used is the 3-sec, 1-min, 10-min, or mean hourly speed. The 3 sec average was adopted because it is the standard in the U.S.A (see ASCE7, 2002).

A possible resulting damage matrix is summarized in Table 2.The wind field model will come into play when the results of the simulation are used to calculate annualized damage probabilities, as

discussed in the following sections. The resulting probabilities of the 217 combined damage states will be assessed as necessary to ascertain the extent to which they are physically realizable. This will provide useful guidance to the future development of the simulation procedure.

4.0 STATISTICAL ANALYSIS OF THE BUILDING STOCK

The goal of this research is to estimate hurricane losses over a large geographical area with a building population composed of different structural types. Although Figure 1 represents a standard masonry house with gable roof, the methodology described above can be applied to any other type of residential houses. It is therefore important to identify all the structural types that make up the building stock of the different regions of Florida. For each structural type, a model will be built and a Monte Carlo simulation performed, so that each structural type will end up with its own damage matrix. Finally, when computing the overall damage in any given area, as explained in the next section, it will be necessary to know the probability of occurrence of each structural type in that region.

The first step in the analysis of the building stock is therefore to identify the most common structural types in the target area. The authors obtained the property tax appraiser databases of 9 Florida Counties, which contain structural information for most single family residential houses, including exterior wall types, roof types and roof cover. These counties are distributed among four different regions of Florida with different building characteristics, as shown in Figure 4.

These counties include: Escambia, Walton, and Leon in the Northern region; Brevard, Pinellas, and Hillsborough in the Central region; Palm Beach, and Broward in the Southeast region; and Monroe County for the Keys. Besides, they have also obtained information for 1691 houses in the Miami-Dade county in Southeast Florida. The statistical significance of the samples (in terms of population covered) in each of the four regions is highlighted in Table 3.

Based on the information contained in the databases, four known plus one unknown or generic structural types were defined in each region. In addition, due to the variety of the building stock in the Keys, four additional types were defined for the Keys. They are all listed in Table 4. Table 5 lists their probability of occurrence per region. It should be noted that for types 1 to 4 the statistics could be divided between structures with tiles and structures with shingles.

5.0 DAMAGE ESTIMATION

Consider a residential community consisting of total number of n homes of different structural types m in a zone with specified surrounding terrain conditions. .

Assume the probability of occurrence of a storm with a peak 3-second gust wind speed within the interval $\{v- \Delta v/2, v + \Delta v/2\}$ m/s is $P(v)=p(v)\Delta v$, where $p(v)$ is the probability density distribution of the largest yearly wind speed (such information will be provided by the associated probabilistic wind field development team). Assume that the repair/replacement cost data for each possible damage state listed in Table 2, e.g. $O_3T_2S_1W_0C_0$, is obtained from insurance adjusters, and that the probabilities of occurrence of damage states, e.g. $P(O_3T_2S_1W_0C_0)$, are estimated conditional upon wind speed. The probable expected damage, expressed as a percentage, can be estimated as follows.

Step 1. The probable damage for a structure of type m in the zone subjected to a wind speed in the interval $\{v- \Delta v/2, v + \Delta v/2\}$ m/s is the sum of all the relative possible damage states listed in Table 2 for speed v in that interval multiplied by their probabilities of occurrence. For example, for v=60 m/s, Δv=10 m/s, the following equation results:

$$\text{damage}_{(60\text{m/s, type } m)} = [P_{\text{type } m}(O_3T_2S_1W_0C_0 | 60 \text{ m/s} - 5 \text{ m/s} < v < 60 \text{ m/s} + 5 \text{ m/s}) \times c(O_3T_2S_1W_0C_0)$$

$$+ [P_{\text{type } m}(O_3T_2S_2W_0C_0 | 60 \text{ m/s} - 5 \text{ m/s} < v < 60 \text{ m/s} + 5 \text{ m/s}) \times c(O_3T_2S_2W_0C_0) + \ldots] + \ldots =$$

$$\Sigma_i P_{m,i}(subdamage\_state_i | 60 \text{ m/s}) \times c(subdamage_i) \quad (1)$$

In Eq. 1, $c(O_3T_2S_1W_0C_0)$ denotes the repair cost corresponding to subdamage state $O_3T_2S_1W_0C_0$ as a percentage of the building replacement value, and $c(subdamage_i)$ is similarly defined.

In modeling the repair cost, the procedure needs to incorporate the fact that, the combined repair cost of components cannot exceed the replacement cost of the facility. In practice, the combined repair costs taper off to reach the replacement cost. Moreover, if the repair cost of the combined structure exceeds 50% to 60% of the replacement value of the building; it is considered economical to demolish the building. For this case the cost of demolishing and removal of debris must be used in the estimates.

It was stated at the end of section 3 that our 5-mode model is decomposed into 217 combined damage states. It is not reasonable to expect that a distinct cost can be assigned to each of these states. Rather, the many combinations will be associated with a handful of classes of damage. For example, 128 states, say, may all lead to 20% of replacement cost, 56 states may lead to 40 % replacement cost, and so forth. The simplification inherent in this observation is to be incorporated into the estimation procedure, and will require the input of experienced insurance adjusters.

Step 2. An expression similar to Eq. 1 applies to each of the wind speeds. Table 2 takes into account the probability of occurrence of wind speeds in the intervals of interest. The damage equation is

$$\text{Annual\_damage}_{\text{type } m} = \sum_{windspeed\ i} \text{damage}_{(vi,\text{type } m)} \times P(v_i-\Delta v/2<v_i<v_i+\Delta v/2) \qquad (2)$$

Step 3. The damages for types 1, 2, ... are multiplied by the respective relative frequency of those types in the building population of the zone (see Table 5). The damage equation becomes:

$$\text{Average\_Annual\_Damage} = \text{Annual\_damage}_{\text{type 1}} \times P(\text{type 1}) + \text{Annual\_damage}_{\text{type2}} \times P(\text{type2}) + \ldots. \qquad (3)$$

Step 4. The total estimated expected damage to buildings for a particular zone is the damage calculated by using Eq. 3 times the total number n of houses in the zone. The process is repeated for each zone, and the results for each zone are added to obtain the estimated expected hurricane-induced annual damage to buildings for the entire state.

6.0 UNCERTAINTIES

The purpose of this paper is to illustrate the conceptual framework of the methodology used for damage computation. A detailed discussion of the uncertainties involved will be the focus of a follow-up paper. Main types of uncertainties include selection of the types of structural models for the simulations, repairment cost uncertainties, the properties or parameter inputs into the Monte Carlo simulations and relationship between wind speed and resultant force on roof. The estimates of the wind speed itself involve a significant degree of uncertainty that affects the final damage estimate. As noted earlier, the probabilistic wind model, including the uncertainties associated with it, is being developed in parallel with the effort reported here. Sensitivity studies are being conducted to define the influence of the different parameters on the outputs of the models and to identify the most critical sources of uncertainty.

7.0 CONCLUSIONS

This paper presents a probabilistic framework for the estimation of annual damages due to windstorms in the state of Florida. The framework is illustrated for the case of five basic damage modes, although additional modes could be considered. The framework assures that no type of damage is counted more than once, no type of possible damage is omitted from the calculations, and interactions between various types of damage are accounted for. The costs are calculated by correctly accounting for the dependence between various damage modes (e.g., window breakage and roof uplift). The damage is appropriately modeled as a stepwise process, as damage to openings gives sudden rise to increases of internal pressures, and sudden collapse of the roof results in immediate damage to walls.

A key ingredient of the proposed procedure is the development of a Monte Carlo simulation approach that relates probabilistic strength capacities of building components subjected to wind action through a detailed aerodynamic and structural engineering analysis. The results of the Monte Carlo simulation are used to fill in the cells of damage matrices used for the estimation of expected damage due to a windstorm event, and of expected annual damage, both at a specified location and over a larger geographical area.

An important component of the methodology is the determination of the right mix of structural types or models that characterize the building population in any given area. The definition of these structural types was achieved through statistical analyses of building databases for several counties throughout the state of Florida. A more accurate definition could be obtained in the future if all the counties were surveyed.

Work is in progress on the development of the Monte Carlo simulation methodology and its application to the various types of structures defined through the county surveys. Work is also in progress on quantifying the uncertainties in loss calculations, based on uncertainties in the estimation of probability matrices, associated conditional probabilities, hurricane wind speeds, structural behavior, component properties, and building population. Work is in progress on the development of the probabilistic wind field model. Preliminary predictions of annual vulnerability are planned once such development is completed.
One of the main advantages of this methodology is its transparency. The probabilities in the damage matrices are based on engineering models that will be continuously updated and refined as more knowledge on the strength of the component, load path, and wind effects becomes available.

8.0 ACKNOWNLEDGMENT

The authors wish to acknowledge with thanks valuable advice from Mark Vangel, Department of Biostatistical Sciences, the National Institute of Standards and Technology, and Dana-Farber, Cancer Institute. This work was done with the financial support of the Florida Department of Insurance (FDOI). Dr. Shahid Hamid, from Florida International University, served as project manager. Portions of this work were also supported in part by NSF grant CMS-9984663. The opinions, findings, and conclusions expressed in this paper are not necessarily those of the FDOI.

9.0 REFERENCES

1. American Association for Wind Engineering, "Wind Engineering: New Opportunities to Reduce Wind Losses and Improve the Quality of Life in the USA", August 1997.

2. American Society of Civil Engineering, "Minimum Design Loads for Buildings and Other Structures," 2002, USA.

3. Federal Emergency Management Agency, "Building Performance: Hurricane Andrew in Florida," report FIA-22, 1993.

4. Huang, Z., Rosowsky, D. V., and Sparks, P. R., (2001), "Long-term hurricane risk assessment and expected damage to residential structures," *Reliability Engineering and System Safety*, **74**, 239-249.

5. Landsea, C. W., Pielke, Jr. R. A., Mestas-Nunez, A. M. and Knaff, J.A. (1999), "Atlantic Basin Hurricanes: Indices of Climatic Changes", *Climatic Change*, 42, 89-129.

6. Minor, J. E. and P. J. Schneider (2001), "Hurricane Loss Estimation – The HAZUS Preview Model," *America's Conference on Wind Engineering*, Clemson, SC June 4-6 2001.

7. Mitsuta, Y., T. Fujii and I. Nagashima (1996), "A Predicting Method of Typhoon Wind Damages", *Probabilistic Mechanics and Structural Reliability: Proceedings of the 7th Specialty Conference*, 970-973.

8. Pielke, Jr., R. A., and Landsea, C. W., "Normalized Atlantic Hurricane Damage, 1925-1995," Weather Forecasting 13, 621-631, 1998.

Table 1. Assumed probabilities of occurrence of sub-damage modes O_i conditional on wind speed intervals associated with the speeds v.

v(m/s)	45	50	55	60	65	70
$P(O_1\|v)$	6%	10%	5%	5%	5%	0%
$P(O_2\|v)$	4%	30%	40%	35%	20 %	10%
$P(O_3\|v)$	0%	10%	40%	60%	75 %	90%

Table 2: Example of estimated probabilities of damage states, conditional on wind speed intervals associated with the speeds v

v (m/s)	45	50	55	60	65	70
P (O_0T_0)	82 %	38. %	6.0%	0.0 %	0.0 %	0. %
$P(O T_0)$	9.1 %	40. %	54.0 %	20.0 %	0.0 %	0. %
P(O_0 T S_0)	7.6 %	10. %	3.7%	0.0 %	0.0 %	0. %
P(O_0 T S)	0.5 %	0.5 %	0.3%	0.0 %	0.0 %	0. %
P(O T S_0)	0.4 %	2.0 %	6.3%	30. %	20. %	0. %
P(OTSW_0C_0)	0.5 %	0.5 %	0.33 %	1.0 %	10. %	0. %
P(OTSCW_0)	0.%	3. %	3.87 %	6.0 %	0.%	0. %
P(OTSWC_0)	0.%	0. %	3.57 %	9.0 %	0.%	0. %
P(OTS CW)	0.%	6. %	21.9 %	34. %	70. %	10 0%

Table 3. Population information for each area

Region	Northern	Central	Southeast	Keys
Total number of counties	34	27	5	1
Number of sample counties	3	3	2	1
Total population	2,885,559	7690240	5,326,990	79589
Sample population	574,463	2396660	2,754,202	79589
% of population in sample	20%	30%	54%	100%

Table 4: Structural types definitions

	Structure	Roof Materials	Roof Type
Type 1	concrete blocks	Shingle/Tile	Gable
Type 2	concrete blocks	Shingle/Tile	Hip
Type 3	timber	Shingle/Tile	Gable
Type 4	timber	Shingle/Tile	Hip
Type 5	concrete blocks	Metal	Gable
Type 6	concrete blocks	Metal	Hip
Type 7	timber	Metal	Gable
Type 8	timber	Metal	Hip

Table 5: Percentage of each type for 4 regions.

	Northern	Central	Southeast	Keys	
Type 1	25%	43%	46%	22%	Type5 . 12%
Type 2	12%	29%	23%	11%	Type6 . 6%
Type 3	32%	12%	13%	12%	Type7 . 9%
Type 4	16%	6%	6%	6%	Type8 . 5%
Unknown Type	15%	10%	12%	17%	

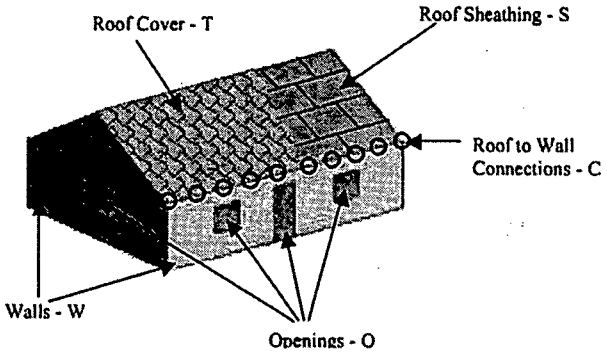


Figure 1: Components of a single family home

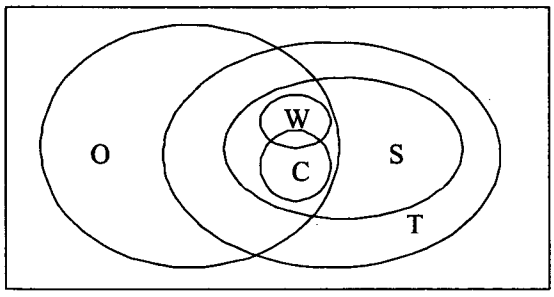


Figure 2: Venn diagram for the basic damage modes of a masonry home

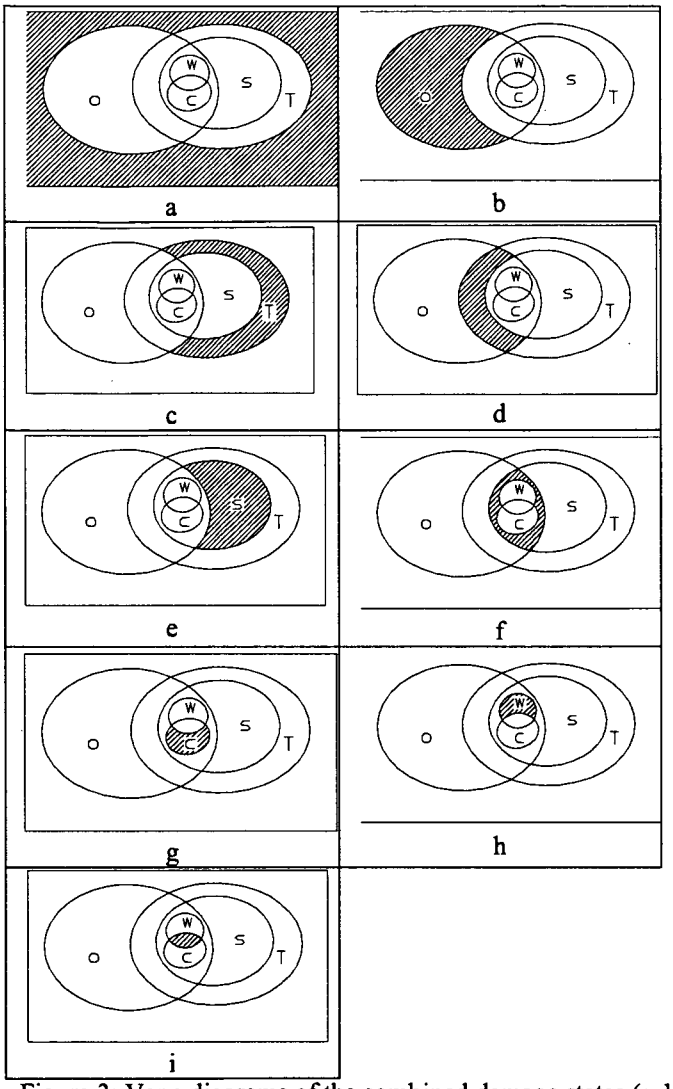


Figure 3: Venn diagrams of the combined damage states (subsets of Figure 2)

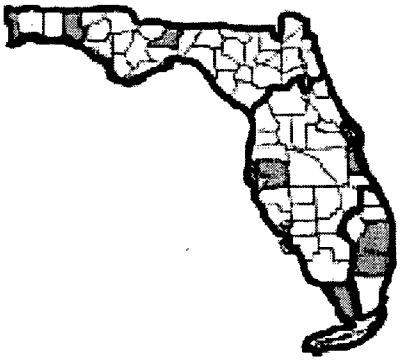


Figure 4. Florida counties and regions

Calculation of Unsteady Aerodynamic Forces by CFD and Their Comparison with Measured Values

by

Hiroshi Sato[1], Jun Murakoshi[2], Koichiro Fumoto[3] and Masao Miyazaki[4]

ABSTRACT

Unsteady aerodynamic forces were calculated for cross sections such as flat plate, box girder and slotted box girder. Seven methods of CFD were applied. The calculated values were compared with theoretical values or measured values from wind tunnel tests. In the case of the flat plate and the box girder, the calculated values agree well with the theoretical or measured values. In the case of the slotted box girder, however, the calculated values did not agree well with the measured values. The methods should be improved for them to be applied for slotted box girders.

KEYWORDS: CFD, Super Long-span Bridges, Unsteady Aerodynamic Forces,

1. INTRODUCTION

Public Works Research Institute has been conducting cooperative research on super long-span bridges with Honshu-Shikoku Bridge Authority, Public Works Research Center, and eight private companies. The research goal is to propose super-long span bridges that have excellent properties in aerodynamic stability and economy. One of our results is the super-long span bridge with the slotted box girder, which has been already presented [1].

Aerodynamic forces on bridge girders are usually measured in wind tunnel. On the other hand, recent progress in computer technology has advanced reliability and applicability of computational fluid dynamics (CFD). Therefore, applicability of CFD to wind resistant design of super long-span bridges was studied as the part of the research.

In the research, unsteady aerodynamic forces were calculated for cross sections such as flat plate, box girder and slotted box girder. Seven methods of CFD were applied. The calculated values were compared with theoretical values or measured values. In this paper described are the cross section of girders, applied CFD methods and the comparison between calculation and measurement.

2. CROSS SECTION OF BRIDGE GIRDER

The cross sections subjected to CFD analysis are shown in Figure-1. It was found that slotted box girder has better flutter characteristics than flat plate or single box girder, and that its characteristics can be improved by some devices like center barrier and guide vane[2]. The slotted box girder used in this research did not have the center barrier or guide vane.

3. CFD ANALYSIS METHODS

The CFD analysis methods in our research are shown in Table-1

The direct method directly calculates an unsteady N-S equation without a turbulence model. We obtained a numerical solution from acoustic, momentum conservation, mass conservation, and state equations. This method ensures tracking of instantaneous values of the turbulent field since it can directly solve the N-S equation without the use of a turbulent model. However, as the number of grid points increases, the time required for calculation sharply rises. The behavior of the vortex below the calculated grid is ignored at the same time. Method 4 was based on this technique[3].

[1] Director, Structures Research Group, Public Works Research Institute, Tsukuba-shi, Ibaraki-ken 305-8516 Japan

[2] Team Leader, Bridge Structures Research Team, ditto

[3] Senior Researcher, Bridge Structures Research Team, ditto

[4] Secretary of Cooperative Research, Sumitomo Heavy Industries Ltd, Shinagawa-ku, Tokyo 141-8686 Japan

When calculation is made according to the Reynolds-Averaged Navier Stokes Equation, turbulence model is required. The k-ε model, the representative model of differentiation method, obtains turbulent stress by solving the transport equation of the modeled turbulent energy k and ε. The k-ε model was applied to the Method 3 and 5. In Method1[4], k-ω SST model[5] was used among double equation models because of Bardina's performance evaluation[6]. In Method 2[7], q-ω model[8] which was based on the k-ε model was used.

Large eddy simulation (LES method) does not use Reynolds' equation. This method takes an in-grid space average of the N-S equation. Smagorinsky's model is frequently used. Method 6 adopted the LES method [9]

The vortex point method introduces the basic solution of a differential equation, instead of solving the differential equation for fluid motion, to formulate an integral equation and divide the boundary into a finite number of elements for boundary integration. The advantage of this method over alternative analysis methods is its small number of unknowns, whose number of dimension is less by one than the other methods. However, the method is invalid unless that the basic solution required to convert the differential equation into an integral equation is already obtained. Method 7 was based on this technique[10]

In FDM, the coordinate system which suits an object boundary well must be used to increase accuracy.(Method1, 3 and 4)[11][4]. The merits of FVM are its easiness to take boundary conditions and to acquire preservation (Method 2 and 5) [12][7]. In FEM, complicated boundary conditions can be treated and accuracy can be increased locally (Method 6).[9]

4. COMPARISON OF CALCULATED FORCES

4.1 Definition of Unsteady Aerodynamic Forces

The calculated unsteady aerodynamic forces were compared with theoretical values and experimental values. The definition of unsteady aerodynamics forces are as follows:

$$L = \pi\rho\left\{B^2\left[L_{ZR}\omega^2 z + L_{ZI}\omega z'\right] + B^3\left[L_{\theta R}\omega^2\theta + L_{\theta I}\omega\theta'\right]\right\} \quad (1)$$

$$M = \pi\rho\left\{B^3\left[M_{ZR}\omega^2 z + M_{ZI}\omega z'\right] + B^4\left[M_{\theta R}\omega^2\theta + M_{\theta I}\omega\theta'\right]\right\} \quad (2)$$

where L: lift; M: aerodynamic moment; ρ: air density; B: girder width; V: velocity; z: vertical displacement; θ: torsional displacement; and ω: circular frequency.

4.2 Flat Plate

Fig.4 compares the calculated and theoretical values of unsteady aerodynamic forces of the flat plate. Although there are some errors in the real part of lift during bending excitation obtained and the imaginary part of lift during torsional excitation, the calculated and theoretical values are almost identical. As for the flat plate, the accuracy of the CFD methods seems relatively high. This accuracy is probably caused by its flatness of the section. Because of its flatness, the effect of viscosity appears only in the upstream and downstream ends of the section. Therefore the difference in calculation methods or in turbulence modeling does not affect much.

4.3 Box Girder

Fig.5 compares the calculated and measured values of unsteady aerodynamic forces of the single box girder section. Although CFD-analyzed and experimental values do not agree as well as they do in the case of the flat plate, an approximate trend can be estimated from the CFD methods. The reasons seem to be as follows: firstly, the handrails at the upstream and downstream ends of the section and the protective fence in the median strip zone were excluded from the present research; secondly, the section of the box girder was very flat.

4.4 Slotted Box Girder

Fig.6 compares the calculated and measured values of unsteady aerodynamic forces of the slotted box girder section. The difference between the CFD-analyzed and wind tunnel experimental values tends to be larger than that of the single box girder.

Among the CFD methods, values calculated according to the Method 6 agrees fairly well with the measured values. Method 6 adopted the LES Method as the turbulence model. The LES Method seems applicable even where flow is strongly unsteady.

As shown in Fig.3, the section of the double box girder forms a very complicated vortex from mutual interference between a vortex discharged from the upstream girder end and a shear layer separated from the front edge of the downstream girder. Therefore, the vortex behavior needs to be simulated accurately. Since vortex behavior is seriously affected by the turbulence model, improvement of the turbulence model seems to be important.

5. CONCLUSIONS

Unsteady aerodynamic forces were calculated for the flat plate, box girder and slotted box girder. Seven methods of CFD were applied. The calculated values were compared with theoretical values or measured values from wind tunnel tests.

It was found that unsteady aerodynamic forces of the flat plate and the flat single box girder can be predicted fairly well by the CFD analysis. The CFD analysis can be applicable to the relatively flat single box section.

On the other hand, satisfactory results were not obtained for the slotted box girder, probably due to the complicated flow in the slot. Improvement of the turbulence model seems to be effective to improve the accuracy of calculation.

This paper is part of the results of the cooperative research conducted by Public Works Research Institute, Honshu-Shikoku Bridge Authority, Public Works Research Center, and eight private companies. We would like to take this opportunity to mention that the CFD analysis for the flat plate, single box girder, and slotted box girder were conducted by Mr. S. Kuroda at Ishikawajima-Harima Heavy Industries Co., Ltd., Mr. H. Kawamoto at Kawasaki Heavy Industries, Ltd., Dr. K. Shimada at Shimizu Corporation, Mr. D. Ichishima at Sumitomo Heavy Industries, Ltd., Mr. S. Shirai at Hitachi Zosen Corporation, Mr. S. Watanabe at Mitsui Engineering & Shipbuilding Co., Ltd., and Mr. S. Sugiyama at Mitsubishi Heavy Industries, Ltd. We would like to acknowledge and thank them for their cooperation.

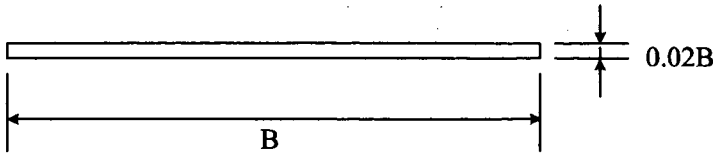
6. REFERENCES

1. H. Sato, N. Hirahara, K. Fumoto, S. Hirano and S. Kusuhara.: Full aeroelastic model test of a super long-span bridge with slotted box girder, *Journal of Wind Engineering and Industrial Aerodynamics, Vol. 90,* 2002.
2. H. Sato, S. Kusuhara, K. Ogi and H. Matsufuji.: Aerodynamic characteristics of super long-span bridges with slotted box girder, *Journal of Wind Engineering and Industrial Aerodynamics,* Vol. 88, 2000.
3. D.Ichishima.: Unified Theory for Solving Multi－Flow Problems, *J. of Technical Paper Vol.45 No.134, Sumitomo Heavy Industries Ltd.*
4. S.Kuroda.: Numerical Computations of Unsteady Flows for Airfoils and Non-airfoil Structures, *Proc. 31st AIAA Fluid Dynamics Conference & Exhibit, Anaheim, C,* 2001.
5. Menter,F.R.: Two-Eqation Eddy-Viscosity Turbulance Models, *AIAA journal*, vol.32,No.8, 1994.
6. Bardina,J.E Huang,P.G and Coakley.T.J.: Turbulence Modeling Validation, Testing and Development, *NASA Techinical Memorandum 110446,*1997.
7. H.Kawamoto, H.Yoshida and T.Oryuu.: 2-Dimensional Steady Turbulent Flow Simulation of Static Aerodynamic Forces of Bridge Girder Sections, *Proc. 16th National Symposium on Wind Engineering, Tokyo,* 2000
8. Coakley.T.J.: Turbulence Modeling Method for the Compressible Navier － Stokes Eqations, *AIAA paper* 83-1693,1983.
9. S.Watanabe,H.Inoue and K.Fumoto.: A Study on Static Aerodynamic Forces of Box Girders Using Computational Fluid Dynamics, *Proc. The Second International Symposium on Advances in Wind and Structures,* 2002.

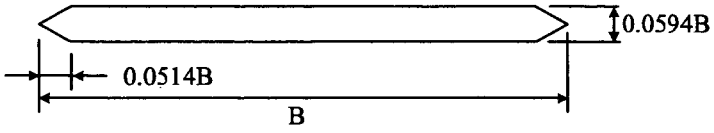
10. T.Inamuro. T.Adachi and H.Sakata.: A Numeral Analysis of Unsteady Separated Flow By Vortex Shedding Model, *Bulletin of JSME, vol.26,* No.222, 1983.
11. K.Shimada, T.Wakahara and H.Sato.: Prediction of Unsteady Wind Force acting on the Separated Box Girder Cross-Section, *In J. of Wind Engineering, No.89, Proc. The Fifth Asia-Pacific Conference on Wind Engineering, Kyoto,* 2001.
12. S.Shirai, and T.Ueda,.: Aerodynamic Simulation By CFD on Flat Box Girder of Super-Long Span Suspension Bridge, *In J. of Wind Engineering, No.89, Proc. The Fifth Asia-Pacific Conference on Wind Engineering, Kyoto*, 2001.
13. N.Hirahara, et al.: An Investigation on Wind-Resistance and Economic Improvements of Super Long Span Suspension Bridges Synoptic Report, *Cooperative Research Report of PWRI,* No.279, 2002.

Table 1 CFD Approaches

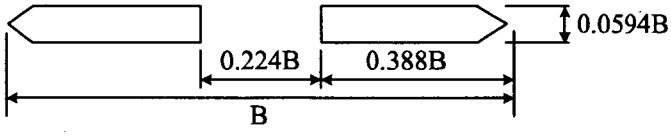
Methods Number	Basic Equation	Turbulence Model	Calculation
1	Reynolds-Averaged Navier Stokes Equation	k-ω	Finite Difference Method
2	Reynolds-Averaged Navier Stokes Equation	q-ω	Finite Volume Method
3	Reynolds-Averaged Navier Stokes Equation	k-ε	Finite Difference Method
4	Navier Stokes Equation	-	Finite Difference Method
5	Reynolds-Averaged Navier Stokes Equation	k-ε	Finite Volume Method
6	Reynolds-Averaged Navier Stokes Equation	Large Eddy Simulation	Finite Element Method
7	Laplace Equation (Vortex points method)	-	Boundary Element Method



Flat Plate



Box Girder



Slotted Box Girder

Fig.1 Cross Section

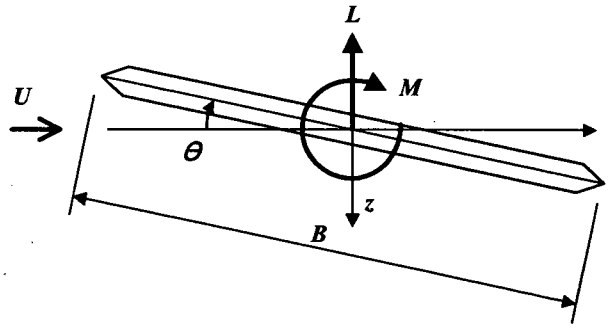


Fig.2 Definition of Forces and Displacement



Fig.3 Flow around Slotted Box Girder

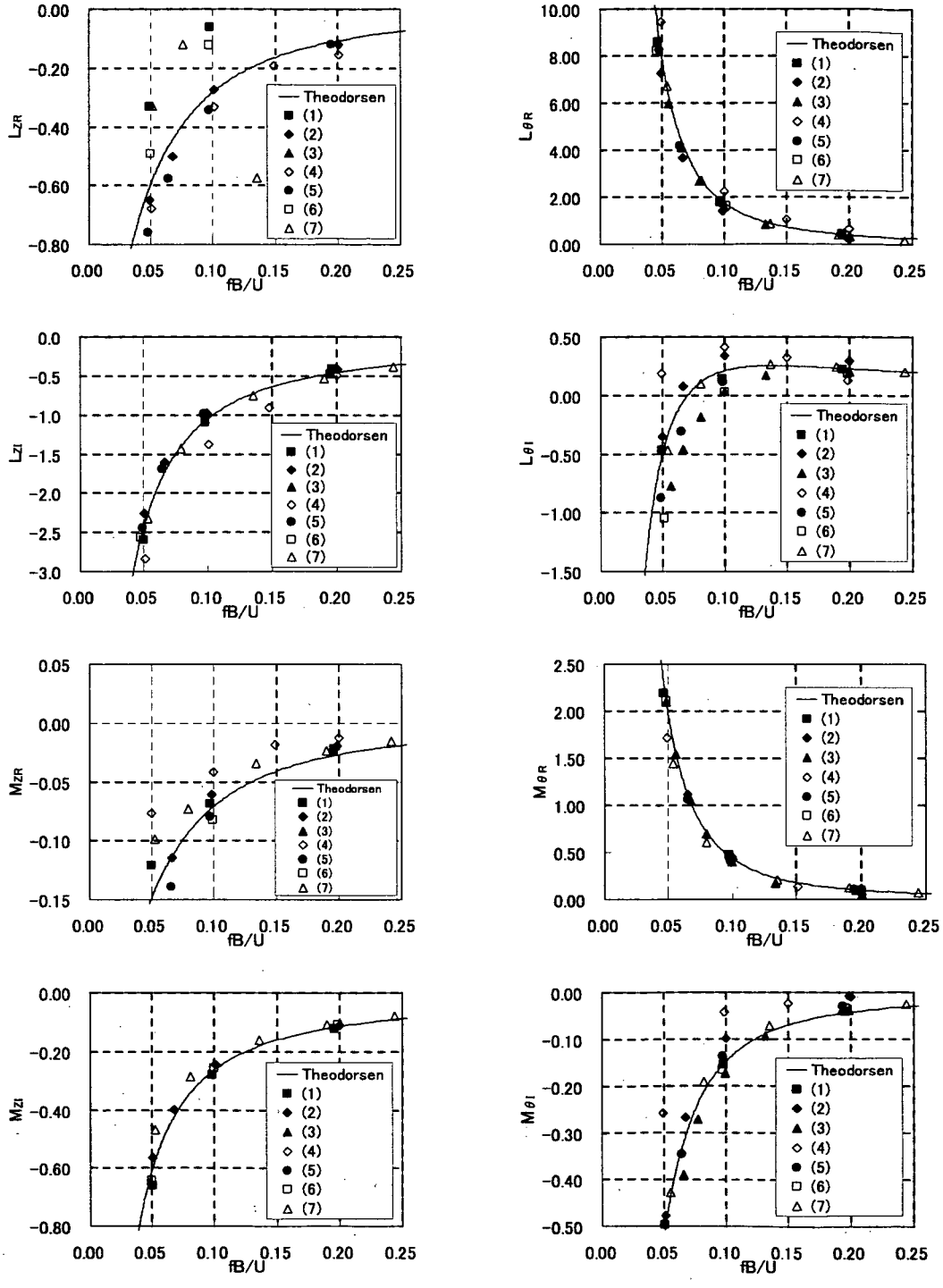


Fig.4 Comparison between Experimental and CFD values for the Unsteady Aerodynamics of a Flat Plate

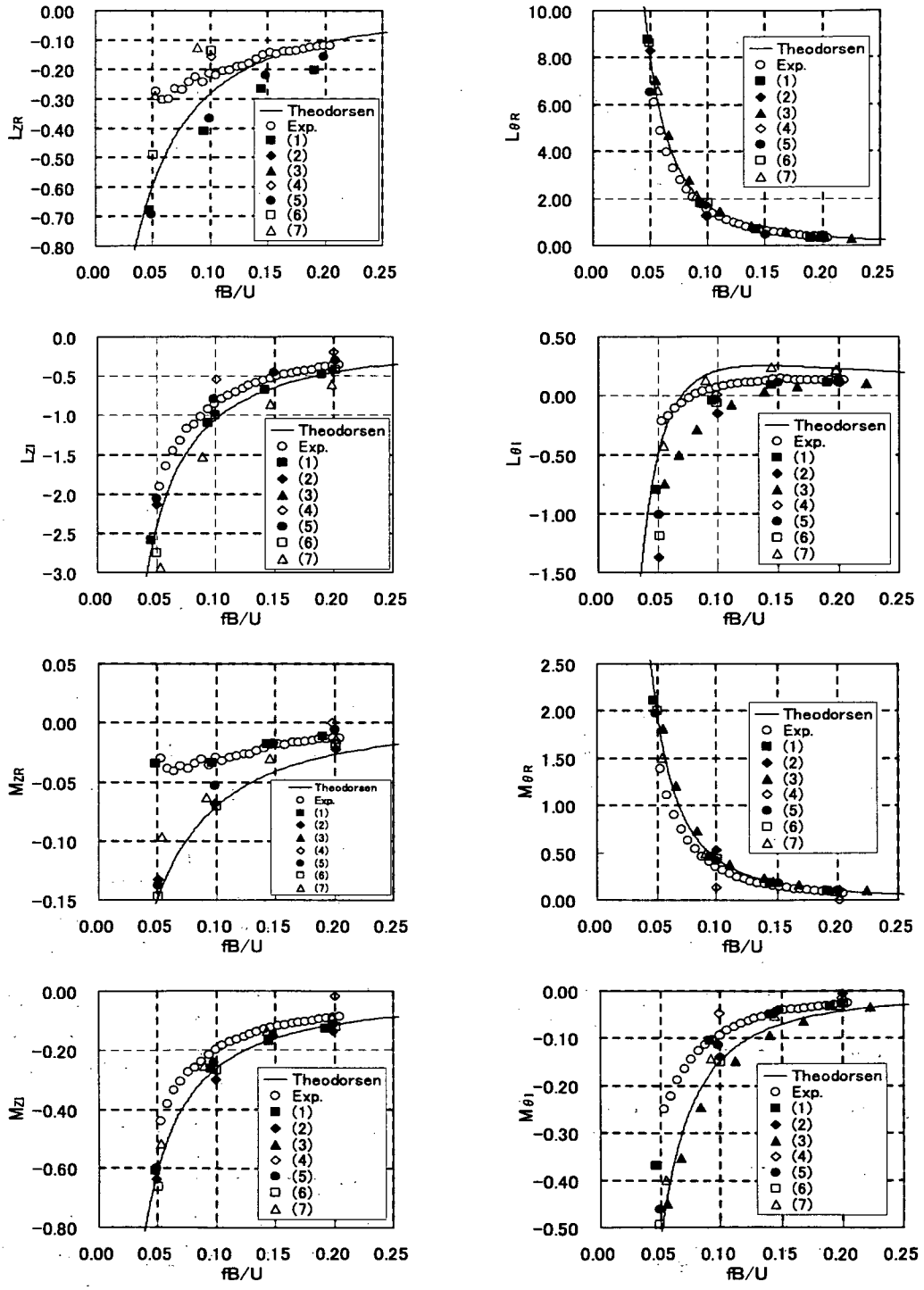


Fig.5 Comparison between Experimental and CFD values for the Aerodynamics of a Single Box Girder

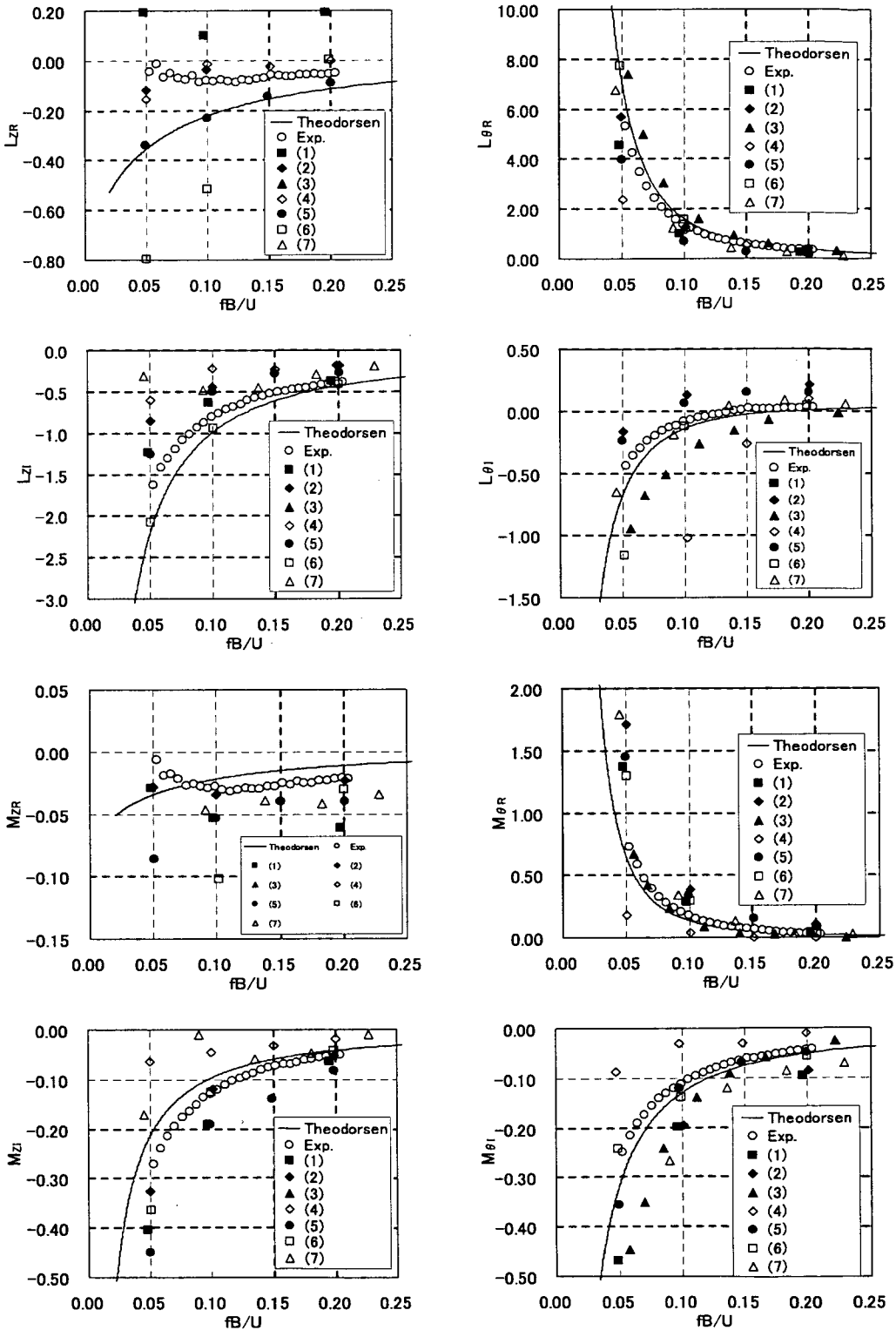


Fig.6 Comparison between Experimental and CFD values for the Unsteady Aerodynamics of a Slotted Box Girder

THEME 7

Progressive Collapse of Buildings

FIRE RESISTANCE OF STEEL FRAMES

Yoshifumi Sakumoto [1], Taro Nishigaki [2], Kenichi Ikeda [3] and Mamoru Kohno [4]

[1] NIPPON STEEL CORPORATION, Tokyo, 100-8071, Japan

[2] TAISEI CORPORATION, Yokohama, 245-0051, Japan

[3] SHIMIZU CORPORATION, Tokyo, 105-8007, Japan

[4] BUILDING RESEARCH INSTITUTE, Tsukuba, 305-0802, Japan

ABSTRACT

This paper verifies analytically the fire resistance of the World Trade Center's steel frames and also examines precautions to be taken in designing skyscrapers.

In the analysis, the temperature increase of steel members for the columns (perimeter and core columns) and the floor trusses of the World Trade Center, when subjected to heating by hydrocarbon fire and standard fire, was calculated in case the steel members were adequately fire-protected and in case they were not fire-protected (or in case the fire protection was blown off). The fire resistance of these steel members was also verified by thermal deformation analysis.

The analysis revealed that, compared with the columns (core columns) of heavy sections, the floor trusses composed of light-gauge steel members, even if fire-protected or not, experienced a temperature increase at a more rapid pace, that the increase in steel temperature posed restraint on thermal deformation, thereby causing the steel members to buckle and leading eventually to the failure of the floor trusses at a relatively low temperature, and that a larger restraint acted on the end connections.

Based on the findings, this paper advances the following three suggestions:

(i) Elaborate care should be exercised in using light-gauge steel members for skyscrapers.

(ii) When hinged connections are to be used, the existence of any fractures at joints should be checked for especially at elevated temperatures and after cooling.

(iii) For designing skyscrapers, fire engineering is essential in addition to traditional structural calculations.

Further, the use of steels with superior heat resistance is recommended to improve fire resistance of steel frames. This does not mean that the fire protection can be deleted, but that given the same or similar protection, the length of time that the steel can tolerate fire is extended. Or, if the fire protection system is destroyed, the unprotected steel will have a longer survival time.

This paper will describe the characteristic of the steel and fire resistance of columns made by the steel compared to the conventional steel. In addition, some of the important major structures in which it has bee used in Japan, will be presented.

Keyword : Steel, Safety, Structure, Fire-Safe Design, Failure

1. Foreword

The collapse of the World Trade Center Towers (hereafter referred to as "WTC," Photo 1 : at the time of construction") was caused by damage to the structures due to aircraft impact and ensuing fire exposure that led to loss of the structures' load-bearing capacity.

The WTC, like other high-rise buildings, was required to have three-hour fire resistance for its columns and two-hour resistance for its floor system members. Its steel frames were protected from fire with insulating materials (hereafter referred to as "fire protection") to meet the requirements.

The lengths of time between the aircraft impact and total collapse were fifty-six minutes for WTC1 and one hour forty-three minutes for WTC2. Indeed, there is little point in discussing the precise details of the collapse time, since damage to the structures due to both aircraft impact and the burning of the aviation fuel were extraordinary events—radical departures from the conditions expected by fire laws and regulations. But, to clarify the cause for the collapse can be considered extremely useful for designing high-rise buildings in the future.

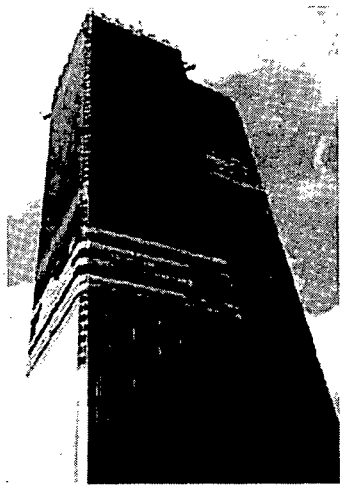


Photo 1. WTC under construction

From this point of view, this paper examines the fire resistance of WTC's steel frames by referring to the report [1] made public by the Federal Emergency Management Agency (hereafter referred to as "FEMA Report").

2. Fire Exposure

The Boeing 767-200ER aircraft that impacted the WTC carried about 10,000 gallons (about 38,000 liters) of jet fuel. The FEMA report assumes: of the total jet fuel carried, 1,000 to 3,000 gallons were exhausted as fire balls, 3,000 gallons flowed onto other floors and the remaining 4,000 gallons were burnt within the impact floors.

The calorific value of the jet fuel was 1 to 1.5 GW. If one-third or a half of that energy was released to the structure, gas temperatures reached 900 to 1,100°C around the ceilings and 400 to 800°C at the rest of indoor spaces according to the analysis of the FEMA Report. The jet fuel remaining on the floors burned within about five minutes, with the blaze engulfing combustible materials (4 to 12 psf: 20 to 60 kg/m^2) in the floor areas.

The fire exposure assumed to occur in typical buildings is called the "standard fire" and the resulting gas temperature is specified in ISO835 [2] (the same as JIS A1304 [3]). The same may be said, within very close limits, of the U.S. specifications (ASTM E119 [4]).

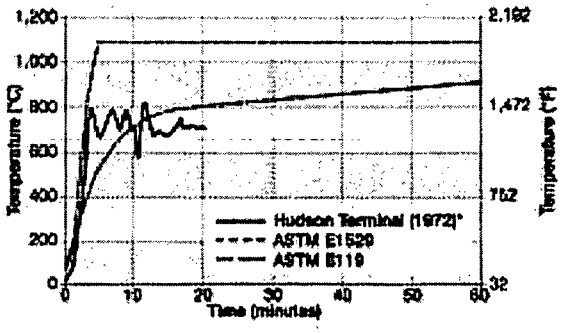


FIG. 1. Comparison between Standard Fire and Hydrocarbon Pool Fire

For buildings other than typical buildings, the gas temperature for a petrol spill fire is also specified in the United States (ASTM E1529 [5], hereafter referred to as "hydrocarbon pool fire"). Fig. 1 shows the comparison of gas temperature between standard fire and hydrocarbon pool fire. In the case of a hydrocarbon pool fire, the temperature at first rises more rapidly to a high of about 1,100°C in the first five minutes (than for the case of a standard fire) and, afterwards, the temperature remains constant according to the U.S. specifications.

3. Fire Protection and Steel-Frame Temperature

Fire protection for WTC1 was originally asbestos-containing spraying up to the 39th floor, but later it was changed to vermiculite plaster insulation. WTC2 was fire-protected wholly with vermiculite plaster insulation. The fire-protection thickness for the floor trusses was originally 3/4 in. but, as a retrofit during tenant changes, was later redoubled to 1-1/2 in. For the columns and beams, the thickness was not specified because of variations in member sizes, but the thicknesses adequate to meet the specified two and three-hour protection requirements were adopted.

Photo 2 shows the core column of ultra-jumbo H-shape before fire protection and Photos 3 and 4 show the floor trusses before and after fire protection. The motion damper inserted between the outer wall and the end of the lower chord of the truss was not fire-protected, as it was not a load-carrying member of the main structure. It can be assumed from the photo that spraying to such a small cross-section members posed great difficulties.

According to the FEMA Report, the aircraft incursion supposedly blasted away the vast majority of fire protection on the impact floors. Photo 5 shows the steel frames of adjoining Bankers Trust Building that was hit directly by the columns falling from WTC2. Their fire protection was largely blown away, and it is not hard to imagine that the same phenomenon occurred at the impact floors of WTC1 and WTC2.

The temperature of heated steel frames varies, depending on heating conditions (standard fire or hydrocarbon pool fire and heating duration), existence of fire protection, insulative properties of protective materials and thermal capacity of steel members.

In this study, an analysis similar to that of the FEMA Report was made on the columns plus the diagonal members (rods) of the floor trusses. The analysis results are shown in Figs. 2 and 3. The sizes of the members adopted are as follows:

Core column	H-455.2 x 418.5 x 42.04 x 67.56	Hp / A = 35.7
Perimeter column	□-355.6 x 355.6 x 6.35 x 6.35	Hp / A = 173.4
Floor truss rod	ϕ-1.09" (27.7mm)	Hp / A = 144.6

The sizes of the columns (core and perimeter) are only those assumed because the FEMA Report gives no specified dimensions for them at and around the impact floors. Hp/A is the indicator of a member's thermal capacity (the rate of a member's temperature increase), with Hp = circumferential length and A = sectional area. The larger the Hp/A, the higher the rate of steel-frame temperature increase.

Figs. 2 and 3 clearly reveal the following:

(i) The increase of the steel-frame temperature corresponds to thermal capacity (Hp/A), regardless of fire protection. In the case of the floor truss rod and the perimeter column with smaller thermal capacity (Hp/A is larger), the temperatures rise more rapidly, reaching as high as 900°C in five minutes especially when the y are not fire-protected.

(ii) By comparison, in the case of the core column that has extremely large thermal capacity, the speed at which the temperature rises is moderate even when it is not fire-protected (or when fire protection is blown off). The temperature increases to about 600°C in approximately 20 minutes.

(iii) In the case of a hydrocarbon pool fire, the temperature of steel frames (fire-protected or unprotected) increases faster than in the case of standard fire, especially in the first five minutes. A hydrocarbon pool fire causes the gas temperature to rise rapidly and that is why, when steel frames are not fire-protected,

the difference between a hydrocarbon pool fire and a standard fire is more pronounced in terms of the rate of the steel-frame temperature increase.

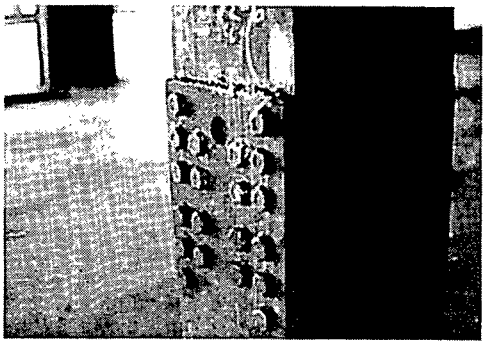


Photo 2. Core column (ultra-jambo H-shape)

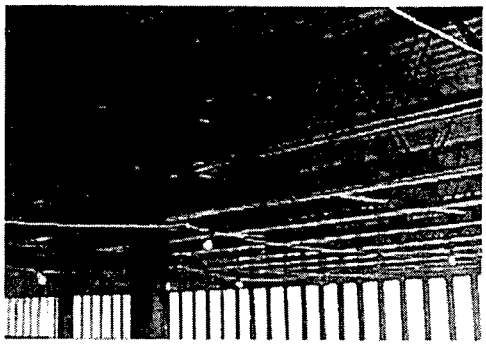


Photo 3. Floor truss (before protected)



Photo 4. Fire Protection of floor truss



Photo 5. Fire protection at Bunker Trust Building

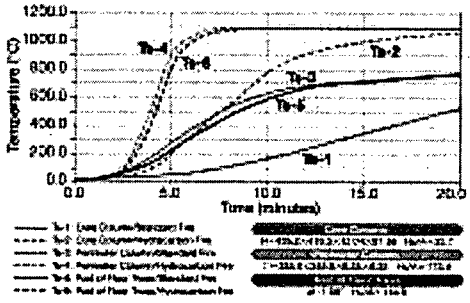


FIG. 2. Steel Temperature Rise Subjected to Heating (No fire protection)

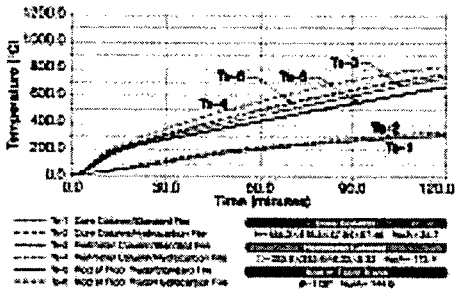


FIG. 3. Steel Temperature Rise Subjected to Heating (3/4-inch thick sprayed fire protection)

4. Fire Resistance of Steel Frames

Steel strength is reduced at high temperatures. A36 steel's high-temperature strength and its stress-strain relationship at high temperatures are shown in Figs. 4 and 5, respectively (FEMA Report). A36 steel's yield point lowers by nearly half at 550°C, as shown in Fig. 4 (A36 steel [6]).

The fire resistance of columns and beams can be verified by a fire test. There are two methods for fire test: one is to obtain the time of failure (fire resistance hours) through loaded heating (the loaded heat test) and the other is to obtain the period of fire resistance from the temperature of steel materials only through

heating (the heat test). The condition of failure immediately after a loaded heat test made on a column is shown in Photo 6. The proof stress of steel frames decreases with the increase of temperature, leading to the loss of the frame's load-bearing capacity.

For the ASTM E-119 fire test in the United States [4], the heat test is prevalent for columns, and the critical temperatures for steel members are specified at:

Column: 538°C (1,000F average, 1,100 maximum)

Beam: 593°C (1,100F average, 1,200 maximum)

As for fire testing in Japan [3], the heat test traditionally has been applied with the critical temperatures specified as follows:

Column: 350°C average, 450°C maximum

Beam: 350°C average, 450°C maximum

But, today, the loaded heat test is also in practice. The load applied is specified as a load equivalent to the long-term critical stress (2/3 of the yield point).

Fig. 6 shows the integration of the critical temperatures in the two countries with Fig. 4 (high-temperature strength of steel materials). The difference between the two countries is about twice in the critical temperature, eventually leading to a wide difference in the thickness of fire protection required.

This study obtained analytically the fire resistance of the columns (core and perimeter) of the WTC at and around the impact floors. The sizes of the columns adopted were identical to those used for the analysis of steel-frame temperatures in Section 3. The steel grade was A36 and the ratio of axial force was set at 0.5, although no reference is made to the columns' ratio of axial force in the FEMA Report. However, since the stress applied on the diagonal members of the floor trusses was estimated, on calculation, at about 50% of the yield point, the ratio was assumed to be the same.

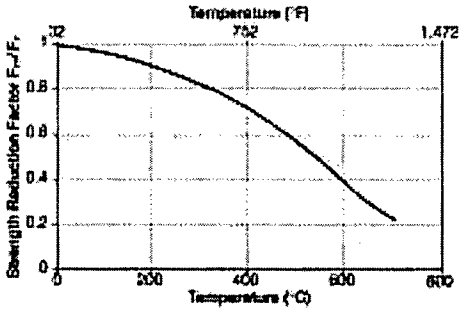


FIG. 4. High-temperature Strength of A36 Steel

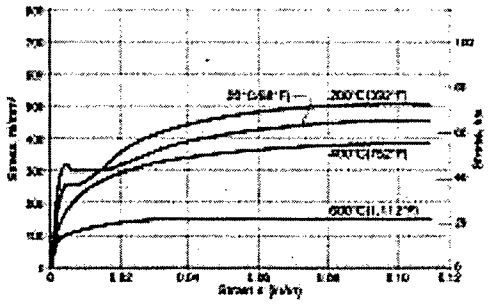


FIG. 5. Stress-strain Curves of A36 Steel At High Temperatures

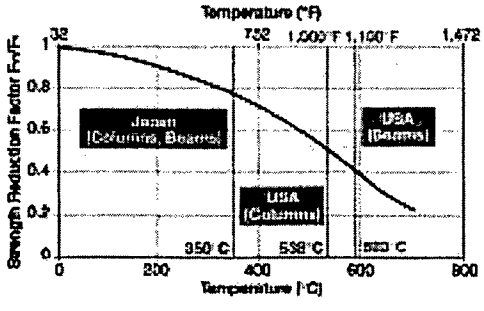


FIG. 6. Relationship between Strength of Steel Materials and Critical Temperature

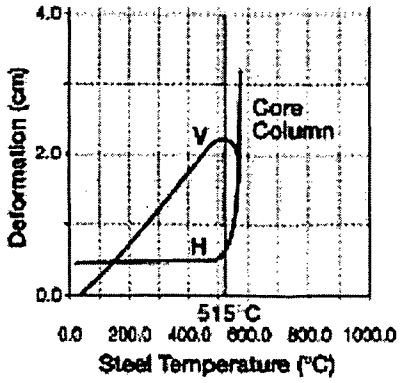


FIG. 7. Analysis of Fire Resistance of Column

Fig. 7 shows the results of the analysis. The columns underwent thermal expansion as the temperature increased (vertical elongation: V), buckled due to the lowering of steel strength and the loss of their load-bearing capacity (horizontal deflection at the middle of the columns: H). The calcula ted buckling temperatures were 515°C for a core column and 520°C for a perimeter column.

A comparison between the above analysis results and the critical temperature shown in Fig. 6 reveals:

(i) The buckling temperature of the columns virtually corresponds to steel's high-temperature strength and the columns' ratio of axial force.

(ii) The U.S. critical temperature, 538°C, is considered almost equivalent to the ratio of axial force of 0.5.

The failure temperature of beams is related to the presence of the floor. It is higher than that of the columns, because the temperature of the steel frames in contact with the floor increases at a slower rate and also because the floor itself shares the applied load. The critical temperature of 593°C for beams, as specified in the United States, is considered to put a restriction on the load applied.

Attention should also be paid to the fact that the high-temperature strength of steel materials shown in Figs. 4 and 6 is the average. Fig. 8 shows the results of examining the high- temperature strength of steel materials, made by the Japan Iron and Steel Federation (JISF) [7]. The high-temperature strength varies widely, as shown in the figure. In addition, there are cases where columns and beams are restrained by peripheral frames due to thermal expansion, resulting in failure at lower temperatures than expected, as discussed later. It is considered that, with such indefinite factors in mind, the critical temperature of 350°C adopted in Japan secures a higher level of safety.

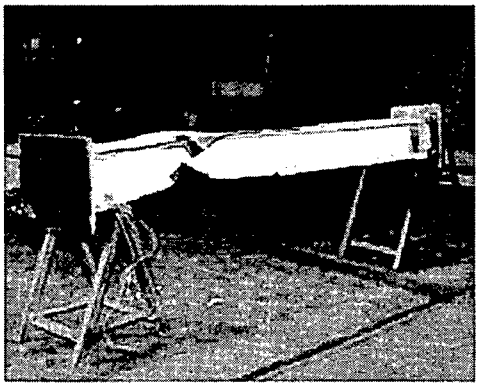


Photo 6. Buckling of Column after Loaded Heat Test

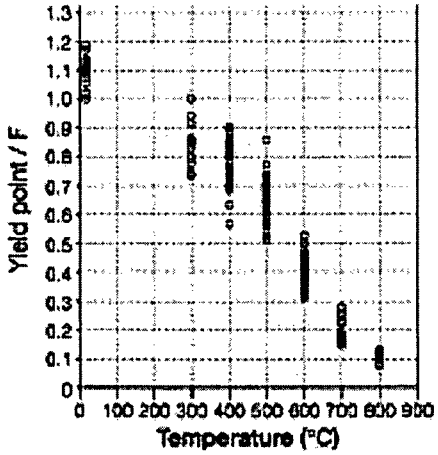


FIG. 8. Variations in High-Temperature Strength of Steel Materials

Fig. 9 shows the schematic diagram of the WTC's floor structure. The floor is of a structure designed to support lightweight concrete (10 cm thick) on steel decking by trusses arranged at a spacing of 6 ft. 8 in. (about 2 m). Their maximum length is 60 ft. (18.3 m). The trusses are lightweight, using angles for the upper and lower chords and round bars for the diagonal members. Their ends are linked to the perimeter columns and the core girders by two high-strength bolts (A325 bolt, 5/8 in. dia.) followed by welding after erection. Fig. 10 shows the details of the truss end (FEMA Report).

Fig. 11 analyzes the failure process of the floor truss by raising the steel-frame temperature.

The FEMA Report gives no reference to the dimensions of the upper and lower chords. For this analysis, two angles, each measuring L-3.5 x 3/8 in. (88.9 x 9.525 mm), were overlapped to match the normal-temperature stress level

(about 50% of yield point) of the truss's diagonal member (Ø1.09 in.). Though the floor trusses are the composite structure with the concrete slabs, the concrete slabs were not considered in the analysis. The loads were design loads (dead load and service load).

When the hinged end was adopted for one end of the truss and the roller end for the other end of the truss, the increase of the steel-frame temperature caused the truss deformation to concentrate on the roller end side and the vertical members of the utmost end to buckle at 340°C. Deflection at the time of buckling was 7.50 cm in the middle of the truss, and horizontal deflection on the roll end side was 6.61 cm.

When each end of the truss was hinged, constraints on the thermal expansion of the truss resulted in the truss's large deflection. Constraints concentrated on the upper chord, and the resultant buckling of the chord caused the failure of the truss at 264°C. The central deflection at the time of the failure was 27.9 cm. Fig. 12 shows the truss end's horizontal restraint load. The restraint load was pulled inward at normal temperature. Due to the thermal expansion of the truss, it then turned around but was eased by deformation of the upper chord. Maximum restraint load occurring outwards was about 30 tons. According to the FEMA Report, the shear strength of the high-strength bolts at each end (A325 bolt, 5/8 in. in inside dia. x 2) is as follows (the strength decreases by half at 550°C):

Room temperature: Ru = 232 kips (105.2 tons)

550°C (1,022F): Ru = 116 kips (52.6 tons)

Since the trusses were connected to the perimeter columns and the core girders, it is assumed that approximately the central values of those given in the above two cases must have been applied for actual behavior. Besides, as the floor slabs serve to retard the thermal expansion of the trusses and to constrain the buckling of the upper chords, it can also be assumed that the actual failure temperatures must have been higher than those in the above analyses.

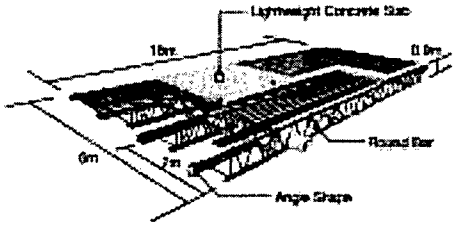


FIG. 9. Floor Structure

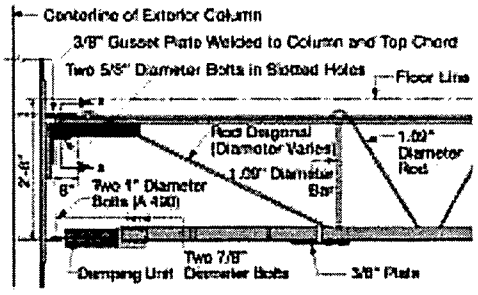


FIG. 10. Details of Floor Truss End

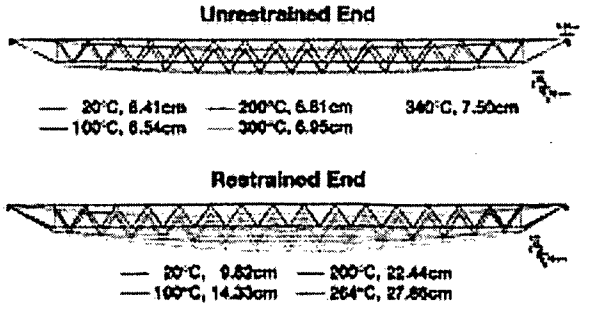


FIG. 11. Analysis of Thermal Deformation of Floor Truss

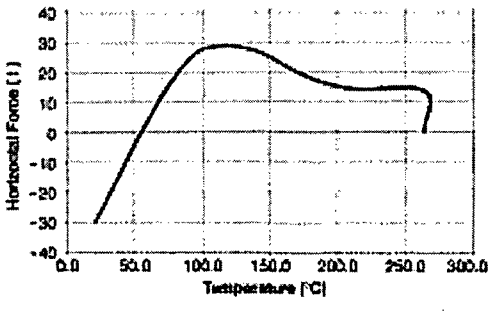


FIG. 12. Restraint Load at Floor Truss End

But, when such a large-span truss is heated and undergoes thermal expansion, it deforms (deflects) due to constraints on its ends and its individual structural members are subjected to large compression stresses. In addition, a large shearing force acts on the end connections. From these, it is quite likely that the failure temperature of the truss is far lower than the critical temperature for beams (593°C: 1,100F) in the fire test.

5. Proposition and the use of Fire Resistant Steel

From the above analytical study and examination of the fire resistance of the WTC's steel frames, the following precautions in the fire-safe design of high-rise buildings are proposed:

(i) When lightweight steel frames are used, a thorough check should be made for the deformation of structural members and the failure of end supports (especially in the case of the hinged end) during the course of fire.

(ii) Adequate fire-protection materials and construction methods should be selected.

Among other effective alternatives is the utilization of steels excelling in high-temperature strength.

Fire resistant steel (Sakumoto et. al, 1992-1, hereinafter referred to as "FR Steel"), containing such alloying elements as molybdenum and chromium, is superior in high-temperature strength to ordinary steels. Fig. 13 shows the yield strength at high temperature of FR steel (Grade 325) and conventional steel. The yield strength at high temperature of conventional steel decreases to two-thirds the specified room-temperature value (217N/mm^2) at around 350°C. On the other hand, this specified value is guaranteed at 600°C for FR Steel.

A yield strength of two-thirds the specified room temperature value corresponds to allowable stress for sustained loads. Because fire and earthquake are not taken into consideration simultaneously, it can be said that yield strength able to support the dead weight of a building, allowable stress for sustained loads, is the strength required at the time of fire.

The elevated yield strength at high temperature is obtained from metallurgy, in which additive elements such as molybdenum precipitate to affect the molecular structure and, therefore, the yield strength.

Table 1 shows mechanical properties of FR Steel (Grade 325) with comparison of conventional steel ASTM A992 [9]. The performance of FR steel at room temperature corresponds to that specified in the standards for Japanese anti-seismic structural steel (JIS G3136 [10]), with yield ratio under 80%, Charpy absorption energy 27J or over at 0°C. Furthermore, it has the same weldability as that of conventional steel.

TABLE1. Mechanical Properties of FR Steel

Standard	Grade	Yield strength		Tensile strength	Yield ratio	Elongation	Charpy
	N/mm^2 (ksi)	N/mm^2 (ksi)		N/mm^2 (ksi)	%	%	energy J
		at 0 C	at 600 C	at 0 C	at 0 C	at 0 C	at 0 C
		min / max	min	min / max	max	min	min
(1)	(2)	(3)	(4)	(5)	(6)	(7)	(8)
FR Steel	Grade 325	325/445	217 min	490 / 610	80	21	27
ASTM A992	Grade 345 (50)	345/450 (50/65)		450 min	85	18	1)

Note 1) : charpy absorption energy is a supplementary requirement for use at the option of the purchaser

Application of FR Steel

Whether FR Steel is used with or without protection is determined by building application and design concept.

Fig. 14 shows numbers of buildings using FR Steel provided by Nippon Steel since 1989. Car parks, atriums, sport facilities, art galleries and a station building have been the major applications without protection. External steel-frame buildings also are a major application.

In case of buildings with high combustible loads, such as office buildings, warehouses, department stores and collective dwellings, thickness of protection can be reduced or the redundancy of a steel frame can be improved by extending fire resistance time with FR Steel protected with the same thickness as conventional steel.

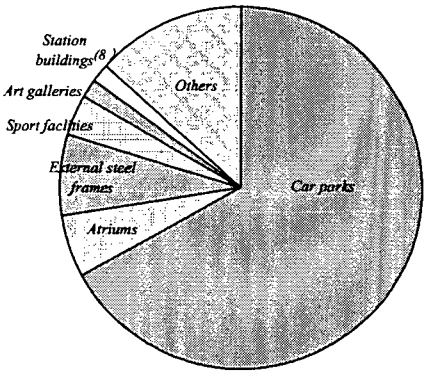


FIG. 14. Application of FR Steel

Car park

Photos. 7 and 8 show the application of FR Steel to a multi-story car park. This 17-story car-park building, constructed close to Chiba Station, is one of the largest of its kind in Japan. It will accommodate 1,800 vehicles. Conventional steel-frame car parks present a dark and dirty appearance because the steel-frame protection blackens by exhaust gases and exfoliates when exposed to rain and wind. With FR Steel, no protection is required for the frame and making the columns slender enlarges the parking area.

Sport facilities

For this gymnasium, constructed at Tokoname Park (Aichi Prefecture), a dynamic structure was adopted in which the roof, a space truss structure measuring 100.8 x 50.4 m, is supported on four sides by large truss structures (Photo 9). For the large truss structures, prestressed concrete was at first considered because protection is necessary when a steel-frame structure is adopted. However, FR Steel that matches the design intention was adopted as the material for this large truss structure.

Station building

East Japan Railway Company constructed a commercial building spanning the tracks of Oimachi Station in Tokyo (Photos. 10 and 11). In the case of constructing a large-scale building spanning a railway, it is necessary to provide protection for steel frames in the vicinity of the tracks. However, because of the exfoliation of maintenance, steel-frame construction without protection was required for this building.

Office building (external steel-frame building)

This 31-story building in Kobe houses offices and research laboratories (Photo 12). A suspended mega-structure, in which six stories are structured as one unit, was adopted for the construction of the building. It features a structural design in which the mega-structure is presented as the building's structural design element. In the building construction, FR Steel was adopted to give the impression of slenderness of the structural members through the application of lighter protection to columns and beams.

In addition, it is important to verify the fire resistance of steel frames by means of fire-safety design.

Fire tests address such structural members as columns and beams, as stated in section 4, and they do not reflect the behavior of steel frames as a whole during a fire. Steel frames expand thermally due to heating by fire and the structural members are exposed to large additional stress by constraints. Especially lightweight structural members not only undergo rapid temperature increases within a short time, but also lose their load-bearing capacity even at a relatively low temperature due to buckling and the like. Besides, load concentrates in connections, so hinged end and similar connections can fracture during the course of heating or cooling.



Photo. 7. View of Sen City Car Plaza



Photo. 8. Steel Frame of Sen City Car Plaza

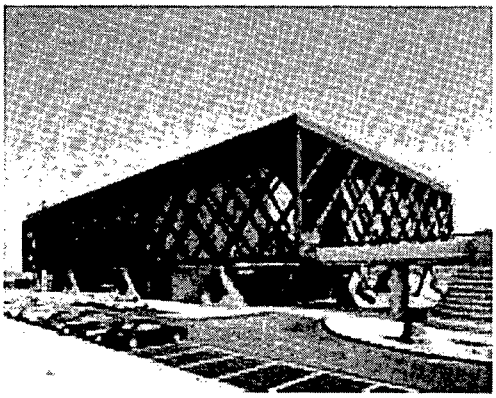


Photo. 9. View of Tokoname Park Gymnasium

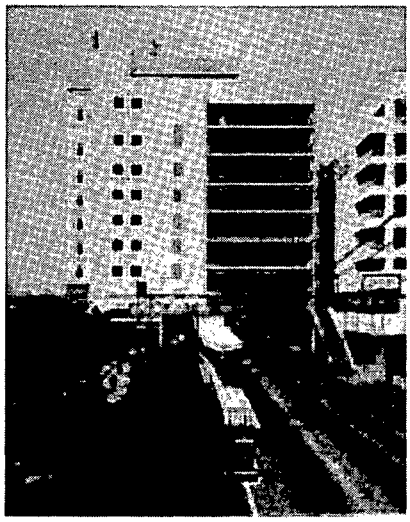


Photo. 10. Steel Frame of Sen City Car Plaza

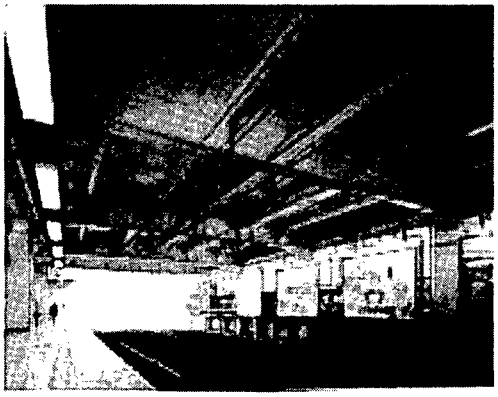


Photo. 11. View of Oimachi Station Building

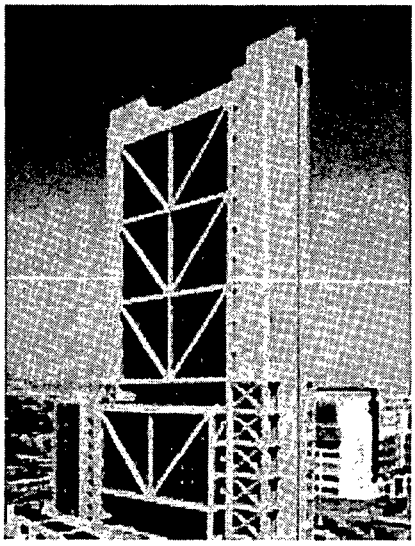


Photo. 12. View of P&G Building

5. Summary

In Japan, the number of such failure analyses have been increasing since around 1990, where fire-safety designs are used to verify the fire resistance of steel frames, targeting buildings adopting FR steel and concrete-filled steel tube columns. Henceforth, imperative is the active adoption of fire-safety designs particularly for high-rise buildings and publicly important buildings. The adoption of fire-safety design for high-rise steel buildings ensures greater safety in fire. FR Steel, used successfully in Japan for a decade, is an option to be considered.

ACKNOWLEDGMENT

The photos of the WTC at the time of construction, shown in this paper, were provided by Mikio Kasajima, former president of Daiken Sekkei Co. His cooperation is highly appreciated.

REFERENCES

[1] World Trade Center; Building Performance Study, (2002), Federal Emergency Management Agency, New York, U.S.A.
[2] ISO834 (1975), Fire-Resistance Tests, Elements of Building Construction, International Organization for Standardization
[3] JIS A1304 (1975), Method for Fire Resistant Tests for Structural Part of Buildings, Japan Standards Association, Tokyo, Japan
[4] ASTM E119 (1983), Standard Methods for Fire Tests of Building Construction and Materials, American Society of Testing and Materials, Philadelphia, U.S.A.
[5] ASTM E1529, Standards Test Methods for Determining Effects of Large Hydrocarbon Pool Fires on Structural Members and Assemblies, American Society of Testing and Materials,
[6] ASTM A36, Standard Specification for Carbon Structural Steel, American Society of Testing and Materials, Philadelphia, U.S.A.
[7] Zakoh, R., et al, (2000), High-temperature Strength of Steel Products for Building Structures, Summary of Technical Papers of Annual Meeting, Architectural Institute of Japan
[8] Sakumoto, Y., Yamaguchi, T., Ohashi, M., and Saito H. (1992), High-Temperature Properties of Fire-Resistant Steel for Buildings, ASCE Journal of Structural Engineering, 118(2), pp.392-407
[9] ASTM A992 (2001), Standard Specification for Structural Shapes, American Society of Testing and Materials, Philadelphia, U.S.A.
[10] JIS G3136 (2001), Rolled Steels for Building Structure, Japan Standards Association, Tokyo, Japan

Best Practices Guidelines
For
Mitigation of Building Progressive Collapse

by

H. S. Lew [1]

ABSTRACT

This paper presents current design approaches found in the U.S. and European building codes and standards for the prevention of progressive collapse due to abnormal loading. Because the definition of abnormal loading is not well established, design provisions are based on an approach that protects buildings by means of strength, ductility and redundancy. The effectiveness of seismic detailing on structural resistance to avert progressive collapse is discussed. Finally, a rational design approach is suggested.

KEYWORDS: Abnormal loading; buildings; codes; collapse; failure; progressive collapse; standards;

1. INTRODUCTION

The dramatic partial collapse of the Ronan Point apartment building in London, England in 1968 generated widespread concern for potential collapse of high-rise buildings in a chain- be designed so that they are capable of resisting abnormal loads. Following the promulgation of and Local Government issued a set of guidelines to aid the designer. To limit the propagation of failure the building must be designed to provide an alternate load path in the event of loss of a single critical member or the critical building members must be designed to withstand a 34 kN/m^2 (5 psi) pressure. This specified pressure was based on a gas-type explosion.

reaction mode, triggered by a local failure. The Ronan Point collapse was brought about by a gas explosion in an apartment on the 18th floor of a 22-story precast concrete building. The explosion blew out the exterior bearing wall of the apartment that caused the upper floor slab to fall on the floor below, thereby initiating the collapse of one corner of the building "progressively" almost to the ground (Figure 1). Since the Ronan Point collapse, the term "progressive collapse" has been widely used to describe an incremental type of failure, both in the vertical and horizontal directions, that leads to a total or a disproportionately large failure relative to an initiating local failure.

In response to the collapse of the Ronan Point, the Building Regulations [HMSO, 1976] were changed in the United Kingdom to require that buildings five stories and higher should not sustain failure disproportionate to an initial local failure due to an abnormal load such as a gas explosion. The intent of this requirement could be met by tying the building together or, if tying is not feasible, design the building so that failure is localized. If neither of these procedures is possible, all critical building elements should the progressive collapse prevention regulation, the Ministry of Housing
In the United States, similar requirements were adopted by the Department of Housing and Urban Development (HUD) in the early 1970s for its housing industrialization program known as "Operation Breakthrough." In 1973 progressive collapse provisions were also adopted by rule and were incorporated into the New York City Building Code [NYC, 1973].

[1] Senior Research Engineer, Building and Fire Research Laboratory, National Institute of Standards and Technology, Gaithersburg, Maryland, U.S.A 20899-8611, hsl@nist.gov

The NYC provisions were very similar to the then European approach.

The HUD design requirements for progressive collapse prevention and the NYC code provisions were not readily accepted by design professionals for several reasons. Firstly, very little documentation was published on progressive collapse of occupied buildings since the Ronan Point incident. Secondly, design professionals felt that the U.S. practice would be considerably more conservative than that of England. Thirdly, very little factual data were available as to the economic consequences of incorporating the progressive collapse provisions. Thus, U.S. design professionals did not embrace the regulatory requirements that are simply based on the European approach.

The concern over progressive collapse had waned considerably during the 1980s as hardly any multistory buildings collapsed due to abnormal loading except for those collapsed during construction. Beginning with the bomb explosion at the World Trade Center in 1993, a number of U.S. owned and occupied buildings have become targets of terrorist attacks. These include the Murrah Federal Building, Oklahoma City in 1995; the Khobar Towers, Saudi Arabia in 1996; the U.S. embassies in Kenya and Tanzania in 1998. These attacks have generated considerable concern over whether current U.S. building codes and standards are adequate to protect buildings and their occupants from progressive collapse. The complete collapse of the World Trade Center Towers on September 11, 2001 following the impacts of the large aircraft clearly showed that American buildings are vulnerable to terrorist attacks. It is prudent to consider a potential threat of terrorist attack in the design of critical and high profile structures so that resulting damage would be localized.

The National Institute of Standards and Technology in cooperation with the National Institute of Building Sciences and several other federal agencies[2] held a workshop on July 10–12, 2002. The purpose of the workshop was to develop a comprehensive action plan that will lead to the development of design and rehabilitation standards for mitigating progressive collapse of new and existing buildings. This paper presents the summary of the papers presented and the conclusions and recommendations reached at the workshop.

2. CURRENT APPROACHES

It is not possible to design structures for absolute safety, nor is it economical to design for abnormal events unless they have a reasonable chance of occurrence. Some of the incidents causing abnormal evens might be: explosions due to gas, explosions of highly flammable liquids or bombs, vehicle impacts, foundation failures, failures resulting from construction and design errors. These events are not usually considered in the usual design process. On the other hand, events such as earthquakes, fires, high winds are part of building code requirements but they should not also cause progressive collapse.

At present, provisions for mitigating progressive collapse in most building codes and standards around the world are based either on explicit design requirements or on general structural integrity requirements. Most European, including the U.K., building codes follow the former approach and U.S. codes and standards the latter approach. Several U.S. government agencies have developed specific design guides for progressive collapse mitigation closely resembling the requirements in the U.K. and European codes

2.1 U.S. Approach

The American Society of Civil Engineers (ASCE) maintains a standard, which deals with design loads [ASCE 7-02]. The section that covers general structural integrity (Section 1.4) of this document states:

[2] Defense Threat Reduction Agency, Department of Defense; U.S. General Services Administration; and U.S. Army Engineering Research and Development Center

"Buildings and other structures shall be designed to sustain local damage with the structural system as a whole remaining stable and not being damaged to an extent disproportional to the original local damage."

ASCE 7 requires that structural integrity be achieved by providing sufficient continuity, redundancy, and ductility in the members of the structure. It does not provide specific design criteria to minimize the risk of progressive collapse. However, the commentary discusses three design alternatives: indirect design, alternate path direct design and specific local resistance direct design. The **indirect design** considers resistance to progressive collapse by providing strength, continuity and ductility to key structural members. The **alternate path direct design** recommends explicitly providing resistance to progressive collapse by requiring the structure to sustain the loss of primary load-carrying members by means of alternate load paths. The **specific local resistance direct design** considers explicitly resistance to progressive collapse by requiring the key members of a structure to withstand a postulated abnormal load. This approach requires that the design intensity of the abnormal loading must be specified for critical load carrying members.

To calculate the local resistance required to resist a postulated abnormal load, the following load combinations are given in the Commentary Section (C2.5) of ASCE 7-02 .

$$1.2\ D + A_k + (0.5\ L \text{ or } 0.2\ S)$$

$$(0.9 \text{ or } 1.2)\ D + A_k + 0.5\ L + 0.2\ W$$

where D is dead load; L is live load; S is snow load; and A_k is the value of the load resulting from an abnormal event, which should be specified by the authority having jurisdiction [Burnett, 1975].

For concrete structures, the American Concrete Institute's Building Code Requirements (ACI 318-02) [ACI 318] provides prescriptive requirements for structural integrity. These requirements are based on the philosophy that tying the building together and continuing top and bottom beam reinforcement through the column and providing moment resisting beam-column connections would improve the integrity of the overall structure.

Questions have been raised as to the effectiveness of seismic detailing of reinforcement for concrete members for mitigating progressive collapse. In general, the seismic detailing requirements in Chapter 21 of ACI 318 Code will improve the ductile behavior in response to strong ground motions, and allow the structure to undergo large inelastic deformation. Thus, it would be reasonable to assume that the ACI seismic detailing would enhance the ability of the structure to behave in a ductile manner and would enhance the resistance to progressive collapse. However, it is recognized that the locations of plastic hinge formation and the degree of ductility demands in seismic events are different from those resulting from abnormal events. Thus, the failure mode of a structure from a seismic event would be different from that resulting from an abnormal event such as blast.

2.2 U.K. and European Approaches

The U.K. and European approaches for mitigating progressive collapse are similar. Their mitigation strategy is to apply one or more of the following criteria into the design process:

1) Eliminate or reduce exposure to abnormal loads,
2) Provide continuity and redundancy to the structure, or
3) Design critical members explicitly for abnormal loading.

The fist criterion is accomplished by eliminating potential hazards altogether such as forbidding the use of gas and storing explosive materials in the building, by erecting protective barriers against vehicular impacts, or by increasing standoff distance against ground-level bomb threats.

The second criterion is accomplished by both tying the building components together and incorporating bridging capability in the structural system. Placement of effective horizontal ties around the periphery and internal beams and vertical ties to columns and walls create a structure with a high degree of redundancy, thereby providing the building with **alternative load paths** should the part of the building be removed by an abnormal event.

When tying is not feasible the structure should be designed to **bridge** over a loss of a supporting member (such as column or wall) by catenary action so that the area of damage is limited and localized. The structure can be analyzed by notionally removing one untied structural member at a time to check for progressive collapse potential. The provisions specified that progressive collapse potential is limited if the damaged area is smaller of the following:

a. 15% of the area of the story or
b. 70 m^2 (750 ft^2).

Third criterion is applied if it is not possible to develop the catenary action or bridge over the missing (notionally removed) member. Therefore, that member must be designed as a **key member** to withstand the load generated by an abnormal event in addition to the gravity loads. This additional load is derived from 34 kN/m^2 (5 psi), which is an estimated pressure that caused the exterior wall panel to fail due to the gas explosion at the Ronan Point apartment.

In recent years, both the U.K. and European building regulations have introduced a risk-based design approaches for abnormal incidents. Depending upon building type and occupancy, buildings are assigned to "consequences classes." Examples of consequences classes are shown in Table 1. Depending upon the assigned consequence class, a building must be design for abnormal loading according to the recommended procedure. These are described below:

Consequences class 1 is defined, as "*Low*" and no specific consideration is necessary with regard to accidental actions.

Consequences class 2 is defined as "*Medium*" and no specific consideration is necessary with regard to accidental actions except to ensure that the robustness and stability rules given in Eurocodes 1 to 9, as applicable, are adhered to.

Consequences class 3 is defined as "*High*" and depending upon the specific circumstances of the structure, a simplified analysis by static equivalent actions models may be adopted or prescriptive design/detailing rules may be applied.

Consequences class 4 is defined as "*Severe*" and a more extensive study recommended, using dynamic analysis, non-linear models and load structure interaction if considered appropriate.

This risk- consequence based approach provides more specific guidance than a general level of robustness.

3. Rational Design Approach

It is difficult to determine the progressive collapse potential of a building. To start with the probability of occurrence and magnitude of a postulated hazard is not well defined. At the present time, analytical tools to determine initial damage and to predict subsequent progressive collapse potential due to a postulated abnormal load is not readily available. Although there are high-performance finite element analysis tools are available, they are not widely used due mainly to the lack of familiarity with the structural behavior associated with progressive collapse, and also the lack of sufficient skills to develop complex structural models and interpret computational results. Until more experimental data become available, it would be realist to adopt "event independent" design criteria for the mitigation of progressive collapse. The design requirements should produce more robust structures which are more resistant progressive collapse due to various causes.

One design approach would be to enhance structural continuity by means of vertical and horizontal ties. This process will allow the structure to develop alternate load paths should a

part of the structure sustain failure. Furthermore, tying horizontal and vertical members improve overall integrity of the structure. If the tying method is not feasible, key structural members should be designed for postulated accidental loads. Finally, as an alternative to the key member design approach, the entire structure system should be designed for "missing (notionally removed) supports" such that the catenary action could be developed to prevent the development of collapse mechanisms.

4. CONCLUSION

The design requirements for progressive collapse mitigation are found in the U.S. and European codes and standards. The U.S. code approach is to require the buildings to possess general structural integrity. For concrete structures, the ACI Building Code provides prescriptive requirements to achieve continuity, redundancy and ductility. The U.K. Building regulations have specific design methods to guide the designer to ensure structures are designed for a minimum level of strength to resist abnormal loads. Because, at the present time, postulated hazards are not well defined, "event- independent" design criteria should be developed for the mitigation of progressive collapse.

REFERENCES

ACI 318, "Building Code Requirements for Structural Concrete and Commentary, ACI 318-02" American Concrete Institute, Detroit, MI, 2002

ASCE 7-02, "Minimum Design Loads for Buildings and Other Structures, 2002 edition," American Society of Civil Engineers, Reston, VA, 2002

Burnett, E.F. P, "The avoidance of progressive collapse: Regulatory approaches to the problem," National Bureau of Standards, Gaithersburg, MD 20899, 1975

HMSO, 1976, Ministry of Housing and Local Government, "Building Regulations, Statutory Instrument 1976, No. 1676" Her Majesty's Stationary Office, London, 1976

NYC, 1973, "Chapter 18, Resistance to Progressive Collapse Under Extreme Local Loads, Appendix A – Rules of the City of New York, Building Code of the New York City," Gould Publications, Binghamton, NY 13901, 2001

Table 1 Examples of Consequences Classes

Class	Building Type and Occupancy
1	Houses not exceeding 3 stories. Single storey storage/warehousing of less than 200 m^2 floor area which in normal use is occupied infrequently by a small number of operatives.
2	Houses exceeding 3 stories but less than 6 stories. Flats, apartments and other residential buildings not exceeding 3 stories. Offices not exceeding 4 stories. Industrial buildings not exceeding 3 stories. Retailing premises not exceeding 3 stories of less than 200m^2 floor area in each story. Single story educational buildings
3	Residential buildings not exceeding 10 stories. Educational buildings not exceeding 10 stories. Retailing premises not exceeding 10 stories. Hospitals not exceeding 3 stories. All buildings to which members of the public are admitted in significant numbers and which contain floor areas within permanent wall enclosures not exceeding 200 m^2. Non-automatic car garage not exceeding 6 stories. Automatic car garage not exceeding 10 stories.
4	All offices, retailing, hospital and car-parking buildings that exceed the limits on area and number of stories described for Class 3 buildings. All buildings to which members of the public are admitted in significant numbers and which contain floor areas within permanent wall enclosures exceeding 200 m^2. Stadia.

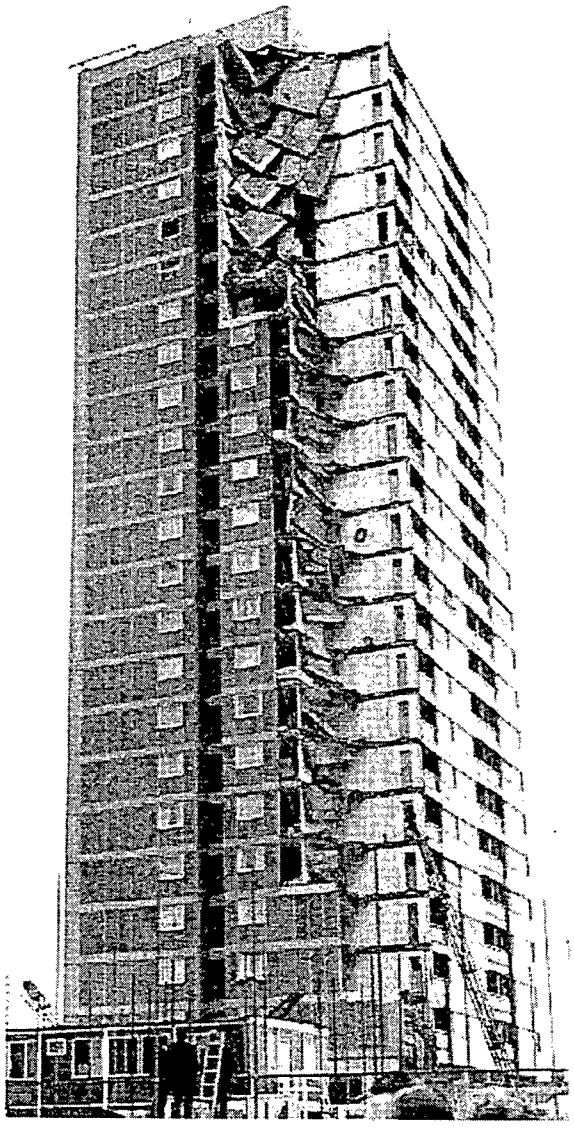


Figure 1 Ronan Point Collapse

Study on High-rise Steel Building Structure that Excels in Redundancy
by

A. Wada[1], K. Ohi[2] , H. Suzuki[3], I. Nishiyama[4], T. Hasegawa[5], Y. Sakumoto[6], M. Fushimi[6], and H. Kamura[7]

ABSTRACT
The collapse of the WTC towers may be taken to be an alert that a local failure can trigger a progressive collapse, and a landmark event that alerted the construction engineers to the importance of preventing progressive collapses of similar structures. Prevention of progressive collapse requires development of design technologies for frames that excel in redundancy. The Japan Iron and Steel Federation and the Japanese Society of Steel Construction established June this year the committee on "Study on Redundancy of High-Rise Steel Buildings". This paper discusses the high-rise steel building structures that excel in redundancy, and outlines the themes of this research project and then investigates analytically the resistance of the steel frames against heat induced by fire and loss of columns by accident such as an explosion and a impact of a crash considering structural parameters which are axial load utilization ratio of columns and structural type of frames, which are moment resistant frame, braced frame by hysteretic dampers and frame by hysteretic dampers and outrigger truss system. A non-linear analysis is conducted to estimate redundancy of various types of frames considering heat induced by fire and loss of columns. Based on the findings of the analysis, this paper advanced that steel frame structures using load-carrying capacity joints can withstand large-scale fires and loss of vertical load resistant members if the axial load utilization ratio of columns is held under 0.25, for prevention of progressive collapses.

KEYWORDS: collapse temperature, critical axial force ratio, high-rise steel building, redundancy, progressive collapse

1. INTRODUCTION

The direct causes for the collapse of the World Trade Center (WTC) Towers on September 11, 2001 were damages on the columns caused by aircraft impact, and large-scale fires. WTC1 and WTC2 kept standing 102 and 56 minutes after the impacts, respectively, during which periods many lives were saved. The great plastic deformation capacity or transferring load capacity of the steel structures reportedly saved a large number of human lives[1]. From the above the WTC towers might be considered to have some redundancy. However, the collapse of the WTC towers may be taken to be an alert that a local failure can trigger a progressive collapse, and a landmark event that alerted the construction engineers to the importance of preventing progressive collapses of similar structures.

Prevention of progressive collapse requires development of design technologies for frames that excel in redundancy. The Japan Iron and Steel Federation and the Japanese Society of Steel Construction established June this year the committee on "Study on Redundancy of High-Rise Steel Buildings". For the purposes of improving safety of high-rise buildings, the committee has begun working on the following two themes. These are: (1) a study on collapse-control design, on the bases of Japan's earthquake resistant and fire prevention technologies, and (2) quantification of redundancy of Japan's high-rise steel building structures and a work to propose frames that excel in redundancy.

1 Tokyo Institute of Technology, 4259, Nagatsuda-Cho, Midori-ku, Yokohama 226-8503, Japan
2 University of Tokyo, 4-6-1, Komaba, Meguro-ku, Tokyo 153-855, Japan
3 Tsukuba University, 1-1-1, Tenno-dai, Tsukuba, 305-8573, Japan
4 Building Research Institute,1, Tatehara, Tsukuba, 305-0802, Japan
5 National Institute for Land and Infrastructure Management,1, Tatehara, Tsukuba, 305-0802, Japan
6 Nippon Steel Corporation, 6-3, Otemachi 2-Chome, Chiyoda-ku, Tokyo 100-8071, Japan
7 JFE R&DCorporation, 1-1, Minamiwataruda-cho, Kawasaki-ku, Kawasaki 210-0855, Japan

2. OUTLINE OF RESEARCH THEMES OF THE COMMITTEE ON "REDUNDANCY OF HIGH-RISE STEEL BUILDINGS"

2.1 High-rise Steel Building Structure of High Redundancy

The WTC towers, both of them, could resist the intentionally created aircraft impacts and kept standing for some time, sparing time that permitted many people to evacuate. In this sense, the WTC towers should be credited with saving many lives. This indicates that the structures of two WTC towers had some redundancy. It is also true that the collapses that occurred some time afterward killed a large number of lives, including firemen who rushed to the towers for the trapped people's rescue. The process in which the collapse of the story that suffered from the aircraft impact lead to the collapse of the entire building may be interpreted as indicating that the structure did not have sufficient redundancy to prevent the total collapse.

Against such a background, necessity of designing buildings that could resist total collapse even in the case of accidental load actions caused as a result of an act of terrorism or accident is being discussed by various concerned parties. This committee considers that structures designed assuming increased external force by a large margin to resist total collapse are different from what the true redundant structure should be, though such structures in effect could be redundant structures. One example of redundant structures is a structure in which its redundant strength in aerodynamic design or seismic design, and its redundant strength at load carrying-capacity joints, both for the stationary load, combine to provide redundancy against the accidental load action created by an aircraft crash or explosion. In other words, the concept of redundant structure should evaluate redundant strength inherent in the subject structure, or should realize high-rise steel building structures excellent in redundancy with a proper selection of structural features, arrangement of members and proportioning of sections at a minimum of additional cost.

2.2 Objectives and Research Theme

The research committee has the following two objectives; namely, (1) Development of collapse control design standards or design recommendations based on the seismic and fire resistant design technologies of Japan, to prevent the progressive collapse; (2) Presentation of a recommendation for construction of high-rise steel building structures with adequate redundancy, based on the collapse control design standards or design recommendations.

The committee has established Structure Design Working Group and Fire-resistant Design Working Group to study the following themes on the basis of the results of studies shown in the preceding chapter. The study themes comprise those common to both groups and those unique to each group.

< Common themes >

1. Establishment of clear definition of the terms "local collapse" and "progressive collapse" as design terminology to be considered in design work
2. Evaluation of difference in redundancy according to the frame type (moment resistant frame, moment resistant frame with hat-bracing, moment resistant frame with hat-and-core-bracing, superframe structure, cf. Fig.1)
3. Proper redundancy of steel structure building from the viewpoint of risk management
4. Development of collapse control design recommendations or guidelines

< Structure Design Working Group >

5. Evaluation of resistance to the story collapse and to the loss of main structures to prevent total collapse
6. Evaluation of the effect of the load-carrying-capacity joint and full penetration welding of joints connecting columns on the above-mentioned stability of frames
7. Clarification of the behaviors of members under explosion and impact load conditions
8. Approach to redundancy of such space structures as shell, dome, etc.

< Fire-resistant Design Working Group >

9. Accuracy improvement of thermal analysis through acquisition of loaded heat test data on the cross-sections of large and thick members used for high-rise buildings, and numerical

simulation based on such data

10. Study on fire-resistive specification and construction of floor, and systems and methods for connecting the floor and the main building structure
11. Evaluation of fire resistance efficiency of high strength bolted connections
12. Study on technical measures for improvement of fire resistant redundancy (use of CFT structure, fire resistant steel and fire partition, etc.)

The Structure Design Working Group will divide the progressive collapse mode of seismically and aerodynamically designed high-rise steel structure building into two types as mentioned below, and analyze stability of frames to each collapse mode. The analysis will use the region for which the main member is conceived lost, strength and deformation capacity of joints as parameters, and obtain the critical axial force ratio of columns at the time of collapse for each type of frames. Further, the working group will clarify behaviors of members under explosion and impact load conditions, referring to the high-speed-loading test on the members and joints connecting columns and beams after the Hyogo-Ken-Nanbu Earthquake 1995 (Southern Hyogo Prefecture Earthquake). In this way, the working group will have clarified stability of members and joints against accidental loads. The working group will also study approaches to redundancy of such large space structure as shell, dome, etc., one of the main structure themes of this committee.

The Fire-resistant Design Working Group is promoting a study on the degree of redundancy (patterns of damage) of high-rise steel structure buildings of seismic and fire-resistant design, with the burning area as parameter. More specifically, the study aims to clarify structural stability at elevated temperatures suited to each frame type. In this study accuracy of evaluation on high temperature resistance of steel parts is important. Data on loaded heating tests on the cross-sections of thick steel members used for high-rise steel structure buildings are virtually nonexistent. Accordingly, the working group is conducting a loaded heat test on the standard heating temperature-time curve/hydrocarbon curve of ISO834 to acquire data. The working group intends to increase the accuracy of thermal analysis by conducting numerical simulations using these data.

The working group considers the effects of the fire-resistive specifications of floor, type of joint connecting the floor with the main structure, joint structure between columns and beams upon the redundancy of total structure very great. The working group studies the fire-resisting performance of the floors and high strength bolted connection in friction type used in Japan (rigid joint), and also presents recommendation on upgrading of redundancy.

The above study should identify members and connecting parts constituting key elements to securing good redundancy from both structural viewpoint and fire-resisting viewpoint. In effect, these key elements should be preferentially protected. The working group presents recommendations for designs of steel structure buildings excellent in redundancy, the objective the committee is expected to achieve, after some study on technical measures with suppressed incremental costs such as use of CFT columns, fire resistant steel, methods for installing fire partitions.

3. PREVENTION OF PROGRESSIVE COLLAPSE

3.1 Mode of Progressive Collapse

The committee classifies the modes of progressive collapses into two modes as shown in Figure 1, and is promoting researches into conditions for preventing progressive collapses for each of the modes. Mode 1 of Fig. 2 illustrates propagation of the story collapse to the lower stories. This mode represents a case when a collapse occurs on a certain story (called initial collapse story, can be more than one story), all stories above this story fall perpendicularly in a mass, and the vertical load resistant members (columns) of the story or stories just beneath cannot sustain the impact. Mode 2 represents progressive collapses that occur on stories above the initial collapse story. If a vertical element of the load bearing strength of the initial collapse story is lost and transferring of load occurs, and if the members adjacent to the lost vertical resistance can sustain the rearranged loads, the progressive collapse of this mode does not occur. This mode occurred to the exterior

columns of the WTC towers. In the case of the WTC towers, a collapse of Mode 1 occurred following a collapse of Mode 2. The WTC tower case is being evaluated without clear distinction of these two modes, because these two modes of collapses occurred consecutively. In studying conditions for preventing collapses of these two modes from occurring, it is necessary to study such conditions, with the two modes clearly segregated.

3.2 Prevention of Mode 1 Progressive Collapse

Regarding prevention of Mode 1 progressive collapse, the following study will be done, considering robustness of Japan's seismically designed high-rise buildings, referring to the studies by Bažant et al [3].

For the sake of simplicity, let it be assumed here that a certain given story (initial collapse story) of a building collapses, and all stories above the initial collapse story fall in a rigid body. The question is whether or not the vertical load resistant members (columns) of the weakest story below the initial collapse story can withstand the load.

The story collapse occurs as a result of a loss of strength of vertical load resistant members (columns) by a fire, or a loss of vertical load resistant members (columns) themselves by an accident like explosion, buckling of vertical load resistant members (columns) as a result of a loss of such buckling-confining members as beams. In case the stories above do not fall in a rigid body but the dead load and the live load of the story immediately above the collapse story alone rest on the floor of the collapse story, the load carrying capacity of the collapse story should be examined. If the load carrying capacity is insufficient, or the oneness of the floor system is not secured, the floor of the collapse story falls and rests directly on the floor of the story immediately below the collapse story. In this case, the progressive collapse cannot be prevented. Therefore, it is assumed here that the ultimate load carrying capacity should be enough to support the load equivalent to those of two stories at least, and oneness of the floor is secured.

The story collapse occurs as a result of a loss of strength of vertical load resistant members (columns) by a fire, or a loss of vertical load resistant members (columns) themselves by an accident like explosion, buckling of vertical load resistant members (columns) as a result of a loss of such buckling-confining members as beams. In case the stories above do not fall in a rigid body but the dead load and the live load of the story immediately above the collapse story alone rest on the floor of the collapse story, the load carrying capacity of the collapse story should be examined. If the load carrying capacity is insufficient, or the oneness of the floor system is not secured, the floor of the collapse story falls and rests directly on the floor of the story immediately below the collapse story. In this case, the progressive collapse cannot be prevented. Therefore, it is assumed here that the ultimate load carrying capacity should be enough to support the load equivalent to those of two stories at least, and oneness of the floor is secured.

Let M and g represent the mass of the entire portion above the initial collapse story and acceleration of gravity, and the load equivalent to Mg is placed on the collapse story before collapse occurs. The collapse story begins collapsing when the strength of its vertical load resistant members (columns) becomes equal to Mg. Let the average axial force ratio of columns of the story just beneath the initial collapse story be p, the vertical strength, Py, of the story just beneath the initial collapse story is given by Equation (1).

$$P_y = \frac{Mg}{p} \quad (1)$$

If the length of the vertical load resistant members (columns) of the story just below the initial collapse story is decreased by, Δ_{max}, the decrease in potential energy, ΔE_h, is given by the following equation.

$$\Delta E_h = Mg(n \cdot h + \Delta \max) \quad (2)$$

where n and h represent the number of collapse stories and story height, respectively.

The amount of energy that can be absorbed by the entire vertical load resistant members (columns) of the building, E_A, is given by the following equation.

$$E_A = Mg(\Delta_{max} - \frac{1}{2}\Delta_y) + P_y(\Delta_{max} - \frac{1}{2}\Delta_y) + E_e \quad (3)$$

where Δ_{max} represents the maximum displacement of the vertical load resistant members (columns) to the limit of maintaining the yield strength, Δ_y represents displacement of the deformation of the

elastic limit of the vertical load resistant member (column), and E_e represents the elastic strain energy of vertical load resistant members (columns) of stories other than the weakest story. The first term of the right-hand side of Equation (3) represents the amount of energy absorbed before the initial collapse story begins collapsing, the second term the amount of energy the story just beneath can absorb. The critical deformation of the initial collapse story is assumed to be equal to the maximum deformation of the story just beneath the collapse floor, or Δ_{max}. If the following inequality holds, the story immediately beneath the collapse story does not collapse.

$$\Delta E_h < E_A \quad (4)$$

By substituting Equations (2) and (3), and, further, Equation (1) into the above equation, the following equation is obtained.

$$Mg(n \cdot h + \Delta \max) < Mg(\Delta_{max} - \frac{1}{2}\Delta_y) + P_y(\Delta_{max} - \frac{1}{2}\Delta_y) + E_e = Mg(\Delta_{max} - \frac{1}{2}\Delta_y) \cdot (1 + \frac{1}{p}) + E_e \quad (5)$$

By solving the above equation for Δ_{max}, the following equation is obtained.

$$\Delta_{max} > ph[n + (1 + \frac{1}{p})\frac{\Delta_y}{2h} - \frac{E_e}{Mgh}] \quad (6)$$

In Equation (5), let n = 1 assuming one story alone to collapse, and neglecting the term, Δ_y/h, because $\Delta_y/h << 1$, the following equation holds.

$$\Delta_{max} > ph(1 - \frac{E_e}{Mgh}) \quad (7)$$

This inequality gives the required capacity for deformation of the vertical load resistant members (columns) required to prevent the progressive collapse. The first term in the parenthesis of the above equation is the product of the average axial force ratio of columns of the initial collapse story, p, and the story height (falling distance), h. The second term is the ratio of the elastic strain energy of the vertical load resistant members (columns) of stories other than the weakest one to the decremental portion of the potential energy of the upper stories equivalent to the distance of fall. According to Bažant'2002) et al., this value is about 1/8.4. If the representative value of p for Japan's high-rise buildings is taken to be 0.2, the following definition of Δ_{max} is obtained from Equation 7.

$$\Delta_{max} > 0.2 \cdot (1 - 1/8.4)h \approx h/5.7 \quad (8)$$

Equation (8), indicates that the required capacity for deformation of the vertical load resistant members (columns) of the story just beneath the collapse story is 1/5.7 the story height. If plastic deformation is not limited to the story just beneath the collapse story but is extended to more than one story or considering the plastic deformation of seismic members such as hysteretic dampers, the required capacity for deformation becomes smaller than this value. To prevent the Mode 1 progressive collapse, the committee will first study the present states of Japan's high-rise steel structure buildings, and second see whether it is possible to make these buildings satisfy Equation (7), and conditions that achieve this at minimum costs.

3.3 Prevention of Mode 2 Progressive Collapse

The following pages compare a moment resistant frame equipped with hysteretic dampers installed for the purpose of reducing responses to seismic movements and a moment resistant frame, in the stability of entire frame structure against a local collapse, by means of static analysis. The study includes a static analysis simulating a condition in which main members are lost by an explosion and an analysis on stability of the frame at high temperatures, assuming the frame to be heated by a fire.

3.3.1 Structural Stability after Loss of Main Members or at the Time of Fire

This sub section presents an analysis of behaviors of the entire steel frame structure, of which columns have been lost, or buckled at high temperatures, of steel frame structures, of which such main members as columns and beams are lost or being exposed to heat of a fire. Here, steel frame structures, of which such main members as columns and beams have been lost are subjected to an ordinary statistical analysis against the vertical load, without the main members that have been assumed lost.

Regarding the steel frame structure exposed to the heat of a fire, collapse temperatures of the frames heated by the fire are calculated to study the structural stability at elevated temperatures of the steel frame structure.

Furumura et al[4]. have shown that plastification

of members caused by temperature rise does not lead directly to the collapse of the entire frame structure. They also have shown that elevated temperatures far exceeding the allowable temperature in the Building Standard Law of Japan do not harm the structural soundness of steel frame structures. While on the other hand, the collapse of the WTC towers indicates a possibility that, if a very large portion of the frame structure is exposed to high temperatures, the frame structure can eventually become totally and destructively, unstable[3]. Considering that, there is conceivably real need to study structural stability at elevated temperatures to prevent the progressive collapse against fire load.

This study regards the unstable process of the frame represents a process of snap through from a certain condition of static balance to another condition. In a stable process where the temperature of members can rise without causing buckling of columns, the behavior of frames can be analyzed from the standpoint of load control. While in an unstable process, temperature rise is suspended until the process of snap through is finished, the frame is analyzed from the standpoint of displacement control. This approach has made it possible to solve a number of problems on structural stability at elevated temperatures, and the ultimate states or collapse temperatures of the frame at the time of fires have been clarified. Regarding theories on dynamics governing behaviors of frames after column buckling at elevated temperatures, reference should be made to the literature[5][6].

The following section presents a study on the axial load utilization ratio that can alleviate the unstable conditions of frame caused by the loss of major members and instability of frames at elevated temperatures, and also structural forms that can prevent the Mode 2 progressive collapses.

3.3.2 Numerical Analysis Model and Method of Analysis

The numerical analysis designs four types of frames for 10 stories; namely, moment resistant frame, moment resistant frame with hat-bracing/with hat-core-bracing, super-frame structure (cf. Fig.1). The brace contemplates use of hysteretic dampers of buckling-restraint braces, increasingly used in Japan recently. The members are regarded as having been joined by load-carrying-capacity joints.

The process of collapse is studied for four assumed patterns of main member losses shown in Fig. 3 in six assumed types of fire shown in Fig. 4. Fig. 3 shows patterns of main member losses in super-frame structures, but the same patterns of losses (location where losses occur) are applied to other types of frames. Figure 4 shows the locations of fires using the moment resistant frame, but the same locations apply to other types of frame.

In Fig. 3, the design stationary loading is proportionally distributed, and axial load utilization ratios of columns at the time of collapse are calculated for each analysis case. In the cases for analysis assuming fires where the axial load utilization ratio of the interior column is $\bar{p} = N / A\sigma_y = 0.225, 0.3, 0.35, 0.4, 0.45$, collapse temperature is calculated for each case. For both cases assuming fires or losses of main members, slenderness ratio of columns is set at $\lambda = l / i = 25.5$ and the column load utilization ratio of exterior columns is set at 1/2 that of the interior columns. Also, uniformly distributed loadings on beams are set by the following normalized load, $\tilde{q}$.

$$\tilde{q} = \frac{ql^2}{16M_p} \quad (9)$$

where l and M_p respectively represent length of span and full plastic bending moment of the beam. $\tilde{q}$ indicates the load factor with respect to the collapse load of the fix-supported beams under a uniform load, and $\tilde{q} = 0.15$ when $\bar{p} = 0.45$. This means that a load equivalent to 15% of the ultimate collapse load under uniform load is normally placed on the beam.

The amount of brace used is the same for the moment resistant frame with hat-and-core-bracing and the superframe structure. The steel materials are all JIS G 3136 SN400 ($\sigma_y = 235 N / mm^2$). Table 1 gives cross-sectional dimensions of the member and load conditions.

In calculating the collapse temperature, used an assumed condition of fires in which temperature of the portions indicated by bold lines of Fig. 4 is uniformly raised and other portions are held at the

room temperature. The rate of thermal expansion of steel, α, is assumed not to vary with the temperature but to remain constant at $\alpha = 12 \times 10^{-6}$ / °C.

Collapse temperature due to fire is calculated with FEM, incorporating elasto-plasticity, linear expansion of the steel material at elevated temperatures, and finite displacements of frames. In this analysis, the yield strength and the stress-strain relationships[4] are assumed to follow the assumptions given in Table 2. The strength of the steel material declines as temperature rises, and the stress-strain relationships vary accordingly. Fig. 3 shows stress-strain relationships of a structural steel, JIS G 3136 SN400, at different temperatures. It may be noted from the figure that the strength of the steel begins lowering as the temperature exceeds 400°C, and becomes 1/3 and 1/7 the strength at the room temperature at 600°C and 700°C, respectively. Naturally, it follows that steel columns buckle under lower load at high temperatures than at the room temperature.

This analysis defines the total collapse as either of the following two conditions. One is a condition in which the vertical displacement of the burning story or of the story where the main members reached the story above ((a) of Fig. 9). The other is the condition where the analysis begins unable to obtain a convergent solution and unable to redistribute the load.

3.3.3 Result of Analysis and Discussion

Figs. 6 and 7 show the results of analysis for fire cases. Fig. 6 shows collapse temperatures produced by each analytical model versus scale of fire. Results are shown for two cases of axial load utilization ratio of the interior column, $\bar{p} = 0.225, 0.45$. It may be noted from the figure that, in case the load utilization ratio of the interior column is $\bar{p} = 0.225$, the collapse temperature is about the same, irrespective of the type of frame. In case the axial load utilization of the interior column is $\bar{p} = 0.45$, under relatively high axial force of ordinary load, the collapse temperatures are higher for the frame structures equipped with seismic members than for moment resistant frame, for localized fire scales of Cases 1 to 4, or analytical cases where exterior columns do not yield to buckling. However, in Cases 4-2 and 5 where large fires are so large that even the exterior columns yield to buckling, the collapse temperature does not vary with the frame structure. Fig. 7 shows fire collapse temperature of each case versus the frame structure. When the scale of fire is larger, the collapse temperature is higher for structures equipped with seismic members than for the moment resistant frame. Figure 10 shows the obtained relationship between the axial load utilization ratio of the interior column and collapse temperature for each frame structure. The bold line on the figure is a series of normalized numbers obtained by the stress values that give one percent strain on the stress-strain curve for each assumed temperature divided by the yield stress (235N/mm^2) at room temperature. The distance between the curve for each frame structure and this bold lime may be considered to indicate the degree of redundancy of each structure. It may be noted that frame structures equipped with seismic members and frames with smaller axial load utilization ratios have greater allowances. It is also indicated that the frame structure with greater axial load utilization ratios and frame structures equipped with fewer seismic members are more in danger of total collapse as simulated by distorted structures shown on Fig. 9.

Regarding the analyses for cases assuming losses of major members (Case 2), Fig. 10 shows the distortion caused by the loss of three interior columns of the first story and the axial load utilization is $\bar{p} = 0.45$. In the case of moment resistant frame, the beam of the second story comes down to the ground, meaning that the collapse of the first story leads to the total collapse. By contrast, despite the loss of interior columns and the brace, the collapse of the first story does not extend to the total collapse. Figure 13 and 14 show the values of axial load utilization ratio versus frame structure type and versus cases for main member loss, respectively. It is evident from Figs. 11 and 12 that the collapse critical axial force ratio is higher for the super-frame structure than for other structures. The moment resistant frame can withstand loss of a considerable number of vertical load supporting members, provided that the axial load utilization is not greater than 0.3. In the case of moment

resistant frame with hat-bracing and with hat-and-core-bracing, the collapse critical axial force ratio is larger than the moment resistant frame, indicating higher resistance of the former to loss of the vertical load supporting members.
As discussed above, it is possible to estimate resistance to the Mode 2 progressive collapse from the value of axial load utilization ratio of columns under ordinary load. Regarding the Mode 1 progressive collapse, Equation (7) of part 1 presents a function of axial load utilization ratio of column under ordinary load, and therefore permits estimation of resistance against progressive collapse from axial load utilization ratio of column under ordinary load.
The analysis presented here uses hypothetical models that use load-carrying capacity joints, and assumes the cross-sections of the members to be uniform with respect to the story height, to study stability against the progressive collapse. This analysis was done as a preliminary study. Hereafter, the committee intends to study such themes as effects of load-carrying capacity joints, for high-rise buildings constructed according to the A seismic Code of the Building Standard Law of Japan.

4. CONCLUSIONS

This paper outlines the joint research program of the Japan Iron and Steel Federation and the Japanese Society of Steel Construction, the committee on "Study on Redundancy of High-Rise Steel Buildings". The study broke down the progressive collapses into two modes, and conducted for both modes a study on the prevention of progressive collapses.
Japan's high-rise buildings designed to resist great earthquakes use a large number of braced members as seismic members. And very few are of moment resistant frame structure that is inferior in stability in case main members are lost by fires or accidents. Recently, hysteretic dampers, excellent in plastic deformation capacity and intended to absorb input earthquake energy, are increasingly used as seismic members. The seismic design also increases the ability to withstand progressive collapses. However, this is not the result of designs that intend to prevent progressive collapses. In other words, seismic design, fire resistant design and the design to prevent progressive collapses should be promoted concurrently. This may be interpreted as indicating that, by this approach, structures excellent not only in earthquake resistance but also in fire resistance and progressive collapse resistance may be constructed, with no great difficulty nor significant increase in cost.
And the study was done by numerical analyses of the effects of the reduction of strength of members as a result of fire and the loss of members by such accident as an explosion on redundancy of steel structure buildings, for different types of frame structure, with axial load utilization ratio of column under ordinary load as parameter.
Further studies are necessary to produce more detailed and practical results. Notwithstanding, the following conclusions have been obtained from the preliminary scope of this study.

(1) Steel frame structures using load-carrying capacity joints can withstand large-scale fires and loss of vertical load resistant members, if the axial load utilization ratio of columns is held low.
(2) Super-frame structures reinforced for earthquake resistance by using hysteretic dampers has a higher stability of the entire structure against the local collapse than the moment resistant frame, in case the strength of member is reduced by fires or structural members are lost by such accidents as an explosion.
(3) The axial load utilization ratio of column under ordinary load can be an effective parameter in the study for prevention of progressive collapses. As far as the results of this study are concerned, a measure of the limit to the axial load utilization ratio of column under ordinary load is about 0.25, for prevention of progressive collapses.

The committee concludes this presentation by expressing the deepest condolence to more than 3,000 people who have been killed by the attach of terrorism to the WTC towers and their families, including 479 men and women of emergency services who sacrificed their lives in pursuit of their noble missions, and aircraft crew of 157 people. The committee also hopes that this research will contribute to the upgrading of safety of steel structures.

Table 1

Section of frame	
• Beam	: H-596x199x10x15 (for all structure)
• Column	: □-350x350x16 (all)
• Hat-bracing	: H-200x200x8x12 (all)
• Hat-and-core bracing	: H-200x200x10x15 (Hat-and-core-bracing) H-200x200x8x12 (Superframe)
Load condition	
• Normalized loading on beam	: $\tilde{q} = \frac{ql^2}{16M_p} = 0.15$
• Column force ratio(The lowest story)	: $\bar{p} = N / A\sigma_y = 0.225, 0.3, 0.35, 0.45$

Table 2 Assumption for formulating yield strength and stress-strain relationship of SN400

$$\sigma(\varepsilon, T) = \max\left\{\sigma^{(1)}(\varepsilon, T), \sigma^{(2)}(\varepsilon, T)\right\}$$

$$\sigma^{(1)}(\varepsilon, T) = \min\left\{E_t \cdot \varepsilon, \sigma_{yt}\right\}$$

$$\sigma^{(2)}(\varepsilon, T) = f^{(1)}(\varepsilon, T) + f^{(2)}(\varepsilon, T)$$

$$f^{(1)}(\varepsilon, T) = \frac{E_{lt} \cdot \varepsilon}{\left\{1 + \left(\frac{E_{lt}}{\sigma_{ot}} \cdot \varepsilon\right)^n\right\}^{\frac{1}{n}}}, \quad f^{(2)}(\varepsilon, T) = \frac{E_{pt} \cdot \varepsilon}{\sqrt{1 + \left(\frac{\varepsilon}{\varepsilon_2}\right)^2}}$$

$$E_{lt} = E_t - E_{pt}$$

$$E_t = \left(1.0 - 0.905 \cdot 10^{-6} \cdot T^2\right) \cdot E_{RT} \qquad E_{RT} = 2100 t / cm^2$$

$$\sigma_{yt} = \left(1.001 - 3.592 \cdot 10^{-6} \cdot T^2\right) \cdot \sigma_{yRT} \qquad \sigma_{yRT} = 2.4 t / cm^2$$

$$E_{pt} = Line\ \text{connecting}\left(0℃, 50.0 t / cm^2\right), \left(400℃, 50.0 t / cm^2\right), \left(600℃, 5.0 t / cm^2\right) and \left(850℃, 0.0 t / cm^2\right)$$

$$\sigma_{ot} = \begin{cases} where\ T \le 600℃ \\ \left(0.759 + 1.933 \cdot 10^{-4} \cdot T - 5.944 \cdot 10^{-6} \cdot T^2 + 2.179 \cdot 10^{-8} \cdot T^3 - 2.305 \cdot 10^{-11} \cdot T^4\right) \cdot \sigma_{yRT} \\ where\ T > 600℃ \\ \quad Line\ \text{connecting}\left(600℃, \sigma_{ot}(600℃)\right) and \left(850℃, 0.0 t / cm^2\right) \end{cases}$$

$$\varepsilon_2 = 0.05 \qquad n_t = 1.7$$

E_t : Young's modulus at T℃ σ_{yt} : Yield strength at T℃
E_{pt} : Plastic Modulus at T℃ σ_{ot} : Reference plastic stress at T℃
n_t : Shape parameter at T℃

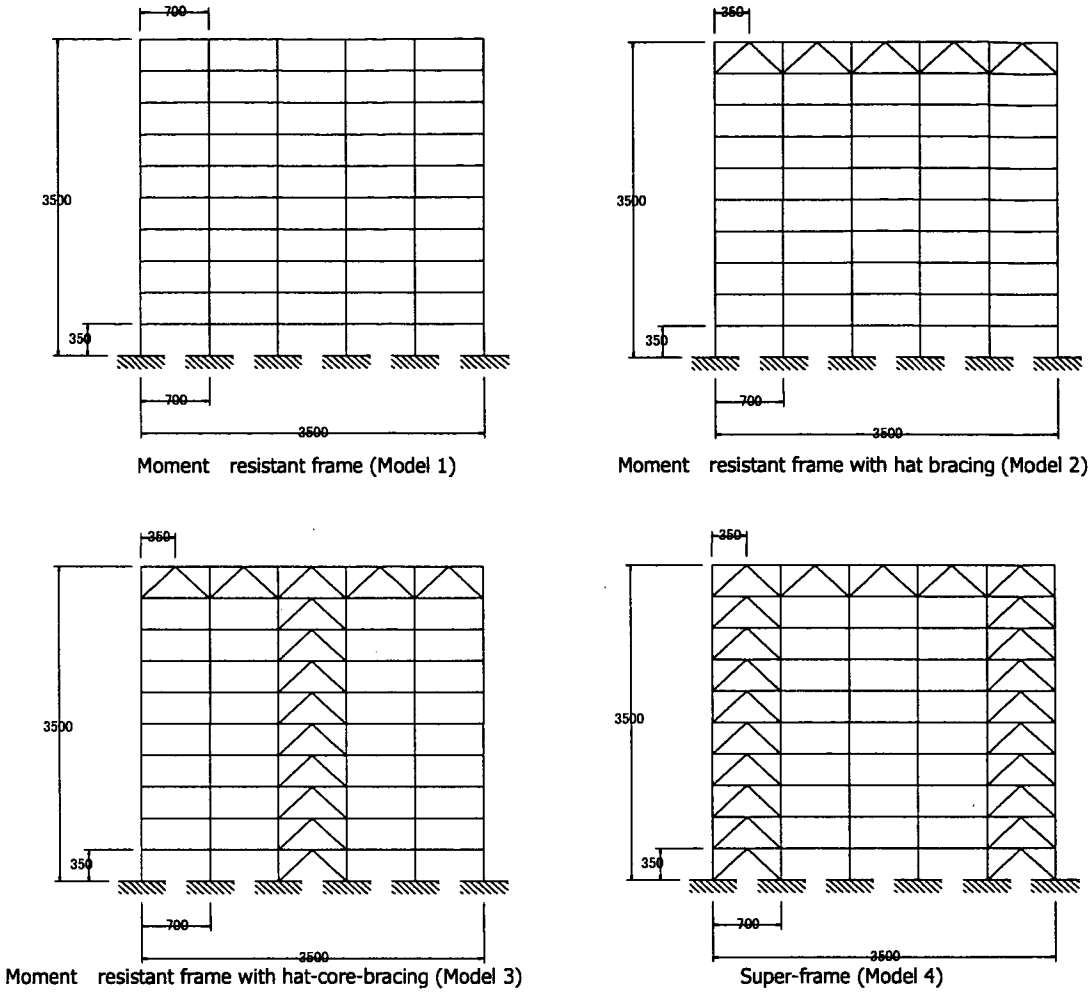


Fig. 1 Analytical Models

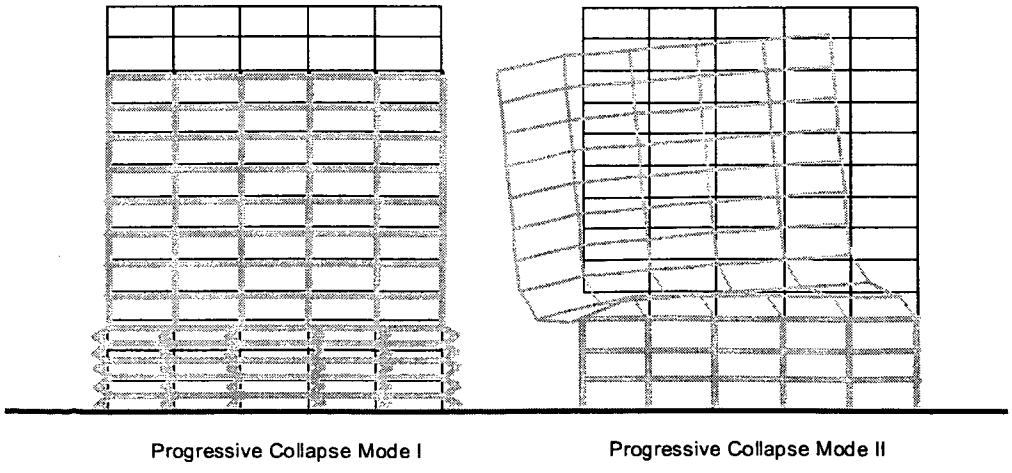


Fig. 2 Modes of progressive collapses

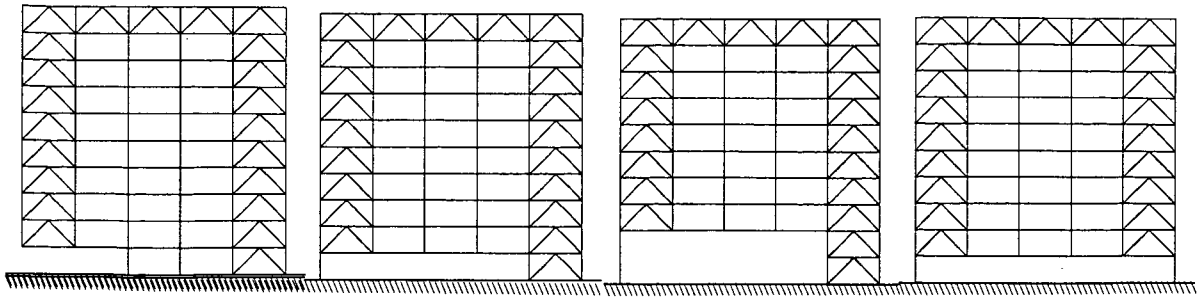


Fig. 3 Analytical models of main member losses

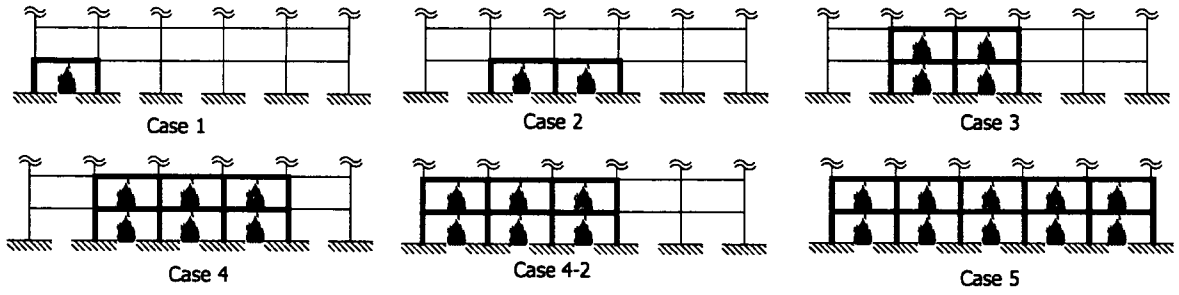


Fig. 4 Location of fires in analytical models

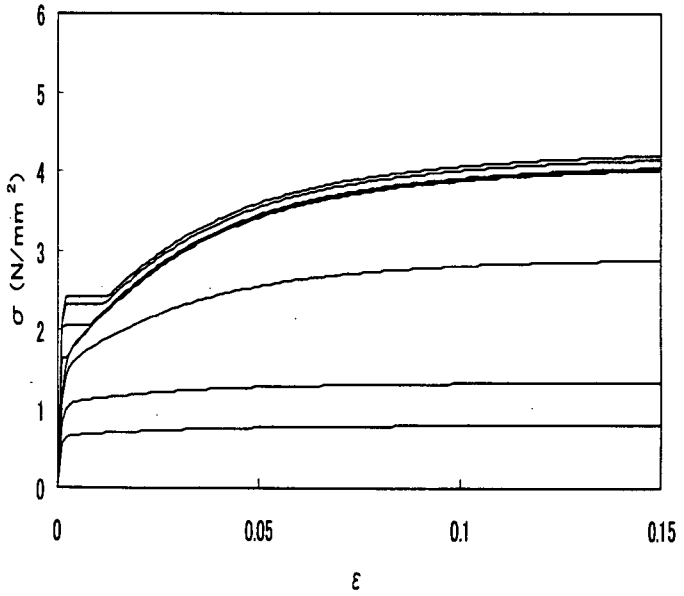


Fig. 5 Stress-strain relationship of SN400 at different temperature

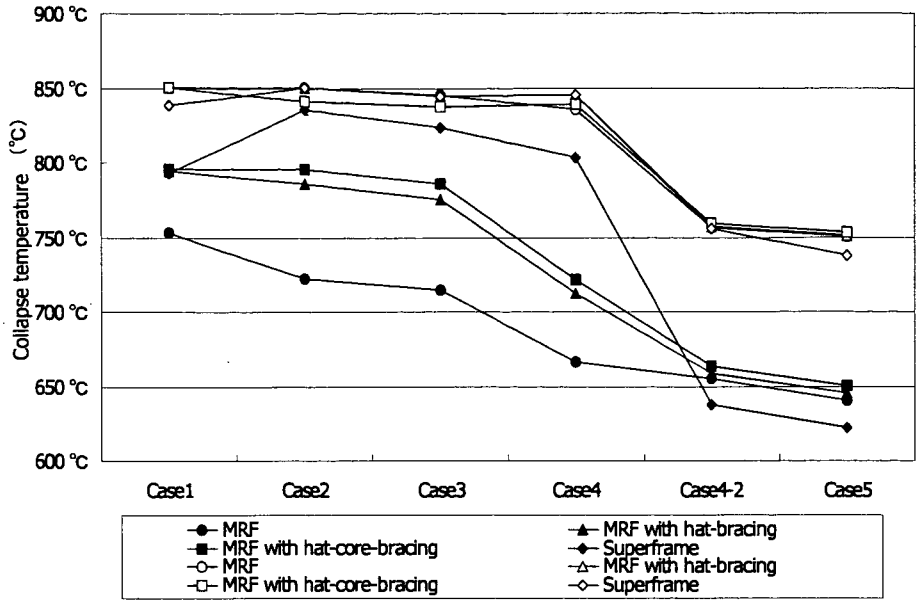


Fig. 6 Collapse temperatures produced by each analytical model versus scale of fire

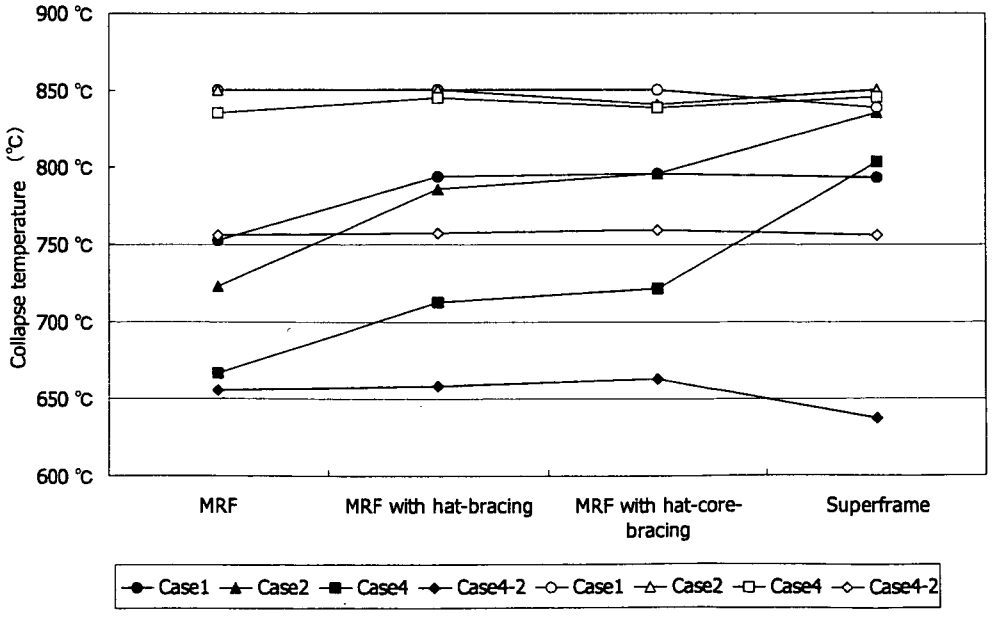


Fig. 7 Fire collapse temperature of each case versus the frame structure

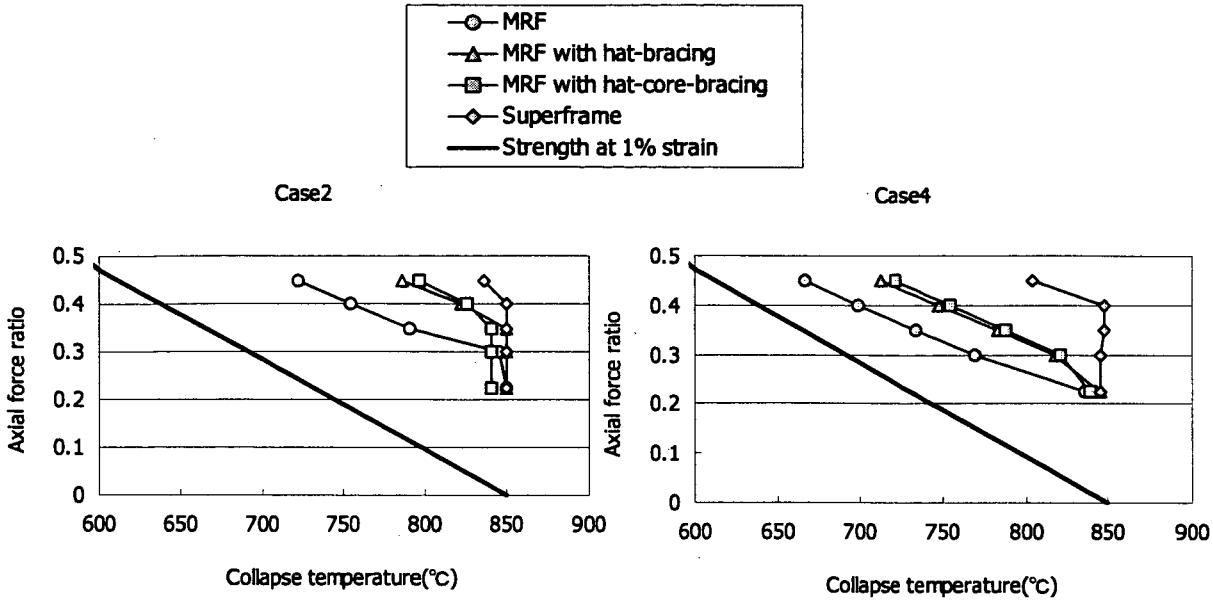
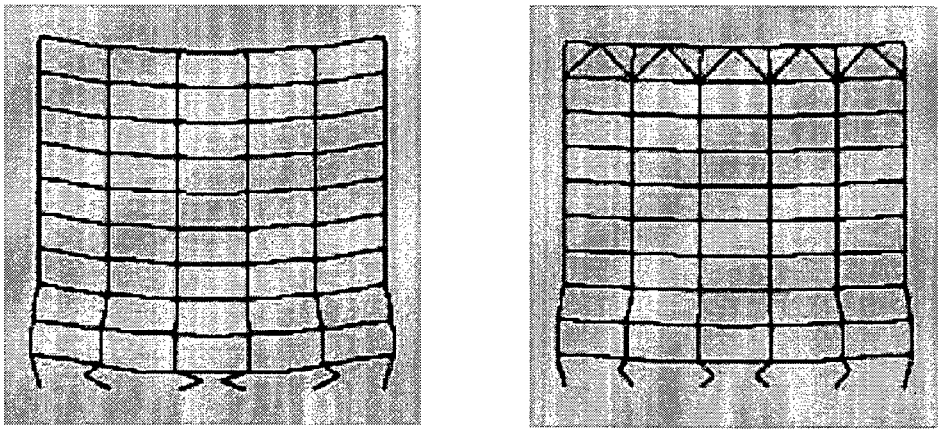
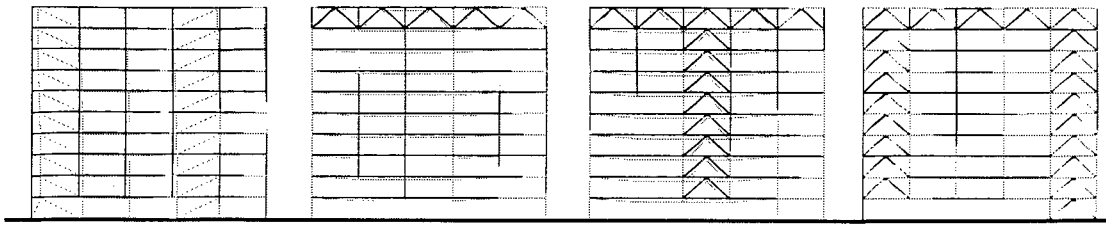


Fig. 8 Relationship between axial load utilization ratio of interior column and collapse temperature



(a)MRF (b)MRF with hat-bracing

Fig. 9 Distorted structures (fire case4: $\overline{p} = 0.45$)



(a)MRF (b)MRF with hat-bracing (c)MRF with hat-core bracing (d)Super-frame

Fig. 10 Distorted structures (less of major members case 2: $\overline{p} = 0.45$)

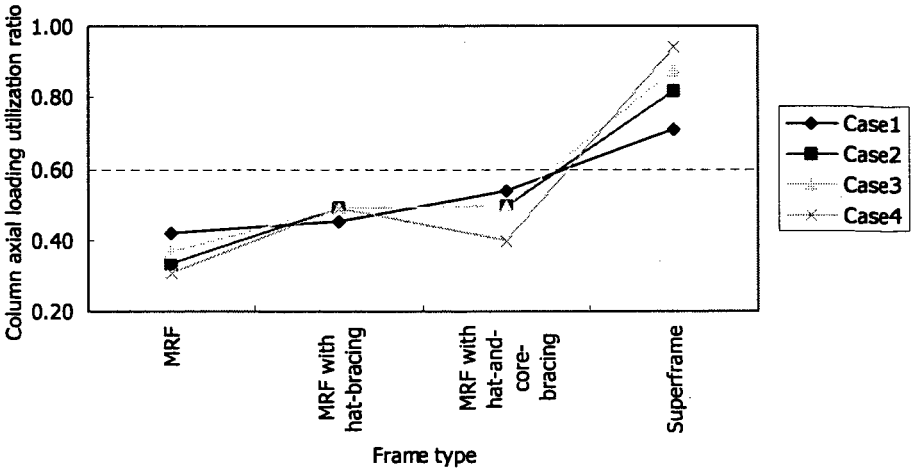


Fig. 11 Collapse axial load utilization ratio in case of loss of major members

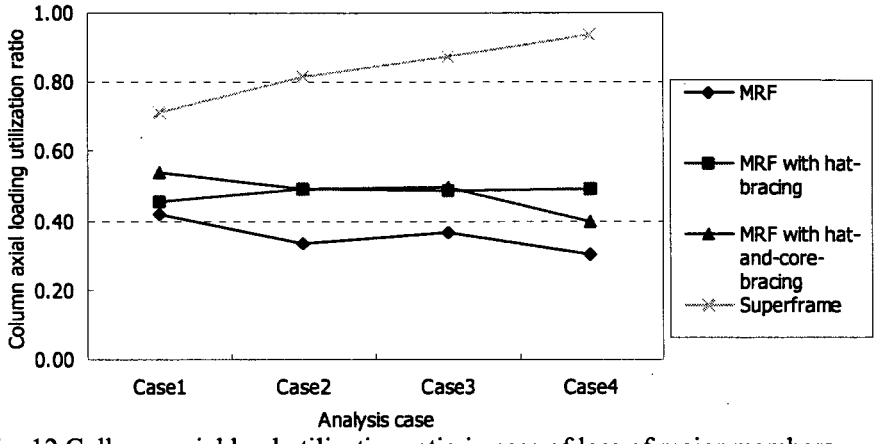


Fig. 12 Collapse axial load utilization ratio in case of loss of major members

5. REFERENCES

1. FEMA: World trade center building performance study, FEMA 403, 2002.5.
2. BS CODE, BS5950 PART1 SECTION2 , 1990.
3. Bažant, Z. P. , Zhou, Y. : Why did the world trade center collapse? - Simple analysis, Journal of Engineering Mechanics, ASCE, pp.2-6, 2002.1.
4. Furumura, H., Shinohara, Y.: inelastic behavior of protected beams and columns in fire, Journal of Structural and Construction Engineering, AIJ, No.300, January 1981.5.
5. Suzuki, H., Ultimate temperatures of steel frame subject to fire, Journal of Structural and Construction Engineering, AIJ, No.477, pp.147-156, 1995.11. (in Japanese)
6. Suzuki, H., Study on the structural failure on the New York world trade center, Symposium on shock wave, 2002.3. (in Japanese)

Acknowledgements

This research is part of a joint research program of the Japan Iron and Steel Federation and the Japanese Society of Steel Construction, the committee on "Study on Redundancy of High-Rise Steel Buildings" headed by Professor Akira Wada of Tokyo Institute of Technology. This paper incorporates various advice from committee members. Mr. Yukio Murakami of JFE Steel Corp. and Mr. Kei Nakagawa of JFE R&D Corporation contributed greatly to the numerical analysis. The authors express deepest appreciation to all men and women who generously extended cooperation to the development of this report.

Applicability of Seismic Design in Mitigating Progressive Collapse

by

W. Gene Corley[1]

ABSTRACT

A Building Performance Assessment Team (BPAT) composed of American Society of Civil Engineers (ASCE) and Federal Government engineers investigated damage caused by the malevolent bombing of the Alfred P. Murrah Federal Building in Oklahoma City, Oklahoma. The purposes of the investigation were to review damage caused by the blast, determine the failure mechanism, and identify engineering strategies for reducing damage to new and existing buildings. Specifically, mechanisms for multi-hazard mitigation, including mitigation of earthquake effects, were considered. Among the strategies evaluated were use of seismic detailing for the structural concrete. This report describes results of the investigation, makes recommendations for design of buildings to be more blast-resistant, and discusses how these details might have changed results of damage in Oklahoma City. The paper also reviews requirements for structural integrity reinforcement after 1989, refers to a case study of blast-damage to the Murrah Federal Building in Oklahoma City, describes how earthquake detailing can reduce losses, and shows how the use of full capacity butt splices could have further reduced the casualties in that blast. Finally, it questions whether seismic detailing can protect buildings where brisance is the failure mode.

KEYWORDS: Blast damage, earthquakes, failure mechanism, multi-hazard mitigation, progressive collapse, seismic design.

1.0 INTRODUCTION - OKLAHOMA CITY BOMBING

In 1995, the Murrah Federal Office Building in Oklahoma City was heavily damaged by a terrorist bomb blast [1]. During the period, May 9 through 13, 1995, 3 weeks after the blast occurred on Wednesday, April 19, 1995, the BPAT visited the area around the Murrah Building in Oklahoma City. While in Oklahoma City, the BPAT took photographs, collected structural drawings, shop drawings, photographs, and samples of structural components, including concrete and reinforcing bars; and obtained an audio tape of the blast recovered from a damaged building across the street from the Murrah Building. The team also conducted interviews of individuals involved in design, construction, and cleanup of damaged buildings. Physical inspection of the Murrah Building was limited to visual observation.

Upon completion of the site visit, data collected were analyzed and the most probable response of the building to the blast was determined. Using knowledge of building performance, an evaluation was made of the use of Special Moment Frame detailing to enhance the resistance of buildings to blast loading. Further details are provided in reference 1.

2.0 ALFRED P. MURRAH FEDERAL BUILDING

Design of the Murrah Building project, shown in figure 1, was done for the Design & Construction Division, Region 7, Fort Worth, Texas, of the GSA Public Buildings Service, Washington, DC. A contract for the design of the project was signed in the early 1970's, and the contract drawings that were issued for construction were dated May 6, 1974. Construction documents for the project consist of architectural, structural, mechanical, and electrical drawings, plus specifications for construction. The general contractor for the project was J. W. Bateson, Inc. Shop drawings for reinforcing bars were prepared by The Ceco Company between December 1974 and May

[1] Senior Vice President, Construction Technology Laboratories, Inc., Skokie, Illinois

1975. A spot-check of the Ceco reinforcing bar shop drawings shows compliance and good correlation with the structural contract documents. Construction was completed in 20 months, between late 1974 and early 1976.

The Murrah Building project included a nine-story office building, shown in figure 1 (hereafter referred to as the nine-story portion of the Murrah Building), with one-story ancillary east and west wings and an adjacent multi-level parking structure, partially below grade and partially above grade, south of the office building.

Focus of this report is performance of the nine-story portion of the Murrah Building and on use of seismic detailing to provide improved resistance to bombing. The nine-story portion of the building sustained significant damage and progressive collapse as a result of the April 19, 1995 bombing as shown in figure 2. Remaining portions of the nine-story and one-story buildings were demolished shortly after completion of the investigation. The parking structure sustained little damage and was not immediately demolished.

The nine-story frame of the Murrah Building was an Ordinary Moment Frame of reinforced concrete supported on columns. Overall plan dimensions were approximately 61 m (220 ft) in the east-west direction and approximately 30.5 m (100 ft) in the north-south direction.

In plan, the structure for the nine-story portion consisted of ten 6.1 m (20 ft) bays in the east-west direction and two 10.7 m (35 ft) bays in the north-south direction, plus shear walls and other localized columns and walls in the core area at the midpoint of the south side of the building. Exposed reinforced concrete with a vertical-board-formed finish served as the exterior architectural treatment. Four large, prominent, vertical circular tube columns, one at each of the four corners of the building, acted as air intake/exhaust shaft for the ventilation system, as seen in figure 1. An elevator shaft and stair wells were located in the south central portion of the building.

Details of Murrah Building—Structural drawings that were obtained confirmed that the Murrah Building consisted of cast-in-place ordinary reinforced concrete framing with conventionally reinforced columns, girders, beams, slab bands, and a one-way slab system. Exterior spandrels supporting the exterior curtainwall were exposed concrete with a vertical-board-formed finish. The lateral load resisting system for wind forces was composed of reinforced concrete shear walls located within the stair and elevator systems on the south side of the building. Although neither the governing building code nor the owner required consideration of blast loading or earthquake loading, the required wind-load resistance provided substantial resistance to lateral load.

According to general notes on the structural drawings, the Murrah Building project was all reinforced concrete that was proportioned, fabricated, and delivered in accordance with the American Concrete Institute (ACI) *Building Code Requirements for Reinforced Concrete* (ACI 318-71 [2]. The yield strength for ties, #3 bars, and concrete reinforcing for stirrups was 275.8 MPa (40,000 psi). The yield strength for all other deformed bars and all welded wire fabric was 413.7 MPa (60,000 psi). The 28-day concrete compressive strengths included 20.7 MPa (3,000 psi) foundation and equipment bases and 27.6 MPa (4,000 psi) for structural beams, slabs, columns, walls, counterforts, pilasters, spread footings, and parking garage exterior walls. General notes also required all reinforcing bar splices to be lapped 30 bar diameters unless otherwise noted.

Plans showed that the design live loads followed requirements of the Oklahoma Building Code. Wind loads were included but no blast or earthquake loads were required.

Concrete and reinforcing bar samples were obtained from materials moved to the Oklahoma County Sheriff's Firing Range. During this visit, the BPAT reviewed photographs taken soon after the explosion by several law enforcement organizations. Also, several pieces of building debris were inspected.

Analysis of Materials and Determination of Blast Size—Five of the cores taken from the concrete from the Murrah Building were selected for compression testing. Compression test results indicated that the concrete strength was well in excess of the 27.6 MPa (4,000 psi) called for in the design specifications. Petrographic evaluation indicated that the concrete contained normal-weight aggregate and was of the quality required in the design specifications.

Several pieces of reinforcing bars were recovered from the debris of the building. A few lengths of straight bar were tested in tension. In all cases, the yield stresses and strengths measured for the bars were greater than the minimums specified and easily met the requirements of the design specifications.

Using forensic engineering techniques, it was possible to determine the blast size. These findings provided a means for assessing response of the building and potential mitigation techniques. Soil test boring data obtained along N.W. Fifth Street was found in the architectural plans. The borings were taken approximately 5.9 m (19.5 ft) south of the street centerline. Crater survey measurements located the center of the crater to be approximately 8.5 m (28 ft) south of the street centerline.

During the crater survey, pavement thickness was measured to include approximately 275 mm (11 in) of asphalt over 175 mm (7 in) of concrete at the north tip of the crater. Borings provided the soil properties below the concrete layer.

Based on observations made of the crater and other damage, the blast that damaged the building had a yield equivalent to approximately 1814 kg (4,000 lb) of TNT [2]. This extremely large explosion was centered approximately 4.8 m (15.6 ft) from Column G20 (see fig. 2 and fig. 3). The blast caused a crater approximately 8.5 m (28 ft) in diameter.

While the north face of the building sustained the brunt of the effects of the blast, structural damage to the remaining exposures was more limited. Most of the damage was caused by progressive collapse following loss of three columns nearest the blast.

Ray Blakeney, Director of Operations for the Oklahoma Medical Examiner's Office, has estimated that up to 90 percent of the fatalities were the result of crushing caused by falling debris.

3.0 PROBABLE FAILURE MECHANISM

A forensic investigation of damage to the Murrah Building disclosed that failure occurred in three columns supporting a transfer girder on the north side of the building. One of these columns was destroyed by brisance or shattering while the adjacent two failed in shear. After losing support from the three columns, approximately 50 percent of the floor area of the building collapsed, producing a large number of casualties.

A photo of the Murrah Building prior to the terrorist attack is shown in figure 1. The transfer girder supported on four intermediate columns can be seen just below the glass curtain wall.

Figure 3 shows a drawing of the building north elevation with the explosive-laden truck parked in the street beside it. Also shown in the figure is the resulting crater. Figure 4 shows a plan view of the crater and location of the column nearest the truck. As reported in reference 1, a bomb having an explosive power equal to approximately 1814 kg (4,000 lb) of trinitrotoluene (TNT) was detonated in the truck.

Analysis of damage in the field and calculation of effects of the explosion determined that the nearest column, G20 as identified in figure 2 and figure 3, would have been destroyed by brisance or shattering. Approximately 12.2 m (40 ft) each side of the column that was destroyed, adjacent columns were found to have exceed their shear strength, but been approximately at their flexural capacity. As a result, the adjacent columns failed in shear, thereby leaving the spandrel beam without

support for distance of approximately 48.8 m (160 ft).

Transfer girder reinforcement is shown in figure 5. Three of the transfer girder top bars were continuous but none of the bottom bars were. A similar pattern was present in spandrel girders above the third floor as shown in figure 5. Consequently, there was no effective integrity reinforcement in the spandrels of this building. It must be noted that at the time the building was built, no integrity reinforcement was required. Analyses show that this building met or exceeded code requirements in every way that was checked.

Reference 1 indicated that shear failures of two of the three columns could have been prevented if only a small amount of hoop steel had been provided. It is also possible that the column nearest the bomb could have been saved if full confinement reinforcement had been provided. However, for purposes of this discussion, it will be assumed that the column nearest the truck would be destroyed by brisance.

In reference 1, an analysis is made with one column removed. The three mechanisms that could develop after removal of one column are shown in figure 6. Calculations indicate that Mechanism 2 results in a capacity of approximately 2.9 kPa (60 psf) to 3.4 kPa (70 psf) floor above the spandrel beam. This is significantly less that the approximately 5.3 kPa (110 psf) of self-weight plus live load that existed in the building. Consequently, removal of any one column supporting the as-built transfer girder would cause failure of all of the floors above over a length of about 24.4 m (80 ft).

4.0 APPLYING EARTHQUAKE DETAILING TO REDUCE LOSSES

Ordinary Moment Frames have limited capacity for dissipating energy from extreme loading such as earthquake and blast. However, Special Moment Frames and Dual Systems with Special Moment Frames, as defined in the 2002 edition of *NEHRP (National Earthquake Hazards Reduction Program) Recommended Provisions for Seismic Regulations for New Buildings*, provide structural systems with much higher ability to dissipate energy. Special Moment Frames are detailed with continuity of top and bottom reinforcement, shear strength to resist maximum probable moments, and confinement at potential hinging locations. It is noted that the NEHRP recommendations for design of Special Moment Frames and Dual Systems were not widely available until 1985, approximately 10 years after the Murrah Building was constructed.

If detailing currently used for Special Moment Frames had been present at the time of the blast, Columns G16 and G24 would have had enough shear resistance to develop a mechanism without failure. Consequently, it is likely that G16 and G24 would not have failed abruptly due to the blast loading if Special Moment Frame detailing had been used. With these columns in place, a mechanism consisting of a combination of vierendeel, catenary, and transfer girder flexure can develop to minimize the loss of structure.

Due to its close proximity to the very large explosive device, Column G20 would be likely to have been destroyed by brisance even if it were detailed as a Special Moment Frame. However, the heavy confinement reinforcement that would have been present would have increased the chances of survival for Column G20.

If Special Moment Frame detailing had been used, the following results could have been expected:

1. If Column G20 survived the blast, loss of structure would have been limited to those floor slabs destroyed by air blast. This would reduce the loss of floors by as much as 85 percent.

2. If Column G20 were removed by the blast, normal detailing for Special Moment Frame design would provide reinforcement in the transfer girder at the third floor that would greatly increase the possibility that the slabs

above would not collapse. Consequently, destruction could be limited to only those areas destroyed by air blast. Although use of a Special Moment Frame would not completely eliminate loss of portions of the building, it is estimated that losses would be reduced by as much as 80 percent.

3. If Column G20 were removed by the blast and failure occurred in the spans between Columns G16 and G24, loss of the structure would be limited to those panels destroyed by air blast and those panels located between Column Lines F to G and Column Lines 16 to 24. Resulting loss of floor space to either air blast or collapse would be reduced by more than 50 percent.

4.1 Integrity Reinforcement

Since 1989, requirements for structural integrity reinforcement have been listed in Section 7.13 of the ACI Building Code [3]. In general, Section 7.13 requires one-sixth to one-quarter of the reinforcement in perimeter beams to be continuous about the building. In addition, Section 13.4.8.5 requires two bottom bars in each direction be carried through columns continuously or anchored within the columns.

The purpose of integrity reinforcement for both spandrel beams and slab column intersections, is to provide a small capacity, even after failure of a column or slab at any one location.

In Chapter 21, toughness is required throughout the structure for seismic resistance. to obtain required toughness, Section R21.3.2 states the following:

> "Lap splices.....are prohibited at regions where flexural yielding is anticipated because.....splices are not reliable under.....cyclic loading into the inelastic range."

Based on this analysis, it is concluded that use of Special Moment Frame detailing has the potential for significantly improving blast resistance.

4.2 Full Capacity Mechanical Butt Splices

In the 1999 ACI Code [4], full capacity mechanical butt splices were recognized for the first time. Classified as Type 2 mechanical splices in Section 21.2.6.1(b), they are required to "develop the specified tensile strength of the spliced bar." ACI 318-99 permits use of Type 2 splices at any location, including hinging regions. Consequently, Type 2 full capacity mechanical butt splices can be used to connect integrity reinforcement and improve the blast and/or seismic resistance of concrete structures.

If integrity reinforcement in the spandrel beams of the Murrah Building was maximized by making all of the bars continuous with full capacity mechanical butt splices, significant increase in the capacity of Mechanism 2 of figure 6 would be realized [5]. Using Mechanism 2 with 100 percent of the bars spliced with full capacity mechanical butt splices, calculated capacity of the building would be at least 6.7 kPa (140 psf). Unit weight of the building, including some live load, is approximately 5.3 kPa (110 psf). Consequently, even if one column had been removed the building would not have collapsed.

Although collapse of the building frame would have a high probability of being prevented by making all of the reinforcement in spandrels continuous, several of the floors would be destroyed as a result of brisance. Consequently, the reduction in catastrophic damage to the building would not be 100 percent, but is estimated to be approximately 80 percent.

As indicated in reference 1, almost all of the casualties were the result of building collapse, not air blast. Consequently, if building collapse is reduced by 80 percent, casualties would be reduced by a similar amount.

4.3 Cost Analysis

To determine what the additional cost might be if full capacity mechanical butt splices had been

used in the Murrah Building, a review of cost studies done by Cagley and Associates and reported in reference 5 was made.

Cost analyses done by Cagley and Associates [4] show that the increased cost of mechanical butt splices over lap splices in a 12-story parking deck was less than ¼ of 1 percent of the cost of the building. In an office structure, such as the Murrah Federal Building, the cost of mechanical splices would be even a smaller percentage of the total cost. Considering that use of full capacity butt splices could be limited to only that portion of the building exposed to the street where the bomb was detonated, estimated total cost differences are approximately 1/8 of the total cost of the building. This cost difference is insignificant.

5.0 SUMMARY

This paper discusses the potential for using earthquake resistant detailing and mechanical full capacity butt splices to increase blast and earthquake resistance of buildings. With seismic detailing, it is shown that damage due to blast can be significantly reduced. The need for integrity reinforcement to reduce damage in a building when unanticipated intense loads destroy a single element is also discussed.

Terrorist bombing of the Murrah Federal Building in Oklahoma City is used as a case study. It is shown that without fully continuous integrity reinforcement, strengthening of columns with seismic detailing could reduce damage by about 50 percent. However, if full capacity mechanical butt splices had been used to make all of the spandrel beam reinforcement continuous, collapse of the building would have been reduced by an estimated 80 percent with a similar reduction in casualties. The estimated additional cost to provide this continuous reinforcement is approximately 1/8 of 1 percent, much less than the variation in estimating the cost to construct the building.

6.0 REFERENCES

1. Corley, W. Gene; Sozen, Mete A.; Thornton, Charles H.; and Mlakar, Paul F., "The Oklahoma City Bombing: Improving Building Performance Through Multi-Hazard Mitigation," FEMA-277, Mitigation Directorate, August 1996, U.S. Government Printing Office, Washington, DC, 90 pp.
2. American Concrete Institute, *Building Code Requirements for Reinforced Concrete* (ACI 318-71), ACI Committee 318, Detroit, Michigan, 1971.
3. American Concrete Institute, *Building Code Requirements for Structural Concrete* (ACI 318-01), ACI Committee 318, Farmington Hills, MI, 2001.
4. American Concrete Institute, *Building Code Requirements for Structural Concrete* (ACI 318-99), ACI Committee 318, Detroit, Michigan, 1999.
5. Cagley, James R., and Apple, Richard, "Economic Analysis—Mechanical Butt Splices vs. Lap Splicing, ERICO, Inc., Solon, Ohio, 5 pp.
6. Corley, W. G., Smith, R.G., and Colarusso, L. J., "Structural integrity and the Oklahoma City bombing," Concrete Construction, A Hanley-Wood Publication, Addison, Illinois, December 2001, Vol. 46, No. 12, pp. 29-30.

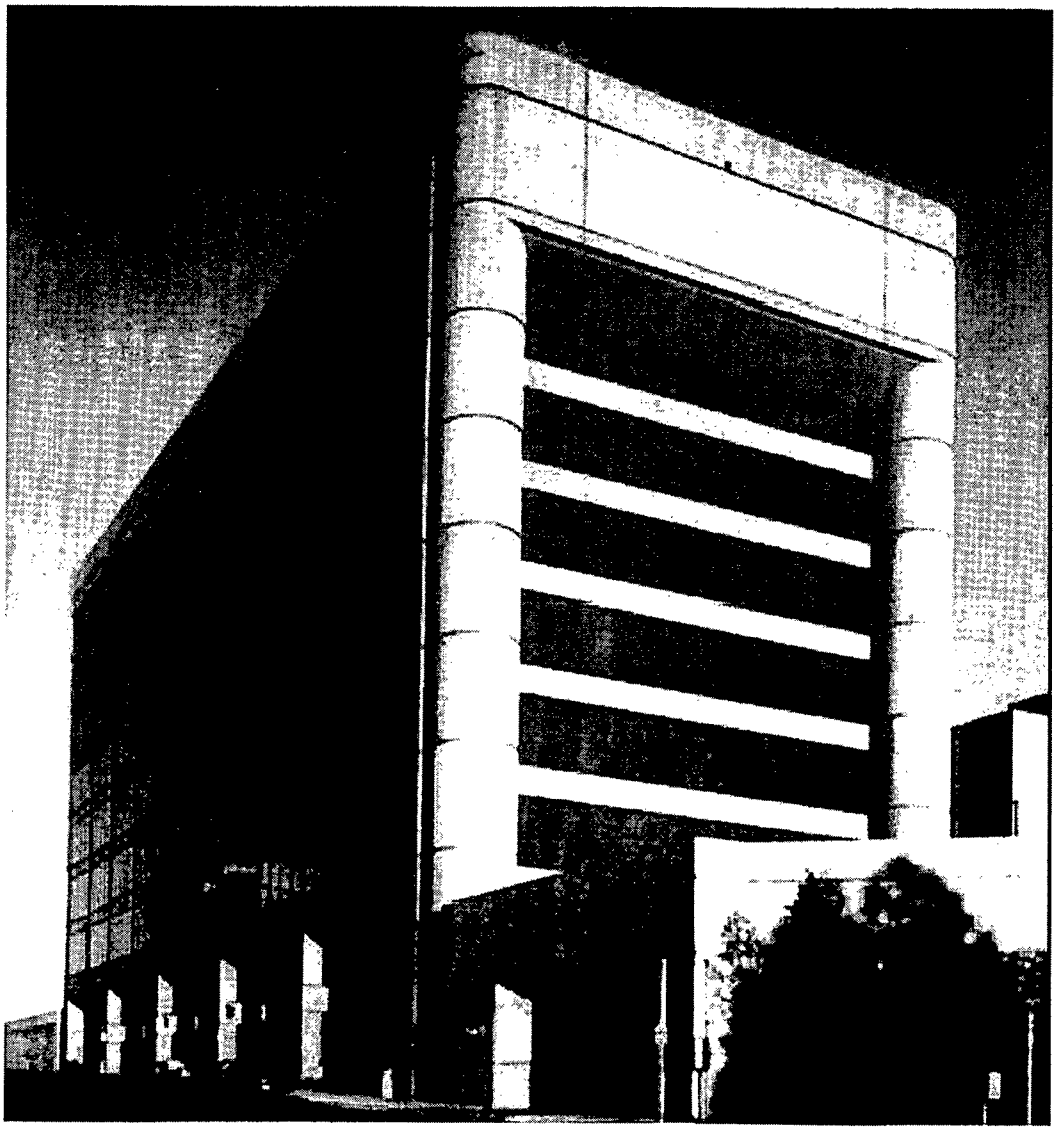


Figure 1. Murrah Building Prior to Blast.

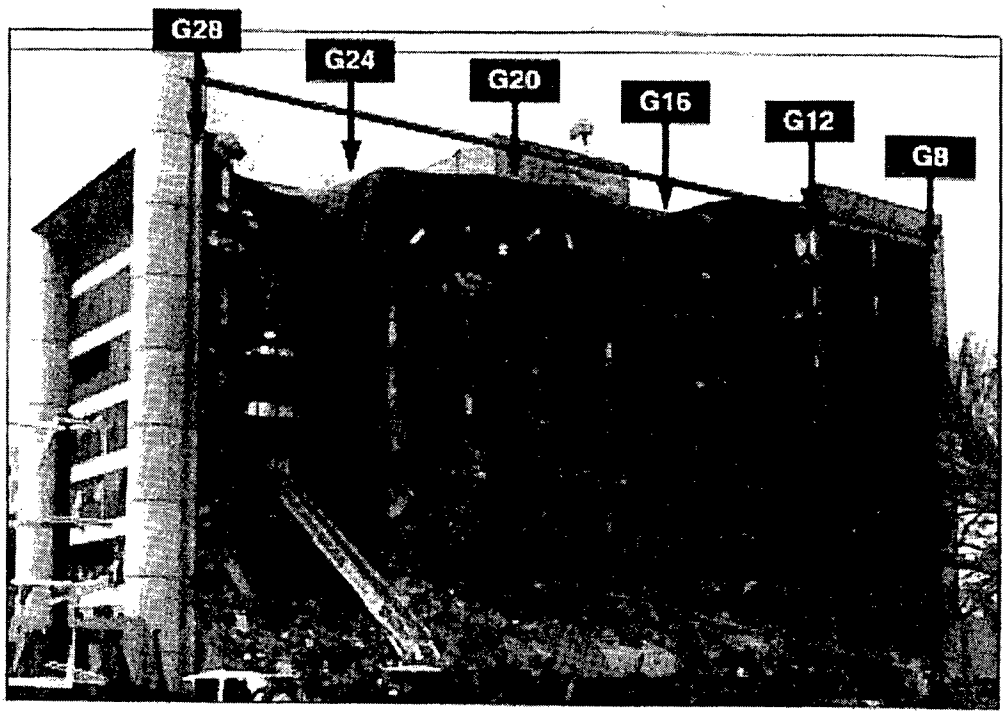


Figure 2. Damage to North and East Sides of Murrah Building

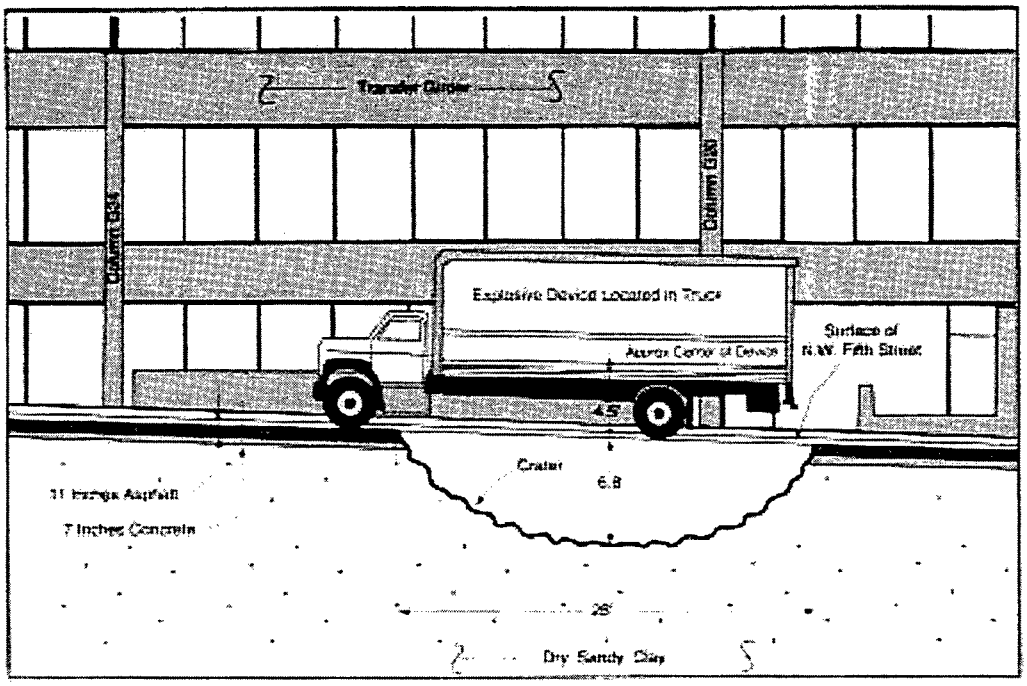


Fig. 3 Approximate Dimensions of Crater at North Face of Murrah Building

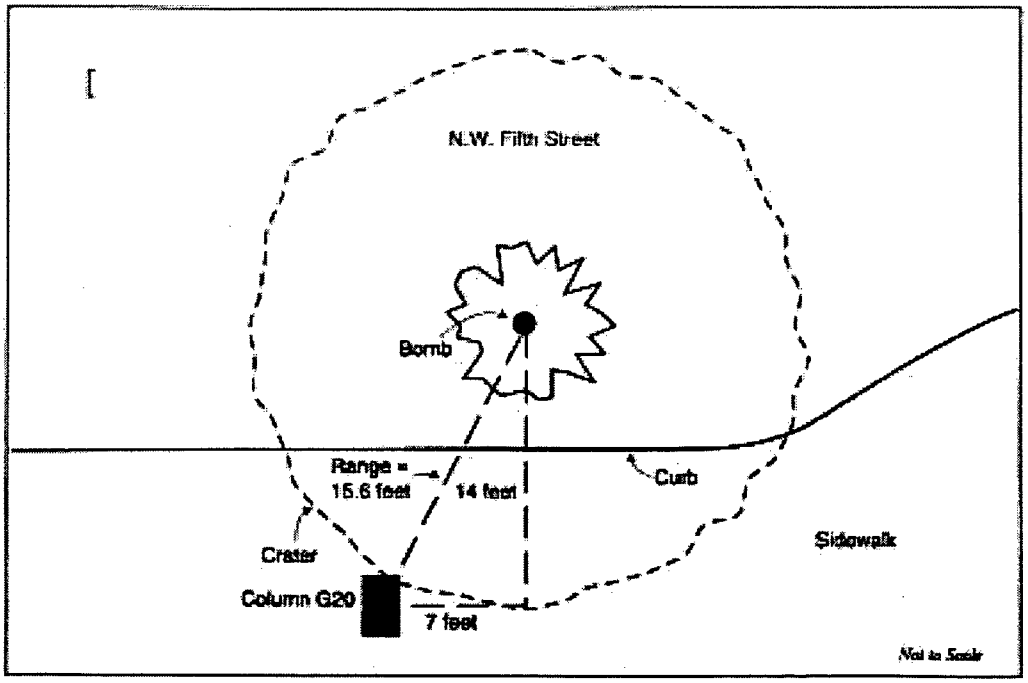


Figure 4. Proximity of Column G20 to Location of Bomb (Plan View).

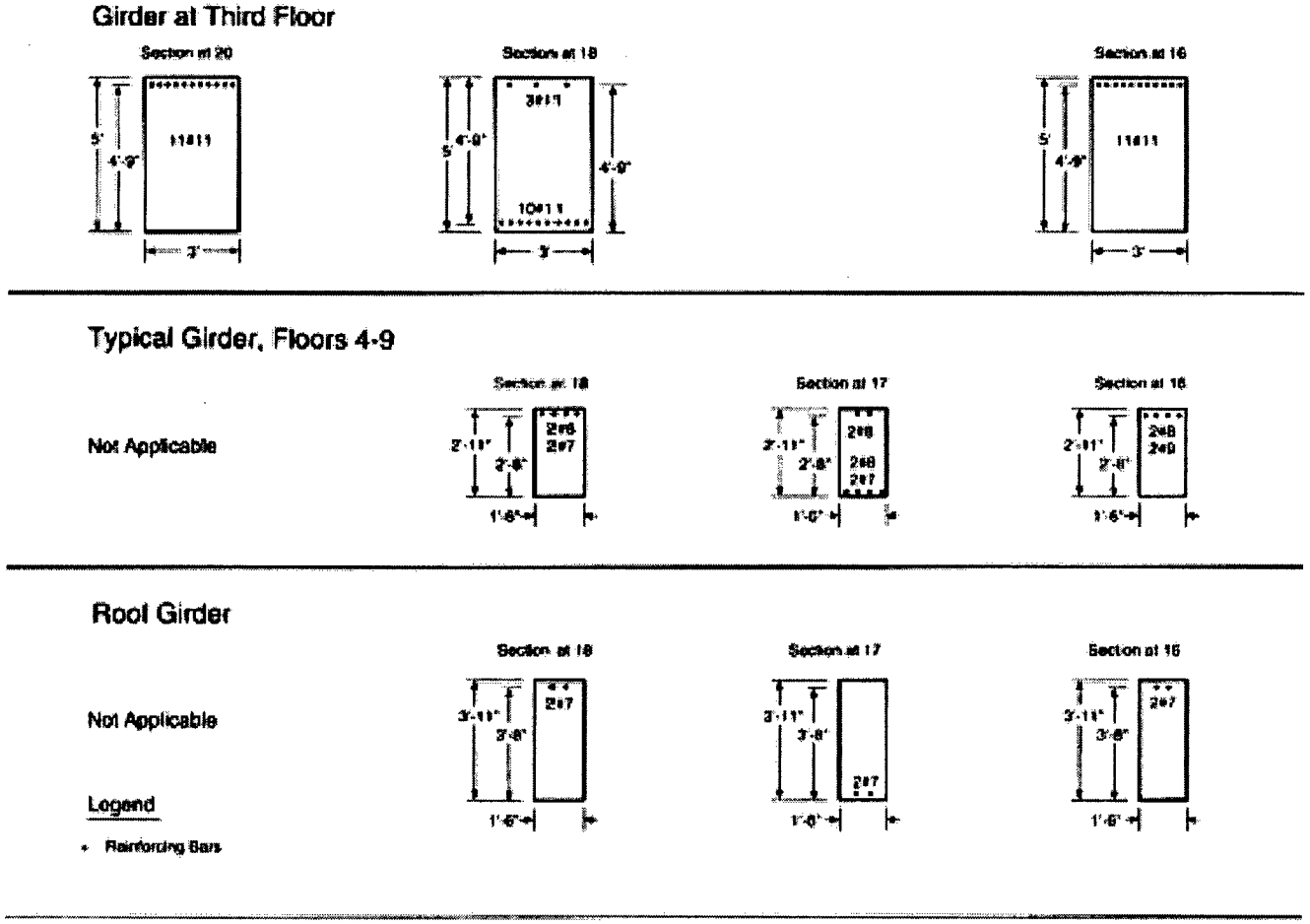


Fig. 5 Cross-Sectional Distribution of Girder Reinforcing Bars.

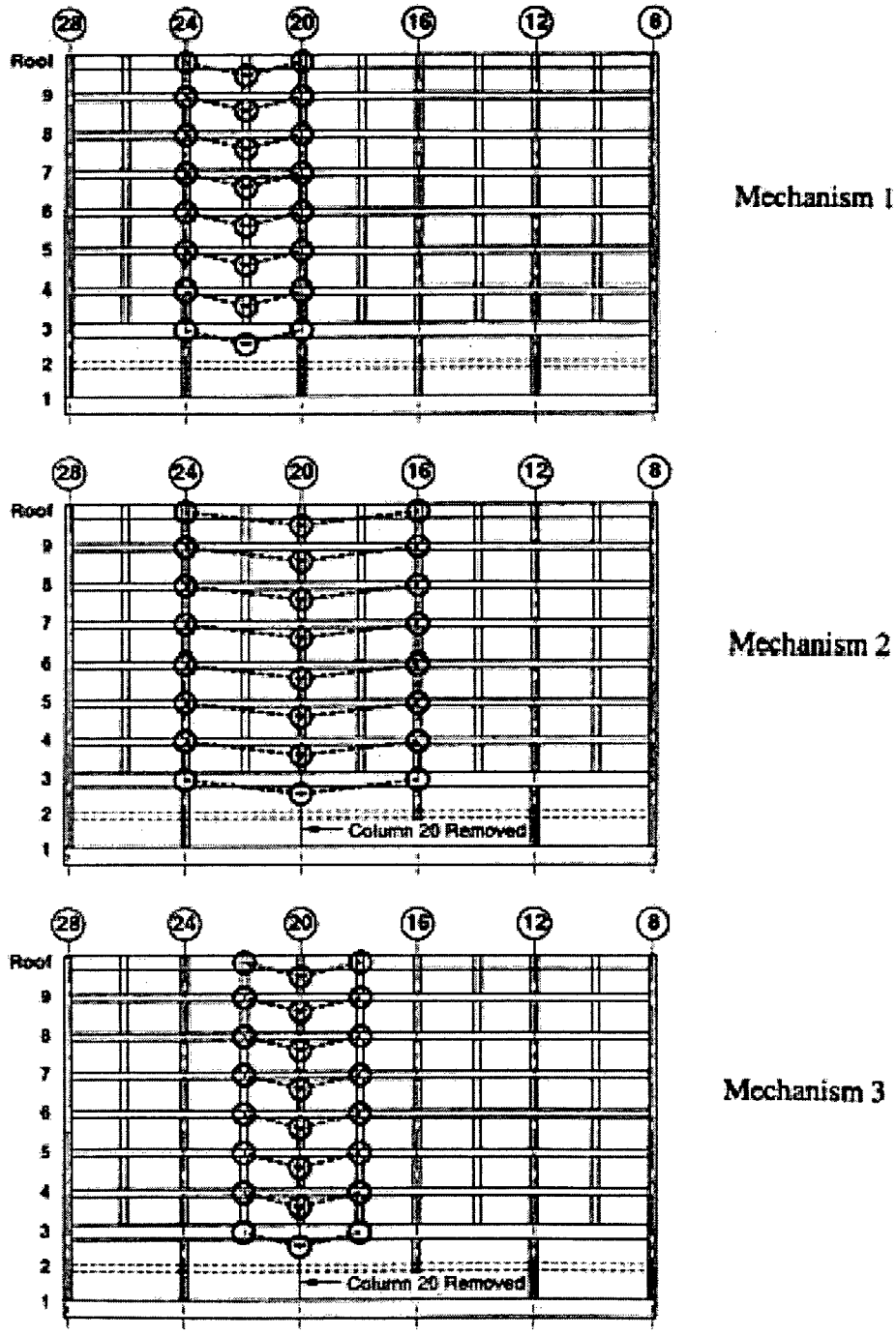


Figure 6. Possible Mechanisms with No Columns Removed and One Column Removed.

Plastic Deformation Capacity of Welded Beam-end Limited by Brittle Fracture

by

Takahiko Suzuki[1], Takumi Ishii[2], Yoshifumi Sakumoto[3] and Akiyoshi Mukai[4]

ABSTRACT

This paper proposes a method of assessing the plastic deformation capacity of welded beam-ends limited by brittle fracture. The phenomenon of brittle fractures in welded beam-ends was first observed in the 1995 Hyogo-ken Nanbu Earthquake, because a practical design method for preventing such fractures had yet to be established. It was, however, confirmed that the fracture toughness of the beam-end welds is one of the many factors controlling the initiation of fracture through full-scale tests conducted after the earthquake. This paper presents a relationship between fracture toughness and fracture strength of beam-end welded joints, which is obtained from the test results, and indicates that the plastic deformation capacity of beams can be calculated from the fracture strength. Further, a simple design expression for calculating the plastic rotation of the beams up to the fracture is presented using the representative stress-strain relation models of steel for buildings. The application of these approaches will allow structural designers to prevent beam-end brittle fractures, even during severe earthquakes, through the selection of suitable steels.

KEYWORDS: Brittle Fracture, Fracture Toughness, Plastic Deformation Capacity, Welded Beam-to-Column Connections

1. INTRODUCTION

In the Hyogo-ken Nanbu Earthquake, there was only limited damage of the collapse of steel buildings. Many fractures, however, were observed, mainly in the welded beam-to-column connections of square tube columns and H-shape beams. These fractures, which occured with buckling and plastification of the beams, were different from the fracture observed in the Northridge Earthquake. Further, it was confirmed that the fractures initiated from the end of beam-flange welded joint or the toe of weld access hole.

In the "strong column-weak beam" seismic design, the beam-end plastic deformation capacity is expected. Further, the deformation capacity was thought to be limited by local buckling, and then the method of calculating the deformation capacity, which is currently used in practical design, was proposed [1]. However, the damage in the Hyogo-ken Nanbu Earthquake presented that the deformation capacity is occasionally governed by fracture, and therefore a new method is needed.

It is possible to predict beam's deformation behaviors from the sectional shape and dimension of the beams and from stress-strain relations. In addition, it can be thought that the beam-end plastic deformation capacity is decided by ending the beam's deformation behavior due to the brittle fracture of beam-end flange. That is, if the fracture strength of beam-flange welded joint is known, the deformation capacity can be assessed by calculating the plastic deformation at the point where the tension force acting on the beam flange reaches its fracture strength.

Prior to the Hyogo-ken Nanbu Earthquake, the importance of fracture toughness, which is evaluated by the Charpy V-notch impact absorbed energy in this paper, was recognized, but experimental data concerning the influence of fracture toughness on the brittle fracture at beam-end were not

[1] Senior Researcher, Steel Structure Development Center, Nippon Steel Corporation, Futtsu-shi, Chiba-ken, 293-8511 Japan

[2] Senior Researcher, Civil Engineering Department, JFE R&D Corporation, Kawasaki-shi, Kanagawa-ken, 210-0855 Japan

[3] General Manager, Building Products Construction Materials Development Division, Nippon Steel Corporation, Chiyoda-ku, Tokyo, 100-8071 Japan

[4] Senior Research Engineer, Structural Engineering Department, Building Research Institute, Tsukuba-shi, Ibaraki-ken, 305-0802 Japan

available. After the Hyogo-ken Nanbu Earthquake, the conditions leading to the fracture were investigated through many full-scale tests and the importance of fracture toughness has become clear.

In this paper, the relationship between fracture strength and fracture toughness of the beam-flange welded joints is quantitatively determined based on data from existing full-scale tests. Next, a method is presented to assess beam-end plastic deformation capacity based on the fracture strength. In addition, a simple design expression for calculating the maximum plastic rotation of beams, which is decided by beam-end fracture, is introduced in the practical design and its validity is verified.

2. EFFECTS OF FRACTURE TOUGHNESS ON BEAM-FLANGE FRACTURE STRENGTH

Tension tests of welded joints with defect were conducted to specify the factors affecting the brittle fracture at beam-ends [2]. As shown in Fig. 1, the test specimens were prepared by forming beam-to-column connections composed of a square tube column and an H-shape beam with through-diaphragm; artificial defects of different sizes were created in the end of welded joints. The test specimens were manufactured in three combinations using different steel plates and welding wire, and the test was conducted using loading velocity and test temperature as parameters. Brittle fractures occured in the vicinity of the defect with ductile cracks in each specimen. Fig. 2 shows the test results. The maximum strength (P_{max}) obtained in the test was normalized by the product of the flange sectional area (A_f) and the tensile strength (σ_u) of steel or weld metal, which was calculated taking into account the change in strength induced by the strain velocity and temperature. P_{max} was compared to the Charpy absorbed energy (${}_vE_{br}$) at the test temperature where brittle fracture occured. ${}_vE_{br}$ was found from the respective energy transition curves of the base metal, the heat-affected zone and the weld metal. These curves had previously been obtained by conducting impact tests on test specimens extracted from welded joints manufactured using the same steel plates, welding wires and welding conditions as those of

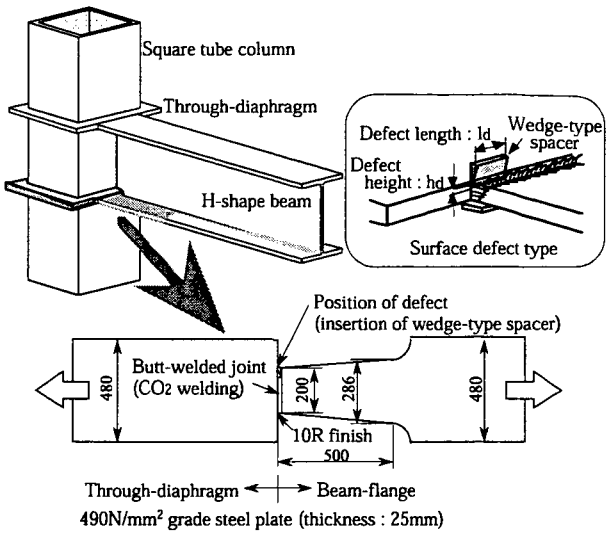


Fig. 1 Tension Tests of Welded Joints with Defect

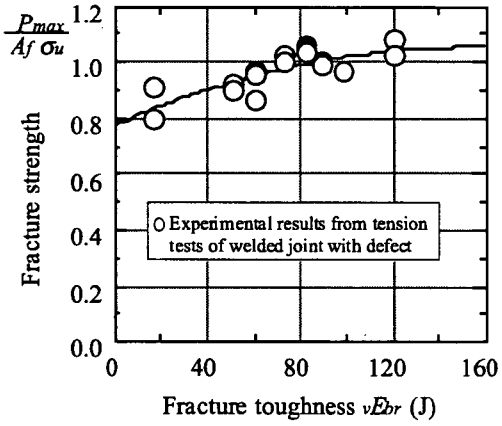


Fig. 2 Relationship between Fracture Toughness and Fracture Strength of Welded Joints

the tension tests. From Fig.2, it was confirmed that there is a positive correlation between ${}_vE_{br}$ and $P_{max}/(A_f \cdot \sigma_u)$.

Cyclic bending tests were also conducted on the T-shaped beam-column subassemblage shown in Fig. 3 [3, 4]. The test specimens, different in the beam-end weld details (type of weld access hole and type of tack welding procedure for backing bar), were manufactured using steel plates and rolled H-shapes having different base metal toughness, and investigations are underway on the ef-

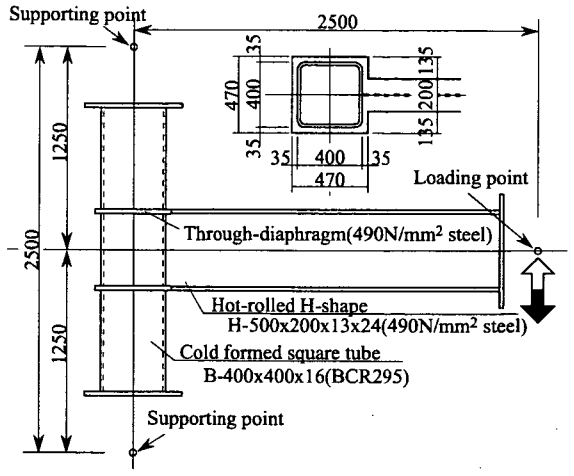


Fig. 3 Cyclic Bending Tests for T-shaped Beam-Column Subassemblages

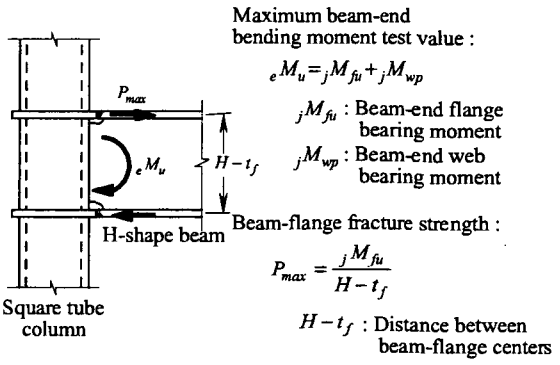


Fig. 4 Estimation of Beam-flange Fracture Strength in the Cyclic Bending Tests

fect of the fracture toughness and weld detail on the fracture strength of the beam-end flange. The beam-end flanges of each test specimen fractured in a brittle manner, and the starting point of fracture was the end of beam-flange welded joint or the toe of the weld access hole. The relationship between maximum tension strength (P_{max}) of beam-flange and fracture toughness ($_vE_{br}$) was investigated as in the following.

P_{max} is found from the maximum beam-end bending moment ($_eM_u$) obtained by the tests, using the method shown in Fig. 4. In the figure, symbol $_jM_{fu}$ indicates the bearing moment of beam flange, H the beam height, t_f the beam flange thickness and $_jM_{wp}$ the assumed value for beam-end web bearing moment calculated based on the literature [5]. $_vE_{br}$ is found from the Charpy impact test on the welded joints manufactured separately, as in the tension tests.

The relationship between $_vE_{br}$ and $P_{max}/(A_f \cdot \sigma_u)$ thus found is shown in Figs. 5 and 6. These figures include the data obtained from the tension test and the existing test results in which $_vE_{br}$ was already been confirmed [6]. Fig. 5 shows the relationship from the test results of specimens in which fracture occurred at the end of beam-flange welded joint, and Fig. 6 those in which fracture occurred from the toe of the weld access hole. Both figures

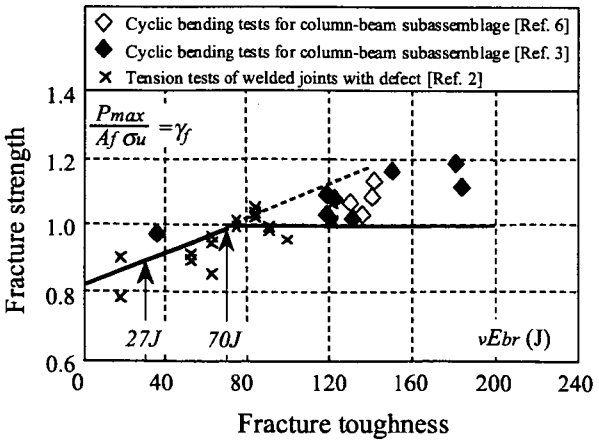


Fig. 5 Relationship between Fracture Toughness and Fracture Strength of Welded Joints (Fracture Initiating from the Beam-flange Weld)

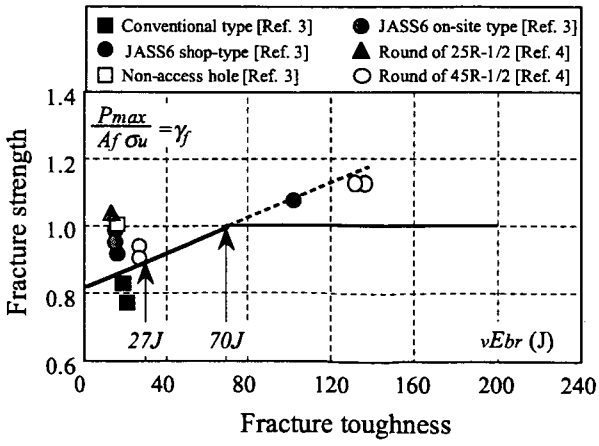


Fig. 6 Relationship between Fracture Toughness and Fracture Strength of Welded Joints (Fracture Initiating from the Toe of the Weld Access Hole)

show that as ${}_{v}E_{br}$ becomes large, $P_{max}/(A_f \cdot \sigma_u)$ tends to become large. Further, it has been found from Fig. 6 that the fracture strength significantly lowers in the conventional type which was the combination of the weld access hole to cause high stress concentration and the tack welding to lower the fracture toughness of base metal.

From these test results, it is considered that the fracture strength of the beam-flange welded joints is decided by the fracture toughness with the adoption of improved-type weld access hole for reducing stress concentration and the restiriction for tack welding on the toe of weld access hole. After all, structural designers can set the beam-flange fracture strength by adopting the appropriate weld details and further by adopting appropriate steels, welding wires and welding conditions so as to secure the fracture toughness of welded joints.

3. ASSESMENT FOR DEFORMATION CAPACITY OF BEAMS

As shown in Fig. 7, when the bending moment of triangle distribution occurs at the beam due to the action of shear force during earthquake, the expansion of beam-end plastic region is decided by the ratio ($\alpha = {}_{j}M_u / {}_{b}M_p$) of the maximum beam-end bending strength (${}_{j}M_u$) to the beam's full plastic moment (${}_{b}M_p$). As α becomes larger, that is, as ${}_{j}M_u$ becomes larger, the plastic region expands and the deformation capacity of beams becomes larger. ${}_{j}M_u$ is expressed as

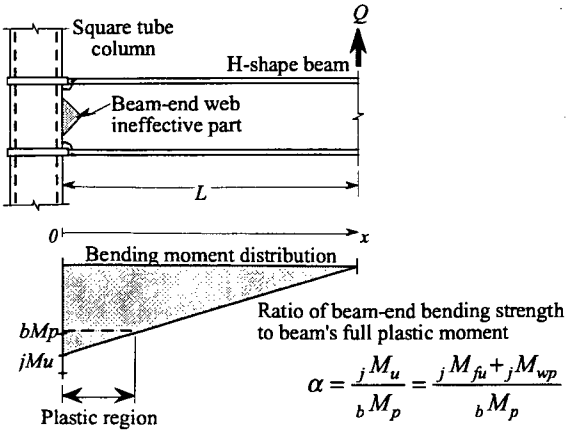


Fig. 7 Assessment Method for Deformation Capacity of Beam-end

$$ {}_{j}M_u = {}_{j}M_{fu} + {}_{j}M_{wp} \quad (1) $$

where ${}_{j}M_{fu}$ and ${}_{j}M_{wp}$ are the maximum bending moment which the beam-flange and the beam-web can bear respectively.

${}_{j}M_{fu}$ is calculated from the plastic section modulus of beam-flange (${}_{f}Z_p$), the tensile strength of beam (σ_u), and the welded joint fracture strength coefficient (γ_f), where γ_f is defined as the normalized fracture strength $P_{max}/(A_f \cdot \sigma_u)$ in this paper.

$$ {}_{j}M_{fu} = {}_{f}Z_p \cdot \sigma_u \cdot \gamma_f \quad (2) $$

On the other hand, ${}_{j}M_{wp}$ is affected by the shape and dimension of columns to which beams are attached. It is known that, in the case of square tube columns, the out-of-plane deformation is generated on the column skin plate section to which the beam-web is attached and the beam-web's bending moment to be transferred to the column becomes small. In the literature [5], the expression to calculate the effective height (χ) and ${}_{j}M_{wp}$ at the beam-end is shown. Here, when using β, the ratio of ${}_{j}M_{wp}$ to the full plastic moment of beam web, ${}_{j}M_{wp}$ is expressed as

$$ {}_{j}M_{wp} = {}_{w}Z_p \cdot \sigma_y \cdot \beta \quad (3) $$

where ${}_{w}Z_p$ is the plastic section modulus of beam-web, and σ_y the yield point of beam.

${}_{b}M_p$ is expressed as

$$ {}_{b}M_p = Z_p \cdot \sigma_y = ({}_{f}Z_p + {}_{w}Z_p) \cdot \sigma_y \quad (4) $$

and therfore, the following expression to calculate α is obtained from Eqs. (1) to (4), using the yield ratio ($YR = \sigma_y / \sigma_u$).

$$ \alpha = \frac{{}_{j}M_u}{{}_{b}M_p} = \frac{\gamma_f}{YR} \cdot \frac{{}_{f}Z_p}{Z_p} + \beta \cdot \left(1 - \frac{{}_{f}Z_p}{Z_p}\right) \quad (5) $$

According to Navier's assumption, the relation between the moment (M) and the curvature (ϕ) at any section of beam can be found from the stress-strain relation of the steel. Further, the deflection of beams can be calculated by integrating two times along the axis of beam the curvature (ϕ) at respective sections, which conforms to the acting moment (M). As shown in Fig. 7, in the case when

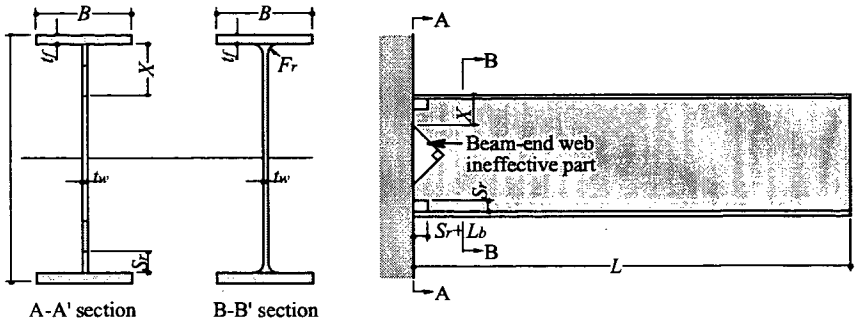


Fig. 8 Cantilever Beam Model Taking into Account the Effective Height of Beam-end Web

the shear force (Q) acts on the cantilever beam-tip without axial force, the beam-end bending moment ($_bM$) and the beam's relative rotation ($_b\theta$) can be found from

$$_bM = Q \cdot L \tag{6}$$

$$\theta_b = \frac{\delta}{L} = \int_0^L \int_0^x \phi \cdot dx \cdot dx = \int_0^L \frac{L-x}{L} \cdot \phi \cdot dx \tag{7}$$

$$\phi = F^{-1}(M) \tag{8}$$

where L indicates the cantilever beam length, and $F(\ )$ the function for the $M-\phi$ relation.

Using the above numerical integral (7), the beam's relative rotation decided by the beam-flange fracture is calculated at the time when the beam-end reaches the maximum bending strength. Meanwhile, it has been confirmed by comparing to the test value that the Q-$_b\theta$ relation of the beam attached to the square tube column can be found by use of the beam model for which the sectional defect, as shown in Fig. 8, is assumed to exist on the beam-end web [2].

4. EXPRESSION TO CALCULATE DEFORMATION CAPACITY LIMITED BY FRACTURE

In the following, a simple expression that can calculate the beam's relative rotation without numerical integral in expression (7) is introduced.

4.1 Basic Expression to Calculate Deformation Capacity of Beams

In this paper, the modified Menegotto-Pinto model proposed in the literature [7], as shown in Fig. 9, is used as the stress-strain (σ-ε) relation of beam.

In the figure, symbol E is the Young's modulus, and R and γ the material constant. Various kinds of models were set for 5 kinds of YR=60, 65, 70, 75 and 80% for 400 N/mm^2 grade steels and 4 kinds of YR=65, 70, 75 and 80% for 490 N/mm^2 grade steels. Material constants of each model is shown in Table1.

Concerning the beam sections, the sections shown in Fig.10 were chosen from among those widely used in the current structural designs, and the M-

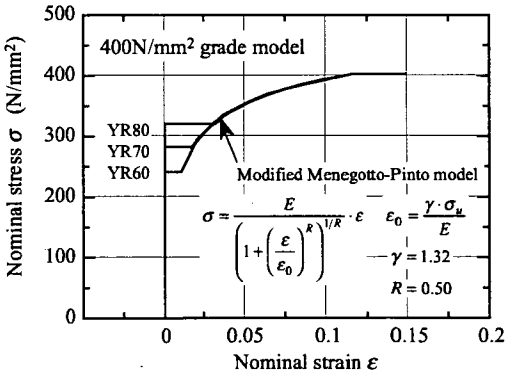


Fig. 9 Stress-Strain Curve Models

Table 1 Assumed Mechanical Properties of Beams

Grade	Yield ratio YR (%)	Yield point σ_y (N/mm^2)	Tensile strength σ_u (N/mm^2)	Uniform Elongation ε_u (%)	Material constant γ	Material constant R
400 N/mm^2	60	240	400	15	1.32	0.50
	65	260				
	70	280				
	75	300				
	80	320				
490 N/mm^2	65	319	490	15	1.26	0.56
	70	343				
	75	368				
	80	392				

ϕ relation of beams was calculated for that sections using the σ-ε relation. The results, which were normalized by the yielding curvature ($\phi_y = 2\varepsilon_y/H = 2\sigma_y/(H \cdot E)$) and ${}_bM_p$, are shown in Fig. 10. Because the M-ϕ relation is nearly same regardless of the beam section, the part of the rise in yield strength due to strain hardening (A-B point in Fig. 11) is approximated using the Ramberg-Osgood function

$$\frac{\phi}{\phi_y} = \frac{M}{{}_bM_p} + a \cdot \left(\frac{M}{{}_bM_p}\right)^b \tag{9}$$

where a and b are the coefficient settled by the yield ratio YR, and as a result of approximation became the value shown in Table 2.

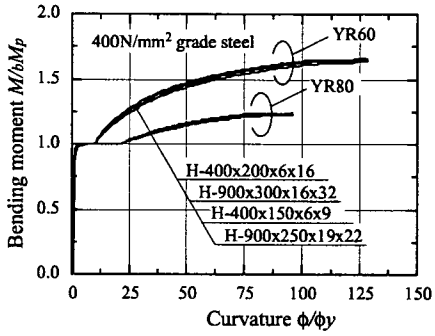


Fig. 10 Bending Moment-Curvature Relation of Beams

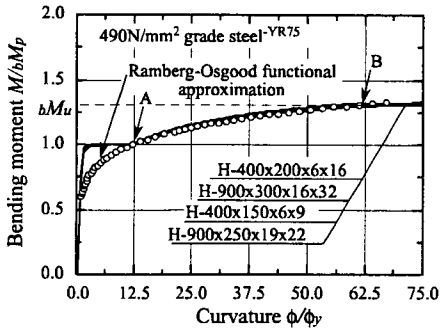


Fig. 11 Mathematical Expression of Bending Moment-Curvature Relation

Table 2 Coefficient of Ramberg-Osgood Function

【400N/mm² grade steel】			【490N/mm² grade steel】		
YR	a	b	YR	a	b
0.60	8.25	5.22	—	—	—
0.65	11.2	5.34	0.65	7.41	5.47
0.70	13.4	5.63	0.70	9.31	5.74
0.75	16.0	6.21	0.75	11.2	6.21
0.80	20.1	6.73	0.80	13.8	6.78

The relative plastic rotation θ_{bp} excluding the elastic deformation from ${}_b\theta$ obtained by Eq. (7), is found from

$$\theta_{bp} = \phi_y \cdot \int_0^L \frac{L-x}{L} \cdot \frac{\phi_p}{\phi_y} \cdot dx \tag{10}$$

where ϕ_p is the plastic element of ϕ.

As shown in Fig. 12, the vertical axis (M-axis) of the M-ϕ relation (in Fig. 11) is squared with the axis of cantilever beam (x-axis in Fig. 12). From the figure, the curvature's plastic element (ϕ_p/ϕ_y) and the plastic region (L_p) are expressed as

$$\frac{\phi_p}{\phi_y} = a \cdot \left(\frac{L-x}{L} \cdot \alpha_1\right)^b \tag{11}$$

$$L_p = L - \frac{L}{\alpha_1} \tag{12}$$

where $\alpha_1 = {}_bM_u/{}_bM_p$, ${}_bM_u$ is the beam's own maximum bending strength.

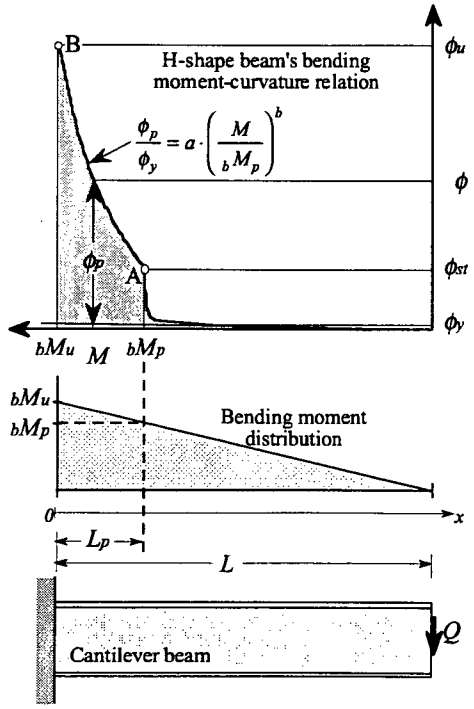


Fig. 12 Cantilever Beam Subjected to Shear Force

When setting the integral range in Eq. (10) up to the range from ${}_bM_p$ to ${}_bM_u$ and substituting Eqs. (12) and (15) for Eq. (10), the expression to calculate the beam's maximum relative plastic rotation (${}_a\theta_{bpm1}$) at the time when the beam-end reaches ${}_bM_u$ is obtained.

$$ {}_a\theta_{bpm1} = \frac{2}{H}\cdot\frac{\sigma_y}{E} \times\int_0^{L_p}\frac{L-x}{L}\cdot a\cdot\left(\frac{L-x}{L}\cdot\alpha_1\right)^b\cdot dx \quad (13) $$

This expression is to indicate the geometrical moment of area around the $M=0$ axis in the section colored pertaining to the M-ϕ relation in Fig.12.

4.2 Expression for Deformation Capacity Limited by Brittle Fracture

Examinations were made on the case in which the brittle fracture occurs at the beam-end before the beam-end reaches the beam's own maximum bending strength (${}_bM_u$). When the full section of the beam web at the beam-end is effective, the ultimate bending moment of beam-end (${}_jM_{u0}$) is expressed by

$$ {}_jM_{u0} = \gamma_f\cdot\sigma_u\cdot{}_fZ_p + \sigma_y\cdot{}_wZ_p \quad (14) $$

In this case, the maximum relative plastic rotation limited by fracture (${}_a\theta_{bpm0}$) can be calculated by replacing ${}_bM_u$ in Fig. 12 with ${}_jM_{u0}$.

$$ {}_a\theta_{bpm0} = \frac{2}{H}\cdot\frac{\sigma_y}{E} \times\int_0^{L_{p0}}\frac{L-x}{L}\cdot a\cdot\left(\frac{L-x}{L}\cdot\alpha_0\right)^b\cdot dx \quad (15) $$

$$ L_{p0} = L - \frac{L}{\alpha_0} \quad (16) $$

$$ \alpha_0 = \frac{{}_jM_{u0}}{{}_bM_p} = \frac{\gamma_f}{YR}\cdot\frac{{}_fZ_p}{Z_p} + \left(1-\frac{{}_fZ_p}{Z_p}\right) \quad (17) $$

4.3 Expression Taking into Account the Lowering of Bending Strength at Beam-end Web

In the case of joining the H-shape beam with the square tube column, the M-ϕ relation in the vicinity of column surface becomes different from the M-ϕ relation in Fig.11. Here, as shown in Fig. 13, it is assumed that as the target sectional area separates from the column, the web section that does not contribute to the bending strength decreases. The figure shows that the M-ϕ relation has changed at the general beam section ($a-a'$ section in the figure) and the beam-end section ($c-c'$), and further at their intermediate section ($b-b'$). In order to calculate the beam's maximum plastic rotation (${}_a\theta_{bpm}$) using the method mentioned above, it is necessary to find the curve that connects the intersection of the x coordinate and the M-ϕ relation at each section (ex. points A, B and C in the figure). Here, if the beam-web bending strength decreases linearly between the points A and C in the figure, ϕ_p is to be expressed as

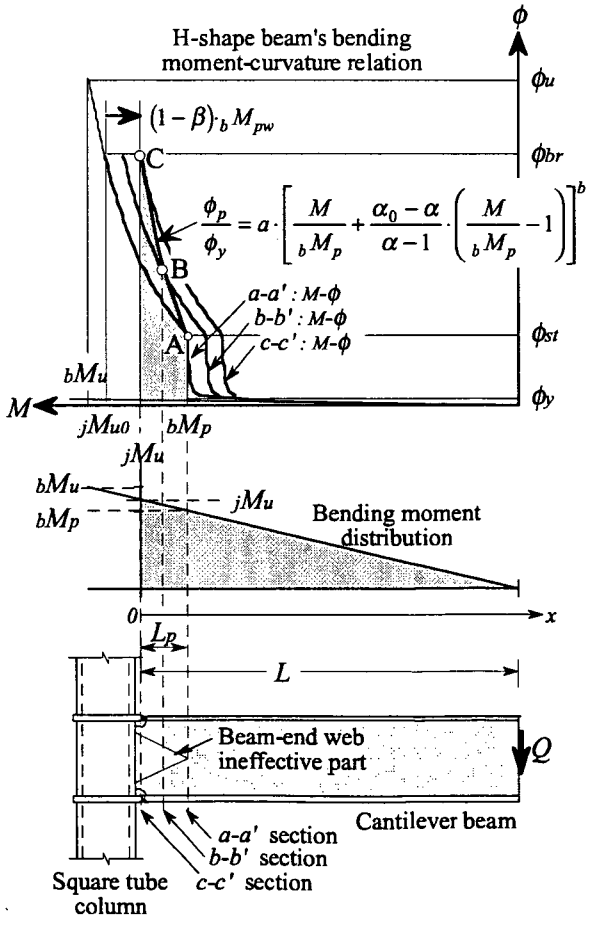


Fig. 13 Cantilever H-shape Beam Joined with Square Tube Column Subjected to Shear Force

$$\frac{\phi_p}{\phi_y} = a \cdot \left[\frac{M}{{}_b M_p} + \frac{\alpha_0 - \alpha}{\alpha - 1} \cdot \left(\frac{M}{{}_b M_p} - 1 \right) \right]^b \qquad (18)$$

where, using α defined by Eq. (5), L_p is given by

$$L_p = L - \frac{L}{\alpha} \qquad (19)$$

With these, the maximum relative plastic rotation of H-shape beam connected to square tube column (${}_a\theta_{bpm}$) can be calculated using the following expression.

$$\begin{aligned} {}_a\theta_{bpm} &= \frac{2}{H} \cdot \frac{\sigma_y}{E} \cdot \int_0^{L_p} \frac{L-x}{L} \cdot a \\ &\times \left[\frac{L-x}{L} \cdot \alpha \cdot \left(1 + \frac{\alpha_0 - \alpha}{\alpha - 1} \right) - \frac{\alpha_0 - \alpha}{\alpha - 1} \right]^b \cdot dx \\ &= \frac{\sigma_y}{E} \cdot \frac{2L}{H} \cdot \frac{a \cdot (\alpha - 1)}{(b+1) \cdot (b+2) \cdot (\alpha_0 - 1)^2 \cdot \alpha^2} \\ &\times \{ \alpha_0{}^{b+1} \cdot [(b+1) \cdot (\alpha_0 - 1) \cdot \alpha + (\alpha_0 - \alpha)] \\ &\quad - [(b+1) \cdot (\alpha_0 - 1) + (\alpha_0 - \alpha)] \} \end{aligned} \qquad (20)$$

5. EFFECTS OF DESIGN FACTORS ON THE DEFORMATION CAPACITY OF BEAM

The numerical calculation was made to investigate the effect of γ_R and γ_f on the deformation capacity of beam limited by beam-end fracture, which is defined by the maximum relative plastic rotation (${}_a\theta_{bpm}$) in this paper. In parallel with this, verification was made of the simple expression to calculate ${}_a\theta_{bpm}$. For the stress-strain relation of steels, the model in Fig. 9 was used. For each combination of square tube columns and H-shape beams shown in the Table 3, $\alpha = {}_j M_u / {}_b M_p$ and ${}_a\theta_{bpm}$ were computed by Eqs. (5) and (7) respectively. The plots in the Figs. 14 to 16 show the calculation results obtained by numaerical integral. It was found from any figure that the increase of ${}_a\theta_{bpm}$ accompanied by the rise in α is clearly indicated and thus α is effective as one of the parameters to evaluate the plastic deformation capacity.

Fig. 14 indicates the effect of the shear span ratio (L/H) at γ_f=1.0. It is clear from the figure that when L/H becomes small, ${}_a\theta_{bpm}$ becomes small. Fig. 15 indicates the effect of γ_R at γ_f=1.0 and L/H=10. Already, the effect of γ_R is included in α at the abscissa. As a result, as γ_R becomes smaller, the calculation results shift to the righter side, and along with this shift ${}_a\theta_{bpm}$ too becomes larger. Further, Fig. 16 indicates the effect of γ_f, in which ${}_a\theta_{bpm}$ significantly lowers at γ_f=0.8. In addition, it is recognized that in the case of high γ_R it has become nearly impossible to expect the plastic deformation capacity.

In Figs. 14 to 16, the calculation results of ${}_a\theta_{bpm}$ by means of the simple expression (20) proposed in this paper are shown using the solid line. The solid lines and the plotted groups show favorable correspondences, thus verifying the validity of the expression.

6. CONCLUSION

This paper shows that the fracture toughness of welded joints is a main factor to affect the occurrence conditions for beam-end brittle fracture and decides the beam-flange fracture strength with certainly restricting the weld detail. Further, the simple design expression based on the beam-flange

Table 3 Sectional Shape/Dimension and Yield Strength/Tensile Strength of Columns and Beams

Calculation target	Square tube column	H-shape beam
BCR295+SN400	Roll-formed square tube (a total of 46 kinds) B-200x6 ~ B-550x22 $_c\sigma_y$=295N/mm²	Rolled H-shape (a total of 212 kinds) H-400x150x6x9 ~ H-900x300x19x32 σ_u=400N/mm², σ_y : set using YR
BCP325+SN490	Press-formed squre tube (a total of 133 kinds) B-300x9 ~ B-1000x40 $_c\sigma_y$=325N/mm²	Rolled H-shape (a total of 212 kinds) H-400x150x6x9 ~ H-900x300x19x32 σ_u=490N/mm², σ_y : set using YR

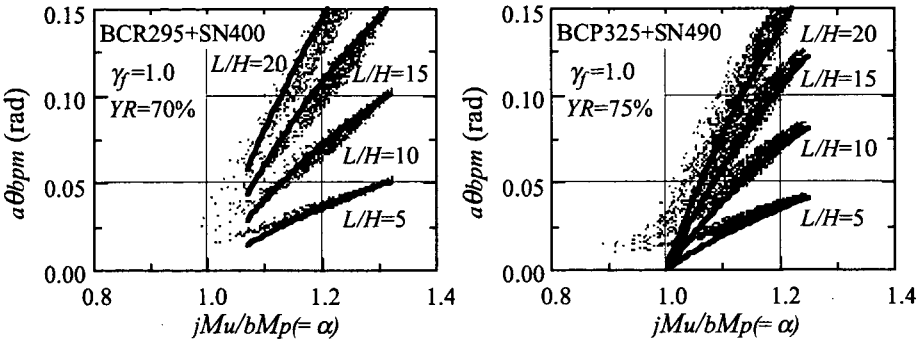


Fig. 14 Effects of Shear Span Ratio on Maximum Plastic Rotation

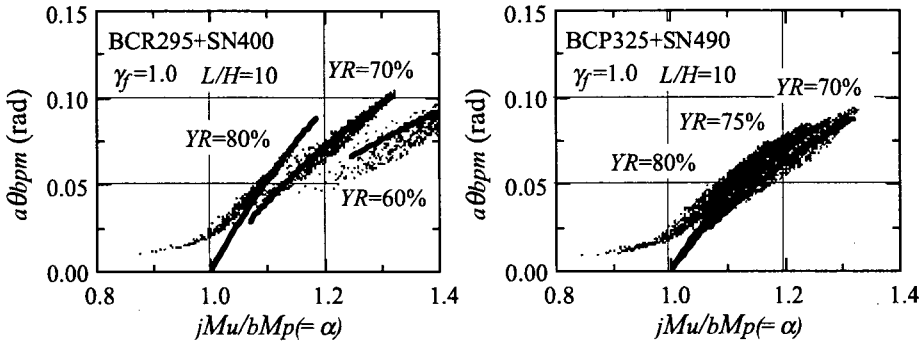


Fig. 15 Effects of Yield Ratio on Maximum Plastic Rotation

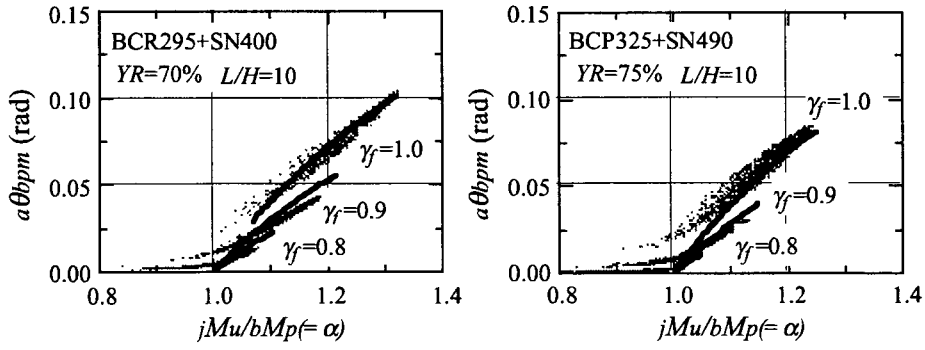


Fig. 16 Effects of Welded Joint Fracture Strength Coefficient on Maximum Plastic Rotation

fracture strength was proposed for calculating the plastic deformation capacity of welded beam-ends limited by brittle fracture. The validity of the expression was also shown.

It has become possible to forecast the rotation demand of beam-end during a severe earthquake using dynamic analysis and so on. Accordingly, it is now possible for structural designers to calculate the rotation of beam-end retained up to the fracture using the approach proposed in this paper and to prevent the brittle fracture that was observed in the Hyogo-ken Nanbu Earthquake by confirming that the retained rotation is larger than the demand.

The use of steels with a low yield ratio for beam is important in order to provide a larger retained rotation than the demand. Further, in order to gain the expected beam-flange fracture strength, it is necessary to select steels and welding wires for

which the fracture toughness of the beam-end welded joint (weld metal, base metal and heat-affected zone) can be secured.

8. REFERENCES

1. Kato, B. and Nakao, M. : Strength and Deformation Capacity of H-shaped Steel Members Governed by Local Buckling, J. Struct. Constr. Eng., AIJ, 1994.
2. Suzuki, T., Ishii, T., Morita, K. and Takanashi, K. : Experimental Study on Fracture Behavior of Welded Beam-to-column Joint with Defects, Steel Construction Engineering, JSSC, 1999.
3. Ishii, T., Kikukawa, S., Morita, K. and Takanashi, K. : Experimental Study on Fracture Behavior of Beam-to-column Connection, Steel Construction Engineering, JSSC, 1999.
4. Azuma, K., Suzuki, T. and Morita, K. : Experimental Study on Fracture Behavior of Built-up H-shaped Beams Connected with Rectangular Hollow Section Columns, Steel Construction Engineering, JSSC, 2000.
5. AIJ : Recommendation for Limit State Design of Steel Structures, 1998.
6. Harada, Y., Morita, K., Yamaguchi, D. and Ishii, T. : Experimental Study on Brittle Fracture in Beam-to-column Connections, Steel Construction Engineering, J. Struct. Constr. Eng., AIJ, 1999.
7. Aoki, H., Kato, B. and Ding, F. : Mechanical Properties of Thick Steel Plates by Blast Furnace and Mathematical Expression for the Stress-strain Diagrams, J. Struct. Constr. Eng., AIJ, 1989.

ACKNOWLEDGEMENTS

The authors' research has been conducted under General Technology Development Project of the Ministry of Construction (currently Ministry of Land, Infrastructure and Transport) entitled Development of Structural Safety Improvement Technology Utilizing New Generation Steel. The authors wish to express their sincere gratitude to all researchers involved in the Project.

APPENDIX

TASK COMMITTEE REPORTS

Report of Task Committee A
GEOTECHNICAL ENGINEERING AND GROUND MOTION

Date: 12 May 2003

Place: National Institute for Land and Infrastructure Management, Tsukuba, Japan

Attendees:	U.S. Side --	Mehmet Celebi (Chair)	USGS
		Jon Ake	USGS
		Donald Yule	CORPS
	Japan Side --	Osamu Matsuo (Chair)	NILIM
		Takahiro Sugano (Chair)	PARI
		Izuru Okawa	BRI
		Mitsu Okamura	PWRI

1. Objective and Scope of Work

The objectives of work include:
(1) To promote sharing of strong motion earthquake data among researchers and practicing engineers, and enhance the availability of technology for evaluating the destructive effects of earthquake motion, and
(2) To promote research on the dynamic behavior of soils, foundations and earth structures during earthquakes.

The scope of work includes:
(1) Exchange strong motion data regularly and identify significant issues.
(2) Exchange information on technological developments, state-of-the-art and practice related to strong motion recording, hazard mapping, soil-structure interaction, soil behavior and stability during earthquakes,
(3) Exchange field data related to geotechnical engineering, and
(4) Plan and conduct programs of cooperative research and/or workshops in coordination with the proposed or ongoing programs.

2. Accomplishments

(1) The task committee held "The Sixth U.S.-Japan Workshop on Geotechnical Earthquake Engineering" with a subtitle "U.S.-Japan Symposium on Seismic Performance of Urban, Reclaimed and Port Area - Full Scale Experiment at Tokachi Port", in conjunction with Port and Airport Research Institute and University of California, San Diego, at San Diego on 27-28th February, 2003.
(2) The Task Committee members continued the following cooperative research projects:
   a) Physical and Numerical Simulation of Structural Damages Due to Liquefaction and Development of Countermeasure Techniques, 1994-2004, by the National Research Institute for Earth Science and Disaster Prevention (NIED), Building Research Institute (BRI) and Wayne State University (WSU), and
   b) Application of the Nuclear Magnetic Resonance Imaging (NMRI) Method to the Study of Soil Behavior and Stability During Earthquakes, by Port and Airport Research Institute (PARI) and Colorado School of Mines and the New Mexico Resonance (Non-profit organization).

3. Future Plans

The future plans include:
(1) Plan the 3rd US-Japan Workshop on Soil-Structure Interaction for 2004. Responsible members will be

Dr. Celebi of USGS and Dr. Okawa of BRI.

(2) Plan a workshop on Real-Time Instrumentation of Densely Urbanized Areas and Instrumentation of Civil Engineered Structures. Temporary committee will include Dr. Fujiwara of NIED, Dr. Okawa of BRI, Mr. Kusakabe of NILIM, Dr. Borcherdt, Dr. Wald and Dr. Celebi of USGS. The committee will explore cooperation with Panel on Earthquake Research.

(3) Continue the cooperative research "Physical and Numerical Simulation of Structural Damages Due to Liquefaction and Development of Countermeasure Techniques, 1994-2004", by the National Research Institute for Earth Science and Disaster Prevention (NIED), Building Research Institute (BRI) and Wayne State University (WSU).

(4) Explore the possibility of joint research and/or workshop on site response issues. The responsible members will be Mr. Matsuo of NILIM and Dr. Borcherdt of USGS.

4. Related Activities

(1) The College of Engineering, University of California at Davis and the Public Works Research Institute made the Specific Working Agreement in the area of geotechnical earthquake engineering. Responsible coordinators are Keiichi Tamura, PWRI and Bruce Kutter, UC Davis.

(2) The US members, J. Ake, M. Celebi and D. Yule provided information on a new organization founded in the United States-Consortium of Organization for Strong Motion Observation Systems (COSMOS). This new organization promotes enhancement of strong motion networks and databases. A virtual database (www.cosmos-eq.data.org) is established and is being maintained at UC, Santa Barbara. COSMOS requests the organizations in Japan that operate strong motion networks and maintain databases to join COSMOS. Japan side will provide a list of possible Japanese organizations for COSMOS organization to contact with.

Report of Task Committee B
NEXT-GENERATION BUILDING AND INFRASTRUCTURE SYSTEMS

Date: 12 May 2003

Place: National Institute for Land and Infrastructure Management, Tsukuba, Japan

Attendees:			
	U.S. Side --	Steven McCabe (Chair)	NSF
		K. Thirumalai	DOT
		Gary Dargush	SUNY
	Japan Side --	Masaomi Teshigawara (Chair)	BRI
		Keiichi Ohtani (Chair)	NIED
		Takashi Kaminosono	NILIM
		Isao Nishiyama	BRI
		Hiroshi Fukuyama	BRI

1. Objective and Scope of Work

(1) Objective
The objective of the task committee is to enhance the development and implementation of innovative and new 1) materials; 2) enabling technologies; 3) evaluation, analysis, design, construction and maintenance methods; through cooperative individual and organized and networked analytical and experimental approaches for the next-generation building and infrastructure systems.

Opportunities during the next few years include experimental observations on the performance of model and near full-size structures using large scale testing facilities and networked earthquake engineering experimental facilities, and the development of innovative technologies and approaches to address the newly obtained analytical conclusions and observed experimental evidences and to formulate various performance based engineering guidelines for building and infrastructure systems.

(2) Scope of Work
a) Enhancement of exchange of information and personnel.
b) Coordinate joint research including the utilizing experimental facilities.
c) Coordinated development of database, test procedures, guidelines for test result interpretation and application.
d) Development of new materials and technologies for condition assessment, retrofit of existing buildings and design of new buildings.
e) Conduct joint workshops and joint meetings to identify research opportunities, new projects, and make recommendation for UJNR Panel.

2. Accomplishments

(1) A new US-side task committee B was established, with George Lee and Steven McCabe as co-chairs and six members (Fu-Kuo Chang of Stanford University; Peter Chang of University of Maryland; Mete Sozen of Purdue University; B.F. Spencer of University of Illinois at Champaign-Urbana, K. Thirumalai of Department of Transportation and Ming Wang of University of Illinois at Chicago).
(2) The Third Joint Technical Coordinating Committee (JTCC) Meeting of the U.S.-Japan Cooperative Research Program on Smart Structural Systems (Auto adaptive Media Applied to Civil Infrastructures) was held at the Building Research Institute (BRI) in Tsukuba, Ibaraki, Japan on October 19, 2002. Fifteen U.S. and ten Japanese JTCC members, plus 22 observers participated in the meeting.
(3) The construction of buildings for E-Defense (3-D Full-scale Earthquake Testing Facility) is almost

completed (95%).

(4) Construction of the NEES sites is progressing; the system will be operational on October 1, 2004. The NEES Consortium has been officially established as of late January 2003.

3. Future Plans

(1) Task Committee B will continue to support the development of joint activities relative to NEES (Network of Earthquake Engineering Simulation).

(2) Task Committee B will continue to plan for the establishment of a US-Japan Coordinated research plan to accelerate the NEES program in the US and E-Defense and other research equipments in Japan for performance-based design, focusing on building functions, and health monitoring.

(3) Task Committee B will recommend an establishment of a US-Japan planning committee to make a long-term US-Japan cooperative research program, in which cooperation between U.S. and Japan within NEES, E-Defense and other research equipments is essential. Professor M. Sozen is nominated as a coordinator for the US-side and Building Research Institute will act as a Japan-side coordinating Institute. It will be proposed that the first workshop should be held by the beginning of October 2003.

(4) Task Committee B will support the activity of new task committee F (ADVANCED INFORMATION AND COMMUNICATION TECHNOLOGY FOR DISASTER PREVENTION AND PUBLIC HEALTH EVALUATION) through cooperative activities that are common to both task committees.

4. Others

AIJ has decided to honor Dr. S. C. Liu with "The Appreciation Prize of Architectural Institute of Japan, 2003", which is the special prize for non-members who have given an excellent contribution to the architecture. His achievement is laying the foundation for and support of pioneering research cooperation between the U.S. and Japan in the broad area of Earthquake Disaster Mitigation over two decades, that is supported by UJNR.

Report of Task Committee C
DAMS

Date: 12 May 2003

Place: National Institute for Land and Infrastructure Management, Tsukuba, Japan

Attendees:	U.S. Side --	Enrique Matheu (Chair)	LSU
		Anjana Chudgar	USACE
		Jon Ake	USBR
		Donald Yule	USACE-ERDC
	Japan Side --	Yoshikazu Yamaguchi (Chair)	PWRI
		Akira Nakamura	NILIM
		Isao Nagayama	PWRI
		Takashi Sasaki	PWRI
		Hiroyuki Satoh	PWRI
		Ken-ichi Kanenawa	PWRI

1. Objective and Scope of Work

To develop technical insights into better understanding of the response of dams to seismic effects, the T/C will plan, promote, and develop research initiatives to assist in assuring seismic safety and economical protective countermeasures against earthquake loading for these critical structures.

The scope of work includes:

(1) Develop methods of analysis for seismic design of dams including outlet works.
   a) Comparative analysis of design methods and evaluation criteria used by U.S. and Japan.
   b) Development of "Design Earthquake Ground Motions" for analysis and evaluation of dams.
   c) Assessment of models and numerical procedures used for seismic dynamic analysis.

(2) Perform research to better understand the dynamic characteristics of dam construction materials and site conditions.
   a) Strength and deformation characteristics of concrete, soil and rock materials during earthquakes.

(3) Evaluate observed performance of dams and outlet works during earthquakes.
   a) Develop a database that contains measured ground accelerations and dynamic response of dams and outlet works during earthquakes, and other related information necessary to evaluate their seismic behavior, such as experimental and/or analytical data with description of test and analysis procedures used.
   b) Investigation of damage mechanisms due to earthquake loading.
   c) Application of the analysis of the observed dynamic behavior to the improvement of design criteria.

2. Accomplishments

(1) The Task Committee developed a database that contains measured ground accelerations and dynamic response of dams and outlet works during earthquakes. The database has been expanded to include other relevant information necessary to evaluate their seismic behavior, such as experimental and/or analytical data with description of test and analysis procedures used. Additional analysis modules have been implemented to facilitate processing of field test data.

(2) The Task Committee held the "***3rd U.S.-Japan Workshop on Advanced Research on Earthquake Engineering for Dams***", in San Diego, USA, on June 22-23, 2002. The workshop was part of the pre-conference activities of the ***22nd USSD (U.S. Society on Dams) Annual Meeting and Conference***,

held at the same location on June 24-28, 2002. The workshop proceedings have been completed and they will be distributed in electronic and hardcopy formats by July 2003.

3. Future Plans

(1) The Task Committee will continue the current efforts focused on the development of improved mechanisms to facilitate the continuous exchange of results of research activities and general technical information related to dam earthquake engineering.

(2) The Task Committee will coordinate exchange visits of scientists and engineers from the U.S. and Japan. A series of case histories of mutual interest will be identified and prioritized and they will serve as the focus for this exchange program.

(3) The Task Committee will promote the development of joint research programs. The following topics have been identified as areas for future collaborative research:

a) *Non-linear stress analysis of concrete dams:*
The Task Committee will take advantage of the recent advances in this area achieved by the Japan side. The Task Committee will share the available analytical results, as well as experimental data collected during the shake table testing of a 1/20-scale model of a gravity dam conducted by the U.S. side.

b) *Global stability analysis of concrete dams:*
The Task Committee will conduct a review of the minimum requirements for sliding and overturning stability currently in use in the U.S. and Japan. The Task Committee recognizes the importance of this collaborative effort, as the corresponding guidelines will be subject to revision and update both in the U.S. and Japan.

c) *Criteria for seismic analysis progression:*
The Task Committee will review and compare the state of practice in the U.S. and Japan regarding current recommendations for progression of seismic analysis based on stages of increasing complexity.

d) *Seismic evaluation of embankment dams:*
The Task Committee will review criteria and guidelines for post-earthquake stability and deformation analysis of embankment dams.

The activities corresponding to the four areas indicated above will be addressed sequentially and the corresponding schedule will depend on the progress of the corresponding guidance documents, some of which are currently under discussion, development and/or review in the U.S. and Japan.

(4) The results of the joint research activities mentioned above will be reported as a series of joint papers to be submitted for presentation at recognized international conferences such as the ***WCEE (World Conference on Earthquake Engineering)***.

(5) Following large earthquakes in the US or Japan, the Task Committee will assemble a reconnaissance team to investigate the performance of dams and outlet works.

(6) The Task Committee will hold the "***4th U.S.-Japan Workshop on Advanced Research on Earthquake Engineering for Dams***" in the year 2004 in Japan. Specific location and time of the Workshop will be determined through correspondence between the Chairs of the Task Committee on Dams of the UJNR Panel on Wind and Seismic Effects.

Report of Task Committee D
WIND ENGINEERING

Date: 12 May 2003

Place: National Institute for Land and Infrastructure Management, Tsukuba, Japan

Attendees:			
	U.S. Side --	Nicholas Jones (Chair)	University of Illinois
		Noel Raufaste	NIST
	Japan Side --	Hisashi Okada (Chair)	BRI
		Jun Murakoshi (Chair)	PWRI
		Yukio Takemura	MRI
		Yasuo Okuda	BRI
		Koichiro Fumoto	PWRI
		Hitomitsu Kikitsu	BRI

1. Objective and Scope of Work

To exchange technical information and to jointly plan, promote, and foster research and dissemination, to improve understanding of wind and its effects on structures, establish more rational wind resistant design procedures for structures, and to contribute synergistically to wind hazard mitigation. Specific objectives for the Task Committee include:

(1) Facilitate collaborative research and cooperation between U.S. and Japanese researchers in the wind engineering.
(2) Identify success in wind engineering and wind hazard mitigation.
(3) Identify research needs in wind hazard mitigation, including development of new technology, basic and applied research in wind and structural engineering, and in social and economic impacts of wind hazards.

The scope of the US-Japan collaboration includes:

(1) Characterization of strong wind, especially boundary layer extreme winds.
(2) The study of wind effects including wind loading on and wind-induced response of structures.
(3) Performance of experimental and analytical research to predict wind effects.
(4) Performance of damage surveys, and wind hazard and risk assessments.
(5) Development of new technologies for wind hazard mitigation.

2. Accomplishments

The 3rd US-Japan Workshop was held in Seattle, 2-5 October 2002. The workshop emphasized development of data and information on wind characteristics, hazards, and effects on buildings and bridges and evolving technologies to serve as a technical basis to revise US and Japan wind standards/codes. 25 technical papers were presented in the workshop.

3. Future Plans

(1) As a follow-up to the workshop on "Reducing Losses from Wind: Collaborative Opportunities for the 21st Century." (third U.S.-Japan Workshop) held in Seattle, U.S. in October 2002, a future meeting is being planned for Japan in 2005.
(2) Pursue collaborative research on the following topics
    a) Wind characteristics and wind hazard mitigation
        i) Wind characteristics in complex terrain
        ii) Validation of wind models with full-scale data (joint field studies)

iii) Cooperative quick-response post-storm damage assessments

b) Wind effects on buildings
   i) Development of reliable and consistent aerodynamic loads for performance-based structural design
   ii) Comparison of wind tunnel data sets and CFD results to full-scale measurements

c) Wind effects on bridges
   i) Benchmark study on flutter derivatives
   ii) Prediction and mitigation of wind-induced vibration of stay cables
   iii) Full-scale measurements

d) Evolving Technologies
   i) Next generation wind tunnels: Improvement of methods to simulate non-stationary wind (straight-line, tornado and microburst)
   ii) Structural control

(3) Exchange technical information on the following topics
   a) Wind characteristics and wind hazards
   b) Wind pressures, loadings and dynamic characteristics of buildings
   c) Wind-induced response of flexible, cable-suspended bridges and their components
   d) Prediction and mitigation techniques for wind effects

(4) Prospective technical collaboration on several researches
   a) Distribution of airborne chemical and biological agents
   b) Development of a distribution model for volcanic gas

(5) Collaboration with fire engineering researchers by making use of unique facilities: Fire Research Wind Tunnel and Wind and Rain Test Laboratory

Task Committee F Charter

1. Name of Task Committee

Advanced Information and Communication Technology for Disaster Prevention and Public Health Evaluation

2. Lead Agency and Task Committee Chairmen

US-side :	William Roper	GWU
	Josephine Malilay	CDC
Japan-side :	Akihiko Nunomura	Cabinet Office
	Takaaki Kusakabe	NILIM

3. Participating Agencies and their Representatives

US-side :	Andrew Bruzewicz	USACE
	Jennifer Mesienberger	NIMA
	Rick Olsen	ERDC
	Daniel Shnyder	USGS
	Kim Shoaf	UCLA
	K. Thirumalai	DOT/RSPA
Japan-side :	Hiromichi Maruyama	GSI
	Osamu Matsuo	NILIM
	Hiroaki Miyatake	Cabinet Office
	Takaaki Ohyama	NIID

4. Function of Task Committee

1) Purpose

The purpose is to support and enhance application of advanced information technologies to emergency management and response operations by providing a decision support system for disaster/hazard preparedness. Advanced remote sensing technologies are enabling science and technology for: weather, climate, land classification, change detection and natural and technological disasters and to assess exposure to public health threats. Such technologies provide disaster management tools for community preparedness. Timely emergency management decision-making demands accurate and timely data detection, assemblage, analysis, interpretation, and dissemination of information about natural and technological disasters. To meet this need, it is necessary to use advanced information and communication systems including remote sensing technologies.

2) Scope of Work

1. Plan and conduct Task Committee workshops and joint meetings to identify state-of-the-art for advanced disaster information techniques such as the components of data integration and identify public health issues following wind and seismic events.
2. Exchange information related to rapid assessment of infrastructure change and condition assessment methods and processes that will assist emergency decision makers during the multiple stages of an emergency.
3. Exchange information related to public health assessments to be better prepared

immediately following a disaster to know the status of affected populations during emergencies e.g., adverse health and environmental conditions, medical supplies, equipment, and personnel for immediate and delayed response.

4. Exchange information on technological development, and state-of-the-art and practice, identify research topics, and develop joint research programs.
5. Exchange information related to rescue, recovery and rehabilitation of lives as a result of disasters.
6. Encourage exchanges of guest researchers between institutions of the US and Japan and the sharing of research findings, publications, and recommended practice.

3) Future Plan of Cooperative Activities

The Task Committee members will identify relevant topics for exchange of research findings and discuss near term cooperative research in the following technology topics:

1. Technology for Gathering and Analyzing Information:
   - Remote sensing technologies: geospatial intelligence (analysis of imagery and geospatial information through data fusion).
   - Monitoring technologies: Multispectral, Hyperspectral, RADAR/SAR, Thermal, Atmospheric and Surface LIDAR, Microwave and RADAR and others,
2. Technologies for transferring information:
   - Satellite telecommunication, cell phone and hand-held computer, fiber optics, Monitoring Camera.
3. Technology for sharing and providing information:
   - GIS, Internet systems, database, mobile communication tools
   - Surveys and GPS referred airborne video imagery to determine the scope and magnitude of the disaster impact on the community to determine appropriate actions.
4. Technology to assess the characteristics of the environment for projecting mortality, disease, injury, and amount of damage on public health infrastructure.

Report of Task Committee F
ADVANCED INFORMATION AND COMMUNICATION TECHNOLOGY FOR DISASTER PREVENTION AND PUBLIC HEALTH EVALUATION

Date: 12 May 2003

Place: National Institute for Land and Infrastructure Management, Tsukuba, Japan

Attendees:			
	U.S. Side --	William Roper (Chair)	GWU
		Josephine Malilay (Chair)	CDC
		K. Thirumalai	DOT
	Japan Side --	Takaaki Kusakabe (Chair)	NILIM
		Hiroaki Miyatake	CO
		Akihiro Sanada	NILIM

1. Objective and Scope of Work

(1) Objective
The objective is to support and enhance application of advanced information technologies to emergency management, response operations, and public health evaluation. Timely emergency management decision-making demands accurate and timely data detection, assemblage, analysis and interpretation, and dissemination about natural and technological disasters. To meet this need, it is necessary to use advanced information & communication technologies including remote sensing technology.

(2) Scope of Work
a) Plan and conduct Task Committee workshop and joint meetings to identify state-of-the-art for advanced disaster information techniques and public health issues following wind and seismic events,
b) Exchange information related to rapid assessment of infrastructure change and condition assessment methods and processes that will assist emergency decision makers during multiple stages of an emergency,
c) Exchange information related to public health assessments to be better prepared immediately following a disaster to know the status of affected populations during emergencies,
d) Exchange information on technological developments, state-of-the-art technology, and their practice, identify research topics and develop joint research programs,
e) Exchange information related to rescue, recovery and rehabilitation of lives as a result of disasters.
f) Encourage exchange of guest researchers between institutions of the U.S. and Japanese and sharing of research findings, publications, and recommended practice.

2. Accomplishments

(1) Two Japanese researchers visited George Washington University in February 2003 to exchange information between US and Japan. The first draft of T/C-F charter was formulated upon this activity.
(2) Following the Resolutions of the 34th Joint Meeting, the Task Committee F charter was developed and submitted for approval of the Joint Meeting. The Task Committee F involves the Theme F and the Theme I which are a listed in "3.2 Task Committee Charters and Recommended Committee", in the Strategic Plan.

3. Future Plans

(1) A Japanese visiting researcher will stay at George Washington University for approximately one year from September 2003.
(2) The Task Committee will plan a workshop on "Utilization of IT for Crisis Management and Disaster

Mitigation (Tentative)". This workshop is scheduled in May 2004.

(3) The Task Committee will continue to exchange research findings and to develop future cooperative research topics in the following technologies:

a) Technology for gathering and analyzing information
b) Technology for transferring information
c) Technology for sharing and providing information
c) Technology to assess the characteristics of the environment for projecting mortality, disease, injury, and the amount of damage on public health infrastructure

(4) The Task Committee will undertake collaboration with Task Committee G on health monitoring of transportation infrastructure.

Report of Task Committee G
TRANSPORTATION SYSTEMS

Date: 12 May 2003

Place: National Institute for Land and Infrastructure Management, Tsukuba, Japan

Attendees:			
	U.S. Side --	W. Phillip Yen (Chair)	FHWA
		David Sanders	UNR
		K. Thirumalai	DOT
	Japan Side --	Hiroshi Sato (Chair)	PWRI
		Kenichi Tokida	PWRI
		Jiro Fukui	PWRI
		Shigeki Unjoh	PWRI
		Masuo Kondo	PWRI
		Junichi Hoshikuma	PWRI

1. Objective and Scope of Work

The objectives of work include:

(1) To plan, promote and foster research on the behavior of transportation facilities when subjected to wind and seismic forces, and

(2) To disseminate research results and provide specifications and guidelines based on the Task Committee's findings.

The scope of work includes:

(1) To investigate existing and new bridges design, the behavior of whole bridge systems and/or single component of a bridge without limitation on their size and function, and

(2) To investigate offshore, coastal and airport facilities' behavior during earthquake.

2. Accomplishments

(1) The US-Japan cooperative research project in Seismic Performance Testing Guideline for Bridge Piers has completed first draft report for both sides. The first panel meeting of this project for the US side was conducted during 28 - 30 August, 2002 in San Francisco. Three Japanese Delegation (Prof. Kawashima, Dr. Hoshikuma and Mr. Nishida) participated in this panel meeting and provided very valuable comments.

(2) The 18th U.S. - Japan Bridge Engineering Workshop was held during 22 - 24 October 2002, at St. Louis, U.S. 25 U.S. and 23 Japanese participants attended the workshop. 37 technical papers were presented and discussed on the following main topics: a) seismic technology and b) bridge management technology. The proceedings of the Workshop was published and distributed by the U.S.-side in January 2003.

(3) Mr. Arata Hiromatsu (NILIM) visited the FHWA on 15 - 18 January 2003, to discuss the state of bridge management with Mr. James Cooper and Mr. Raymond McCormick, and he visited the laboratories of the Turner - Fairbank Highway Research Center.

(4) Dr. Ahmad Itani (University of Nevada, Reno) was invited to the PWRI during 2 - 23 March 2003, to discuss earthquake protective systems for long-span bridge structures.

3. Future Plans

(1) The 19th U.S. - Japan Bridge Engineering Workshop will be held in 27-29 October 2003 in Tsukuba, Japan. The main topics will be a) seismic technology and b) technologies to extend bridge life.

Specific program, and itinerary will be proposed by the Japan-side Task Committee G with the concurrence of the U.S.-side Task Committee.

(2) Conduct the following cooperative research:

a) Seismic Performance Testing of Bridge Structures. This program is to establish Guidelines for seismic performance testing of bridge structures. The objective of this program is to establish Uniform National Guidelines for Testing Bridge Components, which will increase comparability of test results and reduce the duplication of similar testing. On 26-27 June 2003, the US side will hold the second panel meeting in LA to finalize the US side guidelines. In 2003, FHWA and PWRI will meet to develop draft common Guidelines for the experimental methods.

(3) Following a devastating earthquake or hurricane (typhoon) in the U.S. or Japan, the committee will form a joint reconnaissance team to investigate the performance of transportation systems.

(4) Exchange technical information on the following topics:

a) Seismic design and retrofit of highway bridges including the development of seismic response modification devices, smart materials such as SMA, seismic retrofit for long-span bridges, and the development of damage evaluation methods using sensor systems.

b) Seismic and aerodynamic response of long-span bridges including suspension and cable stayed bridges, with emphasis on behavior of composite materials, cable inspection, vibration control, and corrosion protection.

(5) Encourage coordinated research on the following topics:

a) Bridge design methodologies which enhance performance based design concepts, limit state design concepts and life cycle cost analyses.

b) Modeling of seismic isolator and the seismic isolation design methods.

c) System identification techniques, non-destructive evaluation of bridge structures, use and performance of structural materials including new materials, and performance of jointless bridges.

d) Bridge response due to near fault effects.

e) Bridge foundation performance-based design methods.

f) Post-earthquake damage evaluation methods for seismic retrofitted bridges.

g) Remote sensing technologies for bridge health analysis.

TECHNICAL SITE VISITS

HIGHLIGHTS OF TECHNICAL SITE VISITS

The delegation visited seven technical sites during 15-17 May 2003.

1. Tsukuba Express Train Construction Project

A new express railway is being constructed from Tokyo (Akihabara) to Tsukuba by the Japan Railway Construction (Public) Corporation (JRCC) called the Tsukuba Express Joban Shin-sen Line. The 58.3 km line has 20 stations, and will allow 6-car trains to traverse the line at speeds of up to 130 km/hr in 45 minutes. The route was designed to provide a significant number of connections with the Japan Rail (JR) and other train and subway lines. The new line is expected to go into service in Fall, 2005, with an anticipated usage of 280,000 passengers per day (22,000 passing through the Tsukuba Station, the northeastern terminus station). The system is designed for future expansion to eight-car trains, and to operate at higher speeds.

The purpose of constructing this express line is to: enhance the transportation system between Tokyo and Tsukuba (Japan's Science City) and this region in Tokyo's northeastern metropolitan area; reduce the congestion of other rail lines; and encourage construction of industrial and residential infrastructure within this metropolitan/rural area.

The total project cost is expected to be 940 B yen ($8 B). Financing was provided through a combination of public (local, regional, and national governments) and private sources to the JRCC. When operational, the line will repay the investors over a (planned) 40-year period. Major construction is almost complete over most sections of the line, and test trains are running over a portion of track near the main vehicle depot.

The line consists of elevated and underground portions for much of its length. Elevated sections are generally 4-unit precast girders, or arch-slab concrete structures. Tunneling in the Tsukuba area featured the use of "super adjacent" parallel shield tunnels. These tunnels are at some locations separated by only 300 mm at mid-height.



Figure 1. Delegation at the Tsukuba Underground Station

Eight of the stations are underground, including the Tsukuba Station. This station, along with others on the line, exhibits state-of-the-art features including better accessibility for persons with disability, and 1.3 m high walls that separate the riders from the arriving trains. The station has a maximum depth of 20 m below the surface (at Akihabara the depth is 40 m) and features for aesthetic purposes an open plaza area of dimension 19 m x 50 m at one end. Underground tunnels were formed with 7.3 m diameter shield tunnel boring machines and at the Tsukuba Station they cut at the rate of 3 cm/min.

2. Seismic Isolated Building, Kawasaki City

Taisei Corporation, Japan designed and constructed this high-rise residential building. The material used was high-strength concrete with strength of 100 N/mm^2. The building, features a 41-story 135 m tall reinforced concrete tower with plan dimensions of approximately 40 m x 33 m, is supported by a combination of rubber and sliding bearings. This currently represents the tallest base isolated building in the world. The combined use of both rubber and sliding seismic isolation devices also represents a unique feature.

The isolators are placed between an underground parking garage and the 41-story superstructure. A total of 10-1.35 m diameter flat sliding isolators are used beneath the central columns, while 26-1.5 m diameter rubber isolators are positioned under the peripheral columns (see Fig. 2). Each isolator carries about 2 300 tons of weight. The flat sliding bearings are designed for 50 cm displacement; expect only 36 cm displacement during a major earthquake. The superstructure consists of precast beams and columns, with the beam-column connections completed on-site.

Based upon analysis performed by Taisei Corporation, the fundamental natural period of the structure is 3.5 s. The period elongates to approximately 6.5 s for the post-sliding condition. As a result, the relative displacement response of the superstructure is reduced by approximately 30 % to 40 % with the addition of the seismic isolators under design level earthquake ground motions. The corresponding maximum displacement at the isolators is approximately 35 cm. However, the devices are designed for translations of 50 cm with a design life of 100 years. Unfortunately, there is reportedly no instrumentation to record the actual response of the structure.

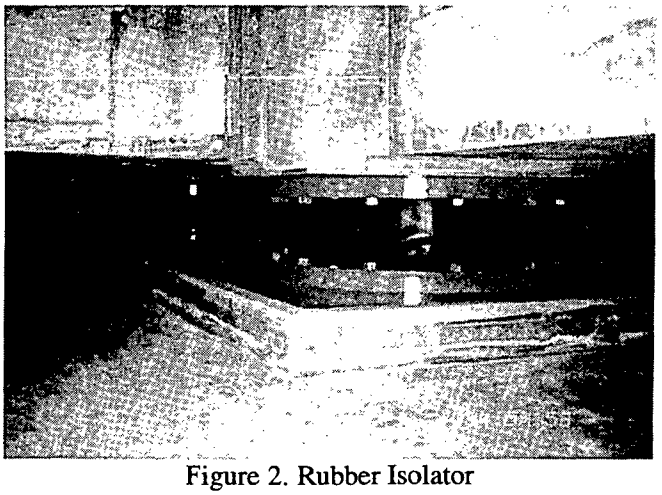


Figure 2. Rubber Isolator

3. Muroran Institute of Technology (MIT), Hokkaido

Muroran Institute of Technology (MIT), Muroran is in the southwestern part of Japan's northern most island of Hokkaido. MIT was founded in 1949 (by consolidating two schools founded in 1887 and 1939) and is one of five National Institutes of Technology in Japan. There are approximately 3,400 students including 550 graduate students at the Institute within six departments:

- Civil Engineering and Architecture,
- Mechanical Systems Engineering,
- Computer Science and Systems Engineering,
- Electrical and Electronic Engineering,
- Materials Science and Engineering, and
- Applied Chemistry.

The delegation was hosted by Professor Norimitsu Kishi, Head of the Department of Civil Engineering and Architecture (see Fig. 3). Professor Kishi's research includes: the development of impact resistant reinforced concrete members, seismic retrofitting and upgrading of steel and reinforced concrete members using FRP sheets and development of the limit state design method for frames. Facilities in the Department's Structural Division include hydraulic and screw jacks with capacities of 500 kN and 300 kN respectively and specimen capacity of 2.5 m x 1 m x 7 m in length. In addition to posters highlighting the Department's research, Professor Kishi conducted a test on a steel pipe column that was wrapped with an aramid fiber reinforced plastic sheet (see Fig. 4). A constant axial load was applied followed by a cyclic lateral load. The purpose of the test was to determine if the aramid fiber sheets are effective in increasing the strength and ductility of the steel pipe columns. Depending upon the number of sheets applied, the strength can be increased by 30 % and the displacement ductility level from 3.9 to 5.9.

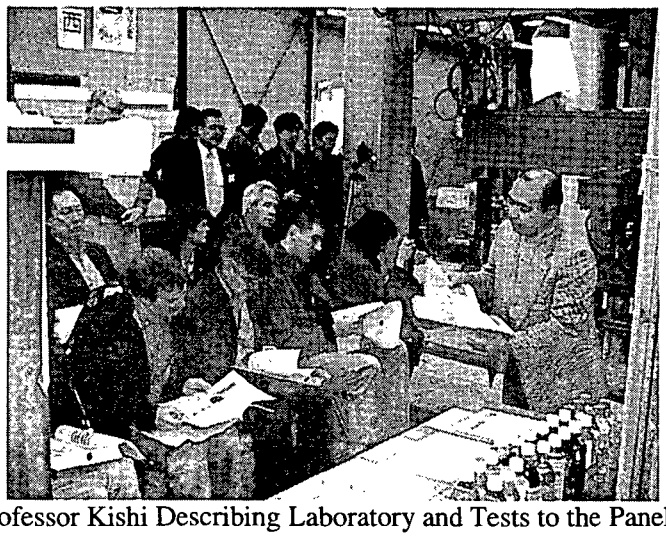


Figure 3. Professor Kishi Describing Laboratory and Tests to the Panel Delegation

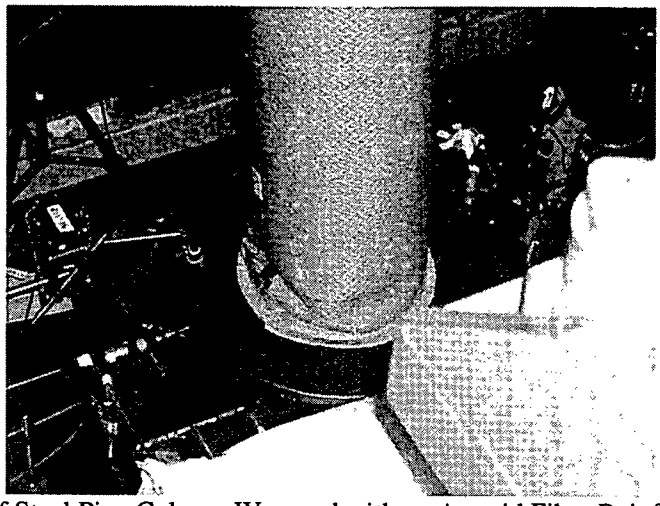


Figure 4. Failure of Steel Pipe Column Wrapped with an Aramid Fiber Reinforced Plastic Sheet

4. New Muroran Highway, Muroran, Hokkaido – Weather Resistant Steel

The delegation transited the New Muroran Highway, Muroran, Hokkaido, Japan then inspected the weather resistant steel used in the superstructure in parts of the elevated highway section. The highway was constructed in 1975. This 27-year old urban four lane divided highway is 8.23 km with a 600 m tunnel section and 4.18 km of elevated sections restricted to vehicular traffic. The highway design speed is 60 km/hr.

The environmental conditions in this marine coastal city of high humidity and salts provide a challenging environment for maintaining exposed corrosive steel members. Also, considering this region's significant winters, maintaining an ice-free driving surface on elevated sections cause addition corrosive conditions, especially, when road salt is used. The designers of this highway decided to use steel beams in selected sections with a new surface treatment developed in Japan between eight of the pier sections. A total of 7 800 tons of this surface treated weather resistant steel was used.

The section visited was selected because it was the poorest performing section yet it was remarkably free of corrosion damage especially considering the extremely corrosive environment and the length of exposure of 27-years. Areas that were moderately corroded were where there was concentrated water leakage from the highway (see Fig. 5).

The highway department is considering remediation of the corroded areas. However, they have not decided how they will accomplish this maintenance. This is surface treated steel and once the protection is breached a different surface treatment is necessary, as the original treatment cannot be replicated.

The highway department is satisfied with the performance of this weather resistant steel. Although this is a weather resistant steel there may be some issues to address in treating corroded areas. Another issue that may exist is any environmentally detrimental releases from this surface treatment or its interaction with adjoining materials. Staining of the concrete piers was not noticed. The steel's color is a dark brown similar to weathered steel. This may be an esthetic limitation in its use. It is interesting to note that none of this

type steel was used in the new Hakucho suspension bridge constructed nearby (see highlight 6 below).

This may be a good case history and should be considered for presentation in the next UNJR Bridge Workshop.

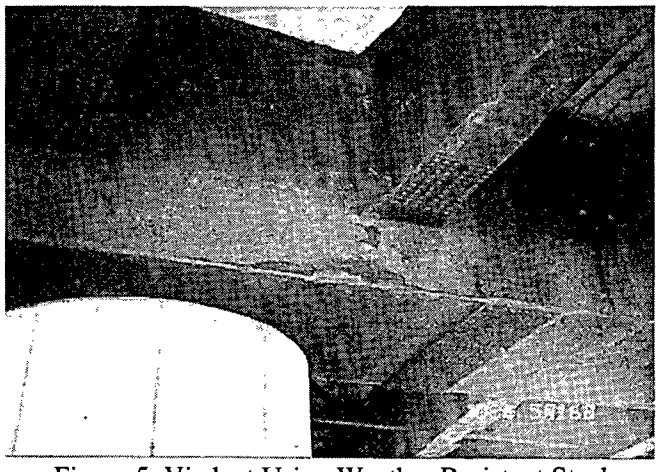


Figure 5. Viaduct Using Weather Resistant Steel

5. Japan Steel Works Ltd., Muroran Plant

The Japan Steel Works (JSW) first steel mill, the Muroran Plant, was completed in 1907 on reclaimed land facing the Muroran Harbor and the Hakucho Suspension Bridge. JSW was founded as a joint venture by three companies: Hokkaido Colliery Steamship Company of Japan; Armstrong Whitworth Co., Ltd., UK; and Vickers Sons and Maxim, Ltd, UK. In 1919 it merged with Hokkaido Steel and Iron Company and started the business of mining and iron-making. In 1947 it was privatized and became incorporated in 1950. The Company produces materials and components and supplies large forged and cast steel products, steel plates, pressure vessels for the chemical and petrochemical industries, and a wide range of industrial machinery. Nine hundred persons are employed at the Muroran Plant.

A video presentation showed a profile of JSW's current work focusing on research into new materials including supper-alloys and powder metallurgy. The main products are steel castings and forgings (up to 600 tons), steel plates, welding assembly, environment and plant engineering, industrial machinery, hydrogen absorbing alloys, medical care and welfare as well as maintenance and inspection services, including a variety of NDT technologies. Other products include rolling mill component, large castings and forging for bridge applications, and powder metallurgy applications. JSW has a long history of providing steel forgings for hydroelectric and nuclear power plants. Their visitor room displays some JSW research activities. Included were posters illustrating development of:

- manufacturing process for an ultra large ingot weighing more than 600 tons,
- magnesium alloy injection molding machine as a more durable substitute for plastics for automobile components, personal computers, mobile phones, etc.,
- high corrosion resistance alloy clad steel plate for environmental protection equipment,

- manufacturing techniques for Ni-base super alloy for large gas turbine forgings,
- hydrogen absorbing alloy and its applications,
- methane fermentation technology,
- clad (stainless + carbon) steel plates for reactor vessels and boilers,
- Stainless steel plates for reactor vessels and boilers.

Recent activity has included a focus on environmental technologies including composting, methane fermentation, wind power, recycling of used tires and gasification methods.

Core Technology	Present and Future areas of interest for JSW	Future Technology
Energy related Materials		Human Life
Industrials Machinery		Ecology
Defence Equipment		Waste Control
		Recycle
		New Technologies

A review was provided on JSW's research on metal hydrides as a substitute for fossil fuels through development of various metal hydride alloys. Hydrogen absorbing alloys have the promise to hold up to 1000 times its weight for use as fuel cells. Metal hydride storage systems have applications for use as heat pumps, refrigeration systems, hydrogen purifiers, actuators and static compressors, magnesium alloy injection molding machines. JSW is seeking an entrée into the green environmental by building on a hydrogen society. See http://www.jsw.co.jp/msb_f/msb_index_e.htm for more information.

The delegation visited JSW's museum, a 1911 building that served as accommodations for the Crown Prince who later became Emperor Taisho, and was father of Emperor Hirohito, when he visited JSW (see Fig. 6). Today the building is a guesthouse for members of the Imperial family and high level dignitaries. Also, the delegation visited JSW's Japanese Sword Smith Shop, founded 1918, where the traditional and cultural heritage of making Japanese swords continues. These traditional Japanese swords require 12 months to become born and cost about $9 000.

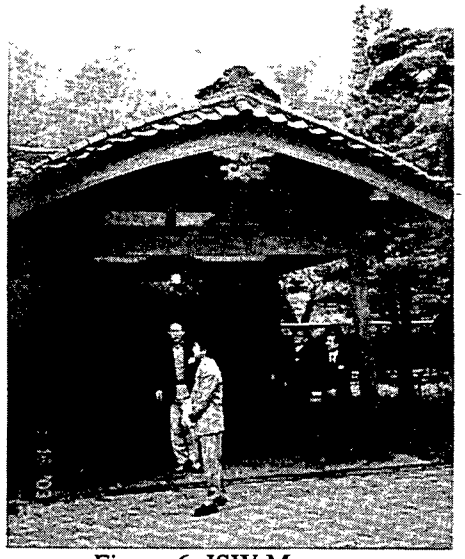


Figure 6. JSW Museum

6. Muroran-Highway Traffic Control System and the Hakucho Suspension Bridge

The Hakucho Ohashi Bridge (Swan Bridge) is a 3 span 1 380 m continuous steel box girder suspension bridge spanning the Muroran Port in Japan's northern prefecture, Hokkaido. Muroran is a major commercial port. The city's commerce is known for its iron and steel industry and its protected deep draft harbor. The bridge was proposed in 1955 by the Muroran Development & Construction Bureau, Hokkaido Development Bureau to provide a ring road around the city of Muroran. To accommodate the growth of Muroran's economy, along with concerted efforts by the municipal government and businesses, and to facilitate urban access officially led to the approval of its construction in 1981. Ground was broken in 1985. Construction commenced in 1985, was completed in 1997, and the bridge opened on 13 June 1998. The Hakucho Bridge's total length is 1 380 m; its end spans are 330 m and a center span measures 720 m. The towers are 140 m high. This is the longest suspension bridge in eastern Japan.

The bridge owner is the Hokkaido Development Bureau. It was constructed by Kawasaki Heavy Industries. Matsuo Bridge Co. Ltd. provided 13 500 tons of steel. This is the first Japanese suspension bridge constructed in a heavy snowy cold area; it required new design technology to handle elimination of snow accumulation on the bridge and control vibration.

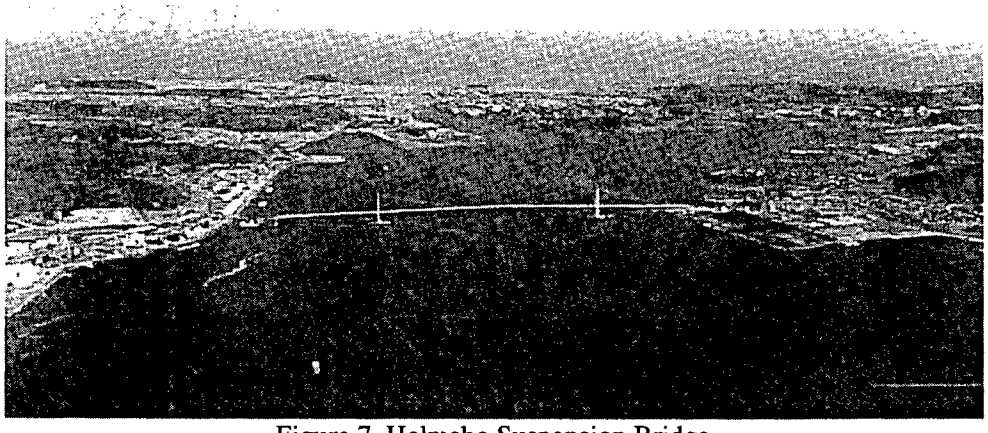


Figure 7. Hakucho Suspension Bridge

The foundation is 73 m below sea level. They are constructed within a cast in place 34 m diameter 50 000 tons of concrete artificial islands. The 140 m towers consist of 15 segment units. Tuned mass dampers were installed at the top of each pylon to dampen sway from high winds. During its erection, the bridge towers employed active control to dampen wind induced vibrations but are limited to a small amplitude range. Such systems don't generally increase seismic safety during severe ground motion. Wind tunnel tests were performed by the Public Works Research Institute under the leadership of Dr. Hiroshi Sato who also is a Panel Member.

The 0.5 m thick cables are comprised of 52 strands of 127 lines of 5.2 mm piano wires. An innovative S-shaped cable wrapping method ties the cables together. That process

was followed by a coating of fluoresin to protect the steel wires from moisture penetrating the cable and cable corrosion. Testing was performed on ½ scale models. Because of the special shape, this type of wrapping minimizes potential exposure due to thermal expansion-contraction cycles. An aeration system also was provided for the main cable, with several dehumidifiers and corresponding inlets and outlet points with the objective of maintaining internal relative humidity levels below 40 percent. Bridge instrumentation includes several anemometers.

The bridge deck is on a stiffening girder – streamlined flat box girder 18 m wide and 2.5 m high – that was selected to better resist winds. The girder has an airfoil-shaped fairing on both sides for aerolastic stability. Ultrasonic testing was performed to assess the welds.

The anchorage consists of 40 000 m^3 of cement. Since the 11 September 2001 World Trade Center/Pentagon Building terrorist attacks, Japan bridge security has been increased. Fences were installed around critical bridge entry locations and motion sensitive cameras were installed at each anchorage.

Many measures were taken to provide for the extreme cold and heavy snows that effect Hokkaido every year. Special procedures were used during the welding processes to account for the brittle nature of steel in cold temperatures. Additions also were made to the steel deck to protect the expansion joints from damage during snow plowing. Because of the demanding requirements to remove snow from the large accumulations, a special snow-removal vehicle was developed for this bridge. Standard snow-removal devices could be operated along the bridge lanes, but removal of significant snow accumulations on the fairings beyond the railing posed significant challenges. The special vehicle operates as a blower, with air speeds up to 150 m/sec with airflow of 500 m^3/min from two nozzles on the left side. A telescopic brush device facilitates snow-removal from the pylons and main cables. The cost of the vehicle was $1 M.

The traffic control office operates an information monitoring system staffed by personnel working in four six-hour shifts. This real time system is employed for the 83-km highway ring-road system using 23 cameras. Seven cameras are at the Hakucho Bridge. Earthquake and wind sensors are installed in the bridge. The bridge is put on alert status when winds exceed 15 m/sec and traffic is halted when wind speeds exceed 25 m/sec. Highest wind speed recorded to date was 30 m/sec resulting in no bridge damage. The design wind speed is 40 m/sec.

7. Mt. Usu, Overview of the Volcanic Effects, Disaster Countermeasures, and Recovery

Mount Usu volcano is located in south eastern Hokkaido on the southern rim of Lake Toya. Usu is a 737 m stratovolcano located about 68 km southeast of Sapporo City. Five small communities totaling approximately 55,000 people live in the vicinity of the volcano. On Friday 31 March 2000, Usu erupted for the first time in 22 years, forcing the evacuation of 16 000 residents by helicopter, truck, and boat. Historical eruptions have been recorded, eleven times with a mean recurrence of 25-years: 1611, 1626, 1638, 1663, 1769, 1822, 1853, 1910, 1943-1945, 1977-1978, and 2000.

The region was shaken by thousands of tremors before the eruption. The field research group of Hokkaido University and Geological Survey of Hokkaido found small fractures in the northern part of the Usu Volcano. Although no lava flowed from the mountain, rocks and ash fell after the eruption. Ash was spewed 3 200 m and coated surrounding towns. No deaths or injuries were reported because the residents followed the recommendations of the Japan Meteorological Agency and the Mayor of the closest community to Usu to evacuate their houses and businesses. The Government invoked the Disaster Relief Law for the neighboring towns at 29 March requesting residents to evacuate immediately. The local headquarters for disaster prevention acted quickly using their video conferencing system to monitor the conditions of affected areas promptly and provide instructions for evacuation and later for rebuilding. A continual degassing continues at various points throughout the area. Although no known health effects have been reported for this eruption, an investigation of the long term human health effects of gases and ash may be in order.

Crustal movements created gaps and mudflow triggered by rainfall and melting snow caused much damage to the infrastructure and to the adjacent National Highway 230. The 2000 eruption mudflow destroyed much of the neighboring infrastructure and covered much of the developed area. A 650 ton bridge on National Highway 230 was washed 120 m away from its site (see Fig. 8). A public bath, apartment, and other structures were destroyed. This area will be created into a future museum to educate visitors about the dangers of such eruptions and stress preventative measures.

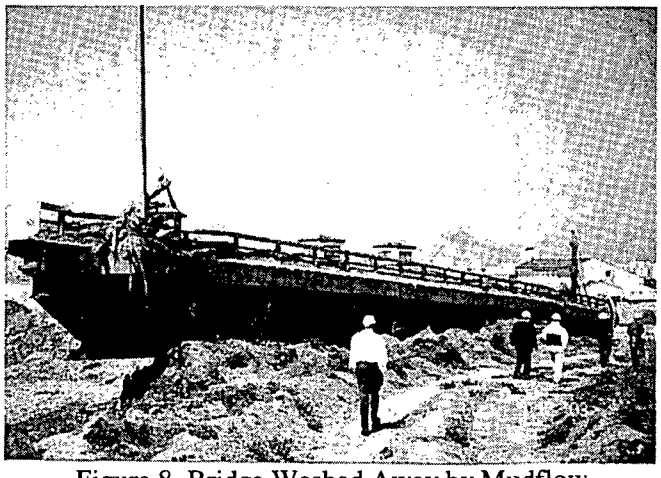


Figure 8. Bridge Washed Away by Mudflow

Following the 1978 eruption, mud flow walls were constructed in several areas of this site to serve as water courses based on data suggesting the most highly probable areas for future mud flows. These flow channels limited the damage from the 2000 eruption. However, the national highway was destroyed in the 2000 event. In anticipation of future eruptions a tunnel is under constructed through the raised ground from crustal movement of the 2000 volcano eruption that will serve as a protected area and an evacuation locations during future eruptions.

The actions performed just prior to and immediately after the volcanic eruption of Mount Usu showcases three key disaster reduction practices:

- An in-place early warning system that monitored the increase in earthquake tremors allowed for timely warnings of the communities residing close to the volcano,
- Effective coordination between the national government, the local authorities, and the private sector allowed for efficient information flow and smooth logistical evacuation procedures,
- A pilot project instigated by the Asian Disaster Reduction Center and the National Space Development Agency of Japan allowed for the live observation of the disaster, as it was unfolding, by satellite.

8. Hokkaido Dams

During the site visits in Hokkaido the delegation was briefed on six dams in the Hokkaido Prefecture. The Hokkaido government manages 20 dams. Detailed information about Japan's large dams, over 50 m high, is available in the publication, *Current Activities On Dams in Japan - 2003*, Japan Commission on Large Dams, Tokyo http://www.jcold.or.jp and email secretariat@jcold.or.jp. The dams highlighted during this visit included:

- Kanayama Hollow Gravity Dam, constructed from 1961 to 1967 for flood control, potable water, hydroelectric power is 57.3 m high, 288.5 m long, and volume of 220 x 10^3 m^3.
- Sasanagare Reinforced Concrete Buttress Dam, constructed during 1920 to 1923 for water supply is 25.3 m high, 199.4 m long, and volume of 36.4 x 10^3 m^3 was reinforced in 1943 and 1968.
- Taisetsu Rock-filled Dam, constructed during 1968 to 1975 as a multi-purpose dam for flood control, electric power, and potable water is 86.5 m high, 440 m long, and volume of 3,740 x 10^3 m^3.
- Jozankei Concrete Gravity Dam, constructed during 1978 to 1989 as a flood control, hydroelectric power, and water supply is 117.5 m high, 410 m long, and volume of 1,185 x 10^3 m^3.
- Pirika Concrete Gravity and Rock-fill Dam, constructed during 1978 to 1991 and later widened to accommodate a fish ladder is 40 m high, 1,480 m long, and volume of 360 x 10^3 m^3.
- Hoheikyo Concrete Arch Dam, constructed from 1967-1972 for flood control, hydroelectric power, irrigation, and potable water is 102.5 m high, 305 m long, and volume of 285 x 10^3 m^3.

STRATEGIC PLAN

U.S.-Japan Joint Panel on Wind and Seismic Effects

Strategic Plan

1.0 Introduction

1.1 Context

The U.S. and Japan must maintain an awareness of international developments in earthquake and wind mitigation technology. The international exchange of information is achieved through a combination of formal and informal mechanisms, including: attendance at conferences and workshops; cooperative research projects and programs; and exchange of scientists and engineers. There is a long-established tradition of joint research activities between Japan and the United States. The U.S.-Japan Cooperative Program in Natural Resources (UJNR) Panel on Wind and Seismic Effects (WSE Panel) provides a formal government-to-government mechanism for cooperation between the two countries in the area of earthquake and wind mitigation technology.

At the 32nd Joint Panel Meeting, a resolution was passed to establish a joint Ad-Hoc Committee for the purpose of developing a strategic plan for the WSE Panel. The catalyst for this effort was the need to address immediate issues related to cost and participation. While the Panel recognized the importance of addressing these immediate issues, it also realized that an opportunity existed to strengthen the WSE Panel's focus on its core mission and foster greater collaboration between researchers in the U.S. and Japan while streamlining the overall operation of the Panel. It was with this goal in mind that the ad-hoc committee developed the strategic plan contained in this document.

1.2 Approach

Before meeting to develop the strategic plan, each side held domestic panel meetings and conducted one-on-one meetings with participating agencies to identify issues that needed to be addressed by the strategic plan and to understand which features of the Panel and its operation should be retained and which needed to be changed or adapted to meet current and future needs. Each side developed a concept paper to capture these ideas. The concept papers, however, tended to focus on addressing the immediate issues rather than positioning the Panel to address the needs and challenges of the future. Through the exchange of the concept papers and subsequent discussion, the two sides moved close to agreement on near-term changes to the Panel's operation. Thus, the strategic plan emphasizes longer-term goals for the operation and growth of the Panel and a time-phased approach to implementation of steps to achieve these goals.

The strategic plan is intended to establish a course for the WSE Panel over the next 5-10 years. It recognizes that there are many ways in which the Panel may work to achieve the goals identified, and so while some steps in the implementation process are clear, others are left open to be determined through experimentation. However, the Panel believes working toward the goals identified will strengthen its role in engineering and scientific communities of the

U.S. and Japan and will allow our countries to make more efficient use of resources to conduct research and disseminate results to the benefit of both countries.

2.0 Role of the Panel

2.1 Guide Research Agendas

As a government-to-government mechanism for collaboration, the WSE Panel is in a unique position to guide the development and execution of each country's research agenda. Currently, each country defines its own research priorities, projects are formulated in a fragmented manner, and results are reported through vehicles such as the Annual Joint Panel Meeting. By strengthening its ties to industry and academia, the Panel will be able to identify specific research needs and align those with government priorities. The Panel shall work toward a coordinated research agenda that permits the efficient use of human resources, funding, and research facilities to achieve mutual research objectives.

The new Task Committees formed through implementation of this strategic plan shall work to identify areas where joint research projects can be established and conducted as a part of a coordinated research agenda. Joint research projects may include participation by university or industry researchers in addition to member agency researchers.

2.2 Leverage Resources

The U.S. and Japan each possess significant expertise in the fields of earthquake and wind engineering and have a substantial investment in equipment and facilities to perform testing and measurements in support of research in these fields. Historically, the WSE Panel has facilitated the exchange of researchers between the U.S. and Japan but has not made a concerted effort to leverage the resources of the two countries. There is an opportunity for the Panel to coordinate research activities to efficiently utilize testing and measurement facilities in both countries to address mutual research needs and avoid duplication. This is an area in which the Panel can significantly strengthen its efforts and provide a tangible benefit to each country by working to establish strong partnerships for coordinated research.

2.3 Foster Cooperation

From its founding, the WSE Panel has promoted cooperation between the U.S. and Japan through annual Joint Panel Meetings, Task Committee activities, and exchange of researchers. One of the hallmarks of success for the WSE Panel through the years has been the high level of cooperation. The model these cooperative efforts have been built around, however, is one of information exchange. While the exchange of information and research results is an important facet of the WSE Panel's work, there is the opportunity to greatly expand the scope and importance of cooperative efforts to leverage resources (people, funding, facilities) through joint research projects of bilateral importance. Additionally, the Panel should look beyond the government agencies that participate to be more inclusive of universities and the private sector. At a minimum, this will include broadening participation in the Joint Panel Meetings to include industry and university participants. As industry and universities become more engaged, exchanges of researchers

among government, university, and industry participants may be possible. Joint programs that include participation by government, industry, and university partners shall also be considered. These activities would broaden the reach of the Panel and provide a means for more rapid diffusion of research results into practice.

2.4 Technical Exchange

The WSE Panel has, throughout its history, been an effective mechanism for the exchange of technical information between Japan and the United States. Further, the WSE Panel has provided a means for disseminating measurements and research results to other nations affected by earthquake, wind, tsunami, and storm surge hazards. Annual Joint Panel Meetings, Task Committee Meetings and Workshops, researcher exchange programs, and personal relationships among researchers have fostered this exchange. The Panel recognizes this as one of its strengths and should seek to broaden its reach to include participation by researchers in other nations. The Panel should explore means of increasing collaboration with other countries through inclusion of representatives from other nations in Joint Panel Meetings, encouraging joint projects through the Task Committees that include partners outside the U.S. and Japan, and through the exchange of researchers with other countries.

2.5 Engage Private Sector

The WSE Panel has engaged the private sector to a limited extent in its activities during its history, although the work of the Panel and the participating agencies can have a direct benefit to industry and ultimately the public in our respective countries. Further, some larger companies have research capabilities and programs that could enrich the Panel. More actively engaging the private sector will provide a means for obtaining input in setting priorities and for more rapidly diffusing the results of research activities into practice within Japan and the United States. The involvement of the private sector may include participation in the development of coordinated research agendas and dissemination of information perhaps through special sessions at the annual Joint Panel Meetings. The Panel should also consider involving the private sector in research projects coordinated at the Task Committee level that will have broad-based benefits to industry in both countries. Longer-term, the involvement of the private sector will facilitate dialogue between practicing engineers and builders in Japan with their counterparts in the U.S. The Joint Panel will examine ways to increase industry participation, initially by inviting key industry representatives to participate in Joint Panel Meetings and to speak about the work of their company or organization and explore possibilities for greater collaboration.

2.6 Web Page Development

The Joint Panel will explore ways to increase utilization of the Internet as a means of communication both among Panel members and with outside organizations. The Japan-side has offered to take the lead in developing an Internet presence for the Joint Panel and has begun work on an initial concept for the site. Once the site is established, the Task Committees will be relied on to provide, maintain, and update content related to their activities. The Joint Panel will

also explore ways of using Internet resources as a means of facilitating communication among researchers as well as the exchange and dissemination of information and research results.

3.0 Implementation

3.1 Strategic Plan Development and Approval

This strategic plan was prepared through the efforts of the Joint Ad-Hoc Committee appointed by the Chairmen following the 32nd Joint Panel Meeting. The Joint Panel shall work toward approval of the Strategic Plan during the 33rd Joint Panel Meeting May 28-30, 2001. The approved document will reflect comments received from Panel members on the draft. Implementation of the strategic plan will begin with approval and require 12-24 months for full implementation.

3.2 Task Committee Charters and Recommended Committees

The US- and Japan-side Panels have agreed on the following seven themes around which Task Committees may be formed:

Theme A: Geotechnical Engineering and Ground Motion
Theme B: Buildings
Theme C: Dams
Theme D: Wind
Theme E: Lifelines
Theme F: Seismic Information and IT
Theme G: Transportation
Theme H: Storm Surge and Tsunami
Theme I: Public Health

Task Committee formed to address one of these themes will be approved by the Joint Panel on annual basis, provided that the Task Committee remains active. The criteria for active Task Committees are following:

a) Conducts joint workshops or technical meetings on a regular basis for the purpose of exchanging technical information, research results, or data for the mutual benefit of both countries.
b) Engages in frequent exchange of researchers for the purpose of technical interchange and collaboration on research.
c) Conducts one or more joint research projects having clearly defined technical objectives, finite duration, and shared responsibility for producing technical results.

Task Committees will report results through papers presented during the joint panel meeting and through task committee reports. The Joint Panel will review task committee results and future plans on an annual basis and will approve task committees for the next year based on this information.

For this year, new task committees may be established by requesting approval through the Secretary-Generals at any time before the 34th Joint Panel Meeting.

3.3 Transition to New Annual Panel Meeting Format

A number of alternative formats for the annual Joint Panel Meeting were considered. Based upon the input received from Panel members, the basic format of the Joint Panel Meeting be retained. Session topics will be principally driven by the Task Committees. Each Task Committee would be given one session during which it would be able to present research results. This Task Committee-driven format should strengthen the role of the Task Committees and is intended to stimulate greater cooperation among researchers in each country. This format will foster the exchange of information that many have expressed is a desirable feature of the Joint Panel Meeting.

The Joint Panel meeting will be shortened by one day (from 4 days to 3 days). The shorter meeting, coupled with a shorter Technical Site Tour will reduce the time commitment for participants to one week. This is intended to encourage greater participation in the Panel Meetings and Site Tours, particularly by members of the visiting Panel.

Finally, the Joint Panel will explore streamlining the Joint Panel Meeting to maximize the opportunity for technical exchange.

The shortened Panel Meeting/Technical Site Tour format is implemented for the first time at the 33rd Joint Panel Meeting. The Task Committee-driven technical meeting format will be implemented at a later date when the revised Task Committee organization is in place.

4.0 Conclusion

The plan outlined above represents a strategic plan for positioning the Joint Panel to meet the challenges of the future, while retaining those aspects that have contributed to its success through it 32 year history. This plan is intended to address the current realities of the Panel, as well as increase the value and contribution of the Panel to the U.S. and Japan. Full implementation of the strategic plan will take approximately two years.